AUGUST · 1955

Proceedings OF THE IRE

GATEWAY TO WESCON

Trans World Airlines Photo

Golden Gate Bridge, longest single span in the world, arches the Strait which separates the Pacific from San Francisco Bay. And San Francisco will this month be the gateway to WESCON, second largest IRE convention.

Volume 43 Number 8

IN THIS ISSUE

Table of Contents, Indicated by Black-and-White Margin, Follows Page 96A

The Institute of Radio Engineers

LEADERS IN MINIATURIZATION FOR OVER TWENTY YEARS . . .

MINIATURIZED TRANSFORMER COMPONENTS FROM STOC

Items below and 650 others in our catalog A.

HERMETIC SUB-MINIATURE AUDIO UNITS

These are the smallest hermetic audios made.

Dimensions . . . 1/2 x 11/16 x 29/32 . . . Weight.8 oz.

TYPICAL ITEMS

Type No.	Application	MIL Type	Pri. Imp. Ohms	Sec. Imp. Ohms	DC in Pri MA	Response ±2 db (Cyc.)	Max. level dbm
H-30	Input to grid	TF1A10YY	50*	62,500	0	150-10,000	+13
H-31	Single plate to single grid, 3:1	TF1A15YY	10,000	90,000	0	300-10,000	+13
H-32	Single plate to line	TF1A13YY	10,000*	200	3	300-10,000	+13
H-33	Single plate to low impedance	TF1A13YY	30,000	50	1	300-10,000	+15
H-34	Single plate to low impedance	TF1A13YY	100,000	60	.5	300-10,000	+ 6
H-35	Reactor	TF1A20YY	100 Henries-0 DC, 50 Henries-1 Ma. DC, 4,400 ohms.				
H-36	Transistor Interstage	TF1A15YY	25,000	1,000	.5	300-10,000	+10

*Can be used with higher source impedances, with corresponding reduction in frequency range and current

COMPACT HERMETIC AUDIO FILTERS

UTC standardized filters are for low pass, high pass, and band pass application in both interstage and line impedance designs. Thirty four stock values, others to order. Case 1-3/16 x 1-11/16 x 1-5/8—2-1/2 high . . . Weight 6-9 oz.

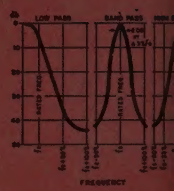

HERMETIC MINIATURE HI-Q TOROIDS

MQE units provide high Q, excellent stability and minimum hum pickup in a case only. 1/2 x 1-1/16 x 17/32 . . . weight 1.5 oz.

TYPICAL ITEMS

Type No.	Inductance		DC Max.
MQE-1	7	mhy.	135
MQE-3	20	mhy.	80
MQE-5	50	mhy.	50
MQE-7	100	mhy.	35
MQE-10	.4	hy.	17
MQE-12	.9	hy.	12
MQE-15	2.8	hy.	7.2

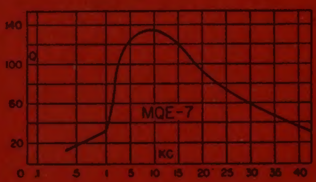

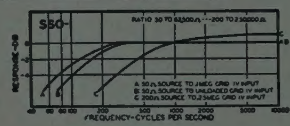

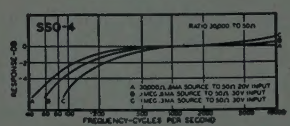

SUB-SUBOUNCER AUDIO UNITS

UTC Subouncer and sub-subouncer units provide exceptional efficiency and frequency range in miniat size. Constructional details assure maximum re bility. SSO units are 7/16 x 3/4 x 43/64 . . . We 1/50 lb.

Type	Application	Level	Pri. Imp.	MA D.C. in Pri.	Sec. Imp.	Pri. Res.	Sec.
*SSO-1	Input	+ 4 V.U.	200 50	0	250,000 62,500	13.5	
SSO-2	Interstage /3:1	+ 4 V.U.	10,000	0-.25	90,000	750	
*SSO-3	Plate to Line	+20 V.U.	10,000 25,000	3 1.5	200 500	2600	
SSO-4	Output	+20 V.U.	30,000	1.0	50	2875	
SSO-5	Reactor 50 HY at 1 mil. D.C. 4400 ohms D.C. Res.						
SSO-6	Output	+20 V.U.	100,000	.5	60	4700	
*SSO-7	Transistor Interstage	+10 V.U.	20,000 30,000	.5 .5	800 1,200	850	

* Impedance ratio is fixed, 1250:1 for SSO-1,1:50 for SSO-3. Any impedance between the values shown may be employed.

OUNCER (WIDE RANGE) AUDIO UNITS

Standard for the industry for 15 yrs., these units provide 30-20,000 cycle response in a case 7/8 dia. x 1-3/16 high. Weight 1 oz.

TYPICAL ITEMS

Type No.	Application	Pri. Imp	Sec. Imp
O-1	Mike, pickup or line to 1 grid	50, 200/250, 500/600	50,000
O-4	Single plate to 1 grid	15,000	60,000
O-7	Single plate to 2 grids, D.C. in Pri.	15,000	95,000
O-9	Single plate to line, D.C. in Pri.	15,000	50, 200/250, 500/600
O-10	Push pull plates to line	30,000 ohms plate to plate	50, 200/250, 500/600
O-12	Mixing and matching	50, 200/250	50, 200/250, 500/600
O-13	Reactor, 300 Hys.—no D.C.; 50 Hys.—3 MA. D.C., 6000 ohms		

HERMETIC VARIABLE INDUCTORS

These inductors provide high Q from 50 - 10,000 cycles with exceptional stability. Wide inductance range (10 - 1) in an extremely compact case 25/32 x 1-1/8 x 1-3/16 . . . Weight 2 oz.

TYPICAL ITEMS

TYPE No.	Min. Hys.	Mean Hys.	Max. Hys.	DC Ma
HVC-1	.002	.006	.02	100
HVC-3	.011	.040	.11	40
HVC-5	.07	.25	.7	20
HVC-6	.2	.6	2	15
HVC-10	7.0	25	70	3.5
HVC-12	50	150	500	1.5

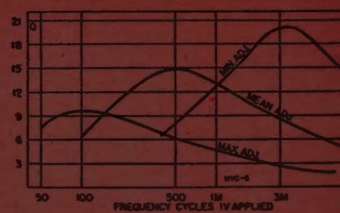

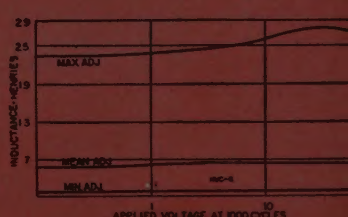

LET US MINIATURIZE YOUR GEAR.

UNITED TRANSFORMER CO

150 Varick Street, New York 13, N. Y. • EXPORT DIVISION: 13 E. 40th St., New York 16

NEW GERMANIUM POWER RECTIFIERS REDUCE VOLUME AND WEIGHT 75%

...and actually cost less!

TYPE
4JA3011

GERMANIUM POWER RECTIFIERS

Ratings to 85°C

Because of the higher efficiency of germanium, these new G-E rectifiers achieve a full 75% saving in size and weight—and yet actually cost less than any conventional type dry rectifier in use today. This sharply-reduced weight and volume is a result of greatly-increased power per cell in G.E.'s unique low-loss rectifier.

Compare and see! For new efficiency in your 1955 designs go the limit with new G-E Germanium Power Rectifier. Tell your rectification problem to the G-E application engineer—write today to: *General Electric Company, Semiconductor Products, Section X5285, Electronics Park, Syracuse, New York.*

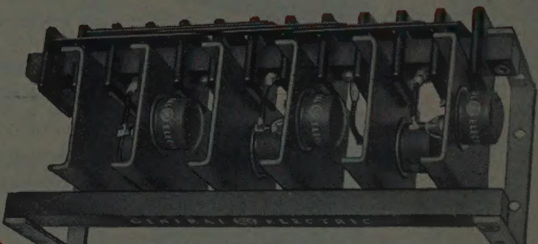

OVERALL SIZE IS 4″ x 5″ x 10″

NOW AVAILABLE IN PRODUCTION QUANTITIES

These rectifiers are available in standard combinations consisting of one or more rectifying elements. A few of the typical ratings are listed below.

CIRCUIT	D-C OUTPUT AT 55°C (Resistive Load)
Half Wave	24 amps @ 60 V 12 amps @ 94 V 8 amps @ 140 V
Full Wave Center Tap	24 amps @ 60 V 10 amps @ 140 V
Full Wave Bridge	10 amps @ 125 V
Three-Phase Half Wave	17.8 amps @ 93 V 11.2 amps @ 139 V
Three-Phase Bridge	11.2 amps @ 188 V

Be "money-wise" and "pound-wise" too, with these stand-out design features:

- Weight and volume reduced 75%
- Rectifier losses have been reduced to ⅓ or less
- No forward aging effects...no need for age-compensating devices

Progress Is Our Most Important Product

GENERAL ELECTRIC

Meetings with Exhibits

As a service both to Members and the industry, we will endeavor to record in this column each month those meetings of IRE, its sections and professional groups which include exhibits.

Aug. 24-26, 1955
Western Electronic Show & Convention, Civic Auditorium, San Francisco, Calif.
Exhibits: Mr. Mal Mobley, 344 N. La-Brea, Los Angeles 36, Calif.

SAN FRANCISCO, CALIFORNIA

Sept. 12-16, 1955
Tenth Annual Instrument Conference & Exhibit, Shrine Exposition Hall & Auditorium, Los Angeles, Calif.
Exhibits: Mr. Fred J. Tabery, 3442 So. Hill St., Los Angeles 7, Calif.

Sept. 26-27, 1955
IRE Sixth Annual Meeting of the Professional Group on Vehicular Communications, Hotel Multnomah, Portland, Ore.
Exhibits: Mr. Henry S. Broughall, General Electric Co., 2727 N.W. 29th Ave., Portland, Ore.

October 3-5, 1955
National Electronics Conference, Sherman Hotel, Chicago, Ill.
Exhibits: Mr. G. J. Argall, c/o DeVry Technical Institute, 4141 Belmont Ave., Chicago 41, Ill.

Oct. 31-Nov. 1, 1955
IRE East Coast Conference on Aeronautical & Navigational Electronics, Lord Baltimore Hotel, Baltimore, Md.
Exhibits: Mr. C. E. McClellan, Westinghouse Electric Corp., Air Arm Div., Friendship International Airport, Baltimore, Md.

Nov. 3-4, 1955
Annual Electronics Conference, Kansas City Section, Town House Hotel, Kansas City, Kans.
Exhibits: Mr. Charles V. Miller, Bendix Aviation Corp., P.O. Box 1159, Kansas City 41, Mo.

Nov. 7-9, 1955
Eastern Joint Computer Conference (IRE-AIEE-ACM), Hotel Statler, Boston, Mass.
Exhibits: Mr. J. D. Porter, Digital Computer Lab., Barta Building, M.I.T., Cambridge, Mass.

Nov. 28-30, 1955
Instrumentation Conference & Exhibit, Atlanta Biltmore Hotel, Atlanta, Ga.
Exhibits: Mr. W. B. Wrigley, Engineering Experiment Station, Georgia Institute of Technology, Atlanta, Ga.

Feb. 9-11, 1956
Eighth Annual Southwestern IRE Conference and Electronics Show, Municipal Auditorium, Oklahoma City, Okla.
Exhibits: Mr. Charles E. Harp, P.O. Box 764, Oklahoma City, Okla.

New, low cost, versatile

INDUSTRIAL COUNTER

Measures frequency, speed, rpm, rps, random events
Measures weight, pressure, temperature, acceleration*
Direct numerical readings 1 cps to 120 KC
High accuracy, simple operation, compact, rugged

-hp- 521A—$475.00

New *-hp-* 521A is designed to be the most useful, accurate low cost industrial counter ever offered. It measures frequency, speed, rpm, rps, and counts random events within a selected time interval. With transducers, it measures weight, pressure, temperature, acceleration and other phenomena which can be converted to frequency. It is direct reading in cps, rpm or rps, and can be used readily by non-technical personnel. Period of count is 0.1 or 1 second; display time can be varied.

The 50/60 cycle power circuit is used as the time base; or, for greater accuracy, a plug-in crystal controlled time base is available at extra cost. There are accessory power supplies of —150 v dc, +300 v dc and 6.3 v ac. Connections are also supplied for photocells and an external 60 cycle standard. Lightweight, compact, sturdy; particularly useful with *-hp-* Optical Tachometer Pickups and Tachometer Generators. *-hp-* 521A, $475.00 (with plug-in crystal time base, $575.00).

Other versatile -hp- Counters

-hp- 524B Electronic Counter with 525/526 series Plug-Ins. Revolutionary all-purpose, direct-reading counter. Buy basic counter, plug-ins giving measuring coverage you need now. Later add other inexpensive plug-ins to double, triple counter's usefulness. Basic counter range: Frequency 10 cps to 10 MC, period 0 cps to 10 KC, stability 1/1,000,000. *-hp-* 524B, $2,150.00Δ.

-hp- 525A/B Frequency Converters extend 524B's range to 100 or 220 MC, increase video sensitivity. *-hp-* 525A/B, $250.00.

-hp- 526A Video Amplifier increases counter's sensitivity to 10 mv, 10 cps to 10 MC. $150.00.

-hp- 526B Time Interval Unit permits counter to measure interval 1 μsec to 100 days with accuracy of 0.1 μsec, ±0.001%. $175.00.

-hp- 522B Electronic Counter. Compact, moderate price; frequency, period or time measurements. 10 cps to 100 KC. Reads direct in cps, KC, seconds, milliseconds. Automatic count reset, repetitive action. Stability 5/1,000,000, display length variable. Easily used by non-technical personnel. $915.00Δ.

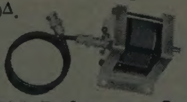

-hp- 508A Tachometer Generators. Use with electronic counters, frequency meters to measure directly 15 to 40,000 rpm. Produces 60 cycle output frequency per revolution; (*-hp-* 508B produces 100 cycles) *-hp-* 508A or 508B, $100.00.

-hp- 506A Optical Tachometer Pickup. For measuring rotation 300 to 300,000 rpm. Ideal for moving parts of small energy or where mechanical connection is impractical. $100.00.

*Data subject to change without notice. Prices f.o.b. factory. ΔRack mount slightly less. *With transducers.*

Electronic Test Instruments

Quality, value, complete coverage

HEWLETT-PACKARD COMPANY
3342D Page Mill Road • Palo Alto, Calif. • Cable "HEWPACK"

PLEASE SEND INFORMATION ON:

___521A ___522B ___524B & Plug-Ins ___506A ___508A/B

Name___

Company___

Street___

City___ Zone___ State___

CORRECTION

High Temperature Tantalum Capacitors

Cornell-Dubilier Electric Corp. has announced the development of a new Tantalum slug type electrolytic capacitor designed to operate under wide temperature ranges.

These new type "TH" Tantalums are rated from −55°C to +125°C. Units rated to +175°C can be supplied on specific order. Standard case size $\frac{1}{2}$ inch × $\frac{7}{8}$ inch to 120 μf; only slightly larger to 240 μf. Series combinations can be supplied at higher capacities and voltage ratings. These new capacitors are suited for operation under conditions of high G shock, high thermal cycling, and severe vibration.

Standard units range from 25 to 120 μf with a voltage range of 18 to 100 volts dcw. Higher capacitances and voltages to 630 volts dcw, can be supplied. For further information send for Engineering Bul etin No. 529.

Welwyn Forms American Sales Company

Welwyn Electrical Laboratories, Ltd. (England) and **Welwyn Canada, Ltd.,** have announced the formation of a new American company to handle the sale of Welwyn products on a national basis. Operations of the new company are effective as of 1955.

Both the English and Canadian companies are engaged in the manufacture of high stability resistors in the following types: deposited carbon, miniature potentiometers—glass sealed, high value Welmegs—vitreous—enamel coated wire-bound—encapsulated—deposited carbon—and deposited carbon meter multipliers. The American sales of Welwyn resistors were handled by Rockbar Corporation as national distributors.

The new company, **Welwyn International, Inc.,** has established offices at 3355 Edgecliff Terrace, Cleveland 11, Ohio. John Buchspice, formerly associated with Welwyn sales at Rockbar, has been appointed Sales Manager.

These manufacturers have invited PROCEEDINGS readers to write for literature and further technical information. Please mention your I.R.E. affiliation.

Thermistor Compensated Pyrometers

Three sizes of sealed and ruggedized instruments have been added to the line of pyrometers made by **Assembly Products, Inc.,** Chesterland, Ohio. There are 4 black bakelite cases ($2\frac{1}{2}$ and $3\frac{1}{2}$ inch round and square) and 3 clear plastic case models. All have automatic bimetal cold junction compensation and thermistors for high accuracy over wide variations of ambient temperatures.

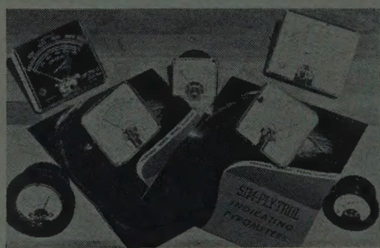

Each has a screwdriver adjustor for setting the reading, when installed, to within 1 per cent accuracy. 17 temperature ranges are listed as standard covering from −400°F to 3,000°F. The corresponding Centigrade is shown on each dial. Sensitivity is 4 ohms per millivolt. The new ruggedized models 255 ($2\frac{1}{2}$ inches) 355 ($3\frac{1}{2}$ inches) and 455 ($4\frac{1}{2}$ inches) offer the same choice of many temperature ranges and have the same electrical specifications.

A thermocouple calibrating resistor is supplied with each pyrometer. Additional resistors are available for installations where one meter is used with several thermocouples and a selector switch. Prices range from \$20.00 to \$50.00. Write for Bulletin G-9.

Guided Missile Timer

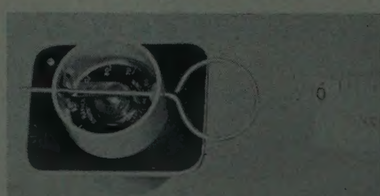

This small timer by **Raymond Engineering Laboratory, Inc.,** Smith St., Middletown, Conn., is specifically suited for airborne equipment or missiles. The unit contains a spring wound timer and a single-pole double-throw switch which is thrown at the end of the set time. The unit is available with three different types of actuators: Pull wire, dimple (explosive) motor, or g weight actuators, which start the timing cycle. The unit is suitable for mounting on a panel or plate in a manner similar to the way small potentiometers are mounted.

Maximum time delays vary from 1 second to 6 minutes in the various models. The switch is rated at 5 amperes, 250 volts, non-inductive. The unit will operate at 40 g, −60°F to +200°F with an accuracy of ± 10 per cent. It is $1\frac{1}{2}$ inches in diameter and $1\frac{3}{16}$ inches deep behind the panel. Finishes and materials conform to Military Specifications.

The photograph shows a pull wire actuated unit.

Multiplier Phototube Catalog

"Du Mont Multiplier Phototubes," a comprehensive catalog of operational theory, data on applications, and specifications for standard and special multiplier phototubes—has just been published by the **Technical Sales Dept., Allen B. Du Mont Laboratories, Inc.,** 760 Bloomfield Ave., Clifton, N. J.

The 64 pages of this illustrated catalog have been divided into three sections. The first section contains a simplified technical discussion of photo and secondary emissions, and their effect on design and operation of multiplier phototubes.

The second section describes the utility of multiplier phototubes for the major sciences and industries with details of specific applications in the mechanical, chemical, electronic, and nuclear fields.

In the third section, full specifications on Du Mont standard and special multiplier phototubes are given, together with complete information on their accessories.

Requests for this catalog should be on company letterheads and addressed to the Technical Sales Department.

(Continued on page 16A)

News-New Products

These manufacturers have invited PROCEEDINGS readers to write for literature and further technical information. Please mention your I.R.E. affiliation.

(Continued from page 14A)

R-C Oscillator

Two new features are made available on the Type 1210-B Unit R-C oscillator designed by **General Radio Co.,** 275 Massachusetts Ave., Cambridge 39, Mass. Square wave output is provided over the entire frequency range from 20 cps to 500 kc in addition to two sine-wave outputs. The square-wave output is 0 to 30 volts peak-to-peak with about $\frac{1}{4}$ μs rise time. Output impedance is 2,500 ohms. A sine-wave output of 0 to 7 volts is available from a 50-ohm output impedance with no-load distortion less than 1 per cent from 200 cps to 200 kc. A maximum of 45 volts is available from a 12,500-ohm output.

Automatic recording of frequency characteristics is made possible by means of the second new feature. The gear-drive precision dial is arranged so that it is driven automatically by a Type 908-P synchronous dial drive. This motor drive can sweep any portion of each of the 5 decade frequency ranges. Several methods of synchronizing the sweeping with pen recorders can be used to give permanent records of frequency response. With a cathode-ray oscillograph the frequency characteristics of a network can be displayed when a Type 1210-P1 detector and discriminator is used with the oscillator to provide a horizontal-deflection voltage proportional to frequency.

The frequency calibration accuracy of the Type 1210-B Unit R-C oscillator is ± 3 per cent. The output control is logarithmic and is calibrated from 0 to -50 decibels. The Type 1210-B Oscillator is priced at $140 less power supply. The Type 1203-A unit power supply is priced at $40 and the Type 1210-P1 Detector and Discriminator at $75. All prices are net f.o.b. Cambridge, Mass.

(Continued on page 152A)

IRE People

Estill I. Green (A'27–M'36–SM'43–F'55), director of military communication systems at Bell Laboratories, has been elected Vice-President in charge of systems engineering.

E. I. Green

Mr. Green, a veteran of 34 years of service with the Bell System, brings to his new assignment a long record of engineering experience and achievement, including some 75 patents.

He began his telephone career in 1921 with the American Telephone and Telegraph Company's Development and Research Department, and with that department transferred to Bell Laboratories in 1934. For a considerable time he specialized in toll transmission systems, with particular interest in multiplex telephone and telegraph systems. During World War II he was engaged in development work on radar testing apparatus and other electronic equipment. He was appointed Director of Transmission Apparatus Development in 1948 and in 1953 was named Director of Military Communication Systems.

Mr. Green received the Bachelor of Arts degree from Westminster College in 1915 and the Bachelor of Science in electrical engineering degree from Harvard in 1921. He is a Fellow of the American Institute of Electrical Engineers.

❖

E. F. Shell (M'51) has been appointed Development Engineer in the Airborne Computer Laboratory at International Business Machines Corporation, Endicott, New York. He came to IBM in 1952 as an Associate Engineer in the Airborne Computer Laboratory, and the following year was appointed Project Engineer. He held the latter position until the time of his appointment as Development Engineer.

Mr. Shell received his early education in Toledo, Ohio. He has attended the University of Toledo where he studied electrical engineering and Wilmington College where he completed courses in mathematics.

During World War II, he served with the U. S. Navy.

❖

The appointment of **R. D. Chipp** (A'34–SM'43) as director of engineering for all manufacturing divisions of Allen B. DuMont Laboratories, Inc., has been announced.

Mr. Chipp, who has directed engineering for the DuMont Television Network

since 1948, will coordinate the engineering activities of DuMont's Television Receiver Division, Cathode-ray Tube Division, Communication Products Division, Instrument Division, and Government Division. He will also serve as liaison between divisional engineering departments and DuMont's Research Laboratories. He will continue to be available to the DuMont Network for consultation and engineering help.

Mr. Chipp has been active in radio and television engineering since 1928. Prior to his association with the DuMont Television Network he was radio facilities engineer for the American Broadcasting Company and the National Broadcasting Company from 1933 to 1941. Since 1938 he has been closely identified with the design and development of television broadcasting techniques and equipment.

During World War II Mr. Chipp was an officer in the U. S. Navy and saw service with the Bureau of Ships. He was cited for "development engineering of the early radar equipment in the desperate early months of the war, and, later, for the splendid design of radar repeaters and equipment." Mr. Chipp has also served as consulting engineer to the U. S. Navy, Hazeltine Electronics, and a number of broadcasting stations.

Holding the B.S. degree, he attended Massachusetts Institute of Technology and Newark College of Engineering.

Mr. Chipp is an associate member of the Association of Federal Communications Consulting Engineers, a member of the National Society of Professional Engineers, the Society of Motion Picture and Television Engineers, the U. S. Naval Institute, the Veteran Wireless Operators Association, and the Cum Laude Society,

❖

The appointment of **W. R. Sinback** (M'47) as Navy sales manager for the G.E. Heavy Military Electronic Equipment Department has been announced.

W. R. Sinback

In his new position he will be responsible for all HMEE sales to the Navy for such products as radar, sonar, and communications equipment.

Formerly the department's district sales manager in Washington for sales to the Army, he will now have his office at HMEE headquarters in Syracuse.

Mr. Sinback, a native of Shannon, Alabama, was graduated from Alabama Polytechnic Institute with the bachelor's degree in electrical engineering.

(Continued on page 34A)

DESIGNERS

ELECTRON TUBES
SEMICONDUCTOR DEVICES
BATTERIES
TEST EQUIPMENT
ELECTRONIC COMPONENTS

GENERAL-PURPOSE 3" FLAT-FACE OSCILLOGRAPH TUBE

RCA-3RP1-A . . . has small, brilliant, focused spot and high deflection sensitivity for its relatively short length. The screen is of the medium-persistence, green-fluorescence type. This tube provides a trace having high brightness when operated with an ultor voltage near the maximum of 2500 volts, and good brightness at relatively low ultor voltage. The flat face facilitates use of an external calibrated scale and minimizes parallax in readings.

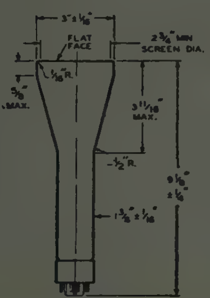

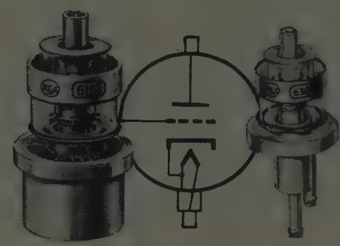

TWO UHF POWER TRIODES FOR FREQUENCIES UP TO 2000 Mc

RCA-6383 . . . liquid- and forced-air-cooled for UHF transmitter service. Has 600 watts plate dissipation and can be operated at full input ratings at frequencies up to 2000 Mc. **RCA-6161** . . . forced-air-cooled, with radiating fin construction. For UHF service in TV and cw applications. Has maximum plate dissipation of 250 watts. Operates at full input ratings up to 900 Mc, reduced ratings up to 2000 Mc. Both types for circuits of the coaxial cylinder type. Particularly suited for cathode-drive circuits. For service in aircraft and other applications where light weight, compactness, and high power output are prime design considerations.

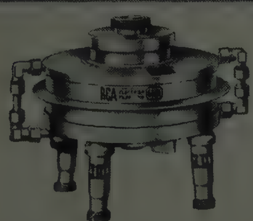

12 KILOWATTS OUTPUT AT 900 Mc

RCA-6448 . . . a water-cooled beam power tube with a unique design—is intended for operation as a grid-driven power amplifier at frequencies up to 1000 Mc. In color or black-and-white TV service, it is capable of delivering a synchronizing-level power output of 15 Kw at 500 Mc or 12 Kw at 900 Mc. The 6448 is also capable of giving useful power output of 14 Kw at 400 Mc or 11 Kw at 900 Mc as a cw amplifier in class C telegraphy service.

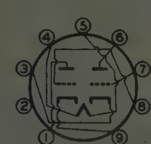

NEW DUAL TRIODE WITH TWO DISSIMILAR UNITS

RCA-6CM7 . . . a medium-mu dual triode of the 9-pin miniature type containing two dissimilar triodes in one envelope. Unit No. 2 is a high-perveance triode designed especially for use as a vertical deflection amplifier. Unit No. 1 is designed for use as a conventional blocking oscillator in vertical deflection circuits. The RCA-6CM7 also features a 600-milliampere heater with controlled warmup time, separate cathodes for the two units, and a basing arrangement which facilitates use in printed circuits.

RCA®

RADIO CORPORATION of AMERICA
TUBE DIVISION HARRISON, N. J.

IRE People

(Continued from page 19A)

He served as a Naval officer during World War II, and during his tour of duty was assigned to the Naval Ordnance Laboratory as an electrical engineer. Following his release from active duty in 1945 he returned to the NOL as a civilian electrical engineer.

He later was engaged in consulting radio engineering before joining G.E. as a sales representative for military electronic equipment in 1950. In 1953 he was appointed district sales manager in Washington for Army electronics sales, a position which he held until his present appointment.

❖

E. J. Bradley (A'51) has been made Sales Manager of Color Television Incorporated.

For the past five years Mr. Bradley has been associated with the Airpax Products Company of Middle River, Maryland where, as General Sales Manager, he successfully increased the company's sales. Since 1935, Mr. Bradley, has been employed in a technical or sales capacity by the Glenn L. Martin Company, General Electric Company, Westinghouse Electric, the U. S. Air Force and a wholesale radio parts distributor.

Mr. Bradley was born in Baltimore, Maryland, March 24, 1917, and graduated from Baltimore Polytechnic Institute, The Maryland Institute and the Commercial Radio Institute in Baltimore.

❖

A. J. Spriggs, USN (Ret.), (SM'47), former Director of Electronics, Office of the Chief of Naval Operations, has been elected a Vice-President of Packard-Bell. In his new post, Commodore Spriggs will be stationed in Washington, D. C., and will represent Packard-Bell with the Armed Services and other customers for the varied electronic products of the company's Technical Products Division.

As Director of Electronics for the Office of the Chief of Naval Operations, Commodore Spriggs was in charge of directives and priorities relating to procurement and distribution of electronics equipments. Prior to his appointment to that post, he was head of the Electronics Division, Bureau of Ships. A graduate of the United States Naval Academy, he received his Master of Science degree in radio engineering from Yale University in 1926. He retired from the Navy in August, 1946 and joined the Packard-Bell Company in September 1950, as production manager of the Technical Products Division.

❖

The appointment of **R. I. Gaines** (S'44–A'49) as assistant director of the International Division of Allen B. DuMont Laboratories, Inc., has been announced. Mr. Gaines will assist in the management

(Continued on page 38A)

Eimac

THE WORLD'S
LARGEST MANUFACTURER
OF TRANSMITTING TUBES

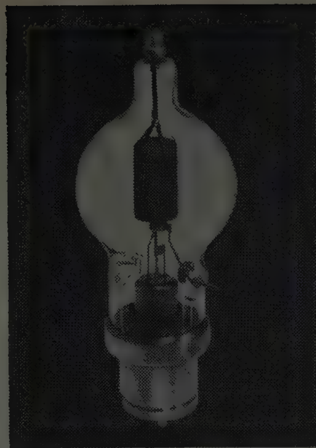

250w Triode

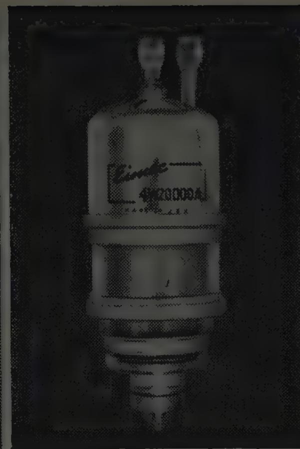

20kw Tetrode

High Vacuum Rectifier

10kw/cw UHF Klystron

EIMAC TUBES

For All Types of Communications, Industrial and Pulse Application!

Eimac offers a complete line of over seventy triode, tetrode, pentode, klystron and rectifier tube types to cover all types of electronic communications, industrial and pulse applications. The versatile Eimac electron-power tube family is second to none in frequency and power coverage. Even at ultra high and microwave frequencies, high power is no problem with Eimac amplifier klystrons. Up through the VHF region, Eimac negative grid tubes have been performance proved in every type of service. Internal or external anode, water or air cooled, metal, ceramic or glass construction, there is an Eimac tube to meet the most exacting requirements.

For further information contact our Technical Services Department.

EITEL-McCULLOUGH, INC.
SAN BRUNO • CALIFORNIA

Reflex Klystron

5kw Tetrode

250w Tetrode

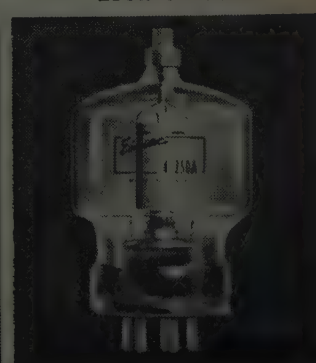

IRE People

(Continued from page 34A)

of the International Division, whose activities involve the foreign sale of products manufactured by DuMont as well as the licensing of foreign companies to manufacture DuMont products.

Mr. Gaines brings to his new position a background of engineering and sales administration in the electronics industry. He previously was export manager of the International Division and sales engineer in the Instrument Division, DuMont Laboratories. Prior to his association with DuMont, Mr. Gaines was an engineer with Communications Measurements Laboratory and with Semco Services.

He holds a degree in electrical engineering from Columbia University and has also done graduate study at Harvard University and Massachusetts Institute of Technology. A member of the American Institute of Management, Mr. Gaines also serves as a member of the electronics committee of the International Department of RETMA.

❖

F. A. Foss (S'43–A'45) has been appointed Development Engineer in the International Business Machines Corporation's Airborne Computer Laboratory at Endicott, N. Y. He began his employment in December, 1950 as an Associate Engineer in the Physics Laboratory. In May, 1951 he was assigned to the Airborne Computer Laboratory, and in February, 1954 he was made Project Engineer, the position he held until his appointment as Development Engineer.

In 1944, he was graduated *Summa Cum Laude* from Tufts College with a Bachelor of Science degree in electrical engineering; he received his Master's degree in Electrical Engineering from the Massachusetts Institute of Technology in 1940. He has completed courses in IBM Products I, Mechanical and Electrical Principles 604–607, and Semiconductor Electronics I in the IBM School.

During World War II, Mr. Foss served with the U. S. Signal Corps. He is a member of the Association for Computing Machinery, Tau Beta Pi, and Sigma Xi.

❖

J. B. Fisk (SM'52–F'55), Vice-President in charge of Research at Bell Telephone Laboratories, has been elected Executive Vice-President. In his new post Dr. Fisk will be directly responsible for all technical activities of Bell Laboratories, as well as continuing his present responsibilities in charge of research.

J. B. Fisk

Dr. Fisk, who joined Bell in 1939,

(Continued on page 40A)

REVERSIBLE SILICON MIXER DIODES

Here's another step forward by Bomac — a *reversible* silicon mixer diode. The 1N415 and 1N416 series are the first silicon diodes to have selective polarity.

Polarity is indicated by the letters REV located at one end of the diode. To change the polarity, just switch the position of the end cap.

With the end cap attached to the contact pin at the unmarked end of the cartridge, the diode will be of normal polarity. With the end cap attached to the end marked REV, the diode will be of reverse polarity. The complete assembly, with either polarity, is electrically the same as its equivalent type of regular silicon diodes.

The Bomac 1N415 and 1N416 series will meet all conditions of JAN 1A specifications.

1N415 - 1N416 SERIES

NORMAL POLARITY

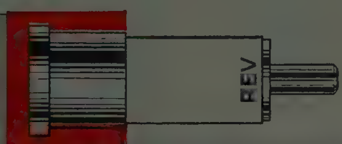

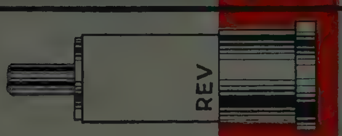

REVERSE POLARITY

Band	Type	Equivalent Type	Frequency (Mc)	Max. Conversion Loss (db)	Noise Ratio (Times)	Max. (VSWR)	IF Imped. (OHMS)	Burnout (erg)
X	1N415B	1N23B	9375	6.5	2.7	—	—	1.0
		1N23BR	9375	6.5	2.7	—	—	1.0
X	1N415C	1N23C	9375	6.0	2.0	1.50	325–475	1.0
		1N23CR	9375	6.0	2.0	1.50	325–475	1.0
X	1N415D	1N23D	9375	5.0	1.7	1.30	350–450	1.0
		1N23DR	9375	5.0	1.7	1.30	350–450	1.0
S	1N416B	1N21B	3060	6.5	2.0	—	—	2.0
		1N21BR	3060	6.5	2.0	—	—	2.0
S	1N416C	1N21C	3060	5.5	1.5	—	—	2.0
		1N21CR	3060	5.5	1.5	—	—	2.0

UNIQUE PACKAGE PROTECTION

For complete protection during shipment and storage Bomac has designed a reusable RF Protective Package* which conforms with MIL-E1B specification. Diodes stored in this package are completely protected no matter how many times they are handled after the original seal is broken.

*PAT. APPLIED FOR

BOOTH 215, 216—WESCON SHOW

We invite your inquiries regarding
- ENGINEERING
- DEVELOPMENT
- PRODUCTION

Bomac Laboratories, Inc.
BEVERLY, MASSACHUSETTS

GAS SWITCHING TUBES · TR, ATR and Pre-TR · DUAL TR and ATR TUBES · SILICON DIODES · WAVEGUIDE SWITCHES · REFERENCE CAVITIES · MAGNETRONS · PRESSURIZING WINDOWS · SHUTTER TUBES · HYDROGEN THYRATRONS · REFLEX KLYSTRONS · TRAVELING WAVE AMPLIFIER TUBES · SYSTEMS

Catalog on request. Write (on your company letterhead) Dept. P-8 BOMAC Laboratories, Inc. Beverly, Mass., or phone Beverly 6000.

IRE People

(Continued from page 38A)

previously served two years as Director of Research of the Atomic Energy Commission and simultaneously as Gordon McKay Professor of Applied Physics at Harvard University. He is currently a member of the General Advisory Committee of the Atomic Energy Commission as well as the Science Advisory Committee of the Office of Defense Mobilization.

During World War II when the potentialities of the microwave magnetron for high-frequency radar were discovered, Dr. Fisk was selected to head the development group at Bell Laboratories. After the war, he was placed in charge of electronics and solid state research. In 1949 when he returned to Bell from the Atomic Energy Commission and Harvard, Dr. Fisk was placed in charge of research in the physical sciences. He has served as Vice-President in charge of research since March, 1954.

Dr. Fisk received the bachelor's and doctor's degrees from Massachusetts Institute of Technology. From 1932 to 1934 he was a Proctor Travelling Fellow at Cambridge University, England, and from 1936 to 1938 a Junior Fellow in the Society of Fellows at Harvard. He also served as Associate Professor of Physics at the University of North Carolina.

Dr. Fisk has served on several government committees and advisory boards. He is a Fellow of the American Physical Society, the American Academy of Arts and Sciences, and was formerly a Senior Fellow of the Society of Fellows at Harvard. He is a member of the National Academy of Sciences.

Industrial Engineering Notes*

FCC Actions

Chairman George McConnaughey of the Federal Communications Commission has revealed that it has been suggested to the FCC Staff that it obtain information on the possibility of improving the sensitivity of UHF receivers and tuning mechanisms. The staff also has been instructed to initiate a rule-making proceeding looking toward increasing the maximum rated power output of UHF stations to five megawatts. These two proposals were revealed by the FCC Chairman during an address presented at the convention of the National Association of Radio and Television Broadcasters in Washington. Al-

(Continued on page 42A)

* The data on which these Notes are based were selected by permission from *Industry Reports*, issues of May 16, 23, 30, and June 6, published by the Radio-Electronics-Television Manufacturers Association, whose helpfulness is gratefully acknowledged.

Sprague on request will provide you
with complete application engineering service
for optimum results
in the use of electrolytic capacitors.

Sprague

LITTL-LYTICS*

for

transistor circuitry

HERE ARE THE SMALLEST *aluminum electrolytic capacitors ever made to Sprague's rigid quality standards.* Add to that their low leakage current, high reliability, and moderate price, and you have a new series of *miniature* electrolytic capacitors ideal for use in transistorized pocket radio receivers, wireless microphones, personal-style wire recorders, and similar equipment.

Their ultra-low leakage current is particularly important for it means minimum drain and long battery life when used in filtering applications across a battery, and excellent circuit performance when used in coupling applications.

Sprague Littl-Lytics are available in a full range of capacitance ratings from 1 to 110 mf, and in standard working d-c voltages of 1, 3, 6, 10, 12, and 15. Sizes range from 3/16"D x 1/2"L to 3/8"D x 3/4"L. Maximum operating temperature of the new Type 30D capacitors is 65°C.

Performance characteristics, sizes and ratings of metal encased, hermetically sealed Littl-Lytics are all in Engineering Bulletin 320, available on letterhead request to the Technical Literature Section, Sprague Electric Company, 235 Marshall Street, North Adams, Massachusetts.

typical ratings

Cat. No.		30D6	30D16
WVDC		6	6
μF		3	60
Leakage Current (μA Max.)		2.0	3.0
Can Size	D"	3/16	3/8
	L"	1/2	3/4

*Trademark

world's largest capacitor manufacturer

SPRAGUE

Export for the Americas: Sprague Electric International Ltd., North Adams, Massachusetts. CABLE: SPREXINT.

SEE US AT THE WESCON SHOW—BOOTHS 1001-1002

(Continued from page 40A)

though Mr. McConnaughey did not amplify on the request that the staff investigate the possibilities of increasing the sensitivity of UHF sets, it is expected that when this work gets under way it will involve consultation with representatives of various set manufacturers. He said the proposal looking toward increased power for UHF stations "was authorized in an effort to explore the practical possibilities of making UHF and VHF comparable. This rule-making proceeding will offer industry the opportunity to provide practical assistance." . . . **The FCC has completed its proposal in Docket 11263 and amended Part 12 of its rules so as to increase the band available for use by Novice Class radio amateurs from 7175–7200 kc to 7150–7200 kc.**

Federal Personnel

The President has nominated Mr. Mack, of Coral Gables, Fla., to a seven-year term as a member of the FCC. He succeeds Frieda Hennock of New York, whose term expired at the end of June. Mr. Mack is Second Vice-President of the National Association of Railroad and Utility Commissioners.

Technical

The Office of Technical Services, Commerce Department, has announced the publication of several research reports of interest to the electronics industry, including one on mass production of harmonic mode crystals, methods for determining the most effective types of seals for making air-tight the containers of electronic components in aircraft, and the development of a diode coincidence circuit for amplitude selection. "Fabricating Techniques for Crystal Unit"—CR-23/U (49.9 to 51.1 mc)—is a Signal Corps research report which points up a program of the Signal Corps Engineering Laboratories to fabricate third-mode crystal units in the range of 49.9 to 51.1 mc on a production-like basis and to explore some of the difficulties existing in the manufacture of this type of crystal unit. The conclusive results of the research are based entirely on the outcome of finished crystal units after production testing. The report, No. PB 111557, is available from the OTS, Commerce Department, Washington 25, D. C., for 75 cents per copy. After testing some 450 representative seals for the Air Force, the Bjorksten Research Laboratories, Inc., issued a report to the Wright Air Development Center which discusses the most effective types of seals for making airtight the containers of electronic components in today's high-speed, high-altitude aircraft. The results are contained in the report "Determination of Leakage Values of Seals," which is available from the OTS,

(Continued on page 44A)

Industrial Engineering Notes

(Continued from page 42A)

Commerce Department, for $4 each. Order by number PB 111545. "Diode Coincidence Gate for Amplitude Selection" contains information about the development of a diode coincidence circuit to select instantaneously the smallest amplitude signal from a group of input signals, and which is capable of handling signals having rise and fall times of 1 microsecond. This report, available from the OTS, Commerce Department, is No. PB 111543, and is priced at 50 cents. . . . **Two reports of government research developments in the field of oscillography have been released for distribution to industry by the Office of Technical Services, the Commerce Department announced They are:** "A Wide-Band Pulse Amplifier for High Speed Oscillography," (Order No. PB 111542 from OTS, Commerce Department, Washington 25, D. C.). This report notes that the amplification of low level signals is required in many applications, and these signals are frequently fast-rising nonrecurrent pulses which require amplifiers having large bandwidth. The design procedure for a wide-band, push-pull distributed amplifier to drive the deflection plates of a cathode ray tube is presented. Also, a complete description of the equipment, including performance characteristics and photographs of pulse response, is given in the report. "Development of the Optical Imaging Oscilloscope," (Order No. PB 111554 from OTS, Commerce Department, Washington 25, D. C.). This report states that the Optimascope is a cathode ray tube modified to combine the presentation of an optically projected image and the normal electron-beam trace on the phosphor coating of the inner face. A system of small plane mirrors is employed in the neck of the tube which may be used to project images optically or to photograph scope information, or to do both simultaneously. The Optimascope may be used to provide aircraft pilots with a radar tracking scope on which various optical images can be displayed. It also has other uses, it was pointed out. . . . **The Federal Communications Commission said last week that it had no objection to the transmission of a color television test signal to accompany monochrome telecasting as proposed last March by RETMA (RETMA Industry Report, Vol. 11, No. 9). . . . Transistor theories, properties, circuit design principles, applications, and the characteristics of transistor types are treated in an 800-page compilation of selected reference material now available to industry through the Office of Technical Services, U. S. Department of Commerce.** Compiled by the Bell Telephone Laboratories, under an Army Signal Corps contract in late 1951, to supply information to those engaged in the military transistor effort, the volume brings together representative material from the enormous amount of information

(Continued on page 46A)

Industrial Engineering Notes

(Continued from page 44A)

on physics, device properties and circuit applications evolved to the date of publication. "The Transistor: Selected Reference Material on Characteristics and Applications," PB 111054, may be obtained from OTS, U. S. Department of Commerce, Washington 25, D. C., at $20. . . . **The Office of Technical Services has announced the availability of a new publication covering a case study of production control through the use of electronic data processing.** The publication was written by an electronic data systems engineer to give business management a better picture of the use of such systems. "Production Control Through Electronic Data Processing: A Case Study" was prepared under an Office of Naval Research contract. It is designed especially for management, and requires no previous knowledge of electronic computers on the part of the reader. Rather, it describes and illustrates through the case study technique the types of clerical operations which these machines can be expected to perform. The publication is available through the Office of Technical Services. U. S. Department of Commerce, Washington 25, D. C. at $1.50 per copy and should be ordered by No. PB 111580.

Professional Group Meetings

Aeronautical and Navigational Electronics

Philadelphia Chapter—May 12, 1955

"Environmental Conditions in Guided Missile Flight," by Captain Grayson Merrill, U.S.N.

Antennas and Propagation and Microwave Theory and Techniques

Albuquerque-Los Alamos Chapter—April 6, 1955

"Microwave Papers Given at the IRE National Convention," by G. A. Arnot, Sandia Corporation.

Audio

Philadelphia—April 7, 1955

"A New Electrostatic Loudspeaker," by Arthur A. Janszen, Janszen Laboratory.

Broadcast Transmission Systems

Houston—April 12, 1955

Tour of inspection of KTRK-TV transmitting facilities.

(Continued on page 48A)

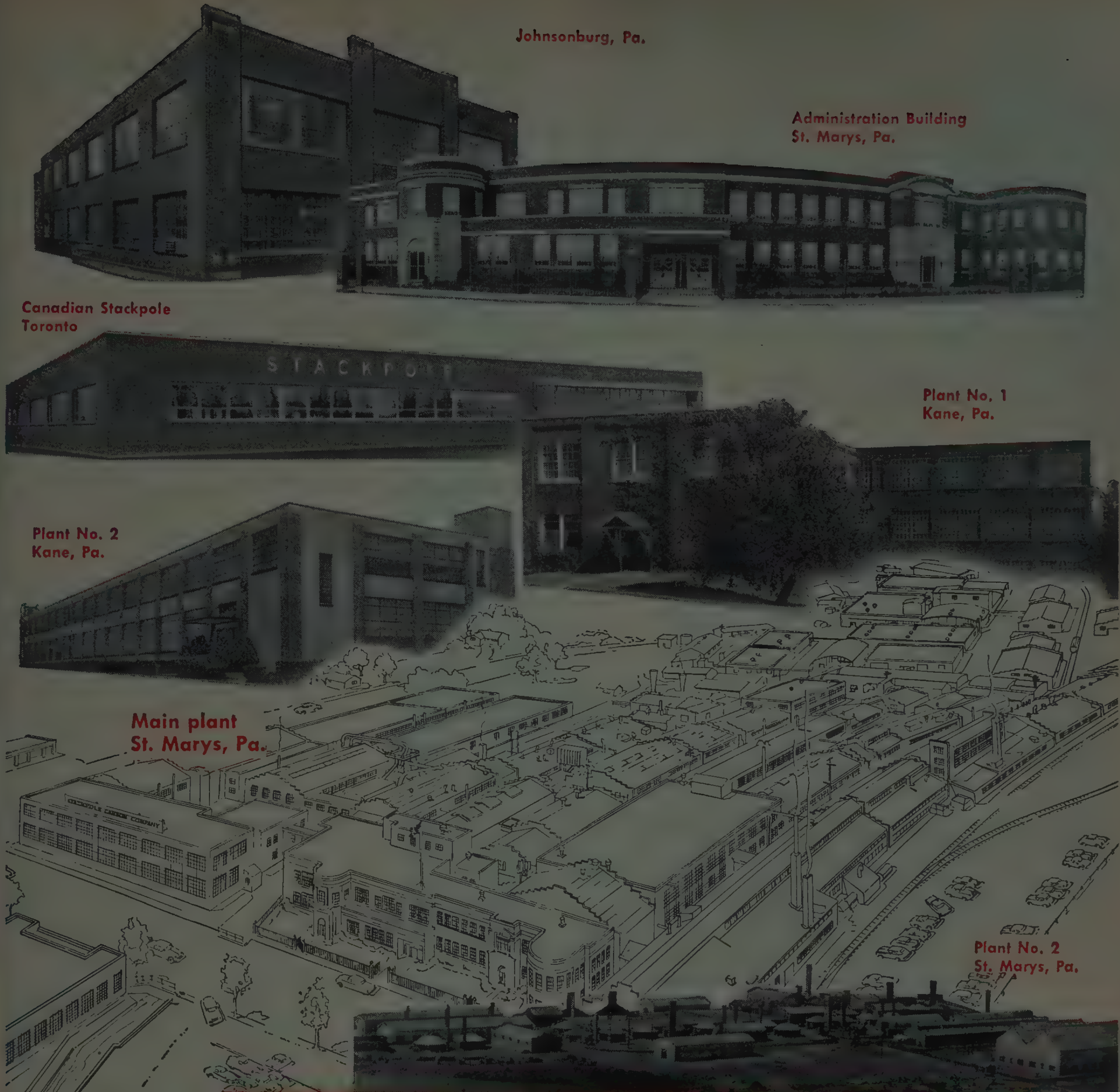
Johnsonburg, Pa.
Administration Building
St. Marys, Pa.
Canadian Stackpole
Toronto
STACKPOLE
Plant No. 1
Kane, Pa.
Plant No. 2
Kane, Pa.
Main plant
St. Marys, Pa.
Plant No. 2
St. Marys, Pa.

Professional Group Meetings

(Continued from page 46A)

Circuit Theory

Albuquer Chapter—April 27, 1955

"Loading Error Correction in an Analogue Network," by R. M. McGehee, Sandia Corporation.

Philadelphia Chapter—April 14, 1955

"Signal-Flow-Graphsmanship," by S. J. Mason, M.I.T.

Syracuse Chapter—April 21, 1955

"Multistage Maximally Flat Video Amplifiers," by Glenn Glasford, Syracuse Univ.

Communications Systems

Washington Chapter—May 9, 1955

"The Navy 'Jim Creek' Transmitting Station," by R. G. Bywater, USN, Office of Director of Naval Communications and Harold E. Dinger, Naval Research Laboratory.

Electronic Computers

Detroit Chapter—April 21, 1955

"A High Performance Table Top Differential Analyzer," by Robert M. Howe, University of Michigan.

Dallas-Fort Worth Chapter

The following officers have been elected for one year terms: Chairman—L. E. Heizer, Senior Aerophysics Engineer, Convair, Fort Worth; Vice-Chairman—C. C. Calvin, Lead Systems Design Engineer, Chance Vought Aircraft, Dallas; Secretary—J. W. Sanders, Senior Aerophysics Engineer, Convair, Fort Worth.

Philadelphia Chapter—April 19, 1955

"Electronic Computers in Commercial Data Processing Applications," by John Spellman, Arthur Anderson and Co.

Electron Devices

Los Angeles—May 20, 1955

"Transistor Physics," by William Shockley, Visiting Professor at California Institute of Technology on leave from Bell Telephone Laboratory.

New York Chapter—February 2, 1955

"Ultra-High Vacuum," by D. Alpert, Westinghouse Research Laboratories.

New York Chapter—May 12, 1955

"Solar Thermoelectric Generators," by Maria Telkes, N.Y.U.

Philadelphia—April 4, 1955

"The Magnetron Beam Switching Tube," by Saul Kuchinsky, Burroughs Corp., Research Div.

Professional Group Meetings

San Francisco Chapter—April 13, 1955

"Problems of Organizing and Operating a Tube Manufacturing Activity," by Farrell McGhie, Elec. Res. Lab., Stanford University.

Washington, D. C. Chapter—April 25, 1955

"Traveling-Wave Tubes," by Henry D. Arnett, Naval Research Lab.

"The Willys Flat-Screen TV Tube," by Moses C. Long, Office of Naval Research.

Engineering Management

Dayton Chapter—April 7, 1955

"Top Level Managers Need Little Technical Skill," by Tom C. Rives, General Electric Company.

Los Angeles—March 16, 1955

"Some Problems in Selecting Management Personnel for Industrial Research Organizations," by William W. Allen, North American Aviation, Inc.

Los Angeles Chapter—April 20, 1955

"The WCEMA Engineers Salary Survey" by Donald Duncan, Helipot Corporation.

San Francisco Chapter

"Symposium on Business Organization of a Tube Manufacturing Activity'" by Richard Huggins, Huggins Labs.; H. M. Stearns, Varian Associates; R. Leng, Sylvania Microwave Tube Laboratory.

Information Theory

Albuquerque-Los Alamos Chapter—April 13, 1955

"A comparison of Feinstein's and Shannon's Proofs of 'A Fundamental Theorem in Information Theory,'" by B. L. Basore.

Los Angeles Chapter—March 31, 1955

"Linear Predictors with Constrained Outputs," by J. C. Gurley, Hughes Aircraft Company. "The Effect of AGC on Radar Tracking Noise," by I. Pfeiffer, Ramo-Wooldridge Corporation.

Washington Chapter—May 16, 1955

"Some Applications of Information Theory" by Thomas P. Cheatham, Jr., Melpar, Inc. At the same meeting the following officers were elected: Chairman—Harold Goldberg; Vice-Chairman—Ben S. Melton; Secretary—Charles R. Tieman.

Nuclear Science

Albuquerque-Los Alamos—March 18, 1955

"Crystal Growth" by Earl Fullman, Group J-13, LASL.

Connecticut Valley Chapter—April 21, 1955

"A Review of the History and Problems of Sonar" by J. W. Horton, U. S. Navy Underwater Sound Laboratory.

(Continued on page 50A)

Professional Group Meetings

(Continued from page 49A)

Oak Ridge Chapter—March 16, 1955

"Radiation Injuries in Man" by A. C. Upton, Oak Ridge National Laboratory.

Oak Ridge Chapter—April 20, 1955

"Stable D.C. Amplifiers" by Ray Dandl, Instrumentation & Controls Division, Oak Ridge National Laboratory.

Microwave Theory and Techniques

Baltimore Chapter—April 20, 1955

"The Antenna Crossover Problem in Conical Scan Radar" by Myron S. Wheeler, Westinghouse Electric Corporation.

"Boresight Radome-Antenna-System as a Unit" by Karl Undesser, Glenn L. Martin Company.

Long Island Chapter—May 17, 1955

"Microwave Applications of Gaseous Discharges" by Roger White, Roger White Electron Devices, Inc.

Northern N. J. Chapter—April 20, 1955

"Microwave Applications of Gaseous Discharges" by Patrick E. Dorney, Roger White, Electron Devices, Inc.

Philadelphia Chapter—April 21, 1955

"Constant K Filters in Waveguide" by Dan Hochman, RCA. At this meeting, the the following officers were elected: Chairman—R. A. Dibos, Philco Corporation; Vice-Chairman—H. R. Reiss, RCA; Secretary—D. Hochman, RCA.

Telemetry and Remote Control

Dayton Chapter—April 7, 1955

"Development Trends in Remote Control" by Andrew B. Henderson, Crosley Division, AVCO.

Los Angeles Chapter—April 19, 1955

"The NACA Telemetering System" by G. M. Truszynski and M. R. Franklin, NACA.

"Telemetry as a Flight Test Instrument" by J. J. Dover, Edwards Air Force Base.

Vehicular Communications

Detroit—February 16, 1955

"Maintenance Problems and Techniques in Vehicular Systems" by T. P. Rykala, Mich. Consolidated Gas Co.; F. M. Hartz, Detroit Edison Co.; O. L. Santi, Mich. Bell; J. E. McFatridge, City of Detroit Mobile Comm.; and F. L. Kahle.

Detroit—March 16, 1955

"Low Power Base Station Operation in the Detroit Edison System" by Frank Hartz, Detroit Edison Company.

(Continued on page 52A)

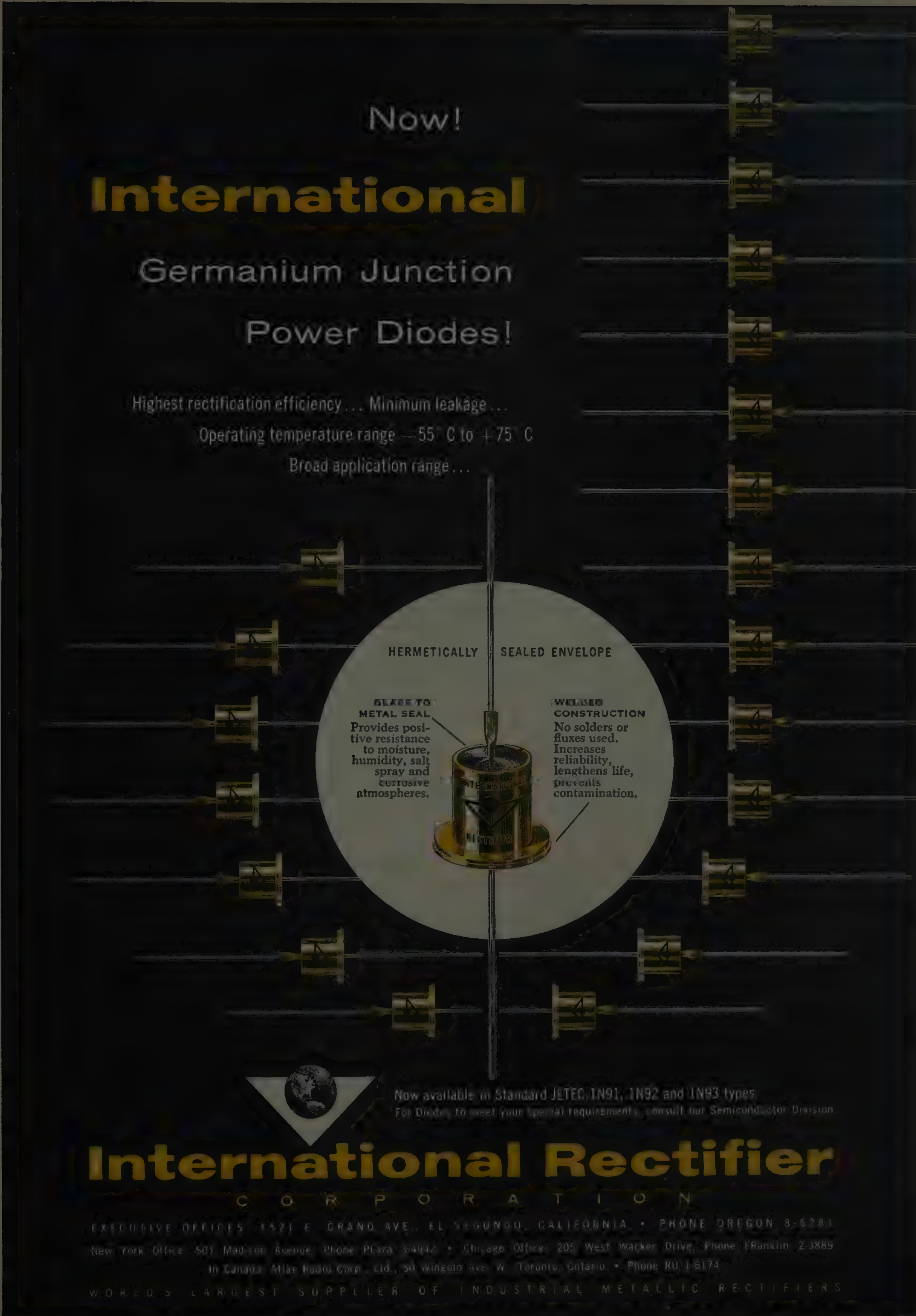
Now!
International
Germanium Junction
Power Diodes!
Highest rectification efficiency . . . Minimum leakage . . .
Operating temperature range −55° C to +75° C
Broad application range . . .
HERMETICALLY SEALED ENVELOPE
GLASS TO METAL SEAL
Provides positive resistance to moisture, humidity, salt spray and corrosive atmospheres.
WELDED CONSTRUCTION
No solders or fluxes used. Increases reliability, lengthens life, prevents contamination.
Now available in Standard JETEC 1N91, 1N92 and 1N93 types.
For Diodes to meet your special requirements, consult our Semiconductor Division.
International Rectifier
CORPORATION
EXECUTIVE OFFICES: 1521 E. GRAND AVE., EL SEGUNDO, CALIFORNIA • PHONE OREGON 8-6281
New York Office: 501 Madison Avenue, Phone PLaza 3-4942 • Chicago Office: 205 West Wacker Drive, Phone FRanklin 2-3889
In Canada: Atlas Radio Corp., Ltd., 50 Wingold Ave. W., Toronto, Ontario • Phone RU 1-6174
WORLD'S LARGEST SUPPLIER OF INDUSTRIAL METALLIC RECTIFIERS

Professional Group Meetings

(*Continued from page 50A*)

Los Angeles Chapter—March 10, 1955

"Radio Interference—Some Causes and Effects'" A Panel Discussion.

Los Angeles Chapter—May 3, 1955

"Progress in Land Mobile Communications" by John F. Byrne, Motorola, Inc.

Los Angeles Chapter—
January 13, 1955

"Some Problems of Closely Spaced Radio Systems" by L. E. Ludekins, Southern Calif. Edison.

Washington Chapter—April 28, 1955

Panel discussion on split channels: Harry Wells, Carnegie Institute; E. W. Allen, Federal Communications Commission; L. E. Delafleur, RETMA; Stuart Meyer, A. B. DuMont; H. A. Radzikowski, Bu. Public Roads.

Section Meetings

Atlanta

"Storage Devices for Digital Computers," by R. J. Klein, Oak Ridge National Laboratory; May 13, 1955.

Baltimore

"Missile Test Instrumentation," by R. V. Godfrey, RCA; May 11, 1955.

Binghamton

"Travelog of Southern and Western United States," by Ralph Carroll, WNBF-TV; June 13, 1955.

Boston

"An Experimental Transistorized Auto Receiver," by Larry Freedman, RCA Labs.; May 19, 1955.

"UHF Long Range Scatter Circuits," by W. E. Morrow, Jr., M.I.T.; June 16, 1955.

Buffalo-Niagara

"The Buffalo-Ithaca Microwave Link," by Prof. Nelson Bryant, Cornell University; May 18, 1955.

Chicago

"VHF System Considerations," by Lloyd Morris, Motorola; April 15, 1955.

"Recent Advances in the Theory of TV Sweep Circuits with Single Multiple Beams, Including Tri-color Tubes," by Dr. Kurt Schlesinger, Motorola; May 20, 1955.

Cincinnati

W. C. Osterbrock Memorial Annual Paper Competition held at University of Cincinnati; May 17, 1955.

Cleveland

"Radio Teletype Operation," by Samuel Davis; "Feedback and Transient Response of an Electromechanical Transducer," by R. A. Grimsey and "Basic Transistor Theory," by J. R. Huntley; May 26, 1955.

(*Continued on page 54A*)

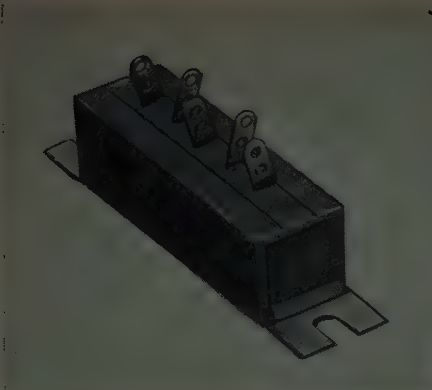

Potted (sealed) Vac-u-Sel rectifier

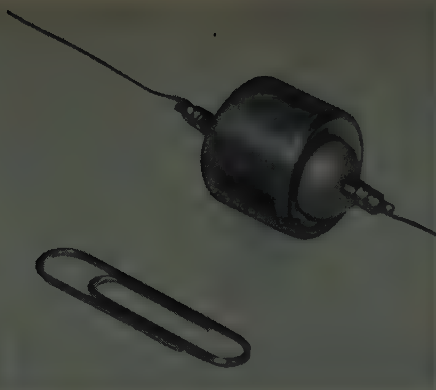

Vac-u-Sel rectifier with metal-clad housing

Tube-mounted Vac-u-Sel rectifier

Textolite* tube construction

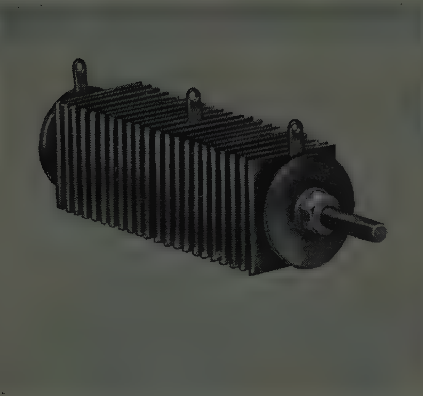

Standard (stud) Vac-u-Sel stack

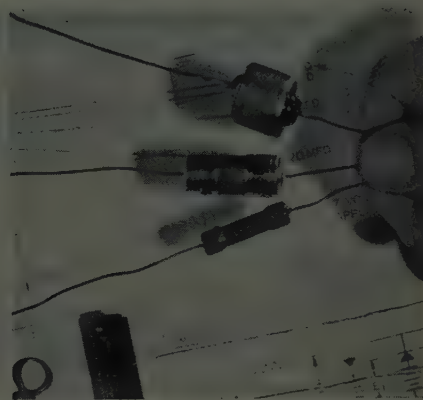

Miniature Vac-u-Sel rectifiers

TO HELP YOU DESIGN QUALITY INTO YOUR PRODUCTS . . .

NEW G-E Application Approach That Selects The Exact *Vac-u-Sel** Rectifier You Need

This new application approach, recently developed by General Electric, assures you of getting the correct Vac-u-Sel rectifier to meet your exact requirements. Now you are assured of getting the full advantage from the long life and outstanding technical characteristics inherent in all the many sizes and types of Vac-u-Sel rectifiers. In addition, in practically all cases, the sales engineer can give you the exact identification and price of your stack on the spot, without the inconvenient delay involved in getting data from the factory.

THIS NEW APPLICATION APPROACH brings top quality to your products by permitting complete and efficient utilization of the outstanding electrical characteristics, dependability, and predictable operation found in the many sizes, housings, finishes, and ratings of Vac-u-Sel component rectifiers.

FOR MORE INFORMATION on this new application approach, or the outstanding Vac-u-Sel line of rectifiers, contact your nearest G-E Apparatus Sales Office, or write Section 461-38, General Electric Co., Schenectady 5, N. Y.

G-E SALES ENGINEERS are able to determine, on the spot, the exact Vac-u-Sel stack to suit your particular application.

**Reg. Trade-mark of General Electric Co.*

Progress Is Our Most Important Product

GENERAL ELECTRIC

Section Meetings

(Continued from page 52A)

Connecticut Valley

"Servomechanisms," by Harold Chestnut, General Electric Company; May 19, 1955.

Dallas-Fort Worth

"The Application of Transistors to Broadcast Radio Receivers," by R. R. Webster, Texas Instruments Inc.; March 1, 1955.

"The Status of Traveling Wave Tube Development," by A. K. Wing, Federal Telecommunications Labs.; March 30, 1955.

"Magnetic Amplifier Operation and Application," by R. W. Roberts, Westinghouse Electric Company; April 5, 1955.

"Nuclear Magnetic Resonance," by Dr. John Zimmerman, Magnolia Petroleum Company; May 3, 1955.

"Aircraft Antenna Performance as Affected by Location," by D. G. Harman, Convair; May 10, 1955.

Election of Officers; June 3, 1955.

Denver

"Applications of Magnetic Recordings," by R. M. Strassner, Ampex Electric Corp.; March 14, 1955.

"The Mars Problem," by Dr. A. W. Recht, Denver University; April 15, 1955.

Informational Report of the Committee on Unity; May 19, 1955.

Des Moines-Ames

"Radar Systems," by C. J. Marshall, Director, IRE Region 5; May 6, 1955.

El Paso

"Test Equipment and Service Adjustments for Color TV," by Jack Croft, RCA Service Co.; May 25, 1955.

Fort Wayne

"Nuclear Power Reactors," by Dr. W. J. McGonnagle, Argonne National Laboratory, and "The IRE" by C. J. Marshall, Director, IRE Region 5; May 5, 1955.

Hawaii

"How Much Distortion Can You Hear?"—tapescript by IRE Professional Group on Audio; March 9, 1955.

"Concepts of Electric Fishing," by R. R. Hill, Pearl Harbor Naval Shipyard; April 13, 1955.

Field trip to New Hawaiian Electric Power Plant; May 11, 1955.

Election of officers; June 8, 1955.

Indianapolis

"Power Transistors, Their Use in a Voltage Regulator with Zener Reference," by Gerald M. Ford, and "Low Power Transistor Applications, in Radar Range Computer," by E. S. McVey, both of U. S. Naval Ordnance Plant; May 19, 1955.

Inyokern

"Applications of Industrial Television," by John Day, Kalbfell Labs.; June 20, 1955.

Ithaca

"High Fidelity," by Dr. F. H. Slaymaker, Stromberg Carlson; May 23, 1955.

Long Island

Field Trip through Long Island Lighting Company Central Operating Headquarters; June 21, 1955.

(Continued on page 56A)

Stand Pat with CLAROSTAT

"Humdinger" Series MH ultra-compact potentiometer. 10 to 200,000 ohms. 1 watt.

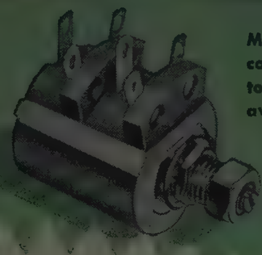

Miniaturized Series 49 wire-wound controls in single and dual units. 10 to 20,000 ohms. 1.5 watts. Switches available.

"Humdinger" Series 39 shaftless, screwdriver-adjusted potentiometer. 4 to 5000 ohms. 2 watts.

Series 58 3-watt wire-wound controls. 1 to 50,000 ohms. With or without switch.

Wire-Wound CONTROLS

Your wire-wound control needs – *usual* or *unusual* –are readily met by specifying CLAROSTAT. Here's why:

For *usual* needs, the Clarostat line is outstandingly complete. It includes 2-watt (1-1/8" dia.), 3-watt and 4-watt (1-21/32" dia.) types; 25- and 50-watt power rheostats; miniaturized (3/4" dia.) 1.5-watt controls; and the handy, space-saving, cost-reducing "Humdingers"*. All these types, and many more, are *standard and stocked*, available for your convenience at the local Clarostat distributor or in quantities from Clarostat factory stock.

And for *unusual* needs, Clarostat can design and put into production those *special* types – quickly, satisfactorily, economically – often based on ingenious adaptations of standard features and tooling.

Send those wire-wound control requirements to us for engineering service and quotations. Literature on request.

Smaller or Series 43c 3-watt wire-wound controls. 5 to 10,000 ohms. With or without switch.

Series 10 4-watt wire-wound controls. 1 to 100,000 ohms. With or without switch.

Power rheostats, Series 25 and 50, 25 and 50 watts. 5,000 and 10,000 ohms max., respectively. Also aircraft type, encased in metal housing.

CLAROSTAT®

Controls and Resistors

CLAROSTAT MFG. CO., INC., DOVER, NEW HAMPSHIRE

In Canada: Canadian Marconi, Co., Ltd., Toronto 17, Ont.

*Reg. U.S. Pat. Office

Section Meetings

(*Continued from page 54A*)

LOS ANGELES

"Control of Transistor Electrical Parameters," by D. E. Combs, Hydro-Aire, Inc.; and Vendor Certification of Electronic Components," by G. H. Beck, Hughes Aircraft; March 1, 1955.

"Mathematical Methods to Predict Biological Behavior," by Dr. H. H. Zinsser, University of Southern California; June 7, 1955.

MIAMI

"Magnistors and Magnetic Amplifiers," by Dr. Craig, Invex, Inc.; May 31, 1955.

NEW ORLEANS

Tapescript: "The Bell Solar Battery,"—speaker: Dr. Gordon Raisbeck, Bell Telephone Labs., May 27, 1955.

NEW YORK

"An Inside Look at Engineering Education in Soviet Russia," by Edward Kenojian, General Electric Company; June 1, 1955.

OMAHA-LINCOLN

"Problems Involved in the Transmission of the Color TV Signal," by Mr. Marston, Bell Telephone Labs.; March 22, 1955.

"Counter Tubes and Circuits," by Rev. W. R. Luebke, S.J.; April 25, 1955.

PHOENIX

"Solar Energy," by C. A. Scarlott, Stanford Research Institute; May 13, 1955.

(*Continued on page 58A*)

TUNG-SOL "Magic Mirror" ALUMINIZED PICTURE TUBE

BRIGHTER–SHARPER
MORE DETAIL
MORE CONTRAST

The "Magic-Mirror" Aluminized Picture Tube produces the brightest, most realistic picture ever seen in the American home. The "Magic-Mirror" tube effectively utilizes *all* the light generated by the phosphor screen.

Tung-Sol has developed a unique "fogging" method of backing up the phosphor screen with a mirror-like aluminum reflector. This reflector prevents light radiating uselessly back into the tube. It brings out all the detail of which the receiver circuit is capable. So smooth and true is the Tung-Sol aluminum reflector that mottling, streaks, swirls, "blue-edge", "yellow center" and other objectionable irregularities are eliminated.

Tung-Sol pin-point-focused electron gun assures a steady, brilliant picture—free from alternate fading and overlighting. Tung-Sol's exacting standards of quality control, manufacture and testing further guarantee the high uniformity and maximum performance of the "Magic-Mirror" TV Picture Tube.

Let the superior qualities of "Magic-Mirror" Picture Tubes add selling advantages to your set.

ORDINARY TUBE—Only *half* the light produced by the phosphor screen is utilized in the picture. Other half radiates wastefully back into tube.

RESULT—A light background within the tube which reduces picture contrast.

MAGIC-MIRROR ALUMINIZED TUBE — Aluminized reflector allows electron beam through. Blocks wasted light from backing up into tube. Reflects *all* the light into picture.

RESULT—Pronounced increase in contrast to make a bright, clear, more realistic picture.

TUNG-SOL ELECTRIC INC., Newark 4, N. J.

Sales Offices: Atlanta, Chicago, Columbus, Culver City (Los Angeles), Dallas, Denver, Detroit, Montreal (Canada), Newark, Seattle.

Tung-Sol makes All-Glass Sealed Beam Lamps, Miniature Lamps, Signal Flashers, Aluminized Picture Tubes, Radio, TV and Special Purpose Electron Tubes and Semiconductor Products.

Section Meetings

(*Continued from page 56A*)

Pittsburgh

"Mechanized Intelligence," by W. O. Fleckenstein, Bell Telephone Labs., Inc., May 9, 1955.

Portland

"Application and Manufacturing Problems in the Transistor Industry," by D. E. Combs, Hydro-Aire, Inc.; May 19, 1955.

"Design and Development of Bonneville A. C. Network Analyser," by Marshall Shelton, Bonneville Power Administration, and "Manufacturing Problems Involved in Bonneville Network Analyser," by Dick Raupach, Electronic Contractors; June 9, 1955.

"Deposited Carbon Resistor Developments," by R. Wilton, Welywn Canada Ltd.; June 23, 1955.

Princeton

"Analog Computers," by J. D. Strong, Electronic Associates, Inc., May 12, 1955.

Rome-Utica

"The Fast Growing Field of Medical Electronics," by Dr. Stanley Briller and Nathan Marchand, both of New York University Bellevue Medical Center; June 7, 1955.

Schenectady

"Doppler Direction Finding," by R. E. Anderson, General Electric Company; March 14, 1955.

"The Limits of Fidelity," by N. C. Pickering, Pickering and Company; April 11, 1955.

"Television Today," by A. G. Zink, WRGB; May 9, 1955.

Syracuse

"Distant Early Warning Line in the Arctic, by J. A. Aschoff, Western Electric; May 5, 1955.

Tulsa

"Bell System Solar Battery," by H. J. McMains, Southwestern Bell Telephone; May 19, 1955.

Twin Cities

Field Trip to Setchell-Carlson, Inc., May 24, 1955.

Washington

Annual Student competition awards and presentation of new Section officers; June 13, 1955.

Winnipeg

Tour of Pelissier's Brewery and Talk,

"Use of Electronics in Brewery Products," by A. Robson, March 15, 1955.

"Automatic Electronics Production," by Dr. J. D. Ryder, President, IRE; April 15, 1955.

SUBSECTIONS

Amarillo-Lubbock

"Analog Computers," by J. W. Sanders, Convair, April 14, 1955.

"Multi-Loop Self Balancing Amplifier," by Dr. J. R. MacDonald, Texas Instruments, Inc.; May 12, 1955.

Berkshire County

"Industrial Application of Radio-Isotopes," by Dr. Liechenstein, General Electric Company; April 26, 1955.

Buenaventura

"Guided Surface Wave Antennas," by Dr. N. J. Ehrlich, Microwave Radiation Co.; May 12, 1955.

Fort Huachuca

Talk by William R. Hemlett, election of officers; June 2, 1955.

Orange Belt

"Domesticating the Traveling Wave Tube," by Dr. Peter D. Lacy, Hewlett-Packard; June 8, 1955.

COMPLETE POWER SUPPLY DEPENDABILITY FOR AS LITTLE AS $57⁵⁰

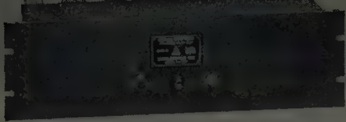

AMERICA'S MOST WIDELY USED POWER SUPPLIES, MANUFACTURED AND GUARANTEED BY LAMBDA

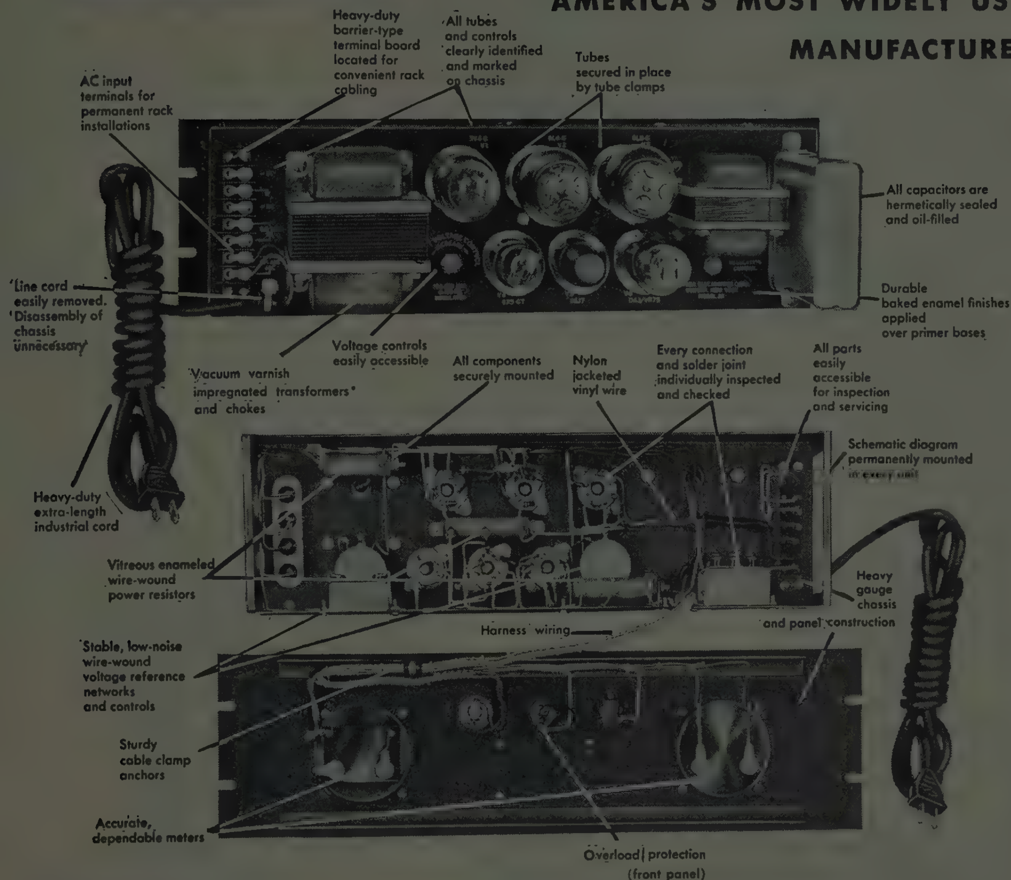

Model 28
200-325 VDC, 0-100 MA
$57.50

Model 29
100-200 VDC, 0-100 MA
$67.50

Model 28M (with meters)
200-325 VDC, 0-100 MA
$87.50

Model 29M (with meters)
100-200 VDC, 0-100 MA
$97.50

Rack models 28, 28M, 29 and 29M are long-lasting, dependable sources of power that deliver "workhorse" service . . . yet cost as little as $57.50 (for Model 28).

Intended primarily for fixed voltage use, these compact supplies are precision-built, as carefully engineered and quality-controlled as the most intricate models. They provide a convenient, low-cost power source for auxiliary equipment, also are well suited to production line applications.

SPECIFICATIONS

DC OUTPUT (regulated for line and load):
Voltage and Current

Models	Voltage Range[1]	Current Range[2]
28, 28M	200-325 VDC	0-100 MA
29, 29M	100-200 VDC	0-100 MA

[1]Voltage is continuously variable over entire range.
[2]Current rating applies over entire voltage range.

Regulation (line) . . . Better than 1%. For input variations from 105-125 VAC.

Regulation (load) . . . Better than 1%. For load variations from 0 to 100 MA.

Internal Impedance . . . Less than 10 ohms.

Ripple and Noise . . . Less than 10 millivolts rms for Models 28, 28M. Less than 5 millivolts rms for Models 29, 29M.

Polarity . . . Either positive or negative may be grounded.

AC OUTPUT (unregulated): 6.5 VAC at 3A (at 115 VAC input) . . . Allows for voltage drop in connecting leads. Isolated and ungrounded.

AC INPUT . . . 105-125 VAC, 50-60 CPS, 120 watts.[3]
[3]With all outputs loaded to full ratings and input at 125 VAC.

AMBIENT TEMPERATURE AND DUTY CYCLE . . . Continuous duty at full load up to 50°C (122°F) ambient.

OVERLOAD PROTECTION:
External Overload Protection . . . AC fuse, front panel.

INPUT AND OUTPUT CONNECTIONS: Heavy duty barrier terminal block, rear of chassis. 8 foot heavy duty rubber covered line cord with integral molded plug, also supplied.

METERS:
Output Voltage . . . 3½" rectangular voltmeter on meter models.
Output Current . . . 3½" rectangular milliameter on meter models.

CONTROLS:
DC Output Control . . . Screw driver adjusting control, rear of chassis.
AC Switch . . . Front panel.

PHYSICAL DATA: Mounting . . . Standard 19" rack mounting.
Size . . . 5¼" H x 19" W x 8" D.
Weight . . . 19 lbs. net, 23 lbs. shipping weight.
Panel Finish . . . Black ripple enamel (standard). Special finishes available to customer's specifications at moderate surcharge.

λ LAMBDA Electronics Corp.
THE FIRST NAME IN POWER SUPPLIES
103-02 NORTHERN BLVD. • CORONA 68, NEW YORK

Membership

The following transfers and admissions were approved and are now effective:

Transfer to Senior Member

Aas, E. A., 2115 Utah St., N.E., Albuquerque, N. Mex.
Altschuler, H. M., 160 West 77 St., New York 24, N. Y.
Anderson, F. J., 58 Fuller Brook Ave., Needham 92, Mass.
Anderson, T. N., 1539 Deer Path, Mountainside, N. J.
Baker, W. L., 1184 Oneida St., State College, Pa.
Bartley, G. A., 11602-76 Ave., Edmonton, Alta., Canada
Boden, E. H., R.F.D. 1, Emporium, Pa.
Brooks, W. O., 9385 Colegio Dr., Los Angeles 45, Calif.
Chasnov, B., 6012 N. 25 St., Arlington 7, Va.
Clarke, L. G., Stanford Research Institute, Menlo Park, Calif.
Cooper, H. W., Maryland Electronic Manufacturing Corp., 5009 Calvert Rd., College Park, Md.
Cullman, F. A., 501 Commonwealth Ave., Orlando, Fla.
Dalton, J. L., 710-14 St., S.E., Cedar Rapids, Iowa
DeWitz, G. H., Box 141, 3814 Domal La., La Canada, Calif.
Dickinson, R. H., R.F.D. 1, Ludlowville, N. Y.
Donsbach, W. R., 2519 Wilkens Ave., Baltimore 3, Md.
Doremire, F. E., 1013 Iris St., A-4, Los Alamos, N. Mex.
Drayner, A. H., 4520-62 St., San Diego 15, Calif.
Endres, R. O., 273 New Jersey Ave., Collingswood, N. J.
Felsen, L. B., Microwave Research Institute, 55 Johnson St., Brooklyn 1, N. Y.
Finkelstein, M. B., RCA Victor TV Division, Sec. 219, Bldg. 204-2, Camden 2, N. J.
Friedman, H., 109 Victory Dr., Rome, N. Y.
Fuqua, H. G., Box 95, Tobyhanna, Pa.
Goodfriend, L. S., Harwood Bldg., Scarsdale, N. Y.
Groce, J. C., 45 Joerg Ave., Nutley 10, N. J.
Grund, J. B., Sylvania Electric Products, Inc., Emporium, Pa.
Hadsell, G. C., 5103 Capitol Ave., Omaha, Nebr.
Hamer, H., 19 N. Locust Ave., Long Branch, N. J.
Hansen, J. R., Westinghouse Research Laboratories, Ardmore Blvd., East Pittsburgh, Pa.
Hax, D. H., 4802 W. 78 Ter., Prairie Village 15, Kans.
Hubbard, M. R., 1841 C Ave., N.E., Cedar Rapids, Iowa
Huggins, W. H., 2813 St. Paul St., Baltimore 18, Md.
Irick, J., Lloyd Harbor Hills, R.D. 3, Huntington, L.I., N. Y.
Jacobson, R. E., Jr., c/o J. Wherry, 10202 Pangborn Ave., Downey, Calif.
Johnson, R. D., 15625 Hart St., Van Nuys, Calif.
Kerfoot, B. P., 115 Hopkins Ave., Haddonfield, N. J.
Luntz, J. D., Nucleonics, 330 W. 42 St., New York 36, N. Y.
May, J. C., Dunham Laboratory, Yale University, New Haven, Conn.
McKnight, G. P., 25 Oakwood Ave., Bradford, Pa.
McMasters, P. A., 3403 Flagler Ave., Key West, Fla.

(Continued on page 62A)

Membership

(Continued from page 60A)

Mosier, R. R., 2700 W. Olive Ave., Burbank, Calif.
Muckenhirn, O. W., Electrical Engineering Department, University of Minnesota, Minneapolis 14, Minn.
Mumma, H. A., Jr., Burroughs Corp. Research Center, Paoli, Pa.
Murthi, J. K., Assistant Radio Engineer, Government of Andhra, No. 3, Crescent Park St., Gandhi Nagar, Madras 20, S. India
Needle, J. S., Electrical Engineering Department, Northwestern University, Evanston, Ill.
Patterson, H. H., Jr., 2619 Arnold St., N.E., Albuquerque, N. Mex.
Pile, D. H., Box 302, Claremont, Calif.
Randolph, J. P., Jr., 2807 Elnora St., Wheaton Hills, Silver Spring, Md.
Reynolds, C. L., 1511 Linden Ave., Owensboro, Ky.
Roberts, E. G., Jr., 111 Patricia La., N. Syracuse, N. Y.
Robbins, J. D., 513 Wood St., Emporium, Pa.
Shuey, R. L., Rm. 433, General Electric Research Laboratory, Schenectady, N. Y.
Sims, D. S., Research Laboratories, Westinghouse Electric Corp., E. Pittsburgh, Pa.
Smith, W. A., Jr., 36 Brandon Rd., Milton 87, Mass.
Stewart, H. H., 288 Collingwood St., Kingston, Ont., Canada
Strum, P. D., National Co., Inc., 61 Sherman St., Malden 48, Mass.
Thomas, M. W., 1400 N.E. 45, Oklahoma City 11, Okla.
Thorpe, R. W., 303 S. Louise Ave., Azusa, Calif.
Tice, T. E., 2214 Jarvis Rd., Columbus 21, Ohio
Turrentine, R. E., 1242 Frantzke Ave., Schenectady 9, N. Y.
Van Meter, D., 197 Prospect St., Cambridge 38, Mass.
Widenor, P. E., Jr., R.F.D. 1, Blairstown, N. J.
Willson, K. R., 1100-17 Ave., Seattle 22, Wash.
Wixson, F. C., 62 Hillcrest Dr., Packanack Lake, N. J.

Admission to Senior Member

Anderson, E. P., 215-12 Stanford Village, Stanford, Calif.
Brill, T., Box 299, Lemont, Ill.
Clark, J. E., 100 Thames Dr., Leigh on Sea, Essex, England
Cooper, H. W., 9315 Crosby Rd., Silver Spring, Md.
Coulombe, R. A., 15 Colliston Rd., Brookline 46, Mass.
Davis, L., Jr., 2 Winthrop Ter., Wayland, Mass.
Gilson, R. J., 780 Nela La., Los Altos, Calif.
Harris, K. E., Cossor House, Highbury Grove, London, N. 5, England
LeVine, H. D., 767 Union Blvd., Totowa, N. J.
Mitchell, H., 106 Memorial Dr., Cambridge, Mass.
Pashler, P. E., General Electric Research Laboratory, Box 1088, Schenectady, N. Y.
Rauch, S. E., Department of Mathematics, University of California, Goleta, Calif.
Robertson, O. F., 2476 S. Federal, Los Angeles 64, Calif.
Sattro, R. L., Sr., 5642 Meade Ave., San Diego 15, Calif.
Temple, J. M., Engineering-Aero 13 Project, Westinghouse Electric Corp., Friendship International Airport, Baltimore, Md.
Tischer, F. J., 114 Hillandale Rd., Huntsville, Ala.

(Continued on page 64A)

Membership

(Continued from page 62A)

Tomberg, V. T., 84-25 Elmhurst Ave., Elmhurst 73, L. I., N. Y.
Tyler, S. R., 2804 W. 74 St., Prairie Village 13, Kans.

Admission to Member

Arcoraci, L. J., Haselton Branch P.O., Rome, N. Y.
Bastian, L. R., 237 W. Kerr Dr., Oklahoma City 10, Okla.
Benafel, R. C., 1044 W. 78 St., Los Angeles 44, Calif.
Bohn, J. T., Hq. AAFCE, APO 11, New York, N. Y.
Bolger, R. L., 101 Tuttle Ave., Clarendon Hills, Ill.
Brennan, P. A., 5 Newman St., River Plaza, Red Bank, N. J.
Brown, A. G., 3 Mostyn Ave., Old Roan, Liverpool 10, England
Budnick, J. A., 3465 S. Bentley Ave., Los Angeles 34, Calif.
Burgess, P. R., 43 Fidler Ave., Winnipeg 12, Manit., Canada
Burk, W. A., 1141 Ninth St., Manhattan Beach, Calif.
Carey, J. J., 37 Garden Pkwy., Henrietto, N. Y.
Carlson, A. R., 1012 Ave. H-14 W., Lancaster, Calif.
Chen, R. K., 844 Custer, Evanston, Ill.
Clark, N. R., General Electric Co., Hudson Falls, N. Y.
Darwin, A. J., 4405 Glacier St., Fort Worth, Tex.
Deards, S. R., The College of Aeronautics, Cranfield, Bletchley, Bucks., England
Distelzweig, F. J., 1687 S. High St., Columbus 7, Ohio
Dooley, M. N., 311 N. Fullerton Ave., Montclair, N. J.
Eidson, R. A., Hoskins Pk., Apt. 61D, Quonset Point, R. I.
Evans, D. J., 1138 McClure St., Victoria, B. C., Canada
Feinstein, L., General Electric Laboratory at Stanford, Palo Alto, Calif.
Flan, A., 1050 Hinman Ave., Evanston, Ill.
Fratkin, B., RCA Victor Co., Ltd., 1001 Lenoir St., Montreal, Que., Canada
Friedrichs, G., Compagnie Generale de Metrologie, Annecy, France
Geffe, P. R., 12411 Washington Pl., Los Angeles 66, Calif.
Gorton, R. M., Hq. 64th Air Division, DCS/P, APO 862, New York, N. Y.
Graeter, R. J., 260 Rigi Ave., Syracuse 6, N. Y.
Hammil, R. B., 307 E. Markham St., Little Rock, Ark.
Hardesty, R. D., 1814 S. Bleckley Dr., Wichita 18, Kans.
Hesselgrave, D. H., Bell Telephone Laboratories, Murray Hill, N. J.
Hilsabeck, D. A., Jr., 2404 Glenhaven Dr., Oklahoma City 10, Okla.
Karpisek, W. J., 5520—70 St., Sacramento 20, Calif.
Kime, K. L., 8405 Melvin Ave., Northridge, Calif.
Layton, H. M., John Ould (U. S. A.), Ltd., 519 S. Fifth Ave., Mount Vernon, N. Y.
Lenker, J. N., 114 Orient Way, Apt. 2B, Rutherford, N. J.
Lupton, W. H., 2510—23 St., Boulder, Colo.
Mannix, J. F. X., West Coast Branch Office, Signal Corps Engineering Laboratories, 75 S. Grand Ave., Pasadena, Calif.
Martin, D. W., 1986 Euclid Ave., Palo Alto, Calif.
McKinney, J. C., 2352—13 Pl., N.E., Washington, D. C.

(Continued on page 66A)

MALLORY

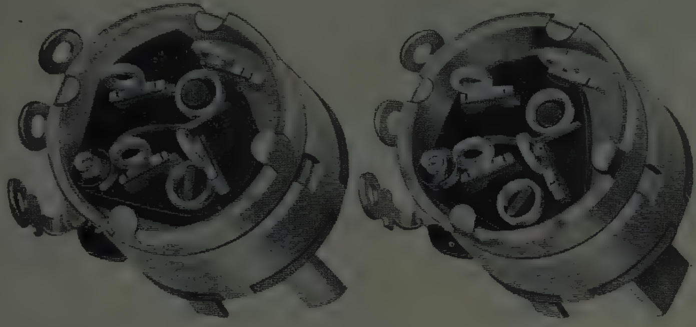

ON   OFF

Switch life is greatly increased by this new contact action. Note how "floating" rings of special Mallory alloy make and break the line circuit as the shaft is rotated—providing a continually changing contact surface.

Long-lasting "Floating Ring" Switch* Now Available on Mallory Controls

NEW CONTROL SWITCH WITH PUSH-PULL ACTION

Try this sales-worthy feature in your new set designs. The on-off switch works by push-pull action. Push the shaft and the set turns off . . . pull, and the set turns on *at the same volume setting*. The set owner doesn't have to re-adjust volume, and the control element lasts far longer because it is moved only for minor volume changes. This switch uses the same type of "floating ring" contacts as the new rotary switch. It is available for use with all Mallory carbon controls.

A NEW TYPE rotary switch, embodying unique contact action, is now available on Mallory carbon controls. Make and break is accomplished by spring-snapped motion of rings of special Mallory contact alloy, with positive self alignment. The rings "float" on pins so they can rotate with each operation.

Extremely long service life, proved on actual tests. The floating action spreads wear and arc erosion around the whole circumference of the rings . . . gives cleaner make and break.

Protection against overload damage. The snap spring which moves the contacts carries no current . . . won't heat and anneal when overloads occur.

Positive "feel". Positive snap action "feel" provides definite assurance of switch operation, with minimum torque requirement.

Available for use with all Mallory carbon controls, the new switch *costs no more* than conventional designs. In combination with high stability, long-wearing, low-noise Mallory resistance elements—in values from 250 ohms to 10 megohms—it gives you unequalled control performance. For full facts, write or call Mallory today.

Expect more . . . Get more from

P.R. MALLORY & CO. Inc.
MALLORY
P. R. MALLORY & CO., Inc., INDIANAPOLIS 6, INDIANA

Serving Industry with These Products:

Electromechanical—Resistors • Switches • Television Tuners • Vibrators
Electrochemical—Capacitors • Rectifiers • Mercury Batteries
Metallurgical—Contacts • Special Metals and Ceramics • Welding Materials

Parts distributors in all major cities stock Mallory standard components for your convenience.

*Patent applied for

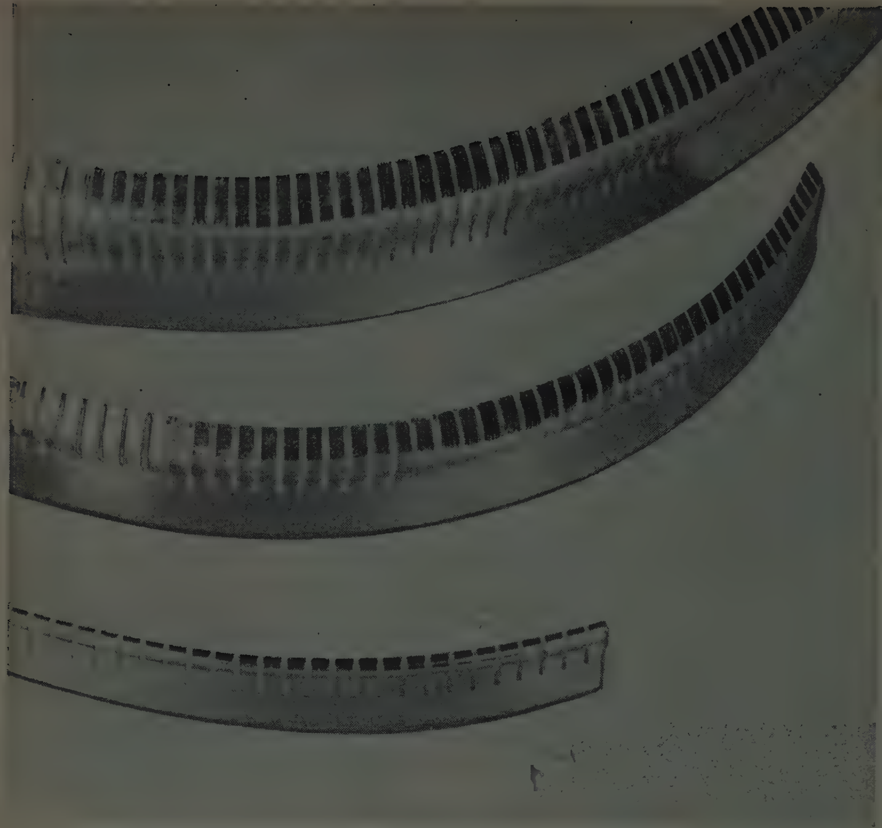

Membership

(*Continued from page 64A*)

McLean, J. B., Apt. 1D, Leland Gardens, E. Front St., Plainfield, N. J.
Mechlin, R. N., Burnam Rd., Bolton, Mass.
Mills, M. E., 11771 Country Club Dr., Los Altos, Calif.
Moore, H. I., 54th Ftr-Intcp Sqdn., Ellsworth AFB, S. Dak.
Murad, E. M., Research Chemist, Electronics Division, Hydro-aire, Inc., 3000 Winona Ave., Burbank, Calif.
Nakamoto, T., 914 Sea View Dr., El Cerrito, Calif.
Nigro, J. P., 9510 Milstead Dr., Bethesda, Md.
Novak, J. F., Jensen Manufacturing Co., 6601 S. Laramie, Chicago 38, Ill.
Oblinger, J. T., 1135 Old Boalsburg Rd., State College, Pa.
Pawlus, J., 1942 N. Springfield Ave., Chicago 47, Ill.
Perineau, M. C., French Air Attache Office, 1759 R. St., N.W., Washington 9, D. C.
Peterson, N. C., 950 Boranda Ave., Mt. View, Calif.
Porter, V. J., Remington Rand, Inc., Echert-Mauchley Division, Box 5616, Philadelphia 29, Pa.
Rastorgoueff, V., 3, Brandon Mansions, Queen's Club Gardens, London, W. 14, England
Rau, J. M., Jr., 3581 N. Stowell Ave., Milwaukee 11, Wis.
Robinson, T. O., 30 Vine Rd., Medway, Ohio
Rogers, D. E., Civilian Mail Rm., Box 71, APO 994, San Francisco, Calif.
Rogers, H. H., Jr., 4715 Westchester Mall, Apt. 75, Dallas 19, Tex.
Roth, J. H., 430 Princeton Rd., Haddonfield, N. J.
Rowe, W. A., 231 Belford, Ottawa 3, Ont., Canada
Ruehlemann, H. E., 1804 Jordan Park Apts., Fullerton, Pa.
Salzer, E., 737 Chestnut St., Waban 68, Mass.
Schmidt, E., 671 Hope St., Springdale, Conn.
Schwartz, E. S., 250 Miami St., Park Forest, Ill.
Shoquist, M. C., Forest Lake, Minn.
Solem, R. J., 1048 N. Walter Ave., Chicago 51, Ill.
Tarver, A. L., R.F.D. 1, Quitman, Ark.
Thain, R. S., Box 474, 54 Rossland Ave., City View, Ont., Canada
Timms, R. J., 806 Glen Cove Ave., Glen Head, L. I., N. Y.
Turkheimer, P. M., 226 Long Hill Rd., Little Falls, N. J.
Wrye, W. C., Jr., 2045 Welch, Houston, Tex.
Vanschaemelhout, A., University of Detroit, Detroit, Mich.
Widmann, L. C., R.F.D. 3, Cold Springs Rd., Baldwinsville, N. Y.

Transfer to Member

Abbitt, C. W., 637 S. 24 St., Arlington 2, Va.
Aberer, J. C., 215 E. North Ave., Elmhurst, Ill.
Aburano, P. F., 3110-24 S., Seattle 44, Wash.
Ackerman, N. A., 6154 N. Talman, Chicago 45, Ill.
Ackworth, D. L., c/o R. D. Thompson, R.F.D. 1, Battle Ground, Ind.
Aderhold, H. J., 1611 W. Peachtree St., N.E., Box 4357, Atlanta, Ga.
Ahlbeck, W. H., Box 394, R.F.D. 1, Boulder, Colo.
Albin, F. I., 1926 E. Joppa Rd., Baltimore 34, Md.
Albright, C. M., Jr., E. I. DuPont de Nemours & Co., Experimental Station, Wilmington 98, Del.
Alden, R. M., 4761-A Matsonia Dr., Honolulu, T. H.

(*Continued on page 68A*)

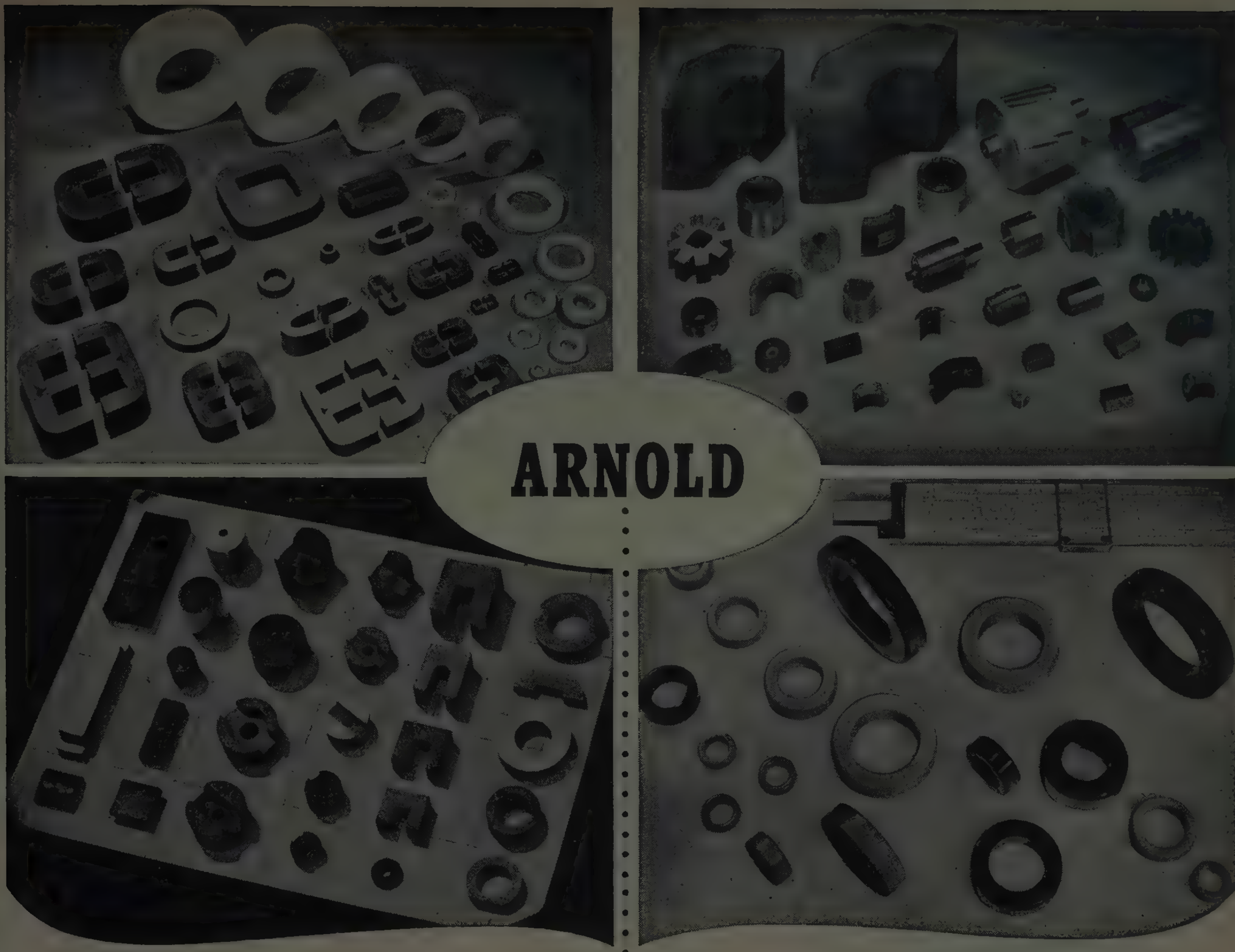

YOUR ONLY SOURCE

of a <u>Complete</u> Line of MAGNETIC MATERIALS

TECHNICAL DATA ON ARNOLD PRODUCTS . . . Write for your copy.

Bulletin GC-106 A . . . General information on all Arnold magnetic materials: permanent magnets, tape-wound and powder cores, etc.

Bulletin TC-101 A . . . "Properties of Deltamax, 4-79 Mo-Permalloy and Supermalloy"—28 pages of technical data on Arnold Tape-Wound Cores.

Bulletin PC-104 A . . . "Molybdenum Permalloy Powder Cores"—16 pages, complete technical data.

Bulletin SC-107 . . . "Arnold Silectron Cores"—52 pages of valuable data, covering a complete range of core shapes, sizes, tape gauges, etc.

ADDRESS DEPT. P-58

Arnold products include all grades of Alnico permanent magnets (cast and sintered) . . . tape-wound cores of high-permeability alloys, such as Deltamax, Permalloy and Supermalloy . . . types "C" and "E" cut cores of Silectron in any size or weight range from a fraction of an ounce to hundreds of pounds (50 lbs. max. on 12-mil C cores); also round, square and rectangular Silectron cores . . . powdered Mo-Permalloy cores . . . Cunife, Vicalloy, Permendur and other magnetic materials. Special magnetic components can be produced to meet your specific requirements; and such products as powder cores, tape-wound cores, and C and E cores are carried in stock in a wide range of standard sizes for immediate delivery. Many sizes of cast and sintered Alnico magnets also are stocked.

In other words, Arnold magnetic materials can answer *any* requirement you may have. It is the *only* complete line in the industry; and in addition, Arnold maintains complete control over every production step from raw materials to finished products. Such a source can bring you advantages in long experience and undivided responsibility, and in unequalled facilities for quality production and control. ● ***Let us supply your needs.***

THE ARNOLD ENGINEERING COMPANY

SUBSIDIARY OF ALLEGHENY LUDLUM STEEL CORPORATION

General Office & Plant: Marengo, Illinois

DISTRICT SALES OFFICES . . . New York: 350 Fifth Ave.

Los Angeles: 3450 Wilshire Blvd. Boston: 200 Berkeley St.

Membership

(Continued from page 66A)

Alderson, R. C., 4134 Wooddale Ave., S., Minneapolis 16, Minn.
Aldous, C. N., 315 Dewey La., Alamogordo, N. Mex.
Alexander, E. M., 8512 Michener Ave., Philadelphia 19, Pa.
Alexander, S. N., 4120 Stanford St., Chevy Chase, 15, Md.
Allen, J. R., 1266 W. Sixth St., Pomona, Calif.
Alley, R. E., Jr., Box 26, University of Richmond, Richmond, Va.
Alley, R. P., 1297 Parkwood Blvd., Schenectady, N. Y.
Allison, D. M., Jr., Othoridge Rd., Towson 4, Md.
Alter, R. S., 59 Vreeland Ave., Clifton, N. J.
Altieri, J. R., 107 ¾ N. Sweetzer Ave., Los Angeles 48, Calif.
Ambos, C., 2608 N. Neva Ave., Chicago 35, Ill.
Andersen, J. F., Box 954, Ventura, Calif.
Anderson, A. W., 321 Old Orchard La., York, Pa.
Anderson, C. A., 1829 Lewis Pl., Waukegan, Ill.
Anderson, C. M., Box 13A, R.F.D. 3, McMinnville, Ore.
Anderson, C. W., Box 202B, R.F.D. 4, Xenia, Ohio
Anderson, G. J., 1157 Parkwood Blvd., Schenectady, N. Y.
Anderson, L. D., 8107 Hammond Ave., Takoma Park, Md.
Anderson, M. K., John Brown University, Siloam Springs, Ark.
Anderson, R. W., 1970 Oakwood St., Pasadena 7, Calif.
Anderson, S. R., C.A.A., Experimental Station, Indianapolis, Ind.
Andrew, R. T., 2320 Peabody Dr., Pimmit Hills, Falls Church, Va.
Andrews, E. G., 463 West St., New York 14, N. Y.
Andrews, G. B., Bendix Aviation Corp., Pacific Division Development Laboratories, 166 W. Olive, Burbank, Calif.
Angell, J. B., Winthrop Rd., Huntingdon Valley, Pa.
Ankrum, P. D., Franklin Hall, Cornell University, Ithaca, N. Y.
Antell, S., 3824 DuRay Pl., Los Angeles 56, Calif.
Anthony, J. P., 3546 Ozark, Houston 21, Tex.
Applegate, C. J., 1816 Grove St., Boulder, Colo.
Applin, R. H., 5055—55 Pl., San Diego 15, Calif.
Arce-Blanco, R., Radio Laboratory, University of Puerto Rico, Rio Piedras, P. R.
Archard, F. H., Jr., USCG Hq., c/o EEE-2, Rm. 5120, Washington 25, Calif.
Armstrong, A. B., 10114 Lanett Ave., Whittier, Calif.
Armstrong, M. M., 421 Wisconsin, Oak Park, Ill.
Armstrong, T. R., 492 River Rd., Nutley, N. J.
Aronoff, M., 901—73 St., Brooklyn 28, N. Y.
Aronow, S., 58 Quincy St., Watertown, Mass.
Aronowitz, L., Department of Physics, New York University, University Heights, New York 53, N. Y.
Arthur, G. M., 15 Warren St., Fitchburg, Mass.
Aster, A. K., 48 Beech St., East Orange, N. J.
Atherton, J. B., 2234 Kamehameha Ave., Honolulu 5, T. H.
Augenblick, H. A., Microlab, 71 Okner Pkwy., Livingston, N. J.
Auriema, R. C., 54 Schmidts La., Staten Island 14, N. Y.
Ayer, D. R., 5 Arlington St., Nashua, N. H.
Ayers, J. B., R.D. 1, Emporium, Pa.
Babcock, D. F., 2700 W. Olive Ave., Burbank, Calif.

(Continued on page 72A)

PROCESS CONTROL—Askania controls regulate speed of the ten turbines which develop compression to maintain gas suction pressure in Creole Petroleum Corporation's giant, pile-supported oil drilling operation on Lake Maracaibo, Venezuela.

SUBMARINE OPERATION — Controls developed and produced by Askania Regulator Company are utilized to govern operation of U. S. Navy's modern Guppy type submarines.

MISSILE GUIDANCE —One of the many guided missiles equipped with Kearfott basic gyro reference systems, the B-61 Matador—U. S. Air Force's first successful ground-to-ground tactical weapon.

GPE CAPACITIES

● Manufacturing
●● Manufacturing and product development
●●● Manufacturing, product development and research
□●● Pilot manufacturing, product development and research

	KEARFOTT COMPANY, INC.	INTERNATIONAL PROJECTOR CORPORATION	BLUDWORTH MARINE DIVISION	GENERAL PRECISION LABORATORY INCORPORATED	THE GRISCOM-RUSSELL COMPANY	LINK AVIATION, INC.	THE HERTNER ELECTRIC COMPANY	THE STRONG ELECTRIC CORPORATION	J. E. McAULEY MFG. CO.	ASKANIA REGULATOR COMPANY	AMPRO CORPORATION	LIBRASCOPE, INCORPORATED
PRECISION MECHANICS, OPTICAL DEVICES, CERAMICS	●●●	●●	●●	□●●	●●	●●●	●●	●●●	●●	●●	●●	●●●
ELECTRICAL EQUIPMENT and COMPONENTS	●●●	●	●			●●●	●●●	●●	●	●●	●	●●●
ELECTRONICS	●●●	●●	●●●	●●●		●●●	●	●●		●●●	●●	●●●
HYDRAULICS, LIQUIDS PROCESSING, HEAT EXCHANGE		●●			●●●					●●●		
TELEVISION Studio, Theatre, Educational, Business, Industrial	●	●		●●●		●				●		
INSTRUMENTS, SERVOS, CONTROLS Hydraulic, Pneumatic, Magnetic, Electronic	●●●	●	●●	□●●		●●●	●●	●●		●●●	●	●●●
AIRCRAFT and MISSILE GUIDANCE, CONTROL, SIMULATION	●●●	●		●●●		●●●	●			●●	●	●●●
AUTOMATIC COMPUTERS and COMPONENTS	●●●	●	●	□●●		●●●				●●●		●●●
RADAR, MICROWAVE, ULTRASONICS	●●●	●	●●	●●●		●●		●		●		
MOTION PICTURE and AUDIO EQUIPMENT		●●●		□●●			●●	●●●	●●●		●●●	
NUCLEAR POWER COMPONENTS and CONTROLS	●●●				●●					●●		●●●
SYSTEMS ENGINEERING Aeronautical, Naval, Industrial	●●●			●●●	●●●	●●●				●●●		●●●

themselves, as well as in systems and equipment developed and produced by other manufacturers of advanced technological equipment.

All GPE Producing Companies work in the advanced areas of highly specialized fields and are engaged in the design, development, manufacture and sale of equipment which is closely related from a technical point of view. It is all precision equipment; it derives from similar fields of technical competence; it saves labor, increases productivity or achieves results which cannot be achieved with even limited use of on-the-spot manpower. The chart here shows the specialized fields in which the key GPE Producing Companies work.

and fields of technical competence, each of these companies has at its command, as required, the facilities and specialized techniques of the other GPE Companies in their respective fields. Interrelation of their resources is achieved through GPE's basic operating policy, GPE Coordinated Precision Technology. In all areas in which GPE Companies work, this coordination has been responsible for a wide variety of precision equipment of superior design and performance, embodying new, advanced principles.

A brochure relative to the work of the GPE Companies and GPE Coordinated Precision Technology is available. Address your request, or specific inquiries, to: General Precision Equipment Corporation — 92 Gold Street,

IRE Membership

(Continued from page 68A)

Bachhuber, R. A., Sylvania Electric Products, 2001 N. Cornell Ave., Melrose Park, Ill.
Bacon, J., 422 Richards Rd., Columbus 14, Ohio
Bagnall, J. J., 33 Kimball Rd., Watertown 72, Mass.
Bailey, C. B., Jr., 625 Arlington Dr., Inkster, Mich.
Bailey, R. L., 2030 Westview Dr., Owensboro, Ky.
Baird, J. A., Bell Telephone Laboratories, Whippany, N. J.
Bairos, C. A., 1225—28 St., Sacramento 16, Calif.
Baldwin, A. L., Jr., 51 Golden Hill, Milford, Conn.
Baldwin, E. G., Bell Telephone Laboratories, Whippany, N. J.
Baldwin, E. V., Biagonal Norte 520, Buenos Aires, Argentina
Ballieu, H. L., 8 Park Ter., Corvallis, Ore.
Barash, L. F., 67-18K—195 La., Fresh Meadows 65, L. I., N. Y.
Barnaby, R. H., 112 Willow St., Garden City, L. I., N. Y.
Barrett, A. M., Jr., 1950 Telegraph Rd., Lake Forest, Ill.
Barrett, C. S., 7710 Seaview Ave., Wildwood Crest, N. J.
Bartholomew, H. C., 554 Edgewood Rd., San Mateo, Calif.
Bartolomei, G. G., Box 403, Bayville, L. I., N. Y.
Baruch, S. N., 1476 Broadway, New York 36, N. Y.
Barus, C., Electrical Engineering Department, Swarthmore College, Swarthmore, Pa.
Bash, I. F., 5245 Roosevelt Blvd., Philadelphia 24, Pa.
Basham, R., Parkview Apts., Fayetteville, Ark.
Bashe, C. J., 5 Jane St., Red Oaks Mill, Poughkeepsie, N. Y.
Bateman, L. J., Hughes Aircraft Co., Los Angeles, Calif.
Battocletti, J. H., Loyola University of Los Angeles, 7101 W. 80 St., Los Angeles 45, Calif.
Baylis, G. F., 5000 Trenholme Ave., Montreal, Que., Canada
Beach, J. B., 540 Longmeadow Rd., Eggertsville, N. Y.
Bean, R. N., 1706 Hughey Dr., Longview, Tex.
Beatty, C. G., US Naval Ord. Test Sta. P 8048, 3202 Foothill Blvd., Pasadena 8, Calif.
Beaver, W. L., 360 S. Charleston Rd., S. Palo Alto, Calif.
Beaverson, W. A., 92 River St., Niles, Mich.
Beck, E. A., 4352 N. Henderson Rd., Arlington, Va.
Becker, S., 432 Peters Blvd., Brightwaters, L. I., N. Y.
Beehler, J., 48 Parkside Ave., Lawrenceburg, Ind.
Behagen, E. L., 2325 N. Fourth St., Milwaukee 12, Wis.
Bell, A. N., 53 Gorton St., Corning, N. Y.
Bell, R. E., 2904 Jodore, Toledo 6, Ohio
Bell, W. L., c/o Westrex, 111 Eight Ave., New York 11, N. Y.
Beltz, G. E., 54 Fairfield Ave., S. Norwalk, Conn.
Benaglio, R. V., 1291 Melton Rd., Birmingham 27, Mich.
Benesch, E. J., 28-06—46 St., Astoria, L. I., N. Y.
Benham, M. J., Phoenix College, Phoenix, Ariz.
Bennett, R. R., 6378 W. 79 St., Los Angeles 45, Calif.
Benns, W. E., Jr., 3738 Kanawha St., N.W., Washington 15, D. C.
Bercaw, O. M., Jr., 741 Eighth St., Wilmette, Ill.

(Continued on page 74A)

Don't be a "Catalog Snatcher"!

Write for your own 2 new additions to Encyclopedia Hermetica—they're Free!

Hermetic Catalogs Now Available
On Vac-Tite* Compression Plugs (No. 300)
And Single Terminal Feed-Thru's And Stand-Offs (No. 400)

Hermetic's two new catalogs are so handy as desk-top references that they'll drive any engineer who hasn't requested or received his copies to "Catalog Snatching"!

These two latest additions to Encyclopedia Hermetica, a continuing catalog series that has become industry's most helpful source of design and purchasing data, provide every significant innovation in hermetically sealed plugs, feed-thru's and stand-offs.

You'll find these two new catalogs indispensable and so easy to use that you'll be able to locate and identify the preferred type needed by its Hermetic part number in second's time. You'd better guard them well against the "Catalog Snatcher" because they contain the most complete line of plugs, stand-offs and feed-thru's ever offered!

*VAC-TITE is Hermetic's new vacuum-proof, compression construction, glass-to-metal seal.

Write **for your copies *today*! Also, request Vac-Tite* Compression Multi-Headers Catalog No. 200, MS Series.**

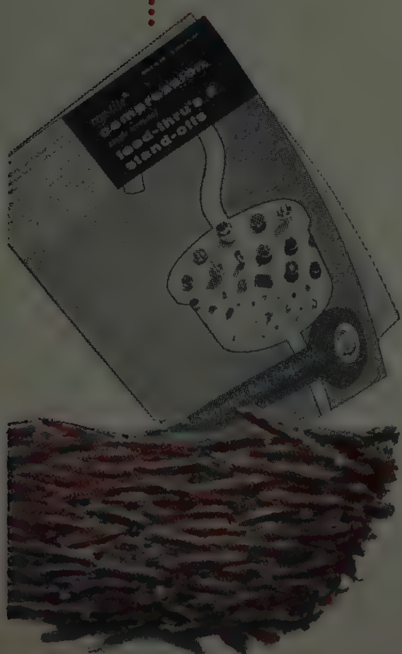

Hermetic Seal Products Company

29 South 6th Street, Newark 7, New Jersey

Visit us at the Wescon Show... Booth #1101.

SEALED IN HERMETIC HEADERS

FIRST AND FOREMOST IN MINIATURIZATION

Membership

(Continued from page 72A)

Beresford, D. R., 200 A Byrnes N.O.T.S., China Lake, Calif.

Bergen, H. A., c/o Industry & Power, 420 Main St., St. Joseph, Mich.

Bernbaum, B., 8327 Williams Ave., Philadelphia 19, Pa.

Bernstein, B., 1004 Laredo Rd., Silver Spring, Md.

Berntsen, W. H., 8250 E. Washington St., Indianapolis, Ind.

Berry, F. G., 86 Gormley Ave., Toronto 12, Ont., Canada

Bertan, L. L., 1255 Stratford Ave., New York 72, N. Y.

Berte, D. W., 957 Stannage Ave., Albany 6, Calif.

Beter, R. H., 154 Sumac St., Philadelphia 28, Pa.

Beymer, E. H., Box 302, Somis, Calif.

Bickel, R. C., 200 E. Ridgewood Ave., Ridgewood, N. J.

Billups, E. E., Box 106, Moutain Park, N. Mex.

Bishop, J. G., Radio Station CHSJ, 14 Church St., St. John, N. B., Canada

Bjerke, J. O., 953—19 St., Newport News, Va.

Black, J. C., Box 1704, R.F.D. 1, Bellevue, Wash.

Blackert, R. O., 4207 E. Montecito, Phoenix, Ariz.

Blackman, W. S., 1215 Daveric Dr., Pasadena 8, Calif.

(Continued on page 76A)

Membership

(Continued from page 74A)

Blackstock, R. S., 117 Brookfield Rd., N. Syracuse, N. Y.
Blanchard, C. K., 189 Main St., South River, N. J.
Blashfield, W. H., 602 Grand St., Galion, Ohio
Blight, A. F., Jr., 8400 Encino Ave., Northridge, Calif.
Block, E., 2017-B S. John Russell Cir., Elkins Park 17, Pa.
Block, E. J., 4353 Elliot Ave., S., Minneapolis 7, Minn.
Blow, T. C., 913 Grandin Ave., Rockville, Md.
Bobeck, A. H., 41 Ellers Dr., Chatham, N. J.
Bocast, D. R., 6415 W. 89 St., Los Angeles 45, Calif.
Boecker, A., Joseph La., E. Norwich, L. I., N. Y.
Bogart, P. M., Sylvania Electric Products, Emporium, Pa.
Bogossian, Z., 77 Lafayette Ave., Brooklyn 17, N. Y.
Bohanske, T. A., 46 Mathias Ave., Amsterdam, N. Y.
Bonwit, S. E., 12915 Flack St., Silver Spring, Md.
Borsarelli, C., Via Pancaldo 7, Milano, Italy
Borth, L. A., R.F.D. 1, Kettleby, Ont., Canada
Boulet, L., Engineering Department, Laval University, Quebec, Que., Canada
Bourret, C. J., 390 Hillside Ave., Hartford, Conn.
Bowman, H. A., 2619 Newton St., Silver Spring, Md.
Boyce, J., 18 Donald La., 'Torbank', Ossining, N. Y.
Boyle, G. G., 69 Fairmount Rd., Ridgewood, N. J.
Boziwick, G. E., 924 N. Fifth St., New Hyde Park, L. I., N. Y.
Bradford, C. E., 902 Jordan Park Apts., Fullerton, Pa.
Branch, B. S., 1401 Hurt Bldg., Atlanta, Ga.
Brand, C. W., 6244 San Jose Blvd., Jacksonville 7, Fla.
Braun, W. E., 205 Crest Dr., Paramus, N. J.
Braverman, R., 1138 Kenesaw Dr., S.E., Grand Rapids, Mich.
Bresler, A. D., 34 E. 68 St., New York 21, N. Y.
Bright, R. L., Westinghouse Electric Corp., 7325 Penn Ave., Pittsburgh 8, Pa.
Bridgman, A. D., Jr., Electronic Defense Laboratory, Box 205, Mountain View, Calif.
Brincka, J. J., 3147 W. 94th St., Cleveland 2, Ohio
Brinda, J., Jr., Electrical Engineering Bldg., University of Pittsburgh, Pittsburgh 13, Pa.
Brockway, R. M., Universal Broadcasting Co., Inc., 1440 N. Meridian St., Indianapolis 2, Ind.
Brodwin, M. E., 2412 Eutaw Pl., Baltimore 17, Md.
Brooks, L. P., 81 Lincoln Ave., Tuckahoe 7, N. Y.
Broudy, R. M., National Carbon Research Laboratory, Box 6087, Cleveland 1, Ohio
Brown, E. M., 88 Emerald Ave., Westmont, N. J.
Brown, J. N., 16 Parkway, Oaklihurst, R.F.D. 2, Langhorne, Pa.
Brown, P. M., 10036 Molly Knoll, Whittier, Calif.
Brown, W. G., 43 Madison St., Pequannock, N. J.
Bruggeman, J. T., Pines Lake Dr., E., Pines Lake, R.F.D. 1, Paterson, N. J.
Bruno, A. R., 1304 Susquehanna Ave., W. Pittston, Pa.
Brussel, E. H., 44 Tennyson Pl., Passaic, N. J.
Bryan, J. F., Box 160, R.F.D. 1, Long Branch, N. J.
Bubb, F. W., Jr., 1199 S. Glenwood La., Kirkwood 22, Mo.

(Continued on page 78A)

These DRIVER-HARRIS alloys do most to improve the quality of

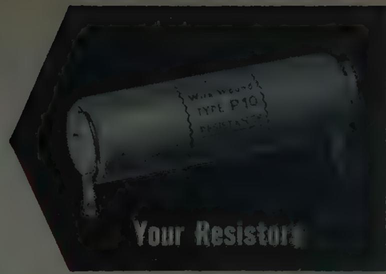

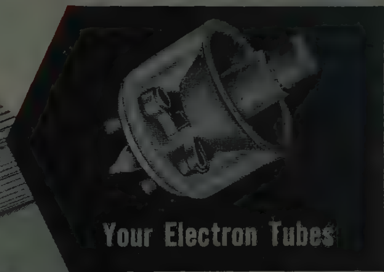

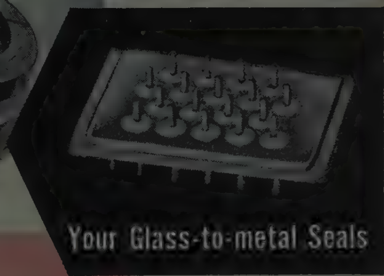

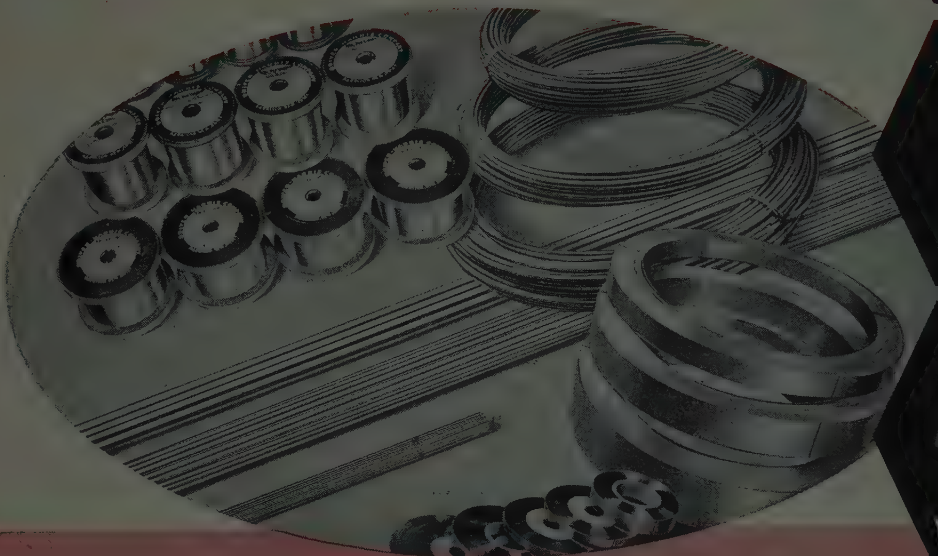

DRIVER-HARRIS RESISTANCE WIRE ALLOYS

NICHROME* V (Nickel-Chrome) Essential for resistor elements in the higher temperature applications such as electric furnaces, electric ranges, radiant heaters, etc.

KARMA* (Nickel-Chrome-Aluminum-Iron) Permits the manufacture of miniaturized wire wound precision resistors of best temperature coefficient of resistance at low cost per ohm; also resistance standards.

NICHROME* (Nickel-Chrome-Iron) The internationally accepted material for heating devices operating up to 1700°; also industrial applications for rheostats and resistance units.

CHROMAX* (Nickel-Chrome-Iron) A lower cost alloy for electrical heating under conditions less critical than those satisfied by Nichrome.

ADVANCE* (Copper-Nickel Series including MIDOHM*, 95 ALLOY, LOHM*, 30 ALLOY) Possess a number of properties which make them useful for winding heavy duty industrial rheostats, precision resistors, thermocouples, and thermocouple leads. Specific resistance range of this series is from 294 to 30 ohms/cmf.

MANGANIN (Manganese Copper) Most stable resistance wire known at ambient temperature. Indispensable for resistors used in many types of precision direct current apparatus such as Wheatstone Bridges, National Bureau of Standards type resistance standards, etc.

HYTEMCO* (Nickel-Iron) Combines high temperature coefficient of resistance with high specific resistance; ideal for winding compensating or ballast resistors.

DRIVER-HARRIS GLASS SEALING ALLOYS

THERLO* (Nickel-Cobalt-Iron). For sealing glasses such as Corning 7052 and 7040.

142 ALLOY (Nickel-Iron). For sealing glasses such as Corning 776, also 8160.

52 ALLOY Contains 50% nickel. It provides a slightly higher coefficient of expansion than 142 Alloy and seals successfully with 0120 glass.

146 ALLOY Contains 46% nickel. It offers special expansion properties, permits seals with ceramic coated resistors.

DRIVER-HARRIS ELECTRON TUBE ALLOYS

The Driver-Harris Company, since the inception of radio, has been making alloys for this field, supplying the industry with alloys for support wires, plates, grids, cathodes, and lead-throughs.

All Alloys are available in:

WIRE
(Sizes as fine as .0005)
ROD
RIBBON
STRIP
(Foil as thin as .00045)

Insulations:

ENAMEL
COTTON
SILK
NYLON
GLASS
FORMVAR

Singly or in combination

Every Driver-Harris alloy is made to the most precise metallurgical checks and controls known to the industry. And each of these highly specialized alloys is custom-made . . . produced exactly to the specifications of our customers.

Send us *your* specifications. If your needs are in any way unusual, and cannot be met by one of our current 112 alloys, our engineers will be happy to start tomorrow to devise a new one, custom-made for you. Just tell us exactly what you wish to accomplish.

*T.M. Reg. U.S. Pat. Off.

Nichrome and Nichrome V are made only by

SPECIAL PURPOSE ALLOYS SINCE 1899 — TRADE MARK REG. U. S. PAT. OFF.

Driver-Harris Company HARRISON, NEW JERSEY

BRANCHES: Chicago, Detroit, Cleveland, Louisville, Los Angeles, San Francisco

In Canada: The B. GREENING WIRE COMPANY, Ltd., Hamilton, Ontario

MAKERS OF THE MOST COMPLETE LINE OF ELECTRIC HEATING, RESISTANCE, AND ELECTRONIC ALLOYS IN THE WORLD

VISIT US AT THE WESCON SHOW. BOOTH #1821.

Membership

(Continued from page 76A)

Buchalter, M., Superex Electronics Corp., 23 Atherton St., Yonkers, N. Y.
Buchanan, W. D., 3725 Nelson St., Riverside, Calif.
Buck, R. F., 2221 W. Fifth, Stillwater, Okla.
Budd, M. A., 251 Emporia Blvd., Apt. 4, San Antonio 9, Tex.
Bueche, H. S., University of Delaware, Newark, Del.
Bukofzer, R., 458 Pacific Ave., Massapequa Park, L. I., N. Y.
Burak, M., 50 Woodward Ave., Quincy 69, Mass.
Burchill, G. H., N. S. Technical College Library, Halifax, N. S., Canada
Burg, K. E., Box 7144, Dallas 9, Tex.
Burger, E., 210 W. 17th St., New York 11, N. Y.
Burrell, W. P., 5836 Ashcroft Ave., S., Minneapolis 10, Minn.
Burton, R. G., 432 Allegheny, Tulsa 12, Okla.
Butenhoff, R. L., 4016 Everett St., Kensington, Md.
Buzzard, C. R., 20 N. Wacker Dr., Rm. 1650, Chicago 6, Ill.
Byrd, E. W., 3529 Beechgrove Rd., Dayton 9, Ohio
Cady, R. T., 17 Verbena Ct., Hicksville, L. I., N. Y.
Callaghan, J. W., 719 S. 52 St., Philadelphia 43, Pa.
Callahan, J. P., 94 Central Pkwy., Mt. Vernon, N. Y.
Calnon, D. C., 2835 N.E. 55 Ave., Portland 13, Ore.
Campbell, D. B., Mount Zion, Iowa
Campling, C. H. R., 306 Frontenac St., Kingston, Ont., Canada
Cancro, C. A., Naval Ordnance Laboratory, Rm. A-004, White Oak, Silver Spring, Md.
Capen, G. A., 812 S. Indiana Ave., Auburn, Ind.
Caporaletti, G. A., 4040 Oak Crest Dr., San Diego 5, Calif.
Cardella, O., 2274 Piche St., Montreal 9, Que., Canada
Carlson, D. J., 18-08 Sylvan Ave., Haddon Heights, N. J.
Carpenter, M. M., Jr., 320 Washington Ave., Haddonfield, N. J.
Carter, C. J., 39 W. Maynard, Columbus 1, Ohio
Carter, D. F., c/o Vinson-Carter Electric Co., 325 N. Fourth St., Phoenix, Ariz.
Cash, W. I., 3536 Hull Ave., New York 67, N.Y.
Casper, S., 30 Newmarket Rd., Syosset, L. I., N. Y.
Cattermole, G. B., 113 Upside Ct., Falls Church, Va.
Chang, S. Y., 2116-B N. John Russell Cir., Elkins Park 17, Pa.
Chapman, J. M., 400 Greenmount Blvd., Dayton 9, Ohio
Chase, R. C., 741 Hazelwood Dr., Walnut Creek, Calif.
Cheng, K. Y., 234 N.W. 36 Ct., Miami, Fla.
Cherry, W. L., Jr., Cherry-Channer Corp., 1488 Skokie Blvd., Highland Park, Ill.
Christensen, R. T., Zenith Radio Corp., 6001 Dickens Ave., Chicago 39, Ill.
Chruney, M., 124 Rutgers Ave., Berkeley Heights, N. J.
Chuan, C. J., Argonne National Laboratory, Box 299, Lemont, Ill.
Church, S. E., Bell Telephone Laboratories, Murray Hill, N. J.
Ciletti, V. J., 3407 Hartel Ave., Philadelphia 36, Pa.
Clark, H. L., 5096 Spring Dr., S.E., Washington 22, D. C.
Clark, M. M., 205 Elm St., Groton, N. Y.
Clark, R. U., 4 Orchard Dr., W. Acton, Mass.
Clark, R. V., 267 Wagner Rd., Northfield, Ill.
Clarke, I. A., 1064 Lindsay La., Rydal, Pa.

(Continued on page 80A)

Collins Mechanical Filters

SUPERIOR SELECTIVITY, SMALL SIZE

Collins Mechanical Filters are now available in six series for design needs where superior selectivity and small cubic volume are important. Permanently-tuned, hermetically-sealed and not affected by wide variations in ambient temperature, the Filters have greatly improved the selectivity characteristics of many commercial and military equipments. Mechanical Filters of special design can be supplied for most requirements in the range of 60 kc to 550 kc center frequencies and your inquiry is invited.

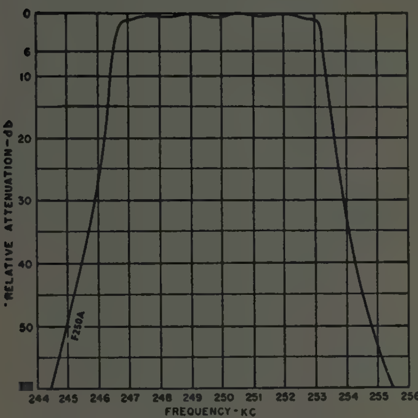

F250A A filter for double sideband signals at a center frequency of 250 kc. Bandwidth 6.7 kc at 6 db attenuation. Transmission loss 13 db.

Write for Technical Bulletin 201.

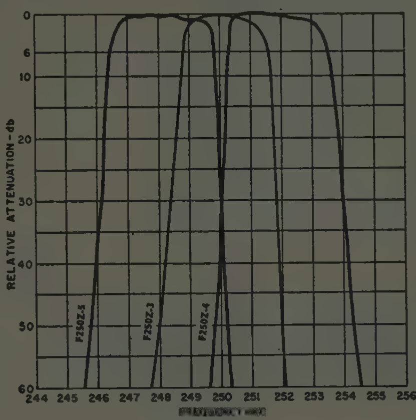

F250Z For single sideband signals at a carrier frequency of 250 kc. Bandwidths of 2.7 and 3.2 kc at 6 db attenuation. Transmission loss, 10 db.

Write for Technical Bulletin 202.

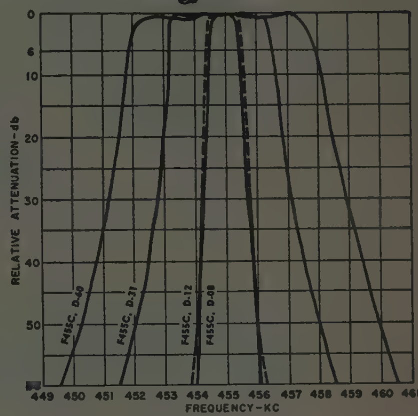

F455C, F455D Low insertion loss filters for AM, CW, RTTY and FSK signals at 455 kc. Bandwidth of 0.8, 1.2, 3.1 and 6.0 kc at 6 db attenuation. Transmission loss, 12 db.

Write for Technical Bulletin 203.

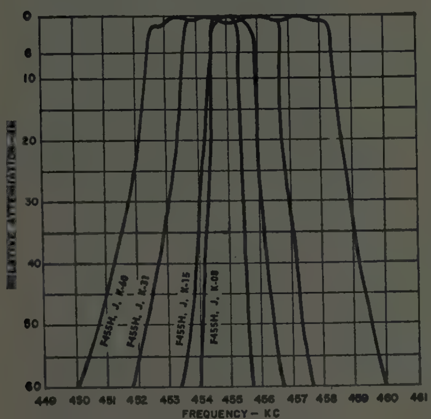

F455H, J and K New tubular case mounting, temperature compensated for signals at 455 kc. Bandwidths of 0.8, 1.5, 3.1 and 6.0 kc at 6 db attenuation. Transmission loss, 10 db.

Write for Technical Bulletin 204.

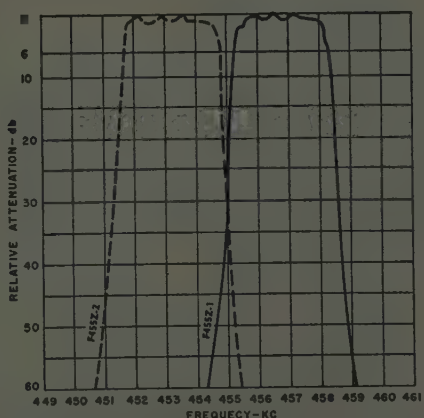

F455Z Mechanical Filters for single sideband signals at a carrier frequency of 455 kc. Bandwidth 3.3 kc at 6 db attenuation. Transmission loss, 10 db.

Write for Technical Bulletin 205.

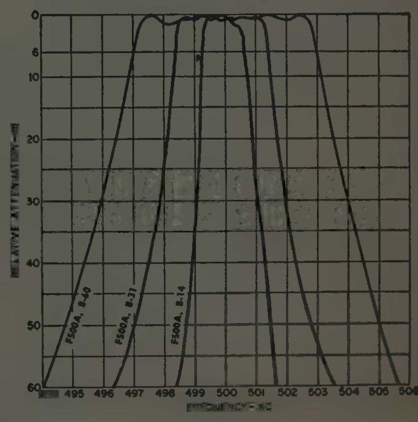

F500 Mechanical Filters for AM, CW, RTTY signals at 500 kc. Bandwidths of 1.4, 3.1 and 6.0 kc at 6 db attenuation. Nominal transmission loss, 23 db.

Write for Technical Bulletin 206.

Write for a copy of Collins Mechanical Filter Theory and Application Bulletin #200 and for any of the Technical Bulletins described above.

COLLINS RADIO COMPANY | **CEDAR RAPIDS, IOWA**

COLLINS

261 Madison Avenue, NEW YORK 16, NEW YORK
1200 18th Street N. W., WASHINGTON, D. C.
1930 Hi-Line Drive, DALLAS 2, TEXAS
2700 W. Olive Avenue, BURBANK, CALIFORNIA
COLLINS RADIO COMPANY OF CANADA LTD.
74 Sparks Street, OTTAWA, ONTARIO

VISIT COLLINS EXHIBIT AT WESCON AUG. 24-26 IN SAN FRANCISCO

IRE Membership

(Continued from page 78A)

Clayton, V. E., 1525 Browning Ave., Salt Lake City 5, Utah
Clements, C. C., Box 213, Fairfield, Ala.
Clotworthy, J. H., 346 Third Ave., Indialantic, Melbourne, Fla.
Clutts, C. E., 463 West St., New York 14, N. Y.
Coan, E. M., 45 Overlook Rd., Cedar Grove, N. J.
Cockrill, M. S., 366 Boyer Ave., Seattle 2, Wash.
Codel, M., Television Digest, Wyatt Bldg., N.W., Washington 5, D. C.
Cohen, C. L., 6804 Randolph St., Radiant Valley, Hyattsville, Md.
Cohen, G., 92 Rowe Ave., E. Rockaway, L. I., N. Y.
Cohen, N. L., 318 Lacey Dr., New Milford, N. J.
Coler, B. A., 381 W. Hazelwood Ave., Rahway, N. J.
Collins, G. S., Box 476, Kerwood Cres., Agincourt, Ont., Canada
Coltin, A. H., 521 N. Fermoore St., San Fernando, Calif.
Comitz, P., 306 E. 31 St., New York, N. Y.
Conley, P., 2 Prescott St., Combridge 38, Mass.
Cook, R. M., Research Department, Ferranti Electric, Ltd., Mount Dennis, Toronto 15, Ont., Canada
Cooper, G. R., Electrical Engineering Department, Purdue University, W. Lafayette, Ind.
Cooper, S., 719 C Parkview Apts., Collingswood 6, N. J.
Corkran, R. L., Jr., U. S. Navy, Underwater Sound Laboratory, New London, Conn.
Cornwall, E. A., Jr., Apt. 7, 10405 Eastborne Ave., Los Angeles 24, Calif.
Corporon, R. P., 609 Emerson St., Goshen, Ind.
Costa, H., Caixa Postal 5025, Rio de Janeiro, Brazil
Cottrell, B. P., 4221 Linden Ave., Western Springs, Ill.
Covert, J. L., 3104 S. Preston, Louisville 13, Ky.
Cowan, C. D., 1077—27 St., Marion, Iowa
Craft, C. J., III, 34 S. Franklin Ave., Valley Stream, L. I., N. Y.
Craig, D. R., Jr., 3 Plymouth Rd., Port Washington, L. I., N. Y.
Cravis, H., 186 Riverside Dr., New York 24, N. Y.
Crissinger, W. W., Crawford Dr., Galion, Ohio
Cromer, E. G., Victor Adding Machine Co., 3900 N. Rockwell St., Chicago 18, Ill.
Cronauer, E. A., 34 Linwood Pl., Massapequa, L. I., N. Y.
Crooke, V. E., 3659 Purdue Ave., Los Angeles 34, Calif.
Crows, H., 2538 Milton Rd., Cleveland 18, Ohio
Csepely, J. A., Westinghouse Electric Corp., Friendship International Airport, Baltimore, Md.
Cummings, K. C., 111 S. Ottawa Ave., Minneapolis 5, Minn.
Cunningham, R. E., Box 85, 7490th Tech Tng Sqdn, APO 207, New York, N. Y.
Curtis, L. B., 101 Forest Ave., Verona, N. J.
Curtis, R. W., 275 Arlington Ave., Ottawa, Ont., Canada
Dadant, P. M., 6604 McLennan Ave., Van Nuys, Calif.
Daggett, N. L., 211 Massachusetts Ave., Cambridge 39, Mass.
Dale, E. H., 6827 Wentworth Ave., S., Minneapolis 23, Minn.
D'Amato, R. J., 195 E. 35 St., Brooklyn 3, N. Y.
Dame, R. O., 6279 E. Bell St., Ventura, Calif.
Daniels, T. E., Box 161, Neptune, N. J.
David, J., 685 Rim Rd., Pasadena 8, Calif.
Davidson, R. A., 224 Hillcrest Ave., Collingswood 7, N. J.

(Continued on page 82A)

A NEW LINE OF BROADBAND MICROWAVE COMPONENTS

MICROWAVE TEST ANTENNAS

Covering 1,000 to 26,600 mc. Rugged, portable units built especially for field intensity measurements, antenna pattern recording, leakage measurements and other communications use. Supplied complete with tripod mount, adjustable pan head, and convenient carrying case.

Each of these Polarad test antennas is highly directional with excellent front to back ratio, and is supplied with flexible waveguide or coax couplings.

MODEL No.	FREQUENCY RANGE	MAX. VSWR
A-L	1,000 to 2,300 mc	3:1
A-S	2,150 to 4,600 mc	2:5
A-R	4,450 to 8,000 mc	2:5
A-X	7,850 to 12,400 mc	2:7
A-KU	12,400 to 18,000 mc	1.5:1
A-K	18,000 to 26,000 mc	1.5:1

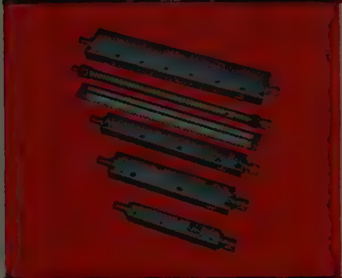

BROADBAND-PASS FILTERS

Covering 650 to 13,000 mc. These Polarad Broadband-Pass filters are the first of their kind commercially available. They feature sharp skirt selectivity and low pass band insertion using standard 50 ohm co-axial connections. Curves showing typical bandpass characteristics are available on request.

MODEL No.	FREQUENCY RANGE
F 650	650 — 1,300 mc
F 1100	1,100 — 2,200 mc
F 1800	1,800 — 3,600 mc
F 3500	3,500 — 7,400 mc
F 6100	6,100 — 13,000 mc

MICROWAVE WAVEMETERS

Covering 500 to 4000 mc. Precision, adjustable, cavity-type meters designed for measuring frequency with ± 0.2% accuracy over the range 500 to 4000 mc. Each meter in the series has a 2:1 frequency range. Specific frequency metering is accomplished by adjustment of micrometer head until a dip of at least 20% in output occurs when input or output impedance is nominal 50 ohms. Micrometer head readings are easily converted to frequency by using calibration chart furnished with each instrument. Utilizes Type "N" coax connectors.

MODEL	FREQUENCY RANGE
FR	500 — 1,000 mc
FL	1,000 — 2,000 mc
FS	2,000 — 4,000 mc

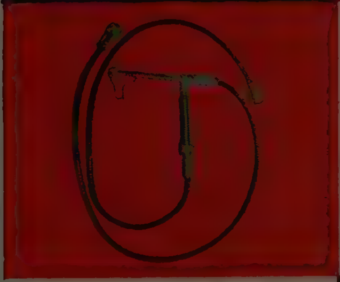

MICROWAVE ATTENUATOR—Model SIJ

Covering 4,000 to 12,400 mc. A continuously variable, stub-tuned, mutual inductance attenuator (waveguide beyond cut-off) designed for external use in making microwave measurements with spectrum analyzers, signal sources, receivers and for power measurements. The Model SIJ can be used as a standard calibrated attenuator; for circuit protection; or for monitoring and measuring. It will insure RF circuit isolation. It may be used to convert signal source or laboratory oscillator into a signal generator.

SPECIFICATIONS:

Frequency Range:	4 to 12.4 kmc
Impedance:	50 ohms
Attenuation Range:	130 db
Minimum Insertion Loss:	Approximately 10 db depending on frequency.

AVAILABLE ON EQUIPMENT LEASE PLAN

FIELD MAINTENANCE SERVICE AVAILABLE THROUGHOUT THE COUNTRY

POLARAD
PROVEN RELIABILITY

ELECTRONICS CORPORATION

43-20 34th STREET • LONG ISLAND CITY 1, N. Y.

REPRESENTATIVES: • Albuquerque • Atlanta • Baltimore • Bayonne • Bridgeport • Buffalo • Chicago • Dayton • Fort Worth • Los Angeles • New York Newton • Philadelphia • San Francisco • Syracuse • Washington, D. C. • Westbury • Winston-Salem • Canada, Arnprior, Toronto—Export: Rocke International Corporation

Membership

(Continued from page 80A)

Davidson, S., 18 S. Bay Pl., Massapequa, L. I., N. Y.
Davis, A. P., 3019 Second St., S.W., Calgary, Alta., Canada
Davis, D. A., Box 2097, Denver, Colo.
Davis, D. C., 3645 Cartwright St., Pasadena 8, Calif.
Davis, J. C., Box 77, Carlisle, Mass.
Davis, J. F., 56 Beaumont St., W., St. Bruno, Que., Canada
Davis, J. I., 1770 Orchid St., Apt. 109, Hollywood 28, Calif.
Davis, R. E., University of Western Ontario, Physics Department, London, Ont., Canada
Davis, W. L., 1100 Copley La., Silver Spring, Md.
Davy, L. H., 1226 Ortega St., San Francisco 22, Calif.
Dawley, R. L., 5 Rosemary La., Santa Barbara, Calif.
Decuir, L. E., 3609 W. 44 Pl., Hawthorne, Calif.
Deichert, R. W., Allen B. DuMont Laboratories, 2 Main Ave., Passaic, N. J.
DeJong, P. G., 1470 Calvin Ave., S.E., Grand Rapids 7, Mich.
DeJonghe, J. J., 352 N. Elm St., Fairborn, Ohio
Delany, E. B., Washington Park Estates, R.F.D. 3, Ridgefield, Conn.
Delany, F. J., 24 Vanderbilt Dr., Lake Success, L. I., N. Y.
Del Camp, S. M., 1820 S. 20 Ave., Maywood, Ill.
De Leon, J., 252 Emmett Pl., Ridgewood, N. J.
Del Giorno, A. E., 53-43—190 St., Flushing, L. I., N.Y.
Dell, H. R., Marchant Research Inc., 5303 Adeline St., Oakland 8, Calif.
Denney, J. M., 284 Prospect St., E. Orange, N. J.
Dennis, J., 130 Ridge Cir., Erlton, Haddonfield, N.J.
Depew, H., Jr., 722 W. 8 St., Claremont, Calif.
De Remer, K. R., Princeton Junction, N. J.
De Rienzo, F., Jr., 18 Irving Pl., Summit, N. J.
De Satnick, S., 10 Montgomery Pl., Brooklyn 15, N. Y.
De Size, L. K., 8639—77 St., Woodhaven 21, L. I., N. Y.
Desnoes, A. B., 140 West St., New York, N. Y.
De Tar, J. B., 15844 Coyle, Detroit 27, Mich.
Detwiler, S. P., 46 Hillside Ave., Bedford, Mass.
Deutsch, L., 1333 President St., Brooklyn 13, N. J.
Deutsch, S., 41 Peachtree La., Roslyn Heights, L. I., N. Y.
Devaney, R. G., 930 Walnut Ave., Sevier Ter., Kingsport, Tenn.
De Voe, L. M., 4010 Washington Blvd., Indianapolis, Ind.
Dicke, A. H., 4792 Burkhardt Ave., Dayton 3, Ohio
Dickson, D. C., Jr., 12 Brookside Ave., Basking Ridge, N. J.
Dillow, J. C., Air War College, Maxwell AFB, Ala.
Dilson, J., 535 E. 14 St., New York 9, N. Y.
Dimond, J., Magnavox Co., Bueter Rd., Fort Wayne 4, Ind.
Dingwall, R. A., 793 Eastbourne Ave., Ottawa 2, Ont., Canada
Distler, J. E., 57 A Middle Ave., Summit, N. J.
Dittenhoefer, H. F., 1010 Maple Ave., New Hyde Park, L. I., N. Y.
Dodd, A. E., 26 McKelvey Rd., Pittsburgh 18, Pa.
Doherty, D. T., 3217 Villanova, Dallas, Tex.
Dolce, S. L., Wheelock Rd., Wayland, Mass.
Dold, C. W., 4433 Clifford Rd., Cincinnati 36, Ohio
Dosch, T. J., 31 Turtle Cove La., Huntington, L. I., N. Y.

(Continued on page 84A)

Membership

(Continued from page 82A)

Dossey, J. L., 2804 Texas St., N.E., Albuquerque, N. Mex.
Doto, N. J., 5949 Nassau Rd., Philadelphia 31, Pa.
Douglas, J. C., 3440 Peel St., Apt. 17, Montreal, Que., Canada
Douglass, F. W., 1242 Westmont Ave., Roslyn, Pa.
Dowell, K. P., 4059 Lomita La., Dallas, Tex.
Downey, R. L., Woodland Dr., R.F.D., Baldwinsville, N. Y.
Doyle, W. T., 315 S. Irving St., Arlington, Va.
Drazy, E. J., Bell Telephone Laboratories, Inc., Murray Hill, N. J.
Duff, J. E., 5102 Jackson Blvd., Canton 9, Ohio
Duffin, J. D., 610 Park Ave., Collingswood 7, N. J.
Dunbar, E. E., 9814—35 Ave., S.W., Seattle 6, Wash.
Duncan, D. B., 5349 Danroth Ct., Cincinnati 24, Ohio
Dunlap, R. H., 710 N.E. 32 St., Grand Prairie, Tex.
Durham, B. H., 4600 Cedar Garden Dr., Baltimore 29, Md.
Dworkin, A. E., 127 Ranee Ave., Wilson Heights, Toronto, Ont., Canada
Eachus, W. J., Mackay Radio & Telegraph Co., Inc., 350 Mission St., San Francisco 5, Calif.
Eager, G. S., Jr., General Cable Corp., Bayonne, N. J.
Eash, J. J., 249 Fourth St., Beaver, Pa.
Ebaugh, P., Department of Engineering Research, Pennsylvania State University, State College, Pa.
Echtman, L., 181 E. 93 St., New York 28, N. Y.
Eckdahl, D. E., 3924 Via Nivee, Palos Verdes Estates, Calif.
Eckert, E. R., Box 254 A, R.F.D. 1, Curwensville, Pa.
Edell, J. J., 199-07—100 Ave., Hollis 7, L. I., N. Y.
Edwards, H. T., 3419 Ewing Ave., Dallas 16, Tex.
Edwards, P. L., 1204 Lebanon St., Apt. 1, Silver Spring, Md.
Egert, S. S., 11 Park Pl., New York 7, N. Y.
Egger, R. J., 132 Oak Knoll Dr., Dayton 9, Ohio
Eglin, J. M., Bell Telephone Labs., Inc., Murray Hill, N. J.
Eikelman, J. A., Jr., 1162 Pine Dr., El Cajon, Calif.
Einsohn, I. A., 1524 Nelson Ave., New York 52, N. Y.
Eisenberger, A. J., 125 Crestview Dr., Red Bank, N. J.
Eisenhard, S. E., Jr., 17 Walnut La., Camp Hill, Pa.
Elderkin, C. D., Box 83, Navy 3923, FPO, San Francisco, Calif.
Eldridge, D. F., 19268 Occidental Ave., S., Seattle 88, Wash.
Elliott, L. W., Essex Electronics of Canada, 99 Wragg St., Toronto, Ont., Canada
Elliott, N. J., 1420 Madison St., N.E., Albuquerque, N. Mex.
Ellis, C. R., 205 Oakdale Dr., Syracuse, N. Y.
Elmendorf, D. E., Lamp Department, General Electric Co., Nela Park, Cleveland 12, Ohio
Englund, R. A., 1943 E. Marshall Ave., Phoenix, Ariz.
Engman, G. E., 34 Florissant Ave., Saxonville, Mass.
Enright, D. J., 219 Alicia Dr., Apt. D, El Paso, Tex.
Epprecht, G. W., 44 Eichholzweg, Muri-Bern, Switzerland
Escher, P. H., 27 Latimer Rd., Santa Monica, Calif.
Evans, A. G., 1109 N. Beville Ave., Indianapolis 1, Ind.

(Continued on page 86A)

HUGHES

SILICON JUNCTION

DIODES

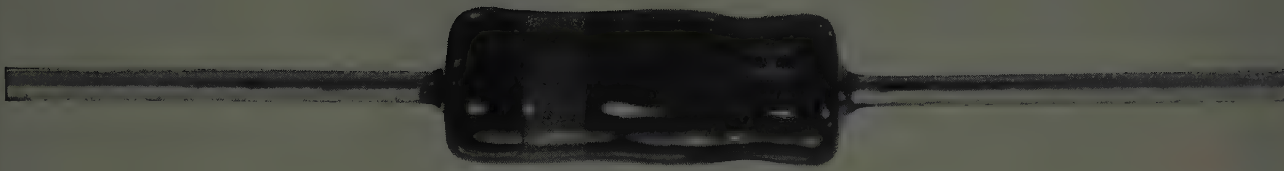

Dimensions are maximum for standard
Hughes Silicon Junction Diodes.

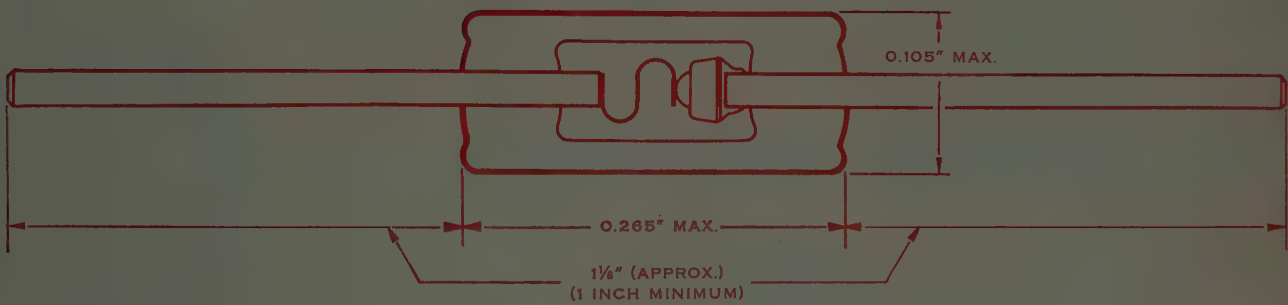

*High Temperature Operation**

Extremely High Back Resistance

Exceptionally Stable Characteristics

FEATURES—High temperature operation . . . *extremely* high back resistance . . . very sharp back voltage breakdown . . . one-piece, fusion-sealed glass body . . . axial leads for easy mounting . . . subminiature size . . . exceptionally stable characteristics.

TESTED—All Hughes Silicon Junction Diodes are subjected to rigorous testing procedures. Specific electrical characteristics are measured and, in addition, each diode is temperature-cycled twice in a moisture-saturated atmosphere. When specified, special tests are also performed.

CONSTRUCTION—Hughes Silicon Junction Diodes are packaged in the famous fusion-sealed glass body, developed at Hughes. This construction is impervious to moisture penetration—*ensures* electrical and mechanical stability, and freedom from contamination.

When high temperatures or high back resistance requirements call for silicon, be sure to specify *Hughes* Silicon Junction Diodes. They are first of all—for RELIABILITY!

Diode glass body is coated with opaque black enamel, color-coded on cathode end. Available now in nine types: HD6001, HD6002, HD6003, HD6005, HD6006, HD6007, HD6008, HD6009, HD6011. Ask for descriptive Bulletin SP-4.

**Characteristics rated at 25°C and at 150°C. Ambient operating range, −80°C to +200°C.*

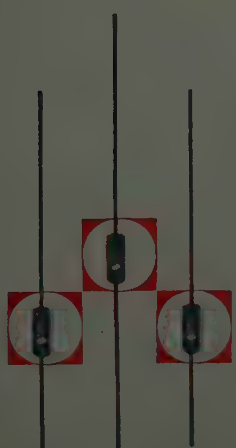

Actual Size

HUGHES Aircraft Company, Culver City, California

SEMICONDUCTOR DIVISION

New York Chicago Los Angeles

Membership

(Continued from page 84A)

Evenson, H. J., 5402—49 Ave., S.W., Seattle 16, Wash.
Ewald, E. R., 1202 James St., Geneva, Ill.
Fales, D., III, 620 Hastings Rd., Towson 4, Md.
Fannin, B. M., 5206 Valley Oak Dr., Austin, Tex.
Fanta, F. A., Jr., 1809 Maple Ave., Berwin, Ill.
Farber, E., WNEX, 2262 Rogers Pl., Macon, Ga.
Farley, B. G., Box 73, Lexington 73, Mass.
Farrall, W. R., 111—18 St., S.E., Rochester, Minn.
Farrell, C., USN, VC-7, NAS, Patuxent River, Md.
Farris, H. W., Cooley Engineering Bldg., University of Michigan, Ann Arbor, Mich.
Faulks, H. R., 1465 N. Sheridan Rd., Lake Forest, Ill.
Faust, A. C., 4237 Greeby St., Philadelphia 35, Pa.
Favreau, R. R., 204 Harrison St., Princeton, N. J.
Fegan, A. A., 17 W. Magnolia St., Stockton 3, Calif.
Fegley, K. A., 6663 Montague St., Philadelphia 35, Pa.
Feinman, G., 154-32—24 Rd., Flushing, L. I., N. Y.
Feitler, J., R.F.D. 1, Hopewell Rd., Wappingers Falls, N. Y.
Fenaughty, A. L., 89 Hudson St., Hastings-on-Hudson, N. Y.
Fenichel, I., 1605 Homestead St., Baltimore 18, Md.
Fennick, B., 8023 Bergenline Ave., North Bergen, N. J.
Ferber, L. W., Gardenside Dr., R.F.D., Willoughby, Ohio
Fetherolf, J. M., 4 Woodland Pl., White Plains, N. Y.
Fialkov, H., 251-14—71 Ave., Bellerose, L. I., N. Y.
Findeis, W. J., 393 Fox Ave., Yonkers 4, N. Y.
Finger, P. R., 728—25 St., N.E., Cedar Rapids, Iowa
Fink, J. H., 26 Hudson St., Bath, N. Y.
Fish, W. Y., Box 274, Cocoa Beach, Fla.
Fisher, C. B., 1080 University St., Montreal 3, Que., Canada
Fisher, E. M., 2303 Calvert St., Lewisdale, Hyattsville, Md.
Fisher, M. R., Jr., 755 Collidge Rd., Birmingham, Mich.
Fishman, M., 114 Paul Revere Rd., Arlington Heights, Mass.
Fisk, R. H., 22354 Cleveland Ave., Dearborn, Mich.
Fitzgerald, R. T., 1317 Coral Sea Dr., Rockcrest, Rockville, Md.
Fivel, M. J., 2715 Sycamore St., Alexandria, Va.
Flackbert, W. D., 6406 Kratzville, Rd., Evansville, Ind.
Flarity, W. H., 5179 W. Point Loma Blvd., San Diego 7, Calif.
Fleissner, C. L., Station 'B', Box 6127, Albuquerque, N. Mex.
Fleming, H. B., 105 Alturas Dr., Burlingame, Calif.
Flemons, R. S., 76 Corbett Ave., Toronto, Ont., Canada
Floyd, R. A., Jr., 1636 Second Ave., N.E., Rochester, Minn.
Flynt, E. R., Engineering Experiment Station, Georgia Institute of Technology, Atlanta, Ga.
Forman, A. H., Jr., P.O. 1-203, N.O.D., General Electric Co., 100 Plastics Ave., Pittsfield, Mass.
Forrest, C. B., 7164 W. 94 St., Los Angeles 45, Calif.
Forst, P. P., Jr., 2016 S. 11 Ave., Maywood, Ill.
Foss, R. N., 1723 E. 91 St., Seattle 5, Wash.
Foster, H. O., 2045 Chelsea Cir., N.E., Atlanta 6, Ga.

(Continued on page 88A)

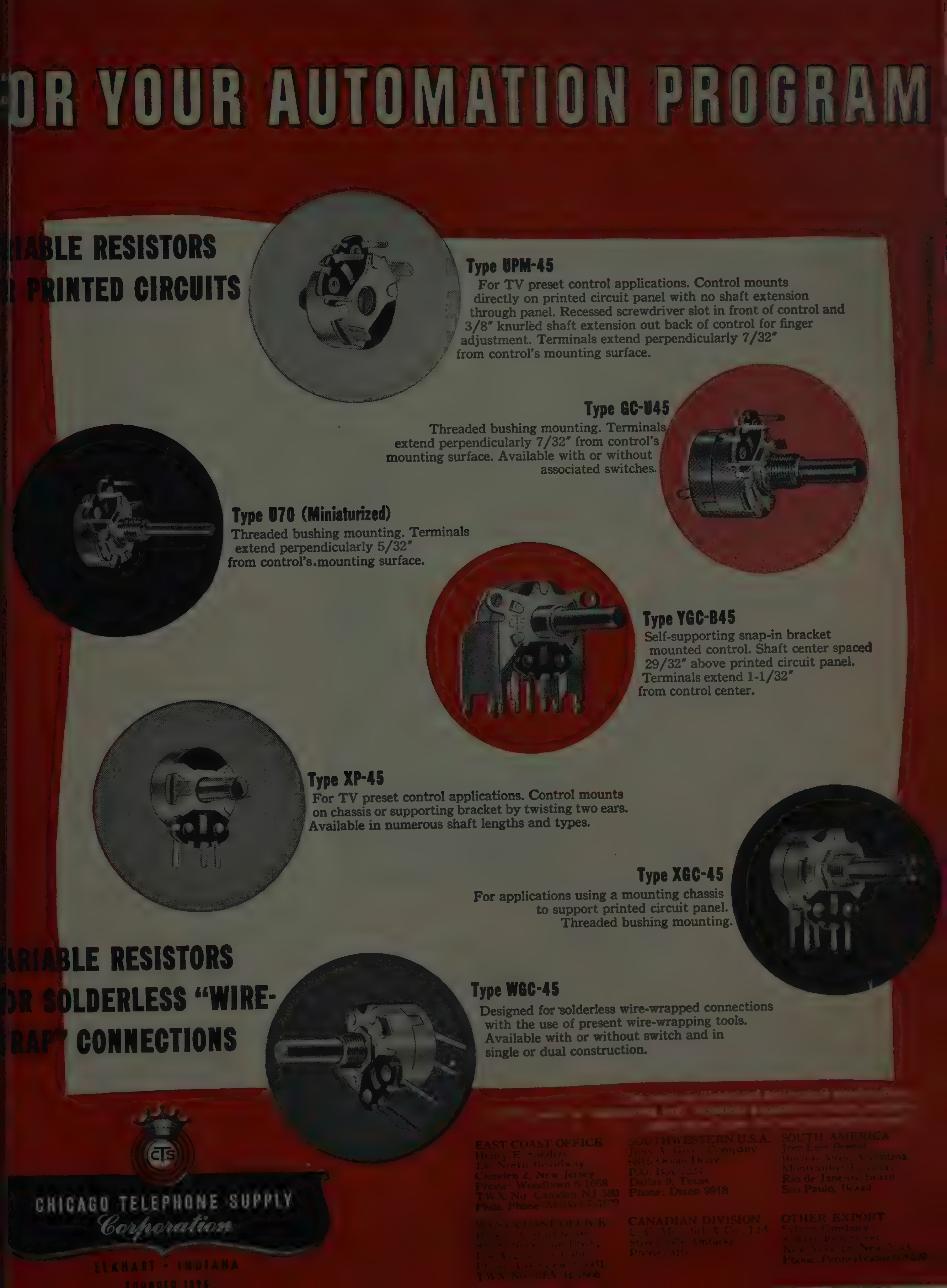

OR YOUR AUTOMATION PROGRAM
IABLE RESISTORS
PRINTED CIRCUITS
Type UPM-45
For TV preset control applications. Control mounts directly on printed circuit panel with no shaft extension through panel. Recessed screwdriver slot in front of control and 3/8″ knurled shaft extension out back of control for finger adjustment. Terminals extend perpendicularly 7/32″ from control's mounting surface.
Type GC-U45
Threaded bushing mounting. Terminals extend perpendicularly 7/32″ from control's mounting surface. Available with or without associated switches.
Type U70 (Miniaturized)
Threaded bushing mounting. Terminals extend perpendicularly 5/32″ from control's mounting surface.
Type YGC-B45
Self-supporting snap-in bracket mounted control. Shaft center spaced 29/32″ above printed circuit panel. Terminals extend 1-1/32″ from control center.
Type XP-45
For TV preset control applications. Control mounts on chassis or supporting bracket by twisting two ears. Available in numerous shaft lengths and types.
Type XGC-45
For applications using a mounting chassis to support printed circuit panel. Threaded bushing mounting.
ARIABLE RESISTORS
OR SOLDERLESS "WIRE-
RAP" CONNECTIONS
Type WGC-45
Designed for solderless wire-wrapped connections with the use of present wire-wrapping tools. Available with or without switch and in single or dual construction.
CTS
CHICAGO TELEPHONE SUPPLY
Corporation
ELKHART • INDIANA
EAST COAST OFFICE
Camden 2, New Jersey
Phone: Woodlawn 6-1668
TWX No. Camden NJ 380
SOUTHWESTERN U.S.A.
Dallas 9, Texas
Phone: Dixon 9918
SOUTH AMERICA
Rio de Janeiro, Brazil
Sao Paulo, Brazil
CANADIAN DIVISION
OTHER EXPORT

Membership

(Continued from page 86A)

Foulks, E. D., R.F.D. 1, Marlboro, Alliance, Ohio
Fowler, B. V., 10435—17 Ave., S., Seattle, Wash.
Foy, R. H., 3521 Beethoven St., Los Angeles, Calif.
Francis, M. C., 2009 Wayne, Topeka, Kans.
Franklin, H. B., 6438 N. Seeley Ave., Chicago 45, Ill.
Frary, R. S., Box 267, Duncanville, Tex.
Frazier, R. K., Box 511-B, R.F.D. 1, Granger, Ind.
Freud, E. L., General Precision Laboratory, 63 Bedford Rd., Pleasantville, N. Y.
Fristensky, C. A., 282 Shaler Blvd., Ridgefield, N. J.
Friswold, F. A., 27027 Russell Rd., Bay Village, Ohio
Fugazzi, C., 150-01 Reeves Ave., Flushing 67, L. I., N. Y.
Fuller, L. C., Jr., 134 Edgewood Rd., Ardmore, Pa.
Furfine, A. L., 812 Lebon Dr., St. Louis 15, Mo.
Furnell, W. W., Jr., Box 638, Garland, Tex.
Gabriel, W. F., 5514 Second St., S.E., Washington 21, D. C.
Gahm, W. L., 351 W. Rosslyn Ave., Worthington, Ohio
Galbraith, H. J., 300 Wendell La., Beverly Gardens, Dayton 3, Ohio
Ganahl, P. J., 813 Lomita, El Segundo, Calif.
Gardner, G. F., 16 S. Dorcas St., Lewiston, Pa.
Gartzke, F. J., 14 Addison Rd., R.F.D. 4, Faifax, Va.
Gates, R. S., Collins Radio Co., Cedar Rapids, Iowa
Gauger, R. H., 26-29—212 St., Bayside 60, L. I., N. Y.
Gauss, H., 2658 N. Quantico St., Arlington 7, Va.
Gebhardt, J. W., 188-50B—71 Cresc., Fresh Meadows 65, L. I., N. Y.
Geiling, H. F., 23-A Bryant Pl., Ridgefield, N. J.
Geisler, H. J., R.F.D. 2, Hillside Lake, Wappingers Falls, N. Y.
Geller, W., 291 Fair St., Paterson 1, N. J.
Gellert, M. E., 1228—109, S.E., Bellevue, Wash.
Gennrich, A., 3343 W. Ruskin St., Milwaukee 15, Wis.
Gens, H. J., 2452 N. California Ave., Chicago 47, Ill.
Germain, R. C., 1405 Parker Rd., Arbutus 27, Md.
Gerten, N., 44 Rue Francois Premier, Paris, France
Geyer, B. H., Jr., 113 Herbert St., N. Syracuse, N. Y.
Gibbs, E. D., 3565 Taft St., Wantaugh, L. I., N. Y.
Gibbs, L. L., 351 Brookfield Rd., Dayton 9, Ohio
Gilbert, R. C., 3601 Marjorie La., Seaford, L. I., N. Y.
Gilford, S. R., 10 S. Prospect St., Oberlin, Ohio
Gilleo, M. A., 849 Springfield Ave., Apt. 18-F, Summit, N. J.
Gillespie, C. N., Woodridge Rd., Wayland, Mass.
Gillette, E. C., Jr., Department of Physics, West Point, N. Y.
Giordano, A. F., 471 Clifton Ave., Newark 4, N. J.
Girdwood, J., Atlantic Sales, McGraw Hill Publishing Co., 330 W. 42 St., New York 36, N. Y.
Giulianelli, R. M., 2360 Lincoln St., N., N. Bellmore, L. I., N. Y.
Glenn, A. J., 1821 Indiana St., N.E., Albuquerque, N. Mex.
Glick, C. L., 1896 Manor Dr., Union, N. J.
Gluck, S. E., Burroughs Corp., Research Center, Paoli, Pa.
Goertz, R. C., 5510 Fairmount Ave., Downers Grove, Ill.
Goetter, W. F., 121 Russell Ave., Liverpool, N. Y.
Gold, J. I., 22 Sussex Ave., Massapequa, L. I., N. Y.

(Continued on page 90A)

INFRA-RED LAMPS RAISE AMBIENT TEMPERATURE TO +125 C.

NEW G-E TANTALYTIC* CAPACITORS OPERATE AT +125°C AMBIENT

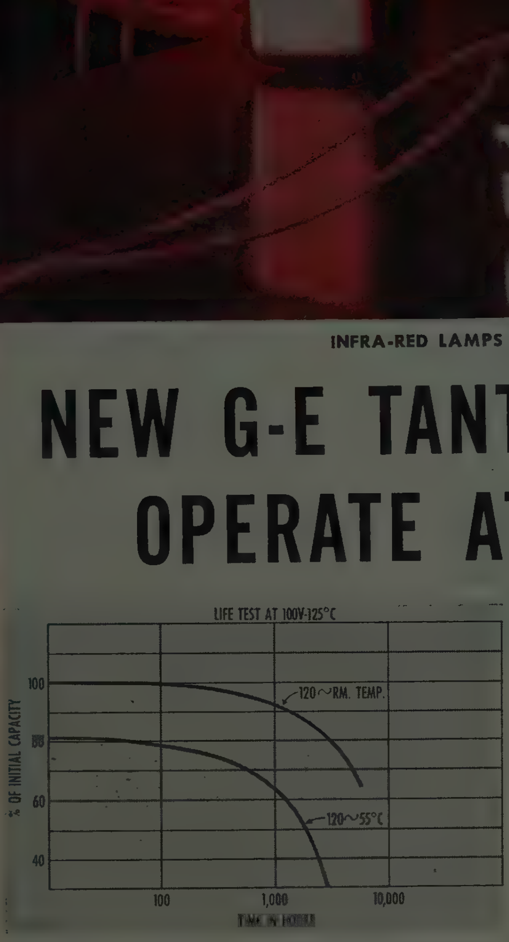

LONG LIFE of G-E high temperature Tantalytic capacitors is shown by this graph of life vs loss of capacitance for typical 100 volt d-c unit.

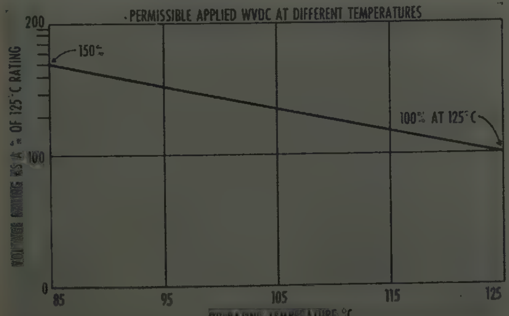

HIGHER VOLTAGES than 100 VDC can be applied . . . with no loss of life . . . at ambient temperatures below rated +125 C as shown above.

Available in ratings from 36 uf at 100 VDC to 180 uf at 30 VDC

Designed to operate at +125 C for 1000 hours with not more than 20% loss in initial +25 C capacitance, General Electric's new high-temperature Tantalytic capacitors meet the tough requirements of miniaturized military equipment.

FOIL CONSTRUCTION assures the same long life, high quality, and stable operating characteristics provided by +85 C Tantalytics. Unlike other types of Tantalytic capacitors, the foil construction also offers:

- **Both polar and nonpolar construction.**
- **Chemically neutral electrolyte . . . minimizes corrosion danger.**
- **Excellent mechanical stability . . . freedom from electrical noise under shock and vibration.**
- **Excellent reliability at rated temperatures . . . extended life at temperatures below +125 C.**

AVAILABILITY: G-E high-temperature Tantalytic capacitors can be obtained now in sample quantities for evaluation and prototype use. Production lots will be available by September in the following standard ratings:

Voltage	uf Case 1 ¾" x ¾" x 1⅛"	uf Case 2 ¾" x ¾" x ⅞"	uf Case 3 ¾" x ¾" x ½"
30	180	110	55
50	100	60	30
75	60	36	18
100	36	24	12

For more information, see your G-E Apparatus Sales Representative or write for Bulletin GEA-6258, General Electric Company, Section 442-27, Schenectady 5, New York.

*Reg. trade-mark of General Electric Co.

Progress Is Our Most Important Product

GENERAL ELECTRIC

Membership

(Continued from page 88A)

Goldfarb, S., 33 Continental Ave., Morristown, N. J.
Goldman, S., RCA Laboratories, 66 Broad St., New York 4, N. Y.
Goldschmidt, K., Bell Telephone Laboratories, 463 West St., New York 14, N. Y.
Goldsmith, A. S., 2830 Schley Ave., New York, N. Y.
Goldstein, R., 805 S. Wa Pella, Mount Prospect, Ill.
Goodfriend, L. S., 6 Harding Rd., Scarsdale, N. Y.
Goodman, H. C., IBM, Research Laboratory—533, Poughkeepsie, N. Y.
Gordon, R. A., 1402 Wilbur St., San Diego 9, Calif.
Gramman, E. G., 8727 Remick Ave., Sun Valley, Calif.
Grammer, R. A., Jr., 139 Bayerest Dr., Rochester 9, N. Y.
Granlund, J., 50 Ashland St., Arlington 74, Mass.
Grannemann, W. W., 209 S. Bedford St., La Habra, Calif.
Gray, M. C., Bell Telephone Laboratories, Murray Hill, N. J.
Graziano, V., 1220 N. East Ave., Oak Park, Ill.
Green, D. W., R.F.D. 2, Easton, Pa.
Green, E. H., Department of Physics, Brooklyn College, Brooklyn 10, N. Y.
Green, S. S., 2629—19 Ave., S., Minneapolis 7, Minn.
Green, W., 59-11 Queens Blvd., Woodside, L. I., N. Y.
Greenwood, D. T., 2917 Sycamore Ave., La Crescenta, Calif.
Gregg, D. P., Southwestern Industrial Electric Co., 2831 Post Oak Rd., Box 15038, Houston 19, Tex.
Gregory, R. M., 1360 High St., Oroville, Calif.
Greig, A. W., 13 Newton Ave., Halifax, N. S., Canada
Griffing, W. W., 1379 Webster St., Elmont, L. I., N. Y.
Griffith, W. A., 53 Ashwood Ave., Whitesboro, N. Y.
Grigg, R. W., 740 S. Olive St., Los Angeles 55, Calif.
Gross, F. A., 612 S. Westmoreland Ave., Los Angeles 5, Calif.
Guia-Monasterio, A. E., 5a Av. y 8a Calle Qta., Los Guia Caracas, Los Palos Grandes, Venezuela
Gunn, L. W., 712 College St., Menlo Park, Calif.
Gunning, W. F., 3538 Greenwood Ave., Los Angeles 66, Calif.
Gutcheon, W. Y., 244A S. Doheny Dr., Beverly Hills, Calif.
Guttwein, G. K., 226 Union Ave., Long Branch, N. J.
Hackley, G. E., 133 Angela Dr., Los Altos, Calif.
Haertig, M. M., General Electric Co., 570 Lexington Ave., New York 22, N. Y.
Haines, B. P., Philco Corp., C & Tioga Sts., Ext. 5778, Philadelphia 34, Pa.
Haines, J. H., 340 E. Olney Ave., Philadelphia 20, Pa.
Hale, C. R., 595 E. Colorado St., Pasadena 1, Calif.
Halina, J. W. O., 1924 Arbor Ave., Belmont, Calif.
Hall, G. O., 2309 Parkwood, Ann Arbor, Mich.
Hall, H. E., 6221 Carew St., Bellaire, Tex.
Hall, J. D., 8 Framer La., Wellesley Hills, Mass.
Hall, T. D., 1244 St. Charles St., Alameda, Calif.
Hallmark, G. D., 1106 Milner St., College Station, Tex.
Ham, N. C., 116 N. 29 Pl., Phoenix, Ariz.
Hamer, H., 19 N. Locust Ave., Long Branch, N. J.
Hamilton, R. E., Jr., 31396 Hathaway, Liavonia, Mich.

(Continued on page 92A)

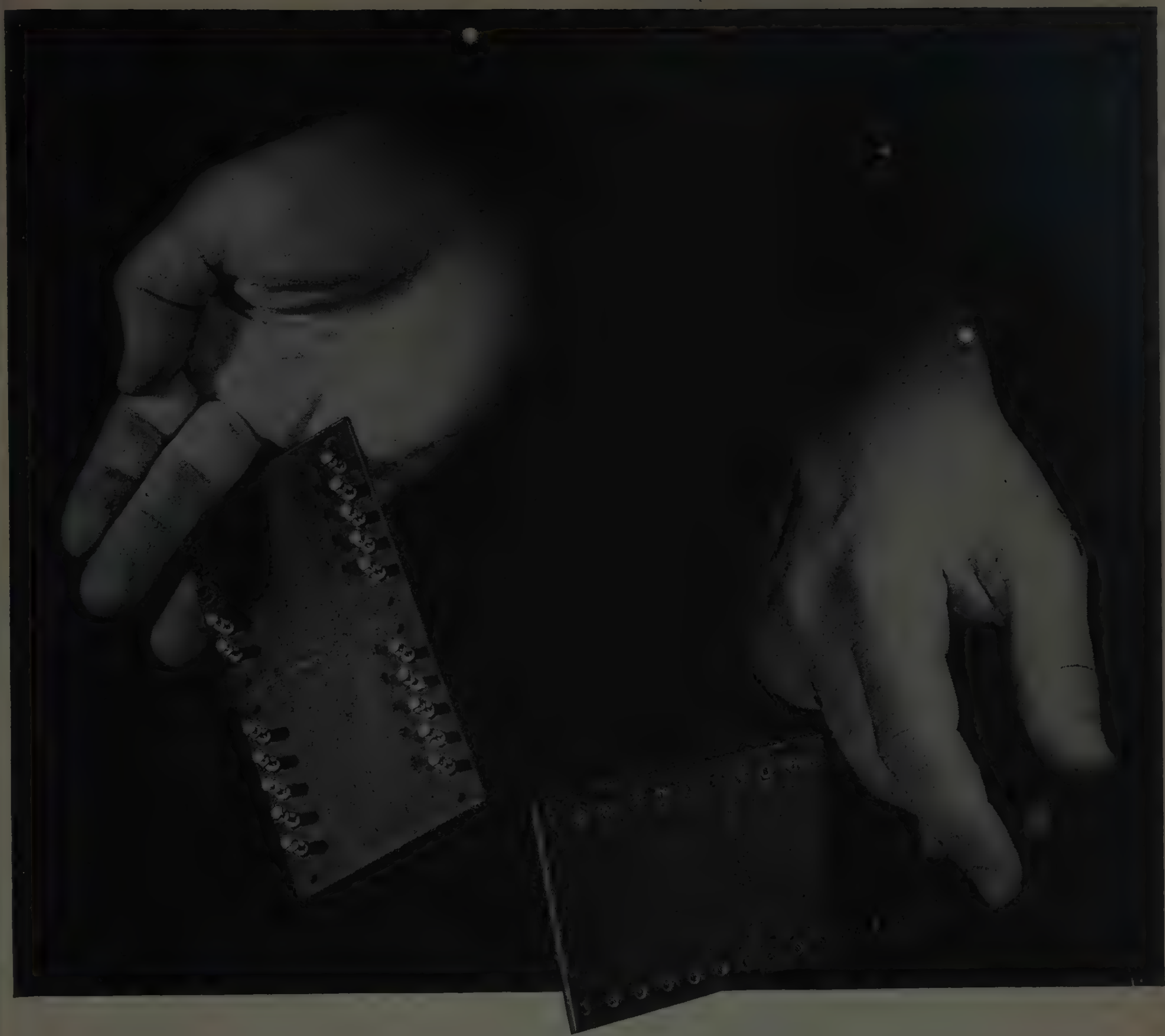

No cracks, please

You'll find no radial cracks in C.T.C. terminal boards, or "cracked" rivet shanks on terminals. And there's a good reason for this.

Our swaging machines use tools that we designed ourselves in order to prevent just such damage. Terminals are fastened securely — *and carefully*. You benefit from a board that has no "weak spots" — that can give you the service you have a right to expect. And, of course, you also benefit from all the other quality control details that enable us to offer our customers *guaranteed* components — custom or standard. Coatings are smoothly applied — no wrinkles, no heavy deposits. C.T.C. terminals are made from certified stock that is free from defects. And the terminals themselves are guaranteed, even to the thickness of the coatings.

This C.T.C. quality control is given to all C.T.C. products including insulated terminals, coil forms, coils, swagers, terminals and capacitors. For all specifications and prices, write to Cambridge Thermionic Corporation, 456 Concord Avenue, Cambridge 38, Mass. West Coast manufacturers contact: E. V. Roberts, 5068 West Washington Blvd., Los Angeles 16 and 988 Market St., San Francisco, California.

Terminal Board Data. C.T.C. makes both standard boards and to your own specifications. Standard boards in cotton fabric phenolic, nylon phenolic or grade L-5 silicone impregnated ceramic. Custom made in cloth, paper phenolic, melamine, epoxy or silicone fibreglas laminates, imprinted as required and lacquered or varnished to specifications MIL-V-173 and JAN-T-152.

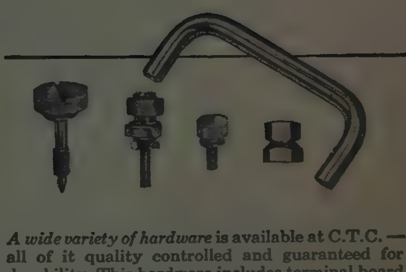

A wide variety of hardware is available at C.T.C. — all of it quality controlled and guaranteed for durability. This hardware includes terminal board brackets, standoff mounts, spacers, tube clamps, panel screws, thumb screws, dial locks, shaft locks, handles and handle ferrules.

See us at Booth 162 at WESCON

CTC

CAMBRIDGE THERMIONIC CORPORATION

makers of guaranteed electronic components, custom or standard

01A

IRE Membership

(Continued from page 90A)

Hammer, H., 110 E. 177 St., New York 53, N. Y.
Hanauer, S. H., 111 Tomlinson Rd., Oak Ridge, Tenn.
Hand, B. P., 3925 El Cerrito Rd., Palo Alto, Calif.
Hannell, F. D., 22 Parkway Dr., Whitesboro, N. Y.
Happell, G. E., 354 S. Grant St., W. Lafayette, Ind.
Harrington, D. C., 2508-B—36 St., Los Alamos, N. Mex.
Harrington, J. V., 3 North St., Lexington, Mass.
Harris, D. L., 560 King St., W., Toronto, Ont., Canada
Harris, E. F., 4729 Farwell, Lincolnwood, Chicago 30, Ill.
Harris, H., 10 Hewett Rd., Rockville Centre, L. I., N. Y.
Harrison, R. I., 1820 Phelan Pl., New York 53, N. Y.
Hartig, D. E., 589½ N. Mentor, Pasadena, Calif.
Hartke, D. C., 11917 Los Arboles, Sunnyvale, Calif.
Harvey, D. M., Air Exchange, OAA, US Navy 100, FPO, New York, N. Y.
Hatch, M. M., 4440 Waldo Ave., New York 71, N. Y.
Hatfield, P. E., 752 Stewart Ave., Evansville 15, Ind.
Hathaway, J. C., Collins Radio Co., 2700 W. Olive Ave., Burbank, Calif.
Hauptschein, A., 1995 Sedgwick Ave., New York 53, N. Y.
Hausman, A. H., 7405—16 Pl., Hyattsville, Md.
Hawk, W. H., 59 Hyde Rd., Bloomfield, N. J.
Hayes, B., 3782B Arizona, Los Alamos, N. Mex.
Hayes, M. H., Jr., 4 Terry Ave., Binghamton, N. Y.
Hazeltine, A. V., 316 Old Forest Rd., Carroll Park, Philadelphia 31, Pa.
Heaton, R. G., 14 Barnesdale Rd., Natick, Mass.
Hedge, L. B., 6219 Massachusetts Ave., N.W., Washington 16, D. C.
Heidgen, B., Jr., c/o 501 Tac. Cont. GP., APO 65, c/o Postmaster, New York, N. Y.
Heintz, R. M., Jr., 601 University Ave., Los Altos, Calif.
Heiser, W. H., 52 Elmwood Dr., E. Paterson, N. J.
Heller, S., 12 Oakway, Scarsdale, N. Y.
Helterline, L. L., Jr., Sorensen & Co., Inc., 375 Fairfield Ave., Stamford, Conn.
Hensel, M. L., 20 Midland Ter., Summit, N. J.
Heritage, J. L., 1125 Moana Dr., San Diego 7, Calif.
Hershler, A., 139-15—28 Rd., Flushing, L. I., N. Y.
Herst, R. J., 5639 N. Talman Ave., Chicago 45, Ill.
Hesselberth, W. M., 1706 Ravinia Rd., W. Lafayette, Ind.
Hessler, W. G., Jr., 111 N. Kensington, La Grange, Ill.
Hetlinger, F. J., 3123 Yearling St., Long Beach 11, Calif.
Hibbert, J. J., Bell Telephone Laboratories, Whippany, N. J.
Hicks, E. P., 5 Wilton St., Burlington, Ont., Canada
Higa, K., 3488 Alani Dr., Honolulu 17, T. H.
Hill, F. E., 110 Englewood Ave., Detroit 2, Mich.
Hillman, P. L., 15 Ridgeland Rd., Yonkers, N. Y.
Hills, E. G., Hills Engineering Co., Box 9, Des Plaines, Ill.
Hines, J. N., 494 Blenheim Rd., Columbus 14, Ohio
Hobbs, N. M., Northern Electric Co., Ltd., Box 6124, Montreal, Que., Canada
Hoberg, G. G., Woodside Rd., Berwyn, Pa.
Hoeflich, A. F., 626—16 Ave., San Francisco 18, Calif.

(Continued on page 94A)

Membership

(Continued from page 92A)

Hoepfner, K. B., 107 Rambling Way, Springfield, Pa.
Hoffman, P. F., 5746 N. Argyle Ave., Milwaukee 9, Wis.
Hoffman, R. R., Jr., 2714 Bainbridge Ave., New York 58, N. Y.
Hogan, H. A., 1022 N. 68 St., Milwaukee 13, Wis.
Hollandbeck, R. F., Westinghouse Research Laboratory, Ardmore Blvd., E. Pittsburgh, Pa.
Hollander, A. G., II, 8552 N.E. Eighth Ct., Miami, Fla.
Hollis, R. H., Box 475, Poulsbo, Wash.
Holmes, D. W., 327—37 St., Cedar Rapids, Iowa
Holmes, D. D., 13 Dorann Ave., Princeton, N. J.
Holmes, W. R., 1680 Monte Vista, Pasadena 4, Calif.
Holt, A. W., 2202 Richland Pl., Silver Spring, Md.
Hom, W. R., 5624 Woodmont Ave., Baltimore 12, Md.
Hommes, H. E., 1019 S. Sixth St., St. Charles, Mo.
Honea, L. W., Box 25, Puunene, Maui, T. H.
Honeiser, V. P., 607 Freeland Ave., Paramus, N. J.
Horak, R. J., 18 Mercer Dr., Brookside, Newark, Del.
Horn, H. T., 4205 W. Armour, Seattle 99, Wash.
Horn, R. H., 224 W. Birch St., Oxnard, Calif.
Horton, D. K., 2312 Carwile Dr., Alhambra, Calif.
Horvath, C., 15 Iby St., S. Burlington, Vt.
Hough, H. O., Oxbow Rd., S. Lincoln, Mass.
Houlihan, R. P., Main St., E. Brookfield, Mass.
Houston, R. W., Chief Engineer, FEN Kyushu, 8213th AU, APO 929, San Francisco, Calif.
Howery, R. W., 106 W. Oak Ave., Moorestown, N. J.
Howitt, G., 212 Voorhis Ave., River Edge, N. J.
Huffman, D. A., 100 Memorial Dr., Apt. 2-2B, Cambridge 42, Mass.
Hughes, J. G., 1441 Crown St., Wantagh, L. I., N. Y.
Hughes, W. L., Electrical Engineering Department, Iowa State College, Ames, Iowa
Hungerford, R. S., 904 S. Wisner, Jackson, Mich.
Hunt, D. F., 39 Remsen St., Apt. 1E, Brooklyn 1, N. Y.
Huntington, W. J., Jr., 1 New Hampshire Ave., Nashua, N. H.
Hurley, R. B., 1629 Thackery St., W. Covina, Calif.
Huskey, H. D., Department of Mathematics, University of California, Berkeley 4, Calif.
Huyett, W. I., 1415 Cleveland Ave., Wyomissing, Pa.
Hylkema, C. G., 1217 El Vago, La Canada, Calif.
Ikerd, H. M., 4652 Dawes St., San Diego 9, Calif.
Ingalls, D., 10 Kimball Cir., Westfield, N. J.
Ingersoll, E. R., 1420 E. Chestnut St., Whittier, Calif.
Ingram, J. H., 2708 Costa Mesa, Dallas, Tex.
Irelan, H. F., 216 S. Aldine, Elgin, Ill.
Irick, J., Lloyd Harbor Hills, R.F.D. 3, Huntington, L. I., N. Y.
Irwin, C. B., Jr., 9919 Bowman Blvd., Dallas, Texas
Jackson, B. B., 7885 Croydon Ave., Los Angeles 45, Calif.
Jackson, S. R., 126 Whitman Rd., Waltham 54, Mass.
Jackson, W., Jr., Standord Oil Co., 2127 Cornell Rd., Cleveland 6, Ohio
Jacob, F., 2116 Kalorama Rd., Washington, D. C.
Jacobi, W. J., 206 Via Alameda, Redondo Beach, Calif.
Jacobs, H., Jr., 60 Paul Revere Rd., Lexington 73, Mass.

(Continued on page 100A)

PROCEEDINGS OF THE IRE

Published Monthly by

The Institute of Radio Engineers, Inc.

VOLUME 43 — *August, 1955* — NUMBER 8

CONTENTS

WESCON

JOSEPH M. PETTIT,

DIRECTOR OF REGION SEVEN

Among the current alphabetical combinations, which by now must number in the thousands, the particular letters appearing in the title above should by this time be familiar to most members of the IRE as the abbreviation for Western Electronic Show and Convention. On the premise, however, that the several thousand new IRE members each year create perennially a new audience, this editorial will tell anew the story of WESCON.

The primary function of the IRE has always been the exchange of technical information, by both the written and the spoken word. The spoken word, in the form of convention papers, reaches full tide every March, of course, at the National Convention in New York, the world's largest technical convention. But did you know that WESCON is the *second* largest IRE convention?

WESCON last year had a convention registration of 2,400, together with an attendance at the apparatus exhibit of 24,000. This year the 570 exhibit spaces were sold out far in advance, and there are enough excellent technical papers to require a schedule of 5 concurrent sessions for a 3-day period.

That is all very well, you may say, but bigness is not a virtue in itself. In this case, however, bigness can serve a useful purpose to you as an IRE member. As a convention goer you will find that WESCON is a truly broad-gage, general-purpose convention, offering a wide range of technical papers, together with a really complete manufacturers' exhibit. Not only do you hear newsworthy papers emerging from the extensive research and development enterprises in the West, but an increasing number of Eastern authors are finding WESCON a highly suitable platform for announcing new progress to the technical world.

As a convention author, you will find your paper in good company, heard by an ample and receptive audience in well equipped meeting rooms. Finally, a publication channel is awaiting in the Professional Group *Transactions*, which receive financial help from WESCON in order to publish the papers presented at the convention.

As an exhibitor you will be mostly interested in the attendance figures and their classified breakdown, all of which are available upon inquiry. In particular you will find that there is a large segment of the electronics industry for whom this is the only convenient annual trade show.

The development of this large segment of the electronics industry, which is now located in the Far West, is amply illustrated by the phenomenal post-war expansion of IRE membership in this region. From the earliest days the IRE has been centered primarily in the East; it was not until 1940 that a President was elected from west of the Atlantic Seaboard states. In 1955, by way of contrast, Region 7, comprising the westernmost states, became the home of over 7,000 members, a greater number than the total IRE membership in any year prior to 1942. Five members of the 1955 Board of Directors come from this Region.

Individual Sections provide further illustration. For example, the Phoenix Section has increased 40 per cent each year for two years. At the end of 1954 the Los Angeles Section had 3,300 members, close behind New York, still the largest Section. Over the last two years Los Angeles has increased by over 1,000 members, a greater increase than most Sections have for a total membership. With 3 Subsections and 14 Professional Group Chapters, Los Angeles provided an outstanding total of 19 Section meetings and 41 Chapter meetings during 1954.

The San Francisco Section also has several Professional Group Chapters together with two Subsections, of which Palo Alto provides another good example of electronics growth in the West. The Palo Alto Subsection started in 1951 with 250 members, and now has over 600. Much of the electronics work in the West is of an advanced

nature, as illustrated by the technical capacities of the people in the field; for instance, there are more than twice the number of IRE Fellows in Palo Alto than the national average on a per capita basis. The West has a major portion of national activity in the development of high performance aircraft, missile systems, atomic weapons, measuring instruments, and microwave tubes, all of which require the greatest technical and scientific skill. There is also, of course, a substantial broadcast and communication industry, together with consumer service to the expanding population, and well established manufacturers of radio and television receivers. Education plays an important role also, with several first class universities in the area, some of which have attracted industrial research and development.

The history of WESCON is interesting, but first consider the present pattern. WESCON alternates yearly between Los Angeles and San Francisco. Last year in Los Angeles the hotel headquarters and the location of the technical sessions was the commodius Hotel Ambassador on Wilshire Boulevard. The size of the technical exhibit necessitated housing it in the nearby Pan Pacific Auditorium, with free bus service to the Ambassador. This year in San Francisco the hotel headquarters will be high atop historic Nob Hill at the well known Fairmont Hotel. Free busses will take the conventioners to the Civic Auditorium (and the Merchandise Mart across the street) where, in one compact location, all of the technical papers will be delivered and where the equipment exhibits will be shown.

WESCON is traditionally held in August which, coming as it does in the vacation season, results in a substantial family attendance. As you read this during the summer, let me remind you that Los Angeles and San Francisco provide refuge from the humid days and nights east of the Rockies.

An event as big and enjoyable as WESCON is not produced in a single year. The organization of WESCON has gone through several phases, and it is not altogether obvious where its history began. In the year 1937, there was held in Spokane, Washington the first Pacific Coast IRE Convention, arranged as an adjunct to the Pacific AIEE meeting. The convention became a yearly event, convening in Portland, San Francisco, Los Angeles, and Seattle through 1941 when the war terminated the series. These pre-war affairs were primarily technical meetings with only incidental manufacturers' exhibits. Then during the war years there came into being a trade association known as the West Coast Electronic Manufacturers' Association (abbreviated WCEMA). This group includes, of course, many IRE members, but acting independently they decided to establish an annual trade show in the post-war period. In 1947 this show was held concurrently with the first postwar rejuvenation of the IRE Pacific Coast Convention. The two groups operated separately but cooperatively for several years alternating the meeting between Los Angeles and San Francisco. These cities were chosen to insure a large trade show attendance.

In the interests of better management, IRE and WCEMA got together on a contractual basis in 1951 to establish a new organization with continuity of administration, and carrying the name WESCON for the first time. The WESCON Board has represented equally the two organizations, and financial backing was guaranteed by both groups. On the IRE side, to establish the affair as a truly West Coast, regionally sponsored event, all the IRE Sections in Region 7 were asked to pledge a portion of their Section funds as part of the financial guarantee. In appreciation of this excess earnings from WESCON have been shared with all these Sections, and hence WESCON has furthered IRE affairs and electronics throughout the entire West. Actual management of IRE aspects of WESCON falls primarily upon the Los Angeles and San Francisco Sections, and hence they are now the official contracting group on the part of the IRE. And finally, in 1955, articles of incorporation are being drawn up which will give complete identity to WESCON.

May we in Region 7 invite you to attend WESCON soon!

Color Television Luminance Detail Rendition*

W. G. GIBSON†, ASSOCIATE MEMBER, IRE, AND A. C. SCHROEDER†, FELLOW, IRE

Summary—**The luminance detail rendition, obtained from a color television signal in which the high-frequency components of the luminance signal are formed in the same way as the lows, is not correct in two respects: (1) The luminance transition amplitude is nearly always reproduced with incorrect amplitude, and (2) the transition is in a dark surround. This paper explains the cause of these two defects and derives an expression for a luminance signal which is free of these defects, and which may be transmitted within the present FCC standards.**

Introduction

Various articles have been written concerning luminance variations at transitions in the color television system, the standards for which have now been adopted by the FCC.[1–3] The luminance signal now used does not accurately reproduce high-frequency luminance detail in colored portions of a picture. The object of this paper is to derive an expression for a luminance signal which will faithfully reproduce high-frequency luminance detail on a color television receiver. Fortunately, this luminance signal also improves detail rendition on a monochrome receiver. It is assumed that the reader is familiar with the general principles and formulations behind the present color television system. "Principles and Development of Color Television Systems," by G. H. Brown and D. G. C. Luck—(*RCA Review*, June, 1953), is an excellent article covering this background material.

The Standard Luminance Signal

The standard luminance signal is

$$\begin{aligned} E_Y' &= a_G E_G^{1/\gamma} + a_R E_R^{1/\gamma} + a_B E_B^{1/\gamma} \\ &= .59 E_G^{1/\gamma} + .30 E_R^{1/\gamma} + .11 E_B^{1/\gamma}; \end{aligned} \tag{1}$$

where E_G, E_R, and E_B are the three voltages representing the green, red and blue signals; $1/\gamma$ indicates that gamma correction has been applied; and a_G, a_R and a_B are the relative luminances of the standard primaries to the eye. The numerical values of the relative luminances have been normalized so that their sum is unity. Gamma has been assigned a system value of 2.2; however, for simplicity in deriving an exact expression for a luminance signal which will faithfully reproduce luminance transitions on a color receiver, a value of 2 will be used. Using a value of 2 for gamma does not yield any serious errors; and the measured gamma values of tri-color kinescopes vary from approximately 2.0 to 2.4.

In gray areas E_Y' yields the proper amount of high-frequency luminance detail. In colored areas, it yields either too much or too little high-frequency detail. The signal applied to a particular kinescope gun is the sum of the luminance signal and the color difference signal. On the blue gun, for example, the applied signal is

$$E_Y' + (E_B^{1/\gamma} - E_Y')_L = (E_B^{1/\gamma})_L + (E_Y')_H. \tag{2}$$

The subscripts L and H represent low and high frequencies, respectively. Low frequencies correspond to those which could be carried in the chrominance channel and high frequencies correspond to those which can only be carried in the luminance channel. The color-difference signal contains only low frequencies since it is transmitted in the narrow-band chrominance channel. Assume, for example, that $(E_Y')_H$ is due solely to a transition in the green channel of the pickup device. If the amplitude of $(E_B^{1/\gamma})_L$ is very small at the transition, $(E_Y')_H$ applied to the blue gun is compressed considerably by the square-law characteristic of the kinescope; or if $(E_B^{1/\gamma})_L$ is very large, $(E_Y')_H$ applied to the blue gun is expanded considerably. For only one low-frequency blue amplitude is $(E_Y')_H$ reproduced correctly in terms of blue light. This nonlinear characteristic causes two defects in the reproduction of luminance detail at a transition in colored areas: (1) the high-frequency components are usually reproduced in improper amounts, and (2) every transition is accompanied by a low-frequency darkening.

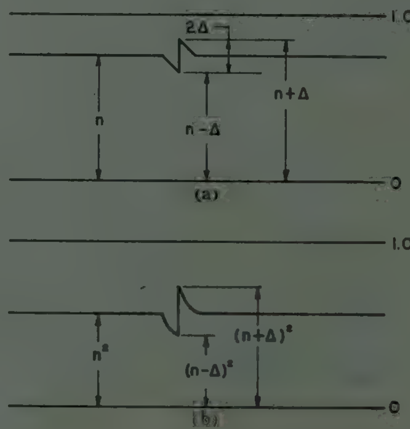

Fig. 1—(a) Signal applied to kinescope gun. (b) Light out.

Reference to Fig. 1 will aid in an understanding of this first defect. Fig. 1 shows a transition composed of a sharp edge superimposed on a nonvarying signal ap-

* Original manuscript received by the IRE, March 3, 1955; revised manuscript received, May 16, 1955.

† RCA Labs. Division, Princeton, New Jersey.

[1] P. W. Howells, "Transients in color television," Proc. IRE, vol. 42, pp. 212–220; January 1954.

[2] J. B. Chatten, "Transition effects in compatible color television," Proc. IRE, vol. 42, pp. 221–228; January 1954.

[3] D. C. Livingston, "Reproduction of luminance detail by NTSC color television systems," Proc. IRE, vol. 42, pp. 228–234; January, 1954.

plied to a kinescope gun. The original transition is assumed to have occurred in another primary. The amplitude of the sharp edge is 2Δ. The transition in light out is

$$(n+\Delta)^2 - (n-\Delta)^2 = 4\Delta n, \tag{3}$$

where n is the fractional height of the center of the transition applied to the kinescope. Note that Δ is not necessarily a small increment. The amplification of the high-frequency transition by the kinescope nonlinearity is

$$\frac{4\Delta n}{2\Delta} = 2n. \tag{4}$$

Therefore, in a three-gun display device which has high-frequency transitions superimposed upon low frequencies, each gun will display more than its share of detail if the low frequencies push the center of the transition more than halfway up on the kinescope transfer characteristic; and less than its share if the low frequencies do not push the transition at least halfway up on the kinescope transfer characteristic. Consequently, transitions where the average luminance is low will be underpeaked and transitions where the average luminance is high will be overpeaked.

This can be expressed analytically. The high-frequency transition as seen by the eye can be expressed as

$$a_R(Y_H')2n_R + a_G(Y_H')2n_G + a_B(Y_H')2n_B. \tag{5}$$

(Y_H') represents the transition. The n's represent the amplitude of the low-frequency components at the transition so that the $2n$'s represent the amplification of the transition due to the kinescope nonlinearities. The increase in high frequencies from original light to reproduced picture is (5) divided by Y_H,

$$2\left(\frac{Y_H'}{Y_H}\right)(a_Rn_R + a_Gn_G + a_Bn_B). \tag{6}$$

This expression can vary from zero to infinity. Usually, however, it does not deviate very far from unity. Table I lists some transitions and the ratios of reproduced luminance detail to initial luminance detail. They are grouped in pairs the arithmetic mean of which is unity. Note that the transition from red to cyan stands alone. This is a transition from a color to its complement. In using (6), it is assumed that kinescopes can deliver negative light. This assumption does not introduce any serious errors.

TABLE I

Transition	Reproduced detail / Original detail
Green to yellow	1.48
Magenta to blue	.52
Yellow to red	1.19
Blue to cyan	.81
Red to magenta	.71
Cyan to green	1.29
Black to blue	.11
White to yellow	1.89
Red to cyan	1.00

Reasoning that part of the information is carried by the chrominance channel which is narrowband and discards any high-frequency information fed to it, many people in the past have concluded that the end result is a soft picture in colored areas. This has been substantiated experimentally by observing transitions from black to a color. However, it has not been generally recognized that a transition from white to a particular color is overpeaked the same amount that a transition from black to the complement of the particular color is underpeaked.

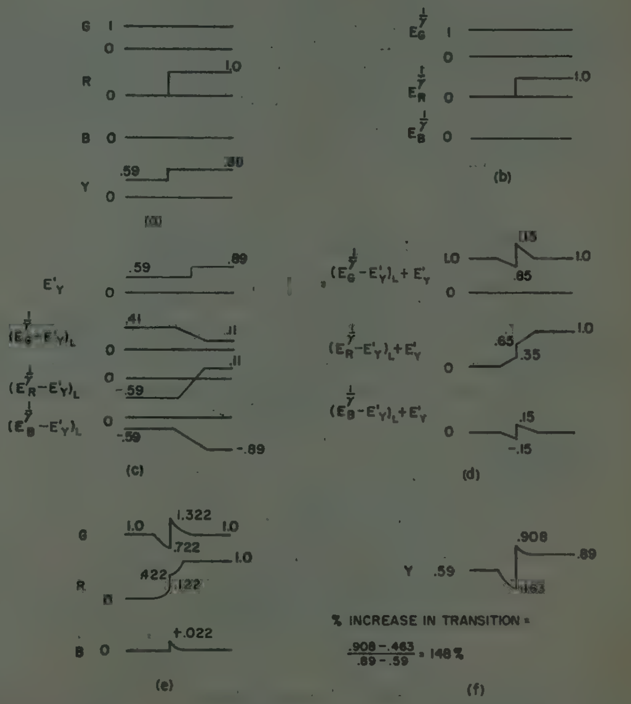

Fig. 2—(a) Light in. (b) After gamma correction. (c) Transmitted information. (d) Applied to kinescope gun. (e) Light out. (f) Luminance component of light out.

The second defect in the proper reproduction of high-frequency luminance detail is the fact that at every colored transition the entire luminance transition is in a dark surround. This can be briefly explained by reference to Fig. 2, which is a green to yellow transition. Fig. 2(a) shows an original scene transition. Fig. 2(b) shows the waveforms after gamma correction. Fig. 2(c) shows the transmitted information. The color-difference signal transitions have been drawn as sloping lines to indicate that only low frequencies are present. Fig. 2(d) shows the combined waveforms applied to the kinescope guns. Fig. 2(e) shows the light out. The straight sloping lines are now curved corresponding to

the kinescope square-law characteristics. Fig. 2(f) shows the output luminance information. Comparing the original Y in Fig. 2(a) to the reproduced Y in Fig. 2(f), note that the steep transition has been increased by 148 per cent (as Table I shows that it should be) but the center of the transition is at .69 rather than at .74; i.e., the transition is in too dark a surround.

It can be shown that a transmitted luminance signal of the form

$$E_{Y_t} = (E_Y')_L + \frac{(E_Y)_H}{2(E_Y')_L} \tag{7}$$

will yield the proper amount of high frequencies on a color receiver. However, as it does not correct for the darkening at a transition it is not important to show its derivation.

An Exact Luminance Signal

We shall now derive an expression for an E_{Y_T} (transmitted luminance signal) which will yield an exact reproduction at the receiver of E_Y as seen by the camera. The signal applied to any kinescope gun is the proper color difference signal plus the luminance signal. These are as follows:

$$\begin{aligned} &\text{Green Gun:} && (E_G^{1/\gamma} - E_Y')_L + E_{Y_T} \\ &\text{Red Gun:} && (E_R^{1/\gamma} - E_Y')_L + E_{Y_T} \\ &\text{Blue Gun:} && (E_B^{1/\gamma} - E_Y')_L + E_{Y_T}. \end{aligned} \tag{8}$$

The above quantities are squared by the square-law characteristic of the kinescope and added as their relative luminances to obtain the brightness signal in light.

$$\begin{aligned} E_Y = a_G\{ &[(E_G^{1/\gamma} - E_Y')_L]^2 \\ &+ 2[(E_G^{1/\gamma} - E_Y')_L]E_{Y_T} + E_{Y_T}^2\} \\ &+ a_R\{[(E_R^{1/\gamma} - E_Y')_L]^2 \\ &+ 2[(E_R^{1/\gamma} - E_Y')_L]E_{Y_T} + E_{Y_T}^2\} \\ &+ a_B\{[(E_B^{1/\gamma} - E_Y')_L]^2 \\ &+ 2[(E_B^{1/\gamma} - E_Y')_L]E_{Y_T} + E_{Y_T}^2\} \end{aligned} \tag{9}$$

$$\begin{aligned} E_Y = {} & a_G[(E_G^{1/\gamma} - E_Y')_L]^2 + a_R[(E_R^{1/\gamma} - E_Y')_L]^2 \\ &+ a_B[(E_B^{1/\gamma} - E_Y')_L]^2 \\ &+ 2[a_G(E_G^{1/\gamma})_L + a_R(E_R^{1/\gamma})_L \\ &+ a_B(E_B^{1/\gamma})_L - (E_Y')_L]E_{Y_T} \\ &+ (a_G + a_R + a_B)E_{Y_T}^2. \end{aligned} \tag{10}$$

The coefficient of $2E_{Y_T}$ is zero. The coefficient of $E_{Y_T}^2$ is unity. Rearranging and taking square roots,

$$\begin{aligned} E_{YT} = (E_Y - \{ &a_G[(E_G^{1/\gamma} - E_Y')_L]^2 + a_R[(E_R^{1/\gamma} - E_Y')_L]^2 \\ &+ a_B[(E_B^{1/\gamma} - E_Y')_L]^2\})^{1/2}. \end{aligned} \tag{11}$$

This expression yields the right amplitude transition and the transition is not surrounded by a darkened area. However, it does not take into account the different cut-off frequencies of E_I' and E_Q'. Eq. (11) may be rewritten, replacing the color difference signals by their E_I' and E_Q' equivalents,

$$\begin{aligned} E_G^{1/\gamma} - E_Y' &= -.280E_I' - .632E_Q' \\ E_R^{1/\gamma} - E_Y' &= .958E_I' + .622E_Q' \\ E_B^{1/\gamma} - E_Y' &= -1.106E_I' + 1.702E_Q'. \end{aligned} \tag{12}$$

This substitution yields

$$E_{Y_T} = (E_Y - [.456(E_I')^2 + .152E_I'E_Q' + .672(E_Q')^2])^{1/2}. \tag{13}$$

Another expression for (11) can be obtained by first writing the second part of the right hand side of (11) in terms of $E_R^{1/\gamma}$, $E_G^{1/\gamma}$, and $E_B^{1/\gamma}$. Next A_c (the amplitude of the subcarrier for a system employing circular chrominance)[4,5] is written in terms of $E_R^{1/\gamma}$, $E_G^{1/\gamma}$ and $E_B^{1/\gamma}$. This is a fairly long and tedious process and will not be done here. Comparing these two expressions where $\gamma = 2$ one can write,

$$.456(E_I')^2 + .152E_I'E_Q' + .672(E_Q')^2 = .529A_c^2 \tag{14}$$

so that

$$E_{Y_T} = (E_Y - .529A_c^2)^{1/2}. \tag{15}$$

Eqs. (13) and (15) give exact expressions for the luminance signal to be transmitted so that a color receiver will reproduce exactly the original luminance detail. A_c of (15) can be obtained by encoding E_I' and E_Q' at the proper angle and amplitudes. E_I' is multiplied by .925 and E_Q' is multiplied by 1.135. E_I' leads E_Q' by 82.1 degrees rather than 90 degrees. This yields the desired circular chrominance subcarrier. This is rectified to yield A_c.

It is, perhaps, worth while to restate the two assumptions that have been made in deriving (13) and (15). The first assumes a system gamma of 2 rather than 2.2 and the second assumes that kinescopes can deliver negative light. Neither of these assumptions causes serious errors.

Luminance Detail on a Monochrome Receiver

It is interesting to examine the effect of this new luminance signal on a monochrome receiver. If the monochrome receiver does not display the subcarrier and its sidebands, then the standard luminance signal reproduces detail faithfully. If the monochrome receiver displays the subcarrier and its sidebands, the subcarrier and its sidebands are rectified (or detected). Since the chrominance channel carries only low-frequency information, its rectified envelope will contain only low frequencies. The addition of these low frequencies, without accompanying high frequencies, to the picture results in distorted detail rendition.

E_{Y_T} of (15) does not correct for rectification due to signal swings beyond cutoff, but it does correct fairly

[4] W. F. Bailey, "The constant luminance principle in NTSC color television," Proc. IRE, vol. 42, pp. 60–66; January, 1954.

[5] A circular chominance subcarrier is one in which no luminance information is carried by the phase of the subcarrier. The phase angles of a color and the color-difference signal of the same color are identical for this type of subcarrier.

well for rectification due only to the tube curvature. This can be shown quite easily. The transmitted signal can be represented as

$$E_T = (E_Y - .529A_c^2)^{1/2} + A \cos(\omega t + \theta), \quad (16)$$

where E_T represents the entire transmitted signal and $A \cos(\omega t+\theta)$ represents the chrominance channel. A monochrome receiver squares this (approximately) to give light out as follows:

$$\text{Light out} = KE_T^2$$
$$= K\left[E_Y - .529A_c^2 + 2A \cos(\omega t + \theta)(E_Y - .529A_c^2)^{1/2} + \frac{A^2}{2} + \frac{A^2}{2}\cos(2\omega t + 2\theta)\right]. \quad (17)$$

The rectified component $A^2/2$ is approximately cancelled by $-.529A_c^2$, since the two A's differ by about only 10 per cent. The cosine terms remaining give the effect of looking through a screen. This new luminance signal does not change this effect appreciably one way or the other. In any event, this effect is not large. These cosine terms will cause additional rectification terms if they cause the signal to swing beyond kinescope cutoff.

This problem of dot rectification is, in general, not encountered on a color receiver. If dot rectification occurs on a color receiver, the amount of light from each gun is changed by different amounts, in general. This affects the hue and saturation of the picture and is quite noticeable. It is usually prevented by filtering out most of the subcarrier and its sidebands from the luminance signal before the luminance signal is applied to the kinescope guns.

On a narrow-band monochrome receiver which does not display the subcarrier and its sidebands, the light out is merely the approximate square of the luminance signal.

$$\text{Light out} = E_Y - .529A_c^2. \quad (18)$$

Some transmitted colored transitions will be underpeaked, some will be overpeaked; and colored transitions will be accompanied by a bright surround. In general, a narrow-band monochrome receiver fed with the luminance signal of (15) will show the inverse effects of a wide-band monochrome or color receiver being fed with the standard luminance signal.

Experimental Work

Fig. 3 is a block diagram of the means used in the laboratory to generate E_{Y_T}. Preliminary work only has been done so far in generating E_{Y_T} but this E_{Y_T} corrects in the direction that is expected of it. Additional experimental work and subjective tests need to be done before the signal can be completely evaluated.

Conclusions

If the luminance signal is formed so that the high-frequency components are formed in the same manner as the low, it does not yield an exact reproduction of high-frequency luminance detail at colored transitions as viewed on a color receiver. A luminance signal of the form

$$E_{Y_T} = (E_Y - .53A_c^2)^{1/2}$$

yields an exact reproduction of high-frequency luminance detail on a color receiver keeping in mind the two assumptions used in its derivation. This signal may be transmitted in accordance with the FCC Standards in view of Reference 21 of those Standards, which states: "Forming of the high-frequency portion of the monochrome signal in a different manner is permissible and may in fact be desirable in order to improve the sharpness on saturated colors." The operation of monochrome receivers varies from no need of this luminance signal (if the subcarrier and its sidebands are not displayed), to a point where this luminance signal corrects fairly well for tube curvature rectification, and to a point (due to subcarrier swings beyond kinescope cutoff) where this luminance signal does not supply enough correction. Therefore this luminance signal is as good a compromise as can be expected for high-frequency luminance detail reproduction on a monochrome receiver.

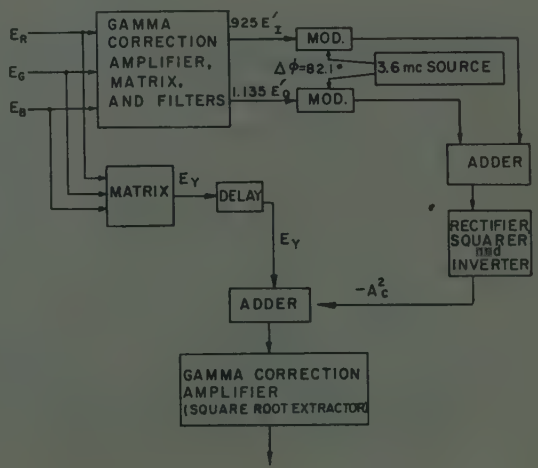

Fig. 3—E_{Y_T} generation.

Appendix

Numerical Calculation of a Transition

In order to compare the standard luminance signal (expressed as E_Y') and the new, derived luminance signal of this report (expressed as E_{Y_T}), a magenta to quarter-level green transition will be calculated at six different points: start and finish of the low-frequency chrominance transition (assuming E_I' and E_Q' to have equal bandwidths for simplicity of analysis), start and finish of the luminance transition (assumed infinitely faster than the chrominance transition for simplicity of analysis), and points halfway between the start (and finish) of the chrominance transition and the start (and finish) of the luminance transition. This will be done for both luminance signals.

The standard system using E_Y' will be considered first. The chosen green, red, and blue light values and the original scene luminance value that they generate are shown in Fig. 4(a).

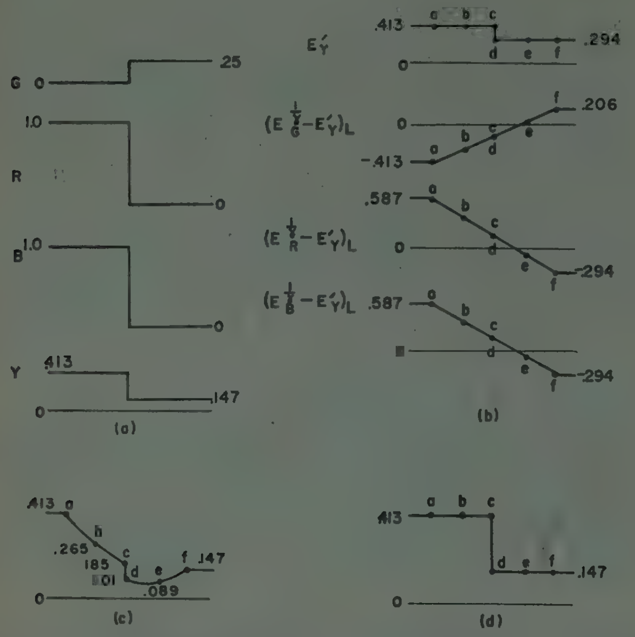

Fig. 4—(a) Original scene light values. (b) Transmitted information using E_Y'. (c) Reproduced luminance using E_Y'. (d) Reproduced luminance using E_{Y_T}.

After gamma correction, matrixing, and low pass filtering of chrominance components, the transmitted information is (remembering that gamma correction changes $E_G=.25$ to $E_G'=.50$) as shown in Fig. 4(b).

At the receiver, the luminance signal is added to each color difference signal and the sum is applied to the appropriate gun which squares the information and converts it into light. The three light signals are then added according to their relative luminances to obtain the reproduced luminance signal. These calculations are shown in Table II.

The reproduced luminance signal is shown in Fig. 4(c). The transition is in a dark surround and its peak-to-peak amplitude has been reduced to 31.6 per cent of its original value, which can be found by using the above calculated values or by using (6) as a check. Using the above calculated values,

$$\frac{.185-.101}{.413-.147}=\frac{.084}{.266}=.316.$$

and, using (6),

$$2\left(\frac{.413-.294}{.413-.147}\right)(.299\times .5+.587\times .25+.114\times .5)$$
$$=2\left(\frac{.119}{.266}\right).354=.316.$$

For the system using E_{Y_T}, the value of the luminance signal must be obtained first and then operations similar to those above can be carried out. The value of A_c^2 is obtained by the relations,

$$A_c^2=E_{I_c}'^2+E_{Q_c}'^2+2E_{I_c}'E_{Q_c}'\cos 82.1°$$
$$E_{I_c}'=.925E_I'=.680(E_R^{1/\gamma}-E_Y')_L-.249(E_B^{1/\gamma}-E_Y')_L$$
$$E_{Q_c}'=1.135E_Q'=.541(E_R^{1/\gamma}-E_Y')_L+.470(E_B^{1/\gamma}-E_Y')$$
$$2\cos 82.1°=.275,$$

so that

$$A_c^2=.462(E_R^{1/\gamma}-E_Y')_L^2-.338(E_R^{1/\gamma}-E_Y')_L(E_B^{1/\gamma}-E_Y')_L$$
$$+.062(E_B^{1/\gamma}-E_Y')_L^2$$
$$+.293(E_R^{1/\gamma}-E_Y')_L^2+.509(E_R^{1/\gamma}-E_Y')_L(E_B^{1/\gamma}-E_Y')_L$$
$$+.221(E_B^{1/\gamma}-E_Y')_L^2$$
$$+.101(E_R^{1/\gamma}-E_Y')_L^2-.037(E_R^{1/\gamma}-E_Y')_L(E_B^{1/\gamma}-E_Y')_L$$
$$+.088(E_R^{1/\gamma}-E_Y')_L(E_B^{1/\gamma}-E_Y')_L-.032(E_B^{1/\gamma}-E_Y')_L^2$$
$$A_c^2=.856(E_R^{1/\gamma}-E_Y')_L^2+.222(E_R^{1/\gamma}-E_Y')_L(E_B^{1/\gamma}-E_Y')_L$$
$$+.251(E_B^{1/\gamma}-E_Y')_L^2.$$

TABLE II

	Transmitted Information				Signals applied to kinescope guns		
	E_Y'	$(E_G^{1/\gamma}-E_Y')_L$	$(E_R^{1/\gamma}-E_Y')_L$	$(E_B^{1/\gamma}-E_Y')_L$	Green gun	Red gun	Blue gun
a	.413	−.413	.587	.587	.000	1.000	1.000
b	.413	−.258	.367	.367	.155	.780	.780
c	.413	−.104	.146	.146	.309	.559	.559
d	.294	−.104	.146	.146	.190	.440	.440
e	.294	.051	−.074	−.074	.345	.220	.220
f	.294	.206	−.294	−.294	.500	.000	.000

	Light signals			Relative luminances			Reproduced luminance
	G	R	B	.587G	.299R	.114B	Y
a	.000	1.000	1.000	.000	.299	.114	.413
b	.024	.608	.608	.014	.182	.069	.265
c	.095	.312	.312	.056	.093	.036	.185
d	.036	.194	.194	.021	.058	.022	.101
e	.119	.048	.048	.070	.014	.005	.089
f	.250	.000	.000	.147	.000	.000	.147

TABLE III

	$.856(E_R^{1/\gamma}-E_Y')_L^2$	$.222(E_R^{1/8}-E_y')_L(E_B^{1/8}-E_y')_L$	$.251(E_B^{1/\gamma}-E_Y')_L^2$	A_c^2	$.529A_c^2$	E_Y	$E_Y-.529A_c^2$	$E_{Y_T}=(E_Y-.529A_c^2)^{1/2}$
a	.295	.076	.086	.457	.242	.413	.171	.413
b	.115	.030	.034	.179	.095	.413	.318	.564
c	.018	.005	.005	.028	.015	.413	.398	.631
d	.018	.005	.005	.028	.015	.147	.132	.363
e	.005	.001	.001	.007	.004	.147	.143	.378
f	.074	.019	.022	.115	.061	.147	.086	.294

TABLE IV

	Transmitted information				Signals applied to kinescope guns		
	E_{Y_T}	$(E_G^{1/\gamma}-E_Y')_L$	$(E_R^{1/\gamma}-E_Y')_L$	$(E_B^{1/\gamma}-E_Y')_L$	G Gun	R Gun	B Gun
a	.413	−.413	.587	.587	.000	1.000	1.000
b	.564	−.258	.367	.367	.306	.931	.931
c	.631	−.104	.146	.146	.527	.777	.777
d	.363	−.104	.146	.146	.259	.509	.509
e	.378	.051	−.074	−.074	.429	.304	.304
f	.294	.206	−.294	−.294	.500	.000	.000

	Light signals			Relative luminances			Reproduced luminance
	G	R	B	$.587G$	$.299R$	$.114B$	Y
a	.000	1.000	1.000	.000	.299	.114	.413
b	.094	.867	.867	.055	.259	.099	.413
c	.278	.604	.604	.163	.181	.069	.413
d	.067	.259	.259	.039	.077	.030	.146
e	.184	.092	.092	.108	.028	.010	.146
f	.250	.000	.000	.147	.000	.000	.147

The calculation for the 6 points of the luminance signal is shown in Table III. Having obtained the luminance signal, E_{Y_T}, the calculation now proceeds as in the first case when E_Y' was used (see Table IV.)

Notice from the tabulated data that this reproduced luminance signal follows the original exactly except for small accumulated errors in the last place of the calculations.

The Design of Stagger-Tuned Double-Tuned Amplifiers for Arbitrarily Large Bandwidth*

M. M. McWHORTER†, ASSOCIATE, IRE, AND J. M. PETTIT†, FELLOW, IRE

Summary—**Double-tuned amplifier stages have a greater gain-bandwidth factor than single-tuned stages, and by stagger-tuning the double-tuned stages the gain-bandwidth factor is better preserved as stages are cascaded than if identical stages were used. This paper presents the results of a study which has yielded accurate design curves for the wide-band case permitting straightforward synthesis of maximally-flat staggered pairs and triples. The theory leading to the design curves is described in the Appendix.**

INTRODUCTION

NUMEROUS articles have appeared dealing with double-tuned circuits; however, many are restricted to bandwidths which are small compared to the center frequency, or do not take up the subject of nonidentical or "stagger-tuned," double-tuned stages which preserve gain-bandwidth product as stages are cascaded.[1] This article shows a method of exact design for maximally-flat amplifiers of arbitrarily large bandwidth, employing stagger-tuned, double-tuned stages. The results, both in gain-bandwidth product and selectivity, are considerably superior to those

* Original manuscript received by the IRE, April 26, 1955.
† Electronics Research Lab., Stanford University, Stanford, Calif.

[1] M. Dishal, "Exact design and analysis of double- and triple-tuned bandpass amplifiers," PROC. IRE, vol. 35, pp. 606–626; June, 1947.
M. Dishal, "Design of dissipative bandpass filters producing desired exact amplitude-frequency characteristics," PROC. IRE, vol. 37, pp. 1050–1069; September, 1949.
G. E. Valley and H. Wallman, "Vacuum Tube Amplifiers," MIT Radiation Lab. Ser., McGraw-Hill Book Co., Inc., New York, N.Y.; 1948.

obtained from either stagger-tuned, single-tuned circuits, or cascaded identical double-tuned stages. Using the graphs presented, the design is not particularly difficult.

The primary advantage of a double-tuned circuit using inductive coupling (Fig. 1) is a two-fold increase in either gain or bandwidth[2] as compared to a single-tuned circuit (Fig. 2) with similar interstage capacitances.

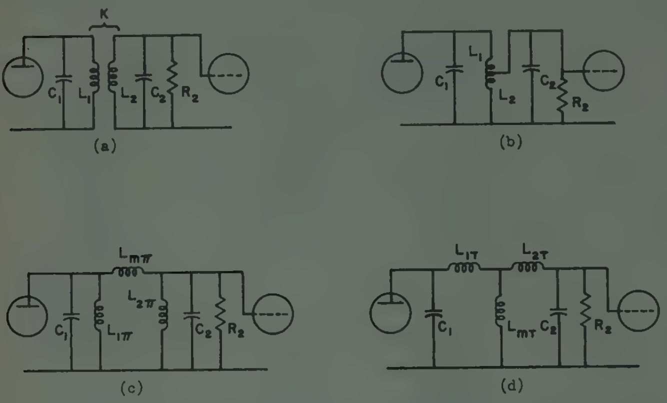

Fig. 1—Various configurations for the double-tuned amplifier interstage. Secondary loading only (R_2); primary Q very high.

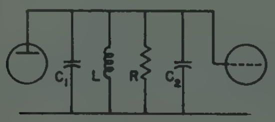

Fig. 2—Single-tuned interstage.

In the single-tuned circuit the product GB of stage gain and 3 db bandwidth (defined as the difference of the frequencies at which the gain is 70.7 per cent of the maximum or midband value) is given by:

$$GB = \frac{g_m}{2\pi(C_1 + C_2)}. \tag{1}$$

For the double-tuned case with loading on one side of the interstage only, the gain bandwidth product is:

$$GB = \frac{g_m}{4\pi\sqrt{C_1C_2}} \times 2. \tag{2}$$

Since $4\pi\sqrt{C_1C_2} \leqq 2\pi(C_1+C_2)$, the gain-bandwidth product of the double-tuned stage is always at least twice that of the single-tuned stage.

A further advantage of double-tuned circuits is better selectivity, i.e., a more nearly rectangular shape of frequency response. This means that the cascading of identical double-tuned stages causes less bandwidth shrinkage than in the case of single-tuned stages. The pass band shape with staggered, double-tuned stages approaches even more closely a rectangle, and groups of staggered stages may be cascaded with very little bandwidth shrinkage.

Quantitative comparison of amplifier interstage circuits is based on a figure of merit, the gain-bandwidth *factor*, *GBF*, which serves as a measure of the relative gain contribution of each stage in any given arrangement, and is defined as:

$$GBF = \frac{(\text{gain of } n \text{ amplifier stages})^{1/n}\,(\text{over-all bandwidth})}{(\text{gain bandwidth product of one single-tuned stage}}. \tag{3}$$

By definition, this is 1.0 for a single-tuned stage and for a double-tuned stage is:

$$GBF = 2\left[\frac{(C_1 + C_2)}{2\sqrt{C_1C_2}}\right] \cong 2 \quad (C_1 \cong C_2). \tag{4}$$

Because of bandwidth narrowing, the GBF diminishes as identical stages are cascaded. The advantage of stagger-tuning, with either single- or double-tuned stages, is that the over-all bandwidth and mean stage gain remain constant as the number of cascaded stages increases. Consequently, the *GBF* remains constant.

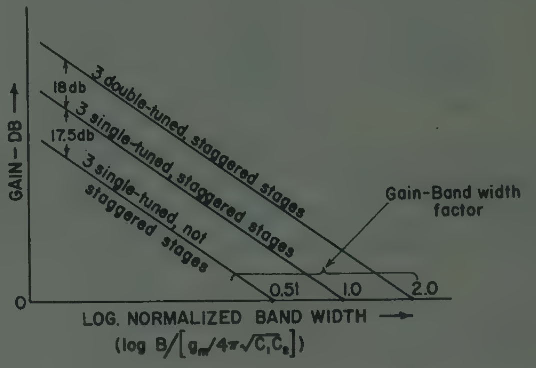

Fig. 3—Comparison of different types of three-stage amplifiers.

A graph which compares the relative merits of the particular case of a three-stage amplifier is shown in Fig. 3.[3] Here the nonstaggered, single-tuned amplifier is compared with the stagger-tuned, single-tuned amplifier and the stagger-tuned, double-tuned amplifier. It is seen that for a given set of tubes and interstage capacitances, the double-tuned amplifier gives 35.5 db more gain than the simplest amplifier for the same bandwidth, or almost four times the bandwidth for the same gain.

Stagger-tuning with double-tuned interstages involves, in general, nonidentical primary and secondary tunings from stage-to-stage, as well as nonidentical Q's. For bandwidths small compared to the center frequency, only the Q's need be different. This simplified case was first described by Wallman,[4] who named the design technique, "stagger damping." The initial determination of the required frequencies and Q's involves some

[2] The capacitance coupled case is not described because in a very wide-band amplifier the gain-bandwidth factor is considerably inferior to the inductively coupled case.

[3] This graph is similar to one for single-tuned stages in the reference: B. A. Wightman, "A Graphical Means for Determining the Number and Order (n) of n-uples in Stagger-Tuned Amplifier Design," National Research Council of Canada, Ottawa, Can.; December, 1951.

[4] Valley and Wallman, *op. cit.*, pp. 221–226.

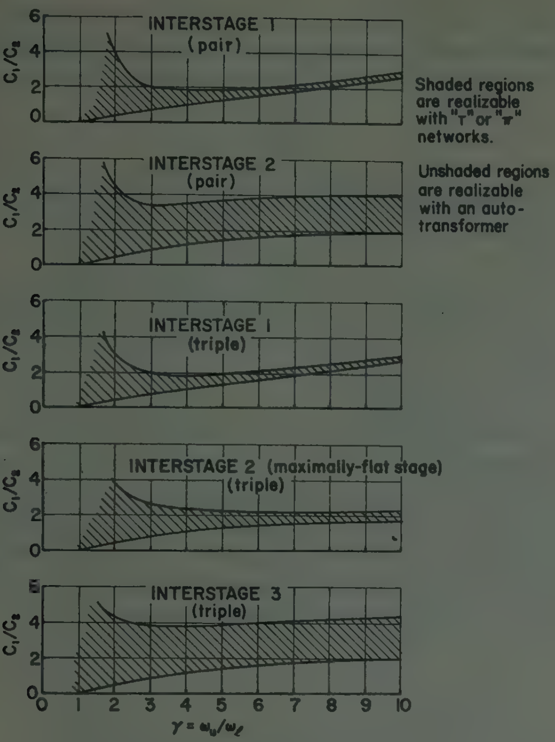

Fig. 4—Regions of physical realizability for the auto transformer and the "T" or "π" equivalents.

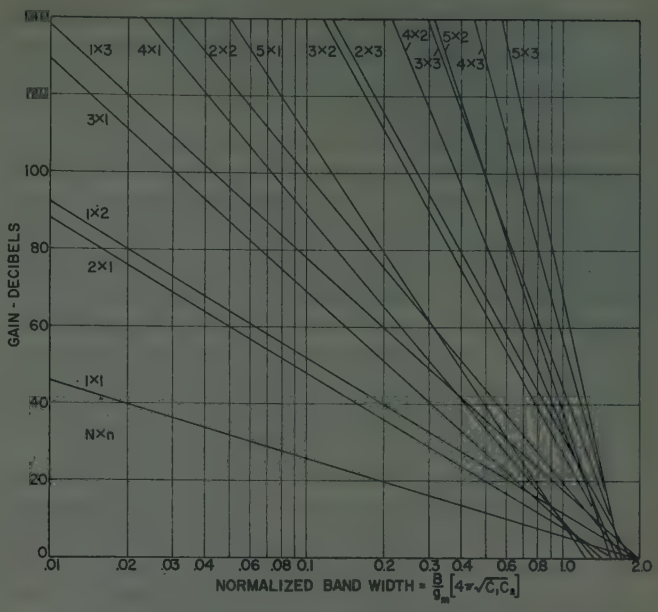

Fig. 5—Gain vs bandwidth for different amplifier configurations.

mathematical insight if an exact frequency response is to result. The derivation is described in the Appendix for those readers who may be interested. Fortunately, however, once this procedure has been carried through for the desired situations, in our case staggered *pairs* and *triples*, the results can be presented in simple graphical form (Figs. 8 to 15 inclusive) for use in circuit design without recourse to the mathematical derivation.

This article is restricted to staggered pairs and triples, because, as in the case of single-tuned pairs and triples, these represent the most widely usable compromises between performance and simplicity. Quadruples, quintuples, etc. give increasingly better selectivity and *GBF*, but with rapidly diminishing return for added complexity. Excessively high Q's are also often encountered.

The graphs are further restricted to the case of loading of the double-tuned circuit on one side only, as opposed, say, to equal primary and secondary Q's because one-sided loading gives the highest gain-bandwidth factor. The loading can be on either the primary or secondary side, but for high-frequency amplifiers the input conductance of pentode tubes constitutes a greater parasitic loading than does the high plate resistance on the primary side. In wide-band situations a loading resistor is added to the secondary to bring the Q to the necessary low value. The resulting secondary Q is usually so low that the primary Q can be considered infinite, without any practical consequences, in spite of the finite plate resistance.

One serious problem with double-tuned interstages is the attainment of the necessary coefficient of coupling concomitant with large bandwidth. The coupling coefficient exceeds 0.9 for $\gamma=5$ in one interstage. (γ is the bandwidth ratio, $\gamma=\omega_u\omega_l$ where ω_u and ω_l are the upper and lower band-edge frequencies respectively.) Such large coefficients cannot be attained with an air-core, two-winding transformer without excessive inter-winding capacitance. Two alternatives are useful: one is to utilize either the "π" or the "T" equivalent of the transformer [Figs. 1(c) and 1(d)]; the second is to utilize an auto-transformer [Fig. 1 (b)]. The two alternatives may not be used interchangeably because with a given capacitance ratio (C_1/C_2) only one alternative is physically realizable, i.e., has all positive inductances. The regions where each type of circuit can be used are shown in Fig. 4 as a function of C_1/C_2 and γ. In general, the auto-transformer is more attractive for large bandwidth ratios because the usual tubes have $C_1/C_2<1$. Also the windings for an autotransformer may be easily calculated and accurately wound.

Procedure

The design of an amplifier usually starts from the desired values of over-all gain, bandwidth, frequency of maximum gain, and perhaps the selectivity required. The necessary number (N) of groups of staggered stages (with n stages per group or n-uple) may be most easily found from the gain-bandwidth chart of Fig. 5. For this graph, which is similar to Fig. 3, the ordinate is normalized bandwidth, i.e., the bandwidth divided by a quantity $g_m/(4\pi\sqrt{C_1C_2})$ which is a figure of merit for the tube with its associated stray capacitances. The values of C_1 and C_2 must include all the wiring, socket and tube capacitances. They should be measured with the tubes in sockets on the amplifier chassis or a similar mock-up, and drawing normal plate current. The accurate determination of these capacitances is essential

to the design and construction of a staggered, double-tuned amplifier.[5] Knowing the desired normalized bandwidth and gain, an amplifier configuration producing the same or more gain can be chosen. For example, if a normalized bandwidth of 0.3 and a gain of 80 db are desired, reference to the graph in Fig. 5 shows either a 3×2 ($N=3$, $n=2$) or a 2×3 might be used. The 2×3 gives more gain, a squarer selectivity curve, but greater difficulty in construction than the 3×2; both require 6 tubes. Reference to Fig. 6 gives the *selectivity ratios*, a measure of the "skirt selectivity," for the two amplifiers as well as for other combinations of N and n. The selectivity ratio is defined as the ratio of the bandwidth at the points of $\frac{1}{2}$ gain to the bandwidth at the points of 10^{-3} midband gain (-6 and -60 db bandwidths referred to midband gain, respectively). For the previous case the 2×3 results in a selectivity ratio of 1.8 whereas the 3×2 gives a ratio of 1.9. It is interesting to note that six, synchronously-tuned, single-tuned stages would give the higher (and thus poorer) selectivity ratio of 5.8, showing the superior skirt selectivity of the double-tuned interstages.

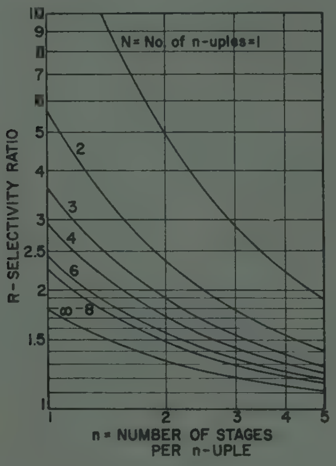

Fig. 6—Selectivity ratio as a function of N, the number of n-uples, and n, the number of stages per n-uple.

If better selectivity is necessary and is more important than economy of gain-bandwidth, then more stages may be used with added capacitance to maintain the stage gain at a value to give the desired total. Any arbitrary value of selectivity ratio cannot be obtained, however, because of the restriction that n be integral.

Knowing N and n, the bandwidth of the individual n-uple (group on n staggered stages) must be found. If N is greater than one, the bandwidth of each n-uple must be greater than the over-all bandwidth; i.e.,

$$\frac{B_{n\text{-uple}}}{B_{\text{over-all}}}=\sigma=\frac{1}{(2^{1/N}-1)^{1/4n}}\qquad N=\text{number of } n\text{-uples.}\qquad (5)$$

[5] The shape of the pass band is sensitive to small changes in tube capacitance. In a typical case a 10 per cent capacitance change can make the gain vary ±1 db from the maximally-flat curve. This effect may make tube selection for capacitance advisable when the shape of the frequency response is critical.

Table I tabulates this equation. The bandwidth of an n-uple is simply σ times the over-all bandwidth. From the bandwidth of the individual n-uple, there may be

TABLE I

VALUE OF σ FOR VARIOUS N AND n

n \ N	1	2	3	4	5	6
1	$\sigma=1.00$	1.25	1.40	1.50	1.61	1.69
2	1.00	1.12	1.18	1.22	1.27	1.30
3	1.00	1.08	1.12	1.15	1.17	1.19

found from Fig. 7 the value of γ, the bandwidth ratio, a parameter which has been found to be especially useful for wide-band analysis. The remainder of the necessary design values may be read directly from Figs. 8 to 15 on the opposite page, and page 928. (For $n=1$, the data for stage 2, Figs. 12 to 15 are used; for $n=2$, Figs. 8 to 11 are used; for $n=3$, Figs. 12 to 15 are used.)

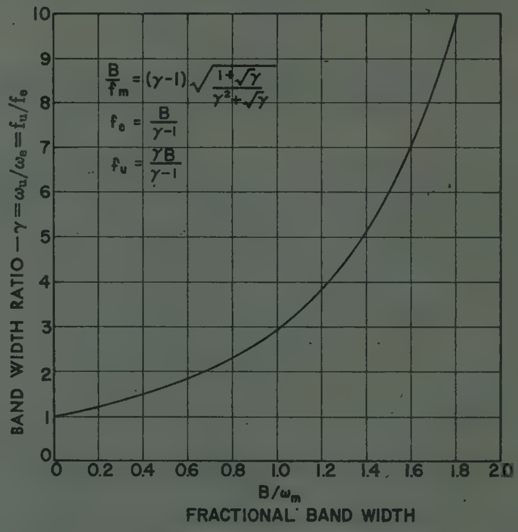

Fig. 7—Bandwidth ratio γ as a function of fractional bandwidth.

The procedure may be summarized:

1. Select the values of N and n from Figs. 5 and 6.
2. Find the value of $B_{n\text{-uple}}=(B_{\text{over-all}})\times\sigma$ (σ is given in Table I).
3. Find γ from $B_{n\text{-uple}}/f_m$ and Fig. 7 (f_m is the frequency of maximum gain or the band-center in narrow-band amplifiers, $\gamma<2$).
4. From the appropriate figures for the value of n chosen, read off ω_1/ω_m, ω_2/ω_m, K_r and Q_2 for each stage of the n-uple.
5. These values are for the transformer coupled circuit Fig.1(a) and (b). Transformation eqs. (6)–(9)[6]

[6] The "π" is somewhat more useful than the "T" equivalent since the latter requires two ungrounded inductors with relatively high stray capacitances to ground.

may be used if the "π" equivalent circuit is necessary:

$$L_{1\pi} = \frac{L_1 L_2 - M^2}{L_2 \pm M} \tag{6}$$

$$L_{2\pi} = \frac{L_1 L_2 - M^2}{L_1 \pm M} \tag{7}$$

$$L_{m\pi} = \frac{L_1 L_2 - M^2}{\mp M} \tag{8}$$

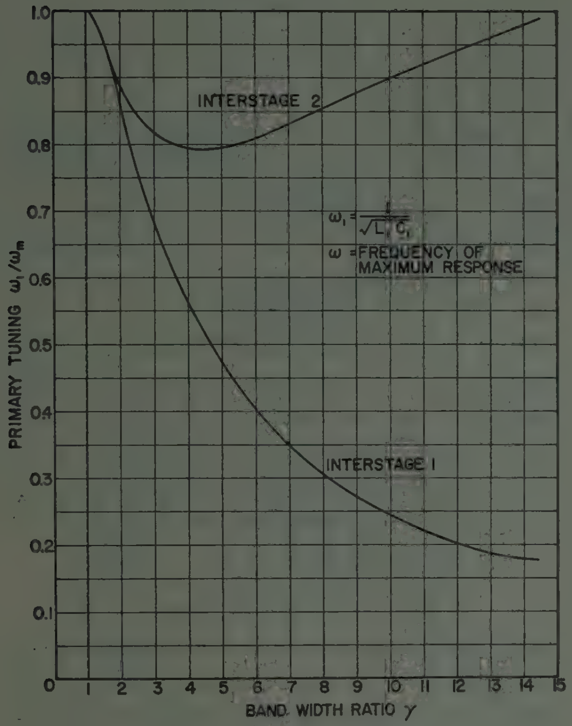

Fig. 8—Primary tuning ω_1/ω_m vs bandwidth ratio γ for a staggered double.

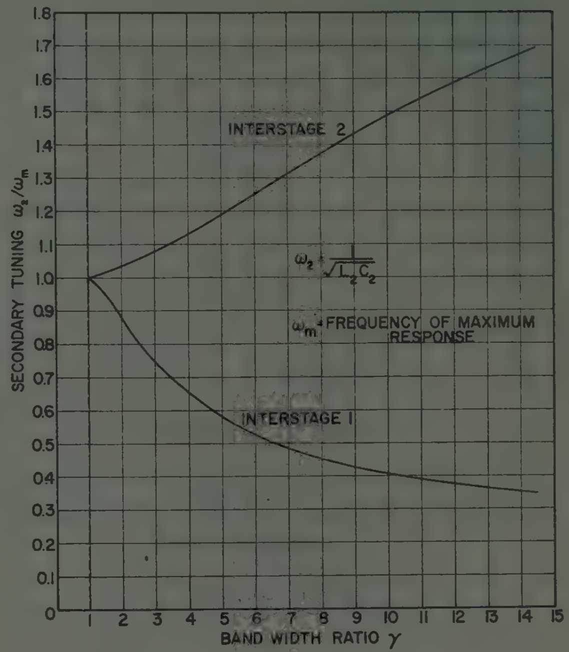

Fig. 9—Secondary tuning ω_2/ω_m vs bandwidth ratio γ for a staggered double.

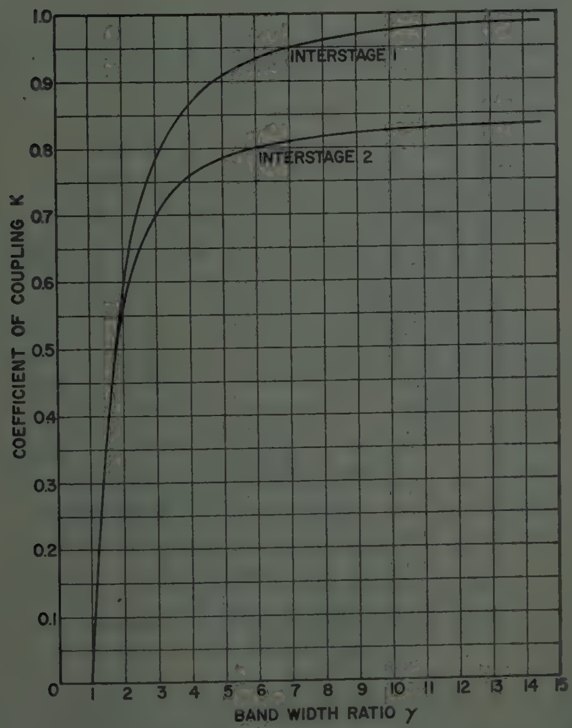

Fig. 10—Coefficient of coupling K vs bandwidth ratio γ for a staggered double.

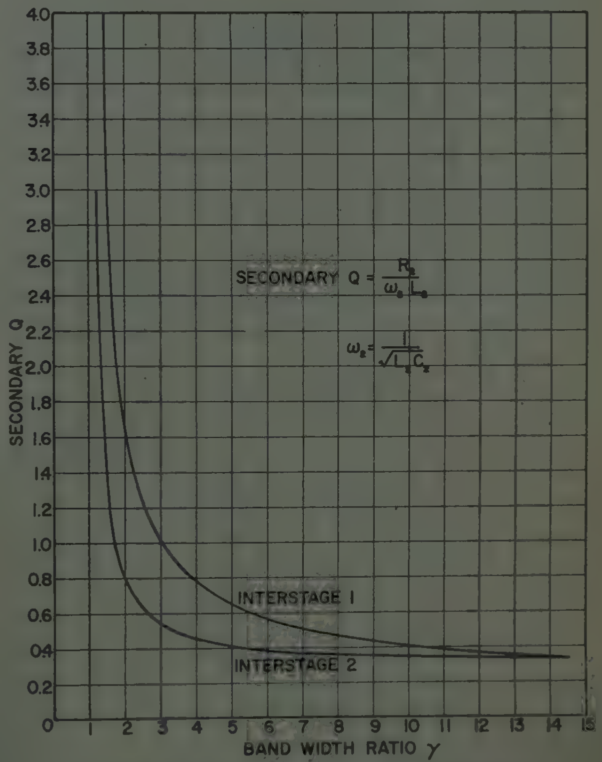

Fig. 11—Secondary Q vs bandwidth ratio γ for a staggered double.

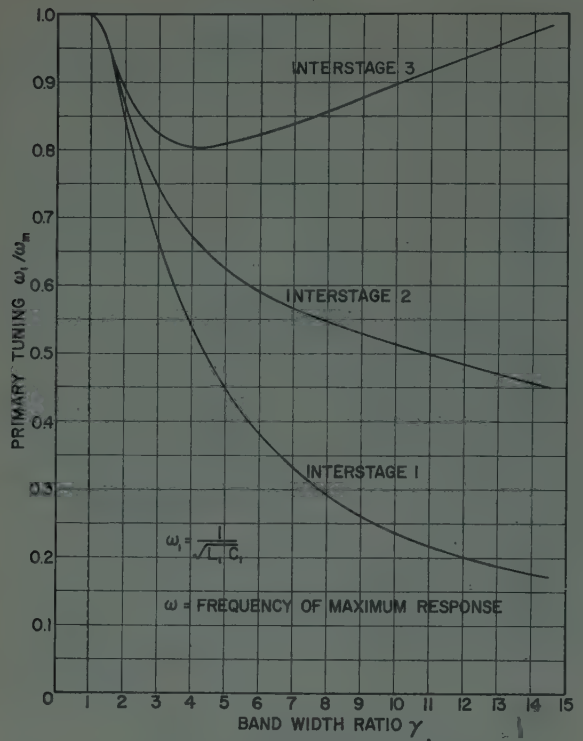

Fig. 12—Primary tuning ω_1/ω_m vs bandwidth ratio γ for a staggered triple.

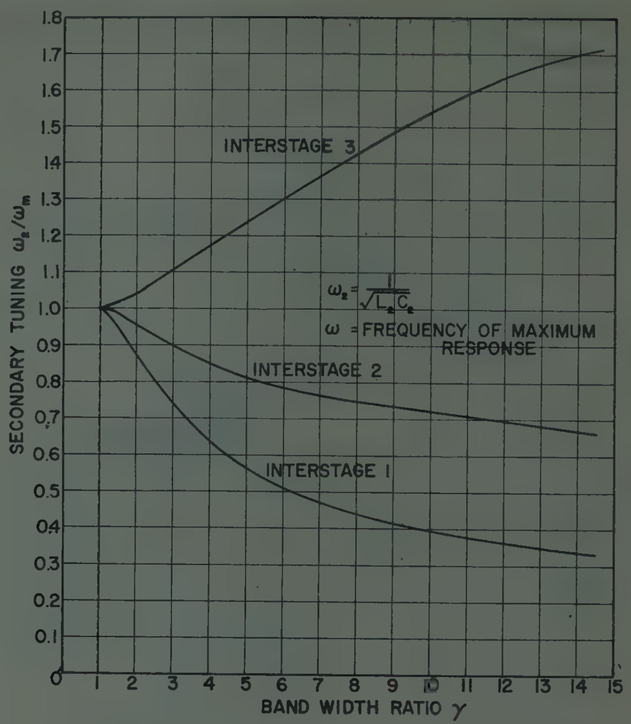

Fig. 13—Secondary tuning ω_2/ω_m vs bandwidth ratio γ for a staggered triple.

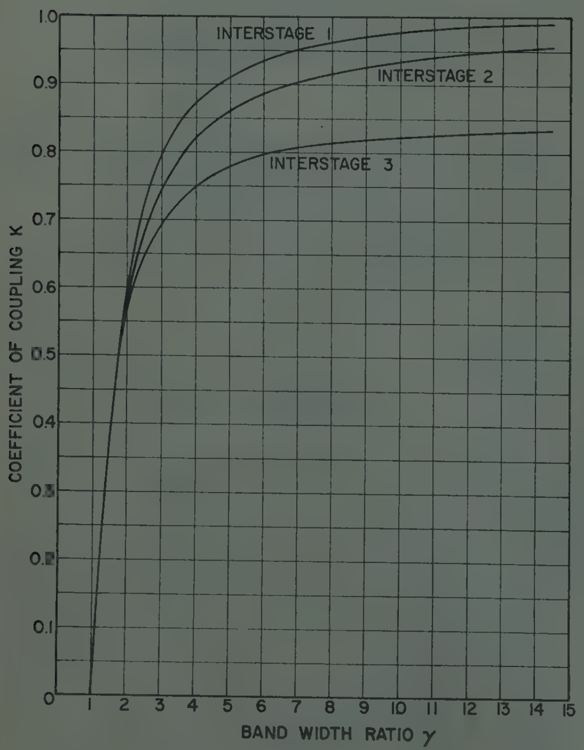

Fig. 14—Coefficient of coupling K vs bandwidth ratio γ for a staggered triple.

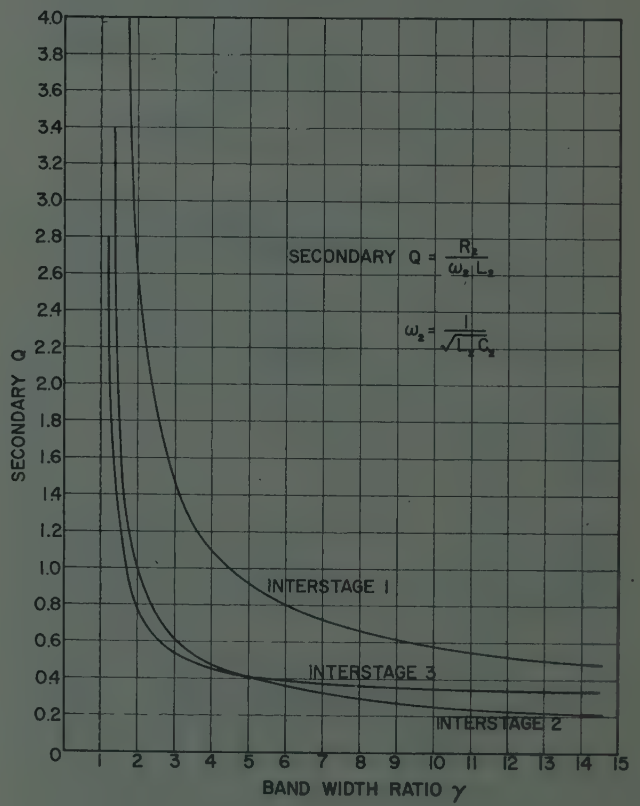

Fig. 15—Secondary Q vs bandwidth ratio γ for a staggered triple.

$$M = k\sqrt{L_1 L_2} \tag{9}$$

The above process yields all the element values necessary for the amplifier. The coils for the "π" equivalent circuit may be calculated from the usual inductance formulas. Care should be used in mounting to minimize unwanted coupling between coils. The coils for the two-winding transformer and the autotransformer may be calculated most easily from the curves of Edson.[7]

[7] W. A. Edson, "The single-layer solenoid as an rf transformer," Proc. IRE, vol. 43, pp. 932–936; August, 1955.

Example

To illustrate the design proedure, a two-stage amplifier was designed with band-edge frequencies of 10 and 30 mc and as much gain as possible with 6CB6 tubes. The first step was to measure C_{in} and C_{out}, with the tubes mounted in the amplifier and drawing normal plate current. These were found to be 10.2 and 3.9 $\mu\mu$f on the average. (Note the disparity with the published values of 6.3 and 1.9 $\mu\mu$f which do not include the socket, and are measured with the tube cold.) To each of these values a capacitance of 1.5 $\mu\mu$f was added to account for leads and coil capacitances.[8] The tuning frequencies, Q's and coefficients of coupling for $\gamma=3$ were obtained from the graphs, Figs. 8 to 12. These values and the element values are tabulated in Table II.

TABLE II

Stage 1	Stage 2
$\frac{\omega_1}{\omega_m}=0.678$	0.817
$\frac{\omega_2}{\omega_m}=0.74$	1.075
$k=0.79$	0.705
$Q_2=1.02$	0.55
$C_1=$ 5.4 $\mu\mu$f	5.4 $\mu\mu$f
$C_2=11.7$ $\mu\mu$f	11.7 $\mu\mu$f
$L_1=26.4$ μh	18.2 μh
$L_2=10.3$ μh	4.86 μh
$R_2=955$ ohms	354 ohms

Since the necessary coupling coefficients were 0.79 and 0.705, a two-winding transformer was impractical, but reference to Fig. 4 shows that an auto-transformer is possible. The transformers were calculated from Edson.[9] The resulting transformers were within 3 per cent of the design values as measured on a Q meter.

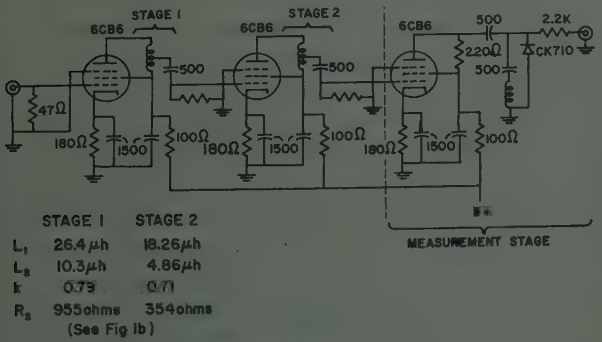

Fig. 16—Schematic diagram for an amplifier employing a staggered pair giving a 20-mc bandwidth centered at 20 mc.

These transformers and associated damping resistors were incorporated into the amplifier circuit (Fig. 16), giving the frequency response shown in Fig. 17, where the calculated response is shown for comparison. The gain per stage may be simply calculated as:

$$G=\frac{GB}{B}=\frac{g_m}{(2\pi\sqrt{C_1C_2})B}$$
$$=\frac{6100\times10^{-6}}{(2\pi)\sqrt{(11.7)(5.4)(10^{-24})}(2\times10^7)}=6.13\ (15.8\ \text{db}),\quad (10)$$

or 31.6 db for two stages. The measured gain was 31 db. It should be emphasized that these results were obtained by measuring the components only—no tuning was done on the assembled amplifier.

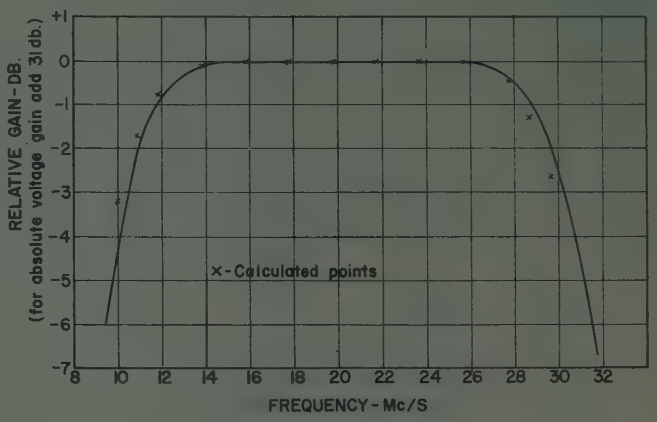

Fig. 17—Measured frequency response of double-tuned staggered pair.

Conclusion

The curves and methods presented make the design of wide-band, stagger-tuned, double-tuned amplifiers relatively simple and very straightforward. For wide-band applications this type of amplifier is greatly superior to either the staggered, single-tuned amplifier or a nonstaggered double-tuned amplifier. Indeed, to produce significant gain with bandwidths approaching the gain-bandwidth figure of the tubes available, the staggered double-tuned amplifier is the best available method of realizing a bandpass amplifier. Consequently, it is hoped that the design information presented herein will facilitate the production of amplifiers where either a minimum number of tubes must be used, or where the bandwidths required are large.

Appendix

The gain function of a double-tuned stage with secondary loading (Fig. 1) is:

$$G(s)=Z_2(s)g_m=\frac{g_mk\omega_1\omega_2}{(1-k^2)C_1C_2}$$
$$\left[\frac{s}{s^4+\frac{\omega_2}{Q_2}s^3+\frac{(\omega_1^2+\omega_2^2)}{1-k^2}s^2+\frac{\omega_1^2\omega_2}{Q_2(1-k^2)}s+\frac{\omega_1^2\omega_2^2}{1-k^2}}\right].\quad (11)$$

For several stages, the gain function becomes:

$$G(s)=G_1(s)\cdot G_2(s)\cdot G_3(s).$$

There are four poles and one zero per stage in this function, and in the case of interest in amplifier design the poles are complex, lying in the s-plane as shown for a

[8] The value of 1.5 $\mu\mu$f was obtained by measuring the capacitance of typical signal wiring in the amplifier and then adding the estimated distributed capacitance of the coils.

[9] Edson, *op. cit.*

single stage in Fig. 18. Since the gain function for cascaded stages is the product of the individual stage gain functions, the pole-zero diagram for the cascaded stages contains the poles and zeros from each separate stage. These poles are to be arranged so that the gain function, $|G(j\omega)|$, along the $j\omega$ axis has maximal flatness about the band-center frequency, $j\omega_0$; i.e., as many derivatives of $|G(j\omega)|$ with respect to ω are made equal to zero as possible within the limited freedom of the gain function. This is the maximally-flat condition which has been treated by Landon,[10] Wallman,[11] and others.

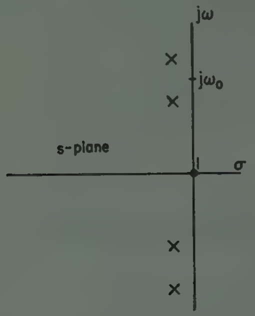

Fig. 18—Typical pole-zero diagram for a double-tuned interstage.

It is now well established that where the gain function has only poles and no zeros, maximal flatness is achieved by placing these poles with uniform spacing on a semicircle having a diameter equal to the desired 3 db bandwidth. An approximate way to synthesize a bandpass gain function is to translate the circular pole locus upwards in frequency so that the circle is centered at $j\omega_0$. This condition is implicit in all the standard formulas for narrow-band stagger-tuning. The "narrow band" situation is as though the upper cluster of poles in Fig. 18 were so far up the $j\omega$ axis that the existence of the zero at the origin and the lower cluster of poles could be ignored in determining the behavior of $|G(j\omega)|$ in the vicinity of $j\omega_0$. This is a reasonable procedure as may be seen by reference to the potential analogy wherein the poles and zeros are considered to be unit positive and negative line charges, respectively, and electrostatic potential along the $j\omega$ axis is proportional to the log $|G(j\omega)|$. In the "narrow band" case the zero at the origin and the cluster of poles on the $-j\omega$ axis are so far removed from the band of interest that the potential caused by them is practically constant across the band. Consequently, the *shape* of the pass band is almost entirely determined by the pole cluster adjacent to the pass band. However, in the general, or wide-band case, all the poles and zeros must be accounted for; consequently, the simple semicircular pole contour must be altered to yield maximal flatness. Trautman[12] has developed a conformal mapping function which transforms a situation like Fig. 18 into that of Fig. 19 where the upper and lower pole clusters of Fig. 18 now overlie each other and the zero of Fig. 18 has moved out to infinity. It is now possible to arrange the poles in the p-plane on a semicircle as in Fig. 20, and thus give in the p-plane a maximally-flat response centered at the origin, or in the analogy, a maximally-flat electrostatic potential. Since the potential is invariant in a conformal mapping, it is possible to transform the pole locations back to the s-plane, retaining the maximal flatness, but centered now, not at the origin, but at $s = \pm j\omega_0$, which is actually the transformed origin from the p-plane.[13]

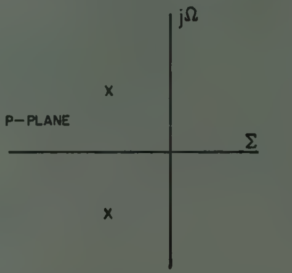

Fig. 19—The pole locations of Fig. 18 as transformed into the p-plane.

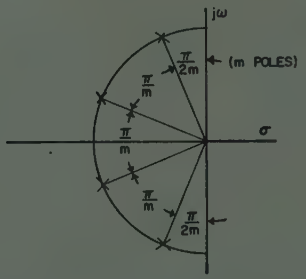

Fig. 20—The pole locations for a maximally-flat gain function corresponding to two double-tuned stages.

Because the transformation equation is relatively complex to apply for each case, the job is best done once for all by mapping the pole locus which is known in the p-plane onto the s-plane. The result is shown in Fig. 21 where the pole loci in the third quadrant of the p-plane are shown. In this figure the frequency of maximum gain is normalized to be equal to 1.0. The lines radiating from $\omega=1$ are the loci of the poles of the gain function as the bandwidth of the amplifier is increased. The lines c_6 and d_6 are the loci for the poles of a single, maximally-flat, double-tuned stage ($n=1$). Lines $a_4 \cdots d_4$ are the pole loci for a staggered-double ($n=2$) (i.e., two stages, stagger-tuned to give a maximally flat response). Lines $a_6 \cdots f_6$ are the pole loci for a staggered triple ($n=3$). More complicated designs than a triple may be made, but the physical realization becomes very difficult. The lines surrounding $\omega=1$ are the loci of the poles with constant γ but increasing n. The pole positions for an amplifier with a given value of γ and n may be easily found from the graph.

[10] V. D. Landon, "Cascade amplifiers with maximal flatness" *RCA Rev.*, vol. 5, pp. 347–362; January, 1941.
[11] Valley and Wallman, *loc. cit.*
[12] D. L. Trautman, "Maximally-Flat Amplifiers of Arbitrary Bandwidth and Coupling," Tech. Rep. No. 41, Elec. Res. Lab., Stanford Univ., Stanford, Calif.; February 1, 1952.

[13] It should be mentioned that only contours and pole distributions possessing circular symmetry in the p-plane will yield physically realizable pole arrangements in the s-plane. Thus the ellipse, which produces an equal-ripple response, cannot be used with this transformation.

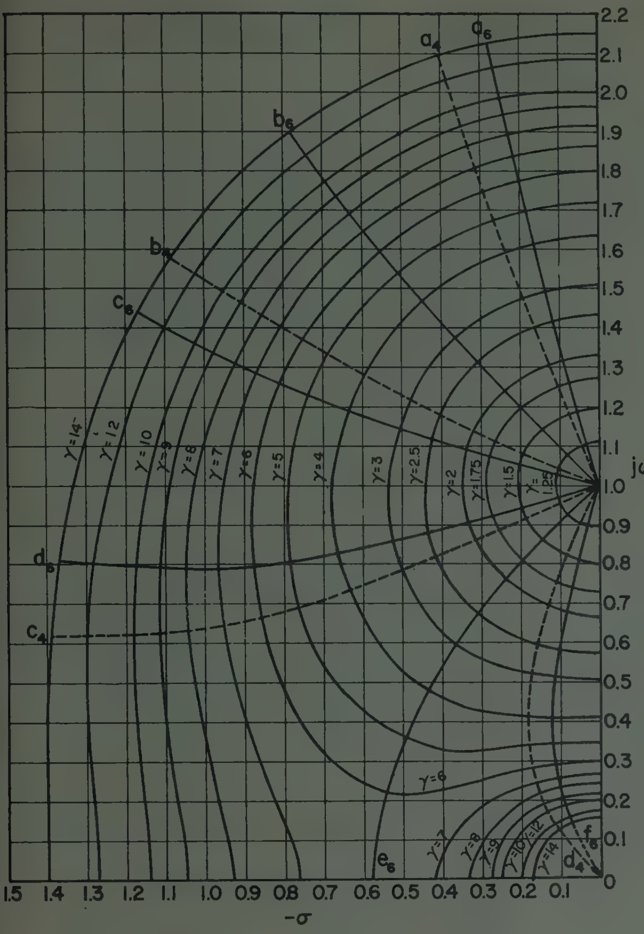

Fig. 21—Loci of s-plane pole positions for staggered doubles and triples.

From the s-plane pole positions the element values for the actual interstages are found. Since the transfer impedance, Z_T, of the double-tuned circuit is an equation of fourth degree, the element values must be found by equating coefficients; i.e.,

$$Z_T = \frac{Hs}{(s + a_1)(s + \bar{a}_1)(s + a_2)(s + \bar{a}_2)}, \tag{12}$$

where a_1, $\bar{a}_1$, a_2, $\bar{a}_2$ are the known pole locations (from Fig. 22). From the standpoint of obtaining the greatest gain-bandwidth factor, it is necessary to pair the poles on nearly vertical lines for use in a single interstage; i.e., poles a and f, b and c, c and d are paired in the three interstages of a staggered triple. Eq. (12) is multiplied as indicated to give:

$$Z_T = \frac{Hs}{s^4 + b_3 s^3 + b_2 s^2 + b_1 s + b_0}. \tag{13}$$

The element values for the circuit of Fig. 1(a) and 1(b) are then given by the equations:

$$\omega_1 = \sqrt{\frac{b_0 b_3}{b_2 b_3 - b_1}} \tag{14}$$

$$\omega_2 = \sqrt{\frac{b_0 b_3}{b_1}} \tag{15}$$

$$Q_2 = \sqrt{\frac{b_0}{b_1 b_3}} \tag{16}$$

$$k = \sqrt{1 - \frac{b_0 b_3^2}{b_1(b_2 b_3 - b_1)}}, \tag{17}$$

where

$$\omega_1 = (L_1 C_1)^{-1/2} \tag{18}$$

$$\omega_2 = (L_2 C_2)^{-1/2} \tag{19}$$

$$Q_2 = R_c(\omega_2 L_2)^{-1}. \tag{20}$$

Although this procedure is relatively straightforward, it is tedious and time consuming. Consequently, the graphs of Figs. 8 to 15 have been prepared which give the primary and secondary Q, and coefficient of coupling directly. With these graphs the design of a staggered, double-tuned amplifier may be accomplished very quickly.

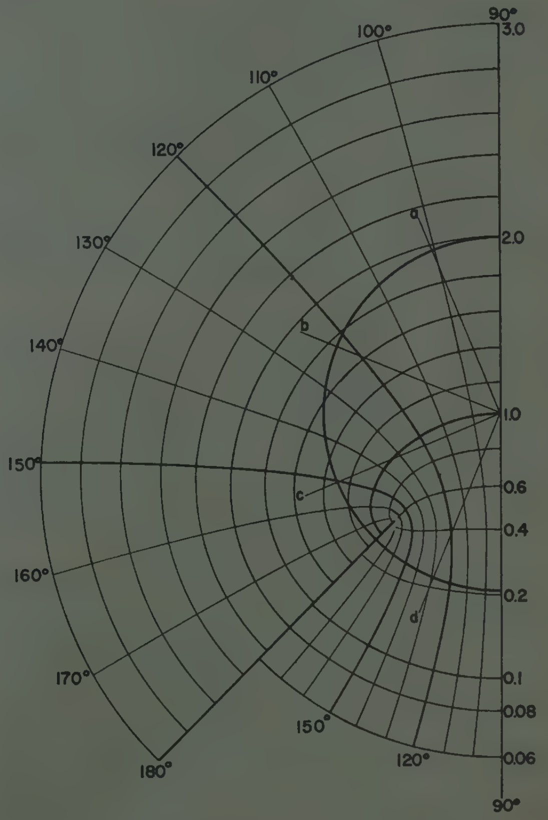

Fig. 22—The polar co-ordinates of the s-plane (bandpass) as mapped onto the p-plane (low-pass).

Acknowledgment

This study was made under an Office of Naval Research Contract N6 onr-251, with joint support by Air Force and Signal Corps. The original work of developing the essential bandpass to low-pass transformation was done by D. L. Trautman[14] and the calculations reducing pole-zero locations to design curves, by J. S. Eddy.[15]

[14] Trautman, *loc. cit.*

[15] J. S. Eddy, "Stagger-tuned amplifiers with double-tuned interstages," Tech. Rep. No. 29, Elec. Res. Lab., Stanford Univ., Stanford, Calif.; January 15, 1951.

The Single-Layer Solenoid as an RF Transformer*

W. A. EDSON†, SENIOR MEMBER, IRE

Summary—A set of curves is presented which makes it relatively easy to design air-core transformers satisfying a majority of engineering needs. Inductances in the range 0.1 μh to 10 mh, coupling coefficients in the range 0.001 to 1.0, and inductance ratios up to 100:1 are covered directly. Certain arbitrary restrictions are placed upon the proportions in order to obtain a single set of charts, but the available electrical characteristics are not limited thereby. The proportions of the resulting coils are compatible with large values of Q, but this is seldom important because heavy damping must usually be provided by associated resistors. The derivation and use of the curves is explained.

Introduction

Cores of laminated iron are rarely useful in transformers operating at frequencies above about 100 kc, and closed cores of powdered iron or ferrite fail at frequencies of only a few megacycles. An air-core design is therefore typical where higher frequencies must be transmitted. Although air-core transformers may have many configurations, it is usually necessary to minimize the self and mutual capacitances of the windings. Because a single-layer solenoid divided into two adjacent sections has low capacitances and is capable of meeting typical requirements on self and mutual inductance, it is the most practical design for most rf transformers.

The designer of an rf transformer usually is given values for the primary, secondary, and mutual inductances derived from filter theory, coupled-circuit theory, or network synthesis. He has also from experience or other sources, information as to how much parasitic capacitance may be tolerated and whether a phase reversal is desirable. The problem is to determine the dimensions and pitch of the two windings.

In typical situations the several requirements can be met in a great variety of ways. This very wealth of possibilities for choice is responsible for the greatest difficulty in preparing design tables or curves. To obtain a set of curves which are convenient to use and which are sufficient in all but exceptional situations it was assumed that *both windings consist of a single layer of wire of a single winding pitch on a common cylindrical form*. In typical applications the coupling coefficient is more important than the selectivity Q. When this is true it is appropriate to use a single size of wire and no spacing between adjacent turns. Because formex enamel wire is now commonly available and provides close spacing in conjunction with low losses and high dielectric strength, its use will be assumed in the numerical examples. However, the curves are applicable to all types of insulation and all degrees of spacing. Evidently the design of coils having three or more windings on the same form can be accomplished by additional use of the same set of curves. Finally, by an appropriate transformation, the curves for two-winding transformers can be used, even when the winding pitches are unequal. This point is illustrated by the fourth numerical example.

Description of the Curves

When a relatively low coupling coefficient is desired, it is appropriate to leave a space between the two windings. Fortunately, quite low coefficients are achieved without going to unreasonable separations: however, a wide choice of proportions is available. To secure a single set of curves it was arbitrarily decided to fix the total winding length equal to the diameter. This choice leads to windings having reasonable proportions, even for inductance ratios as great as 100:1, and is compatible with realizing high values of selectivity. In typical situations the inductance ratio is near unity and both coils have the proportions $b/d \doteq 1/2$. This form is negligibly different from that which produces maximum inductance for a given length of wire. The resulting set of curves is presented in Fig. 1, on the opposite page.

When a moderate-to-high coupling coefficient is needed and a phase reversal is necessary, it is appropriate to use two separate but adjacent windings. Capacitive coupling is minimized if the adjacent ends of the windings are grounded, at least to ac, The curves of Fig. 2 (page 934) show the results obtained when no spacing is left between the two windings and when the shorter winding has a length no greater than the diameter. Because the parameter b_3 is zero in this situation, it is possible to vary b_1 and b_2 independently to secure a wide range of inductance ratios and coupling coefficients.

When a large coefficient of coupling is desired and when a phase reversal is unnecessary, the preferred arrangement is the autotransformer prepared by attaching a tap to a continuous single-layer winding. Fig. 3 (page 934) which applies to this shows that coupling coefficients in excess of 80 per cent may be obtained in coils of reasonable dimensions with substantial transformation ratios.

Numerical Examples

To illustrate the use of these curves let us first assume that we need to design a special interstage transformer having a coupling coefficient $k=0.01$ and self-inductances of 40 and 100 μh respectively. Referring to Fig. 1 we find for $L_2/L_1=2.5$ and $k=0.01$ the value $b_3/d=1.70$. Referring to the upper curve of the same set we find for $L_2/L_1=2.5$ the value $b_1/d=0.35$. Therefore $b_2/d=1-0.35=0.65$.

* Original manuscript received by the IRE, April 26, 1955. This work was supported by the Joint Services under Contract N6onr 251 (07) with the office of Naval Research.

† Applied Electronics Lab., Stanford, Calif.

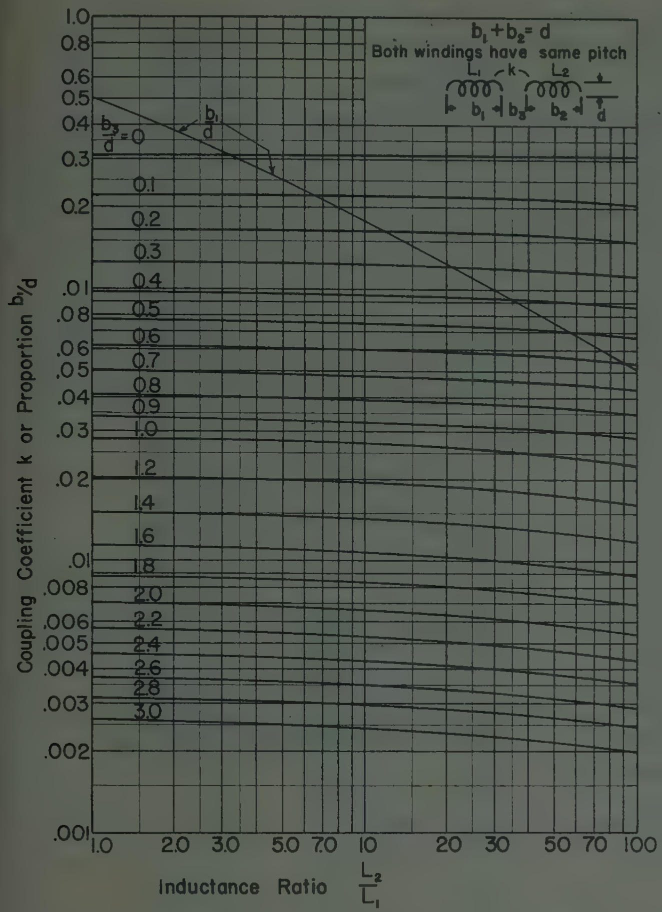

Fig. 1—Two-winding transformer with gap between windings.

The proportions of the windings are now fixed, and it remains only to choose the diameter, wire size, or winding pitch. Referring to Fig. 4 (page 935) and using $b/d=0.35$ we have $L/d^3n^2=3.85\times10^{-3}$. Let us choose a winding pitch $n=290$, which corresponds to No. 40 formex wire, which has a nominal diameter of 0.0034 inch. Substitution of $L=40$ μh with this value yields $d=0.498$ inch. Thus the actual dimensions are $d=0.498$, $b_1=0.174$, $b_2=0.324$ and $b_3=0.847$ inch. The actual winding turns are $N_1=0.174\times290=50.5$ and $N_2=0.324\times290=94.0$.

As a second example let us assume that a double-tuned interstage in an intermediate frequency amplifier for a radar requires self-inductances of 10.0 and 8.0 μh with a coupling coefficient of 0.30. These requirements are readily met by a two-winding transformer without gap. Referring to Fig. 2 we find for $L_2/L_1=1.25$ and $k=0.30$ the proportion $b_1/d=0.49$. The proportions of the second winding may be found in either of two ways. The most straight-forward is to interpolate between the contours of b_2/b_1 to obtain the approximate value 1.2. This procedure, which works well for larger ratios, gives relatively poor accuracy in the present case, and we turn to an alternative procedure.

Referring to Fig. 4 we have for the smaller winding $L/d^3n^2=6.4\times10^{-3}$. Because the inductance of the other winding must be larger by the factor 1.25, we refer to $L/d^3n^2=8.0\times10^{-3}$ and find $b_2/d=0.57$. Thus $b_2/b_1=0.57/0.49=1.16$, which is in good agreement with the value 1.2 obtained above by interpolation.

At this time we are still free to make an arbitrary choice of the form diameter, the wire size, or the number of turns in either winding. Assuming the diameter is fixed at $d=0.500$ inch by the available form we have from the foregoing numbers and the inductance, the winding pitch $n=100$, which corresponds approximately to No. 31 enamel wire which has a nominal diameter of 0.0097 inch. Corresponding to $d=0.500$ we have $b_1=0.245$ and $b_2=0.285$ inch. The actual number of turns in the two windings are now found from $N_1=b_1n$ and $N_2=b_2n$ as 24.5 and 28.5 turns respectively.

As a third example let us assume that for an interstage network in a broad-band, grounded-grid amplifier we need an autotransformer having self-inductances of 1.0 and 0.1 μh and a coupling coefficient of 0.8. Assigning L_2 to the larger inductance we enter Fig. 3 at $L_2/L_1=10$, $k=0.8$ and find $b_1/d=0.029$. That is, the distance from the common end of the coil to the tap shall be 0.029 times the diameter. Interpolating between the cross rulings we find $b_2/b_1=3.75$. Therefore, the total length to diameter ratio is $b_2/d=0.109$.

On the basis of experience or preliminary calculations we anticipate a coil with a rather small number of turns. Consistent with $b_2/b_1=3.75$ let us choose $N_1=2$ and $N_2=7.5$ turns. The design will now be complete provided a suitable diameter and winding pitch can be determined. To this end we write $N_2=b_2n=b_2(dn)/d$, which upon substitution of the chosen numbers yields $(dn)=69$. We now refer to the curves of Fig. 4 which show that for $b_2/d=0.109$ the ratio $L/d^3n^2=5.8\times10^{-4}$. Substitution of the values $L=1$ and $dn=69$ yields $d=0.362$ inch. In turn, $n=69/0.362=190$ turns per inch which corresponds closely to No. 36 formex wire which has a nominal diameter of 0.0055 inch. Tabulating the results we have $d=0.362$, $b_1=0.011$, $b_2=0.041$ inch, $N_1=2$ and $N_2=7.5$ turns, tapped two turns from the end which is common to both circuits.

As a fourth example, let us suppose that for a special application we need a two-winding transformer having a coupling coefficient of 0.10 and self-inductances of 1 and 450 μh respectively. Because the inductance ratio exceeds 100, the problem may not be solved by direct application of the charts. However, we know that the coupling coefficient of two windings depends only upon the relative geometry and not upon the individual winding pitches, whereas the self-inductance of a coil of given diameter and length is proportional to the square of the pitch. Therefore, if the pitch of the longer winding is m times greater than the pitch of the shorter winding, then the effective inductance ratio will be m^2 greater than the effective inductance for corresponding geometry with equal pitches.

In the present case we must set $m^2L_2/L_1=450$. The choice $m=3$ and $m^2=9$ leads to $L_2/L_1=50$. Entering

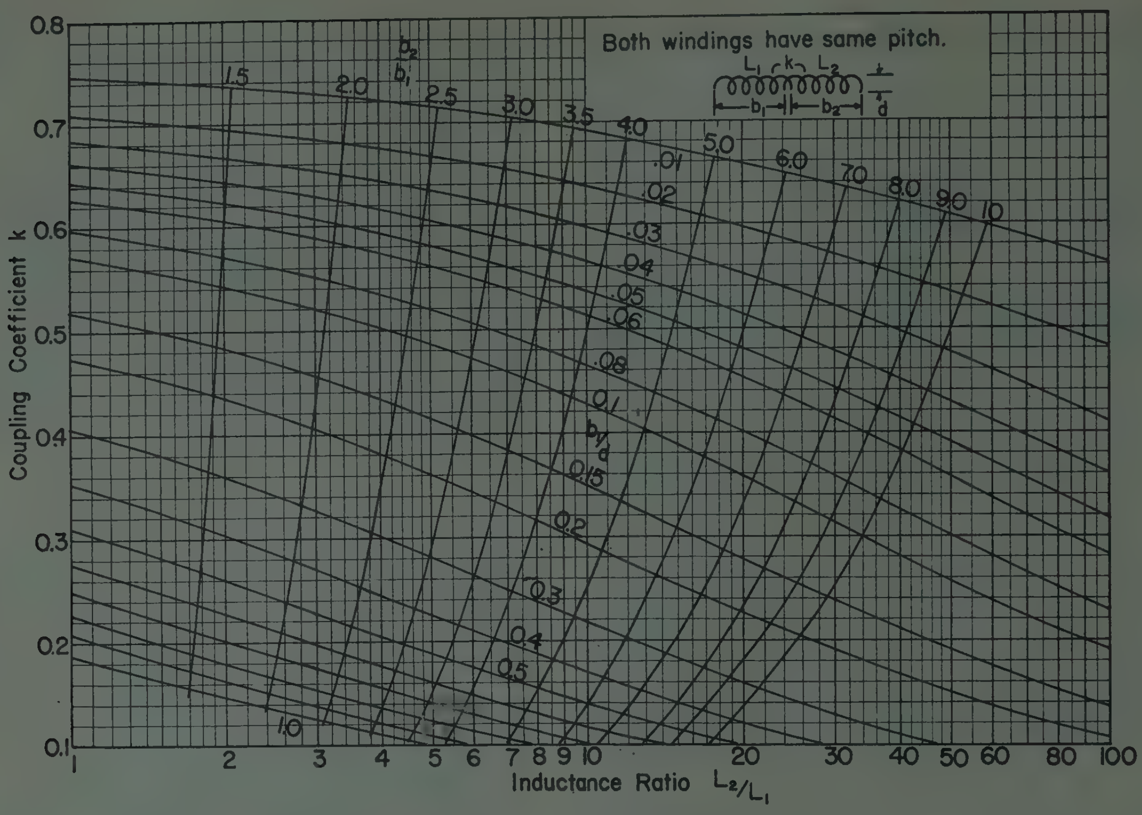

Fig. 2—Two-winding transformer without gap between windings.

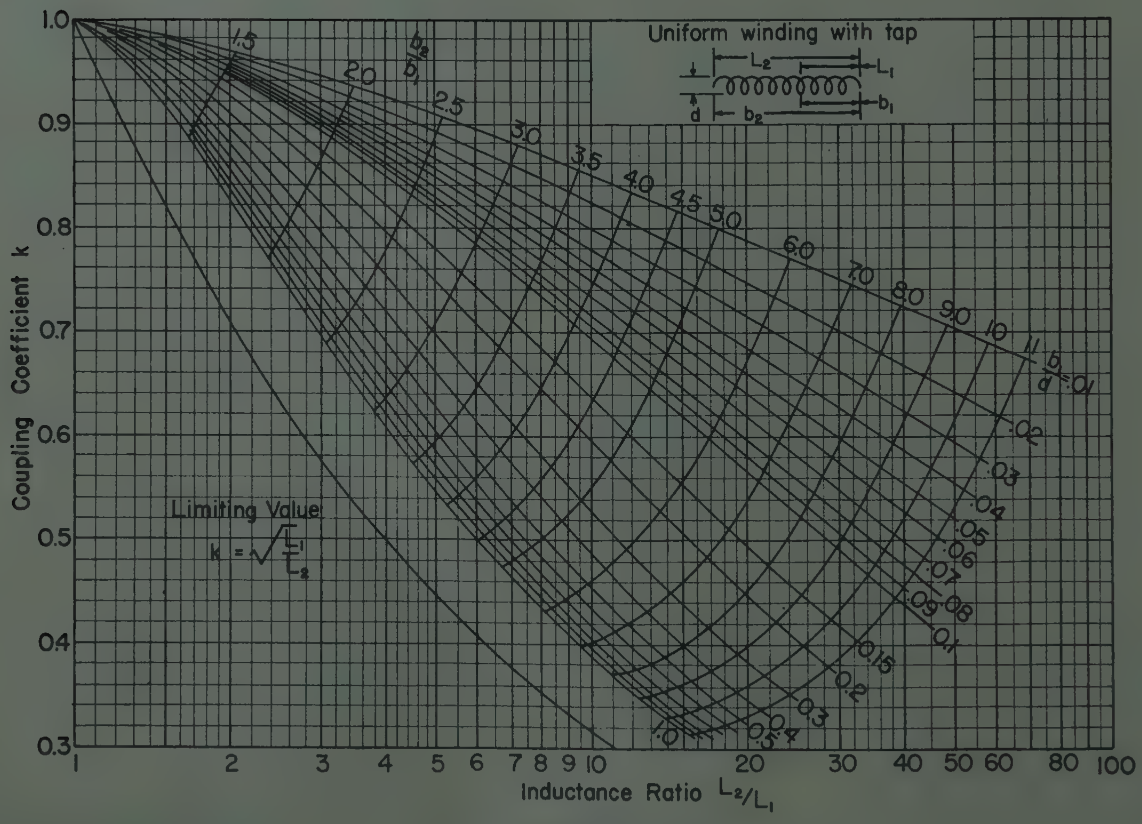

Fig. 3—Auto transformer.

Fig. 1 at $L_2/L_1=50$ and $k=0.1$ yields $b_1 d=0.075$, $b_2/d=0.925$ and $b_3/d=0.36$. Entering Fig. 4 for L_2 at $b/d=0.925$ yields $L/d^3n^2=0.0157$. Choosing $n=356$ corresponding to No. 42 formex wire[1] which has a nominal diameter of 0.0028 inch we have $d=0.610$ inch. Thus, $b_1=0.046$, $b_2=0.563$ and $b_3=0.220$ inch. The longer winding consists of $N_2=356\times 0.563=200$ turns. The winding pitch of the smaller winding is $n/m=356/3=119$ turns per inch, which is approximated by No. 32 wire with a nominal diameter of 0.0088 inch. The number of turns is $N_1=119\times 0.046=5.5$ turns. Alternatively one could use a finer wire wound to the same pitch or a paralleled combination of three strands of No. 42 wire.

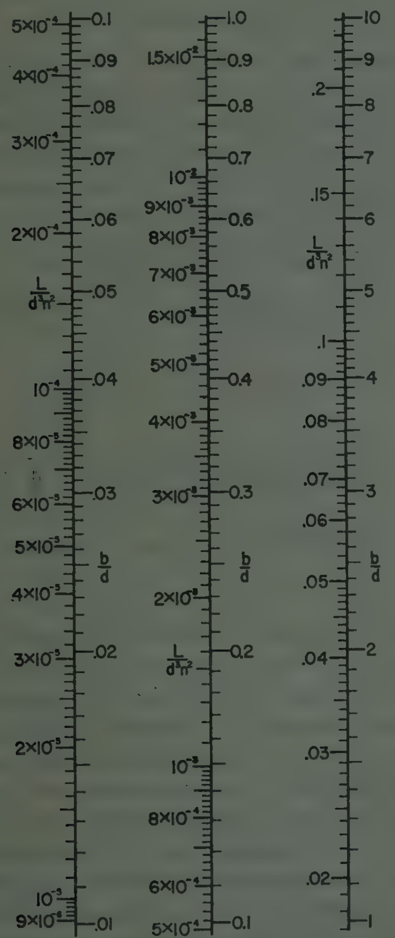

Fig. 4—Normalized self-inductance of a single layer solenoid. L = Inductance in microhenries; d = Diameter in inches; n = Winding pitch in turns per inch; b = Winding length in inches.

Derivation of the Curves

While there exist several excellent formulas for calculating the mutual inductance of coils, they are all rather tedious. Moreover, they commonly involve the relatively small difference of two comparable numbers. Therefore, they give poor results unless the individual terms are calculated to great accuracy. These difficulties are readily avoided in the present case by combining the self-inductances of various component windings. The self-inductance values can be derived with great accuracy from existing tables so the over-all accuracy is quite satisfactory.

Referring to Fig. 1, let us assume that a single, continuous solenoid of diameter d (inches) and uniform winding pitch n (turns per inch) is divided into three sections of length b_1, b_2 and b_3 (inches). The total inductance L_t is evidently expressible as

$$L_t = L_1 + L_2 + L_3 + 2M_{12} + 2M_{13} + 2M_{23}. \qquad (1)$$

Adding L_3 to each side and grouping terms one has

$$L_t + L_3 = 2M_{12} + (L_1 + L_3 + 2M_{13}) + (L_2 + L_3 + 2M_{23}). \qquad (2)$$

However, the terms in parenthesis are recognizable as the inductances of sections 1+3 and 2+3 respectively. Therefore one may write

$$M_{12} = \frac{1}{2}(L_t + L_3 - L_{13} - L_{23}). \qquad (3)$$

This procedure is set forth by Grover,[2] who also gives excellent tables for calculating the several component self-inductances. One finds as one form of Nagaoka's formula[3]

$$L = 0.004\pi^2 a^2 b n^2 K \qquad \mu h, \qquad (4)$$

where a is the radius, b the length, n the winding pitch, and K a tabulated function of b/a. Converting from metric to English units and using $d=2a$ one has

$$L = 0.02507 n^2 d^2 K b = 0.02507 n^2 d^3 K(b/d) \qquad \mu h, \quad (5)$$

where d is the diameter in inches, n is the pitch in turns per inch, and the product $K(b/d)$ is dimensionless and determined from available tables. The relationship $L/d^3n^2=0.02507\ Kb/d$ is plotted vs b/d in Fig. 4 from values given in Grover's tables. A precise table of the product $K(b/d)$, not reproduced here, was also prepared for obtaining accurate results in the operation indicated by (3).

It should be noted that in all cases d is the average diameter of the winding *not* the diameter of the form. The form diameter is thus $d'=d-1/n$. The correction involved is rarely large, but is easily made.

It is emphasized that (4) and, therefore, all the present results are based on the assumption of a uniform current sheet, and take no account of distributed capacitance or the wave properties of a conducting helix. Hence, they are subject to error at high frequencies or if the number of turns is exceedingly small. Fortunately neither of these sources of error is serious in typical situations where transformers are to be used in conjunction with conventional vacuum tubes. The curves

[1] With a little practice, it is possible to wind wire of this size with an ordinary hand drill and very simple guides and pivots.

[2] F. W. Grover, "Inductance Calculations," D. Van Nostrand Co., New York, p. 137; 1946.

[3] Grover, *ibid.*, p. 143.

of Fig. 1 were derived by directly substituting into (3) values of L derived from (5). The separation b_3/d was varied in an orderly manner from 0 to 3.0 while b_1/d and b_2/d were assigned various values such that their sum was always unity. The value of the coupling coefficient k was then determined from the defining relationship

$$k = M_{12}/\sqrt{L_1L_2}. \qquad (6)$$

The curves of Fig. 2 were derived in the same way except that b_3 was set equal to zero, and a wide variety of values of b_1 and b_2 were chosen.

The curves of Fig. 3 were developed from the same calculations used in the preparation of Fig. 2 but involve a change of notation which facilitates their use. The total inductance is now represented by L_2 rather than L_t, and the effective coupling coefficient is given by

$$k = (L_1 + M_{12})/\sqrt{L_1L_2}. \qquad (7)$$

The exceptional feature of the curves of Fig. 3 is that quite large coupling coefficients are available, even for substantial inductance ratios. This fortunate situation stems from the fact that L_1 is physically common to both circuits so that the coupling coefficient is unity for an inductance ratio of unity without regard to magnetic flux leakage.

More generally, in the absence of actual magnetic coupling,

$$k = L_1/\sqrt{L_1L_2} = \sqrt{L_1/L_2}. \qquad (8)$$

This relationship represents the minimum coupling coefficient which may be secured in an autotransformer (unless the pitch is reversed). It is plotted for convenience in Fig. 3.

In closing it should be noted that curves similar to Fig. 1, but restricted to the situation $b_1 = b_2$, have been published by Sulzer[4] and that a chart yielding results equivalent to those of Fig. 4 was published by Wheeler.[5] It is believed that the added convenience and generality of the present curves justifies this partial duplication.

Acknowledgment

The author wishes to thank Dr. M. M. McWhorter of Stanford University for valuable help in designing the various charts as well as for much aid in supervising the detailed work involved in their preparation. Credit is also due to J. C. Hogg of the Georgia Institute of Technology for contributions to the initiation of this work.

[4] P. G. Sulzer, "Coupling chart for solenoid coils," *TV Eng.*, vol. 1, p. 20; June, 1950.

[5] H. A. Wheeler, "Inductance chart for solenoid coils," Proc. IRE, vol. 38, pp. 1398–1399; December, 1950.

A New High-Efficiency Parallax Mask Color Tube*

M. E. AMDURSKY†, R. G. POHL†, AND C. S. SZEGHO†, FELLOW, IRE

Summary—The electron transmission through the parallax masks of present-day tricolor tubes is about 12 per cent, thus placing a limit on picture brightness. This paper describes a new tube employing a parallax mask maintained at a potential much lower than that of the screen and a collector mesh maintained at anode potential intermediate to the screen and mask potentials; the brightness of the tube is increased 3–4 fold by virtue of enlarged mesh holes and the ensuing post-deflection focusing. In addition, secondary emission from the mask, which would dilute color, is minimized. In contrast to other post-accelerating tubes, the mask holes and fluorescent screen dots are uniformly spaced over the entire target area. Nineteen-inch round and twenty-four-inch rectangular tubes incorporating the new principle have been built.

Introduction

COLOR PICTURE tubes have run through the gamut of size in a remarkably short time when compared with monochrome tubes,[1] thus creating a brightness problem. Adequate light output on a 250 square-inch screen can only be achieved, even with three guns, by raising the anode voltage well above the levels used in monochrome tubes. With one gun, the brightness leaves much to be desired. The reason for this, of course, is that the customary shadow-masks have only approximately 12 per cent electron transmission, 88 per cent of the electrons being intercepted by the mask. It has been suggested early in the development of colors tubes[2] to employ post-deflection focusing which permits enlargement of the apertures in the shadow-mask and so increases brightness in the ratio of the increase in electron transmission. The usual practice in post-deflection focusing is to provide an accelerating field between the barrier electrode and the aluminum-backed tri-phosphor screen. The apertures in the barrier electrode followed by the field form an array of tiny electron lenses which focus an electron beam scanning this lens raster down to a fraction of the area of a phosphor element. Certain drawbacks of this customary scheme will now be explained and it will be shown how they can be overcome by a different configuration of the electric field.

* Original manuscript received by the IRE, April 7, 1955; revised manuscript received, June 3, 1955. A condensed version of this paper was presented at the IRE Convention in New York, N. Y., on March 24, 1955.

† Res. Dept., Rauland Corp., Chicago 41, Ill.

[1] H. R. Seelen, H. C. Moodey, D. D. VanOrmer, and A. M. Morrell, "Development of a 21-inch metal-envelope color kinescope," *RCA Review*, vol. XVI, pp. 122–139; March, 1955.

[2] French Pat. No. 866,065 issued June 16, 1941.

Post-Acceleration Tube with a Single Field

In tubes without post-acceleration the screen elements are usually of equal size over the screen area and are laid down by methods utilizing straight optical projection from a point which coincides with the center of deflection of the electrons. In a tube with an accelerating field between the shadow-mask and the screen, the beam arriving from the center of deflection is bent in that field toward the normal to the screen, as shown in Fig. 1. For one given deflection angle a straight line through a mask aperture and a screen element will define a new center of optical projection (0′). For different deflection angles, however, the landing point of the beam on the screen will deviate from the projected point.

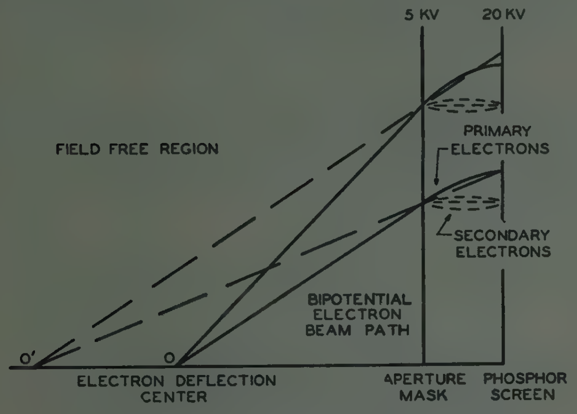

Fig. 1—Path of electron beam in post-acceleration tube with a single field.

This deviation increases rapidly with deflection angle so that at large angles the beam no longer hits the phosphor element of proper color.[3] The situation is analogous to spherical aberration in optics and it is conceivable to use an aspherical lens inserted in the optical path during the photographic part of the process of screen fabrication, to change the center to center distance of the phosphor elements. Another, but even more complicated method, would be to utilize electron exposure of the emulsions which are used in the screen fabrication. One would then have to provide the same accelerating field for the exposing beam as in the final tube. In practice, complete compensation by this method is difficult and at large deflection angles color purity is bound to suffer.

Another drawback of post-deflection focusing with a single accelerating field is that the secondary electrons, which are released by the bombardment of the mask and start out at low velocity from the vicinity of an aperture, do not follow the trajectory of the primary beam but are drawn to the screen at right angles, as shown in Fig. 1. In monochrome tubes, this secondary electron stream limits detail contrast;[4] in color tubes it also dilutes color.

[3] R. Dressler, "The PDF chromatron—a single or multi-gun tricolor cathode-ray tube," Proc. IRE, vol. 41, pp. 851–858; July, 1953.
[4] L. S. Allard, "An ideal post-deflection accelerator c.r.t.," *Electronic Eng.*, vol. 22, p. 461; November, 1950.

The Principles of a Post-Acceleration Tube with Retarding and Accelerating Fields

By providing a retarding field on the cathode side of the mask, in addition to the accelerating field between the parallax mask and screen, the electron trajectories can be altered to make the beam go through the same point in the mask and land on the same phosphor element as it would in the straight parallax case for a large range of deflection angles, since the center of deflection of the electron beam may be made identical with the center of parallax. Consequently, the screen can be fabricated by the customary straight-line optical projection methods with the mask apertures and screen elements uniformly spaced. The new structure then consists of an auxiliary mesh electrode at anode potential, V_a, followed by the parallax mask at a potential V_p lower than that of the anode and the screen, with the latter at a potential V_s much higher than the anode.

The electron path in the tube with both retarding and accelerating fields is shown in Fig. 2. The electron trajectory may be considered as having three parts.

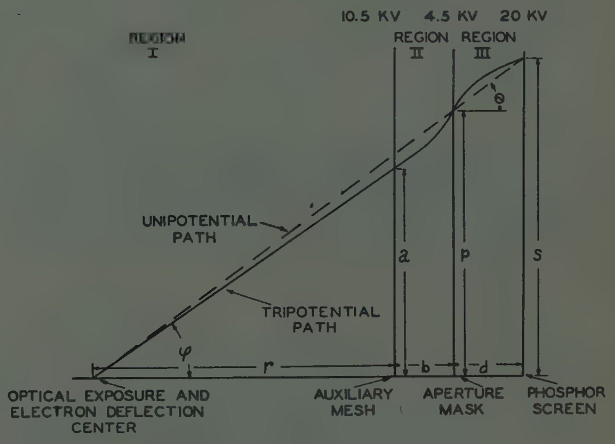

Fig. 2—Path of electron beam in post-acceleration tube with retarding and accelerating fields.

In region I, between the center of deflection and the mesh, the trajectory is straight; in region II, between the mesh and the parallax mask, it is a parabola convex with respect to the tube axis; and in region III, between the mask and the metal-backed screen it is a parabola concave toward the axis. The necessary operating relationships between electrode potentials and spacings for the proper position of the beam on the screen can be derived from geometrical, energy, and transit time considerations. Definitions of the symbols used in the derivations appear in the glossary.

Conventional magnetic deflection is used; consequently, in region I the electron speed is constant. Therefore, from the energy equation

$$v_{x,1}^2 + v_{y,1}^2 = \frac{2e}{m} V_a \qquad (1)$$

$$v_{x,1} = \left(\frac{2e}{m}\right)^{1/2} V_a^{1/2} \cos \phi \qquad (2)$$

$$v_{y,1} = \left(\frac{2e}{m}\right)^{1/2} V_a^{1/2} \sin \phi. \tag{3}$$

As the two electric fields between the auxiliary mesh and the parallax mask, and between the mask and the screen have no components perpendicular to the axis, the vertical component of the electron velocity is constant in the three regions. Consequently,

$$v^2_{x,2,p} + v^2_{y,1} = \frac{2e}{m} V_p$$

and

$$v_{x,2,p}^2 = \frac{2e}{m} [V_p - V_a \sin^2 \phi]. \tag{4}$$

In a uniform field, in which acceleration is constant and is directed horizontally, the average horizontal component of velocity during any time interval equals one-half of the sum of the horizontal velocity at the beginning and at the end of the interval. Therefore,

$$\begin{aligned}\bar{v}_{x,2} &= \frac{1}{2}(v_{x,1,a} + v_{x,2,p}) \\ &= \frac{1}{2}\left(\frac{2e}{m}\right)^{1/2} \{V_a^{1/2} \cos \phi + [V_p - V_a \sin^2 \phi]^{1/2}\}. \end{aligned} \tag{5}$$

Since the transit time in region II is equal to $b/\bar{v}_{x,2}$, the difference of the ordinates of the points where the scanning beam intersects the parallax mask and the auxiliary mesh is

$$\begin{aligned}\overline{p-a} &= \frac{b v_{y,1}}{\bar{v}_{x,2}} \\ &= \frac{b\left(\frac{2e}{m}\right)^{1/2} V_a^{1/2} \sin \phi}{\frac{1}{2}\left(\frac{2e}{m}\right)^{1/2}\{V_a^{1/2}\cos\phi + [V_p - V_a \sin^2 \phi]^{1/2}\}}\end{aligned}$$

$$\overline{p-a} = \frac{2b}{\cot \phi + \left[\frac{V_p}{V_a} \csc^2 \phi - 1\right]^{1/2}}. \tag{6}$$

We require the beam to go through the same point of the mask in the tube with retarding and accelerating fields as in the straight parallax tube; consequently:

$$\begin{aligned}(r+b)\tan\theta &= r \tan \phi + \overline{p-a} \\ &= r \tan \phi + \frac{2b}{\cot \phi + \left[\frac{V_p}{V_a} \csc^2 \phi - 1\right]^{1/2}}. \end{aligned} \tag{7}$$

In region III, from similar reasoning

$$\overline{s-p} = \frac{d v_{y,1}}{\bar{v}_{x,3}}$$

$$= \frac{d\left(\frac{2e}{m}\right)^{1/2} V_a^{1/2} \sin \phi}{\frac{1}{2}\left(\frac{2e}{m}\right)^{1/2}\{[V_p - V_a \sin^2 \phi]^{1/2} + [V_s - V_a \sin^2\phi]^{1/2}\}}$$

and

$$\overline{s-p} = \frac{2d}{\left[\frac{V_p}{V_a}\csc^2\phi - 1\right]^{1/2} + \left[\frac{V_s}{V_a}\csc^2\phi - 1\right]^{1/2}}. \tag{8}$$

The deviation, at the screen, of the point of landing of the beam from the point of intersection of a straight line through the center of deflection and the parallax mask aperture through which the beam passes, is

$$\Delta = d \tan \theta - \overline{s-p}. \tag{9}$$

If the expressions for $\tan \theta$ and the distance $\overline{s-p}$ are substituted from (7) and (8), we obtain the desired relation for the beam deviation as a function of deflection angle, tube geometry, and electrode potentials:

$$\begin{aligned}\Delta = \frac{rd}{r+b}\tan\phi + \frac{2b}{r+b}\,\frac{d}{\cot\phi + \left[\frac{V_p}{V_a}\csc^2\phi - 1\right]^{1/2}} \\ - \frac{2d}{\left[\frac{V_p}{V_a}\csc^2\phi - 1\right]^{1/2} + \left[\frac{V_s}{V_a}\csc^2\phi - 1\right]^{1/2}}. \end{aligned} \tag{10}$$

For small angles of deflection $\csc^2 \phi$ is large so that the "ones" in the denominators can be neglected, and further $\csc \phi \approx \cot \phi$. With these approximations the electrode voltages can be so chosen that the deviation in (10) becomes zero. By setting $\Delta = 0$ in (10) the resulting equation can be solved for the screen voltage, giving

$$V_s^{1/2} \approx \frac{2(r+b)}{\frac{r}{V_a^{1/2}} + \frac{2b}{V_p^{1/2} + V_a^{1/2}}} - V_p^{1/2}. \tag{11}$$

If it is assumed that the spacing between the auxiliary mesh and the parallax mask is much smaller than the distance of the deflection center to the auxiliary mesh, then it can be shown that by neglecting terms in "b" the paraxial equation (11) reduces to:

$$V_s^{1/2} \approx 2V_a^{1/2} - V_p^{1/2}. \tag{12}$$

This relationship is valuable for determining approximate initial values for the various electrode potentials.

Calculation of the deviation Δ with the aid of (10) shows that, with the proper electrode spacings and potentials, the beam goes with negligible error through the same mask aperture and strikes the same phosphor dot as it would in the straight parallax tube with mask and screen at common anode potential. Deviation plots

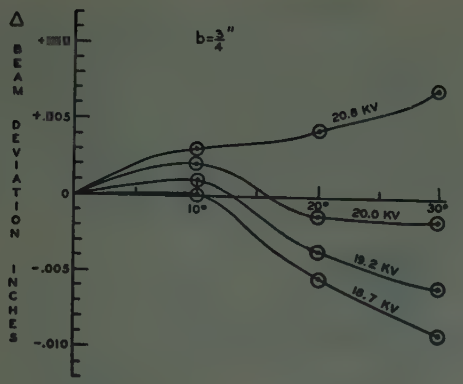

Fig. 3—Beam deviation vs deflection angle as calculated from (10) for various values of V_s. $V_a=9.80$ kv, $V_p=3.60$ kv, $r=12.7$ inches, $b=3/4$ inch, $d=0.400$ inch.

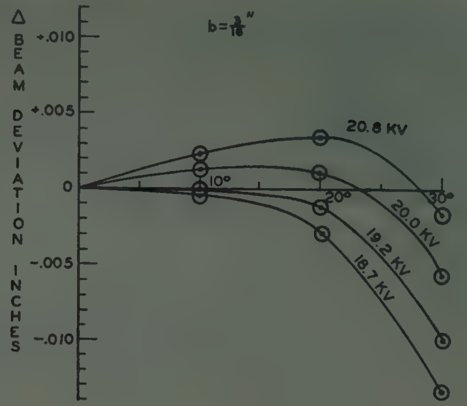

Fig. 5—Beam deviation vs deflection angle as calculated from (10) for various values of V_s. $V_a=9.80$ kv, $V_p=3.60$ kv, $r=12.7$ inches. $b=3/16$ inch, $d=0.400$ inch.

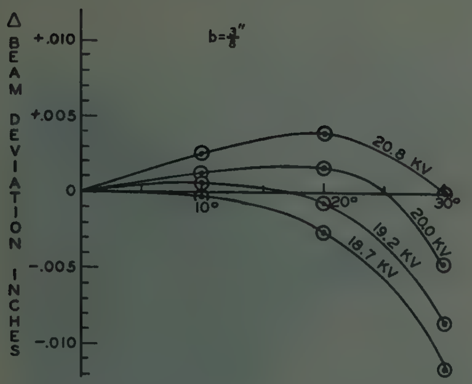

Fig. 4—Beam deviation vs deflection angle as calculated from (10) for various values of V_s. $V_a=9.80$ kv, $V_p=3.60$ kv, $r=12.7$ inches, $b=3/8$ inch, $d=0.400$ inch.

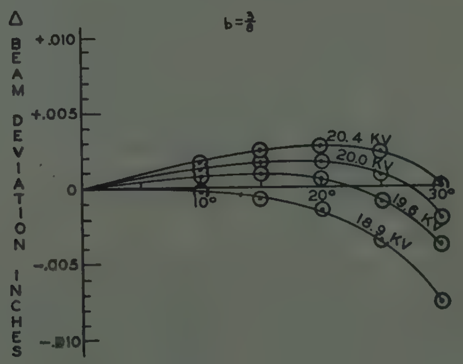

Fig. 6—Beam deviation vs deflection angle as calculated from (10) for various values of V_s. $V_a=10.80$ kv, $V_p=4.80$ kv, $r=14.8$ inches, $b=3/8$ inch, $d=0.416$ inch.

for various screen voltages and spacings between the auxiliary mesh and the parallax mask are shown in Figs. 3, 4, 5 and 6. The mesh and mask voltages were calculated from the paraxial equation (12). It can be seen that up to a scanning half angle of 30 degrees, with certain of the parameters, the maximum deviation is 0.002 inch. At small deflection angles the beam lands somewhat below and at larger angles somewhat above the parallax point but still well within the phosphor dot area.

For adequate collection of secondary electrons, it is desirable that the auxiliary mesh voltage be as high as possible. The magnitude of the operating voltages will now be estimated. The voltages V_a and V_p for a given screen voltage V_s must not only satisfy (12) but must also be chosen so that the beam is focused down by the fields established by the auxiliary mesh, parallax mask, and metal-backed screen to a size smaller than a screen element. For best operation of the tube, the focusing action of the aperture must be controlled so as to provide an illuminated portion of an individual phosphor dot which is neither too large—lest color contamination result, nor too small—to avoid saturation of the phosphor at high current densities. Experimental evidence indicates that a ratio of spot size to aperture size of 1/3 is satisfactory.

For paraxial rays the well-known Davisson and Calbick formula provides the means for obtaining an expression for the focal length of the elementary lenses in terms of the voltage of the aperture electrode and the

fields on both sides of it. As this formula applies only when the field following the aperture is confined to the immediate vicinity of it, a modified expression is derived in the Appendix for the dependence of the ratio of spot size to aperture size (ρ) on the potentials and geometry of the present tube, which yields,

$$\rho = 1 - \frac{V_s + V_a - 2V_p}{2(V_p + \sqrt{V_p V_s})}. \qquad (13)$$

Eqs. (12) and (13) explicitly determine the values of the potentials which must be applied to the auxiliary mesh and the parallax mask once the screen voltage and the focus ratio ρ are specified. Using (12) to eliminate V_p from (13), we obtain

$$V_a(15 - 8\rho) - \sqrt{V_a}(12 - 4\rho)\sqrt{V_s} + V_s = 0. \qquad (14)$$

If a focus ratio $\rho = 1/3$, and a screen potential $V_s = 20$ kv, are inserted in (14), the resulting value of the auxiliary mesh potential is $V_a = 11.4$ kv. The value of the aperture mask potential can then be determined by substituting the above values in (12), which gives $V_p = 5.15$ kv. These calculated values are in reasonable agreement with the experimental values $V_a = 10.5$ kv and $V_p = 4.7$ kv. Since the auxiliary mesh is at high positive potential with respect to the parallax mask and is close to it, it efficiently collects the secondary electrons originating there. This is an indispensable condition for successful operation of the tube as otherwise loss of contrast and color dilution would result.

Secondary emission would be completely absent if the parallax mask could be operated at zero or near cathode potential as in the direct-view storage tubes with electron-lens raster systems described by M. Knoll.[5] In the absence of perpendicular incidence (for which Knoll makes provision) this mode of operation is not possible in the present case since with increasing scanning angle the horizontal component of the electron velocity near the parallax mask soon becomes too low to enable the electrons to reach the saddle point of the potential along the axis of the apertures, and they are reflected back towards the cathode.

If one disregards the penetration of the accelerating field through the parallax mask apertures, the equation for the beam deviation, (10), determines the maximum deflection angle at which the tube will operate for a given voltage ratio V_p/V_a, since if the square roots in the denominator become negative, the equation loses physical significance. Thus maximum deflection angle is:

$$\sin \phi_{\max} = \left(\frac{V_p}{V_a}\right)^{1/2}. \qquad (15)$$

For the values of electrode voltages actually used

$$\phi_{\max} = 42 \text{ degrees}$$

which is a larger angle than necessary to scan the tube completely.

[5] M. Knoll, "Electron-lens raster systems," *Electron Physics*, NBS Circular 527, pp. 329–337; March 17, 1954.

Tube Construction

The new principle has been incorporated into tubes utilizing 24-inch metal rectangular two-part envelopes as well as 19-inch glass round two-part bulbs. A 24-inch rectangular tube is shown schematically in Fig. 7 and a photograph of it in Fig. 8. The phosphor dot screen,

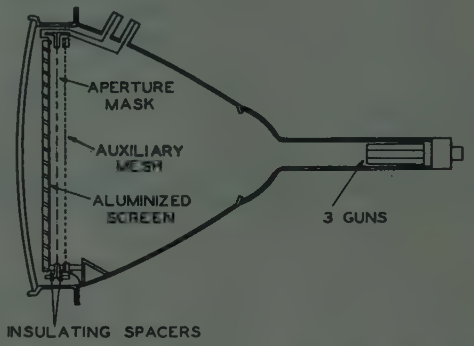

Fig. 7—Schematic cross section of 24 inch metal rectangular tube.

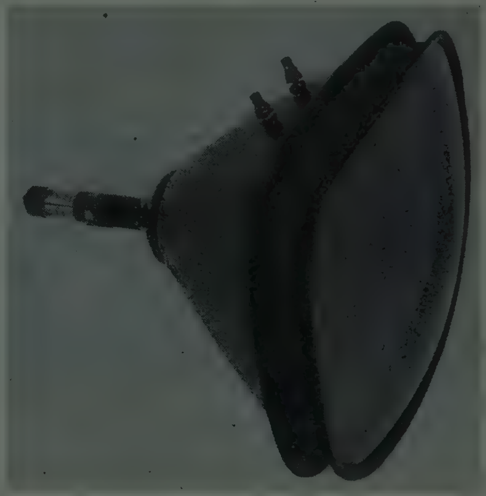

Fig. 8—Photograph of completed 24 inch metal rectangular tube.

parallax mask, and auxiliary mesh are all planar and assembled as an internal pack with a supporting framework and insulating spacers of uniform thickness. The pertinent dimensions and a typical set of the voltages applied to each electrode are given in Table I on the facing page.

The phosphor dot screen for these tubes was made by silk-screening process. As the parallax mask which is normally used to produce the stencil has in this case apertures of double size, the resulting dots on the master positive must be reduced. This is achieved merely by the technique of successive exposures and dodging customary in photoengraving. In aluminizing the screen, a border is left as an insulating section between the frame and the phosphor area. Mykroy insulator spacers provide further insulation between the mask and screen.

The auxiliary mesh used was a woven cloth of 0.003-inch diameter stainless steel wire with 50 meshes per inch. This particular size was chosen from commercially available stock since it has a high transmission (80 per cent) and is quite strong even though the wire diameter is sufficiently small that in the operation of the tube its out-of-focus image is invisible. The mesh was stretched and bolted between two rings supported by insulating bushings at a uniform distance (b) from the mask. The mesh need not be precisely aligned with respect to either the parallax mask or screen; however, in these tubes it was oriented at approximately 45 degrees to the horizontal to eliminate moiré between it and the scanning lines.

Connections to the screen and to the parallax mask were provided through additional buttons in the case of the glass bulb and through insulated connector bushings in the case of the metal envelope. The auxiliary mesh was directly connected to the metal flange and through the customary aquadag coating to the final anode of the gun.

As shown in the previous section, the auxiliary mesh voltage is 0.57 times the screen voltage. The anode voltage of these tubes is therefore twice that of post-deflection focused tubes having an accelerating field alone.[3] Consequently, the conventional 3-gun assembly with mechanical convergence which employs an immersion type focusing electrode can be used. As a result of the higher anode voltage, the focusing electrode voltage is not inordinately low and current limiting in this electrode remains at a permissible value.

TABLE I

	19 inch	24 inch
Picture size	$12\times15\frac{1}{2}$ inches	$13\frac{1}{2}\times18\frac{1}{4}$ inches
Deflection angle (diagonal)	62 degrees	62 degrees
Parallax mask—screen spacing (d)	0.400 inch	0.416 inch
Parallax mask—auxillary mesh spacing (b)	0.375 inch	0.375 inch
Distance—deflection center to auxiliary mesh (r)	12.7 inches	14.8 inches
Parallax mask aperture diameter	0.018 inch	0.018 inch
Parallax mask aperture spacing	0.023 inch	0.023 inch
Phosphor dot diameter	0.014 inch	0.014 inch
Screen voltage	20 kv	20 kv
Parallax mask voltage	4.7 kv	4.7 kv
Auxiliary mesh voltage	10.5 kv	10.5 kv

Performance

In the tubes described the parallax mask has a transmission of 50 per cent; with the auxiliary mesh the overall electron transmission is 40 per cent. Thus a brightness gain of 3 to 4 over that of the straight parallax mask tube can be expected. Fig. 9 shows the measured brightness-versus-cathode current characteristic of the new tube with 20 kv on the anode, and it can be seen that up to approximately 1 milliampere total current, a brightness gain of almost $3\frac{1}{2}$, is realized. At higher currents the characteristic flattens because the focusing electrode draws a portion of the current. The drives of each of the 3 guns were adjusted to give a total current to produce illuminant C white light output. In color pictures highlight brightnesses of 60 foot lamberts have been measured.

To determine how efficiently the auxiliary mesh acts as a secondary emission collector, the ratio between the brightness produced by the primary beam and the secondaries still reaching the screen was measured. This was done on a white screen by first imaging a single line written by the primary beam and by subsequently imaging the line traced by secondary electrons onto a slit in front of a photocell, yielding ratios as high as 70 to 1. If the auxiliary mesh is kept at the same potential as the mask, this ratio drops to 10 to 1.

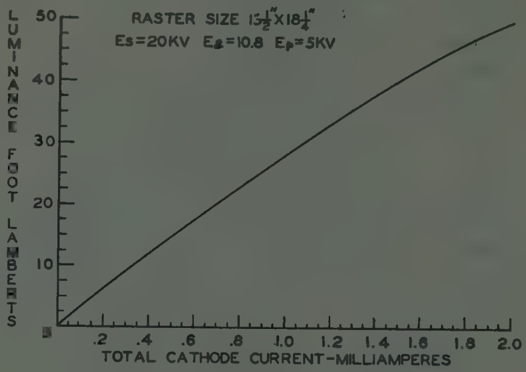

Fig. 9—Luminance vs total cathode current characteristic.

Secondary electrons not only detract from contrast but also desaturate color. For instance, in an area where only a saturated red is to be reproduced, the green and blue dots also become slightly luminous due to secondary electron bombardment. This condition is further aggravated by the red phosphor having the lowest luminous efficiency. Fig. 10 (next page) shows a CIE chromaticity diagram with the color gamuts obtainable on various types of tubes. The triangle indicated as A represents that of the straight parallax mask tube, the one indicated as C that of the post-accelerated tube with a single field, and the one indicated as B that of the post-accelerated tube with both a retarding and an accelerating field. It may be seen that with the latter construction the blue primary is almost identical with that of the parallax tube. The green, however, is somewhat desaturated and the red is slightly more desaturated. A further improvement in color saturation, over what has been achieved by the collection of secondary electrons, can be expected if the phosphor efficiencies could be more closely matched.

In post-accelerated tubes there is another source of stray light, caused by primary electrons reflected at the screen and returned to it by the accelerating field. The intensity of this stray light was found, by the method of contrast measurement described, to be down by a factor of 200 when compared to that of the useful primary-beam light.

The markedly enhanced purity of the color fields is one of the major advantages of this type of tube. The accuracy of landing of the electron beam on the phosphor dots was mapped, with the aid of a microscope, over the entire screen area and was found to be in excellent agreement with the calculated deviation plots of Figs. 4 and 6.

Moiré due to the auxiliary mesh was not visible on a blank raster or on either black-and-white or color pictures.

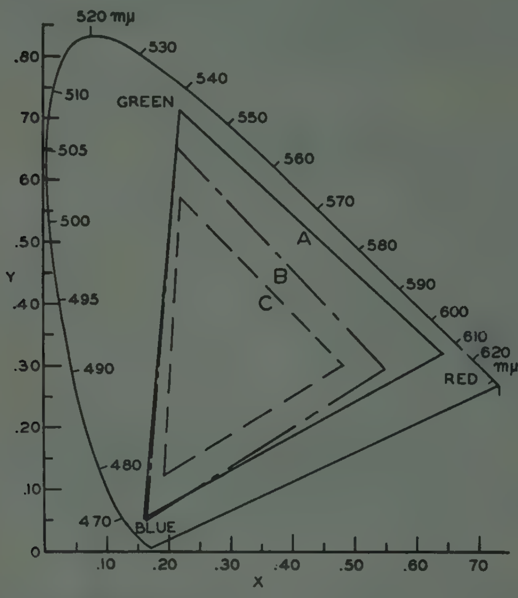

Fig. 10—CIE chromaticity diagram with the color gamuts obtainable on: *A*, straight parallax mask tube; *B*, post-acceleration tube with both retarding and accelerating field; *C*, post-acceleration tube with a single field.

Conclusion

It has been shown that post-deflection focusing with a retarding field preceding the accelerating field considerably extends the brightness range of the parallax mask type tricolor tubes. Up to now this principle has been applied only to tubes with an internal screen pack of inherently complex design. In addition to the fact that in such a tube the phosphor screen is on a separate glass plate which introduces objectionable reflections and contrast loss, the picture must be viewed through a window which is never quite free from striations. This gives rise to a rather disturbing sensation similar to "muscae volitantes" (fleeing flies), to borrow an expression from Physiological Optics. It therefore appears certain that future commercial tricolor tubes will have the fluorescent screen deposited directly on the curved faceplate. Since this curve is usually spherical, a spherically shaped barrier electrode is required.[6] The principle described in this paper, because it employs an apertured sheet barrier electrode which can be formed into a spherical shape, lends itself to this construction while tubes employing wire barriers do not.[7]

List of Symbols

- O Center of magnetic deflection.
- r Distance from center of deflection to auxiliary mesh.
- b Spacing between auxiliary mesh and parallax mask.
- d Spacing between parallax mask and screen.
- V_a Auxiliary mesh voltage, with respect to cathode.
- V_p Parallax mask voltage.
- V_s Metal-backed screen voltage.
- ϕ Deflection angle.
- θ Angle subtended by the phosphor dot and the tube axis at the center of deflection.
- a Ordinate of the point where the beam trajectory intersects auxiliary mesh.
- p Ordinate of the point where the beam trajectory intersects parallax mask.
- s Ordinate of the point where the beam trajectory intersects the screen.
- v_x Horizontal component of the electron velocity.
- v_y Vertical component of electron velocity.
- $\bar{v}_x$ Average velocity in the horizontal direction.
- Δ Deviation at the screen between the point of landing with tripotential operation, and the corresponding point under unipotential parallax operation.

Subscripts 1, 2, 3 indicate the region in which the electron travels while the letter subscripts indicate the electrode nearest the position of the electron.

Appendix

The focal length of a circular aperture in a thin metal plate for an electron beam arriving at normal incidence is given by the Davisson-Calbick formula for electrode structures that establish essentially a field-free region at distances far from the aperture. However, the parallax mask and screen in the present tube establish an approximately uniform electric field between them so that the trajectories are parabolic rather than straight and the actual focal length becomes greater than that given by this formula. Harnwell[8] derives the equation of the parabolic trajectory as

$$y = \frac{2su}{f}\left[\left(1 + \frac{f}{2s}\right) - \left(\frac{x}{s} + 1\right)^{1/2}\right], \qquad (16)$$

[6] S. H. Kaplan, "Theory of parallax barriers," *Jour. Soc. Mot. Pic. Telev. Eng.*, vol. 59, p. 18; July, 1952.

[7] Tubes with post-deflection focusing utilizing a spherical aperture mask, a spherical auxiliary mesh and the phosphor screen on the faceplate have since been successfully operated.

[8] G. P. Harnwell, "Principles of Electricity and Electromagnetism," McGraw-Hill Book Company, Inc., New York, N. Y., First Ed., p. 231, eq. (7.16); 1938.

wherein (x, y) specifies the position of an electron relative to the center of an aperture of radius u, f is the Davisson-Calbick focal length, and, in the notation of this paper

$$f = \frac{4V_p}{\dfrac{V_a - V_p}{b} + \dfrac{V_s - V_p}{d}} \tag{17}$$

and

$$s = \frac{d}{\dfrac{V_s}{V_p} - 1}. \tag{18}$$

The ratio of the spot size at the screen to the aperture size is then easily found by setting $x=d$ in (16), yielding

$$\rho = \frac{y}{u} = \frac{2s}{f}\left[1 + \frac{f}{2s} - \left(\frac{V_s}{V_p} - 1 + 1\right)^{1/2}\right]. \tag{19}$$

For the tripotential tubes actually constructed, we can, to a reasonable order of accuracy, set $b=d$ in (17), so that

$$f = \frac{4V_p d}{V_s + V_a - 2V_p}. \tag{20}$$

Substitutions of (18) and (20) in (19) yields

$$= 1 - \frac{2d(V_s + V_a - 2V_p)\left(1 - \dfrac{V_s}{V_p}\right)}{\left(\dfrac{V_s}{V_p} - 1\right)4V_p d}$$

$$= 1 - \frac{V_s + V_a - 2V_p}{2V_p + \sqrt{V_p V_s}} \tag{21}$$

which is (13) stated earlier.

The new focal length for paraxial rays, f', is determined by setting $y=0$ in (16), and solving for $x=f'$, yielding

$$f' = f + \frac{f^2}{4s}$$

$$= f + \frac{f^2}{4d}\left(\frac{V_s}{V_p} - 1\right). \tag{22}$$

Hence if $V_s > V_p$ then $f' > f$, as mentioned above.

Acknowledgment

The authors wish to thank T. S. Noskowicz for stimulating discussions and J. Wimpffen for taking measurements. The construction of experimental color tubes involves arduous and painstaking efforts and the authors are especially indebted for this to J. Fiore and various members of the Research Laboratory workshops.

Design of Lens-Mask Three-Gun Color Television Tubes*

R. C. HERGENROTHER†, SENIOR MEMBER, IRE

Summary—**This paper discusses a modification of the shadow-mask three-gun color television tube. By applying an electron accelerating field between the mask and the fluorescent screen, the mask apertures act as individual electron lenses causing the individual electron beams to converge. This permits the apertures to be increased in area resulting in improved utilization of the electron beam current and reduced mask heating. The added voltage is applied after beam deflection and therefore increases the energy in the beam without requiring increased scanning power.**

Design formulas pertaining to lens effects at the mask and electron beam refraction effects between the mask and the fluorescent screen are given for both planar mask and curved mask designs.

The effects of fluorescent screen bombardment by secondary electrons produced at the lens mask is described and means for suppressing these effects are discussed.

* Original manuscript received by the IRE, February 28, 1955; revised manuscript received, April 2, 1955; second revised manuscript received, May 26, 1955.

† Raytheon Manufacturing Co., Waltham, Mass.

Introduction

THE SHADOW-MASK three-gun color television tube has reached an advance stage of development and use.[1-3] In these tubes the aperture hole area is required to be of the order of 15 per cent of the mask area to confine each electron gun beam to its respective color. This means that 85 per cent of the potentially useful electron beam energy is intercepted by the shadow mask where it is not only wasted but produces heating of the mask which may cause it to dis-

[1] M. J. Grimes, A. C. Grimm, and J. F. Wilhelm, "Improvements in the RCA three-beam shadow-mask color kinescope," Proc. IRE, vol. 42, pp. 315–325; January, 1954.

[2] N. F. Fyler, W. E. Rowe, and C. W. Cain, "The CBS-colortron: a color picture tube of advanced design," Proc. IRE, vol. 42, pp. 326–333; January, 1954.

[3] H. R. Seelen, H. C. Moody, D. D. Van Ormer, and A. M. Morrell, "Development of the RCA 21-inch metal envelope color kinescope." *RCA Rev.*, vol. 16, pp. 122–139; March, 1955.

tort, resulting in misalignment between the apertures and the phosphor dots.

An electron accelerating electric field between the mask and the fluorescent screen will produce an electron lens effect at each aperture causing the electron beam to converge after passing through the aperture. Because of this, it becomes possible to greatly enlarge the aperture hole area over that required when the only function of the mask is to cast a shadow on the fluorescent screen. By using this arrangement, which we shall describe as a "lens mask," it is possible to use aperture hole areas totaling more than 40 per cent of the total screen area thus more than doubling the useful electron beam energy reaching the fluorescent screen and reducing the heating of the mask by more than a third. In addition, since the electron beam receives a substantial part of its total acceleration beyond the lens mask, the deflection system operates on a lower voltage beam resulting in a considerable reduction in the power required for the deflection circuits.

The design of lens mask systems for both planar mask and curved mask three-gun color television tubes is described below.

Computation of Electron Beam Convergence Produced by an Aperture Lens

The paraxial ray equation for an axially symmetrical electric field is given by Pierce[4] as

$$r'' + \frac{V'}{2V} r' + \frac{V''}{4V} r = 0, \tag{1}$$

where

r = radial distance of electron from the symmetry axis

V = potential measured to cathode.

The prime notations refer to derivatives along the direction Z of the symmetry axis.

We shall apply this to a lens comprising a circular aperture in a thin flat conductor at potential V_1, having parallel to it at a distance l, a plane conducting sheet at potential V_2, as shown in Fig. 1.

We divide the electric field into Region I, which is the field near the aperture, and Region II which extends from the boundary of Region I to the target electrode. In Region I, r and V can be considered to be constant and we can write from (1),

$$r'' + \frac{V''}{4V_1} r = 0 \tag{2}$$

which, when integrated over Region I, gives

$$r_A' - r_B' = \frac{r_B}{4V_1}(V_B' - V_A'). \tag{3}$$

Let us assume that the region to the left of the aperture is field free and that the electrons are entering parallel to the axis. Then $r_A' = 0$ and $V_A' = 0$ leaving

$$-r_B' = \frac{r_B}{4V_1} V_B'. \tag{4}$$

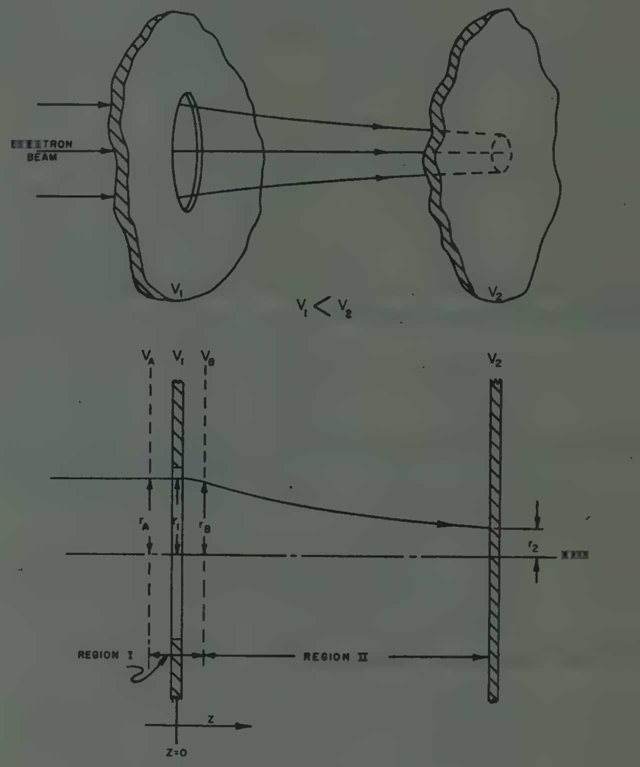

Fig. 1—Diagram of an aperture lens.

In Region II we shall assume a uniform electric field. This means that $V'' = 0$, so for Region II we can write (1) as

$$r'' + \frac{V'}{2V} r' = 0. \tag{5}$$

However, in Region II

$$V = V_1 + ZV_B'. \tag{6}$$

Thus

$$\frac{r''}{r'} + \frac{1}{2}\frac{V_B'}{(V_1 + ZV_B')} = 0. \tag{7}$$

Integrating (7) gives

$$\log r' + \tfrac{1}{2}\log(V_1 + ZV_B') = C_1$$

or

$$r'(V_1 + ZV_B')^{1/2} = C_2. \tag{8}$$

At the boundary between Regions I and II

$$r' = r_B'$$

$$Z = 0.$$

Thus at the boundary (8) gives

[4] J. R. Pierce, "Theory and Design of Electron Beams," D. Van Nostrand Co., Inc., New York, N.Y., p. 77; 1949.

$$r_B'(V_1)^{1/2} = C_2. \tag{9}$$

Substituting (4)

$$-\frac{r_B}{4V_1} V_B'(V_1)^{1/2} = C_2 \tag{10}$$

and (8) reads

$$r'(V_1 + ZV_B') = -\frac{r_B}{4(V_1)^{1/2}} V_B' \tag{11}$$

or

$$r' = \frac{-r_B}{4(V_1)^{1/2}} \frac{V_B'}{(V_1 + ZV_B')^{1/2}}. \tag{12}$$

Integrating (12) gives

$$r = -\frac{r_B}{2(V_1)^{1/2}} (V_1 + ZV_B')^{1/2} + C_3 \tag{13}$$

when

$$Z = 0, \qquad r = r_B$$

and (13) reads

$$r_B = -\frac{r_B}{2(V_1)^{1/2}} (V_1)^{1/2} + C_3 \tag{14}$$

and

$$C_3 = \frac{3}{2} r_B. \tag{15}$$

Thus (13) reads

$$r = \frac{r_B}{2}\left[3 - \left(\frac{V_1 + ZV_B'}{V_1}\right)^{1/2}\right]. \tag{16}$$

Substituting (6) gives

$$r = \frac{r_B}{2}\left[3 - \left(\frac{V}{V_1}\right)^{1/2}\right]. \tag{17}$$

From Fig. 1, when $r = r_2$, $V = V_2$; also $r_B = r_1$. Thus from (17)

$$\frac{r_2}{r_1} = \frac{1}{2}\left[3 - \left(\frac{V_2}{V_1}\right)^{1/2}\right]. \tag{18}$$

If r_1 is taken as the radius of the aperture and r_2 as the radius of the electron spot incident on the target electrode, (18) gives us the ratio of these two quantities which measures the electron beam convergence of the aperture lens.

We make the following observations concerning (18):

1. The electron spot is in focus on the target electrode when $r_2 = 0$, which occurs when $V_2/V_1 = 9$.

2. The electron spot radius increases as V_2/V_1 becomes less than 9, becoming equal to the aperture radius when $V_2/V_1 = 1$, and approaching a maximum value of 3/2 times the aperture radius as V_2/V_1 approaches zero. When V_2 is made negative, the electrons do not reach the target and (18) becomes imaginary.

3. As V_2/V_1 becomes greater than 9, r_2 increases in the negative direction, which means the electron beam has crossed over at the focus before reaching the target.

Experimental Measurement of Electron Beam Convergence of Lens Mask

The cathode ray tube shown in Fig. 2 was constructed using a conventional electron gun which directs an electron beam perpendicular to a target about 12 inches from the cathode. The target comprises a thin metal plate having circular apertures and, parallel to this, an aluminized fluorescent screen deposited on a thin sheet of mica. The electrical connection to the aluminum film was brought out to a separate electrical terminal. The fluorescent spots on the screen could be measured with a microscope having a calibrated eyepiece scale. It was desired to study the properties not only of a single aperture but of a close-spaced triangular array to simulate what we shall define as a lens mask. The aperture diameters were 0.064 inch with a spacing of 0.094 inch from center-to-center.

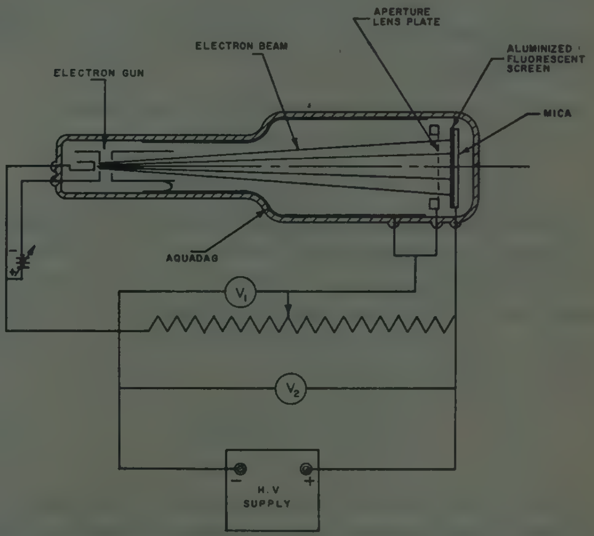

Fig. 2—Diagram of a tube used for studying the aperture lens.

The fluorescent spot diameter of this tube was measured for a series of voltage ratios V_2/V_1 where V_2 was the voltage of the aluminum fluorescent screen coating and V^1 is the voltage of the aperture electrode, taking cathode potential as zero. These data are plotted in Fig. 3 (next page) being normalized at $r_2/r_1 = 1$, $V_2/V_1 = 1$. Note that r_1 is equal to the radius of the apertures so we are here considering the extreme boundary ray.

Also in Fig. 3 is shown the plot of (18). It is seen that the measured data agree quite well with (18) to voltage ratios of 10 which covers the region of major interest. It is also concluded that the field disturbance produced by the close proximity of the apertures causes no appreciable change from that for a single isolated aperture.

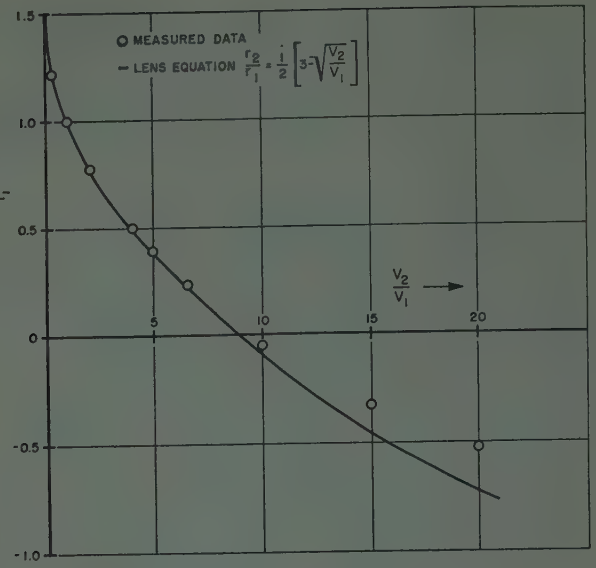

Fig. 3—Aperture lens measurements.

Photographs of the fluorescent spot pattern taken from a number of different values of V_2/V_1 are shown in Fig. 4.

The above analysis can also be successfully applied to a lens comprising a long slot instead of a round hole and this is given in Appendix I.

Electron Beam Transmission Considerations of the Lens Mask

Electron Beam Transmission Efficiency

Consider an electron beam incident upon a lens mask. The beam transmission efficiency η may be defined as the ratio of the hole area of the lens mask divided by the total mask area. If the mask comprises circular holes of diameter D_1 placed in a triangular pattern with a distance of D_3 between hole centers, we can write

$$\eta = \frac{\pi}{2\sqrt{3}}\left(\frac{D_1}{D_3}\right)^2. \tag{19}$$

This equation is shown plotted in Fig. 5 with points A, B, and C, representing three different values of D_1/D_3.

Factors Limiting Aperture Diameter to Aperture Spacing Ratio

In an actual mask D_1/D_3 cannot equal unity since the holes would be tangent and the mask could not hold together. The point C in Fig. 5 represents a practical upper limit for D_1/D_3 for reasons of mask strength. The point B in Fig. 5 represents the maximum ratio of $D_1/D_3=\sqrt{3}/3$ for a shadow-mask tube which is approached as the electron beam diameter at the gun approaches zero. In actual shadow-mask tubes, D_1/D_3 is smaller than value B, usually having a value of about $\frac{3}{8}$ as shown at point A. This is done to allow for the finite size of the beam at the electron gun and to restrict the diameter of the electron spots to a value somewhat smaller than the diameter of the color dots.

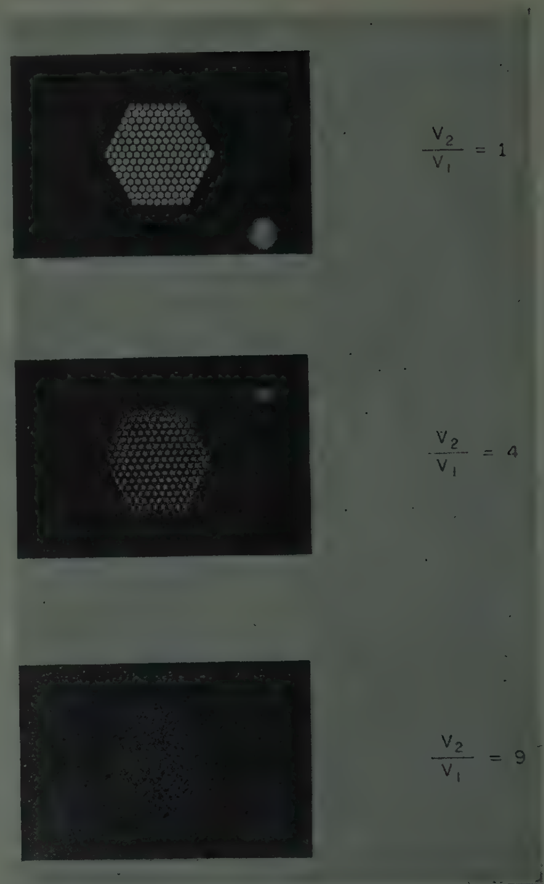

Fig. 4—Photographs of the dot pattern produced on the fluorescent screen of the tube shown in Fig. 2, for various V_2/V_1 ratios.

Light Projection Considerations

Point B on Fig. 5 has a further significance in lens-mask design since it represents the maximum ratio of D_1/D_3 which can be used when the same lens mask is used for producing the phosphor-dot pattern by photographic methods and for final use in the tube. Actually since the light source has a finite size, a value slightly less than that shown at B must be used. In the region between B and C in Fig. 5 it appears necessary to use either an interchangeable mask, as is done in the planar-mask tube, or to restrict the mask hole size below the value B during photographic printing, and then to enlarge it after photographic exposure has been completed.

Application of Lens Formula to Lens-Mask Design

We have shown in (18) above, the relation between the lens voltage ratio V_2/V_1 and the lens convergence ratio r_2/r_1, the latter being equal to D_2/D_1.

The maximum permissible diameter of the electron spot on the target, D_{2max}, is related to the hole spacing D_3 by the expression.

$$\sqrt{3}D_{2max} = D_3. \tag{20}$$

It is desirable to make D_2 smaller than this maximum

value to allow some alignment tolerance without having electron spots overlapping.

If we let the ratio of actual D_2 to D_{2max} equal α, we can write

$$D_2 = \frac{\alpha}{\sqrt{3}} D_3. \tag{21}$$

Combining (21) with (18) gives us the following relation

$$\frac{D_1}{D_3} = \frac{2\alpha}{\sqrt{3}\left[3 - \left(\frac{V_2}{V_1}\right)^{1/2}\right]}. \tag{22}$$

Eq. (22) was used in plotting Fig. 6 which shows D_1/D_3 vs V_2/V_1 for various values of the parameter α.

The horizontal line at $V_2/V_1=1$ represents the design range of the shadow-mask tube. The curves lying between this line and the vertical line at $D_1/D_3=0.9$ represents the design range of the lens-mask tube and shows the possibilities for increased electron beam transmission which is equivalent to increased screen brightness.

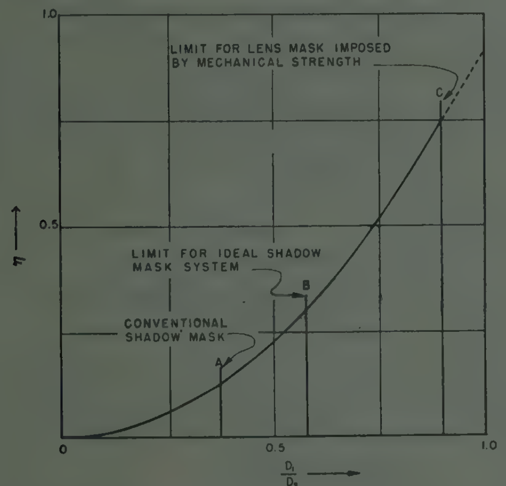

Fig. 5—Electron-beam transmission efficiency η vs D_1/D_3, the ratio of mask-hole diameter to mask-hole spacing.

Factors Limiting the Ratio V_2/V_1

Although it is clear from the preceding discussion that it is desirable to use a large value of V_2/V_1, it must not be assumed that this can be done arbitrarily. Let us consider a given shadow-mask tube design as a prototype for a lens-mask tube. Suppose we keep the mask voltage unchanged and, using a given beam current, increase the value of V_2/V_1 by operating the fluorescent screen at a higher voltage. The fluorescent screen brightness will be increased both because of increased fluorescent screen current (since we may increase D_1/D_3 and therefore increase η) and also because of increased fluorescent screen voltage. At the same time, mask heating will be reduced and scanning power requirements will remain unchanged. The maximum useable value of V_2 will be limited by cold emission effects in the tube and by corona in the external circuit. On the other hand, suppose we increase the value of V_2/V_1 by decreasing the anode and mask voltage V_1. The focused electron-spot size produced by an ideal electron gun at a given beam current will increase[5] as V_1 is reduced. If the upper limit of the beam current is chosen to be such as to produce a given limiting resolving power, we find that for an ideal electron gun this maximum current is proportional to the anode voltage V_1. Thus decreasing V_1 will result in decreased beam current and, although this is partly compensated by increased mask transmission η, there will be no net gain in highlight brightness through using the lens mask with the same electron gun. To reduce V_1 without losing resolving power would require an improvement in electron gun performance which might be achieved, for example, by using a higher cathode current density.

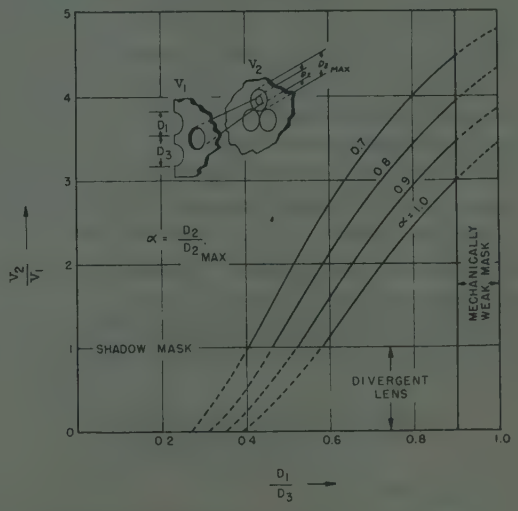

Fig. 6—Voltage ratio V_2/V_1 vs D_1/D_3 for several values of the factor α.

Probably the best compromise for design of a lens-mask tube will include both increase of V_2 above the anode voltage used in a prototype shadow-mask tube and a decrease of V_1 below this value. For example, suppose the prototype shadow-mask tube operates at 24 kv anode voltage. Let V_2 be increased to 36 kv and let V_1 be reduced to 12 kv. Let us assume for the moment that the electron gun performance has been improved to compensate for the lower anode voltage. The ratio of V_2/V_1 is 3 and, choosing an α value of 0.7, we see from Fig. 6 that this calls for D_1/D_3 value of 0.62. From Fig. 5 we see that this corresponds to a beam transmission figure η of 0.38. Assuming the prototype has an η of 0.15, we see that a gain of 2.5 times has been achieved in the current to the fluorescent screen and

[5] R. R. Law, "Factors governing performance of electron guns in television cathode ray tubes," Proc. IRE, vol. 30, pp. 103–105; February, 1942.

TABLE I

RELATIVE PERFORMANCE OF A SHADOW-MASK TUBE AND RELATED LENS-MASK TUBES FOR A VOLTAGE RATIO OF 3

Tube Description	Anode kv	Screen kv	Relative Beam Current	Relative Screen Brightness	Relative Scanning Power	Relative Mask Heating Power
Prototype Shadow-Mask Tube	24 36	24 36	1 1.5	1 2.25	1 1.5	1 2.25
Lens-Mask Tube (Same Electron Gun as Prototype)	12	36	0.5	1.9	0.5	0.18
Lens-Mask Tube (Improved Electron Gun)	12	36	1.0	3.8	0.5	0.36

considering the 50 per cent increase of fluorescent screen voltage, the fluorescent screen brightness is increased to 3.8 times that of the prototype tube. If however the same electron gun as that of the prototype is used in the lens-mask tube, the beam-current limit will be reduced in the same proportion as the anode voltage reduction, which is one-half. The fluorescent screen brightness increase over that of the prototype tube will thus be a factor of 1.9. The scanning power is proportional to the anode voltage and, in the above examples, the lens-mask tube will require only one-half the scanning power required by the prototype tube. By comparison, if we operate the prototype tube at 36 kv anode voltage the screen brightness can be increased by a factor of 2.25 and the scanning power requirement will be increased by a factor of 1.5.

These data appear in Table I above; also the relative power dissipated in the mask for the various cases.

Computation of Electron-Beam Refraction Effects

Planar Lens Mask

In a planar lens-mask three-gun color television tube, the electron acceleration produced by the electric field between the focus mask and the aluminized fluorescent screen causes the electron path to be curved in this region.

Fig. 7 illustrates how the electron ray from the color center C passes through the planar lens mask at A and strikes the fluorescent screen at B. Photographic methods are used to produce the fluorescent dot pattern represented by B from the mask represented by A. In order to project a light ray from A to B its source must be located at a position L which is different from the color center C. It can be seen from Fig. 7 that if A is to be projected into B by both the electron ray and the light ray, then the ratio $(\tan\theta)/(\tan\psi)$, which equals the ratio of the distance $\overline{LM}$ from the projection light source to the lens mask divided by the distance $\overline{CM}$ from the corresponding electron-beam deflection center to the lens mask, must be invariant with θ. The behavior of this ratio as a function of beam deflection angle is computed below.

In Fig. 8 is shown the electron ray incident on the lens mask at an angle θ and striking the fluorescent screen, which is parallel to the mask at a distance h. A rectangular co-ordinate system x, y is used, with the origin 0 at the point of penetration of the focus mask by the electron beam.

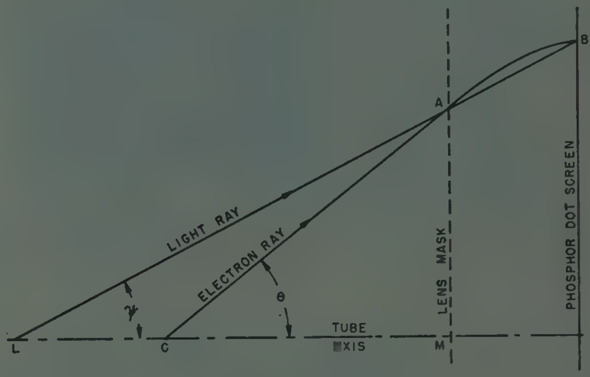

Fig. 7—Diagram to illustrate electron ballistics of the lens mask.

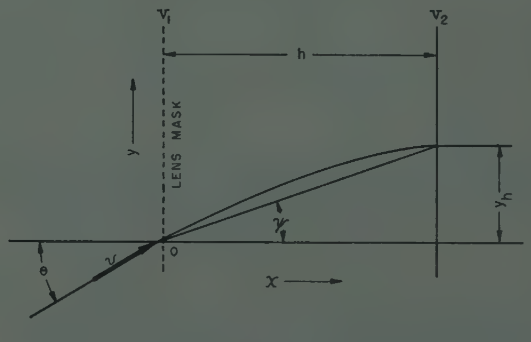

Fig. 8—Comparison of electron ray path and light ray path in a lens-mask system.

The electric field intensity in the region between the lens mask and the screen is $(V_2 - V_1)/h$. The electron motion in the x direction can be expressed by the relation

$$\ddot{x} = \frac{e}{m}\,\frac{V_2 - V_1}{h}. \tag{23}$$

Integrating (23) twice, using the boundary conditions

at the origin which are

$$\dot{x}_0 = v \cos \theta; \qquad \dot{y}_0 = v \sin \theta,$$

we can eliminate "t" and solve for $y = y_h$ when $x = h$ giving for the first intersection of the parabola with the plane $x = h$,

$$y_h = 2h \frac{V_1}{V_2 - V_1} \sin \theta \left[\left(\cos^2 \theta + \frac{V_2 - V_1}{V_1} \right) - \cos \theta \right]. \tag{24}$$

However, from Fig. 8 we see that $\tan \psi = y_h/h$. Thus,

$$\tan \psi = \frac{2V_1}{V_2 - V_1} \sin \theta \cdot \left[\left(\cos^2 \theta + \frac{V_2 - V_1}{V_1} \right)^{1/2} - \cos \theta \right]. \tag{25}$$

Dividing (25) into $\tan \theta$ gives us the equation

$$\frac{\tan \theta}{\tan \psi} = \frac{\frac{V_2}{V_1} - 1}{2 \cos \theta \left[\left(\cos^2 \theta + \frac{V_2}{V_1} - 1 \right)^{1/2} - \cos \theta \right]} \cdot \tag{26}$$

Table II shows computed values of the ratio $(\tan \theta)/(\tan \psi)$ over a range of θ for several values of V_2/V_1.

It is seen that with a planar lens mask and flat fluorescent screen the registry error between the projected light spot and the corresponding electron spot becomes significant when scanning angles are increased beyond 15 or 20 degrees, from the tube axis.

TABLE II

Computed Values of $\tan \theta/\tan \psi$ for Various θ and V_2/V_1 Values

θ In Degrees	$V_2/V_1=3$ $\tan \theta/\tan \psi$	$V_2/V_1=4$ $\tan \theta/\tan \psi$	$V_2/V_1=5$ $\tan \theta/\tan \psi$	$V_2/V_1=6$ $\tan \theta/\tan \psi$
0	1.370	1.500	1.619	1.730
5	1.370	1.500	1.620	1.732
10	1.377	1.512	1.636	1.740
15	1.386	1.520	1.645	1.765
20	1.400	1.550	1.675	1.795
25	1.425	1.578	1.717	1.828
30	1.450	1.620	1.760	1.888
35	1.502	1.675	1.820	1.960
40	1.552	1.731	1.896	2.035
45	1.620	1.822	2.000	2.155

For example, using a V_2/V_1 value of 4 and a deflection angle $\theta = 20$ degrees, we see that if a value of 1.525 is used for $(\tan \theta)/(\tan \psi)$ this will give an error range of ∓ 1.7 per cent over the entire range of θ, which appears to be a practical upper limit.

It is clear that the fluorescent plate dot pattern for the planar lens-mask tube can be made by a single light projection process only at the cost of some error which is small for small scanning angles but increases as the scanning angle increases.

If the light projection process is carried out in a number of concentric zones, each zone being projected with its appropriate angle ψ, the error can be rapidly reduced to negligible proportions.

Spherically-Curved Lens Mask

By using a curved lens mask, the range of *incident angle* in the deflected beam may be greatly reduced. The use of a curved lens mask therefore will permit more accurate photographic register of the required phosphor-dot pattern than will a planar mask.

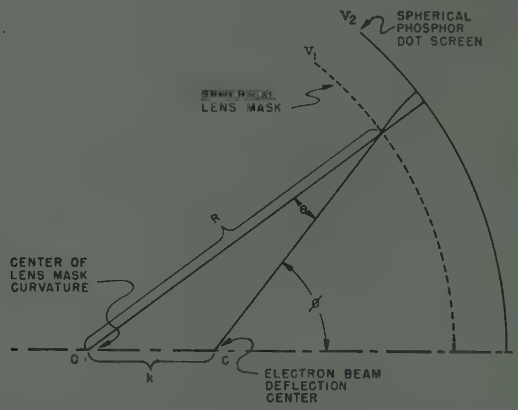

Fig. 9—Diagram of a spherical-lens mask having electron-beam deflection center C closer to the mask than the center of mask curvature, O.

In Fig. 9 the center of deflection C lies closer to the screen than the center of curvature O of the focus mask which has a curvature radius R. It is evident from the figure that

$$\sin \theta = \frac{k}{R} \sin \phi, \tag{27}$$

where

θ = electron beam incidence angle

ϕ = deflection angle.

Thus, whereas the beam-deflection angle equals the angle of incidence of the beam to the mask in the planar lens-mask tube, in the curved lens-mask tube the angle of incidence can be made much smaller than the angle of deflection. The ideal case occurs when the center of curvature of the mask is at the center of deflection so that k = zero and for all deflection angles the beam is perpendicular to the mask and consequently suffers no refraction. The light source for projection is in this case placed in the same position relative to the mask as the electron-beam color center. It is not considered desirable to fulfill this ideal condition with wide angle deflection tubes since it would result in too great a distortion of the picture on the tube face because of the tube face curvature. Values of k/R of about 0.28 have been used and, with this figure, the position of the light source required to make the optical projection of the aperture mask correspond to the electron beam projection varies only very slightly. For example, with k/R

$=0.28$ and deflection angle $\phi=45$ degrees (i.e. 90-degree total deflection angle), we compute θ, the electron beam incidence angle at the mask, to be less than 12 degrees. Referring to Table I we see that the ratio $(\tan\theta)/(\tan\phi)$ (which is required to be constant if the phosphor-dot pattern is to be projected from a single-point light source) is constant within 1 per cent.

Secondary Emission Effects

The lens mask intercepts a fraction of the incident electron beam current which produces secondary electrons at the lens mask on the side facing the electron gun. The secondaries have low initial velocities and random directions, so some of the secondaries will be directed over the lens apertures and will be pulled through the apertures by the electric field. They will fall through a voltage of (V_2-V_1) in bombarding the fluorescent screen, and produce a noticeable illumination of the screen. The secondary electrons will enter a given aperture lens at various incidence angles and low velocities so they will not be focused and will produce a general illumination of all the color phosphor dots.

This is an undesirable condition resulting in an appreciable deterioration of color purity in the lens-mask tube if no means are taken to suppress secondaries. In the shadow-mask tube the secondaries are harmless, since the few which do pass through the apertures strike the fluorescent screen with very low energies and produce essentially no light.

Suppression of Secondary Emission Effects

The general illumination of the phosphor-dot screen produced by secondary electrons from the lens mask can be reduced somewhat by coating the side of the lens mask facing the electron gun with carbon or other material of low secondary emission, but this can never reduce the effect to zero.

It is possible to suppress the passage of the secondary electrons through the lens apertures by applying a small retarding field at the apertures. Tests have been made using a compound lens mask comprising two aligned planar lens masks which were separated by a distance of the order of an aperture radius and which were brought out to separate electrical terminals. By applying a retarding field of 50 volts between the two aperture masks the general illumination of the phosphor-dot screen was completely suppressed whereas the convergent lens action of the compound lens mask was not measurably affected by the weak retarding field. Such a compound lens mask can also be made by coating a lens mask with an insulating material on top of which a thin conducting film is placed by vacuum evaporation.

Conclusion

The three-gun color television tube is capable of substantial improvement in beam efficiency through using a lens mask. The direct benefits of the lens mask are a reduction in mask heating and a reduction in scanning-power requirements. No increase in screen brightness is obtained over a shadow-mask tube operating at the same maximum voltage if the same electron gun is used in each.

The theory and design of both planar and spherical lens masks has been developed. The effects of secondary electrons originating at the mask is described and a method of suppressing these is described.

A number of experimental three-gun color television tubes have been made using planar lens masks by using a mask with small apertures for photographic printing of the phosphor dots and using a similar mask with large holes for the lens mask. To obtain increased screen brightness in the lens mask tube its maximum voltage must be increased over that of the shadow-mask tube or the figure of merit of the electron gun must be improved. The first alternative is limited only by cold emission effects and corona. Improvements in electron gun performance can be taken full advantage of because in the lens-mask tube mask heating is greatly reduced and will not limit beam power.

Appendix I

Design of Lens-Mask Three-Gun Color Television Tubes

The preceding analysis of the aperture lens is readily extended to the case of a two-dimensional aperture lens comprising a longitudinal slot instead of a circular hole.

We note that for a two-dimensional case (1) above is replaced by[6]

$$y'' = \frac{V'}{2V}y' + \frac{V''}{2V}y = 0, \tag{27}$$

which differs only from the circular aperture case in that the third term in (27) is twice as large as the corresponding third term in (1).

Carrying through the same analysis as described above we find that in Region I

$$-y_B' = \frac{r_B}{2V_1}V_B'. \tag{28}$$

Thus y_B' is twice as great as was computed for the circular aperture case.

We note that in Region II the same equation holds as was the case in the circular aperture.

$$y'' = \frac{V'}{2V}y' = 0. \tag{29}$$

The integration of this equation is carried out as was shown above. The integration constant however is evaluated by means of (28) giving as the solution

$$y' = -\frac{y_B}{2(V_1)^{1/2}}\frac{V_B'}{(V_1+ZV_B')^{1/2}}, \tag{30}$$

[6] Pierce, *op. cit.* p. 89.

in which y' comes out to be twice that found for the circular aperture (12).

A second integration gives

$$y = -\frac{y_B}{(V_1)^{1/2}}(V_1 + ZV_B')^{1/2} + K. \qquad (31)$$

Again here the first term on the right-hand side of the equation is double that found in the circular aperture (13).

Solution for the integration of constant K for the boundary conditions $Z=0$; $y=y_B$ gives

$$y = y_B\left[2 - \left(\frac{V}{V_1}\right)^{1/2}\right]. \qquad (32)$$

And taking y_1 as the half-width of the aperture and y_2 as the half-width of the electron spot on the target electrode we get

$$\frac{y_2}{y_1} = 2 - \left(\frac{V_2}{V_1}\right)^{1/2}, \qquad (33)$$

which is the slit lens analog of the aperture lens equation (18).

We see from (33) that

1. $\frac{y_2}{y_1} \to 2$ when $\frac{V_2}{V_1} \to 0$
2. $\frac{y_2}{y_1} = 1$ when $\frac{V_2}{V_1} = 1$
3. $\frac{y_2}{y_1} = 0$ when $\frac{V_2}{V_1} = 4$ (focus on target).[7]

[7] See also J. M. Lafferty, "Beam deflection color television picture tubes," Proc. IRE, vol. 42, pp. 1478–1495 (eq. 23); October, 1954.

The Radio Frequency Coaxial Resistor Using a Tractorial Jacket*

C. T. KOHN†

Summary—**Radio frequency coaxial resistors are usually fitted with an exponential jacket, whose design is based on an approximation by a cylindrical transmission line. This approach is not consistent with the actual field distribution in the termination.**

An approximation which is more appropriate is a conical line, leading to a tractorial jacket. An analysis of this profile is given. It is shown that in the tractorial termination the electric field fulfills the boundary conditions at both the surface of the jacket and the resistor, and that the remaining parts of the field lines are represented fairly well. This ensures a reliable prediction of the properties of the termination. The residual difference between the actual waveform and the assumed TEM wave is expressed by means of a distortion factor.

In the design, the length/diameter ratio of the resistor is the most important parameter. The factors influencing its choice are discussed in detail. For terminations below 80 ohms a length/diameter ratio between 8 and 20 is satisfactory, higher impedances requiring greater ratios.

List of Symbols

C_z = Capacitance per unit length, at distance z.
D = Diameter of outer conductor.
E_r = Resultant field strength on surface of resistor.
E_z = Radial component of field strength on surface of resistor.
E_s = Axial component of field strength on surface of resistor.
F = Field distortion factor [see (26)].
I_z = Current flowing in resistor.
L_z = Inductance per unit length, at distance z.
R = Resistance of resistor per unit length.
R_z = Resistance between $z=0$ and $z=z$.
R_0 = dc resistance of resistor.
Z_{0z} = Characteristic impedance of a lossless transmission line associated with a distance z.
Z_0 = Characteristic impedance of the transmission line to which the termination is to be matched.
Z_{0j} = Characteristic impedance of a lossless transmission line determined by the resistor and a cylindrical jacket.
Z_r = Impedance of resistor.
Z_s = Intrinsic impedance of dielectric.
a = Radius of resistor.
c = Velocity of propagation of electromagnetic waves in dielectric.
d = Diameter of resistor.
l = Length of resistor.
l_{BA} = Length of tractrix.
r = Radius of field lines = length of tangent of tractrix.
t = Thickness of resistive film.
t_{BA} = Propagation time along tractrix.
t_{DA} = Propagation time along resistor.
V_R = Phase velocity along resistor.
w = Width of resistor.
y = Radius of jacket.
z = Distance from end of termination.

* Original manuscript received by the IRE, April 14, 1955.
† British Telecommunications Research Ltd., Taplow, Bucks, Great Britain.

Δ_z = See Fig. 4.
Φ = See Fig. 4.
θ = See Fig. 4.
θ_m = Value of θ at the open end of the termination.
α = Tilt angle of field strength on surface of resistor.
δ = Depth of penetration in resistor.
κ = Relative permittivity of dielectric ($\kappa=1$ for free space).
λ = Free-space wavelength.
ρ = See (5).
ρ_R = Resistivity of carbon film.

I. Introduction

For measurements made on transmission lines it becomes very often necessary to terminate the line with its characteristic impedance. Depending on the transmitted frequency and on the required matching accuracy, various types of resistors are used. At the lowest frequencies (audio frequency) wire wound resistors are satisfactory, expecially if the residual inductance and capacitance of the resistor are minimized by special winding arrangements.[1] At higher frequencies, skin effect becomes important, making the resistance frequency-dependent. This is overcome by using resistors consisting of a ceramic body covered with a thin coating of resistive material, usually metal or cracked carbon. The thickness of the resistive film can be kept so low that it becomes comparable with the depth of penetration of rf currents only at frequencies of thousands of mc. However, the residual reactances make the use of such resistors difficult already in the megacycle region of the frequency spectrum. At still higher frequencies special steps must be taken to eliminate the influence of residual reactances. The most successful way consists in using cylindrically shaped resistors and surrounding them by a coaxial jacket. The jacket serves two purposes; firstly, it eliminates the shunt capacity which is formed by the electric field extending along the length of the resistor in the absence of the jacket;[2] secondly, it forms together with the resistor, a network which can by suitable choice of its parameters, cancel the effect of residual reactances of the resistor. The second point will be now discussed in more detail.

II. Types of Coaxial Terminations

Coaxial terminations, employing a cylindrical resistor as the dissipative element, are used mainly in the vhf band. More precisely they will find application at frequencies at which coaxial lines are commonly used for the transmission of electromagnetic waves. The vhf broadcasting band No. 1 may be considered as the lowest limit where their use is of definite advantage, especially at higher power levels. Such high power terminations, e.g. for 0.5 kw at 100 mc, are commercially available.[3] The main range of application, however, extends from about 300 mc to 3,000 mc in fact, as high up as coaxial lines are used.

In view of the wide frequency band the design will vary. The designs hitherto developed may be conveniently divided in two groups. The first group comprises terminations in which cylindrical elements are used for the cancellation of the input reactance.[4] These resistors give an excellent performance provided their length is short compared with the wavelength. The manufacture is simple, as only cylindrical elements are involved, and also corrections after manufacture are easily made. However, their length being restricted, these terminations are limited to low powers or low frequencies.

The second group consists of terminations built in such a way that all the incoming energy is absorbed completely, without reflections. The absorption process can be carried out over any length of resistor so that there is basically no limitation to the length of the resistor, and hence to the power. This type is therefore used in preference when the power and/or the frequency are high.

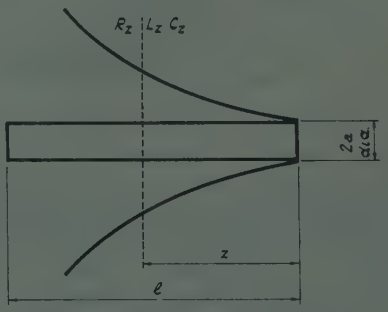

Fig. 1—The principle of jacket design.

To obtain a reflection free performance, the characteristic impedance of the jacket enclosing the resistor is made, at any cross section, equal to the resistance beyond that cross section. If the resistance is assumed to be distributed uniformly over the surface of the resistor, the resistance per unit length being R, the resistance at a distance z from the end of the termination, is $R_z = Rz$ (Fig. 1). The characteristic impedance at this cross section is $Z_{0z} = \sqrt{L_z/C_z}$, L_z and C_z being the inductance and the capacitance respectively per unit length at cross section z of the transmission line formed by the resistor and the jacket. The condition for a reflection free termination is[5]

$$\sqrt{L_z/C_z} = Rz. \tag{1}$$

[1] F. E. Terman, "Radio Engineers Handbook," McGraw-Hill Book Co., Inc., New York, N.Y., Sec. 2; 1943.
[2] G. W. O. Howe, "The behaviour of high resistances at high frequencies," *Wireless Engineer*, vol. 12, pp. 291–295; June, 1935.
[3] "The 'very wide band' dummy load for R.F. power measurements," 37th Physical Society Handbook of Scientific Instruments and Apparatus, The Physical Society, London, p. 101; 1953.
[4] C. T. Kohn, "The design of a radio frequency coaxial resistor," *Proc. IEE* pt. IV, vol. 101, pp. 146–153; February, 1954.
[5] F. A. Harris, "The design of dissipative attenuators for V.H.F. power measurement or other application," Aeronaut. Inspect. Directorate Rep. No. A.I.D. Rad. Elect./5; May, 1950.

For all practical purposes R is made a constant with regard to frequency and to z, i.e., the resistive layer, is thin as compared with the depth of penetration of the rf currents, and it is uniformly applied to the insulating body. So the problem of calculating the profile of the jacket narrows down to determining L_z and C_z.

III. The Exponential Termination

The values of L_z and C_z can be calculated most easily by assuming that over a short length dz the diameter of the jacket is constant, forming together with the re-resistor a *cylindrical* coaxial line; this solution has been described.[6,7] Then

$$L_z = 0.2 \ln \frac{y}{a} \cdots \mu H/m,$$

$$C_z = \frac{55.5\,\kappa}{\ln \frac{y}{a}} \cdots pF/m,$$

where κ is the relative permittivity of the dielectric in the space between the resistor and the jacket.

$$\sqrt{\frac{L_z}{C_z}} = \frac{60}{\sqrt{\kappa}} \ln \frac{y}{a},$$

and

$$y = a \exp \frac{Rz\sqrt{\kappa}}{60}, \tag{2}$$

which gives an exponentially shaped outer conductor.

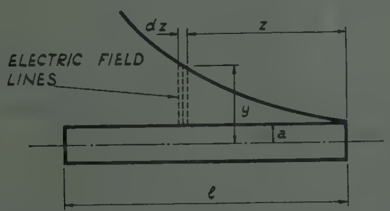

Fig. 2—The assumed field distribution in the exponential termination.

This method of calculating the characteristic impedance is obviously not entirely satisfactory. Fig. 2 shows an element of the outer conductor replaced by the cylindrical approximation dz. The formulas for L_z and C_z are applicable if the electric field between the inner and outer conductor has only a radial component as shown in Fig. 2 and this is so in a cylindrical, coaxial line with negligible losses. In the case here considered the lines must leave the external (perfect) conductor at an angle of 90 degrees, and will reach the surface of the resistor at an angle which differs from 90 degrees. Thus the field lines are curved and do contain an axial component.

In spite of this rather poor approximation to the actual configuration, terminations built on this principle have given voltage standing wave ratios (VSWR) well below 1.2 in a waveband extending from 7.5 to 30 cm.[6] Another source reports terminations with a mismatch of 1–2 per cent at frequencies below 3,000 mc.[8] Exponential terminations have been developed which are suitable for mass production.[9]

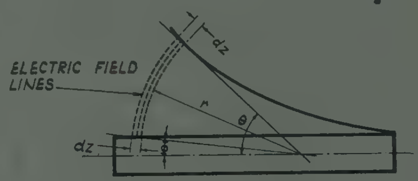

Fig. 3—The assumed field distribution in the tractorial termination.

IV. The Tractorial Termination

A better approximation to the field configuration has been proposed,[5,10] which give also a first order mathematical treatment of the termination. There the characteristic impedance is calculated by treating a short length of the termination as a *conical* coaxial line (Fig. 3), tangent to the outer conductor. In such a transmission line the electric field lines are circular arcs. The characteristic impedance is

$$\sqrt{\frac{L_z}{C_z}} = \frac{60}{\sqrt{\kappa}} \ln \frac{\tan \theta/2}{\tan \Phi/2}, \tag{3}$$

and the profile of the jacket is a tractrix.

This solution deserves closer examination. The assumed field distribution between the jacket and resistor is obviously much nearer the actual configuration than in the exponential termination. At the outer conductor, the boundary conditions are fulfilled, the field lines being perpendicular to the surface. Also the assumption that the field lines are curved will hold better than the straight line representation in the exponential solution. Only at the surface of the resistor the assumed and actual conditions differ. The over-all performance of the termination determined in this way should agree better with the calculation than in the exponential solution. In fact, the definite superiority of this shape as compared with an exponential profile is claimed to have been confirmed experimentally.[11] It is therefore desirable to

[6] C. G. Montgomery, "Technique of microwave measurements," McGraw-Hill Book Co., Inc., New York, N.Y., sec. 12; pp. 722–726; 1947.

[7] Mullard Radio Valve Co., "Improvements in or Relating to High Frequency Resistances," Brit. Patent Spec. No. 554 630; August 13, 1943.

[8] A. Jaumann, "Ein thermischer Leistungsmesser als Spannungsnormal im Frequenzgebiet 0 bis 3000 MHz," *Siemens Zeitschrift*, vol. 27, pp. 416–420; December, 1953.

[9] Bird Electronic Corporation, "Improvements Relating to High Frequency Coaxial Circuit Components," British Patent Specification No. 641 607; August 16, 1950.

[10] I. A. Harris, "Improvements in or Relating to Electric Wave Attenuators and the Like," Brit. Patent Spec. No. 670 339; April 16, 1952.

[11] I. A. Harris, "Discussion," on Ref. 4, *Proc. IEE*, pt. IV, vol. 101, p. 299; August, 1954.

explore the properties of the tractorial profile with greater accuracy than has been done, so that its application to high precision terminations will be made possible.[12]

V. General Analysis of the Tractorial Termination

The geometry of the termination is shown in Fig. 4. The cylindrical resistor has a resistance of Z_0 which is equal to the characteristic impedance of the transmission line to be terminated. The length of the resistor is l,

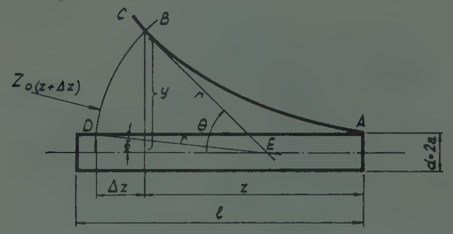

Fig. 4—The geometry of the tractorial termination.

and its diameter is $d=2a$. The jacket AC forms with the resistor a transmission line which will be approximated—at any cross section—by a conical line tangent to the outer conductor. For a point B on the outer conductor the approximation consists of the cones formed by ED and EB. The resistance lying beyond D is

$$Z_0 \frac{z + \Delta z}{l},$$

thus the characteristic impedance at the spherical cross section passing through D and B, which is

$$\frac{60}{\sqrt{\kappa}} \ln \frac{\tan \theta/2}{\tan \Phi/2},$$

must equal

$$Z_0 \frac{z + \Delta z}{l};$$

this gives

$$\tan \frac{\theta}{2} = \tan \frac{\Phi}{2} \exp \rho(z + \Delta z), \tag{4}$$

where

$$\rho = \frac{Z_0\sqrt{\kappa}}{60l}. \tag{5}$$

In (4) only ρ is known, and additional information is required regarding Φ. This can be obtained by taking the logarithm of (4) and differentiating

$$\frac{d\theta}{dz} \operatorname{cosec} \theta - \frac{d\Phi}{dz} \operatorname{cosec} \Phi = \rho\left(1 + \frac{d\Delta z}{dz}\right). \tag{6}$$

[12] A comprehensive treatment of this subject appeared after this paper was accepted for publication. See: I. A. Harris, "The theory and design of coaxial resistor mounts for the frequency band 0–4000 Mc/s," Inst. Elec. Eng., Monograph No. 132 R; May, 1955.

From Fig. 4, $\Delta z = a \cot \Phi - y \cot \theta$, after differentiation

$$\frac{d\Delta z}{dz} = -a \frac{d\Phi}{dz} \operatorname{cosec}^2 \Phi + y \frac{d\theta}{dz} \operatorname{cosec}^2 \theta - \frac{dy}{dz} \cot \theta, \tag{7}$$

where dy/dz is equal to $\tan \theta$ because the profile was postulated to be tangent to the approximating cone. Substituting (7) into (6):

$$\begin{aligned} &\frac{d\theta}{dz} \operatorname{cosec} \theta - \frac{d\Phi}{dz} \operatorname{cosec} \Phi \\ &\quad = \rho\left(y \frac{d\theta}{dz} \operatorname{cosec}^2 \theta - a \frac{d\Phi}{dz} \operatorname{cosec}^2 \Phi\right) \\ &\quad = \rho r\left(\frac{d\theta}{dz} \operatorname{cosec} \theta - \frac{d\Phi}{dz} \operatorname{cosec} \Phi\right). \end{aligned} \tag{8}$$

Now

$$\begin{aligned} &\int\left(\frac{d\theta}{dz} \operatorname{cosec} \theta - \frac{d\Phi}{dz} \operatorname{cosec} \Phi\right) dz \\ &\quad = \ln \tan \frac{\theta}{2} - \ln \tan \frac{\Phi}{2} + \text{constant} \\ &\quad = \rho(z + \Delta z) + \text{constant}. \end{aligned} \tag{9}$$

As the right-hand side is not constant,

$$\frac{d\theta}{dz} \operatorname{cosec} \theta - \frac{d\Phi}{dz} \operatorname{cosec} \Phi \neq 0. \tag{10}$$

Thus cancelling this factor in (8)

$$\rho r = 1, \tag{11}$$

and from (5)

$$r = \frac{60l}{Z_0\sqrt{\kappa}} = \text{constant}. \tag{12}$$

This reveals that all the electric field lines in the termination have a constant radius of curvature. Furthermore, the angle Φ has a constant value of

$$\Phi = \arcsin a/r = \arcsin \frac{Z_0\sqrt{\kappa}}{60} \frac{a}{l}. \tag{13}$$

Also, in any design, the arcs representing the field lines impinge on the surface of the resistor, over all its length, at the same angle 90 degrees $-\Phi$ degrees.

From Fig. 4 the length of the tangent to the profile between its point of tangency and the intercept with the z-axis is equal to r, thus having a constant value. The profile is, therefore, a tractrix. This result has been obtained without making any mathematical approximations, and without imposing any limitations on the values of θ, Φ, ρ, l or Z_0. The angle θ may assume any value between Φ and 90 degrees.

The calculation of the profile for a given resistor consists in assuming suitable values for $z+\Delta z$ and calculating θ from (4). Then y and Δz can be determined from (Fig. 4)

$$y = a\frac{\sin\theta}{\sin\Phi}, \tag{14}$$

$$\Delta z = a\frac{\cos\Phi - \cos\theta}{\sin\Phi}. \tag{15}$$

The parameters Δz, θ and Φ can be eliminated from (4) by substitution from (13), (14), and (15). This gives

$$\frac{z}{l} = \frac{60}{Z_0\sqrt{\kappa}}\left[\ln\frac{1-\sqrt{1-y^2/r^2}}{y/r} + \sqrt{1-y^2/r^2} - \left(\ln\frac{1-\sqrt{1-a^2/r^2}}{a/r} + \sqrt{1-a^2/r^2}\right)\right], \tag{16}$$

or, after expanding the logarithms and the roots,

$$\frac{z}{l} \simeq \frac{60}{Z_0\sqrt{\kappa}}\ln\frac{y}{a} - \frac{15\sin^2\Phi}{Z_0\sqrt{\kappa}}\left[\left(\frac{y^2}{a^2}-1\right) + \frac{\sin^2\Phi}{8}\left(\frac{y^4}{a^4}-1\right) + \frac{\sin^4\Phi}{24}\left(\frac{y^6}{a^6}-1\right) + \cdots\right]. \tag{17}$$

The last equation shows the difference between the exponential and the tractorial shape, the first term on the right-hand side representing the exponential curve, the second the difference. The tractorial profile opens out quicker than the exponential, but the difference becomes small when Φ is small.

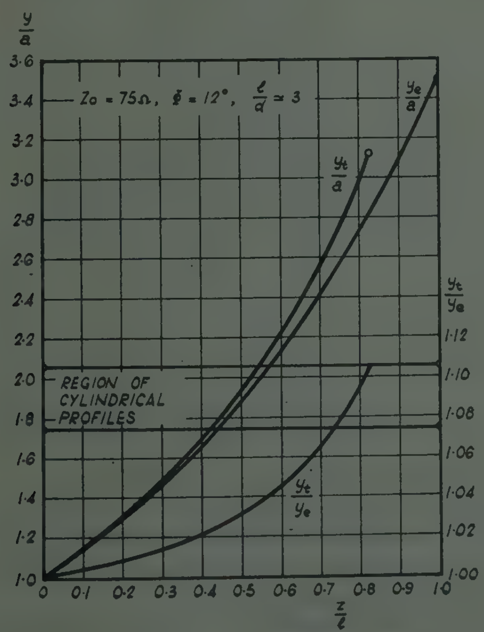

Fig. 5—Profiles of various jackets.

A comparison of the jacket profiles in question will now be made by means of an example. A 75-ohm termination with a resistor having $\Phi = 12$ degrees (length/diameter $=3$), has been calculated from (2) and (4), and the profiles are plotted in Fig. 5, as a function of z/l. The unusually low l/d ratio was chosen to make the difference between the curves more pronounced. The exponential profile (curve y_e/a) extends over all the length of the resistor and reaches a final diameter of $3.49a$ which corresponds to the diameter of a 75-ohm cylindrical line. The tractrix (curve y_t/a) extends only over 83 per cent of the resistor length and the final diameter is smaller. In general, it resembles the exponential line, being however, somewhat steeper. The relationship between both profiles is better seen in the ratio curve y_t/y_e which shows that the difference is small at the beginning, but increases rather quickly towards the open end where it reaches 10 per cent.

It has been mentioned in Section II that cylindrical jackets also can be used in the design of coaxial resistors. The characteristic impedance of such jackets Z_{0j} (with reference to the resistor diameter) varies between $Z_0/\sqrt{5}$ and $Z_0/\sqrt{3}$.[4] These limits are shown, for comparison, in Fig. 5. Cylindrical jackets have considerably smaller diameters than the curvilinear profiles, which is advantageous in designing the transition between resistor and transmission line because the discontinuity reactances are smaller.

VI. Conditions on the Surface of the Resistor

In the derivation of the tractorial profile the greatest discrepancy between assumptions and actual conditions seemed to appear on the surface of the resistor. The conical line substitution requires that the field lines arrive on the surface of the inner, conical, perfect conductor at an angle of 90 degrees, whereas the inner conductor has actually a cylindrical shape, so that the field lines form an angle of 90 degrees$-\Phi$ degrees with its surface. Furthermore, it is not a perfect conductor. It is therefore necessary to examine the effect of this discrepancy on the validity of the analysis.

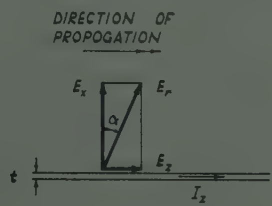

Fig. 6—The field at the surface of the resistor.

When an electromagnetic wave travels along the surface of a plane, perfect conductor, the electric field lines form an angle of 90 degrees with the surface of the conductor. When the perfect conductor is replaced by one of finite resistivity, the current I_z, flowing in the direction of propagation, produces a voltage drop in the resistor. If the total impedance of the resistor is Z_r, the field strength along the resistor E_z (Fig. 6) is equal to the voltage drop per unit length

$$E_z = I_z Z_r / l, \tag{18}$$

where I_z is the current flowing through the resistor. The total field strength E_r just outside the surface of the

resistor is determined as the product of the transverse magnetic field and the intrinsic impedance Z_s of the dielectric surrounding the resistor.[13] As the magnetic field is equal to the current per unit width flowing in the resistor,

$$E_r = I_z Z_s / w, \tag{19}$$

where w is the total width of the resistor. The resulting field E_r is tilted in the direction of the energy flow by an angle α which is determined by

$$\sin \alpha = \frac{E_z}{E_r} = \frac{Z_r w}{Z_s l}. \tag{20}$$

This equation, which was derived for a flat surface, can be also applied to a cylindrical surface, if the thickness of the conducting layer is small compared with the radius of the cylinder. This must be always the case, because otherwise the impedance of the resistor would not be frequency independent.

The impedance of a tubular resistor is[14]

$$\frac{Z_r}{R_0} = \frac{t}{\delta} \frac{\sinh(2t/\delta) + \sin(2t/\delta)}{\cosh(2t/\delta) - \cos(2t/\delta)} + j\frac{t}{\delta} \frac{\sinh(2t/\delta) - \sin(2t/\delta)}{\cosh(2t/\delta) - \cos(2t/\delta)}, \tag{21}$$

where

t is the wall thickness of the tubular conductor,

δ is the depth of penetration of rf currents,

R_0 is the dc resistance of the tubular conductor.

This formula neglects any resistor capacitive currents. Expansion of the functions on the right-hand side yields

$$\frac{Z_r}{R_0} = 1 + \frac{4}{45}\left(\frac{t}{\delta}\right)^4 + j\frac{2}{3}\left(\frac{t}{\delta}\right)^2\left[1 - \frac{8}{315}\left(\frac{t}{\delta}\right)^4\right], \tag{22}$$

which is accurate to 0.1 per cent for $t/\delta < 1$. Making $t/\delta = 0.1$, the impedance of the resistor becomes $Z_r/R_0 = 1{,}000 + j0.007$. The resistive component is equal to the dc resistance, and the reactive component is negligible. Further improvement can be obtained by lowering t/δ. Thus the total impedance is resistive and equals $R_0 = Z_0$. The value of Z_s being $120\pi/\sqrt{\kappa}$ ohms, (20) yields

$$\sin \alpha = \frac{R_0 \pi d \sqrt{\kappa}}{l 120\pi} = \frac{Z_0\sqrt{\kappa}}{120} \frac{d}{l}. \tag{23}$$

On the other hand, from (13)

$$\sin \Phi = \frac{Z_0 \sqrt{\kappa} d}{120 l}. \tag{24}$$

Hence

$$\alpha = \Phi. \tag{25}$$

[13] S. Ramo and J. R. Whinnery, "Fields and Waves in Modern Radio," John Wiley and Sons, New York, N.Y., sec. 8, pp. 280–292; 1948.

[14] *Ibid.*, sec. 6, pp. 218–221.

This is rather a remarkable result. It indicates that the tilt of the field lines at the surface of the resistor, resulting from its finite resistivity, is the same as the angle at which the lines arrive to the resistor, because of its being cylindrical instead of conical. Thus the equations of Section V, based on the conical line approximation, prove to be also a good representation of the electromagnetic conditions on the surface of the resistor. In this way, the last major inaccuracy which seemed to be caused by the approximation of the inner conical line by a cylinder is removed. The equality of α and Φ was obtained without any restriction as to the dimensions of the resistor, to its magnitude, or to the frequency involved. The derivation however is only approximate, and it holds better when the tilt and Φ are small.

VII. Conditions for the Existence of a TEM Wave

The calculation of the tractorial profile in the preceding sections is based on the assumption that the field in the termination has the simple, spherical configuration shown in Fig. 7. Whether such a field actually exists in the termination could be decided only by solving Maxwell's equations for this case. However, transmission line equations can predict at least some conditions, which are necessary for the propagation of a spherical TEM wave, although they may not be sufficient.

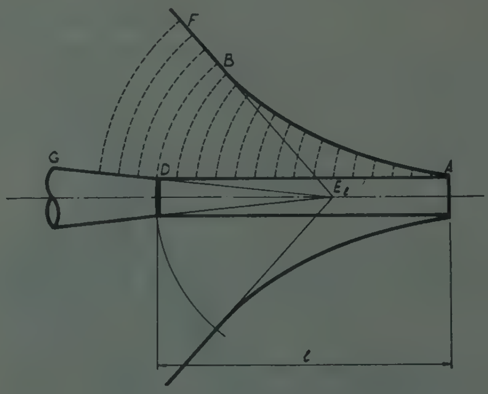

Fig. 7—Transition from resistor to transmission line.

In a TEM wave the wavefront BD (Fig. 7) travels down the termination in such a way that all points of the front arrive to the end of the termination at the same time. In particular, the propagation time from B to A and from D to A must be equal.

Denoting by l_{BA} the length of the tractrix BA, by c the propagation velocity along a perfect conductor, equal to the velocity of light, the propagation time t_{BA} is l_{BA}/c. For the path DA the propagation time $t_{BA} = l/v_R$ where v_R is the phase velocity along the resistor. As the wave propagates with a velocity c towards the apex of the approximation cone and is tilted by an angle α, $v_R = c/\cos\alpha$. The relative time difference $F = (t_{BA} - t_{DA}) t_{DA}$ will be a measure of the field imperfection; it will be called "field distortion factor."

The field distortion factor is

$$F = \frac{t_{BA} - t_{DA}}{t_{DA}} = \left(\frac{l_{BA}}{c} - \frac{l \cos \alpha}{c}\right) \Big/ \frac{l \cos \alpha}{c}$$

$$= \frac{l_{BA}}{l \cos \alpha} - 1. \tag{26}$$

The length of the profile is calculated to

$$\frac{l_{BA}}{l} = \frac{60}{Z_0\sqrt{\kappa}} \ln \frac{\sin \theta_m}{\sin \Phi}$$

$$= 1 - \frac{60}{Z_0\sqrt{\kappa}} \ln \left[1 + (\exp Z_0\sqrt{\kappa}/30 - 1)\sin^2 \Phi/2\right]. \tag{27}$$

Hence the field distortion factor, substituting $\alpha = \Phi$,

$$F = \frac{1}{\cos \Phi}\left\{1 - \frac{60}{Z_0\sqrt{\kappa}} \ln \left[1 + \left(\exp \frac{Z_0\sqrt{\kappa}}{30} - 1\right) \cdot \sin^2 \frac{\Phi}{2}\right\} - 1. \tag{28}$$

Expanding the ln and cos Φ function, and neglecting small terms,

$$F \simeq \tfrac{1}{2} \sin^2 \Phi \left[1 - \frac{30}{Z_0\sqrt{\kappa}}\left(\exp \frac{Z_0\sqrt{\kappa}}{30} - 1\right)\right]. \tag{29}$$

The approximation is accurate within 2 per cent in the range of Z_0, and Φ here considered.

In any particular design the factor in the square brackets is given and is $\neq 0$, so that $F \neq 0$. This means that the wave does not travel down the termination in the assumed manner. To obtain conditions approaching TEM propagation F has to be made small. There is no experimental information available as to the relationship between F and the standing-wave ratio; however it can be expected that F is of the same order as the reflection coefficient. In high quality terminations a value of $F < 0.01$ may be desirable.

When a decision as to the permissible value of F is made the length/diameter ratio of the resistor results from (29) which can be transformed to

$$\frac{l}{d} = \frac{Z_0\sqrt{\kappa}}{120} \sqrt{\left|\frac{1}{2F}\left[1 - \frac{30}{Z_0\sqrt{\kappa}}\left(\exp \frac{Z_0\sqrt{\kappa}}{30} - 1\right)\right]\right|}. \tag{30}$$

Eq. (30) is plotted in Fig. 8 for several values of F. Where the accuracy was not high enough, the accurate formula (28) was used. The design of a termination will usually start with assuming a value for F and reading off the graph the lowest permissible l/d ratio for the specified impedance. It will be seen that (30) follows rather closely the second set of curves for constant angles at the open end of the termination θ_m. This leads to the conclusion that the field distortion depends basically only on the angle the tractrix forms with the axis at the open end of the termination, no matter what the length of the resistor or characteristic impedance. Good terminations can be obtained only when angle θ_m is small.

VIII. Conditions at the Open End of the Resistor

Coaxial resistors are usually designed to work in connection with coaxial lines. For convenience, the resistor is fitted with a plug of suitable diameter, which is as a rule much smaller than the final diameter of the resistor jacket. Between these two diameters a coaxial adapter piece must be fitted, which has to be designed in such a way that it produces no reflections.

The first step in the design of the adapter is to find a reflection-free transition from the resistor to a lossless transmission line. A solution to this problem is shown in Fig. 7. BD is the first field line of the resistor; it is part of a circle of radius r, the center of the circle being in E_l. BD forms obviously an angle of 90 degrees with the jacket BA, and an angle of $90-\Phi$ degrees with the surface of the resistor.

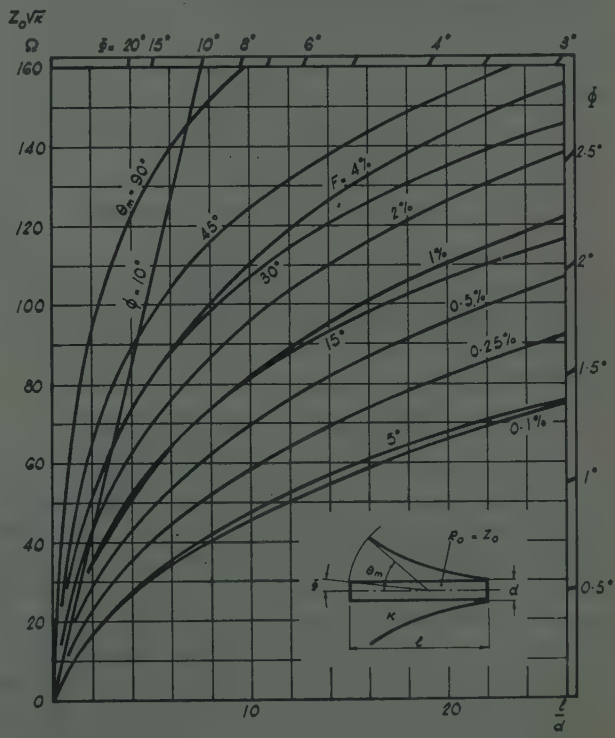

Fig. 8—Dependence of θ_m, F and Φ on the characteristic impedance and on the l/d ratio.

If there are not to be any reflections, the first field line of the resistor must be, at the same time, the last field line of the transmission line to which the resistor is attached. This condition will be fulfilled if the transmission line is a conical line whose apex is in E_l. Of this line only the part BF and DG is utilized. The field line BD which is now considered to be the last field line of the conical line forms right angles with both the outer and inner conductor, this being the boundary condition in perfect conductors. Any preceding field line is again a circle

centered on E_l, the radius being now $r_1 < r$. At point D there is a discontinuity of slope, which is such that it just compensates for the discontinuity of conductivity.

This property of the tractorial termination, to merge with a conical, lossless transmission line without producing reflections, is of definite advantage as it permits any matching operations to be carried out between lossless transmission lines.

The transition from the divergent conical line to the plug diameter can now be done by known methods. Usually a convergent conical line is used for this purpose (Fig. 9), and the transition between both conical lines is made by means of a cylindrical, or barrel-shaped, line.[5,10] If discontinuities appear at the junctions of the lines, compensating elements must be provided.

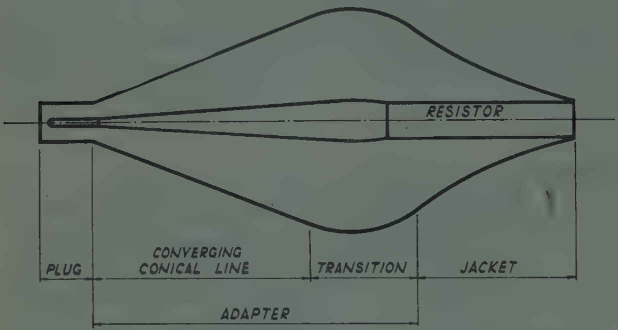

Fig. 9—General layout of a tractorial termination.

The length of the conical line between the tractrix and the transition piece can be kept short, but it should be long enough to produce a pure, spherical wave, centered on E_l.

IX. The Length/Diameter Ratio

It is now possible to examine various points which arise when a termination has actually to be designed. The designer is usually given two quantities, the characteristic impedance Z_0 to be terminated and the power to be dissipated in the resistor. The second quantity determines the cooling surface of the resistor $= \pi dl$, and there is still one degree of freedom in the choice of d and l. For a given Z_0 and heat dissipation a variety of terminations can be built, using short resistors of large diameter or long ones with small diameter. On the correct choice of the slenderness l/d of the resistor depends the performance ultimately obtainable. As the l/d ratio turns out to be the most important design factor, it will be convenient to assume $Z_0\sqrt{\kappa}$ and d as given quantities, and to treat l/d as the quantity to be determined. The effect of the l/d ratio on various design aspects will now be examined in more detail.

The design equations (4), (5), and (11)–(15) developed in Section V, apply to the whole length of a tractrix, i.e., for Φ degrees $< \theta < 90$ degrees, and in principle, terminations could be designed with θ extending up to 90 degrees. This is the limit beyond which the outer conductor cannot be physically expanded. The mathematical formulation for this limit is obtained by substituting $\theta_m = 90$ degrees in (4), which gives

$$\tan \Phi/2 = \exp(-Z_0\sqrt{\kappa}/60), \tag{31}$$

with Φ determined by (13). θ_m is the value of θ at the open end of the termination and is associated with $z + \Delta z = l$. The relationship between $Z_0\sqrt{\kappa}$ and l/d for the maximum possible angle $\theta_m = 90$ degrees is plotted in Fig. 8. It can be seen that there exists a minimum value for l/d below which, for a given Z_0, a tractrix cannot be constructed.

In practice this limit of 90 degrees will not be utilized because of the difficulties arising from the design of the reduction to the plug diameter, Fig. 9. With $\theta_m = 90$ degrees the outer conductor would require a bend of more than 90 degrees to join the convergent taper leading to the plug. In a precision termination the overall VSWR should not exceed 1.01, and therefore reflections in the nonattenuating part of the termination must be kept well below 1 per cent. To achieve this, large or rapid changes of direction must be avoided. For this reason it is suggested that $\theta_m = 45$ degrees should never be exceeded in ordinary resistors, and 30 degrees in precision resistors; the lower θ_m is made the easier it is to design the adapter.

To illustrate the limitations imposed by lower values of θ_m several curves for $\theta_m < 90$ degrees have also been plotted in Fig. 8. It is evident that low values of θ_m can be easily obtained in the practically most important region of $40 < Z_0 < 75$ ohms. At 75 ohms a resistor with an l/d ratio of 6 has $\theta_m = 20$ degrees, but at 105 ohms a similar resistor will require $\theta_m = 45$ degrees. In the latter case a resistor with $l/d = 12$ would be more adequate.

Another limitation may be imposed in some cases by the value of Φ. It has been shown in Section VI that the electric field lines, assumed in the conical line geometry, form with the resistor an angle which is just equal to the tilt angle resulting from the losses in the resistor. In view of the approximations made in the derivation, this equality can be considered to hold only approximately, but the error vanishes when Φ and α become small. It will be, therefore, wise to use, as a precautionary measure, rather low values for Φ, say $\Phi < 10$ degrees. For this value a Φ line is plotted in Fig. 8, and other values are marked along the perimeter of the graph so that further $\Phi = \text{const.}$ lines can be drawn, if required; they are straight lines passing through the origin. From the position of the $\Phi = 10$ degrees line it will be seen that below $Z_0 = 80$ ohms the lowest l/d ratio is determined by Φ, rather than by the $\theta_m = 30$ degrees line.

The designer has also to take steps to prevent the generation of higher-order waves in the termination, because the calculation is based on the presence of the principal (TEM) mode alone. When other modes are present, the termination acquires a reactive component and consequently the VSWR increases. Higher modes

can be generated when the wavelength drops below a critical value. The approximate conditions for non-propagation of other modes are[15]

$$\lambda > \sqrt{\kappa}\,(D - d) \qquad \text{for } TM \text{ waves,} \tag{32}$$

$$\lambda > \sqrt{\kappa}\,\frac{\pi}{2}\,(D + d) \qquad \text{for } TE \text{ waves,} \tag{33}$$

where D and d are the diameters of the outer and inner conductor respectively, and λ is the free space wavelength. It is the second condition which puts greater restrictions on the dimensions of the termination. If a 75-ohm termination is to be used up to a frequency of 3,000 mc, the outer diameter must nowhere exceed 5 cm. The largest diameter of the termination is in the transition piece. To keep this diameter low the diameter of the resistor must be small, and also the value of θ_m must be low. Both conditions will be fulfilled when l/d is large.

Very severe limitations as to the l/d ratio may arise when performance requirements are stringent [(30) and F-curves in Fig. 8]. Inspection of Fig. 8 shows that if for constructional reasons an angle θ_m of 30 degrees is satisfactory, the l/d ratio for $Z_0 = 75$ ohm need be made 4. However, if at the same time a field distortion factor of 1 per cent is specified, the l/d ratio has to be increased to 8.2, corresponding to $\theta_m = 15$ degrees.

It can be seen that all the effects discussed in this section impose a lower limit for the l/d ratio of the resistor. In general, the longer and thinner the resistor the better performance may be expected. This is consistent with the general principle that in any transmission line with a varying cross section the slower the cross section changes, the smaller the reflections become.

Against the electrical arguments favoring long resistors, mechanical reasons have to be considered, calling for a limitation of the length. The longer the resistor the weaker it is mechanically, and the greater are the difficulties in its manufacture and assembly. However, $\frac{1}{4}$-inch diameter ceramic rods of 4-inch length, ground to close tolerances, are readily available, corresponding to $l/d = 16$, and longer pieces can also be obtained.

Another limitation may arise from the resistivity of the film material. According to (22) the film thickness ought not to exceed 0.1 of the depth of penetration. Thus putting

$$\delta = \frac{1}{\pi}\sqrt{\frac{\lambda \rho_R}{120}}, \tag{34}$$

$$t = \frac{l \rho_R}{\pi R_0 d}, \tag{35}$$

where ρ_R is the resistivity of the film in ohm-cm, and λ is in cm, the condition for independence of frequency becomes

$$\frac{t}{\delta} = \frac{l}{R_0 d}\sqrt{\frac{120 \rho_R}{\lambda}} < 0.1, \tag{36}$$

or

$$\frac{l}{d} < 0.1 R_0 \sqrt{\frac{\lambda}{120 \rho_R}}. \tag{37}$$

For cracked carbon ρ_R has a value of 0.2 ohm-cm.[16] Then

$$\frac{l}{d} < 0.2 R_0 \sqrt{\lambda}. \tag{38}$$

If a 75-ohm resistor is to work down to $\lambda = 9$ cm, l/d must remain below 45. This is a high figure and limitation resulting from this factor should not be serious.

In view of the advantages offered by a long resistors, a high l/d ratio should be aimed at in the design. Only when θ and Φ become very low, say 5 and 2 degrees respectively, the directional changes of the profile are so small that no substantial performance improvement can be expected by further reducing θ and Φ. Consequently, subject to the limitations discussed, the practical l/d ratio limits for resistances up to 80 ohms, with air as the dielectric, may be given as

$$8 - 10 < l/d < 20. \tag{39}$$

X. The Influence of Liquid Coolants

In cases where a high power termination is required, cooling by means of an insulating liquid may be considered. In this case the liquid must have a negligible power factor because it is assumed in the calculations here presented that the transverse conductance is zero.

The presence of the dielectric impairs the performance of the termination. From Fig. 8, a 75-ohm air cooled termination with $F = 1$ per cent has an $l/d = 8.2$. When the same resistor is built for operation in a cooling medium with $\kappa = 2$, $Z_0\sqrt{\kappa}$ becomes 106 ohms and F increases above 4 per cent. At the same time the tilt angle goes up from 4.3 degrees to 6.2 degrees, θ_m from 15 degrees to 33 degrees, and the maximum diameter increases by a factor of 1.45, which in turn lowers the maximum frequency at which higher modes can appear, to nearly one half. To restore the original performance, the l/d ratio has to be raised to 18, i.e., 2.2 times.

To keep the adverse effects of coolants small, their permittivity must be as low as possible. Often forced air cooling may be the best solution.

XI. Conclusion

The calculation of the tractorial termination presented in Section V to Section X is based on transmission line theory. Therefore, it cannot supply a rigorous

[15] *Ibid.*, sec. 9, pp. 333–335.

[16] R. O. Grisdale, A. C. Pfister, and W. Van Roosbrock," Pyrolytic film resistors: carbon and borocarbon," *Bell Sys. Tech. Jour.*, vol. 30, pp. 271–314; 1951.

and complete solution, such as would be obtained from Maxwell's equations. However, adopting a conical line as approximation for the termination in place of the usual cylindrical line, the field pattern between jacket and resistor can be represented fairly accurately. The field configuration fulfills the boundary conditions both at the jacket and at the resistor, and the introduction of circular field lines is certainly a close approximation to actual conditions. This is a vast improvement over the exponential resistor which does not fulfill any of the boundary conditions, and which assumes straight field lines.

No method has been found of predicting the residual VSWR of a termination directly from transmission line equations. Instead, the field distortion factor F has been introduced as a criterion of field imperfection. When experimental evidence of the relationship between F and the VSWR becomes available, F may acquire a more quantitative meaning in designing terminations.

The treatment is limited to the jacket only, but it is essential to keep in mind that the quality of the resistor itself is of as much importance as the jacket design. The greatest difficulty seems to be in obtaining resistors with really uniformly distributed surface resistance; this may prove to be the ultimate limitation in the attainable accuracy.

So far, no terminations have been built in accordance with this treatment so that its soundness has yet to be proved experimentally. However, it is expected that the calculated performance of the tractorial resistor will agree with its actual performance much more closely than in the case of an exponential resistor. This should encourage the construction of tractorial terminations, which are likely to supersede, in future, the exponential profile used at present.

XII. Acknowledgment

The author wishes to thank F. O. Morrell, B.Sc., M.I.E.E., Director of Research of British Telecommunications Research Ltd., for permission to publish this paper. He is also indebted to J. R. W. Smith, M.Sc., A. Inst. P., and Miss J. Turner, B.Sc. of the Mathematical Section, for the proof that the profile is a tractrix, for general discussions, and for the numerical calculations.

A Time-Sampling and Amplitude-Quantizing Tube*

R. P. STONE†, SENIOR MEMBER, IRE, C. W. MUELLER†, SENIOR MEMBER, IRE, AND W. M. WEBSTER,† SENIOR MEMBER, IRE

Summary—The possibility of a saving of bandwidth—or of transmitting additional information in a given bandwidth—by means of amplitude quantizing and time sampling is reviewed. The requirements on a tube to simultaneously time sample and quantize a video input, and to produce a residue output, are outlined.

Beam deflection-type tubes were successfully built and tested which perform all of these functions. They will change a continuous signal into a quantized signal having six discrete amplitude levels. The signal may also be simultaneously sampled as often as ten million times per second. A residue signal is also generated. The tube response is sufficiently accurate to meet the requirements of the system outlined. The stability of operation is such that after initial setup no critical operating conditions or adjustments are involved.

Two types of output structure have been used, both of which permit the external adjustment of the output amplitude levels. The tube operates with an anode voltage of 300 volts. While the maximum operating beam current is only 55 microamperes, the signal-to-noise ratio of the tube is computed to be 55 db.

Introduction

The portion of the electromagnetic spectrum which can be used for communication is limited by such practical considerations as the propagation characteristics of the atmosphere. Since, in general, at a given location, each transmission must use exclusively a finite portion of the available spectrum, the number of channels which may be assigned is necessarily in inverse proportion to their average bandwidth. It is therefore highly desirable to reduce the required bandwidth of each channel as much as possible. Until recently it was believed that the bandwidth of a communications channel must be at least as great as the highest frequency component in the information to be transmitted. However, recent mathematical development of communication theory has indicated the possibility of exchanging transmitter power for bandwidth, providing one is willing to eliminate the transmission of superfluous information.[1–8] This actually means a loss in accuracy of the transmitted signal; but neither the ear

* Original manuscript received by the IRE, February 28, 1955; revised manuscript received, May 31, 1955.
† RCA Labs. Div., Princeton, N. J.

[1] F. Okolicsanyi, British Patent 505,673; May 11, 1939.
[2] D. Gabor, "Theory of communications," *Jour. IEE* (*British*), vol. 93, p. 429; September, 1946.
[3] N. Wiener, "The Extrapolation, Interpolation and Smoothing of Stationary Time Series," Cambridge Technology Press; 1949.
[4] C. E. Shannon, "Communication in the presence of noise," Proc. IRE, vol. 32, pp. 10–21; January, 1949.
[5] W. G. Tuller, "Theoretical limitations on the rate of transmission of information," Proc. IRE, vol. 37, pp. 468–478; May, 1949.
[6] G. C. Sziklai and A. V. Bedford, U. S. Patent 2,664,463.
[7] G. C. Sziklai, U. S. Patent 2,643,289.
[8] G. C. Sziklai, U. S. Patent 2,617,879.

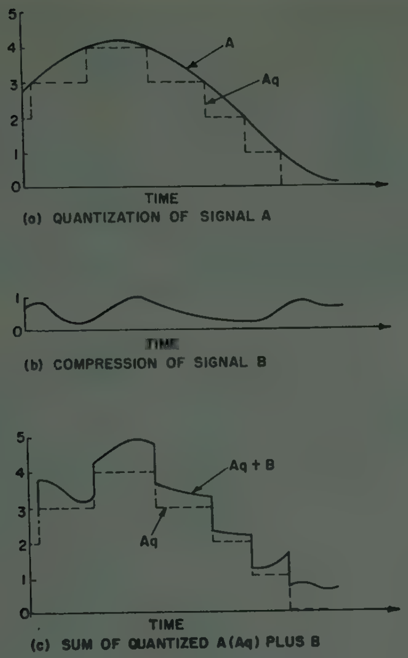

Fig. 1—Quantization and adding of signals A and B.

nor the eye can appreciate subtle changes in signal amplitude and, further, noise is always present in a transmission system. Thus, such a loss of accuracy, if done in appropriate fashion, will not cause a noticeable degradation of the signal. In addition, a form of coding must be involved and a certain amount of intelligence stored in the receiver.

In summary, information can be squeezed into a narrower channel than that previously required and thus save valuable bandwidth providing (1) the transmitter power is increased, (2) a coding system is included in the transmitter and receiver, and (3) some loss in accuracy of signal level definition is tolerated. The third condition is not severe, since, as pointed out before, noise is always present and the individual at the receiver cannot detect inaccuracies providing they are sufficiently small.

In order to facilitate the discussion and description of the sampling and quantizing tube we will first describe a transmission system in which it might be used and which conforms to the conditions listed above. This system will be capable of transmitting two signals simultaneously over a channel which would normally only accommodate one.

Description of Transmission System

In order to separate two signals which are being transmitted over a single channel, we must do something to at least one of these signals which will enable the receiver to distinguish between them. In this case, we will permit one of them (signal A) to exist only at certain discrete amplitude levels. This is called quantization[6] in analogy with the energy states of atomic physics. If the receiver finds that the incoming signal has at any moment an amplitude different from one of the discrete levels of signal A, it concludes that the signal A amplitude is at the next lower allowed level of the discrete set, and that the difference between the received signal and this allowed value for signal A gives information as to the amplitude of signal B. Specifically, suppose we restrict signal A to only six levels, namely: 0 volts, 1 volt, 2 volts, 3 volts, 4 volts, and 5 volts. Six levels will produce a reasonably acceptable picture, for example.[9] We compress signal B to a total range of 1 volt and add it to signal A at the transmitter. If the incoming signal at the receiver should have an amplitude of 3.6 volts, the receiver would conclude that the signal A level was 3 and that the signal B level was 0.6. If now the signal increases to 4.6 volts, the receiver concludes that signal A has increased by one quantum level while signal B has remained unchanged. Similarly, a change in the second digit would indicate a change in signal B amplitude. Fig. 1 illustrates this. In Fig. 1(a) the solid line corresponds to the input signal A and the dotted line is the quantized signal Aq. In Fig. 1(c) the quantized signal Aq is added to signal B which has been attenuated so that its maximum amplitude is equal to one quantum step in signal A [Fig. 1(b)]. Obviously, to perform quantization on a signal, a device whose output vs input characteristics looks like the solid line in Fig. 2 must be used. As the input signal varies continuously from zero to maximum value, the output signal must jump from one discrete level to the next in an abrupt fashion.

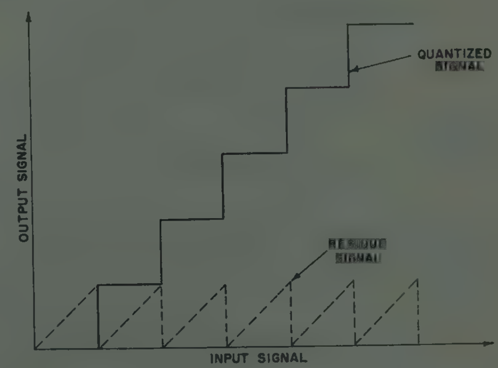

Fig. 2—Output vs input characteristic for a quantizing tube.

However, simply quantizing one of the signals and compressing and adding the other is not enough. Obviously, to transmit the combined signal as it is shown in Fig. 1(c) would require a broad bandwidth, since rounding off of the quantum jump of signal A caused by circuits with insufficient high frequency response will result in an appreciable error in signal B.

The problem is essentially that of eliminating the effect of transients produced by the quantum jumps of signal A on the apparent value of signal B. This can be done in several ways; one of the simplest is used in this system and is called "time sampling" or just "sampling."

[9] W. M. Goodall, "Television by pulse code modulation," *Bell Sys. Tech. Jour.*, vol. 30, p. 33; January, 1951.

The mathematical analysis of sampling has been previously published.[8] It will suffice here to give a qualitative description with emphasis on the operational requirements of the sampling device. Time sampling amounts to a periodic measurement of the amplitude of a signal such as the combined quantized signal A and signal B. The output of a sampler consists of a series of very short pulses, the energy content of each one proportional to the amplitude of the input signal at the moment the sample was taken, as shown in Fig. 3. It has been shown that if these pulses occur at the proper rate and are passed through appropriate filtering circuits a continuous wave results which has no frequency components higher than the highest frequency component in either signal A or B. More important, sampling this wave at the same rate as before gives pulses proportional to the desired signal $(Aq+B)$. This second sampling operation occurs at the receiver. Thus, the transmitted signal requires the same bandwidth as the ordinary transmission of either of its components; but includes two signals, A and B, each having the full bandwidth.

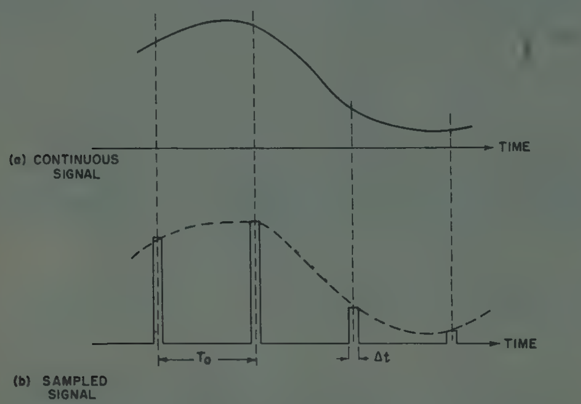

Fig. 3—Time sampling.

Signals Aq and B are separated at the receiver by a device which is nearly identical to the quantizer used in the transmitter. The combined signal $Aq+B$ is requantized. As before, only certain amplitude levels are allowed and the output signal is again the quantized signal Aq. Subtracting this from the input signal gives a residue signal B. Output vs input characteristic for which is shown by the dotted line in Fig. 2.

Thus, for example, we may take two television picture signals, quantize one of them with some loss in accuracy of half-tone reproduction, combine them and transmit them over a channel with a bandwidth no greater than that which would be required for one of them alone. Furthermore, we are able to separate the signals at the receiver with essentially the same device as we used to combine them at the transmitter, and display the two television pictures independently.

A tube has been described by Sears[10] which performs the functions of quantizing and producing a coded signal. However, to accomplish all the above operations in both the transmitter and receiver, a special tube was designed and constructed. It may be used to sample and quantize the input signals in the transmitter, or to sample and separate the two signals in the receiver. It is to be noted that in both the transmitter and receiver a very wide bandwidth must be had between the operations of sampling and quantizing or separating in order that the system work properly. In order to eliminate very wide-band circuits, the tube was designed to accomplish both operations almost simultaneously.

The Coding Tube

Fig. 4 shows the essential design of the sampling and quantizing tube, or coding tube, and its operation will be described with reference to this figure. A cathode and beam-forming structure produces a thin, flat electron beam which passes down the length of the tube. A pair of deflection plates to which is applied a sampling signal sweeps this beam back and forth across a narrow slit. Only when the beam is centered on the slit will electrons pass through to the rest of the tube. Thus, short pulses of electrons are formed. The sampled beam passes between the signal deflection plates and is deflected up and down across the quantizing structure. As shown, this consists of a flat aperture plate in which a step-shaped opening has been punched. If the beam is of essentially

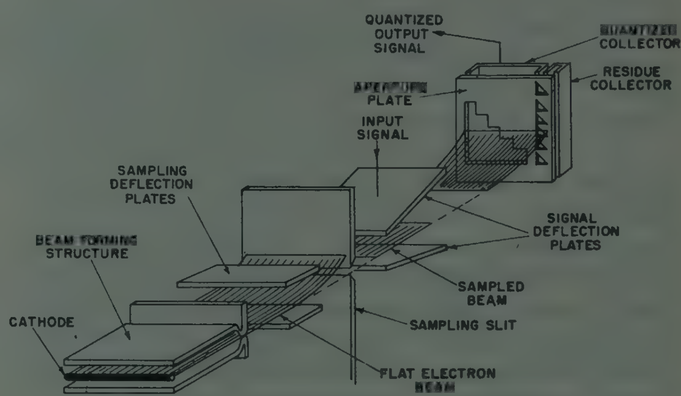

Fig. 4—Arrangement of the elements in the sampling and quantizing tube (suppression and adjustment electrodes have been omitted for simplicity).

constant current density across its width, the current which passes through the aperture increases in abrupt steps as the input signal moves the beam down the quantizing aperture assembly. The beam current which passes through the step-shaped hole is collected and constitutes the quantized output signal. A series of triangular apertures permit a current which is proportional to the difference between the input signal and the quantized signal to be collected on an electrode designated as the residue collector. This signal is used in the receiver.

The method of time sampling which is shown is far to be preferred over gating the total beam current by means of a grid. The signal which passes the beam back and forth across the sampling slit may be sinusoidal,

[10] R. W. Sears, "Electron beam deflection tube for pulse code modulation," *Bell. Sys. Tech. Jour.*, vol. 27, p. 44; January, 1948.

and at one-half the sampling frequency, whereas to pulse the beam on and off by means of a grid would require pulses at the sampling frequency with extremely short rise-and-fall times and short duty cycles.

In addition to deflecting the electron beam, as has been described, both sets of plates serve as lens structures for focusing the beam in the proper fashion. This is accomplished by externally adjusting the dc biases on these plates. The beam is focused by the sampling deflection plates onto the slit and by the signal plates onto the target structure.

Parts from beam deflection tubes[11] were used to form the beam and accomplish the sampling deflection. The beam thus formed has a thickness of a few thousandths of an inch. However, the width of the sampling aperture determines the effective beamwidth at that point, and this was four-thousandths of an inch. Since the imaging action of the signal deflection plates constitutes a lens of a 1:1 magnification, the effective beam thickness upon incidence on the output structure was approximately four-thousandths of an inch. Certain difficulties were encountered in achieving a large deflection across the output structure without having the beam bow in the middle or strike the signal deflection plates. In order to overcome these difficulties, deflection plates were constructed divergent at an angle to the beam as shown, and the surrounding structural members were made of mica and in such a way to minimize distortion of the deflecting field.

It is to be noted that a small deviation from the ideal quantizing characteristic shown in Fig. 2 will produce a large error in signal B when it is separated at the receiver. Thus, it is important that the steps be "flat" and that the amplitude difference between steps be constant. Due to the finite thickness of the beam, a certain amount of rounding is to be expected at the step edges. The amount of rounding which can be tolerated determines the ratio of beam thickness to step dimensions. The practical difficulty of forming an electron beam which has uniform (or even predictable) current density across its width is such as to require some mechanism to adjust the current collected by each quantum step independently and externally.

Two methods were employed to correct for nonuniformity in beam current density, and will be described in detail. The first of these permits one to correct the current gathered by each quantum step in either an additive or subtractive direction. The second permits only a diminishing action.

In order to correct for nonuniformity in beam current density, a system of correcting wires, the potential of each being externally adjustable, was used between the aperture plate and the quantized collector. Fig. 5 shows schematically how this was done. As shown in Fig. 6 these wires could add or subtract from the current which was gathered by the quantized collector, by operating as deflection electrodes and as secondary emitters. If the potential of the correcting wire was negative with respect to the collector, more of the beam current would be deflected to the quantized collector and, in addition, secondary emission from the correcting wire would also go to the quantized collector. If the potential of the correcting wire is positive with respect to the collector, a larger proportion of the beam current is attracted to the correcting wire, as is secondary emission current from the quantum collector, thus diminishing the current to the quantized collector. As a result, it was possible to increase or decrease the current to the quantized collector for each step independently. The secondary emission ratios of the quantized collector and the correcting wire were not always constant along the length of the structure. Hence, if one applied a saw-tooth wave to the input structure, the output wave could be adjusted for equal step heights, but it did not necessarily have perfectly flat steps.

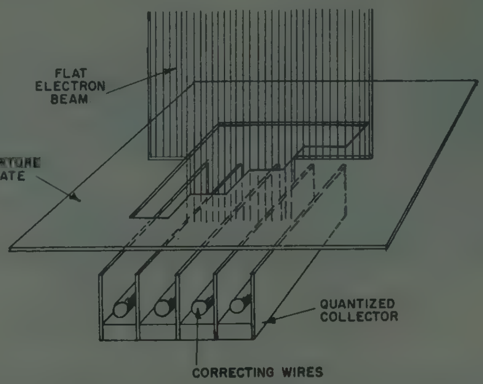

Fig. 5—Target assembly.

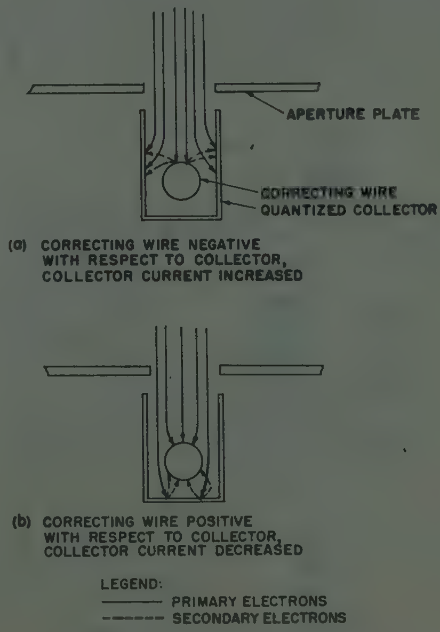

Fig. 6—Action of correcting wires.

[11] E. W. Herold and C. W. Mueller, "Beam deflection mixer tubes for uhf," *Electronics*, vol. 22, pp. 76–80; May, 1949.

A typical input-output characteristic, such as recorded from a tube of the sort just described, is shown in Fig. 7. The roundness of the steps, which is due to the finite width of the beam, is not excessive from the standpoint of the system accuracy. However, it will be noted that the steps are by no means flat.

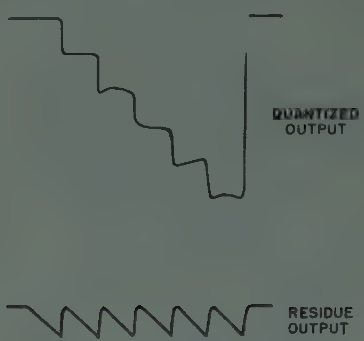

Fig. 7—Output of quantizing tube as observed on scope (system of Fig. 5).

In order to obtain flatter steps, the correcting structure illustrated in Fig. 8 was designed. In this case, the correcting wires serve only to deflect the beam toward or away from the aperture fins which are attached to an aperture plate similar to the one previously described.

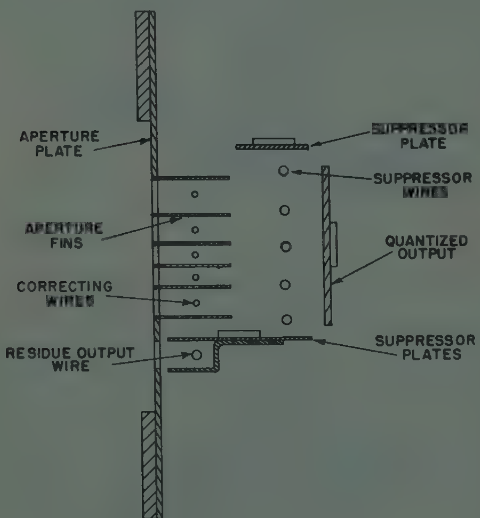

Fig. 8—Revised target assembly.

Suppressor wires are included to minimize the effect of secondary electrons which are generated on the aperture plate and correcting wires and thereby prevent them from reaching the quantized output electrode. If the potential of a given correcting wire is the same as the potential of the aperture plate, the beam which passes through that section remains relatively undisturbed and arrives at the quantized output electrode. If, however, the potential of the correcting wire is negative with respect to the fins on the aperture plate, a large proportion of the current passing through the aperture plate is deflected and strikes the fins, thus diminishing the current which reaches the output electrode. In this way it is possible to decrease continuously the current through each slot. Notice that the slots are of varying width. This was done in an effort to pre-adjust for nonuniformities in the beam current density since the beam current density would be the greatest at the center and the least at the edges.

Fig. 9 shows the output of the revised quantizing structure, and it will be noted that the steps are of essentially equal height and are extremely flat. The rounded portion of the step is less than 10 per cent of the step width. Since the beam thickness was four-thousandths of an inch and the step of the aperture plate was forty-thousandths of an inch, this rounding was to be expected.

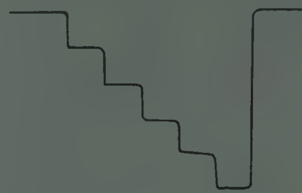

Fig. 9—Quantized output as observed on scope with optimum adjustment of correcting wires (system of Fig. 8).

In both types of collector systems, the residue signal, i.e., the current which passes through the triangular shaped holes, is collected by a small wire which runs through a U-shaped suppressor electrode behind the quantizing aperture plate. The current which passes through the triangular hole is proportional to the width of the triangular hole at the point where the beam passes. The ideal output vs input characteristic of this channel is illustrated in Fig. 2, and is proportional to the difference between the input signal and the quantized output signal.

A few tubes were constructed with only residue output electrodes. Since the most important operation at the receiver is the separation of signals A and B, it was felt that the use of the combined $A+B$ signal for the A signal would not constitute a serious error. Therefore, simply obtaining signal B from the combined signal would be all that was needed. These purely residue tubes worked precisely as one would anticipate, and the response to a linearly increasing signal is shown in Fig. 10.

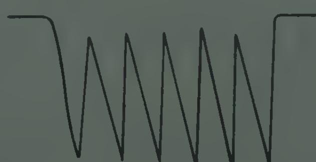

Fig. 10—Output of all-residue tube, as observed on scope.

In order to shield the output from the input, all the leads from the electron gun structure and both sets of deflection plates were brought out through one end of

the tube and the output leads and the individual leads to the correcting wires brought out the other end. The region of the electron beam is surrounded by a cylindrical shield, and a mesh shield surrounds the output leads, in order to further shield the input from the output. These features can be seen in the photographs of Figs. 11 and 12.

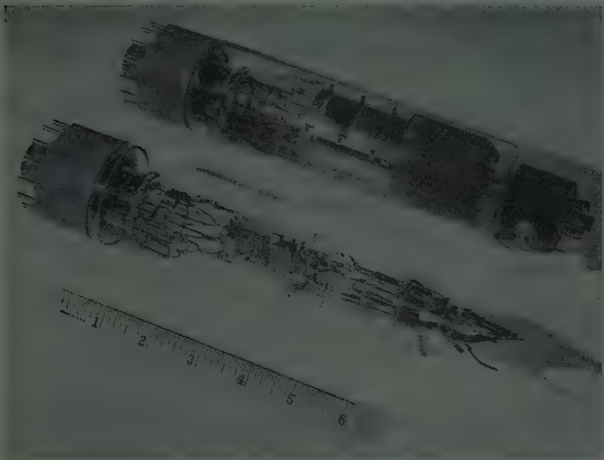

Fig. 11—Photograph of time-sampling and amplitude-quantizing tube.

Performance Data

In the preceding section describing the operation of the coding tube, many of the features of its mechanical design were discussed. In this section typical operating conditions will be described.

The tube whose input-output characteristic was given as Fig. 7 operated under the following conditions:

Heater	6.3 volts, 0.3 amp
Cathode	0 volts
Outer Shield	300 volts
Beam Forming Structure	300 volts
Sampling Deflection Plates	165 volts
Sampling Slit	300 volts
Signal Deflection Plates	75 volts
Aperture Plate	300 volts
Quantized Collector	260 volts
Correcting Wires	Centered about 300 volts
Residue Suppressor Plate	0 volts
Residue Collector Wire	300 volts.

Under these conditions of operation the total current drawn from the cathode is of the order of 10 milliamps, of which about 7 milliamps goes directly to the beam-forming structure in the process of collimating the beam. The actual current in the flat electron beam is of the order of 100 microamps. At the point of focus, this beam is about 0.004-inch thick and 0.300-inch wide.

When the beam is not modulated and is adjusted to fall on the largest step opening in the aperture plate, a current of about 55 microamps reaches the quantized collector output. This indicates a current of 11 microamps per unit step of the quantized output. The current through the widest part of a residue triangle is 10 μa.

This largest step opening in the aperture plate has a dimension of 0.190 inch parallel to the width of the beam. The beam also falls across one of the triangular residue openings, so a total of 0.260 inch of the beam-width is used. The residue openings are right isosceles triangles 0.040 inch on a side. The height of each step opening, in the direction of the thickness of the electron beam, is also 0.040 inch. For the six levels involved in this tube, the total deflection required of the electron beam is thus 0.240 inch.

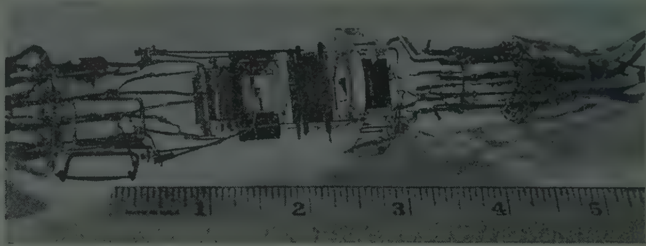

Fig. 12—Photograph of beam-forming and target sections of the quantizing tube.

The deflection sensitivity is such that a voltage of about 35 volts rms applied to the signal deflection plates will swing the electron beam over the whole step pattern on the aperture plate. The sampling voltage required on the first deflection plates is of the order of 6 volts rms to produce pulses with a duty cycle of about 10 per cent. These signal voltages are applied push-pull to the deflection plates and are superimposed on the dc focusing voltages applied to these plates.

The correcting wires were operated so that they were individually adjustable over a range of plus or minus 45 volts about the median value of 300 volts. They were each adjusted in a manner to best equalize the step amplitude in the output.

The tubes were operated successfuly with a 5-megacycle sampling voltage and a microsecond saw-tooth signal on the signal deflection plates.

Signal-to-Noise Ratio

As a first approximation, the predominant source of noise in the tube can be assumed to be shot noise, and noise sources following the tube can be neglected. The approximate signal-to-noise ratio may then be computed from the equation:

$$\frac{S}{N} = \frac{i}{\sqrt{2eI_a\Delta f}},$$

where

i is the signal current
I_a is the average collector current
Δf is the bandwidth of the output circuit
e is the charge on the electron.

In our case, $I_a = I_p/2$, where I_p is the maximum collector current, and $\Delta f = 4$ megacycles.

In the quantized output, the undeflected beam passing through the largest step-opening produces a current of 55 microamps. This current, multiplied by the duty

factor of 0.1, gives $I_p = 5.5$ microamp for the operating tube. The signal current to the smallest step will be $\frac{1}{5}$ this amount, or $i = 1.1$ microamp. When these values are substituted in the above formula, the computed signal-to-noise ratio for the smallest step in the quantized output is about 55 db.

The maximum undeflected current through a residue opening is 10 microamps. To compute the noise in the residue output, this must be multiplied by the duty factor, giving $I_p = 1.0$ microamp. The signal-to-noise ratio is computed for a residue signal of $\frac{1}{5}$ this amplitude, or $i = 0.2$ microamp. This gives a computed signal to noise ratio of about 48 db for this small residue signal.

These computed signal to noise ratios are of such magnitude as to indicate that noise from the tube should not appreciably degrade the signal.

Conclusion

Beam deflection-type tubes have been successfully built and tested which simultaneously perform the functions of time-sampling and amplitude-quantizing of a video input, and producing a residue signal.

Experimental tubes were operated successfully with a 5-megacycle sampling voltage, and a microsecond saw-tooth signal on the signal deflection plates. This closely simulates the conditions of sampling and quantizing which would be required of the tube in operation in a television system of the type described.

It is hoped that this outline of a system of bandwidth saving, and the descritpion of an experimental electron tube which will perform the critical functions required in this system, will help further the thought in this important field.

Noise Power Radiated by Tropical Thunderstorms*

S. V. CHANDRASHEKHAR AIYA†, SENIOR MEMBER, IRE

Summary—**The common types of tropical thunderstorms are described. A synthesis is made of the available information on the subject. Hence, the essential peculiarities and electrical parameters of typical lightning discharges are deduced. These are utilized to explain the radiation that appears as radio noise. An expression is deduced for the average electric field due to a stroke in a flash. This is used to evaluate the power at the source that should correspond to the noise field strength as measured by the noise meter previously described by the author. The noise power is found to vary as the inverse square of the frequency and the expression obtained for the noise power is expected to be valid in the frequency range of 1–20 mc. The theoretical results are compared with values obtained by experiment. There is close agreement between the two.**

Introduction

An OBJECTIVE METHOD of measuring atmospheric noise interference to broadcasting has been reported.[1] The method is evolved from subjective considerations and aims at measuring the parameter required for engineering evaluations of noise interference. The results of experimental investigations by this method can be satisfactorily explained, on the basis of the known distribution of thunderstorm centers and the laws of propagation, by assigning a suitable power at each frequency to the thunderstorm acting as a radiator. The problem of calculating this power from lightning discharge data was examined and the results of such an investigation are reported in this paper. The scope of the paper is, therefore, naturally restricted to examining the effect of the more commonly occurring types of thunderstorms in the tropics. The approximations, etc. made are such that the results can be considered valid in the frequency range 1–20 mc. As far as possible, the assumptions, approximations and the choice of numerical data incorporated in the paper are justified by the experimental results of investigators or on theoretical considerations. For this purpose, the necessary systematic restatement of known facts is given, to bring out clearly the full significance of the final result.

* Original manuscript received by the IRE, November 15, 1954; revised manuscript received, April 4, 1955.

† Electrical Communication Department, College of Engineering, Poona, India.

[1] S. V. C. Aiya, "Measurement of atmospheric noise interference broadcasting," *Jour. Atmos. Terr. Phys.*, vol. 5, pp. 230–242; September, 1954.

Present Position

Frequency distribution of energy radiated by a lightning flash has been evaluated by several investigators. Ollendorff assumed a linear rise and an exponential decay for currents in the discharge channel.[2] By a Fourier analysis of the waveform so obtained, it was concluded that the received field strength is proportional to bandwidth and inversely proportional to frequency. Jaegar made a rough estimate of the frequency distribution of noise power and concluded that the assumption that noise field strength is inversely proportional to frequency cannot be reconciled with lightning discharge data.[3] Thomas and Burgess[4] have attempted to show

[2] F. Ollendorff, "Radiation field of lightning," *Electr. Nachr. Tech.*, vol. 1, pp. 108–119; 1930.

[3] J. C. Jaegar, "Atmospherics and Noise Level," Conn. Sci. Ind. Res. (Aust.), Report 184, 1943.

[4] H. A. Thomas and R. E. Burgess, "Survey of Existing Information and Data on Radio Noise in the Frequency Range, 1–30 Mc/s," *Radio Research Special Report No. 15*, H. M. Stationery Office London, 1947.

that the noise power at the source is proportional to the inverse fourth power of the frequency. Bailey's results show that the noise field strength is inversely proportional to frequency.[5] The assumptions of Ollendorff are not consistent with the now available lightning discharge data and the field strengths obtained are low. The calculations of Thomas and Burgess are based on the data about the return stroke in the case of flashes that strike the ground and they assume the radiation of one impulse per stroke. Further, their choice of recurrence frequency is incorrect. Bailey's calculations appear to give numerical values approaching the measured values.

A lightning discharge radiates an impulse. The magnitude of a quantity like a field strength measured depends, therefore, very largely on the several processes involved in the technique of measurement. A power estimate can, therefore, have significance when this is taken into account. That is, the power estimate should be attempted for a specific purpose. The physical processes involved in the radiation of impulses and their recurrence frequency in relation to the technique of measurement at the receiving end have to be carefully considered and incorporated into the calculation. The statistical aspects of the phenomenon must be given their due weight at each stage of the calculation.

With the available information on lightning discharges, the derivation of a generalized formula for the variation of noise power at the source with frequency presents difficulties. It is, therefore, proposed to approach the problem in stages. Thus, this investigation is restricted to tropical thunderstorms and the frequency range of 1–20 mc. Although this paper is confined to calculating the noise power for a specific purpose, the principles emerging from the calculation may perhaps be useful in a wider field.

Analysis of the Problem

A scientific analysis of a complicated problem like that of this paper can only be undertaken in distinct stages. The procedure adopted for dividing the subject matter of the paper into sections is as follows. Thunderstorms occur all over the world. They are first described briefly with the principal object of bringing out clearly the characteristics of typical tropical thunderstorms. A short account is then given of lightning flashes which accompany thunderstorms, and it is shown that they are intermittent and consist of a number of strokes. The physical nature of a stroke is then discussed and the importance of the stepped leader in a stroke is explained. There follows a detailed description of the stepped leader and its electrical microstructure. In each of the sections, the numerical values of the parameters required for the analysis of the problem are given with reasons for their choice. On the basis of this material, the mechanism of radiation from a tropical thunderstorm is explained and this is utilized in the section to follow for calculating the average electric field due to a stroke in a flash.

The rest of the paper is devoted to the specific problem of evaluating the power at the source that should correspond to the noise field strength as measured by the noise meter described by the author. For this purpose, a brief description of the noise meter is given, and the effect of the meter characteristics on calculations is discussed. The significance of the procedure adopted for the calibration of the noise meter is explained. Finally, a simple expression is obtained for the noise power at the source that corresponds to the noise field strength as measured by the particular noise meter. Numerical values obtained on the basis of this expression are then compared with experimental results. The last section of the paper summarizes the limitations of the expression derived and focuses attention on basic conclusions.

Tropical Thunderstorms

Essentially, a thunderstorm is a localized thermodynamical process in the atmosphere accompanied by electrical discharges. The physical mechanism of the discharge process is still not clearly understood. When the intensity of the electric field at some point in the cloud exceeds the disruptive strength of the dielectric, a discharge occurs, and this leads to the initiation of a lightning flash. Theoretically, such a flash can occur within the cloud, from a cloud to the upper atmosphere, and from a cloud to the earth. At higher latitudes, especially in temperate regions, the third type is common. Extensive investigations have been carried out on this type. Owing to the greater height of the tropopause, thunderstorms occur at a higher altitude in the tropics. Consequently, the most common type of flash in the tropics occurs within the cloud. It is this type of flash that has to be carefully examined. Discharges into the air or the earth also occur in the tropics, but they are less common. References to discharges from cloud to earth will be restricted in this paper only to the extent to which they can reveal information of use for the analysis of the main problem.

Lightning Flashes

As a result of extensive investigations, it is now clear that a lightning flash is intermittent and consists of a number of separate strokes which follow each other in time along very nearly the same path in space.[6,7] The number of strokes per flash has been investigated in detail and shows that it has a statistical variation and has a median value between two and three strokes per flash. The available data appears to indicate that these facts hold good for all types of discharges. The

[5] RPU-140. "Radio Propagation Unit Technical Report No. 5, 1947." Radio Propagation Unit (9463 d-TSU), Holabird Signal Depot, Baltimore, Md.

[6] C. E. R. Bruce and R. H. Golde, "The lightning discharge," *Jour. IEE.*, vol. 88(2), pp. 487–505; December, 1941.

[7] H. H. Hoffert, "Intermittent lightning flashes," *Proc. Phys. Soc. Lond.*, vol. 10, pp. 176–180; 1890.

higher value of 3 for the number of strokes per flash is more probable for flashes in the cloud or into the air as the intense return stroke is absent. It will be assumed, therefore, in this paper, that the number of strokes per flash in a discharge which occurs in the cloud has a median value of 3.

The median value of the duration of a flash is found from lightning discharge experiments to be 0.25 second. A value of 0.2 second is obtained for this quantity by listening experiments,[1] in which it is believed that one is mostly concerned with tropical thunderstorms. It is, therefore, reasonable to conclude that in tropical thunderstorms three strokes occur in 0.2 second in the majority of cases.

The time interval between successive strokes shows a statistical variation and the median value of this time interval is estimated to lie between 35 and 85 milliseconds. When a higher median value is chosen for the number of strokes, the choice of a lower median value for the time interval between strokes in the same period is logical. Further, the median value of the duration of a flash as assumed here is less than what lightning discharge results give. Therefore, 40 milliseconds will be chosen as the median value of the time interval between strokes in a flash in a tropical type of thunderstorm as described in this paper.

Physical Nature of a Stroke

According to Schonland and collaborators, the nature of a stroke is as follows.[8–12] A pilot streamer which travels slowly advances into virgin air. The currents involved are small and the duration is comparatively large. Hence, this pilot streamer is of no real significance from the point of view of radiation. Superimposed on this pilot, there are a succession of leader streamers, each traveling from the cloud downward and getting extinguished after it has traveled a short distance. This is called the stepped leader. If the stepped leader does not approach the ground, as is the case for discharges within the cloud or into the air, there may follow a recoil of low intensity and long duration. This recoil therefore is also of no significance from the point of view of radiation. The principal source of radiation in the more common types of tropical thunderstorms is, therefore, the stepped leader, and it will be described in detail in the section to follow.

If the leader approaches the ground, as in the case of discharges from cloud to earth, a return stroke of high velocity and great intensity travels from the earth to the cloud along the preionized channel. Very high currents are involved and the duration is very short. This may be followed by a discharge of low intensity and long duration from the cloud to the earth. In the case of flashes reaching the ground, only the leader of the first stroke in a flash is ordinarily always stepped; the leader of the second or subsequent stroke is generally not stepped.

It has been observed that the pilot streamer and the stepped leader of the first stroke in a flash reaching the earth are essentially the same as for discharges into the air or within the cloud. This fact justifies the use of data of the first stroke in a flash reaching the ground insofar as they pertain to stepped leaders for purposes of this analysis.

The Stepped Leader

Schonland and collaborators have studied in detail the nature of the stepped leader and their investigations represent the closest approach to the tropics.[12] Results of other investigators generally support the conclusions of Schonland and collaborators. Hence, their results will be taken as quite representative on the subject. The stepped leader is found to have a number of steps. The length of the steps shows a statistical variation. Step lengths between 40 and 100 meters are quite common. This suggests an average value for the length of a step of 70 meters. The time interval between steps shows a statistical variation. It is found, by experiments involving photographic technique, to lie between 31 and 91 microseconds and, from oscillographic studies, to lie between 40 and 65 microseconds. These give broad indications of the orders of magnitude involved. There is probably some relation between the step length l, the number of steps responsible for radiation n, and the average duration of each step T. The final equation derived in this paper requires the value of $nl\sqrt{T}$. The variation of n, l, or T do not matter so long as $nl\sqrt{T}$ is constant. That is, what is actually required is the median value of $nl\sqrt{T}$. It has been difficult to evaluate this quantity and descretion has been exercised, but the close agreement between the theoretical value of power deduced and the value of power obtained experimentally probably justifies the procedure which has been adopted. It is as follows.

A typical photograph of a stepped leader in a discharge into the air taken by Schonland and collaborators has been examined.[13] An air discharge corresponds very nearly to a discharge in the cloud. In this case, the average step length is 67 meters. The average time interval between steps is 74 microseconds. These values are quite consistent with the broad conclusions arrived at in the previous paragraph and they will be assumed as appropriate values.

The number of steps in a stepped leader responsible for radiation or the duration of the radiating part of the stepped leader is a quantity that is required for

[8] B. F. J. Schonland and T. E. Allibone, "Branching of lightning," *Nature*, vol. 128, pp. 794–795; November, 1931.

[9] B. F. J. Schonland and H. Collens, "Progressive lightning," *Proc. Roy. Soc.*, vol. 143, pp. 654–674; February, 1934.

[10] B. F. J. Schonland and J. Craib, "The electric field of South African thunderstorms," *Proc. Roy. Soc.*, vol. 114, pp. 229–243; March, 1927.

[11] B. F. J. Schonland, D. B. Hodges and H. Collens, "Progressive lightning, V," *Proc. Roy. Soc.*, vol. 166, pp. 56–75; May, 1938.

[12] B. F. J. Schonland, D. J. Malan and H. Collens, "Progressive lightning, II," *Proc. Roy. Soc.*, vol. 152, pp. 595–625; November, 1935.

[13] *Ibid.*, p. 610, Plate 18, flash 36 in Fig. 9.

calculations. This quantity is again difficult to evaluate. The radiation due to the stepped leader has been recorded by Watson-Watt and collaborators in the photographs of the waveform of atmospherics.[14] They call this the precursor. They have noticed that there appear to be 10 perceptible oscillations and that the over-all duration of the precursor is about one millisecond. In the records of Appleton and Chapman, the part of the field changes in the stepped leader likely to cause perturbations appear to last one millisecond.[15] These authors further state that "the most frequently observed waveform of the atmospheric ultimately developed is a brief steep fronted train of 6 to 10 half cycles of quasi period 0.1 to 0.15 millisecond."[16] It is possible in these investigations that two impulses following each other in a very short time may not get resolved properly. Therefore, the actual value of the number of oscillations may not be of great significance. But the conclusion that the over-all duration is one millisecond can be accepted without reservation. Hence, it will be assumed that the average duration of the radiating part of the stepped leader is one millisecond.

A time interval of 74 microseconds between the steps gives a value of 13.5 kc for the average recurrence frequency of the steps in the stepped leader.

Electrical Microstructure of the Stepped Leader

Appleton and Chapman have examined the microstructure of the electrostatic field due to a stepped leader at a distance of 3 kms from the source.[15] In view of its extreme importance for the present investigation, Fig. 6 (iv) in Plate I of their paper has been suitably redrawn and reproduced below as Fig. 1.

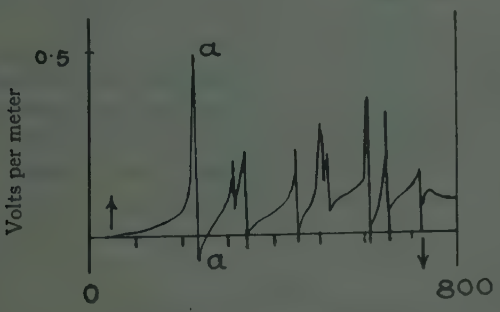

Fig. 1—Electrostatic field due to a stepped leader at 3 km from the source.

Between the arrows in the figure, there are nine changes of field in a total time of 670 microseconds. This gives an average period of 74.4 microseconds between steps, a value which is in striking agreement with the value earlier quoted from Schonland and collaborators and assumed for purposes of this paper. This supports the assumption that the microstructure is due to the stepped leader and supports using the result for drawing conclusions about the stepped leader and its electrical parameters.

An examination of the figure shows that portions like "*aa*" which correspond to discharges are practically parallel to each other. In a stepped leader, therefore, there are a number of discharges and the rate of rise of current is very nearly the same in all these discharges. Each such discharge will naturally be responsible for the radiation of an impulse. There is abundant evidence in the existing literature to justify the assumption that the rise of current in a discharge accompanying a lightning flash is exponential. It is, therefore, reasonable to assume that the current waveform in each of these discharges can be represented by

$$I = I_0(1 - \epsilon^{-\delta t}) \tag{1}$$

where I_0 is the peak current and "δ" is the constant. Hence,

$$\text{Maximum rate of change of current} = (dI/dt)_{\max} = \delta \cdot I_0. \tag{2}$$

Three different drawings of Fig. 1 were made. In each, lines like "*aa*" were produced and the slopes of the seven more distinct lines in the figure were determined. The slopes were of about the same value, showing clearly that the discharge mechanism appears to be the same for all discharges. Hence, using an equation such as (1) as typical for any such discharge is a justifiable step.

The average value of the slope of lines like "*aa*" was determined. Using this, taking the distance of the source as 3 km and assuming as explained earlier that the average value of the length of the discharge path as 67 meters, the value of $(dI/dt)_{\max}$ was evaluated. It was found to be (6.2×10^9) amperes/second. Calculations by such methods cannot possibly be very accurate but they are most useful for giving an idea of the order of magnitude of the quantity involved.

Berger gives the average value of the maximum rate of increase of current as 10^{10} amperes per second.[17] The discharge current in the return stroke of a flash which reaches the ground has been extensively investigated and the results are well summarized by Thomas and Burgess.[4] It has been found that the initial part can be well represented by

$$I = I_0(\epsilon^{-at} - \epsilon^{-bt}).$$

Therefore,

$$(dI/dt)_{\max} = (b - a)I_0. \tag{3}$$

The following average values have been obtained for the quantities involved:

[14] R. A. Watson-Watt, J. F. Herd, and F. E. Lutkin, "On the nature of atmospherics, V," *Proc. Roy. Soc.*, vol. 162, pp. 267–291; September, 1937.

[15] E. V. Appleton and F. W. Chapman, "On the nature of atmospherics, IV," *Proc. Roy. Soc.*, vol. 158, pp. 1–22; January, 1937.

[16] *Ibid.*, p. 22.

[17] K. Berger, "Thunderstorm measurements in Switzerland in 1932 and 1933," *Assoc. Swiss. Elect. Bull.*, vol. 25, pp. 213–229; 1934.

$I_0 = 20$ to 24 kilo-amperes
$a = 4.4 \times 10^4$ second^{-1}
$b = 4.6 \times 10^5$ second^{-1}

Since one is concerned with peak values of impulses, the choice of the higher median value for I_0 is suggested. (The value of I_0 given above as 20 to 24 kilo-amperes is the median value.) If calculations are carried out using these values, it is found that the maximum rate of increase of current is 10^{10} amperes per second.

Looking to the similarity of lines like "aa" in the figure, and the fact that the order of magnitude of $(dI/dt)_{\max}$ is the same, it appears reasonable to conclude that the discharge mechanism is the same in all cases in any lightning discharge. Hence, one average value for $(dI/dt)_{\max}$ can be assumed for all cases. From the discussion above, it follows that this average value should be 10^{10} amperes per second.

Radiation from Tropical Thunderstorms

The discussion so far has made it quite clear that it is the stepped leader that is responsible for radiation. The discharge current in a step gives rise to the radiation of an impulse. There will thus be a train of impulses from a stepped leader. Since the average duration of the radiating part of the stepped leader is one millisecond, this train of impulses is radiated for one millisecond. The recurrence frequency of the impulses is 13.5 kc. Since there will be three strokes on an average in each flash, three such trains of impulses arise from a flash and the average time interval between such trains of impulses is 40 milliseconds. This description can be considered as an idealized, statistically valid representation of a typical flash in a tropical thunderstorm as a noise radiator.

The next question to consider is the form of the radiator. A step in the leader is responsible for radiation. This can be considered to be practically vertical and this is what the photographs of stepped leaders appear to indicate. The ordinary height at which the step appears is such that, for frequencies above 1 mc, the effect of the ground can be neglected in any first approximation. The average length of a step is 67 meters. Since the currents in a discharge are exponential, i.e., involving a wide range of frequencies with a predominance of lower frequencies of higher amplitudes, it is reasonable to assume that the length of the step, viz., 67 meters, is such that the step can be considered to have the equivalence of a short dipole.[18]

This paper is confined to estimating the peak field strengths and hence the peak power. This requires the maximum rate of increase of current during a discharge in a step and this is 10^{10} amperes per second.

Electric Field Due to a Stroke in a Flash

The radiation is due to the stepped leader in the stroke and consists of a number of impulses radiated at random; these impulses arise from the discharge currents in the steps. Let M be the equivalent electric moment corresponding to a step in the stroke and let l be the equivalent length of the step. Then,

$$\frac{dM}{dt} = l \cdot I_0(1 - e^{-\delta t}). \tag{4}$$

Therefore,

$$\frac{d^2M}{dt^2} = \delta I_0 l e^{-\delta t} \tag{5}$$

$$= \phi(t) \tag{6}$$

where $\phi(t)$ represents the form of the impulse radiated. If $q(\omega)$ represents the frequency spectrum of the impulse,

$$\phi(t) = \frac{1}{2\pi}\int_{-\infty}^{+\infty} q(\omega)e^{i\omega t}d\omega \tag{7}$$

where

$$q(\omega) = \int_{-\infty}^{+\infty} \phi(t)e^{-i\omega t}dt. \tag{8}$$

Now,

$$\int_{-\infty}^{+\infty} \phi^2 dt = \frac{1}{\pi}\int_0^{\infty} \overline{|q(\omega)|^2} d\omega \tag{9}$$

where

$\overline{|q(\omega)|^2}$ = average value of the square of the frequency spectrum.

The impulses occur at random. Let ν be the average recurrence frequency of the impulses. Let B represent the frequency interval, i.e., bandwidth of the receiver at a frequency $\omega_0/2\pi$. Then, the mean square amplitude within this bandwidth at $\omega_0/2\pi$ is given by

$$\overline{S}^2 = 2\nu B \, |q(\omega_0)|^2 \tag{10a}$$

But,

$$q(\omega_0) = \int_{-\infty}^{+\infty} \phi(t)e^{-i\omega_0 t} \cdot dt. \tag{10b}$$

$$\therefore q(\omega_0) = \delta l I_0 \int_{-\infty}^{+\infty} e^{-(i\omega_0+\delta)t}dt. \tag{11}$$

$$\therefore |q(\omega_0)| = \frac{\delta l I_0}{\omega_0} \quad \text{if } \omega_0 \gg \delta \tag{12}$$

$$\therefore S(\omega_0) = \sqrt{2\nu B} \cdot \frac{\delta l I_0}{\omega_0}. \tag{13}$$

This may be considered as the statistical amplitude spectrum of a succession of impulses in one stroke in a flash.

[18] When a discharge takes place, the ionized streamer travels through the step with a velocity which is probably the same as in the return stroke of flashes reaching the ground, viz., one tenth the velocity of light. Therefore, the time the streamer takes to travel a step length of 67 meters is about 2.2×10^{-6} seconds, and this is very short. Scientifically, therefore, the step length has the significance of the product of velocity and time. But the ultimate result will not be affected if the step is regarded as an aerial of length, 67 meters, and this conception is simpler and more convenient to work with for engineering purposes. Hence, it will be adopted here.

Since the "step" has been considered as equivalent to a short dipole, it will be logical to suppose that it has a gain factor given by

$$G_\theta = 1.5 \sin^2 \theta \tag{14}$$

where θ is the angle the direction of radiation makes with the axis of the dipole. Then, on the basis of the electromagnetic theory, peak field intensity is given by

$$E_1 = \frac{30}{cr} \cdot S(\omega_0) \cdot \sqrt{1 \cdot 5 \sin^2 \theta}. \tag{15}$$

If all the quantities are expressed in the usual units and r in 10^6 meters, the field intensity will be in microvolts/meter. "c" is the velocity of light, i.e., 3×10^8 meters per second.

Eq. (15) gives the statistical median value of the peak field intensity to be expected from a stroke in a typical tropical thunderstorm and can be used for any calculations requiring this parameter. In the sections to follow, (15) will be utilized to carry out a specific calculation with reference to the noise meter already mentioned. For this purpose, the problem of the measurement of atmospheric noise interference will be first described. This will be followed by a brief description of the noise meter as developed for measuring the noise interference to one service, viz., broadcasting. The effect of meter time constants and calibration on calculations will then be explained and then the final expression required deduced.

Atmospheric Radio Noise

Electrical discharges associated with thunderstorms give rise to the radiation of impulses. These impulses travel via the ground, via the ionosphere, via the troposphere, or as an optical ray in exactly the same manner as other radio waves, and all the laws of propagation are applicable to them. An impulse is really equivalent to a large number of components of different amplitudes and frequencies. Radio waves of different frequencies display different propagation characteristics. This applies equally well to the different components of the impulses radiated by lightning flashes.

Suppose a receiver is tuned to a certain frequency. It can pick up frequencies within a certain bandwidth at this frequency. Therefore, it picks up all the components of the impulse radiated by a lightning flash which are received at the place and whose frequencies lie within the receiver bandwidth. These, after they pass through the different stages of the receiver, appear as noise from the loudspeaker. This noise is called atmospheric radio noise as it arises from sources in the atmosphere. Early investigators who studied this noise found that it corresponded to different types of common sounds on different occasions or different places and classified them as clicks, grinders, etc. It is now known that atmospheric noise is impulsive noise and gives the impression of continuous noise only when the impulses arrive at a very rapid rate.

This atmospheric radio noise is a source of interference and, as such, affects the information handling capacity of a signaling system. It is the principal source of interference to radio communication on frequencies below 20 mc. Measurement of atmospheric noise interference is a complicated problem. It has been found that the number of impulses received per minute, and the magnitude and duration of each impulse shows a statistical variation. Therefore, the collection and assessment of data on atmospheric noise must have a statistical basis so that the result corresponds to the idealized, statistically valid representation of the phenomenon as described. Such a step is also necessary for making the data useful for engineering evaluations. Since atmospheric noise is a form of interference and appears as impulses, its measurement must be based on its interfering effect. The whole problem of what are the different parameters necessary to assess the interference of atmospheric noise to different services is still unsolved. Some criteria have to be developed either experimentally or theoretically for the purpose before measurements of its interference to any one service are carried out.

The usual practice is to measure field strengths in microvolts per meter for specifying the strengths of received signals. It is, therefore, most desirable to measure atmospheric noise field strength, i.e., the noise meter must be a noise field strength meter. Since the field strengths of impulses have to be measured, a decision has to be taken about the parameter to be measured. It is found that the peak value is important as a measure of annoyance and generally the quasi-peak value of the impulse, the value that lasts a small interval of time necessary to affect the ear, is measured. Therefore, the time constants of the measuring system become important.

Noise measurements have significance only when all the factors enumerated above have been taken into account. With data from such measurements, the noise level can be evaluated. Then, the extent to which the signal must be above noise for a desired degree of satisfactory service can be given in the form of standards. Further, it becomes possible to evaluate the noise power that would correspond to the noise field strength as finally assessed and given.

Measurement of atmospheric noise interference to broadcasting has been studied on the lines indicated above and the noise meter developed on this basis will be described in the section to follow.

The Noise Meter

Atmospheric noise is classified in three types: type A noise giving the impression of continuous noise and arising from impulses coming at a very rapid rate; type B noise coming as distinct impulses; and type C noise, a special form of type B noise in which there are large variations of magnitude from impulse to impulse and which appears to arise from a few local thunderstorms,

often only one. The extent to which the signal must be above noise for satisfactory reception depends on the type of noise. Ten impulses per minute are found to have an annoyance value to the listener of broadcast programs. Therefore, the arithmetical average of the ten highest impulses is taken as a measure of noise. Data is collected on a specific statistical procedure and assessed for monthly median and higher decile values of noise.

For carrying out the measurements, a noise meter has been developed. It is designed as a field strength meter. It uses a short vertical aerial which is connected to a superheterodyne receiver through a feeder. The receiver has a bandwidth of 6 kc at 6 db down as this corresponds more nearly to what is found in ordinary commercial receivers. Since the detector can have an effect on the wave form of noise impulses, the af output is taken and fed through a logarithmic amplifier to an impulse recording valve voltmeter. The time constants of the meter were adjusted by trial and error to see that what was read by the meter corresponded to what was heard and that the meter failed to record kicks when the ear got the impression of continuous noise. A million observations have revealed that the time constants are satisfactory for over 50 per cent of the impulses. The time constants chosen are:

charging time constant = 10 milliseconds
discharging time constant = 500 milliseconds.

The calibration procedure follows the usual method adopted for calibrating field strength meters. But, since measurements are taken on the af side, a suitable modulating frequency and a suitable depth of modulation had to be chosen. Following the usual receiver testing practice, signals modulated 30 per cent by a 400 cps note from a standard signal generator are used.

The time constants of the noise meter and its method of calibration both have an effect on calculations of noise power at the source that should correspond to the noise field strength as measured by this noise meter and this is discussed in what follows.

Effect of Noise Meter Time Constants

The charging time constant of the noise meter is 10 milliseconds. The electric field due to a stroke in a flash as calculated in (15) lasts only one millisecond. Therefore, the effective field charging up the condenser of the noise meter, E_2, will be given by

$$E_2 = (0.1)E_1 \tag{16}$$

The discharge time constant of the noise meter is 500 milliseconds. The time interval between the strokes in a flash is 40 milliseconds, and there are three such strokes per flash. The effect as recorded by the noise meter will, therefore, be additive and the net effect of the three strokes will be

$$E_3 = 2.776E_2 = 0.2766E_1. \tag{17}$$

It is extremely important to remember that the noise meter readings correspond to E_3 and not to E_1 as would ordinarily be supposed.

Significance of Noise Meter Calibration

The procedure adopted for estimating noise field strengths for comparison with experimental results is as follows. Suppose that during a certain period, say a month, the thunderstorm activity is spread over a certain area. Then, the mean center of this area is located. At this position, it is supposed that there is a short dipole in free space radiating a power of Q kilowatts carrying a 30 per cent modulation by a 400 cps note. Since the height of the clouds in which the discharges take place is not very great, it is assumed, for long distance calculations, that this dipole is situated practically at ground. Thus the field intensity calculations are carried out by using the following formula:

$$E_4 = \text{Field intensity in microvolts per meter}$$
$$= \frac{212\sqrt{Q}\cdot\sin\theta}{r} \tag{18}$$

where r is the distance of the source in 10^6 meters.

Q represents the carrier power. Therefore, the total power involved, when the 30 per cent modulation by a 400 cps note is taken into account, is $Q(1+0.045)$. This total power has to be equated to the noise power at the source while carrying out calculations.

But, the noise field strength is due to the noise source acting as a radiator at a particular frequency within the limits of the defined bandwidth of the receiver. This noise source is, of course, the idealized, statistically valid representation of the lightning flash as given in this paper. This gives E_3 as the equivalent field strength that the noise meter measures. Therefore, equating E_3 to E_4 after applying the correction for modulation, the following expression is obtained:

$$E_3 = \frac{212\sqrt{Q(1\cdot045)}\cdot\sin\theta}{r}. \tag{19}$$

Power Radiated by the Noise Source

Therefore, Q is the power in kilowatts that the noise source is implied to radiate on the basis of the actual measurement by the noise meter calibrated as previously explained. Using (19), (17), (15), and (13), the following expression is obtained for Q:

$$\sqrt{Q} = \frac{0\cdot2776 \times 30 \times \sqrt{1\cdot5} \times \sqrt{2\nu B} \times \delta l I_0}{212 \times c \times 2 \times \pi \times f \times 10^6 \times \sqrt{1\cdot045}} \cdot \tag{20}$$

The significance and assumed values of the different letters in the above equation are given below:

B = bandwidth of the receiver = 6,000 cps
f = frequency in megacycles per second
c = velocity of light = 3×10^8 meters per second
ν = recurrence frequency of the impulses radiated = 13,500 cps

l = average length of a step in a stepped leader = 67 meters

δI_0 = maximum rate of change of current in a discharge occurring in a lightning flash.
= 10^{10} amperes per second

From (20), Q works out to be

$$\frac{4.506 \times 10^{-2}}{f^2}$$

kilowatts. This gives the power, P, in watts as

$$P = 45.06/f^2 \text{ watts.} \tag{21}$$

This power, P, corresponds to the idealized, statistically valid representation of a lightning flash. It can be used along with known thunderstorm centers and the laws of propagation to estimate a monthly or seasonal median value of atmospheric noise as measured by the particular noise meter described earlier.

A thunderstrom builds up, shows peak activity for a certain number of hours and then decays. It has been observed that there are two distinct types of common thunderstorms on tropical land mass like that of India.[19] In one type, the period of peak activity is about 4 to 5 hours and the maximum is reached before sunset. In another type, the period of peak activity is about 5 to 6 hours and the maximum is reached after sunset. During this period of peak activity, the noise field strength is within about 3 db of a mean value. This power, P, given by (21), refers to such a mean value during the period of peak activity.

Comparison with Experimental Results

Systematic measurements of atmospheric noise by the method[1] referred to earlier have been taken for a complete year and more at Poona (18.31 N, 73.55 E) for the period of day, 18 to 24 hours (Indian Standard Time—5 hours 30 minutes ahead of GMT), at frequencies 2.9 and 4.7 mc, and the results have been analyzed.[20,21] Table I below summarizes the results.

TABLE I
Comparison of Observed and Estimated Noise Field Strengths

f in mc	Source dist. (kms)	No. of months	Mean observed value in $\mu V/m$	Estimated value in $\mu V/m$	Type of noise
2.9	700	8	10.6	13.0	B
2.9	1500	1	6.2	9.2	B
2.9	2000	3	5.3	7.3	B
2.9	4000	4	0.9	2.3	A
4.7	700	9	7.3	8.1	B
4.7	1500	3	5.2	5.7	B
4.7	2000	2	4.4	4.5	B
4.7	4000	3	0.9	1.4	A

The first column gives the frequency in mc. The second column gives the estimated mean distance, d, of the source as explained earlier. The value is given in km. The third column gives the total number of months during which the noise due to the source at this distance has been observed. The fourth column gives the mean of the observed values for all the months in $\mu V/m$. It may be stated that the variation of the monthly median value from month to month is within 10 per cent of the mean value given. The fifth column gives the calculated unabsorbed field intensity in $\mu V/m$. For carrying out the calculations, the power as given by (21) has been used. Since the period corresponds to night conditions, the reflection is assumed to occur in the F_2 layer and the calculations have been carried out using the procedure and data from Circular 462 of the U. S. Bureau of Standards on Ionospheric Radio Propagation. The formula used is as given in (18) in which $r = d/\sin\theta$.

It will be seen that the estimated and observed values agree within 3 db for type B noise and the measured values are always lower than the estimated values. Considering the range of data required, the agreement between measured and estimated values appears to be satisfactory. The wide difference between measured and estimated values for type A noise, which is due to distant sources, and the fact that even for type B noise the measured value is always less than the estimated value, are suggestive of a possible absorption in the ionosphere even when night conditions prevail. An average monthly value for the absorption factor, K, between 0.03 and 0.05 for the complete period of 18 to 24 hours IST can explain all the differences.

Measurements are in progress at 980 kc and 9.0 mc and data for several months are available.[22,23] The results indicate that they can also be explained on the same lines as above.

Type C noise is due to local thunderstorms. Eq. (21) is not applicable to an individual phenomenon but it should give a rough indication of the magnitude. Individual local thunderstorms have been followed by noise measurements at more than one frequency.[19] By using the power given by (21) and carrying out ground or optical ray calculations as required, the distance of the thunderstorm from the point of observation has been calculated from the results at different frequencies. The values agree within 20 per cent.

Conclusion

The satisfactory agreement between measured and estimated values is largely because one is dealing, in both cases, with statistical averages. It is also because of the outstanding excellence of the data on lightning discharges. The values chosen for the different quantities

[19] S. V. C. Aiya, K. R. Phadke, C. G. Khot and C. K. Sane, "Tropical thunderstorms as noise radiators" (to be published).

[20] S. V. C. Aiya and K. R. Phadke, "Atmospheric noise interference to broadcasting in the 3 mc/s band at Poona," *Jour. Atmos. Terr. Phys.*

[21] K. R. Phadke, "Atmospheric noise interference to broadcasting in the 5 mc/s band at Poona," *Proc. 42nd Ind. Sc. Cong.*, part III, section XIII, No. 21, 1955 (to be published).

[22] S. V. C. Aiya and C. G. Khot, "Atmospheric noise interference to broadcasting at 1 mc/s at Poona," *Proc. 42nd Ind. Sc. Cong.*, part III, section XIII, No. 23, 1955 (to be published).

[23] S. V. C. Aiya and C. K. Sane, "Atmospheric noise interference to broadcasting at 9 mc/s at Poona," *Proc. 42nd Ind. Sc. Cong.*, part III, section XIII, No. 22, 1955 (to be published).

required from lightning discharge results and the reasons for their choice have been discussed in detail. They all appear to be essentially correct. The only factor now left is bandwidth. In the receivers employed for noise measurements, the actual bandwidth is 6 kc at 6 db down. This has been used in the calculations as 6 kc. Whether a corrected value should be used is being examined and, if it is concluded that there should be a correction, the details will be reported separately.

Certain assumptions and approximations made in the paper require modification for very low frequencies, and this is obvious from the paper itself. For high frequencies, i.e., above 20 mc, the idealized picture of the step in the leader stroke may require modification. The question of flashes which strike the ground does not strictly fall in the scope of this paper but needs examination not only for tropical thunderstorms as special cases but also for thunderstorms in temperate regions.

The paper makes it abundantly clear that the main source of noise is not, as is commonly believed, the return stroke to the cloud from the ground in flashes which strike the ground. The discharges within the cloud or into the air, particularly the former, are the main sources of noise.

The analysis can, perhaps, be made more rigorous mathematically. The final result will not alter significantly. The principal object of this paper is to bring out clearly the basic physical principles involved in the analysis as they are most fundamental. Such an object cannot be realized by a more rigorous analysis in which the mathematics may mask the basic ideas. Further, the method adopted here should fully meet the requirements of an engineer.

The author's thanks are due to Messers. L. A. Ramdas and K. N. Rao for permission to use the library of the India Meteorological Department.

Rotatable Inductive Probe in Waveguides*

F. J. TISCHER†, SENIOR MEMBERS, IRE

Summary—It is shown by calculation of the field distribution in waveguides with TE waves in the presence of both the forward and the reflected waves that the voltage induced in a pure inductive probe depends on its angular position in the same manner that a probe in a slotted line depends on its axial position. Thus, a rotatable probe consisting of a wire loop and a compensating arrangement extending through an aperture into the waveguide can be used as a standing wave detector. An instrument for S-band waveguides utilizing this principle, its advantages and disadvantages and its error are further subjects of this paper.

Introduction

FROM THE representation of the field distribution in waveguides with TE waves, considering both the forward and the reflected wave, it follows that the amplitude of the voltage induced in a rotatable inductive probe, expressed as a function of the angular position, has under certain conditions the same form as that induced in a probe moved in a slotted waveguide in the axial direction. Thus, such a rotatable probe extending into the waveguide through an aperture in its wall can be used as a standing-wave detector to determine the matching properties of components connected to the guide.

One of the conditions named postulates that only the magnetic field induces a voltage in the probe. This condition is not fulfilled in the case of an ordinary wire loop used as a probe because a part of the probe voltage is induced by the electric field of the waves in the waveguide. Application of a pure inductive probe, investigated in connection with an error study of slotted line sections may offer a way to overcome this difficulty.

A recent publication[1] and its references[2] describe another method of using the presence of the two components of the magnetic field strength for the standing wave measurement. The device utilized consists of a secondary circular waveguide attached at right angles to the main guide and coupled to it by holes or slots. The variation of the electrical field strength in the circular waveguide around the circumference is sampled by a probe and used as a reference for the standing-wave pattern in the primary waveguide.

Rectangular Waveguides with Rotatable Probe

The field distribution of TE waves in a lossless rectangular waveguide in the presence of a reflected wave can be generally represented by (1).

* Original manuscript received by the IRE, March 7, 1955; revised manuscript received May 9, 1955. Statements and opinions advanced in this paper are to be understood as individual expressions of the author, and not necessarily those of Redstone Arsenal.

† Research Div., Ordnance Missile Labs., Redstone Arsenal, Huntsville, Ala.

[1] S. B. Cohn, "Impedance measurement by means of a broadband circular-polarization coupler," Proc. IRE, vol. 42, pp. 1554–1558; October, 1954.

[2] F. E. F. Fertel, R. W. L. Batt, J. A. Barrable, and C. S. Wright, British Patent No. 592,224; September 11, 1947.

$$E_z = E_0 \cos \frac{\pi}{b} y[1 + \rho_L e^{-2i\beta(L-x)}]e^{-i\beta x},$$

$$H_x = i\frac{\lambda_0}{\lambda_c}\sqrt{\frac{\epsilon_0}{\mu_0}}\, E_0 \sin \frac{\pi}{b} y[1 + \rho_L e^{-2i\beta(L-x)}]e^{-i\beta x},$$

$$H_y = \sqrt{1-\left(\frac{\lambda_0}{\lambda_c}\right)^2}\sqrt{\frac{\epsilon_0}{\mu_0}}\, E_0 \cdot \cos \frac{\pi}{b} y[1 - \rho_L e^{-2i\beta(L-x)}]e^{-i\beta x}. \quad (1)$$

Fig. 1 shows the co-ordinate system and the dimensions on which the equations are based.

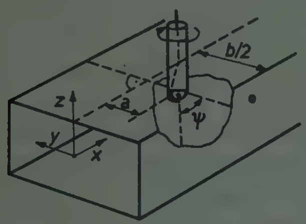

Fig. 1—Rotatable pure inductive probe in a rectangular waveguide.

In (1), E_0 is the maximum amplitude of the electric field strength, b is the internal width of the waveguide, $\beta = 2\pi/\lambda_g$ is the propagation constant and ρ_L the voltage reflection coefficient with respect to a reference plane at $L = x$. The reflection coefficient is defined by the condition that a conducting plane shorting the waveguide at the distance L from the origin produces $\rho_L = -1$. The wavelength in free space is λ_0; and ϵ_0 and μ_0 are coefficients for the relations between the field magnitudes.

Under the assumption that a pure inductive probe is used, the magnetic field component H_n, directed perpendicular to the plane of the loop, induces a voltage in the probe. Its value is

$$V_p = -i\omega\mu_0 H_n F,$$

in which F is the area of the probe loop. Both components of the field strength in the waveguide H_x and H_y contribute to H_n, and the probe voltage V_p becomes

$$V_p = -i\omega\mu_0 F[H_y \cos\psi + H_x \sin\psi]. \quad (2)$$

ψ is the angle between the normal to the loop plane and the transverse direction of the waveguide y. Further, if the substitutions

$$k_1 = \frac{\lambda_0}{\lambda_c} \sin \frac{\pi}{b} y \text{ and } k_2 = \sqrt{1-\left(\frac{\lambda_0}{\lambda_c}\right)^2} \cos \frac{\pi}{b} y \quad (3)$$

are made, V_p is found to be:

$$V_p = -i\omega\sqrt{\epsilon_0\mu_0}E_0F\{ik_1[1 + \rho_L e^{-2i\beta(L-x)}]\sin\psi + k_2[1 - \rho_L e^{-2i\beta(L-x)}]\cos\psi\}e^{-i\beta x}. \quad (4)$$

For $k_1 = k_2$, (4) can be simplified to

$$V_p = V_0\{1 - \rho_L e^{-2i[\psi+\beta(L-x)]}\}e^{i(\psi-\beta x)}. \quad (5)$$

V_0 is the amplitude of the voltage induced in the pure inductive probe if the waveguide is matched.

The consideration of the amplitude factor between the braces of (5) shows that a rotation of the probe by an angle ψ has the same consequence as a movement of the probe over a distance $\overline{\Delta}x = \psi/\beta = \psi\lambda_g/2\pi$. Thus, a rotation by 90 and 180 degrees corresponds to a movement of the probe by $\lambda_g/4$ and $\lambda_g/2$, respectively, in the axial direction. The wavelength in the waveguide, λ_g, is related to λ_0 and λ_c by

$$\frac{1}{\lambda_0^2} = \frac{1}{\lambda_g^2} + \frac{1}{\lambda_c^2} \quad (6)$$

in which λ_c is the cutoff wavelength which is equal to $2b$.

The condition $k_1 = k_2$ can be realized by a proper position of the probe in transverse direction. By equating the right-hand terms of (3), this position is found to be determined by the relation:

$$\frac{a}{b} = \frac{1}{\pi}\tan^{-1}\frac{\lambda_c}{\lambda_g} = \frac{1}{\pi}\tan^{-1}\sqrt{\left(\frac{f_0}{f_c}\right)^2 - 1}. \quad (7)$$

The ratio a/b, the relative distance of the probe from the vertical plane of symmetry, is shown as a function of the frequency quotient f_c/f_0 in Fig. 2.

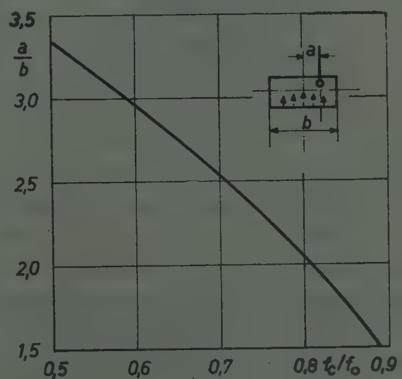

Fig. 2—Frequency dependence of the relative probe position for desired probe properties.

If the waveguide is matched, the relation for the probe voltage becomes

$$V_p = V_0 e^{-i\psi} e^{-i\beta x}.$$

Therefore, the phase of the probe voltage varies in direct proportion to ψ.

Circular Waveguide with Rotatable Probe

The results of the derivation of the field distribution in lossless circular waveguides with TE_{11} waves can be shown to be

$E_z = 0,$

$$E_r = -K\frac{\omega\mu}{r}J_1\left(\sigma\frac{r}{r_0}\right)\sin\phi[1+\rho_L e^{-2i\beta(L-x)}]e^{-i\beta x},$$

$$E_\phi = -K\frac{\omega\mu\sigma}{r_0}J_1'\left(\sigma\frac{r}{r_0}\right)\cos\phi[1+\rho_L e^{-2i\beta(L-x)}]e^{-i\beta x},$$

$$H_x = iK(\omega^2\epsilon\mu-\beta^2)J_1\left(\sigma\frac{r}{r_0}\right)\cos\phi[1+\rho_L e^{-2i\beta(L-x)}]e^{-i\beta x},$$

$$H_r = K\beta\frac{\sigma}{r_0}J_1'\left(\sigma\frac{r}{r_0}\right)\cos\phi[1-\rho_L e^{-2i\beta(L-x)}]e^{-i\beta x},$$

$$H_\phi = -K\frac{\beta}{r_0}J_1\left(\sigma\frac{r}{r_0}\right)\sin\phi[1-\rho_L e^{-2i\beta(L-x)}]e^{-i\beta x}. \quad (8)$$

Eqs. (8) consider either the forward or the reflected waves and are based on co-ordinates and dimensions of the waveguide according to Fig. 3. K is a general amplitude constant, J_1 and J_1' are Bessel functions of the first order and its derivative, and σ a parameter depending on the conditions at the boundary of the cross section. The wave propagation constant β is again related to the wavelength in free space and to the cutoff wavelength by (6). The cutoff wavelength is related to cross-section dimensions of the waveguide by $\lambda_c = 3.41\ r_0$.

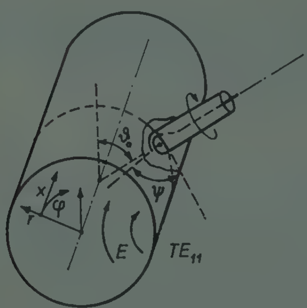

Fig. 3—Rotatable probe in a circular waveguide.

The probe extends through an aperture into the waveguide at a point determined by an angle ϑ between the probe axis and the plane of symmetry of the field distribution. The probe axis and the plane of the probe loop are perpendicular to the wall of the wave guide. The probe loop is considered to be small. Therefore, the approximation may be made that the voltage of the probe is induced by the field occurring in the vicinity of the waveguide wall. With this assumption $r \cong r_0$ and the radial component of the magnetic field strength is zero ($H_r = 0$). Only the components H_x and H_ϕ contribute to the probe voltage. These components are a function of the angle ϑ which determines the position of the probe with respect to the field configuration;

$$H_x = iH_0\frac{\lambda_0}{\lambda_c}\sin\theta[1+\rho_L e^{-2i\beta(L-x)}]e^{-i\beta x},$$

$$H_\phi = -H_0\frac{1}{1.84}\sqrt{1-\left(\frac{\lambda_0}{\lambda_c}\right)^2}\cdot\cos\theta[1-\rho_L e^{-2i\beta(L-x)}]e^{-i\beta x}. \quad (9)$$

To obtain the probe voltage, (2) is to be used. In it, H_y must be replaced by H_ϕ. The angular position of the probe about its axis is measured by the angle between the normal to the loop plane and the ϕ-direction at the point where the probe is placed. Under these conditions, the probe voltage has the value

$$V_p = -i\omega\mu_0 F\{ik_1H_0[1+\rho_L e^{-2i\beta(L-x)}]\sin\psi + k_2H_0[1-\rho_L e^{-2i\beta(L-x)}]\cos\psi\}e^{-i\beta x}, \quad (10)$$

in which

$$k_1 = \frac{\lambda_0}{\lambda_c}\sin\theta \quad \text{and} \quad k_2 = \frac{1}{1.84}\sqrt{1-\left(\frac{\lambda_0}{\lambda_c}\right)^2}\cos\theta. \quad (11)$$

In the case that $k_1 = k_2$, (10) can be simplified and

$$V_p = V_0\{1-\rho_L e^{-2i[\psi+\beta(L-x)]}\}e^{+i(\psi-\beta x)} \quad (12)$$

is obtained. The functional relationship of variables determining the probe voltage is similar to that in the case of the rectangular waveguide.

A rotation of the probe through an angle $\Delta\psi$ yields the same results as a movement of the probe of $\Delta x = \lambda_g\Delta\psi/2\pi$ in the axial direction. Again, rotations through 90 and 180 degrees correspond to a movement of $\lambda_g/4$ and $\lambda_g/2$, respectively. From (12) the conclusion can be drawn that if only one wave proceeds in the waveguide and $\rho_L = 0$, the amplitude of the probe voltage is constant and its phase angle varies linearly as a function of the angle.

Examination of the condition $k_1 = k_2$ shows that the probe must be located at a proper place on the circumference of the waveguide with respect to the plane of symmetry of the field distribution. This position is measured by θ_0 the angle between the radial direction from the center of the waveguide to the probe and the plane of symmetry of the field distribution in the waveguide. From (11) θ_0 is obtained as a function of f_0/f_c:

$$\theta_0 = \tan^{-1}\frac{\sqrt{\left(\frac{\lambda_c}{\lambda_0}\right)^2-1}}{1.84} = \tan^{-1}\frac{\sqrt{\left(\frac{f_0}{f_c}\right)^2-1}}{1.84}. \quad (13)$$

Values of θ_0 are shown graphically in Fig. 4.

Application of a Rotatable Probe for the Standing Wave Detection

Assemblies shown schematically in Figs. 1 and 3 can be used for the standing-wave detection and determination of the reflection coefficient in the same manner as a slotted line section is used. If the probe is rotated, the absolute value of the reflection coefficient can be obtained from the ratio of the maximum to minimum probe voltage. The values for $|V_p|_{max}$ and $|V_p|_{min}$ are calculated from (12) and (5) respectively. It is

$$\frac{|V_p|_{max}}{|V_p|_{min}} = \frac{1+|\rho|}{1-|\rho|}, \quad (14)$$

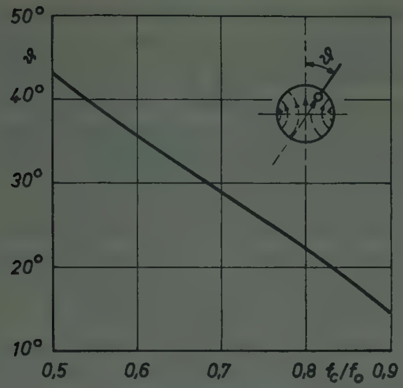

Fig. 4—Frequency dependence of the probe position relative to the field configuration for desired probe properties.

where ρ is the reflection coefficient in the cross-sectional plane of the waveguide containing the axis of the probe. It is to be noted that $|\rho|$ is independent of the position in axial direction or of the reference plane for ρ. In a sense, the ratio $|V_p|_{\max}/|V_p|_{\min}$ can be called the standing-wave ratio swr. In consequence, (14) yields

$$|\rho| = \frac{\text{swr} - 1}{\text{swr} + 1}.$$

For more thorough determination of the reflection properties of an element connected to a waveguide, it is necessary to determine the complete complex reflection coefficient. Representing $\rho = |\rho| e^{i\phi}$, substitution in (5) yields

$$V_p = V_0[1 - |\rho| e^{i(\phi - 2\psi)}] e^{i(\psi - \beta z)}. \tag{15}$$

The minimum of the probe voltage occurs at an angular position at which the term $(\phi - 2\psi)$ equals zero. Thus,

$$\phi = 2\psi_{\min} \tag{16}$$

is obtained, if $\psi_{\min}$ defines the angular position of the probe about its axis for the minimum voltage. Eq. (16) shows as an advantage of the rotatable probe that the phase of the reflection coefficient can be determined directly by $\psi_{\min}$ independent of the frequency under the assumption that the probe is properly placed ($k_1 = k_2$). Note that using a slotted line detector this value has to be determined by comparing the positions of the probe for the minimum probe voltage with that position obtained if the measured object is replaced by a short circuit.

If the section with rotatable probe is used as standing-wave detector, the microwave circuitry is the same as for a slotted waveguide section. The instrument is placed between the object, the matching data of which are to be determined, and the signal generator. The probe voltage can be rectified directly in the probe by a crystal diode and fed to an instrument. Another possibility is the use of a receiver to evaluate the probe voltage.

The Probe Problem

One of the main problems concerns the probe. The investigation of a simple asymmetrical wire loop shows that not only the magnetic field but also the electric field contributes to the probe voltage. The capacitive part of the probe voltage results from a capacitive current induced in the loop by the electric field in axial direction of the probe. This part of the probe voltage can be reduced almost to zero by a compensating wire as shown in Fig. 5. The compensating wire partially shields the loop wire in the region of its transition from probe line to loop. The capacitive current on the compensating wire resulting from the electric field induces a capacitive compensating voltage in the wire loop opposing the directly induced capacitive voltage. Adjusting the length of the compensating wire to a proper value, eliminates the capacitive part of the probe voltage.

Fig. 5—Pure inductive probe with compensation wire.

As a measure of the quality of the compensation, the ratio between the amplitude of the capacitive part of the probe voltage divided by the inductive part can be considered. A special method has been developed for the determination of this ratio $V_{\text{cap}}/V_{\text{ind}}$ by use of a slotted line standing-wave detector. As has been shown in the derivation,[3] this ratio is proportional to the distance between two axial positions of the probe for minimum probe voltage when a short circuit is connected to the output of the slotted section. One axial position occurs in the normal position of the probe and the second is obtained when it is rotated about its axis by 180 degrees. This relation is valid for small values of $V_{\text{cap}}/V_{\text{ind}}$. In the case of an ideally pure inductive probe, the positions of the minima, if the probe is rotated by 180 degrees, coincide and lie at a position $\lambda_g/4$ distant from that which would be obtained with a capacitive probe. With increased capacitive contribution to the probe voltage, the distance between the positions of the minima increases and becomes $\lambda_g/2$ in the case of the capacitive probe.

Fig. 6 (next page) shows ratio $V_{\text{cap}}/V_{\text{ind}}$ as a function of frequency obtained by the above method for a practical design of an essentially pure inductive probe with a loop area of approximately 0.02 square inch. The graph confirms the results of the calculations of an idealized compensated probe and shows that within limits compensation is independent of frequency.

Standing Wave Detector for Rectangular Waveguide with Rotatable Probe

Using the results of the foregoing investigation, a standing-wave detector for S-band waveguides was designed and tested. The prototype is shown in Fig. 7.

[3] F. J. Tischer, "Inductive probe for standing wave meters and field strength meters on microwaves," *Trans. Royal Inst. Tech.*, No. 45, Stockholm, Sweden, p. 12; 1951.

The instrument consists of a section of a rectangular waveguide. On the broad wall of the guide is placed a carriage which is movable in the transverse direction of the waveguide. A probe attached to it can be rotated about its axis and extends into the waveguide through an aperture of elliptical shape to permit the adjustment of the position in the transverse direction. A spring presses the carriage against a micrometer head. The relative position in transverse direction can be precisely determined by readings on the scale of the micrometer. By use of calibration curves of transverse position versus frequency, the probe can be placed with high accuracy to meet the condition $k_1 = k_2$. To facilitate the rotation movement, a disc is attached to the probe on which a scale is engraved. The scale covers an angle of 180 degrees and is divided in 50 parts. One degree on the scale corresponds to an axial translation of the probe by $\lambda_g/100$. A matched flexible cable provides the transfer of the probe voltage to a type-"N" contact affixed to the instrument. The probe voltage can be rectified by a crystal diode, amplified and fed to an instrument to indicate the amplitude of the probe voltage.

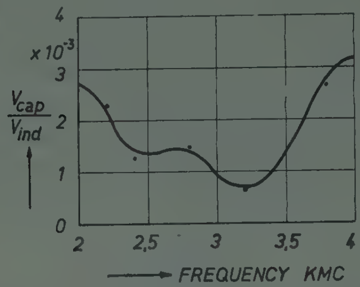

Fig. 6—Ratio of the capacitive to the inductive component of the probe voltage induced in a compensated inductive probe.

The practical measuring procedure is similar to that of a slotted line section. The instrument described in the preceding paragraph is inserted between the signal generator and the object under investigation. By rotation of the probe, maximum and minimum voltages are observed and swr and the absolute value of the reflection coefficient computed. The angular position $\psi_{\min}$ for the minimum probe voltage corresponds directly to the angle $\phi = \angle \rho$ according to (16).

The instrument with rotatable probe has some advantages over a slotted section. One is the simplicity of the rotational movement in the measurement procedure. The mechanical problems in connection with this rotational movement can be solved more easily than the accurate linear movement of a probe along a slotted standing-wave detector. Thus, some errors occurring in the slotted section are avoided by using the rotating probe. For example, errors resulting from mechanical inaccuracy of the probe movement, inaccurate machining of the slot, disturbances resulting from leakage of high-frequency energy through the slot; further, errors resulting from discontinuities attributable to the slot and the moving probe itself do not occur in this instrument. A further advantage is the fact that the angle of the reflection coefficient is directly determined by the angular position of the probe, when the probe voltage is a minimum. This relationship is independent of frequency if the probe is properly placed in transverse direction. The necessity to adjust the transverse position of the probe in the case of a frequency change should be mentioned as a disadvantage. However, the calibration of the frequency of signal generators and the adjustment of the position of the probe by the micrometer head are sufficiently accurate to insure a negligible error for most purposes.


Fig. 7—Prototype of a standing-wave detector with rotatable probe.

As a measure of the accuracy of a standing-wave detector, the indicated swr can be used if the instrument is terminated by a perfectly matched waveguide termination. Fig. 8 (facing) shows the graphs of the relative probe voltage plotted as a function of the angular position of the probe at different frequencies under this condition. The curves show that the residual error lies under ± 1 per cent, thus permitting accurate matching measurements.

Error Analysis of a Rotatable Probe in Rectangular Waveguides

Two errors and their sources must be discussed more thoroughly. The first is originated by improper transverse position of the probe relative to frequency and the other results from the capacitive part of the probe voltage induced by the electrical field in an unsatisfactorily compensated probe.

The first type of error results from an erroneous calibration or setting of the micrometer head which controls the position of the probe. It can occur also if the frequency reading or calibration is inaccurate. The consequence is in both cases that (7) is not satisfied. To investigate the error the assumption is made that the probe is displaced by a relative distance $\Delta a/b$ from the position for which $k_1 = k_2$. Under this condition

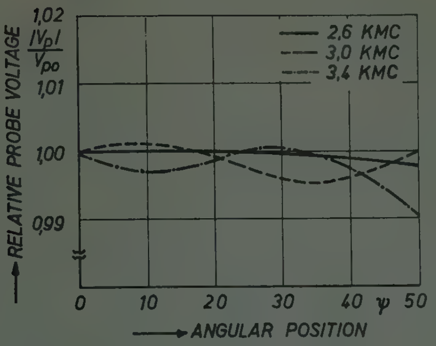

Fig. 8—Probe voltage as a function of the angular position of the probe for matched output ($\rho=0$).

$$k_1 = \frac{\lambda_0}{\lambda_g} \sin \frac{\pi}{b}(a + \Delta a)$$

and

$$k_2 = \sqrt{1 - \left(\frac{\lambda_0}{\lambda_c}\right)^2} \cos \frac{\pi}{b}(a + \Delta a) = k_1 - \frac{\pi}{b}\Delta a \qquad (17)$$

is obtained. This may be substituted in (5) and yields the erroneous probe voltage as a function of the angular position

$$V_p' = V_0 \left[1 - \frac{k_1\rho + \dfrac{\pi}{b}\dfrac{\Delta a}{2}(1-\rho)}{k_1 - \dfrac{\pi}{b}\dfrac{\Delta a}{2}(1-\rho)} e^{-2i\psi} \right] \cdot \left[k_1 - \frac{\pi}{b}\frac{\Delta a}{2}(1-\rho) \right] e^{i(\psi - \beta x)}, \qquad (18)$$

if the reference plane for the reflection coefficient is placed at the probe ($L-x=0$). Eq. (18) shows that the probe voltage is the same as in the case when an object defined by a reflection coefficient

$$\rho' = \frac{k_1\rho + \dfrac{\pi}{b}\dfrac{\Delta a}{2}(1-\rho)}{k_1 - \dfrac{\pi}{b}\dfrac{\Delta a}{2}(1-\rho)} \qquad (19)$$

should be connected to the output, the probe being correctly located. At the same time, ρ' is the erroneous reflection coefficient measured instead of ρ if the probe is displaced by Δa. The error $\Delta\rho = \rho' - \rho$ has the value:

$$\Delta\rho = \frac{\pi}{2k_1}\frac{\Delta a}{b}(1-\rho^2) \Big/ \left[1 - \frac{\pi}{2k_1}\frac{\Delta a}{b}(1-\rho) \right]. \qquad (20)$$

For a matched waveguide and small errors the approximation

$$\Delta\rho_0 \approx \frac{\pi}{2k_1}\frac{\Delta a}{b} \qquad (21)$$

is obtained.

Thus, in spite of correct matching, a value of

$$\text{swr}' \approx 1 + \frac{\pi \dfrac{\Delta a}{b}\left(\dfrac{\lambda_c}{\lambda_0}\right)^2}{\sqrt{\left(\dfrac{\lambda_c}{\lambda_0}\right)^2 - 1}} \qquad (22)$$

is measured.

In the case of total reflection, the positions of the minima of the standing-wave pattern are displaced yielding an error $\Delta\phi$ of the angle of the reflection coefficient. It is:

$$\Delta_\phi \approx -2\frac{\pi}{2k_1}\frac{\Delta a}{b}\sin\phi.$$

In the general case, for an arbitrary value of ρ, the errors caused by the incorrect position of the probe are shown in Fig. 9, relative to the error in the case of matching ($\rho=0$).

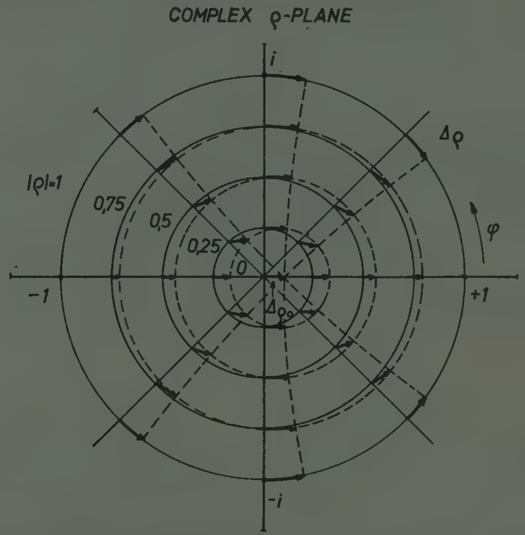

Fig. 9—Error of the measured reflection coefficient ρ resulting from incorrect positioning of the probe.

Numerical calculations show that this type of error for the instrument described is in the magnitude of approximately 3×10^{-3}.

The same type of error results from inaccurate frequency setting or calibration. This part of the total error can be calculated from the frequency dependence of the correct transverse position of the probe. From (7), the differential quotient da/df_0 can be obtained. Further calculation yields

$$\frac{\Delta a}{b} = \frac{1}{\pi}\frac{\Delta f_0}{f_0}\frac{1}{\sqrt{\left(\dfrac{\lambda_c}{\lambda_0}\right)^2 - 1}}. \qquad (23)$$

Eq. (23) shows the necessary change of the relative position of the probe if the frequency is shifted by $\Delta f_0/f_0$. It shows further the value of $\Delta a/b$ which produces the same error as misalignment of the frequency

by $\Delta f_0/f_0$. Thus, the error of the reflection coefficient caused by an incorrect frequency is

$$\Delta\rho_0 \approx \frac{1}{2} \frac{\dfrac{\Delta f_0}{f_0}}{1 - \left(\dfrac{\lambda_0}{\lambda_c}\right)^2}, \tag{24}$$

in the case of matching or in the neighborhood $|\rho| \ll 1$. For other values of ρ, $\Delta a/b$ of (20) must be substituted by the right term of (24). The dependence is the same as shown in Fig. 9.

Substituting numerical values for an S-band instrument, an error of $\Delta\rho_0 \approx \pm 0.3 \times 10^{-3}$ is obtained, if a frequency error of ± 1 per cent is assumed. This latter error is of the magnitude of the usual error of the calibration of signal generators.

A further error is introduced if the inductive probe is not satisfactorily compensated and the electric field induces a voltage in the probe. It was shown that this voltage has a value

$$V_{cap} = V_{0cap}[1 + \rho]e^{-i\beta x}, \tag{25}$$

V_{0cap} being the amplitude of the voltage induced by the electric field of a single forward wave. This voltage is independent of the angular position of the probe. The inductive part of the probe voltage V_{ind} is

$$V_{ind} = V_{0ind}[1 - \rho e^{-2i\psi}]e^{i(\psi - \beta x)}. \tag{26}$$

By addition and with the assumption $\rho = 0$

$$V_p = V_{0ind}\left[1 - \frac{V_{0cap}}{V_{0\,ind}} e^{i(\pi/2 - \psi)}\right] e^{i(\psi - \beta x)} \tag{27}$$

is obtained. Eq. (27) shows that the amplitude of the probe voltage varies for small capacitive voltages according to

$$|V_p| \approx V_{0ind}\left[1 - \frac{V_{0cap}}{V_{0ind}} \sin \psi\right]. \tag{28}$$

The function represented by (28) has a dependence on the angular position of the probe, which is different from that obtained from mismatch ($\rho \neq 0$). The occurrence of this type of error can, therefore, be easily detected. The amplitude ratio V_{0cap}/V_{0ind} can be determined by special measurement methods mentioned above. Typical values for a compensated probe are shown in Fig. 6. With these values, the error resulting from unsatisfactorily compensated probes seems to have an upper limit of approximately ± 0.2 per cent.

The mean value of the total error resulting from all these influences, using the accuracies of conventional equipment, has for an S-band instrument an approximate value of ± 0.6 per cent and is sufficiently low to permit matching and reflection measurements in waveguides with high accuracy.

Acknowledgment

The author wishes to acknowledge the assistance of James E. Norman in the composition of this paper.

The Minimum Noise Figure of Microwave Beam Amplifiers*

H. A. HAUS† AND F. N. H. ROBINSON‡

Summary—**A matrix description of microwave amplifiers such as klystrons, traveling-wave tubes, and backward-wave amplifiers, in which an electron beam interacts with longitudinal RF fields, is developed. Certain relations between the matrix elements are derived as a consequence of the conservation of energy and these relations set a lower limit to the noise figure attainable with amplifiers of this class. It is shown that the minimum noise figure of any amplifier of this type with lossless RF structures is identical with that already found by several authors for the traveling-wave tube and is entirely determined by the noise parameters of the beam. These in turn depend only on conditions in the immediate neighborhood of the cathode. Special cases involving lossy structures are investigated and in each case the presence of loss is shown to increase the noise figure. The method is also applied to calculate the minimum noise figure of a double-stream amplifier.**

I. Introduction

Noise in electron streams has been discussed by various authors[1–3] and their results have been applied to the reduction of noise in traveling-wave tubes by Watkins[2] and Peter.[4] More recent developments due to Pierce,[5] Bloom and Peter,[6] and Haus[7] have led to the realization that there is a lower limit to the noise figure to be obtained in this way.[8–10] All of the authors have based their calculations on a one-dimensional model of the electron beam using also a small signal and single valued velocity approximation. More sophisticated treatments[11] show that except in the immediate vicinity of the potential minimum the small-signal and single-velocity approximations are valid in any case of practical interest. The one-dimensional approximation chosen primarily for its mathematical simplicity is known to lead to results which within its limitations agree with experiment.

An identical result has been found for the minimum noise figure of klystrons, space-charge-wave amplifiers and similar devices[10,12] and it is therefore pertinent to inquire whether this result has more general validity. We shall prove that any amplifier with lossless structures employing arbitrary noise reduction schemes possesses a noise figure at least as great as that of a conventional traveling-wave tube.

Amongst the concepts which we shall employ in this proof there are some which are new and others which may be unfamiliar. These we now outline.

The modulation of an electron stream can be specified by a pair of complex quantities. The choice of the particular pair is arbitrary but most usually the convection current q and velocity modulation v at the same cross section have been chosen. The state of the beam at any subsequent point is then completely determined by the values of these parameters and the dc conditions of the beam. Instead of the velocity modulation a quantity U related to v may be defined

$$U = -\frac{u}{\eta} v, \tag{1}$$

where u is the time average beam velocity at the cross section in question and η is the electronic charge to mass ratio, defined positive. The advantage of using U, which has the dimensions of voltage, rather than v, will become apparent.

We can define a kinetic power

$$P_k = \tfrac{1}{2} U q^* \tag{2}$$

which has the property that its real part is unchanged when the beam undergoes either accelerations or decelerations in static fields.[13] Chu has also shown that if between two reference planes the beam interacts with an RF field the change in $\mathrm{Re}(P_k)$ is algebraically equal to the electromagnetic power extracted from the field (see Appendix I).

A freely drifting beam represents a close analog of a transmission line.[6,14] Modulation of the beam is propagated by two waves, one traveling faster than the

* Original manuscript received by the IRE, April 1, 1955, revised manuscript received, May 27, 1955. This work was supported in part by the Signal Corps, the Air Material Command, and the Office of Naval Research.

† Research Laboratory of Electronics and Dept. of Electrical Engineering, Massachusetts Institute of Technology, Cambridge, Mass.

‡ Bell Telephone Laboratories, Inc., Murray Hill, N.J. (on leave of absence from the Clarendon Laboratory, Oxford, England).

[1] J. R. Pierce, "Travelling Wave Tubes," D. Van Nostrand Co., New York, N. Y.; pp. 145–159; 1950.

[2] L. M. Field, P. K. Tien, and D. A. Watkins, "Amplification by acceleration and deceleration of a single-velocity stream," Proc. IRE, vol. 39, pp. 194; February, 1951.

[3] F. N. H. Robinson, "Space-charge smoothing of microwave shot noise in electron beams," *Phil. Mag.*, vol. 63, pp. 51–62; January, 1952.

[4] R. W. Peter, "Low-noise traveling-wave amplifier," *RCA Rev.*, vol. 13, pp. 344–368; September, 1952.

[5] J. R. Pierce, "A theorem concerning noise in electron streams," *Jour. Appl. Phys.*, vol. 25, pp. 931–933; August, 1954.

[6] S. Bloom and R. W. Peter, "Transmission-line analog of a modulated electron beam," *RCA Rev.*, vol. 15, pp. 95–112; March, 1954.

[7] H. A. Haus, "Noise in one-dimensional electron beams," *Jour. Appl. Phys.*, vol. 26, 560–571; May, 1955.

[8] W. E. Danielson and J. R. Pierce, "Minimum noise figure of traveling-wave tubes with uniform helices," *Jour. Appl. Phys.*, vol. 25, pp. 1163–1165; September, 1954.

[9] S. Bloom and R. W. Peter, "A minimum noise figure for the traveling-wave tube," *RCA Rev.*, vol. 15, pp. 252–267; June, 1954.

[10] F. N. H. Robinson, "Microwave shot noise in electron beams and the minimum noise factor of travelling wave tubes and klystrons," *Jour. Brit. IRE*, pp. 79–87; February, 1954.

[11] A. M. Clogston and L. R. Walker, unpublished. H. A. Haus, Sc. D. Thesis, M.I.T.

[12] H. A. Haus, "Limitations on the noise figure of microwave amplifiers of the beam type," Trans. IRE, vol. ED-1, pp. 238–257; December, 1954.

[13] L. J. Chu, "A kinetic power theorem," 1951 IRE Conference on Electron Devices, Durham, N. H.; June, 1951.

[14] J. R. Pierce, "Coupling of modes of propagation," *Jour. Appl. Phys.*, vol. 25, pp. 179–183; February, 1954.

electrons and one traveling more slowly.[15,16] Thus the current modulation q is the sum of two components q_1 and q_2.

$$q = (q_1 e^{j\beta_p z} + q_2 e^{-j\beta_p z})e^{-j\beta_e z}, \tag{3}$$

where $\beta_p = \omega_p/u$ is the plasma propagation constant and $\beta_e = \omega/u$ is the beam propagation constant.

The kinetic voltage U for the fast mode (1) is

$$U_1 = Zq_1, \tag{4a}$$

while for the slow mode (2) it is

$$U_2 = -Zq_2, \tag{4b}$$

where Z is defined by

$$Z = 2\frac{\omega_p}{\omega}\frac{V_0}{I_0}. \tag{5}$$

In this expression V_0 is the beam potential and I_0 the magnitude of the beam current, so that Z is a positive quantity. Reference to (2) shows that the kinetic power flow is

$$\begin{aligned} P_k &= \tfrac{1}{2}(Zq_1 e^{j\beta_p z} - Zq_2 e^{-j\beta_p z})(q_1{}^* e^{-j\beta_p z} + q_2{}^* e^{j\beta_p z}) \\ &= \tfrac{1}{2}Z(q_1 q_1{}^* - q_2 q_2{}^* + q_1 q_2{}^* e^{2j\beta_p z} - q_1{}^* q_2 e^{-2j\beta_p z}) \end{aligned}$$

and its real part is

$$= \tfrac{1}{2}Z[q_1 q_1{}^* - q_2 q_2{}^*]. \tag{6}$$

Eq. (6) shows that the power flow does not contain cross terms between the modes and also that the fast mode (1) carries positive power while the slow mode (2) carries negative power.[13] A qualitative but by no means rigorous explanation of the negative power carried by the slow mode may be given in the following way. The current and voltage of the slow mode are 180 degrees out of phase. With the definitions we have adopted a positive current means a deficit of electrons, a negative voltage means a positive velocity modulation, i.e., an excess velocity. These regions of highest velocity occur where the electron density is least and vice versa. The energy of the beam is thus reduced by the presence of the slow wave.

Instead of describing the state of the beam by giving the current and kinetic voltage we might equally well give instead the amplitude of the two component waves. It will be convenient to use normalized amplitudes a_1 and a_2 which are related to q_1 and q_2 by

$$a_1 = (\tfrac{1}{2}Z)^{1/2}q_1 \qquad a_2 = (\tfrac{1}{2}Z)^{1/2}q_2, \tag{7}$$

so that the power carried by each wave is $a_1a_1{}^*$ or $-a_2a_2{}^*$ and the total power is $P_k = a_1a_1{}^* - a_2a_2{}^*$.

The kinetic power is not only unchanged when the beam passes through drift regions or regions in which it is accelerated or decelerated by static electric fields; it is also conserved when the beam interacts with an rf field without absorbing energy from the field or transferring power to it, as for example when it passes through the gap of a lossless cavity resonator. Under the assumptions of small signal theory the current q' and kinetic voltage U' in the beam after it has traversed any of these beam transducers can be expressed as a linear combination of the current q and voltage U prior to the transducer.

$$\begin{aligned} U' &= AU + Bq, \\ q' &= CU + Dq. \end{aligned} \tag{8}$$

The coefficients $ABDC$ are subject to certain restrictions imposed by the conservation of power. An equivalent description which is more suitable for some purposes can be given in terms of the normalized amplitudes a_1 and a_2:

$$\begin{aligned} a_1' &= M_{11}a_1 + M_{12}a_2, \\ a_2' &= M_{21}a_1 + M_{22}a_2. \end{aligned} \tag{9}$$

Analogous conditions apply to the M_{ij} elements. These equations can conveniently be written in matrix form if we regard a_1, a_2 and a_1', a_2' as column matrices

$$a' = Ma. \tag{10}$$

We shall find that this notation forms a suitable basis for generalization.

When a beam interacts with a circuit the output quantities can similarly be written as a linear combination of the input quantities. If there is no ohmic loss the sum of the real part of the kinetic power and the electromagnetic[17] (or circuit) power is conserved, and the matrix elements which describe the whole system, beam and circuit, will also be subject to certain restrictions which express this conservation. Thus the existence of a definite kinetic beam power whose real part behaves in this way allows us to treat an amplifier as a generalization of a passive network in which some of the terminals now correspond to the beam. The conversion of the dc beam power into RF power is automatically accounted for by the way in which the kinetic power is defined.

II. Normal Modes and Amplifiers

Any amplifier has at least an input terminal and an output terminal, an ingoing beam and an outgoing beam. It can therefore be represented by the scheme in Fig. 1 (opposite). Since we are working in terms of normalized amplitudes of the beam modes it is natural to define circuit excitation in the same way. For example, if we have a transmission line of impedance Z_0 with a voltage V_i of the incident wave we define the normalized amplitude of this wave by

[15] W. C. Hahn, "Small signal theory of velocity modulated electron beams," *Gen. Elec. Rev.*, vol. 42, pp. 258–270; June, 1939.

[16] S. Ramo, "Space-charge and field waves in an electron beam," *Phys. Rev.*, vol. 56, pp. 276–283; August, 1939.

[17] W. H. Louisell and J. R. Pierce (unpublished) have shown that the electromagnetic power associated with fields due to space charge is negligible being of order ω_p/ω.

$$a_i = (2Z_0)^{-1/2}V_i, \tag{11}$$

the power flow in this channel being then $a_ia_i^*$.

The excitation of the ingoing beam and the incident circuit waves at the input and output can be determined arbitrarily by conditions exterior to the amplifier. The excitations of the outgoing beam and outgoing circuit waves are then linearly related to and determined by the excitations of the input modes.

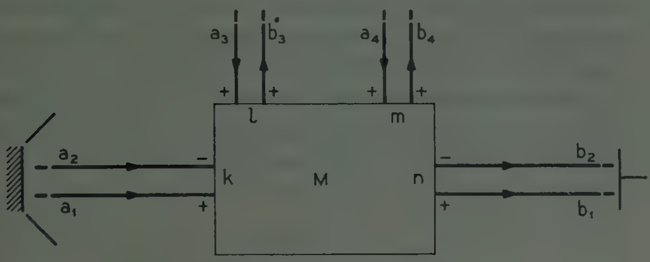

Fig. 1—Schematic diagram of a general beam amplifier.

In the figure we have indicated the waves which can be adjusted by conditions exterior to the amplifier by arrows leading into the amplifier. At point k there are two incident waves a_1 and a_2 associated with the fast and slow modes of the beam. At l, which is the input terminal of the amplifier, there is one inward wave, a_3 (the signal input to the amplifier); at m the output terminal a_4 represents the reverse wave which will be present if there are reflections at the output terminations. At n there are two outward waves which once again are the slow and fast modes of the beam; these we denote by b_1 and b_2. The remaining outward waves are b_3, the reflected mode at the input l, and the output wave b_4 at m.

The properties of the amplifier can be specified by giving the relations between the b_i and the a_j. These can be written in the form

$$\begin{aligned} b_1 &= M_{11}a_1 + M_{12}a_2 + M_{13}a_3 + M_{14}a_4 \\ b_2 &= M_{22}a_1 + M_{22}a_2 + M_{23}a_3 + M_{24}a_4 \\ b_3 &= M_{31}a_1 + M_{32}a_2 + M_{33}a_3 + M_{34}a_4 \\ b_4 &= M_{41}a_1 + M_{42}a_2 + M_{43}a_3 + M_{44}a_4, \end{aligned} \tag{12}$$

or more compactly in matrix form,[18]

$$b = Ma. \tag{13}$$

It will be noticed that in the figure the ingoing mode a_2 and the outgoing mode b_2 are marked with a $-$ sign while the remaining modes are marked $+$. These signs, which we shall refer to as the parity of the mode, relate the direction of power flow to the direction of the arrow associated with the wave. We define the parity p of a mode as $p=+1$ or $p=-1$ according as the power flow is in the direction of the arrow or the opposite direction.

[18] See for example, H. Margenau and G. M. Murphy, "Mathematics of Physics and Chemistry," D. Van Nostrand Co., New York, N. Y., pp. 287–316; 1943.

The power flow in the direction of the arrow associated with any mode j will therefore be $p_ja_ja_j^*$.

The power flowing into the amplifier is

$$\sum_{j=1}^{4} p_ja_ja_j^*,$$

and this, if there are no ohmic losses in the amplifier, must equal the power flowing out

$$\sum_j p_ja_ja_j^* = \sum_i p_ib_ib_i^*. \tag{14}$$

In the present case $p_1 = p_3 = p_4 = +1$, $p_2 = -1$.

Eq. (14) can be expressed in matrix notation if we define a parity matrix P which is a diagonal matrix whose elements are the parities p_i.

$$P = \text{diag}\,(p_1, p_2, p_3, p_4). \tag{15}$$

Eq. (14) then becomes

$$a^+Pa = b^+Pb, \tag{16}$$

where a^+ is a row matrix whose elements are the complex conjugates of those of a. Thus if

$$a \equiv \begin{pmatrix} a_1 \\ a_2 \\ a_3 \\ a_4 \end{pmatrix} \quad \text{then} \quad a^+ = (a_1^*, a_2^*, a_3^*, a_4^*). \tag{17}$$

We shall also need the corresponding operation performed in the square matrix M. The matrix M^+ is formed from the elements of M by transposing them and then taking the complex conjugates

$$(M^+)_{ij} = M_{ji}^*. \tag{18}$$

M^+ is the Hermitian conjugate of M.

The operation of taking the Hermitian conjugate of a product of two matrices AB has the property that

$$(AB)^+ = B^+A^+. \tag{19}$$

Similarly when we take the inverse of a product of two matrices the order of the factors is reversed.

$$(AB)^{-1} = B^{-1}A^{-1}. \tag{20}$$

By inspection it is obvious that the matrix P has the following properties:

$$P^+ = P, \qquad P^2 = PP = I \text{ the unit matrix}$$
$$P^{-1} = P. \tag{21}$$

If in (16) we write "b" in terms of "a" using (13), we have

$$a^+Pa = (Ma)^+PMa = a^+M^+PMa. \tag{22}$$

Since the input quantities "a" are completely arbitrary this equation implies certain relations between the elements M_{ij}. For example, setting $a_2 = a_3 = a_4 = 0$ and $a_1 \neq 0$ we find

$$M_{11}M_{11}^* - M_{21}M_{21}^* + M_{31}M_{31}^* + M_{41}M_{41}^* = 1. \tag{23}$$

Three more conditions of this nature are found by taking each of the other a_i in turn to be nonzero.

If we take $a_1 \neq 0$, $a_2 \neq 0$ and $a_3 = a_4 = 0$, then, since both the amplitudes and phases of a_1, a_2 are arbitrary, we find

$$M_{11}M_{12}^* - M_{21}M_{22}^* + M_{31}M_{32}^* + M_{41}M_{42}^* = 0. \quad (24)$$

Five more equations analogous to (24) are obtained by permutation of the a's.

This whole set of relations can be summarized in the single matrix equation

$$M^+PM = P. \quad (25)$$

This equation is analogous to a theorem applicable to the scattering matrix S describing wave guide junctions.[19]

$$S^+S = I, \quad (26)$$

which is obtained if all the modes have positive parity so that P is the unit matrix.

Although (24) leads to some interesting conclusions it is not in a form suitable for our later applications. We may however derive a related equation which yields results directly applicable to the calculation of noise figures.

The determinant of P is det $P = \pm 1$ and so (24) shows that det M and det M^+ are nonzero. Inverses of M^+ and M therefore exist, and we can premultiply (25) by MP and postmultiply it by $(PM)^{-1}$ to obtain

$$MPM^+PM(PM)^{-1} = MPP(PM)^{-1}.$$

By the use of (20) and (21) this reduces to

$$MPM^+ = P. \quad (27)$$

Although at first sight (27) appears very similar to (25), nevertheless when it is written out element by element it leads to a different set of relations. For example the equation analogous to (23) is

$$M_{11}M_{11}^* - M_{12}M_{12}^* + M_{13}M_{13}^* + M_{14}M_{14}^* = 1. \quad (28)$$

In particular amongst the equations contained in (27) we find

$$M_{41}M_{41}^* - M_{42}M_{42}^* + M_{43}M_{43}^* + M_{44}M_{44}^* = 1. \quad (29)$$

If $M_{44} = 0$, i.e., the amplifier is matched to the output, $M_{43}M_{43}^*$ is the available power gain of the amplifier and (29) shows that if $M_{43}M_{43}^*$ is larger than unity then $M_{42}M_{42}^*$ is greater than zero. If the gain $M_{43}M_{43}^*$ is very large $M_{42}M_{42}^*$ is of the same order. The coefficient $M_{42}M_{42}^*$ specifies the power coupled from the slow mode of the beam to the output terminal of the amplifier. In particular any noise associated with the slow mode must be coupled to the output. We shall see that this has a profound influence on the noise figure of any amplifier.

[19] C. G. Montgomery, R. H. Dicke, and E. M. Purcell, "Principles of Microwave Circuits," Rad. Lab. Ser., McGraw-Hill Book Co., Inc., New York, N. Y., vol. 8, p. 149; 1948.

The generalization of these results to more complicated devices in which there are more terminals or electron beams is simple and will be described later with applications of the theory.

The set of equations implied by (27) can be written in the form

$$\sum_{j=1}^{n} p_j M_{rj} M_{sj}^* = p_r \delta_{rs}, \quad (30)$$

where δ_{rs} is Kronecker's symbol, M_{rj} is the amplitude of the outgoing wave in channel r due to unit input wave amplitude in j, and the quantities p are the parities associated with each channel. The parity p_j is $+1$ or -1 according as the direction of power flow in channel j coincides with the group velocity or is in the opposite direction.

III. Noise

Noise in a conventional transmission line is completely specified by the spectrum of either the current or voltage fluctuations. Since the impedance at any point in the line is determined by the termination of the line there exists a definite phase relation between voltage and current which are, therefore, merely two aspects of the same statistical process.

In an electron beam, on the other hand, since all information is transmitted in one direction only, it is meaningless to speak of an impedance termination. The phase relation between current and voltage at any point is determined by conditions at an earlier point in the flow. Any satisfactory description of noise must therefore include the possibility of a partial or fully random relation between voltage and current. More parameters are therefore needed to describe noise in a beam than a material transmission line.

Haus[7] has shown that in the limit of an indefinitely narrow bandwidth four parameters are sufficient. These parameters defined at one and the same reference cross section are: Φ the self power density spectrum, *SPDS*, of the voltage fluctuations, Ψ the *SPDS* of the current fluctuations and Π and Λ the crosspower density spectra, *CPDS*.

If, for example, the *SPDS* of the voltage is Φ, then the mean square voltage fluctuations in bandwidth Δf are

$$\overline{U}^2 = 4\pi\Phi\Delta f. \quad (31)$$

The factor 4π enters because the power density spectrum which is taken over from correlation theory[20] is defined over positive and negative *angular* frequencies. Thus for a beam displaying full shot noise the current *SPDS* is

$$\Psi = \frac{eI_0}{2\pi}. \quad (32)$$

[20] Y. W. Lee, "Application of statistical methods to communication problems," Mass. Inst. Tech. Res. Lab. of Electronics, Tech. Rep. 181; 1950.

The crosspower density spectra are given in an analogous way by the ensemble average of the kinetic power. If U and q are the instantaneous rms amplitudes of the kinetic voltage and convection current within a band Δf, then

$$\overline{Uq^*} = 4\pi(\Pi + j\Lambda)\Delta f. \tag{33}$$

In dealing with the properties of the beam alone this formulation is most advantageous, but when we have to consider the interaction of the beam with a circuit, an alternative formulation in terms of the power density spectra of the fast and slow beam modes leads to simpler results. Although the matrix formulation of the previous chapter can be written in terms of voltage and current so that the parameters Φ, Ψ, Π and Λ could be used directly, this approach does not lead to useful results.

We therefore define a new set of parameters to replace Φ, Ψ, etc. These are A_1, A_2 and A_{12} defined in such a way that if the normalized amplitudes of the fluctuations in the fast and slow modes are a_1 and a_2 in bandwidth Δf, then

$$\begin{aligned}\overline{a_1a_1^*} &= 4\pi A_1\Delta f\\ \overline{a_2a_2^*} &= 4\pi A_2\Delta f\\ \overline{a_1a_2^*} &= 4\pi A_{12}\Delta f,\end{aligned} \tag{34}$$

where the bars denote mean values. In accord with the terminology of correlation theory, A_1 and A_2 are the *SPDS* of the fluctuations in the fast and slow mode and A_{12} is the *CPDS* of the two modes. A_1 and A_2 are real, A_{12} is complex.

These quantities can be related to Φ, Ψ, Π and Λ using (3), (4) and (7). For example, the peak value of U is

$$U = (2Z)^{1/2}(a_1 - a_2),$$

so that

$$4\pi\Phi\Delta f = \tfrac{1}{2}\overline{U^2} = \overline{Z(a_1 - a_2)(a_1^* - a_2^*)};$$

i.e.,

$$4\pi\Phi\Delta f = 4\pi Z(A_1 + A_2 - A_{12} - A_{12}^*)\Delta f.$$

Thus

$$\Phi = Z(A_1 + A_2 - A_{12} - A_{12}^*) \tag{35a}$$

and similarly

$$\Psi = Z^{-1}(A_1 + A_2 + A_{12} + A_{12}^*) \tag{35b}$$

$$\Pi = A_1 - A_2 \tag{35c}$$

$$j\Lambda = A_{12} - A_{12}^*. \tag{35d}$$

For reference we give the inverse relations

$$A_1 = \tfrac{1}{4}(Z^{-1}\Phi + Z\Psi) + \tfrac{1}{2}\Pi \tag{36a}$$

$$A_2 = \tfrac{1}{4}(Z^{-1}\Phi + Z\Psi) - \tfrac{1}{2}\Pi \tag{36b}$$

$$A_{12} = \tfrac{1}{2}(Z\Psi - Z^{-1}\Phi) + \tfrac{1}{2}j\Lambda. \tag{36c}$$

IV. Invariants of the Noise

Haus[7] has shown that when a beam is subjected to arbitrary lossless transformations of the type discussed in the introduction, there exist two invariant quantities associated with the noise.

Clearly one of these, since the transformations are lossless, is the real part Π of the crosspower. The other, which we shall denote by S, is given by the positive square root of

$$S^2 = \Phi\Psi - \Lambda^2. \tag{37}$$

A qualitative explanation of the existence of this second invariant is that for coherent processes (such as signal modulation) $S = |\Pi|$ and therefore transforms in the same way as Π. A detailed proof of the invariance of these two quantities is simple but lengthy. It is given by Haus.[7]

In terms of the parameters A_1, A_2 and A_{12}, S and Π are given by

$$S^2 = (A_1 + A_2)^2 - 4A_{12}A_{12}^*, \tag{38a}$$

$$\Pi = A_1 - A_2. \tag{38b}$$

For any process, coherent or otherwise, $S \geqq |\Pi|$.

Not all parameters can be varied at will in a lossless beam transformation but the restrictions imposed on the transformation by power conservation are contained in the requirement that S and Π be invariant. We can, therefore, pick certain pairs of parameters as independent variables when the other pair will be determined by (38a) and (38b). A particular convenient pair are the modulus $|A_{12}|$ and the argument arg (A_{12}).

Since S and Π are invariant for lossless transformations, and any operation on the beam in a region where the single velocity approximation is valid can be so described, they are completely determined by conditions in regions where this approximation is not valid; that is, in the immediate vicinity of the cathode and potential minimum.

We have so far considered only lossless transformations. In a lossy transformation, as for example when a beam passes through the gap of a lossy resonator, S and Π are no longer conserved. It may, however, be shown[7] that in this case the difference $S - \Pi$ which, as we shall see, is the quantity which determines noise figures, is always increased.

An example should serve to clarify the meaning of S and Π. Pierce[5] assumes that noise in the beam is due to two incoherent sources, which may be identified as current fluctuations and independent velocity fluctuations[21] at the potential minimum. These two fluctuations set up two independent noise current standing waves in the beam. He shows that the product, $\overline{q_{\max}^2} \times \overline{q_{\min}^2}$, of the maximum and minimum of the resulting over-all standing wave is independent of any transformation to which the beam has been subjected, between its departure

[21] A. J. Rack, "Effect of space charge and transit time on the shot noise in diodes," *Bell Sys. Tech. Jour.*, vol. 17, pp. 592–619; October, 1938.

from the potential minimum and its arrival at the drift region where the standing wave is measured, and is given by

$$\overline{q_{\max}^2 q_{\min}^2} = (4-\pi)\left(\frac{\omega}{\omega_p}\frac{kT_c}{eV_0} eI_0\Delta f\right)^2, \qquad (39)$$

where T_c is the cathode temperature.

This assumption that noise is the resultant of two independent standing waves implies that $\Pi=0$. A pure standing wave carries no power and a combination of two standing waves carries power only if the two waves are at least partially correlated. It is easy to show[7] that S^2 in this case is apart from numerical factors identical with $q_{\max}^2 \times q_{\min}^2$.

$$S = \frac{(4-\pi)^{1/2}}{2\pi} kT_c \text{ and } \overline{q_{\max}^2 q_{\min}^2} = \left(\frac{4\pi S}{Z}\right)^2 \Delta f^2. \qquad (40)$$

V. Noise Figure

The noise figure of any amplifier is defined by

$$F = 1 + \frac{N_b\Delta f}{N_c\Delta f}, \qquad (41)$$

where $N_b\Delta f$ is the noise power in the output wave due to beam noise and $N_c\Delta f$ is the noise power in the output wave due to noise in the input wave within the frequency range Δf.

The denominator of this expression depends only on the characteristics (i.e., the available gain) of the amplifier, while the numerator depends also on the noise parameters of the beam. It may be minimized independently by the use of a suitable beam transducer acting on the beam prior to its entry into the amplifier, as for instance in Watkins'[2] velocity jump noise reduction scheme.

In the matrix notation of Section II the denominator $N_c\Delta f$ is simply $M_{43}M_{43}^* \overline{a_3a_3^*}$. The power density spectrum of the noise in the input wave of a transmission line matched to a termination at temperature T is $kT/4\pi$, and thus the quantity

$$\overline{a_3a_3^*} = kT\Delta f; \qquad (42)$$

and so

$$N_c\Delta f = M_{43}M_{43}^* kT\Delta f. \qquad (43)$$

The numerator $N_b\Delta f$ is due to contributions from noise in both the fast and slow modes at the input. Its value is

$$N_b\Delta f = \overline{(M_{41}a_1 + M_{42}a_2)(M_{41}^*a_1^* + M_{42}^*a_2^*)}. \qquad (44)$$

In terms of the spectral densities introduced earlier

$$N_b\Delta f = 4\pi\Delta f(M_{41}M_{41}^*A_1 + M_{42}M_{42}^*A_2 + M_{41}M_{42}^*A_{12} + M_{41}^*M_{42}A_{12}^*), \qquad (45)$$

which may be written

$$N_b\Delta f = 4\pi\Delta f(M_{41}^2A_1 + M_{42}^2A^2 + 2M_{41}M_{42}A_{12}\cos\theta); \qquad (46)$$

where the M's and A_{12} are now, and henceforth, to be considered as the absolute magnitudes of the corresponding complex quantities and

$$\theta = \arg(M_{41}) - \arg(M_{42}) + \arg(A_{12}).$$

We have already remarked that the magnitude and argument of A_{12} can be varied arbitrarily by lossless beam transformations. The smallest possible value of $N_b\Delta f$ is obtained when $\cos\theta = -1$ and then we have

$$N_b\Delta f = 4\pi\Delta f(M_{41}^2A_1 + M_{42}^2A_2 - 2M_{41}M_{42}A_{12}). \qquad (47)$$

This may be expressed by (38a)and (38b) in terms of A_{12} and the invariants S and Π alone and then minimized with respect to A_{12}.

We have

$$N_b\Delta f = 4\pi\Delta f\left[\tfrac{1}{2}(M_{41}^2 - M_{42}^2)\Pi + \tfrac{1}{2}(M_{41}^2+M_{42}^2)(S^2+4A_{12}^2)^{1/2} - 2M_{41}M_{42}A_{12}\right], \qquad (48)$$

which on minimization yields

$$N_b\Delta f = 2\pi\Delta f(|M_{42}^2 - M_{41}^2|S - (M_{42}^2 - M_{41}^2)\Pi). \qquad (49)$$

The absolute sign appears because (47) is essentially positive. Thus the noise figure after minimization is

$$F_{\min} = 1 + \frac{2\pi}{kT}\,\frac{|M_{42}^2 - M_{41}^2|S - (M_{42}^2 - M_{41}^2)\Pi}{M_{43}^2}. \qquad (50)$$

This expression has the general form

$$F_{\min} = 1 + \frac{2\pi}{kT}|K|\left(S - \frac{K}{|K|}\Pi\right), \qquad (51)$$

where the new parameter

$$K = \frac{M_{42}^2 - M_{41}^2}{M_{43}^2} \qquad (52)$$

It is the difference between the power transfers (power out per unit power in) from the slow and fast modes to the output divided by the available gain.

The form of the result (51) is not limited to the scheme of Fig. 1 nor in its derivation have we needed to assume that the amplifier contains only lossless structures.

We now show, however, that for this particular case and assuming lossless structures, K has a lower bound.

In Section II we proved the relation

$$M_{41}^2 - M_{42}^2 + M_{43}^2 + M_{44}^2 = 1 \qquad (29)$$

as a consequence of power conservation.

From this we find immediately

$$K = 1 - \frac{1}{M_{43}^2} + \frac{M_{44}^2}{M_{43}^2}. \qquad (53)$$

The available gain G of the amplifier is identical with M_{43}^2 if $M_{44}=0$, and

$$K = 1 - \frac{1}{G}. \qquad (54)$$

The equality sign applies when $M_{44}=0$, which will be the case if the amplifier presents a match to the output transmission line.

We have thus proved that the noise figure of any amplifier, whatever circuits it contains, including internal noise reduction schemes provided only that they consist of lossless structures, cannot have a noise figure less than

$$F_{\min} = 1 + \frac{2\pi}{kT}(S - \Pi)\left(1 - \frac{1}{G}\right). \tag{55}$$

It will be noted that the noise properties of the beam appear only in the form $S-\Pi$. It has been proved[7] that this quantity cannot be reduced by the use of lossy beam transducers prior to the amplifier. Thus the use of such transducers leads to no decrease in $F_{\min}$.

The appearance of the term $1/G$ in (55) might suggest that an improvement could be obtained by using a cascade of amplifiers each of small gain G. A straightforward calculation of the over-all noise figure of a cascade of n such amplifiers whose total gain would be G^n gives

$$F_{\min} = 1 + \frac{2\pi}{kT}(S - \Pi)\left(1 - \frac{1}{G^n}\right). \tag{56}$$

Thus the noise figure of the cascade is the same as that of a single tube of the same gain.

With the assumptions about beam noise made by Pierce, (55) becomes

$$F_{\min} = 1 + (4 - \pi)^{1/2}\frac{T_c}{T}\left(1 - \frac{1}{G}\right), \tag{57}$$

which for large gain is identical with the result already obtained for traveling-wave tubes by Danielson and Pierce[8] and others.

VI. Applications

Eq. (55) is immediately applicable to a traveling-wave tube with a lossless helix and matched input and output (M_{44} is then zero). The term in $1/G$ which appears as a correction to the formulas already published[8–10,12] is due to the fact that earlier authors considered only the growing wave at the output. The additional term represents just the effect of the other two waves.

A klystron with infinitesimal gaps and lossless cavities cannot be matched at its output. Therefore $M_{44}{}^2=1$ and so (53) yields $K=1$ in agreement with the results stated by Robinson and Haus.[10,11]

We have so far not considered amplifiers with lossy structures, but we now show how our treatment can be generalized to deal with the presence of loss in certain cases.

An important example is the traveling-wave tube with a lossless helix and a short region of attenuation near the center. The treatment we give is equally applicable to a tube with a severed helix terminated resistively at the break or a tube with a long center attenuator, provided that the interaction between the beam and helix is negligible in this region.

Any of these cases can be represented by Fig. 2. The additional pair of terminals which appear represent connections to the helix at the ends of the attenuating region which lead outside the amplifier to matched loads.

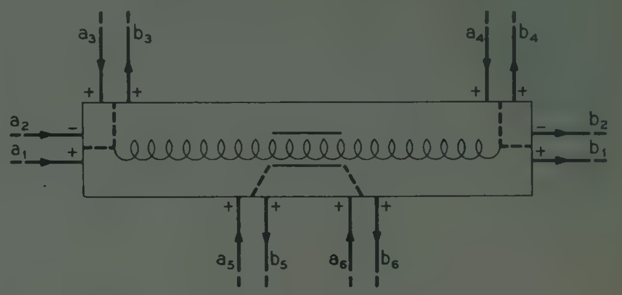

Fig. 2—Traveling-wave tube with center loss.

The additional terminals increase the dimension of the matrix M which describes the amplifier to 6 by 6. The results we have so far obtained can be very simply generalized to this case. Eq. (52) still gives K correctly. Since loss is now external to the amplifier the new 6 by 6 matrix M satisfies conditions for a lossless amplifier and an equation analogous to (29) can be derived;

$$M_{41}{}^2 - M_{42}{}^2 + M_{43}{}^2 + M_{44}{}^2 + M_{45}{}^2 + M_{46}{}^2 = 1. \tag{58}$$

If we assume that the amplifier is matched at its terminations, then $M_{44}=M_{45}=0$. $M_{46}{}^2$ is the available gain G' for a signal introduced at the beginning of the second part of the helix. From (58) and (52) we have

$$K = 1 - \frac{1}{G} + \frac{G'}{G}. \tag{59}$$

Thus the effect of such an attenuator is to increase the attainable noise figure and this increase is least when G'/G is small. This can be ensured by placing the attenuator towards the output end of the tube.

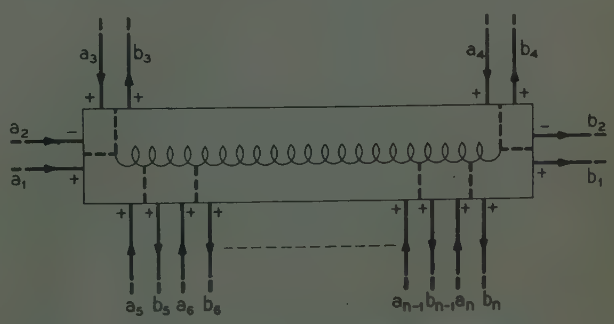

Fig. 3—Traveling-wave tube with distributed loss.

In a similar way distributed loss along the helix can be treated. We suppose that the actual helix is replaced by a lossless helix loosely coupled at a large number of closely spaced points to matched loads external to the amplifier (see Fig. 3).

The new expression for K is then

$$K = 1 - \frac{1}{G} + \frac{1}{G}\sum_{j=5}^{n} M_{4j}^2. \tag{60}$$

The coefficients M_{4j}^2 may be evaluated in the following way. Suppose the connection j is made a distance z from the input across a length dz of the helix and the loss per unit length of the actual helix is λ. Then a fraction λdz of the forward power is coupled to the outgoing mode of the j^{th} connection to the ideal helix. Therefore if power is introduced at the j^{th} terminal a fraction λdz of it is coupled to the forward wave. The coefficient M_{4j}^2 is thus $G(z)\lambda dz$ where $G(z)$ is gain from point z to output.

If we consider only the growing wave at output then

$$G(z) = Ge - 2\beta_e Cx, z \tag{61}$$

where $\beta_e c$ and x_1 have their usual meaning.[1] Thus

$$\frac{1}{G}\sum_{j=5}^{n} M_{4j}^2 = \int_0^l e^{-2\beta_e c x_1 z}\lambda dz,$$

and if G is large this yields $\lambda/2\beta_e c x_1 = d/x_1$ where d is Pierce's loss parameter and x_1 is the real part of the incremental propagation constant associated with the growing wave. Thus

$$K = 1 - \frac{1}{G} + \frac{d}{x_1}\cdot \tag{62}$$

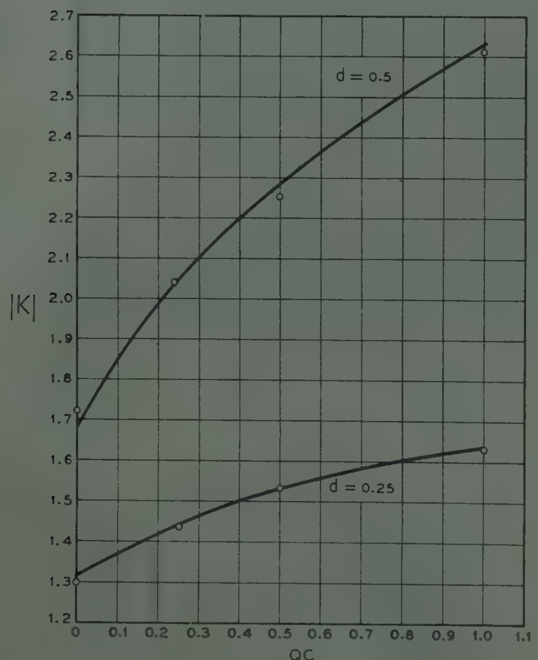

Fig. 4—$|K|$ for a lossy helix. The curves represent Pierce and Danielson's results. The points are calculated from (1) to (6).

In Fig. 4 we exhibit K derived from (62) for two values of d as a function of QC, together with the equivalent quantity obtained numerically by Danielson and Pierce.[8] The agreement is surprisingly good in view of the crude nature of our calculation.

As a final example we calculate the minimum noise figure of a double stream amplifier, which we represent by the diagram of Fig. 5. Terminals 3 and 5 represent the two ends of a short section of helix used to modulate the beam, and 6 and 4 represent the ends of the helix used to pick up the modulation. The second beam is represented by the two new inward channels a_7 and a_8 and the corresponding output channels. The parity matrix for this problem has the diagonal elements $p_1 = +1$, $p_2 = -1$, $p_3 = p_4 = p_5 = p_6 = p_7 = 1$, $p_8 = -1$, and the analogs of (29) is

$$M_{41}^2 - M_{42}^2 + M_{43}^2 + M_{44}^2 + M_{45}^2 + M_{46}^2 + M_{47}^2 - M_{48}^2 = 1. \tag{63}$$

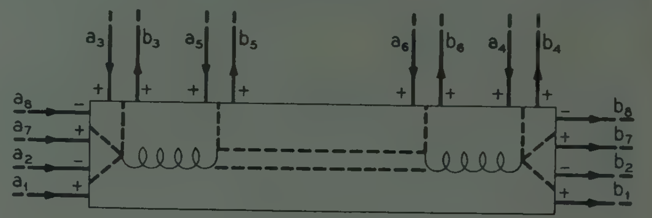

Fig. 5—Double-stream amplifier.

The expression for the noise figure will be

$$F = 1 + \frac{2\pi}{kT}\left[K_1(S_1 - \Pi_1) + K_7(S_7 - \Pi_7)\right], \tag{64}$$

where

$$K_1 = \frac{M_{42}^2 - M_{41}^2}{M_{43}^2}\; K_7 = \frac{M_{48}^2 - M_{47}^2}{M_{43}^2}, \tag{65}$$

S_1 and Π_1 are the noise invariants for the first beam S_7, and Π_7 the invariants for the second beam. In this derivation it has been assumed that the noise from the two beams is uncorrelated, the minimization has been carried out for each beam independently.

From (63) we see that

$$K_1 + K_7 = 1 - \frac{1}{G} + \frac{M_{46}^2 + M_{45}^2}{G}, \tag{66}$$

with $G = M_{43}^2$. If the input is matched $M_{45} = 0$. M_{46} is the gain of the second coupling helix. If the gain G is large and $M_{46}^2 \ll G$ then

$$K_1 + K_7 \simeq 1. \tag{67}$$

The double stream amplifier therefore has, if the noise invariants are identical for the two beams, the same minimum noise figure as any other amplifier.

VII. Conclusions

We have shown that any microwave amplifier with lossless structures, whose operation depends on the interaction of an electron beam with longitudinal electric fields, cannot have a noise figure less than

$$F = 1 + \frac{2\pi}{kT}(S - \Pi)\left(1 - \frac{1}{G}\right). \qquad (68)$$

If we assume with Pierce[5] that the noise is due to uncorrelated and completely random fluctuations of current and velocity at the potential minimum, this simplifies to

$$F = 1 + (4 - \pi)^{1/2}\frac{T_c}{T}\left(1 - \frac{1}{G}\right). \qquad (69)$$

This latter expression has already been derived for the traveling-wave tube with a uniform lossless helix[8-10,12] and our work shows that it is applicable to any other tube of a class which includes klystrons, space charge wave amplifiers, double stream amplifiers, traveling-wave klystrons, or traveling-wave tubes with internal noise compensation circuits. It is also applicable to backward wave amplifiers, for in our formulation of the problem no distinction is made between backward and forward wave tubes. The inclusion of backward wave tubes merely necessitates a renumbering of the terminals.

Although we have not proved an equally general theorem for tubes with lossy elements our treatment of certain specific examples indicates very strongly that the presence of loss has a harmful effect on the noise figure.

The matrix notation for the description of amplifiers in terms of the normal beam modes leads to a very compact statement of the restrictions imposed on the operation of amplifiers by the conservation of power.

Our considerations rest mainly on the concept of a kinetic power for the beam which can be defined unambiguously at any point and whose real part is conserved when the beam does not interact with external fields. The existence of such a kinetic power is proved in Appendix I. In Appendix II we show how the present formalism can be related to a more conventional treatment of the traveling-wave tube with a lossless helix.

Acknowledgment

We have had the benefit of many stimulating discussions with Professor L. J. Chu and Dr. J. R. Pierce. This paper is largely based on their pioneer work. Our thanks are also due to Dr. C. F. Quate for his encouragement and interest in this problem.

Appendix I

A simple solution of Maxwell's equations in the presence of a flow of charged particles can be obtained only when the small-signal assumptions are used; i.e., a sinusoidal time dependence of the time varying part of the velocity and current of the particles is assumed and all squares and cross products of the sinusoidal terms are neglected. Energy and power relations involve squares and cross products of the small signal amplitudes which are of the same order of magnitude as those terms which have been neglected in the small signal approximation. Thus, it seems that a discussion of energy and power in the presence of a flow of charged particles is bound to be inconsistent if it is based on the small signal assumptions.

This is not entirely so, however. An identity analogous to the conventional Poynting theorem can be derived starting from the small-signal equations. One term of the identity can be recognized readily as the complex electromagnetic power flowing through the surface S out of the volume τ through which passes the beam. (See Figure 6.) In the identity, the real part of the complex electromagnetic power flowing out of the volume balances against the real part of what is called the net "kinetic power flow" into the volume. The kinetic power flow at any cross section of the beam depends solely upon the state of excitation of the beam at the cross section. The net flow of kinetic power into the volume is found as the difference between the kinetic power flow through the cross section of entry into the volume and the kinetic power flow through the exit cross section. The concept of the kinetic power flow allows us to treat a system consisting of an RF structure and a one-dimensional electron beam as a passive system. A detailed proof and a discussion of the above statements follows.

Two of Maxwell's equations are:

$$\nabla \times \overline{E} = -\mu \frac{\partial \overline{H}}{\partial t}, \qquad (70)$$

$$\nabla \times \overline{H} = \overline{J} + \epsilon \frac{\partial \overline{E}}{\partial t}, \qquad (71)$$

where $\overline{J}$ is the current density carried solely by the charged particles assuming that the conductivity of the medium through which they flow is zero.

For small signals, (70) and (71) split into a time-independent part and a time-varying part at a frequency ω. This part can be written in complex form

$$\nabla \times \widehat{E} = -j\omega\mu\widehat{H} \qquad (72)$$

$$\nabla \times \widehat{H} = \widehat{J} + j\omega\epsilon\widehat{E}. \qquad (73)$$

The circumflex indicates complex vector quantities which are small compared to the corresponding time average quantities. From (72) and (73) one can obtain identities involving cross products of the complex small signal amplitudes. Scalar multiplication of (72) by $\widehat{H}^*$ and of the complex conjugate of (73) by $\widehat{E}$ gives after subtraction

$$-\nabla\cdot(\widehat{E} \times \widehat{H}^*) = \widehat{E}\cdot\widehat{J}^* + j\omega(\mu\widehat{H}\cdot\widehat{H}^* - \epsilon\widehat{E}\cdot\widehat{E}^*). \qquad (74)$$

Eq. (74) looks like the conventional complex Poynting theorem, but differs from it conceptually in establishing a relation among the approximate small signal solutions of Maxwell's equations.

We assume now that an infinite magnetic field confines the motion of the particles to the z-direction. The velocity and current have then only a z-component.

$$\hat{E}\cdot\hat{J}^* = E_z J_z^*. \qquad (75)$$

The force equation is then

$$-\frac{1}{\eta}\left(j\omega v + \frac{\partial uv}{\partial z}\right)E_z. \qquad (76)$$

The current is given by

$$J_z = \rho_0 v + \rho_1 u, \qquad (77)$$

where ρ_1 is the complex amplitude of the sinusoidal variation of the charge density, u is the time average velocity in the z-direction, v is the complex amplitude of the velocity modulation in the z-direction, and ρ_0 is the time average charge density. The continuity equation is

$$\frac{\partial J_z}{\partial z} = -j\omega\rho_1. \qquad (78)$$

Using (76), (77) and (78) in (75) we find

$$\hat{E}\cdot\hat{J}^* = -\frac{1}{\eta}\left(j\omega\rho_0 vv^* + \frac{\partial}{\partial z}uvJ_z^*\right). \qquad (79)$$

We assume that the time average velocity, u, and the longitudinal E-field are constant across the cross section of the beam (one-dimensional assumption). Then, v is also constant across the beam. Eq. (79) introduced into (74) with a subsequent integration over the volume τ shown in Fig. 6 gives

$$-\oint \hat{E}\times\hat{H}^*\cdot d\bar{A} = Uq^*\big|_{z_1} - Uq^*\big|_{z_2} + j\omega\int\left[\mu\hat{H}\cdot\hat{H}^* - \epsilon\hat{E}\cdot\hat{E}^* - \frac{1}{\eta}\rho_0 vv^*\right]d\tau, \qquad (80)$$

where $q=\int J_z dA$ integrated over the beam cross section and the kinetic voltage, U, is defined by

$$U = -\frac{1}{\eta}uv.$$

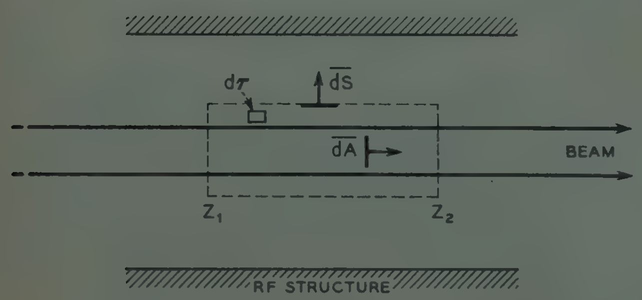

Fig. 6—Volume and surface elements.

The real part of (80) can be written in the form

$$\tfrac{1}{2}\,\mathrm{Re}\oint\left[\hat{E}\times\hat{H}^*\cdot d\bar{S}\right] + \tfrac{1}{2}\,\mathrm{Re}\left[Uq^*\big|_{z_2} - Uq^*\big|_{z_1}\right] = 0. \qquad (81)$$

Eq. (81) shows that a decrease in the real part of the kinetic power, $\frac{1}{2}Uq^*$, as defined by Chu, balances the electromagnetic power delivered by the beam. We shall discuss the significance of (12) in two examples.

In the ac analysis of a diode, which occurs in the noise analysis of a Pierce gun, the one-dimensional assumption is used. The total alternating current is zero, thus $\hat{H}=0$, and the electromagnetic power flowing out of the beam,

$$\tfrac{1}{2}\,\mathrm{Re}\oint\left[\hat{E}\times\hat{H}^*\cdot d\bar{S}\right],$$

is zero. Correspondingly, for any two reference cross sections in the diode the equality holds,

$$\tfrac{1}{2}\,\mathrm{Re}\left[Uq^*\big|_{z_2}\right] = \tfrac{1}{2}\,\mathrm{Re}\left[Uq^*\big|_{z_1}\right].$$

The real part of the kinetic power is conserved during the acceleration. A diode region is a lossless beam transducer.

Next, consider a traveling-wave tube. The term

$$\mathrm{Re}\,\frac{1}{2}\left[\oint \hat{E}\times\hat{H}^*\cdot d\bar{S}\right]$$

is the time average of the RF power delivered to the RF structure between the cross sections z_1 and z_2. According to (80) this power is balanced by a decrease of the real part of the kinetic power between the same cross sections. The amplifier can be represented as a lossless network (or lossy network, if the RF structure has ohmic losses) by incorporating the beam in the network. Such a network must have at least four pairs of terminals. Two pairs of terminals represent the RF input and output of the amplifier. The other two terminals represent the beam entering and leaving the amplifier. The circuit voltages and currents appear at the circuit terminals. The kinetic beam voltages and the beam currents appear at the remaining two pairs of terminals. If the real part of the kinetic power is accepted on equal footing with the electromagnetic power, then (81) reduces to the statement: The sum of the powers entering the amplifier through the four terminal pairs must be equal to zero, if the RF structure is lossless, greater than zero, if the RF structure has ohmic loss.

Appendix II

To show that our treatment is equivalent to that of other authors for the traveling-wave tube we need only calculate the ratio of the coefficients M^2_{42}/M^2_{43} and M^2_{41}/M^2_{43} and show that their difference is unity.

Pierce[1] gives an expression for V_1 the voltage in the growing mode at the output end of a traveling-wave tube due to a signal input V, an initial current modulation q and an initial velocity modulation v which may be written using the kinetic potential U to replace v as

$$V_1 = G\left(V + jC(\delta_2+\delta_3)U - (\delta_2\delta_3 - 4QC)\frac{2V_0C^2}{I_0}q\right). \qquad (82)$$

Expressing U and q in terms of a_1 and a_2 we can identify the coefficients M_{41}, M_{42}, M_{43}, as

$$M_{43}^2 = G$$

$$M_{41}/M_{43} = jC(\delta_2 + \delta_3)\left(\frac{Z}{Z_0}\right)^{1/2} - (\delta_2\delta_3 - 4QC)\frac{2V_0C^2}{I_0}(ZZ_0)^{-1/2}$$

$$M_{42}/M_{43} = -jC(\delta_2 + \delta_3)\left(\frac{Z}{Z_0}\right)^{1/2} - (\delta_2\delta_3 - 4QC)\frac{2V_0C^2}{I_0}(ZZ_0)^{-1/2},$$

where Z_0 is the helix impedance and Z the beam impedance.

This yields after some rearrangement

$$K = \frac{M_{42}^2 - M_{41}^2}{M_{43}^2}$$

$$= j[(\delta_2^*\delta_3^* - 4QC)(\delta_2 + \delta_3) - (\delta_2\delta_3 - 4QC)(\delta_2 + \delta_3^*)]. \quad (83)$$

This expression is already identical with the equivalent one derived by Danielson and Pierce.[8] To complete the proof we show that its value is unity. If we write $\delta = j\epsilon$ the secular equation of the traveling-wave tube becomes

$$\epsilon^2 + b\epsilon^3 - 4QC\epsilon - 4QCb - 1 = 0. \quad (84)$$

This is an equation with real coefficients and therefore has three roots: ϵ_3, which is real and $\epsilon_2 = \epsilon_2^*$, which are complex.

Writing (83) in terms of ϵ_2 and ϵ_3 and using the relations between the roots to eliminate ϵ_2 we find

$$K = 2 - (\epsilon_3^3 + b\epsilon_3^2 - 4QC\epsilon_3 - 4QCb),$$

the term in parenthesis is 1 by (84) and so $K = 1$. The term in $1/G$ does not appear, since by considering only the growing wave at the output we effectively assume G to be infinite.

Television Synchronizing Signal Generator*

WILLIAM WELSH†

***Summary*—This paper deals with the formation of low-frequency rectangular pulses from a train of higher-frequency pulses, using a pulse-coincidence type of frequency-dividing chain. The developed pulse has leading and trailing edges bearing a precise time relationship to the leading edges of pulses of the original train, and a width equal to the period of an integral number of these pulses.**

A second low-frequency pulse, concurrent with the first, and having its leading and trailing edges displaced from those of the first pulse by the period of an integral number of the high-frequency pulses, may also be formed. The rise time and precision of timing of each edge of each developed pulse are of the same order as those of the leading edge of the high-frequency pulse. A 60 cycle wave in which these quantities are within 0.2 microsecond may be readily obtained.

The method is described by reference to a specific application, that of the formation of the keying waves in a television synchronizing signal generator.

Introduction

THE synchronizing signal generator is a vital piece of television studio equipment, and several types have been described in detail elsewhere.[1–3] Although they may differ in detail, these units all operate on essentially the same principle. This paper describes a generator the circuitry of which shows a significant departure from that of conventional equipment, with resultant improvements in stability and reliability.

Incorrect sync generator operation can show up as loss of interlace, selection of incorrect numbers of equalizing pulses or vertical sync pulses, or instability of the intersync group. The end result is an unsteady picture. The generator to be described is inherently free from the above troubles, this improvement arising from the circuitry employed, rather than from precise adjustment and elaborate supply voltage regulation.

The composite sync signal consists of three sync component pulses: the horizontal sync pulses, the vertical sync pulses, and the equalizing pulses. Continuous trains of each of these pulses are formed in appropriate circuits controlled by a train of trigger pulses having a pulse repetition frequency of 31.5 kc, and are selected in the required number at the required times by keying pulses or "Keying Waves" as they are often called. These waves have a repetition frequency equal to the field frequency of 60 cps and must be precisely timed to select the required pulses. It is with the formation of these keying waves that this paper is mostly concerned, as this is the point at which the subject generator departs radically from those in current use.

The requirements demanded of the keying waves in a

* Original manuscript received by the IRE, March 3, 1955; revised manuscript received, May 16, 1955.

† Riverdale Radio, Ottawa, Can.

1 A. R. Applegarth, "Synchronizing generators for electronic television," Proc. IRE, vol. 34, pp. 128w–139w; March, 1946.

2 A. J. Baracket, "Television synchronizing signal generator," *Electronics*, vol. 21, pp. 110–115; October, 1948.

3 D. G. Fink, "Television Engineering," McGraw-Hill Book Co., Inc., New York, N.Y., 2nd ed., pp. 553–567; 1952.

typical sync generator will be described with reference to Fig. 1, a pulse-timing diagram illustrating the function of these waves in the formation of the intersync group of equalizing and vertical sync pulses. A and B are the horizontal sync pulses for the first and second fields respectively, C is the train of equalizing pulses and D is the equalizing pulse keying wave.

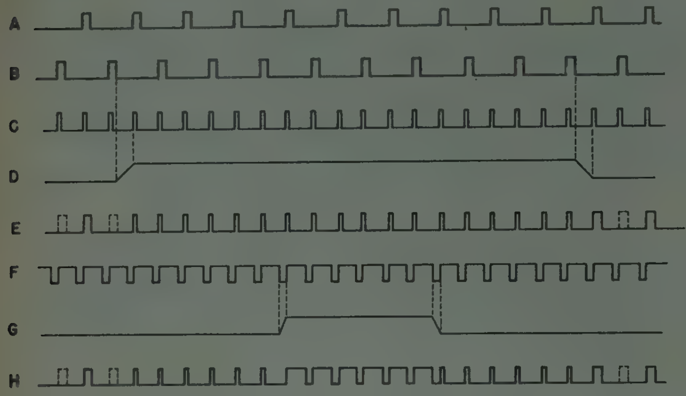

Fig. 1—Formation of the intersync group from continuous trains of each of the sync component pulses by means of keying waves.

It will be seen that the leading edge of this keying wave must be entirely contained within a 26 microsecond interval between two equalizing pulses, and must be of such duration as to select exactly eighteen equalizing pulses. The trailing edge must be entirely confined to a 26 microsecond interval between the eighteenth and nineteenth pulses.

One other requirement which is not obvious from the above is that there must be exactly five hundred and twenty-five equalizing pulses between the leading edges of two successive keying waves. With the frequency-dividing circuits commonly used, a small amount of crosstalk from 60-cycle power circuits introduced into the counter may cause a phase displacement of the output pulse sufficient to cause the leading edges of the keying waves derived from this pulse to occur at five hundred twenty-four pulse intervals in one field, five hundred twenty-six in the other, thus destroying interlace.

The group of eighteen equalizing pulses is shown at E along with adjacent horizontal sync pulses, those of the alternate field being shown in broken lines. Horizontal sync pulses are removed during equalizing pulse interval by the inverse of equalizing pulse keying wave.

The train of vertical sync pulses is shown at F and the vertical sync pulse keying wave at G. When the vertical sync pulse group is added to the center six equalizing pulses, the complete intersync group shown at H is formed. It will be seen that the wave G must be delayed six pulse intervals from the start of the equalizing pulse keying wave and its leading edge must be confined to the four microsecond interval preceding the seventh equalizing pulse. If it occurs sooner, part of a vertical sync pulse will appear after the sixth equalizing pulse. If it occurs later, the first vertical sync pulse will be incomplete. Similar tolerances are required at the trailing edge.

A precise method of forming these waves using a

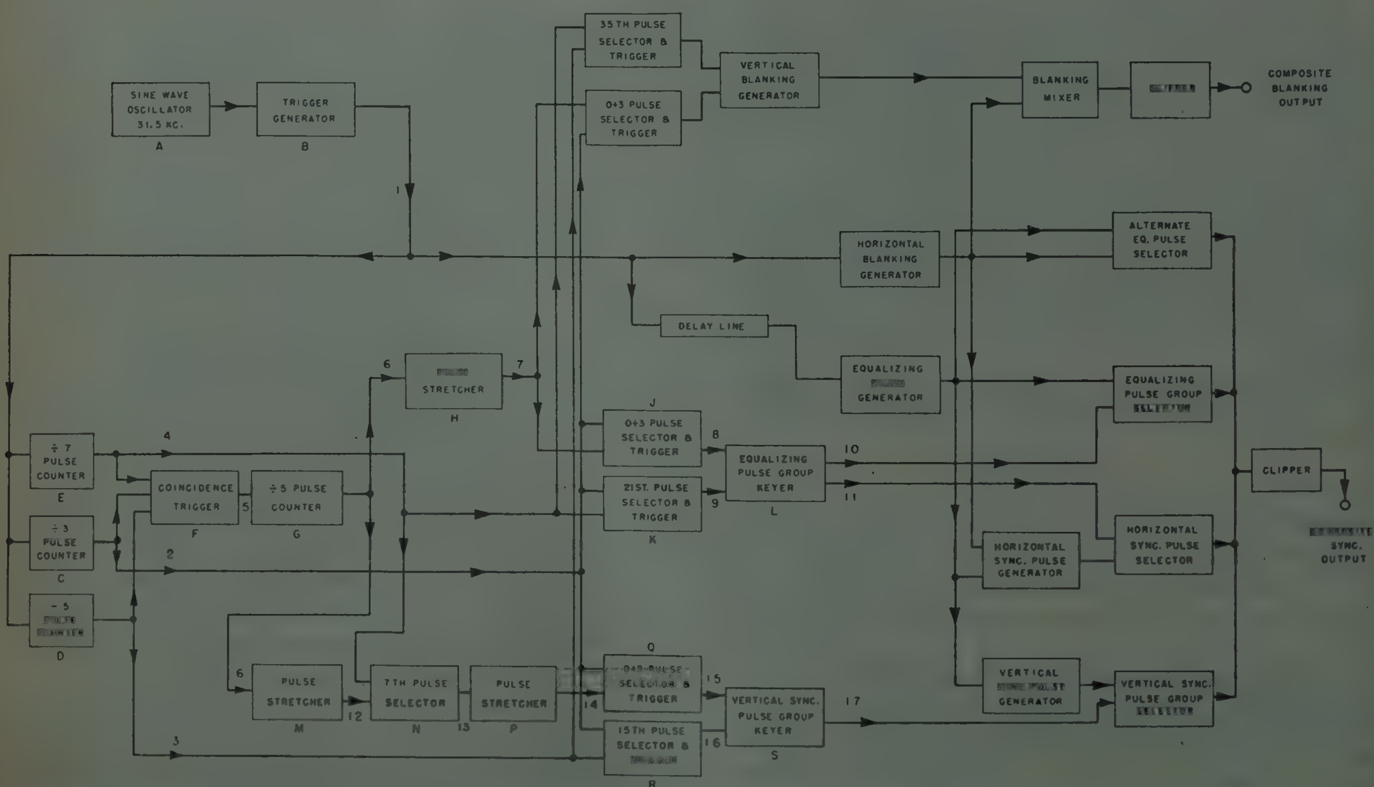

Fig. 2—Block diagram of a sync generator employing a pulse-coincidence counter and pulse selection circuits for the formation of the keying waves. Numbers adjacent to the flow arrows refer to waveforms in Fig. 3.

pulse-coincidence type of frequency-divider[4] and pulse selection circuits will now be described.

Pulse-Coincidence Type Frequency-Divider

Referring to the block diagram, Fig. 2, a source of 31.5 kc sine waves A supplies a trigger shaping circuit B, which, through a process of limiting and differentiation, forms trigger pulses having a rise time in the order of 0.2 microsecond. These are shown as waveform 1 in Fig. 3. The trigger pulses drive three frequency-dividing

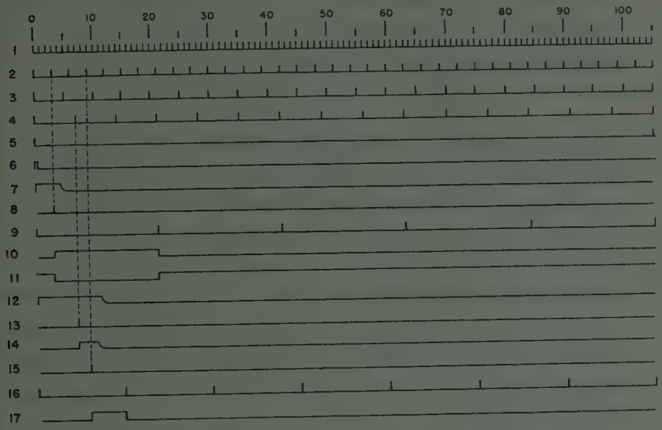

Fig. 3—Pulse-timing diagram illustrating the formation of the keying waves.

(counter) circuits C, D and E operating in unison. C produces an output pulse for every three input pulses and its output is shown as waveform 2. D produces an output pulse for every five input pulses and its output is waveform 3. E similarly divides by seven and its output is waveform 4. A triple-grid coincidence tube F has its circuit constants so arranged as to draw plate current only when pulses appear on all three grids at the one time. This event will occur once for every $3\times5\times7$ or 105 trigger pulses, as shown in waveform 5. These pulses drive a scale-of-five counter G which produces a pulse for every five hundred twenty-five trigger pulses, equivalent to a pulse repetition rate of 60 per second. This pulse has a width of 10 microseconds and is shown as waveform 6. The trigger pulse in waveform 1 which corresponds to this pulse is the Ø (zero) pulse, or starting point, of the timing diagram.

To ensure reliable operation of the coincidence circuit, it is desirable that the three counters produce pulses of identical shape. In the present application this was achieved by using a blocking-oscillator type of counter circuit, all three circuits having identical transformers and grid-blocking condensers.

The circuits were designed to produce pulses with a width of two microseconds, as such a pulse was found to contain sufficient energy to ensure reliable triggering of the following stage and is narrow enough to give precise timing. It has a shape which is characteristic of this type of circuit—a single positive half-cycle of a sine wave. The driving pulses for counter G are thus very narrow (2 microseconds) compared to their period (3,333 microseconds) and their leading and trailing edges are equally sharp. This fast rise time results in very precise timing of the output pulse. For reasons which will be apparent later, this circuit is arranged to trigger on the trailing edge of the driving pulse.

Since little information has appeared on the pulse-coincidence type of counting circuit, and since it forms the heart of this unit, a circuit suitable for the present application is shown in Fig. 4.

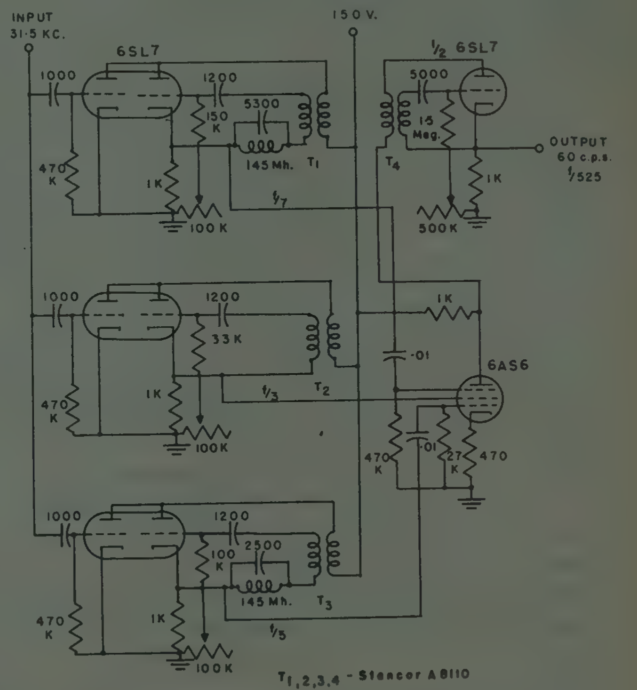

Fig. 4—Schematic diagram of a counter circuit which uses the pulse-coincidence principle. For the transformers indicated, in $T1$, $T2$ and $T3$ the green lead is the plate, and the blue lead the grid connection. In $T4$ the plate lead is blue, and the grid lead is green.

It will be noted that resonant stabilizing elements are used in the $f/5$ and $f/7$ stages. The action of these devices has been described before[1,2,5] and will not be entered into here.

Formation of Keying Waves by Pulse Selection

The output pulse 6 of the counting circuit is applied to a pulse stretching circuit H consisting of a triode biased to plate-current cutoff and having a parallel rc circuit as its plate load. The pulse applied to its grid causes it to draw plate current for the duration of the pulse. The saw-tooth pulse formed at the plate as the capacitor recharges is clipped by a second triode, and a positive pulse of roughly rectangular shape appears at

[4] B. Chance, V. Hughes, E. F. MacNichol, David Sayre and F. C. Williams, "Waveforms," M.I.T. Radiation Lab. Ser., McGraw-Hill Book Co., Inc., New York, N.Y., vol. 19, pp. 625–626; 1949.

[5] *Ibid.*, pp. 595–599.

its plate. The width of this pulse is governed by the constants of the rc circuit and the clipping level of the grid circuit of the second tube.

The "stretched" pulse so produced is not especially precise, and need not be. Its only requirements are that it rise to full amplitude within three trigger pulse intervals from the driving pulse, and decay to substantially zero value during the next three pulse intervals. This has been achieved quite readily in practical circuits.

This pulse 7 is applied to a coincidence tube J along with waveform 2 from the $f/3$ counter. The plate circuit of J will thus contain only the first pulse from Ø of the $f/3$ counter, corresponding to the third trigger pulse. It cannot contain the pulse occurring at Ø because the output pulse of G starts on the trailing edge of the corresponding driving pulse. Due to the pulse width of 7, it cannot contain any of the pulses which follow. This pulse, shown as waveform 8, is used to trigger the Eccles-Jordan "flip-flop" circuit L. The circuit is returned to its former condition eighteen pulse intervals later by the coincidence tube K to which is applied the outputs 2 and 4 from the $f/3$ counter C and the $f/7$ counter E. The output of this circuit K is shown as waveform 9.

The pulse appearing on one plate of L is shown as waveform 10 and is used to select the group of eighteen equalizing pulses. A similar, but inverted pulse 11 appears on the other plate of L and is used to reject nine horizontal sync pulses during this interval. The leading and trailing edges of this pulse are quite sharp, having a rise time in the order of 0.2 microsecond, and bear a precise time relationship to the original 31.5 kc trigger pulses.

It might be noted here that the sync component pulses are delayed 1.25 microseconds from the trigger pulses 1 and they therefore fall well within the keying wave 10.

The formation of the keying wave which selects the six vertical sync pulses and adds them to the center six equalizing pulses will now be described.

Formation of Vertical Sync Pulse Keying Wave

The pulse 6 is applied to a pulse stretcher M which produces a pulse 12 in the same manner as previously described for the formation of pulse 7. This pulse must rise to full amplitude within seven trigger-pulse intervals from the driving pulse and decay to substantially zero amplitude during the next seven intervals. The pulse is applied to a coincidence tube N along with the output 4 of the $f/7$ counter E. The pulse 13 so selected is the first pulse from Ø of the $f/7$ counter and corresponds to the seventh trigger pulse. It is applied to the pulse stretcher P which produces a pulse 14 having a width corresponding to the interval of more than two but less than five trigger pulses.

This pulse is applied to a coincidence tube Q along with the output 2 of the $f/3$ counter C. The tube selects the third pulse from Ø of the counter C, corresponding to the ninth trigger pulse. This pulse, shown at 15 is used to trigger the Eccles-Jordan "flip-flop" circuit S. The circuit is returned to its former condition six pulse intervals later by the coincidence tube R which receives output pulses 3 and 2 from the $f/5$ and $f/3$ counters and conducts on every fifteenth pulse as shown in waveform 16.

The required keying wave appears on a plate of the Eccles-Jordan circuit S and is shown as pulse 17. The leading and trailing edges of this pulse have the same rise time, and display the same accuracy of timing as the equalizing pulse keying wave previously described.

Formation of Blanking Pulses

The leading edge of the vertical blanking pulse coincides with the leading edge of the equalizing-pulse keying wave, and is formed in the same manner. The trailing edge is formed thirty-two pulses later by a coincidence between the $f/5$ and $f/7$ counter outputs 3 and 4. The pulse so produced has a width of 32×31.75 or 1,016 microseconds, which is well within the tolerance limits of eight hundred thirty-four to one thousand three hundred and thirty-four microseconds set in the United States by the FCC.

Referring again to Figs. 2 and 3, the trigger pulse train 1 drives the horizontal blanking pulse generator. This is a conventional multivibrator which produces a 10-microsecond pulse and at the same time counts down by a factor of 2.

The two blanking pulses are combined in the blanking mixer and clipper to form the composite blanking pulse train.

Formation of Sync Component Pulses

The trigger pulse train 1 in Fig. 2 drives the equalizing pulse generator after first passing through a delay line which is adjusted to give a 1.25-microsecond delay interval between the leading edge of the equalizing pulses and the leading edge of the horizontal blanking pulses. This interval later appears in the composite sync output as the "front porch" between the leading edge of the horizontal blanking pulse and the leading edge of the horizontal sync pulse. It also ensures that the sync component pulses will fit inside the keying waves as previously mentioned.

The equalizing pulse generator is a conventional multivibrator and produces pulses of 2.5 microseconds at the trigger frequency of 31.5 kc.

The horizontal blanking pulse is used as a keying wave to select every second equalizing pulse. The pulses so selected drive the horizontal sync pulse generator, a multivibrator which produces pulses of five microseconds width at the line-scanning frequency of 15.75 kc.

The vertical sync pulses are formed from the equalizing pulses in a pulse stretcher similar to those described earlier in this paper, rather than in a multivibrator. These pulses are wide (27 microseconds) compared with

their period (31.75 microseconds) and their trailing edge is not critical. Their formation in a shaping circuit rather than in a multivibrator resulted in a more stable pulse train.

Assembly of the Sync Component Pulses

To ensure that the interval between the leading edges of all sync components be uniform, they are all formed from the equalizing pulse train, the horizontal and vertical sync pulses serving only to broaden the equalizing pulses as required. This is accomplished in the following manner.

The equalizing pulse train is applied to the alternate equalizing pulse selector along with the horizontal blanking pulses. The output of this circuit thus contains every second equalizing pulse. The equalizing pulse train is applied also to the equalizing pulse group selector along with the equalizing pulse group keying wave 10. A group of eighteen equalizing pulses appears in the output of this circuit.

The inverse keying wave 11 is applied to the horizontal sync pulses selector along with the output train of the horizontal sync pulse generator. The output of this circuit contains horizontal sync pulses except during the interval of the group of eighteen equalizing pulses.

The outputs of these three pulse selectors are combined in a common plate load and the overlap between the horizontal sync pulses and the alternate equalizing pulses is removed later in a clipper circuit.

The output of the vertical sync pulse generator is applied to the vertical sync pulse group selector along with the vertical sync pulse group keying wave 17. The output of this circuit contains a group of six vertical sync pulses. These pulses are combined in the common plate load with the center six of the group of eighteen equalizing pulses and as before the overlap is removed in the clipper circuit.

In this manner the leading edge of each sync component pulse is derived from an equalizing pulse, and the possibility of bends in the picture resulting from irregular spacing of the sync components is eliminated.

Conclusion

It is felt that the method of producing precise low frequency pulses from higher frequency pulse trains as used here for the formation of the keying waves in a television synchronizing signal generator may have applications other than the one described, possibly in the field of precision navigation systems, radars, and computers. The writer would welcome suggestions along these lines.

The synchronizing signal generator described here achieves an unusual degree of stability with the use of only a moderate number of vacuum tubes. All of the functions shown in the block diagram, along with the necessary buffers and output stages, are achieved in thirty-four tube envelopes made up of twenty-one twin triodes and thirteen pentodes. A complete sync generator suitable for studio use would, of course, contain additional stages for the formation of the camera driving pulses and for automatic frequency control of the 31.5 kc sine wave oscillator. These have been adequately described in the references cited.

Acknowledgment

The assistance of G. Harbottle of the National Research Council, Ottawa, Canada, in the review of the manuscript and the preparation of the illustrations, is gratefully acknowledged.

Microwave Detection in a Thermionic Diode*

P. A. REDHEAD†, ASSOCIATE MEMBER, IRE

***Summary*—A theoretical analysis of the detection of microwave energy in a thermionic diode is presented assuming a parabolic space-charge potential distribution and that the resultant field acting on the electron is the sum of the static and radio-frequency fields. It is shown that at microwave frequencies the space-charge-limited diode behaves as a velocity-modulated detector. This solution is a valid approximation for signal frequencies in excess of the electron plasma frequency at the potential minimum and for signal amplitudes less than $2V_m/d\ s[1+(\omega^2/\alpha^2)]^{1/2}$. Here s is the diode spacing, d the potential minimum spacing, ω the angular frequency, V_m the potential at the minimum and $\alpha^2=2\epsilon V_m/md^2$.**

* Original manuscript received by the IRE March 14, 1955; revised manuscript received May 30, 1955.

† Radio and Electrical Engineering Division, National Research Council, Ottawa, Canada.

Introduction

When a low-frequency signal is applied to a space-charge-limited diode the detected output is proportional to the curvature of its $I-V$ characteristic (d^2I/dV^2); as the frequency of the signal is increased the detected output is diminished, as Llewellyn[1] has shown. At sufficiently high frequencies another detection mechanism becomes operative making the thermionic diode a relatively efficient detector of microwave energy. This detection effect, henceforth called velocity-modulated detection, was first observed

[1] F. B. Llewellyn, "Electron Inertia Effects," Cambridge University Press, 1941.

by Döhler[2] who explained his experimental results on the basis of a greatly simplified model. Bronwell[3] has recently reported measurements of the same effect. The present paper is an extension of some preliminary results previously reported.[4] Papp[5] has analyzed the problem using the same basic model that is assumed herein.

The space-charge cloud in a thermionic diode, when acted on by an rf field of low frequency, reacts to the variations of electric field in an organized fashion so as to partially cancel the rf field within the space-charge cloud, i.e., the rf field fails to penetrate the space-charge cloud. At very high frequencies the space-charge owing to the inertia of the electrons, no longer behaves like an organized medium,[6] and the rf field within the space-charge cloud approaches the field that would exist in the absence of space-charge. Thus only at very high frequencies is the force on an electron in the space-charge cloud the result of the sum of the static and rf fields. By assuming that the potential distribution between the cathode and the potential minimum (hereafter PM) is parabolic the equations of motion of an electron acted upon by the combined static and rf fields may be solved to yield the initial velocity conditions for an electron to surmount the potential barrier at the PM and reach the anode. It will be shown that the initial velocity condition for the electron reaching the PM at zero velocity contains a term proportional to the rf field, hence the term "velocity-modulated detection."

The velocity distribution of the emitted electrons

$$\left.\begin{aligned} \frac{N(v)dv}{N_0} &= \frac{mv}{kT} \exp\left\{-\frac{mv^2}{2kT}\right\} dv \qquad && (v > 0) \\ &= 0 && (v < 0) \end{aligned}\right\}. \tag{1}$$

(k: Boltzmann's constant $\quad T_0$: cathode temperature
m: electron mass $\quad N_0$: total number of emitted electrons)

is shown in Fig. 1, where v_m is the initial velocity of an electron reaching the PM at zero velocity under dc conditions. The anode current is the area under the curve from v_m to infinity.

$$I = \int_{v=v_m}^{\infty} N(v)dv.$$

When v_m is modulated by applying an rf field it is clear that detection will occur owing to curvature of the I-v_m characteristic; i.e., the derivative of the $N(v)$ curve at $v=v_m$. When the anode current is such that v_m occurs at the maximum of the $N(v)$ curve

$$\frac{dN(v)}{dv} = \frac{d^2I}{dv_m^2} = 0$$

the detected output will go to zero for small signals. This occurs when

$$\tfrac{1}{2}mv_{m0}^2 = \tfrac{1}{2}kT, \quad \text{or} \quad I/I_s = 0.606 \tag{2}$$

(I_s: saturation current density).

This point of zero output is independent of geometry or of frequency.

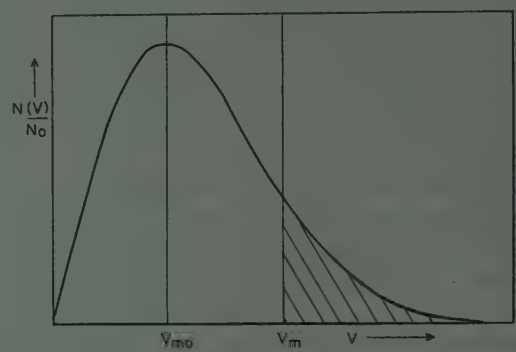

Fig. 1—Maxwellian velocity distribution of emitted electrons.

Since the velocity-modulated detection takes place in the region between cathode and PM the dimensions of the diode and the total cathode-anode transit time are relatively unimportant. Moreover, it is clear that cylindrical geometry will concentrate the rf field near the cathode and thus increase the detection sensitivity. This improvement is particularly marked since the detected output is proportional to the square of the rf field. This theory developed for plane-parallel diodes may be applied with some confidence to cylindrical diodes as the cathode-PM spacing at normal currents will be small compared to the cathode diameter.

Using the model described above an expression will be derived for the detected current on a small-signal basis. Restrictions on the frequency and amplitude of the rf signal imposed by the model will also be derived.

The Detected Current in a Plane Diode

In a plane-parallel diode (see Fig. 2, page 997) the rf field will be assumed constant and the equation of motion of the electrons is given by

$$\ddot{x} = -\frac{\epsilon}{m}(E_0 + E), \tag{3}$$

where ϵ/m is the charge to mass ratio of an electron, and E_0 the static field. E is the rf field given by

$$E = E_1 \sin(\omega t + \phi). \tag{4}$$

It is assumed that the static potential distribution

[2] O. Döhler and C. Hecker, "Ein Neuer Gleichrichtungsmechanismus bei cm-Wellen," *Hochfreq. und Electroak.*, vol. 54, pp. 7–11; July, 1939.

[3] A. B. Bronwell, T. C. Wang, I. C. Nitz and J. May, "Vacuum-tube detector and convertor for microwaves using large electron transit angles," Proc. IRE, vol. 42, pp. 1117–1123; July, 1954.

[4] P. A. Redhead, "Thermionic Microwave Detectors," IRE Conference on Electron Tube Research, 1952.

[5] G. Papp, "Mechanism of rectification in vacuum tube diodes at microwave frequencies," *Elec. Commun.*, vol. 31, pp. 215–219; September, 1954.

[6] D. Bohm and E. P. Gross, "Theory of plasma oscillations," *Phys. Rev.*, vol. 75, pp. 1851–1876; June 15, 1949.

caused by space-charge is parabolic about the PM; i.e.,

$$V_0(z) = az^2, \tag{5}$$

where $z=x-d$, and $a=V_m/d^2$. This approximation is reasonable for small anode currents when the potential minimum is large. Eq. (3) then becomes

$$\ddot{z} - \frac{2\epsilon}{m}az = -\frac{\epsilon}{m}E_1 \sin(\omega t + \phi), \tag{6}$$

which has the solution

$$z(t) = b_1 \exp(\alpha t) + b_2 \exp(-\alpha t) + b_3 \sin(\omega t + \phi), \tag{7}$$

where

$$b_3 = \frac{\epsilon}{m}E_1/(\omega^2 + \alpha^2),$$

and

$$\alpha = \left[\frac{2\epsilon a}{m}\right]^{1/2} = \left[\frac{2\epsilon V_m}{md^2}\right]^{1/2} = \frac{V_m}{d}.$$

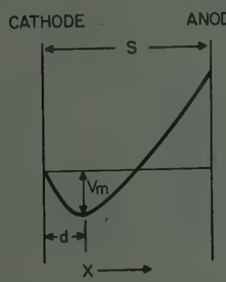

Fig. 2—Assumed potential distribution in a plane diode.

Inserting the initial conditions at time $t=0$,

$$\left.\begin{aligned} z &= -d \\ \dot{z} &= v_0 \end{aligned}\right\}, \tag{8}$$

the coefficients of (7) are found to be

$$\left.\begin{aligned} b_1 &= \frac{v_0 - v_m - c\sin(\phi+\theta)}{2\alpha} \\ b_2 &= \frac{v_0 + v_m + c\sin(\phi-\theta)}{2\alpha} \end{aligned}\right\}, \tag{9}$$

where

$$\left.\begin{aligned} c &= (\omega^2+\alpha^2)^{1/2}b_3 = \frac{\frac{\epsilon}{m}E_1}{(\omega^2+\alpha^2)^{1/2}} \\ \text{and} \quad \theta &= \tan^{-1}(\omega/\alpha) \end{aligned}\right\}. \tag{10}$$

Examination of (7) shows that for large values of t the term $b_2 \exp(-\alpha t) \to 0$ since α is positive: moreover b_2 is always negative for small values of c. The term $b_3 \sin(\omega t+\phi)$ merely causes a small oscillation about the long term tendencies of $z(t)$ provided that b_3 is small. (This limitation will be discussed more fully later.) Thus the solutions to (7) for t large are controlled by the $b_1 \exp(\alpha t)$ term and are of three basic types:

$$\left.\begin{aligned} &1)\ z(t) \to +\infty \quad \text{if} \quad b_1 > 0 \\ &2)\ z(t) \simeq 0 \quad \text{if} \quad b_1 = 0 \\ &3)\ z(t) \to -\infty \quad \text{if} \quad b_1 < 0 \end{aligned}\right\}. \tag{11}$$

Thus electrons with initial velocities and entrance phase angles satisfying the condition $b_1>0$ will reach the anode; those with $b_1<0$ will return to the cathode. For the electrons which pass the PM and contribute to the anode current

$$b_1 > 0$$

or

$$v_0 > v_m + c\sin(\phi+\theta). \tag{12}$$

The current to the anode per unit area is governed by the Schottky equation

$$I = I_s \exp\left(\frac{-\epsilon V_m}{kT}\right) = I_s \exp -\left(\frac{V_m}{V_T}\right), \tag{13}$$

where $V_T = kT/\epsilon$. Eq. (13) may be rewritten in terms of velocities to yield

$$I = f(v_m) = I_s \exp\left(\frac{-v_m^2}{v_T^2}\right) \tag{14}$$

where

$$v_T^2 = \frac{2kT}{m}.$$

The change in anode current produced by applying an rf field may be found by expanding (14) in a Taylor's series and for small signals we may neglect all but the first two terms

$$\Delta I(\phi) = \Delta v f' + \frac{\Delta v^2}{2} f'' + \cdots, \tag{15}$$

where Δv is identified with $c\sin(\phi+\theta)$. From (14) we find that

$$f'' = \frac{4I}{v_T^2}\left[\frac{v_m^2}{v_T^2} - \frac{1}{2}\right]. \tag{16}$$

The change in mean anode current density caused by the rf field is then

$$\begin{aligned} \overline{\Delta I} &= \frac{1}{2\pi}\int_0^2 \Delta I(\phi)d\phi \\ &= \frac{I}{v_T^2}\left[\frac{v_m^2}{v_T^2} - \frac{1}{2}\right]\frac{c^2}{\pi}\int_0^2 \sin^2(\phi+\theta)d\phi \\ &= \frac{I\left[\frac{\epsilon}{m}E_1\right]^2}{v_T^2} \cdot \frac{\left[\frac{v_m^2}{v_T^2} - \frac{1}{2}\right]}{\omega^2+\alpha^2}. \end{aligned} \tag{17}$$

Substituting (14) in (17) we obtain

$$\overline{\Delta I} = \frac{I}{4}\left(\frac{E_1}{V_T}\right)^2 \frac{(\log\beta - \frac{1}{2})}{\frac{\omega^2}{V_T^2} + \frac{1}{d^2}\log\beta} \tag{18}$$

where

$$\beta = \frac{I_s}{I}.$$

The value of d (cathode-PM spacing) may be determined from the Fry-Langmuir[7] analysis of space-charge-limited diodes which yields

$$d^2 = \frac{\xi_c^2 T^{3/2}}{I(9.186 \times 10^5)^2}, \tag{19}$$

where

$$\xi_c = f(\eta_c) \quad \text{and} \quad \eta_c = \log\frac{I_s}{I};$$

these two parameters being evaluated at the cathode surface. Values of ξ as a function η have been tabulated.[8] The critical anode current density (I_∞) at which the PM is located at the anode surface is

$$I_\infty = \left[\frac{\xi_{c\infty}}{9.186 \times 10^5}\right]^2 \frac{T^{3/2}}{s^2}$$

$$= 7.73 \times 10^{-12}\frac{T^{3/2}}{s^2} \text{ amps/cm}^2, \tag{20}$$

(s: anode-to-cathode spacing)

since $I_\infty/I_s \to 0$ in most practical cases and $\xi c_8 \to 2.554$ for small currents.

Thus

$$\left.\begin{aligned} Id^2 &= KI_\infty s^2 \\ K &= \frac{\xi_c^2}{\xi_{c\infty}^2} \end{aligned}\right\}. \tag{21}$$

where

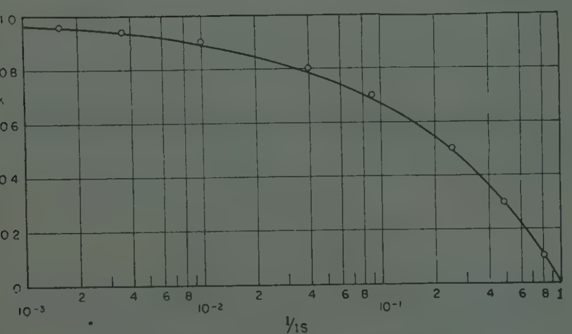

Fig. 3—Variation of $K = d^2I/s^2I_\infty$ with anode current. Circled points indicate values of K from the approximation $K = 1 - \beta^{-1/2}$

Fig. 3 shows the dependence of K on I/I_s computed from tables of Langmuir's functions.

An approximate analytic solution for K may be found by assuming that the space-charge cloud is in thermodynamic equilibrium (c.f. Von Laue[9]). Under these circumstances the space-charge density is given by

$$\rho = \rho_0 \exp(-V/V_T) \tag{22}$$

(ρ_0: space-charge density at the cathode surface), and one obtains with the use of Poisson's equation

$$\cos\left[\frac{\xi_c}{\sqrt{2}}\right] = \beta^{-1/2}. \tag{23}$$

Taking only the first two terms in the expansion of the cosine leads to the approximation

$$K = 1 - \beta^{-1/2}, \tag{24}$$

since $\xi c_8 = \pi/\sqrt{2}$ using the Von Laue approximation.

Values of K derived from (24) are shown as the circled points on Fig. 3. It will be seen that the values are in reasonable agreement with the values of K derived from the Langmuir analysis.

Substituting (21) in (18) leads to

$$\Delta I = \frac{I_\infty}{4}\left(\frac{V_1}{V_T}\right)^2 \frac{\log\beta - 1/2}{\frac{1}{K}\log\beta + \lambda\beta}, \tag{25}$$

where $V_1 = E_1 s$, and the dimensionless parameter

$$\lambda = \frac{\omega^2}{v_T^2} s^2 \frac{I_\infty}{I_s} = 0.993 \times 10^{-9} f^2 \frac{T^{1/2}}{I_s}$$

(f in mc/s., I_s in Amp. cm^{-2}). Eq. (25) can be rewritten

$$\Delta I = \frac{I_\infty}{4}\left(\frac{V_1}{V_T}\right)^2 C, \tag{26}$$

where

$$C = \frac{\log\beta - 1/2}{\frac{1}{K}\log\beta + \lambda\beta}. \tag{26a}$$

The variation of C with current is shown in Fig. 4 for three values of $\lambda^{1/2}$, $\lambda^{1/2}$ being proportional to frequency. It is apparent from (26a) that the detected output goes through zero for all frequencies when $\log\beta = 1/2$ or $I/I_s = 0.606$. For large anode currents ($\beta \to I$) it can be shown with the aid of (26a) and (24) that

$$C_{\beta\to 1} = \frac{-1/2}{2 + \lambda}. \tag{27}$$

Variation of the Detection Effect with Frequency

The maximum value of C ($C_{\max}$) and the value of current at which this maximum occurs ($I_{\max}$) for any value of $\lambda^{1/2}$ may be found from (26a) and (24) by graphical methods. $I_{\max}/I_s$ is plotted in Fig. 5. It will be observed that $I_{\max}/I_s$ varies from zero at low frequencies to a limiting value of 0.225 at very high frequencies. $C_{\max}$

[7] I. Langmuir and K. T. Compton, "Electrical discharges in gases, part II," *Rev. Mod. Phys.*, vol. 13, pp. 191–257; April, 1931.

[8] P. H. J. A. Kleijnen, "Extension of Langmuir's Tables for a Plane Diode with a Maxwellian Distribution of the Electrons," Phil. Res. Rep., vol. 1, pp. 81–96; January 1946. This is the most recent tabulation.

[9] M. Von Laue, "Glühelektronen," *Jahrb. d. Rad. u. Elekt*, vol. 15, pp. 205–256; 1918.

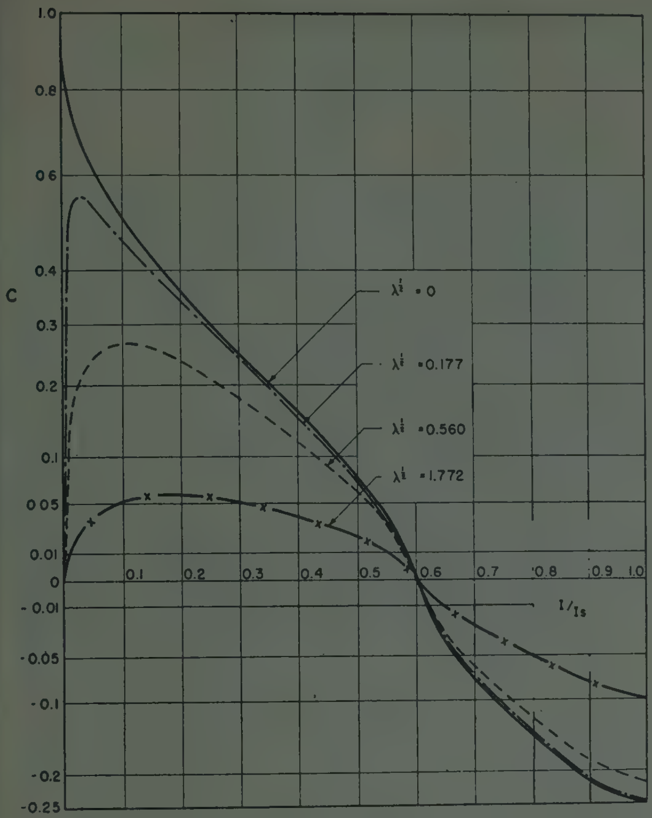

Fig. 4—Detection sensitivity factor C as a function of current for various values of $\lambda^{1/2}$. For $I_s = 1\text{A/cm.}^2$ and $T = 1{,}000$ degrees K., $\lambda^{1/2} = 1.772$ corresponds to a frequency of 10^4 mc., $\lambda^{1/2} = 0.560$ to 3.10^3 mc., $\lambda^{1/2} = 0.177$ to 10^3 mc.

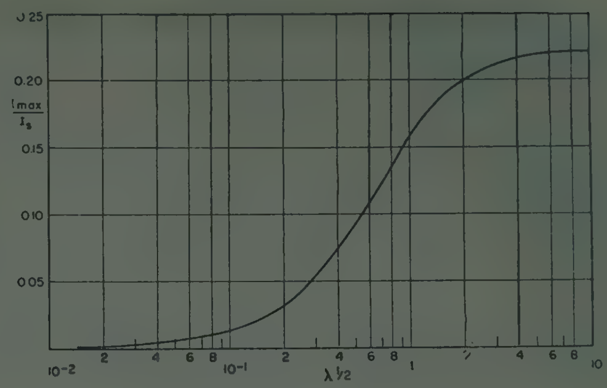

Fig. 5—I_{max}/I_s as a function of $\lambda^{1/2}$ ($\lambda^{1/2}$ is proportional to frequency).

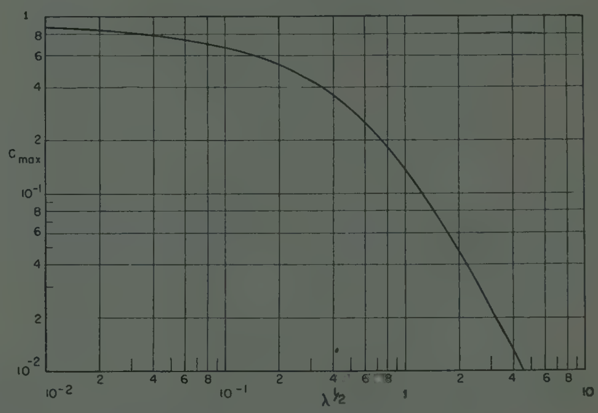

Fig. 6—The maximum detection sensitivity, C_{max}, as a function of $\lambda^{1/2}$ ($\lambda^{1/2}$ is proportional to frequency).

may also be found and plotted as a function of $\lambda^{1/2}$ (see Fig. 6). It will be seen that C_{max} decreases very rapidly at high frequencies.

Limitations of the Model

Signal Amplitude

One upper limit to the amplitude of the rf voltage for which the model is valid occurs when the term $b_3 \sin(\omega_t + \phi)$ [see (7)] becomes large enough to cause electrons which would move to the anode under small-signal conditions to be returned to the cathode. Electrons can most readily strike the cathode owing to a large b_3 term when $b_1 \to 0$. For the limiting electron which grazes the cathode surface it can be shown from (7) that

$$V_{1\max} = \frac{2V_m s}{d}(1 + \omega^2/\alpha^2)^{1/2}. \tag{28}$$

Thus the maximum rf voltage for which the model is valid increases with frequency. The most stringent limitation on V_1 occurs when $\omega^2/\alpha^2 << 1$, then

$$V_{1\max} = \frac{2V_m s}{d}\,. \tag{29}$$

For a tungsten filament at 2,000 degrees K, $I_s = 3 \times 10^{-3}$ amps/cm². With $I/I_s = 0.2$ and $s = 5$ mm then

$$d = 0.26 \text{ mm.}$$

$$V_{1\max} = 10.6 \text{ volts.}$$

The approximation used in (17) that

$$\frac{c^4}{v_T{}^4} < \frac{c^2}{v_T{}^2}$$

leads to a similar limitation, namely,

$$V_1 < \frac{2s}{d}\sqrt{V_T V_m}(1 + \omega^2/\alpha^2)^{1/2}. \tag{30}$$

Signal Frequency

At sufficiently high frequencies the rf field within a space charge cloud of uniform density approaches the field that would exist in the absence of any space charge. At low frequencies the rf field within the space charge cloud approaches zero. The transition between these two regions occurs in the neighbourhood of the electron plasma frequency given by

$$\omega_p = \left[\frac{\rho\epsilon}{\epsilon_0 m}\right]^{1/2}. \tag{31}$$

An approximate lower limit of frequency for which the assumed model is valid may be obtained by equating the signal frequency to the electron plasma frequency at the PM.

The space-charge density at the cathode surface is given by

$$\rho_0 = I_s\left[\frac{2\pi m}{kT}\right]^{1/2}, \tag{32}$$

then from (22) and (13) the space-charge density at the PM is

$$\rho_{\mathrm{PM}} = I\left[\frac{2\pi m}{kT}\right]^{1/2}. \tag{33}$$

Then if λ_{lim} is the value of λ when the signal frequency equals the plasma frequency at the PM it can be shown that

$$\left(\lambda_{\mathrm{lim}}\frac{Is}{I}\right)^{1/2} \simeq 1.8, \tag{34}$$

when $I = I_{\max}$ it can be shown from the data of Fig. 5 that

$$\lambda_{\mathrm{lim}}{}^{1/2} = 0.6$$
$$I = I_{\max}. \tag{35}$$

For $I_s = 1$ amp cm^{-2} and $T = 10^3$ degrees K the frequency corresponding to $\lambda_{\mathrm{lim}}{}^{1/2} = 0.6$ is 3.4 km.

For $I_s = 3$ mA.cm.$^{-2}$ and $T = 2.10^3$ degrees K the corresponding frequency is 159 mc.

Discussion

The foregoing analysis of the detection of microwave energy in a much simplified model of a thermionic diode may be applied to a real diode if the limitations discussed in the previous section are observed. The results of this analysis are in qualitative agreement with the experimental results of Döhler, and others. Although the foregoing results were obtained on the basis of plane-parallel geometry they may be applied to cylindrical diodes with some confidence since cathode-PM spacing will be small compared to cathode diameter.

List of Symbols

$a = V_m d^2$

c = coefficient of v-m term;

$$c = \frac{\epsilon/mE_1}{(\omega^2 + \alpha^2)^{1/2}}$$

C = detection sensitivity factor;

$$C = \frac{\log\beta - 1/2}{\dfrac{\log\beta}{K} + \lambda\beta}$$

d = cathode-PM spacing

E_0 = dc field

E_1 = peak rf field

f = frequency

I = anode current density

I_∞ = critical anode current density

I_s = saturation current density

k = Boltzmann's constant

K = PM spacing factor; $K = d^2I/s^2I_\infty$

m = mass of electron

s = anode-cathode spacing

T = cathode temperature

v_m = initial velocity of electron reaching the PM at zero velocity

v_T = velocity equivalent of cathode temperature; $v_T^2 = 2kT/m$

V_m = depth of PM

V_T = voltage equivalent of cathode temperature; $V_T = kT/\epsilon$

V_1 = rf field gradient

x = distance

z = reduced distance; $z = \kappa - d$

$\alpha = v_m/d$

$\beta = I_s/I$

ϵ = charge on electron

η_c = Langmuir potential function at the cathode surface

$\theta = \tan^{-1}\omega/\alpha$

$\lambda = (\omega_s/v_T)^2\, I_\infty/I_s$

ξ_c = Langmuir current-distance function at the cathode surface

ρ = space-charge density

ϕ = entrance phase angle

ω = angular frequency of applied signal

Acknowledgment

The author gratefully records his indebtedness to J. P. Hobson and C. R. Crowell for many stimulating discussions.

Unilateralization of Junction-Transistor Amplifiers at High Frequencies*

G. Y. CHU†, ASSOCIATE, IRE

Summary—**In designing an amplifier with a bilateral device, unilateralization is one approach which permits use of techniques already developed for unilateral devices, in particular vacuum tubes. A general method for deriving a unilateral circuit based on an equivalent circuit of the device is described, emphasis being placed on junction transistors operating at high frequencies. The principle is: application of external feedback which neutralizes the internal feedback of the device so that the signals at the output end no longer yield a signal at the input end. In general, two types of circuits are used for junction-transistor high-frequency amplifiers: emitter input and base input connections. Measurements of the input characteristics of two singly-tuned amplifiers have verified their unilateral properties. Tolerances of the neutralizing network depend on such factors as: transistor parameter spread, impedance level of the collector circuit, and performance deviations which a designer will accept. Gain and input and output characteristics of the unilateralized high-frequency amplifier may be predicted easily from the transistor parameters (both emitter input and base input connection) in a frequency range below the alpha cutoff frequency.**

INTRODUCTION

INTEREST in unilateral and bilateral amplifiers has been renewed because of the introduction of the transistor in direct competition to the vacuum tube. The superiority of a unilateral over a bilateral amplifier is not defined clearly, because, in general, the primary performance considerations of the amplifier do not depend directly on this property. Yet such considerations as gain, frequency response, and stability have bearing on this property. Thus, in amplifier study, unilaterality vs bilaterality is of much interest.

A vacuum tube triode, used as an audio amplifier, is regarded generally as a unilateral device, because of its negligible internal feedback in that frequency range. It is well-known that such performances as frequency response, stability, and gain can be altered by applying external feedback, either in single or in multiple stages. Thus, for the primary consideration of the mentioned performances, the unilateral amplifier is converted to a bilateral amplifier.

At radio frequencies, a vacuum tube triode is sufficiently bilateral to become unstable as an amplifier without neutralization (neutralization being an old technique to unilateralize the triode amplifier). To eliminate the need for neutralization, pentodes were introduced. They have negligible feedback at radio frequencies, and therefore have been used almost exclusively for all radio frequency amplifiers. Thus, in practice, a unilateral property is obtained with stable amplifiers at radio frequencies, with apparent advantage.

The development of the principle of staggered tuning for wide-band amplifiers and for other bandpass characteristics was based on the unilateral property of vacuum tube pentodes at the frequencies of interest. In order that the bandpass characteristics of an amplifier be controlled by tuning each stage individually, it is generally required that each stage or block be unilateral.

Since the advent of the transistor, it has been discovered that it is a bilateral device because of the inherent internal feedback. In junction transistors, this feedback can be represented approximately by such parameters as the base resistance, the collector capacitance, the collector resistance, and the effect of the space-charge layer widening.[1] At low frequencies and with common base or common emitter connections, the feedback signal is in phase or in phase opposition to the input signal and is relatively small. The effects on stability, frequency response, power gain and input resistance are usually of no great concern. As the frequency of operation is increased, the feedback caused by the collector capacitance and the base resistance becomes increasingly large, and instability problems similar to those of the vacuum tube triode radio frequency amplifier are introduced. Neutralizing circuits for junction transistor amplifiers were subsequently developed tending to unilateralize the stage.[2] Thus, the advantages of unilateralizing these amplifiers are:

1. Improved stability.
2. Ability to apply to transistor amplifier certain design techniques developed in vacuum tube amplifiers.

The above approach has been mentioned by Mason.[3]

Unfortunately, simple neutralizing circuits obtained by direct analogy to vacuum tube triode amplifiers in general will not result in unilateralized circuits. This is because of the more complicated frequency characteristics of the junction transistor.

In this paper, a general method of unilateralization is presented, based on the equivalent circuit of a bilateral device. Some typical unilateralized high-frequency circuits, both for common emitter and common base connections (also called base input and emitter in-

* Original manuscript received by the IRE, August 3, 1954; revised manuscript received, June 2, 1955.
† Sylvania Elec. Prod., Inc., Electronics Div., Ipswich, Mass.

[1] J. M. Early, "Effect of space-charge layer widening in junction transistors," PROC. IRE, vol. 40, pp. 1401–1406; November, 1952.
[2] J. B. Angell and F. P. Keiper, "Circuit applications of surface-barrier transistors," PROC. IRE, vol. 41, pp. 1709–1712; December, 1953.
[3] S. J. Mason, "Power Gain in Feedback Amplifiers," MIT Radiation Lab. Elec. Rep. No. 257; August 25, 1953.

put connections, see last section), are derived by applying the general method. Finally, some practical aspects of the application of these circuits are discussed.

General Method

A general method for deriving a unilateralized circuit using a bilateral device can be outlined as follows:

1. The bilateral device must be such that it can be represented by an equivalent circuit consisting of a linear passive network plus an active generator, which responds to a branch voltage (or a branch current) of the equivalent network.
2. If the device is excited at its output terminals only, then one is required to make the above-mentioned branch voltage (or current) vanish by means of an external passive feedback network. When this is realized, the active generator becomes inactive with respect to the voltage at the output and the equivalent circuit of the device is reduced to a passive network under the condition of zero input.
3. The external passive network which will meet the requirement of (2) may be found by applying the principle of the balanced bridge circuit because the equivalent circuit of the device becomes passive and is known in the absence of input excitation.

This principle will be used in the following sections to derive two unilateralized circuits for junction-transistor high-frequency amplifiers, (emitter and base input connections).

Unilateralized Emitter Input Circuit

One of the well-known equivalent circuits for junction transistors, generally used in emitter input circuits for Class A amplifiers is shown in Fig. 1.[1,4] In this diagram r_e, C_e, r_c, C_c, r_b, and r_b' respectively represent the emitter resistance, emitter capacitance, collector resistance, collector capacitance and the two base resistances of the passive network. The active current generator, αi_e, responds to the emitter current, i_e.

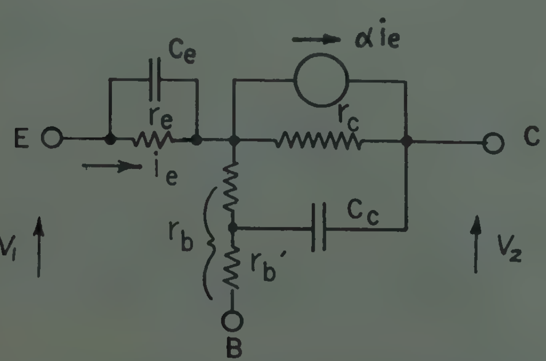

Fig. 1—Equivalent circuit of a junction transistor.

In accordance with the general method, if i_e can be made zero when $V_1=0$ and $V_2 \neq 0$ with the input terminated by any finite impedance, the active generator, αi_e, becomes zero and drops out of the circuit. The output

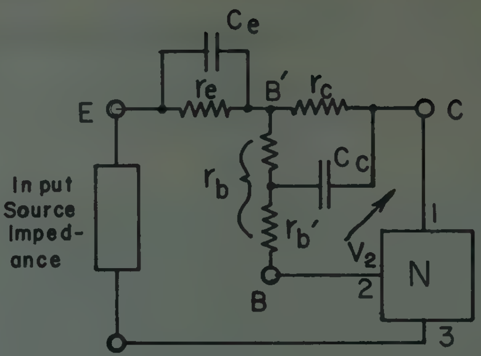

Fig. 2—Transistor equivalent circuit and neutralizing network for emitter input amplifiers.

terminals between which the voltage V_2 exists are the terminals B and C. Thus, an external three-terminal passive network can be achieved readily by using the arrangement illustrated in Fig. 2, where N is three-terminal passive network with any one of the configurations shown in column A of Table I.

TABLE I

N Network for Emitter Input Amplifiers

	A	B
(1)	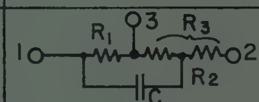	$\frac{R_1}{r_c} = \frac{R_2}{r_b'} = \frac{R_3}{r_b}$ $R_2C = r_b' C_c$
(2)	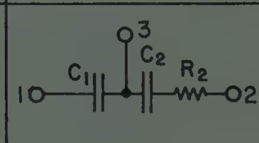	If $r_c >> \frac{1}{wC_c} >> r_b'$, $R_2 C_1 = r_b' C_c$, $\frac{C_1}{C_2} = \frac{r_b}{r_c}$

A set of relations of the elements in Fig. 2 must be satisfied in order to make $i_e=0$. These conditions are listed in column B of Table I.

The configuration (1) for the N network is apparently a direct copy of the equivalent feedback network inside the transistor itself. From a balanced bridge circuit viewpoint, the elements r_c, r_b, r_b', and C_c are the counter parts of R_1, R_3, R_2, and C in the N network with respect to the terminals B' and 3. The configuration (2) is a simplified version of (1) suitable for practical use. Configuration (2) can be derived from (1) by either applying a Pi to Tee conversion for the elements R_1, C and R_3-R_2 or by considering that the feedback network supplies two feedbacks; one in phase with and one in quadrature with V_2. The C_1, R_2 combination supplies the quadrature feedback to compensate for the $C_c r_b'$ combination whereas the C_1C_2 combination supplies the inphase feedback to compensate for the $r_c r_b$ combination. The advantages of (2) are: (a) only three elements are needed; (b) there is less energy loss, because most of the resistive elements in (1) have been replaced by lossless capacitive elements.

For commercial high-frequency junction transistors now available on the market, such as Sylvania's 2N94,

[4] G. Y. Chu, "A new equivalent circuit for junction transistors," 1954 IRE Convention Record, Part 2, "Circuit Theory," vol. 2

the standard broadcast band. Therefore, the accuracy of (2) is sufficiently high for most applications in the above frequency ranges.

Experimental Verification

The circuit in Fig. 2 with an N network of configuration (2) has been adopted for a single-tuned 455kc IF amplifier, using a Sylvania type GT-547 *n-p-n* transistor (this is an early experimental version of the now available 2N94 and 2N94A). The input impedance of the amplifier was measured to verify the theory. This impedance was found to be constant over the pass band and to be equal virtually to the short-circuit input impedance of the transistor. This is as it should be. Fig. 3 shows the input impedance as a function of frequency for a unilateralized single-tuned 455kc IF amplifier.

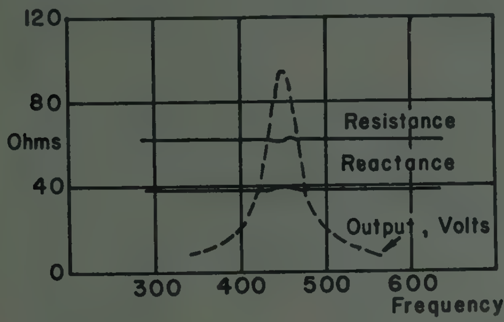

Fig. 3—Input impedance and response of a unilateralized single-tuned amplifier.

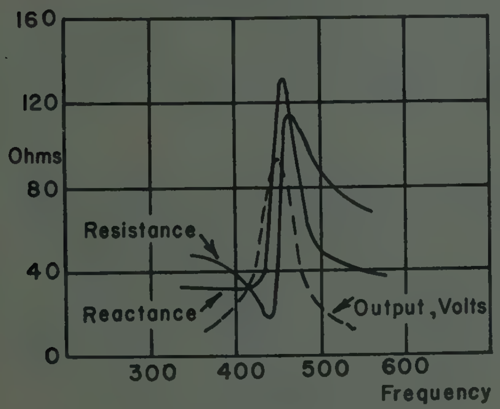

Fig. 4—Input impedance and response of a single-tuned amplifier with no neutralization.

The fact that the input impedance is constant whereas the load impedance varies rapidly with frequency in the vicinity of resonance indicates that the amplifier has been unilateralized. For comparison, the input characteristics of another amplifier using the same transistor with no neutralization are shown in Fig. 4. The large fluctuations both of the resistive and of the reactive components of the input impedance are clearly caused by the transistor's non-neutralized internal feedback.

Unilateralized Base Input Circuit

The equivalent circuit of a junction transistor for base input high-frequency application is shown in Fig. 5,[4,5] where the active current generator responds to the excitation current i_b'. A is the current transfer amplification factor; C_e is the emitter diffusion capacitance; G_e is the emitter conductance in the base input connection; G_c is a leakage conductance across collector barrier; R_2 is an output resistance caused largely by the effect of space-charge widening in the transistor.

$$A = \frac{\alpha}{1-\alpha}$$

$$G_e \cong \frac{1-\alpha_0}{r_e}$$

$$C_e \cong \frac{1}{2\pi f_\alpha r_e}$$

$$G_c \cong \left(\frac{1}{r_c}\right)_{Ie=0}$$

Following the general method of unilateralization already outlined as regards feedback analysis, the active generator can be omitted in the absence of an input. The equivalent circuit of the transistor becomes a passive network. This facilitates finding an appropriate passive network to fulfill the required unilateralized condition.

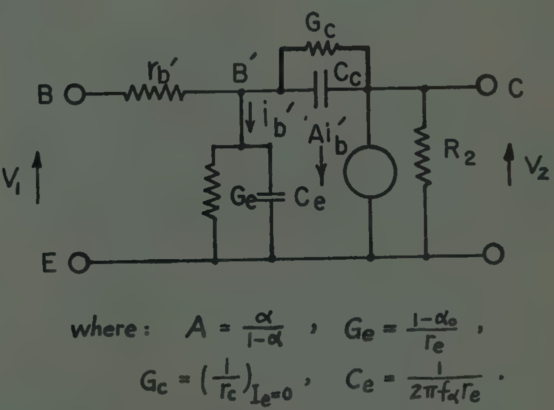

Fig. 5—A high-frequency equivalent circuit for base input applications.

Fig. 6, on the next page, shows the equivalent circuit of a base input transistor amplifier, (with G_c and R_2 neglected), and a neutralizing network. For a balanced bridge, the following conditions must be satisfied:

$$\frac{C_1}{C_3} = \frac{C_e}{C_2} = \frac{R}{r_b'}. \tag{1}$$

In addition, a three-terminal network T must satisfy the following conditions:

$$\frac{V_3}{V_2} = \frac{r_b' + \dfrac{1}{j\omega C_1}}{-\dfrac{1}{j\omega C_e}}, \tag{2}$$

and

$$|Y_3| \ll \omega C_2. \tag{3}$$

For transistors suitable for high-frequency applications, $r_b' \ll (1/\omega C_e)$. Therefore, it is virtually true that

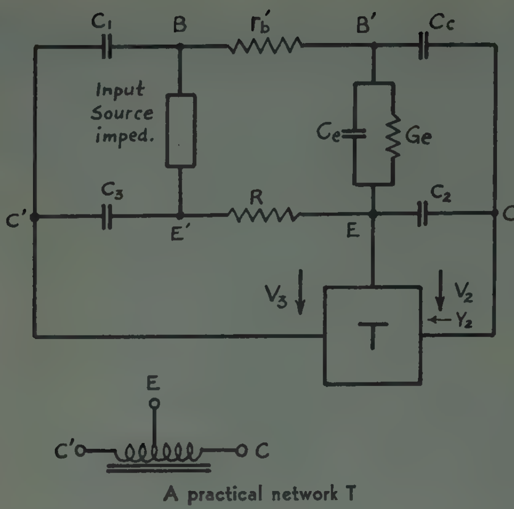

Fig. 6—Transistor equivalent circuit and neutralizing network for base input amplifiers.

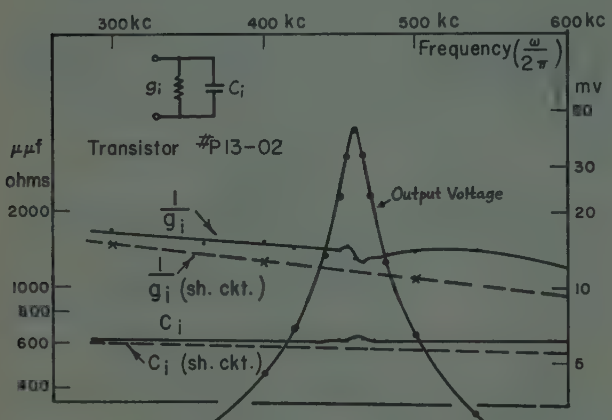

Fig. 7—Input characteristics of a unilateralized base input IF amplifier.

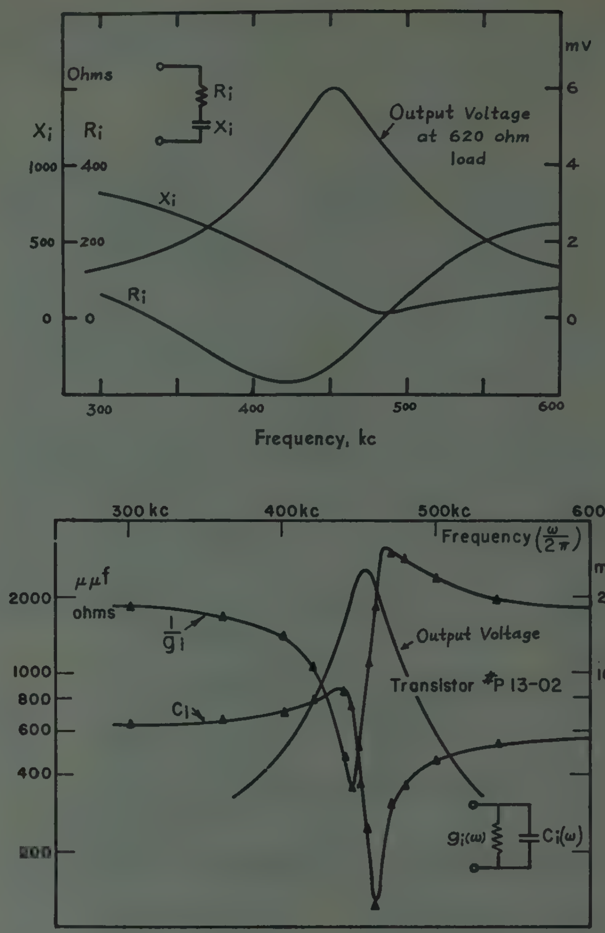

Fig. 8—(a) Input characteristics of a non-neutralized base input 455kc IF amplifier. (b) Input characteristics of a partially-neutralized base input IF amplifier.

Thus, a tapped transformer can be used as the network T, the feedback inside the transistor is neutralized, and the amplifier is essentially unilateralized. Again, the circuit to achieve this end is not unique.

Experimental Verification

The circuit shown in Fig. 6 was adopted to a single-tuned base input 455kc IF amplifier. The circuit elements were chosen such that the approximations made in the above analysis are valid. The input impedances were measured and compared with the short-circuit input impedance of the transistor, as shown in Fig. 7. Their close resemblance verifies that the circuit has been essentially unilateralized.

Shown for comparison in Figs. 8(a) and 8(b) are the input characteristics of a non-neutralized and a partially-neutralized amplifier, using the same transistor. The wide variation occurring in the pass band indicates clearly the effect of internal feedback.

The partially-neutralized circuit was derived by neglecting the influence of r_b' returning the input source and the G_eC_e combination to the tap on the transformer. The C_2C_3 combination can then be replaced by a single condenser C. The resulting circuit is shown in Fig. 9 (opposite), obviously similar to that of a plate-neutralized triode tube amplifier. The partially-neutralized case represents a distinct improvement over the non-neutralized case in that for the former the input resistance does not become negative in the vicinity of resonance as it does for the non-neutralized case.

Accuracy, Tolerance and other Practical Neutralizing Circuits

The accuracy achieved in unilateralizing an amplifier depends on these factors, which are discussed below: frequency range; bandwidth; transistor parameter value and spread; neutralizing circuit element tolerance; and amplifier gain.

Frequency Range

The degree of accuracy obtained in representing a junction transistor by an equivalent circuit with linear lumped elements depends largely on the frequency range. It is known that as the operating frequency is increased to the region of alpha cutoff, the transistor behaves more and more as if it possessed distributed

parameters. Passive networks with distributed parameters may be feasible, for a neutralizing network, but are far less practical.

Bandwidth

Bandwidth is another important factor. As the frequency range of interest is narrowed, accuracy obtained in representing a device by an equivalent circuit with passive elements of constant coefficients is increased

Transistor Parameter Value and Spread; Neutralizing Circuit Element Tolerance; Amplifier Gain.

Because the principle of neutralization depends on a balanced bridge, transistor parameter spread and neutralizing circuit element tolerance obviously influence any unbalance. However, unbalance sufficient to cause significant residual feedback depends upon the gain of the amplifier. Thus, in practice, as the amplifier output collector impedance level is lowered, the tolerance on transistor parameter spread and neutralizing circuit elements can be relaxed. The transistor parameters, C_c and r_b', play a crucial role. As these values are increased, the internal feedback increases for a given gain of the amplifier. It follows that for a given percentage of tolerance on the parameter spread, the amount of feedback is greater for transistors with larger values of the $C_c r_b'$ product.

If the collector circuit impedance level of the amplifier is made sufficiently low, the feedback effect caused by the r_b' and r_e is generally insignificant for good transistors. Thus amplifiers may be essentially unilateralized or stabilized by neutralizing the feedback component caused by the $r_b'C_c$ combination in the emitter input connection, or C_c in the base input connection.

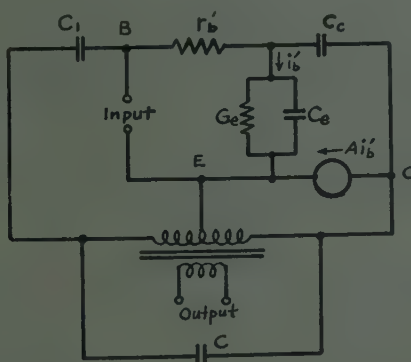

Fig. 9—Partially-neutralized base input IF amplifier.

Such circuits can be obtained simply by omitting C_2 in the N network in Fig. 2 or by using the circuit of Fig. 9 in place of that of Fig. 6. The simplified circuits and their various modifications have stimulated interest recently in the IF and RF stages of transistorized radio receivers.

Properties of the Unilateralized Amplifier

For transistors, there are three possible connections used in practice, namely: common base, common emitter and common collector. Theoretically, the roles of the input and output terminals may be interchanged because of their bilateral properties. This results in a total of six connections. However, the three reversed connections are never used because they are contrary to the amplifier requirement. In the unilateralized amplifier which uses an external feedback network, a three-terminal device is generally expected to become a four-terminal device. Therefore, the terms "base input" or "emitter input" are used more appropriately. Furthermore, because of the inherent transfer characteristic of the junction transistor, in which the transfer occurs mainly in one direction, the unilateralized collector input amplifier is not practical. Thus, although the neutralization circuit may not be unique, there probably will be only two general types of circuits: the base input and the emitter input.

The behavior of a linear unilateral amplifier can be described generally by the following equation:

$$\begin{bmatrix} V_1 \\ I_2 \end{bmatrix} = \begin{bmatrix} Z_1 & 0 \\ A & Y_2 \end{bmatrix} \begin{bmatrix} I_1 \\ V_2 \end{bmatrix}, \tag{5}$$

where

V_1 = input voltage,
V_2 = output voltage,
I_1 = input current,
I_2 = output current,
Z_1 = input impedance with output short circuited,
Y_2 = output admittance with the input open circuited,
A = current transfer ratio in the forward direction with the output short-circuited.

It is clear that both Z_1 and Y_2 can be predicted from the equivalent circuit plus the connected neutralizing circuit. A is characteristic of the transistor alone and is equal to alpha (α) in the emitter input connection and to beta

$$\left(\beta = \frac{\alpha}{1-\alpha}\right)$$

in the base input connection.

Because the power loss in a good neutralizing network is generally a small fraction of the power gain in a unilateralized amplifier, the over-all gain of these amplifiers can be estimated approximately from an amplifier with an ideal unilateral transistor. This ideal transistor has the same parameter values as the one used in the unilateralized amplifier except that $C_c \to 0$, $r_c \to \infty$ and there is no space-charge layer widening effect. Using the equivalent circuits in Figs. 1 and 5, the input impedances are as follows:

$$Z_{ie} = \frac{r_e}{1 + j\dfrac{f}{f\alpha}} + r_b'\left[1 - \frac{\alpha_0}{1 + j\dfrac{f}{f\alpha}}\right] \tag{6a}$$

$$Z_{ib} = r_b' + \frac{r_e}{1 - \alpha_0 + j\dfrac{f}{f\alpha}}, \tag{6b}$$

where the second subscript denotes the type of input connection. For the ideal transistor, the output admittance Y_2 is zero in each case. The transfer characteristics have been stated already, i.e., $A=\alpha$ and β, respectively. For a given load resistance, R_L, connected to the output terminals, the power gain of the two amplifiers is given by the following formulas:

$$G_e = \frac{R_L}{r_b'} \frac{1}{\left(\dfrac{r_e}{r_b'} + 1 - \alpha_0\right) + \left(\dfrac{f}{f\alpha}\right)^2} \tag{7a}$$

$$G_b = \frac{R_L}{r_b'} \frac{1}{(1-\alpha_0)\left(\dfrac{r_e}{r_b'} + 1 - \alpha_0\right) + \left(\dfrac{f}{f\alpha}\right)^2}. \tag{7b}$$

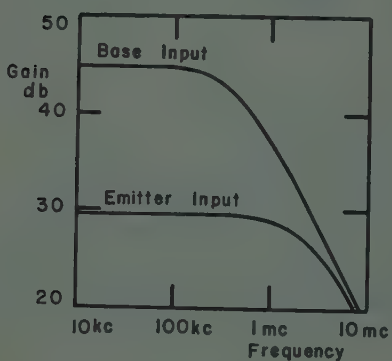

Fig. 10—Gain vs frequency characteristics of unilateralized amplifiers.

Eqs. (7a) and (7b) have been plotted in Fig. 10, using the following parameter values:

$R_L = 50K$ ohms

$r_b' = 100$ ohms

$\alpha_0 = 0.97$

$r_e = 50$ ohms (@ $I_e = 0.5$ ma)

$f_\alpha = 3.5$ mc.

These curves are similar to those illustrating the current amplification characteristics of a junction transistor, although the critical frequencies at which the gain starts to decay at the rate of 6 db per octave are slightly different. The actual gain of a unilateralized amplifier which uses a practical transistor will be a few db lower because of losses in the neutralizing network and the tuning coils. The actual gains measured in the above two single tuned 455kc IF amplifiers have checked calculated gains very closely, as shown in Table II.

TABLE II

Typical Performance of Single-Tuned Unilateralized 455 kc Amplifiers

	Emitter Input	Base Input
Impedance level of the tank circuit referred to the collector-ground terminals	100 K ohms	39 K ohms
Equivalent load resistance referred to collector-ground terminals	180 K ohms	68 K ohms
Input resistance, series equivalent		
Measured	62 ohms	
Calculated	58 ohms	
Input conductance, parallel equivalent		
Measured		770 μmhos
Calculated		720 μmhos
Net power gain,		
Measured	29 db	39 db
Calculated	30 db	39.5 db
Loss in coil and neutralizing network	3 db	2 db
Bandwidth, −3 db points,		
Measured	11 kc	13 kc
Calculated	10.8 kc	13.5 kc

Measured transistor parameters, at $V_c=6$, $I_e=0.5$ ma
$\alpha_0=0.98$ (h_{21}) $C_c=12$ $\mu\mu$f
$f\alpha=4$ m cps $r_c=2$ megohms
$r_b'=90$ ohms $\gamma=2\times10^{-4}$ (h_{12})

As the frequency is increased to and above the alpha cutoff frequency, the performance will deteriorate and become less predictable. This happens for two reasons:

1. The behavior of a practical transistor cannot be approximated accurately by a simple lumped constant equivalent circuit.

2. The loss involved in the neutralizing network becomes more and more appreciable.

Acknowledgment

The above work was done as a part of a development program of the Type 2N94 series transistors at Sylvania Electric Products, Inc. The author wishes to acknowledge the assistance of Miss D. McDonald in preparing this paper, and to thank B. H. Alexander, M. H. Dawson, and L. E. Dwork, for their constant interest.

Correspondence

"A Large-Signal Theory of Traveling-Wave Amplifiers"*

Tien, Walker, and Wolontis'[1] fine article on the large-signal theory of traveling-wave amplifiers is a distinct contribution to the traveling-wave tube field. However, certain limitations must be kept in mind if the results are to be used in designing and predicting the performance of large-signal traveling-wave amplifiers.

The theory as presented is certainly a large-signal theory, since nonlinear effects are considered and the output power reaches a saturation level, but it should be remembered that the Nordsieck equations on which it is based are not valid for C values larger than approximately 0.02. Hence, since efficiency is proportional to C $(\eta=2CA^2(y))$, the results do not extend to high-efficiency operation. For example, the efficiency reaches a maximum of 8 per cent in Fig. 7(a) and 12 per cent in Fig. 7(b), which is considerably lower than typical saturation efficiencies of already existing large-signal traveling-wave amplifiers. Also, the results cannot be applied to the many large-signal tube with gain parameters of 0.1 or higher.

It should also be noted that the computations so far carried out by the authors do not include the optimum relative injection velocity b for maximum saturation efficiency. The maximum efficiency of Fig. 7(a) (more correctly called the saturation efficiency) is obtained by adjusting the stream velocity to give maximum small-signal gain, but since the optimum value of b for maximum saturation efficiency is in general greater than the b for maximum small-signal gain, calculations in Fig. 7(a) do not apply to large-signal tubes operating at maximum power output.

The more general large-signal analysis of the traveling-wave amplifier considering space charge, loss along the helix, and large values of the gain parameter C (i.e., 0.1 and 0.2) is a longer and more difficult problem, but has been solved on the Michigan Digital Automatic Computer for some representative values of the traveling-wave amplifier parameters. It is expected that the results of this study will be published very soon.

J. E. Rowe
Elec. Engrg. Dept.
University of Michigan
Ann Arbor, Mich.

Rebuttal[2]

It is true that for large values of C, a large C theory should be used. However, the ratio of efficiency to C does not depart from small C value as rapidly as one might expect as C is increased. The large C results in Table I illustrate this.

These results are in every case computed for the value of b which gives maximum small-signal gain and for $d=0$ (a loss-free circuit). We used a set of equations different from those used by Poulter,[3] particularly in the methods of computing space charge and the effect of the backward wave. The numerical integration is again being carried out by Miss D. C. Leagus under the direction of Dr. V. M. Wolontis (using 701 type I.B.M. Equipment). It may be seen that the value of Eff/C at saturation decreases slowly with C up to $C=0.1$, particularly when QC is small. This agrees with extensive measurements made by C. C. Cutler[4] at low frequencies using a very accurately constructed 10-foot experimental tube. For practical purposes, we should estimate the saturation efficiency, by using values of Eff/C multiplied by *the actual C of the tube.* (The maximum efficiency of 8 per cent and of 12 per cent stated in Rowe's letter is computed using $C=.02$.) It should also be noted that in our computations, the electric field is assumed to be uniformly distributed over the cross section of the electron beam.

TABLE I

QC	C	k	Saturation Eff/C	Saturation Eff.
0.1	small C	2.5	3.39	
0.1	.1	2.5	3.04	30.4%
0.1	.2	2.5	2.08	41.6%
0.2	small C	2.5	3.72	
0.2	.05	2.5	3.36	16.8%
0.2	.1	2.5	2.93	29.3%
0.4	small C	2.5	3.50	
0.4	.05	2.5	3.18	15.9%
0.4	.1	2.5	2.50	25 %

With regard to the best value of b for high saturation efficiency, Fig. 7(b) of our paper shows the saturation Eff/C versus QC for different values of b. For example, for $QC=0.5$, cases were computed for $b=1.30$, 1.71 and 2.2. For $b=1.30$, the small-signal gain (μ_1 or Pierce's x_1) is maximum and for $b\geq 2.5$, μ_1 is zero. Obviously, since we assume an infinitesimal signal at the input end, the signal will not build up if $\mu_1=0$, so we do not make any computations for $b>2.5$. The picture obtained from small C computations is thus: Eff/C increases continuously with b up to a value such that μ_1 approaches zero. The efficiency then drops suddenly, simply because the small input signal does not build up properly.

P. K. Tien and L. R. Walker
Bell Telephone Labs., Inc.
Murray Hill, N. J.

* Received by the IRE March 22, 1955.

[1] P. K. Tien, L. R. Walker and V. M. Wolontis, "A Large Signal Theory of Traveling-Wave Amplifiers," Proc. IRE, vol. 43, pp. 260–277; March, 1955.

[2] Received by the IRE, April 13, 1955.

[3] H. C. Poulter, "Large Signal Theory of the Traveling Wave Tube," Tech. Rep. No. 73, Electronics Res. Lab., Stanford University, Stanford, Calif.

[4] Paper presented at the 12th Annual Conference on Electron Tube Research, at Orono, Maine, June, 1954.

The Practicality of E-Type Traveling-Wave Devices*

Beam-type amplifiers and oscillators such as the traveling-wave tube, backward-wave-tube, etc., can be separated into categories depending upon the way in which the electrons give up energy to the rf electromagnetic fields which in turn depends on the method of beam focusing employed. One of these categories is characterized by the fact that the electrons give up energy to the rf fields through loss of kinetic energy. The conventional traveling-wave tube presents an example of this mechanism at work. This class of amplifiers or oscillators has been termed "O"-type by French workers and is illustrated schematically in Fig. 1(a).

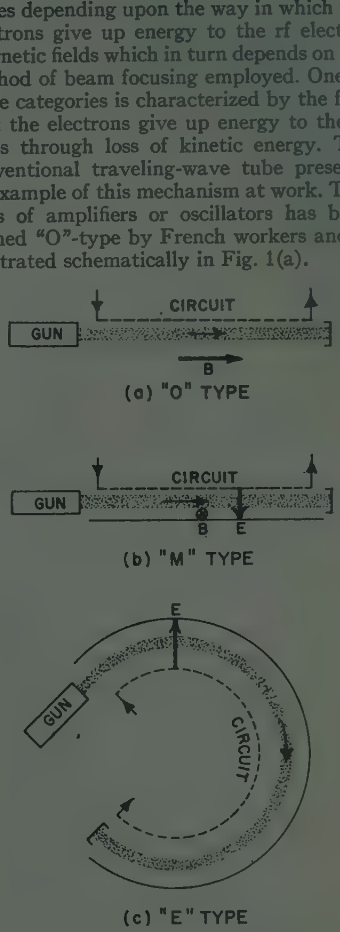

Fig. 1—Schematic representation of three forms of beam-type tubes. In the drawings the symbols E and B indicate static electric and magnetic fields respectively. the "M"-type (b) may also be formed into a circle but here centrifugal force is small compared with electric and magnetic forces.

A second group of beam-type tubes is categorized by the fact that the electrons give up energy to the rf fields not by losing kinetic energy but rather by losing potential energy. One example of this category of tubes is the linear magnetron amplifier. In it a beam of electrons is introduced at an appropriate velocity into a region of crossed electric and magnetic fields. The electrons then have kinetic energy by virtue of their velocity and potential energy by virtue of their positions in the crossed electric field. The closer they are to the positive circuit, the less potential energy they have. In order to keep the electrons on course, however, a transverse magnetic field must be applied to counteract the force of the crossed electric field on the electrons. Because of the presence of the counteracting magnetic field, this form of crossed field tube has been labeled "M"-type.

Electron tubes in which potential energy is lost to the rf fields possess a unique advantage over those in which the rf energy is augmented at the expense of kinetic energy —they are more efficient. The relatively

* Received by the IRE April 2, 1955.

lower efficiency of "O"-type tubes arises because electrons which have lost kinetic energy—or what is equivalent, velocity—drop behind in phase with respect to the traveling wave and eventually congregate in phases which allow them to begin to abstract energy from the rf fields. The amplifier or oscillator in which potential energy is lost can exhibit much greater efficiency since the electron velocity remains unchanged as energy is transferred to the rf fields. Only position is changed while synchronism is maintained. Efficiency then is determined primarily by how great a potential difference exists between the position of the beam at entrance and the circuit.

The "M"-type tube is not the only example of this second class of tubes in which positional or potential energy is utilized. There is a second type which uses the transverse electric field of the "M"-type tube to furnish the potential difference required but does not use the crossed magnetic field to counteract the static force on the electrons which this electric field engenders Instead the electrons are made to traverse a circular path, and the inward force due to the radial electric field is balanced in the static case by the centrifugal force experienced by the electron in its circular orbit. The electron can now give up a portion of its energy by moving to a circular path of somewhat smaller radius but maintaining the same angular velocity. In this way it loses potential energy rather than kinetic energy and by the above arguments should be capable of good efficiency. Versnel and Jonker have proposed this form of tube as a "magnetless magnetron" oscillator.[1] Because the transverse field is purely an electric field we have termed the traveling-wave form an "E"-type tube. Fig. 1(c) shows a diagram of this tube.

Further consideration of "E"-type amplifiers and oscillators indicates that a question arises as to the compatibility of the beam focusing requirements and the rf electrical requirements. In order to answer this question consider the relative "stiffness" of focusing obtained with the radial electric field and centrifugal force in the "E"-type as compared with that obtained with the magnetic and electric fields in the "O" and "M"-types. A measure of this is found by calculating the maximum radial or lateral excursion from the equilibrium trajectory produced by a given lateral or radial velocity. In the case of confined flow or Brillouin flow neglecting space charge as used in the "O"-type tubes the following relationship holds[2]

$$\frac{\Delta r}{v_r} \simeq \frac{1}{\omega_c} \tag{1}$$

where Δr is the maximum radial excursion in a round beam. ω_c is the cyclotron frequency $[\omega_c=(e/m)B]$, and v_r is the initial radial velocity. In the "M"-type, which normally employs a strip beam, we find[2]

$$\frac{\Delta y}{v_y} \simeq \frac{1}{\omega_c} \tag{2}$$

where Δy is the maximum lateral excursion and v_y is the initial lateral velocity. In the case of the "E"-type we have.[3]

$$\frac{\delta}{v_r} \simeq \frac{r_0}{\sqrt{2}v_0} \tag{3}$$

where δ is the maximum radial excursion, v_r is the initial radial velocity, v_0 is the velocity of the beam, and r_0 is the equilibrium radius for the velocity v_0.

Comparing (1), (2), and (3), it appears that in order to have a beam of comparable stiffness in the "E"-type with that normally employed in the "O" or "M"-type we must see that

$$\frac{r_0}{\sqrt{2}v_0} = \frac{1}{\omega_c}. \tag{4}$$

In order to see clearly the limitation imposed by (4) we need one additional relationship concerning the operating frequency of the traveling-wave tube. Either experience or an examination of existing tubes of the "O" and "M"-types tells us that tubes operating at a frequency ω usually employ a magnetic field such that $\omega_c \sim \omega$. In low power tubes, ω_c may be as small as one-fifth ω but not much less. The reasons for this lower limit on beam stiffness have to do with a requirement that the electrons stay within a certain proximity to the circuit measured in electronic wavelengths for useful interaction. If we require a comparable beam stiffness in the "E"-type traveling-wave tube we have,

$$\frac{1}{\omega} \sim \frac{r_0}{\sqrt{2}v_0}, \tag{5}$$

which can be rearranged to say

$$N = \frac{\omega}{v_0} r_0 \sim \sqrt{2} \tag{6}$$

where N is the number of electronic wavelengths along the circle of radius r_0. Eq. (6) says that for usual beam stiffness the total length of the path of the electrons cannot be greater than about $\sqrt{2}$ electronic wavelengths in the "E"-type. Actually, it will be less than this for $\omega=\omega_c$ because part of the path length must be reserved for gun and collector. Practical traveling-wave devices for the "O" and "M"-types are normally about eight to forty wavelengths long ($N=8$ to 40) since the traveling-wave principle requires the cumulative interaction between a beam and a wave over a number of rf cycles. Hence, we conclude that stiffness of focusing and rf interaction are somewhat incompatible in the "E"-type device.

A possible way around this difficulty is to allow the electron beam to go around more than once. If the beam in Fig. 1(c) is given a drift velocity into the paper, the beam will follow a spiral path and could interact with a wave traveling a spiral path. This idea is embodied in a tube invented by L. A. Harris[4] which employs a flattened helix wound again into a helix so as to produce a helically traveling wave. It has occurred to the writers that this complication may not be necessary where interaction with a backward wave is desired since the space harmonic waves on an ordinary single or bifilar helix travel in the spiral direction. This combination of a spiral traveling beam interacting with a spiral traveling backward wave appears to make possible an embodiment of the "E"-type tube having the conversion efficiency approaching that of the "M"-type but without the heavy magnet.

H. Heffner
D. A. Watkins
Stanford University
Stanford, California

[1] A. Versnel and J. L. H. Jonker, "A magnetless magnetron," *Philips Research Reports*, vol. 9, pp. 458–459; December, 1954.

[2] J. R. Pierce, "Theory and Design of Electron Beams," D. Van Nostrand Co., Inc., New York, N. Y.; 1949.

[3] W. W. Harman, "Fundamentals of Electronic Motion," McGraw-Hill Book Co., Inc., New York, N. Y., p. 44; 1953.

[4] W. E. Lear, "Analysis of the spiral beam traveling-wave magnetron," *Technical Report*, College of Engineering, U. of Florida, Gainesville, Fla.; November 1, 1954.

Audio Pentode vs Triode Harmonics*

In the old controversy in the audio field concerning the relative merits of the pentode vs the triode, one point seldom ever brought out is the particular type of harmonic content of these two classes of amplifiers. Old-timers in audio are well aware of the fact that to merely specify the total harmonic and intermodulation content of an audio unit is no guarantee of rating its relative subjective distortion effect. This is aside from more obtuse types of audio distortion such as transient, FM, spatial, frequency-shift, etc. The point is that higher-odd-order harmonics appear to irritate trained (well conditioned) ears more than do the even-order type, particularly where intermodulation is concerned. Hence if we say that a certain super-fidelity amplifier generates 0.001 per cent total harmonics at .15 kw at some particular video frequency, we may find that some other ultra-fidelity unit with an equally modest sine-wave performance index may sound a bit different from it under identical conditions, even though it may possess similar transient characteristics (equivalent phase bandwidth), and even though the listener might possess the auditory equipment of a bat.

Where a few tube harmonic content ratings are given in itemized detail (2nd, 3rd, 4th, 5th harmonics), it appears that the pentodes are blessed with more of the higher-odd-order type. This may be one reason why pentodes seem to please the well-known "golden ears" somewhat less than do the less ambitious triodes. If so, the answer may lie in an irritating higher-odd-order intermodulation content, or else in some metallurgical confusion (Sn instead of Au).

See Tungsol "Technical Data—Electron Tubes" sheets on the 2A3, 2A5, 6A3, 6L6, 6V6, 45 and 70L7 tubes and "RCA Tube Handbook HB-3" sheets on the 6AK6, 6L6, 43 and 70L7. Unfortunately, the smaller though interesting 5th harmonic is no longer shown on the newer curves, as in the past. Note the generally low 3rd (and presumably low 5th) harmonic content of the triodes. The question is, how well does inverse feedback handle this in the case of the high-impedance pentodes under transient and complex-wave conditions where the phase becomes something less than linear?

Hence the suggestion made here is that tube makers kindly supply us with detailed harmonic content curves for tubes more commonly used as audio amplifiers. They might turn out to be rather illuminating as well as acoustically disturbing.

Ted Powell
Great Neck, N. Y.

* Received by the IRE, February 25, 1955.

Measurement at 9,000 Mc of the Dielectric Constant of Air Containing Various Quantities of Water Vapor*

Many researchers[1–4] have measured the dielectric constant of dry air and of water vapor at microwave frequencies. To verify Strichland's[5] empirical formula, the author measured the dielectric constant of air containing various quantities of water vapor by a new method at 9,000 mc. He obtained a modified empirical formula coinciding more exactly with the measured values than the formula referred to.

The author applied his formula to development of an industrial method for determination of humidity content of almost dry air.

The klystron oscillator is doubly modulated by superposing the output of a variable intermediate frequency oscillator (8∼12 mc) on the saw-tooth wave derived from the oscilloscope sweep. The signal from the klystron is divided into two parts by an *H*-plane Tee junction; one part is fed to a measuring cavity, the other to a standard cavity. The detected outputs of these cavities are differentially mixed, amplified and then displayed on the oscilloscope. When the resonant frequencies of the two cavities coincide exactly with each other at f_0 the well-known, typical curve shown in Fig. 1 (a) appears on the oscilloscope screen without modulation by the intermediate frequency.

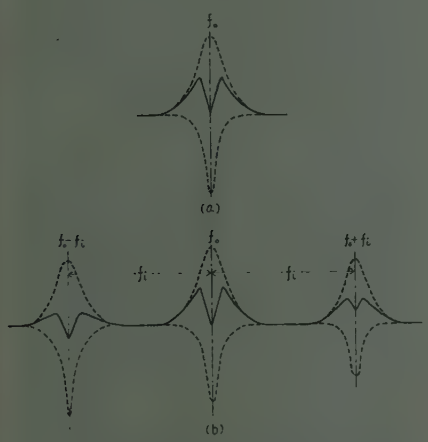

Fig. 1—Differential figures of two resonance curves. (a) Single Modulation. (b) Double Modulations.

Since the output of the klystron involves the sideband frequency components corresponding to the impressed intermediate frequency f_i, the curve shown in Fig. 1 (b) appears on the oscilloscope when IF modulation is present. Here, the upper and lower dotted lines are the resonance curves of the standard and the measuring cavities, respectively; the solid line represents the differential signal corresponding to these two curves. If the resonant frequencies of the standard and measuring cavities are f_0 and f_0-f_i, respectively, a differential curve similar to that shown in Fig. 1 (a) is obtained as shown in the middle of Fig. 1 (b). This is so because the side band $(f_0-f_i)+f_i$ of the measuring cavity frequency coincides with the standard cavity frequency.

When one lets the resonant frequencies of the measuring cavity containing air and vacuum be f_0-f_{i1}, and f_0-f_{i2}, respectively, it follows that the dielectric constant of the air can be calculated from

$$\epsilon - 1 = 2\frac{f_{i1}-f_{i2}}{f_0-f_{i2}}, \qquad (1)$$

where f_0 is the standard cavity frequency. The frequencies f_{i1}, and f_{i2} can be determined exactly from the readings of the variable precision condenser of the IF oscillator. (The condenser scale is divided into 2,500 parts.) These frequencies, in turn, yield the differential curve on the oscilloscope trace, as shown in the middle of Fig. 1 (b). The variable IF oscillator is of the stabilized Clapp type, whose frequency is calibrated with a crystal oscillator. Its short time stability has been verified to be within 10^{-4}. Taking account of the error in reading the oscilloscope trace, the accuracy of the measurement of the dielectric constant of air is considered to be within 4×10^{-7}.

Cylindrical standard and measuring cavities oscillate in TE_{012} mode. Each cavity is enclosed by an evacuation chamber and attached to the chamber at one point to avoid any mechanical distortion which might be caused by evacuation. Since endplates of the two evacuation chambers are in mechanical contact with each other, and the cavities are made of super invar, drift in the difference between the two cavity frequencies (caused by variation in room temperature), could be kept below 1 kc degrees C.

The dry air sample is obtained by passing air through three bottles of 100 per cent H_2SO_4 and through three tubes of P_2O_5.

Air of various humidities is obtained by allowing air to pass slowly through three bottles of H_2SO_4 solution of various percentages. Saturated vapor pressures of solution are determined from the International Chemical Table; 50, 58 and 68 per cent H_2SO_4 solution were used here. Similarly, saturated wet air can be obtained by allowing air to pass through three bottles of water. Pressure in the standard cavity is kept below 10^{-3} mm Hg during experiment.

The dielectric constant of dry air was measured at 9,080 mc in the temperature range from 5 to 20 degrees C. and in the pressure range from 10 to 760 mm Hg. From these measured values, the dielectric constant of dry air at standard conditions (0 degrees C., 760 mm Hg) was determined to be 1.000574 (±0.0000025).

The results obtained in the measurements of air of various humidities at 9,080 mc are plotted in Fig. 2, where the ordinate indicates the difference between the resonant frequencies with and without the air sample, and where the abscissa gives the partial pressure of the water vapor in mm Hg. In this figure, the small circles indicate the measured values and the straight lines are calculated from the following modified formula:

$$\epsilon - 1 = 2.06\times10^{-6}\frac{P_a}{T} + 180 \times 10^{-6}\left(1+\frac{5580}{T}\right)\frac{P_w}{T}. \qquad (2)$$

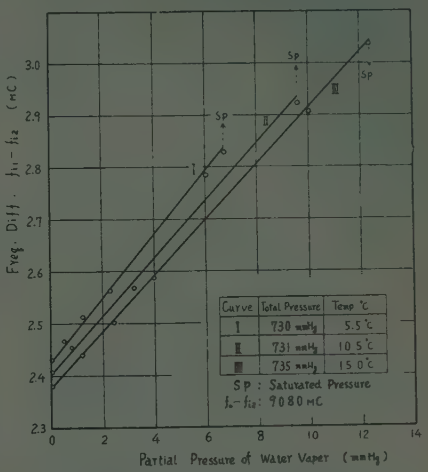

Fig. 2—Relation between frequency difference $f_{i1}-f_{i2}$ and water vapor pressure of the air.

Here, T is the absolute temperature, P_a is the partial pressure of dry air in mm Hg, and P_w is the partial pressure of water vapor in mm Hg. The maximum deviation of the measured from the calculated values is 15 kc. This corresponds to 3×10^{-6} in ϵ, and is considered to be caused mainly by the unreliable values of water vapor pressure. The modified formula given above is slightly different from that given by Strichland, who takes the first term as 2.10×10^{-6} (Pa/T).

On applying this method to industrial measurements, long-time stability is considered to be an important factor. A record of the stability of this equipment over several hours is shown in Fig. 3. In obtaining these

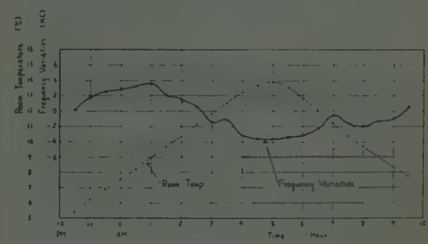

Fig. 3—Long-time stability of this equipment.

data, not only the standard cavity, but also the measuring cavity were evacuated to investigate the drift caused by any possible changes in the measuring equipment. From this and other data obtained by continuous measurements extending over several days, it was found that the stability may be considered to be within 5 kc in the measurement of frequency difference, i.e., within 1×10^{-6} in measurement of the dielectric constant.

The author is now measuring the humidity of air in the process of drying employed in the manufacture of paper cables by means of this measuring method.

Shigefumi Saito
University of Tokyo
Chiba-City, Japan

* Received by the IRE, April 2, 1955.

1 G. Birnbaum, S. J. Kryder, and H. Lyons, "Microwave measurements of the dielectric properties of gases," *Jour. Appl. Phys.*, vol. 22, pp. 95–102; January, 1951.

2 C. M. Zieman, "Dielectric constants of various gases at 9,470 mc," *Jour. Appl. Phys.*, vol. 23, p. 154; January, 1952.

3 G. Birnbaum and S. K. Chatterjie, "The dielectric constant of water vapor in the microwave region," *Jour. Appl. Phys.*, vol. 23, pp. 220–223; Feb., 1952.

4 L. Essen, "A highly stable microwave oscillator and its application to the measurement of the spatial variations of refractive index in the atmosphere," *Proc. IEE*, part III, vol. 100, pp. 19–24; Jan., 1953.

5 A. C. Strichland, "Technique of Microwave Measurement," McGraw-Hill Book Co., Inc., New York, N. Y.; 1947.

Parabolic Transmission Line*

Scott[1] has proposed to use hyperbolic transmission line as a matching section (Fig. 1), which is relatively less frequency sensitive than any other known nonuniform lines. He assumed that the characteristic impedance of the matching section, $Z_0(x)$ is a hyperbolic function of x and calculated the reflection coefficient from

$$\rho = \int_0^l \tfrac{1}{2}[\ln Z_0(x)]' e^{-i2\beta x}dx. \qquad (1)$$

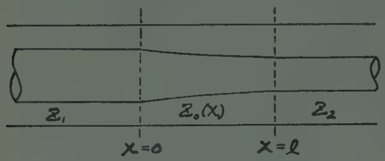

Fig. 1—Matching section between impedances Z_1 and Z_2.

He also gave several numerical examples comparing hyperbolic line with exponential and Bessel lines for the case where $Z_1=50$ ohms and $Z_2=150$ ohms.

Here we propose another line which seems to be better than hyperbolic line (see Fig. 2). Let us assume

$$Z_0(x) = a_0 + a_1x + a_2x^2 + a_3x^3.$$

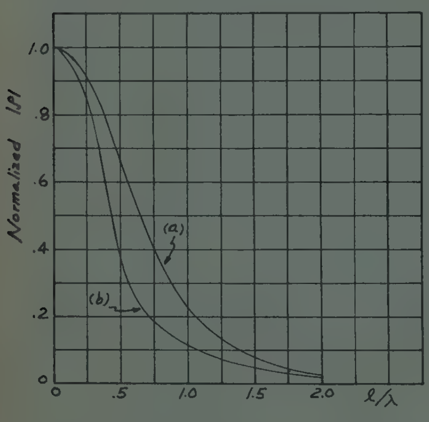

Fig. 2—Amplitude variation of reflection coefficient with l/λ for (a) hyperbolic line section, and (b) parabolic line section, between 50 and 150 ohms.

The a's may be chosen by letting $Z_0(0)=Z_1$, $Z_0(l)=Z_2$ and $Z_0'(0)=Z_0'(l)=0$, where the prime denotes the derivative with respect to x. Thus we have

$$Z_0(\bar{x})=Z_1+3(Z_2-Z_1)\bar{x}^2-2(Z_2-Z_1)\bar{x}^3, \qquad (2)$$

where $\bar{x}=x/l$; a higher parabolic equation. Thus the line may be called parabolic transmission line. Substituting (2) into (1),

$$\rho = \int_0^1 R(\bar{x})e^{-i4\pi\bar{x}l/\lambda}d\bar{x}, \qquad (3)$$

where

$$R(\bar{x}) = 3\bar{x}(1-\bar{x})\Big/\left[\frac{Z_1}{Z_2-Z_1}+3\bar{x}^2-2\bar{x}^3\right].$$

This expression cannot be readily integrated. However numerical result may be obtained by graphical integration. In order to compare the parabolic line with Scott's hyperbolic line, we assume the same case $Z_1=50$ ohms and $Z_2=150$ ohms. The result of the parabolic line is plotted as curve (b) in Fig. (2). Curve (a) is that of the hyperbolic line.

It is noted that $|\rho|$ is normalized by $\frac{1}{2}\ln(Z_2/Z_1)$ which is the value of expression (1) when $l\to 0$. The small difference between $\frac{1}{2}\ln(Z_2/Z_1)$ and the actual value of the reflection coefficient $(Z_2-Z_1)/(Z_2+Z_1)$ when $l\to 0$, is due to the assumption $\rho^2 \ll 1$ and $1-\rho^2 \cong 1$ in the derivation[1] of expression (1).

R. F. H. Yang
Andrew Corporation
Chicago, Ill.

* Received by the IRE, May 16, 1955.

[1] H. J. Scott, "The hyperbolic transmission line as a matching section," Proc. IRE, vol. 41, pp. 1654–1657; November, 1953.

"Fabrication of Airborne Electronic Equipment"*

R. K-F Scal[1] and the National Bureau of Standards are to be complimented for their efforts and accomplishments in creating a unit of airborne electronic equipment that not only meets the environmental requirements of existing specifications, but provides some margin in its high temperature capabilities. Such a margin is essential for any current design, since current specification conditions (55 to 71 degrees C. at sea level) are inadequate for today's high performance aircraft. However, it would appear that more margin could have been designed into the unit with very little extra effort.

Unfortunately, the paper does not give enough specific data about power losses, airflow vs air temperature and pressure-drop requirements, and temperature-altitude characteristics, to permit evaluating the improvement in cooling performance as compared to more conventional or other novel designs. For instance, a curve of required airflow vs air inlet temperature would be much more informative than the single point given (5 lb/min at 100 degrees C.).

The design of the cooling plates indicates that careful attention was given to securing good heat transfer in them, but it appears that this concept was not carried through into the detail component installations. For instance, the use of connection plates mounted on the cooling plates seems to introduce an unnecessary thermal resistance between the heat producing components and the cooling plates. Similarly, no specific provisions seem to have been made for a good heat flow path from the liquid potted tubes to the cooling plates. Finally, the sentence—"A small blower is mounted upon the rf unit to prevent hot air (which would act as thermal insulation) stagnating about the klystron and magnetron"—demonstrates inadequate application of the principles of heat transfer that were used in the cooling-plate arrangement. Blowers should be used, when necessary, to secure specific velocities over specific surfaces, to remove known amounts of heat from those surfaces at a given temperature level, and to transfer that heat in a controlled fashion to some other area. Random circulation of air is too inefficient for use in airborne units; it is even possible that careful consideration of the temperature and heat flow conditions would permit a design without a fan.

The article indicates a significant advance over most current designs in the use of high temperature components, which reduces the required cooling flow, since there is more temperature potential between the components and the coolant. Also mentioned is the very important point that the term "ambient" has very little significance inside an assembly, and that actual component temperatures must be considered. Despite this, references are made to heat producing components as suitable for operation in certain "ambient" temperatures.

If the concepts of controlling component temperatures (instead of ambients), and of heat flow from the components to the cooling plates had been carried through, the required cooling flow might have been reduced by 20 to 40 per cent.

L. J. Lyons
Consulting Engineer
Los Angeles, Calif.

* Received by the IRE, April 14, 1955.

[1] "New techniques for fabrication of airborne electronic equipment," Proc. IRE, vol. 43, pp. 4–11; January, 1955.

Rebuttal[2]

I would like to take up the remarks made by Mr. Lyons, in order, and clarify them as follows:

1. More margin could have been designed into the unit with very little extra effort! While this observation may contain some truth. I am sure that every engineer who has the satisfaction of completing a successful project, nevertheless, always finds some dissatisfaction in the fact that a well-executed project always turns up points where a great deal of additional results could be obtained with little extra effort. Unfortunately, hindsight seems to be better than foresight, and there comes a time when a project must be completed. Some of our engineers worked sixty hours a week on the project; the "little extra effort" just was not available!

2. Unfortunately, the paper does not give enough specific data on various thermal aspects. It should be noted that Mr. Lyons' remarks concern only thermal matters, and it is probable that the circuitry engineer also feels there is not sufficient specific data on circuitry, while the component engineer feels that there is not sufficient specific data included on components. Unfortunately, when an author presents a general article, he is likely to be criticized by the specialist for not having devoted the article to his specialty. On this point it should be obvious (from Mr. Lyons' complimentary remarks on the design of the cooling system) that he realizes that the data is in existence; in fact, it would make a very interesting article on this special subject. However, it is not available for publication due to security considerations.

3. It is very true that a great deal more work could have been and can be done in bringing about more efficient thermal transfer from components to the cooling plates. However, here again one must consider the matter of available time and funds for such a project. It is also of interest that the specific problem of the electronic-connecting plates being mounted on the cooling plates was very carefully studied and this construction was selected as the best compromise between various thermal, electrical, and equipment problems. After all, one must keep in mind that the best thermal design

[2] Received by the IRE, May 2, 1955.

does not necessarily yield the best possible electronic equipment. Similarly, the matter of a good heat-flow pattern from the liquid-potted tubes to the cooling plates, and of the blower, are again results of compromises between thermal and electronic design as well as of time considerations. Let it here be noted that the solutions to the various problems, selected as the best compromise for the over-all equipment, resulted in the desired over-all operation.

4. References to heat-producing components being suitable for operation in certain ambient temperatures. In his previous sentence, Mr. Lyons had stated my reply to his own question (that I, as author, do not consider the terminology as proper), but I might also add that the description of components being useful in certain ambient temperatures is a carry-over of the manufacturer's own description of their products.

Finally, it is probably quite true that, if all the information learned in the end of the project could have been applied at the beginning, the required cooling flow might have been reduced by 20 to 40 per cent. It is also quite possible that had we neglected the electronic operation of the equipment and concentrated on thermal problems all through the project, this same result might have been achieved. Mr. Lyons' letter brings to light the difficulty in compromising mechanical, thermal, and electronic problems. Since we have had about the same sort of remarks from electronic engineers concerned only with circuitry, mechanical engineers concerned only with production of the equipment, and heat transfer engineers concerned only with cooling of the equipment, we conclude an excellent job has been done in pursuing a balanced program to its logical conclusion (i.e., the prototype production of an advanced operational radar set). As is the case in any project, complete final reports were prepared upon completion of the project, and the reports outline the shortcomings noted in the equipment, plus recommendation for further work to be done. But, of course, this detailed design information is classified, and could not be included in the article. However, because a technical article describes work done, these recommendations also should *not* have been included, in any case.

R. K-F Scal
RS Electronics Corp.
Palo Alto, Calif.

Nonlinearity of Propagation in Ferrite Media*

Kittel,[1] Polder[2] and others have developed a theory dealing with the propagation of electromagnetic waves in a magnetized ferrite medium. According to this theory, the propagation will be linear with respect to the rf field strength only if a number of restrictive conditions are fulfilled. One of the limitations is that the rf magnetic field should be small compared to the static magnetizing field. This condition will clearly be violated if the peak power is sufficiently high. Many who are interested in applications of microwave ferrite devices have felt that the nonlinearity is not a significant problem at power levels normally encountered in radar applications. However, experiments conducted at the Naval Research Laboratory, indicate that nonlinear characteristics may appear at relatively low power levels.

The subject of nonlinearity has been treated both theoretically and experimentally in papers by Damon,[3] and Bloembergen and Wang.[4] Insofar as nonlinearity is concerned, the emphasis in these articles is in the region of gyromagnetic resonance. Although some ferrite devices make use of gyromagnetic resonance, there are many other applications where the static magnetizing field is very small compared to that required for resonance. It is not evident that the results obtained in the articles cited can be applied to determine the nonlinear characteristics in a ferrite loaded waveguide far from resonance. In tests conducted by the authors it was found that the ratio of absorbed power[5] to the input power *increased* with the input power level. This may be compared with the ratio of the power absorbed to the magnetic energy density in the cavity measurements of Damon, and Bloembergen and Wang. The results of these cavity studies indicate a *decrease* in the ratio of absorbed power to magnetic energy density, as the magnetic energy density is increased.

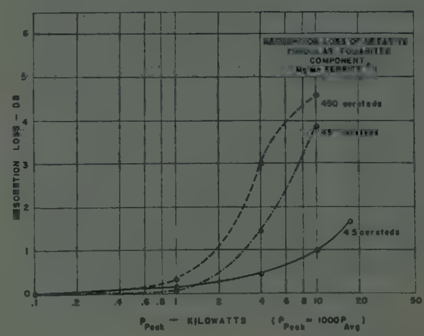

Fig. 1—Power absorbed from a negative circularly polarized wave by a ferrite cylinder (¼ inch diameter ×2 inches length) versus the peak power, the applied longitudinal magnetostatic field as a parameter.

Some of the results, which were obtained at a frequency of 9,375 mc, are shown in Figs. 1–3. In considering the results, it should be kept in mind that the factor which determines the appearance of nonlinear effects is not simply the level of transmitted power, but rather the rf field in the ferrite itself. The data shown were obtained for a round waveguide which contained a longitudinally magnetized ferrite cylinder along its axis. For this configuration, the rf field inside the ferrite cylinder will depend on the diameter of the cylinder and the material constants of the ferrite. Thus, if circularly polarized waves of opposite sense pass through a ferrite section, the effective permeability of the ferrite will be different for the two senses of polarization. This difference in permeability gives rise to a difference in the rf field strength for the two cases. It is clear from the curves shown that the nonlinear effects do indeed depend on the diameter of the ferrite cylinder and the sense of circular polarization.

An interesting feature of the measurements is that even though the percentage of power absorbed depended on the power level, the Faraday rotation remained essentially constant.

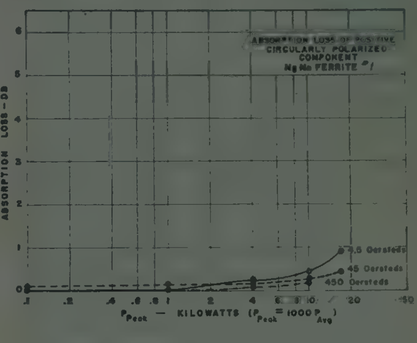

Fig. 2—Power absorbed from a positive circularly polarized wave by a ferrite cylinder (¼ inch diameter ×2 inches length) versus the peak power, the applied longitudinal magnetostatic field as a parameter.

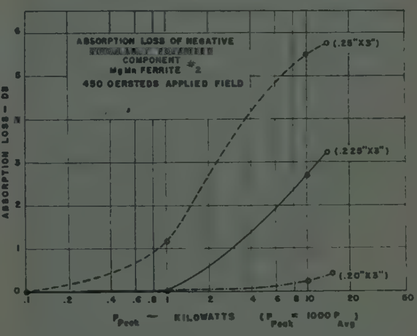

Fig. 3—Power absorbed from a negative circularly polarized wave by a ferrite cylinder versus the diameter of the cylinder as a parameter.

Since the propagation characteristics of a ferrite medium are also temperature sensitive, care had to be taken to insure that the observed variation of attenuation with power level was not due to a rise in temperature of the ferrite. This was checked in a number of ways. One of these is of some interest. It is known that if at a given power level the temperature only is varied, both the attenuation and rotation will vary. Since, in these measurements the rotation did not vary with power level, this corroborates the view that the change in attenuation is due to the increase in power level, rather than an increase in temperature.

These results show that in designing ferrite microwave devices for use at high peak power levels, the nonlinear effects must be taken into account. The possibility of applications which make use of nonlinear devices is being investigated.

N. G. Sakiotis, H. N. Chait, and M. L. Kales
Microwave Antennas and Components Branch
Naval Research Lab., Washington 25, D.C.

* Received by the IRE, March 23, 1955; revised manuscript received, May 11, 1955.

[1] C. Kittel, *Phys. Rev.*, "On the theory of ferromagnetic resonance absorption," 1947 and vol. 73, p. 155; January, 1948.

[2] D. Polder, "On the theory of ferromagnetic resonance," *Phil. Mag.*, vol. 40, p. 99; January, 1949.

[3] R. W. Damon, "Relaxation effects in the ferromagnetic resonance," *Rev. Mod. Phys.*, vol. 25, p. 239; January, 1953.

[4] N. Bloembergen and S. Wang, "Relaxation effects in fera- and feromagnetic resonance," *Phys. Rev.*, vol. 93, p. 72; January, 1954.

[5] Absorbed power = input power − output power − reflected power.

Observation of Electroluminescence Excited by Dc Fields in Cathode-Ray Tubes*

During tests on aluminized cathode-ray tubes with high voltage on the aluminum and a grounded electrode touching the face plate of the tube, light was observed to come from the phosphor screen in the region near this electrode. This occurred only when the face plate was hot and was present when the electron gun was not operating. An improved result, with uniform light emission, was obtained by making contact to the outside of the tube face with a transparent conductive coating on a piece of glass and by uniformly heating the glass and tube face with a controlled stream of hot air.

Under these conditions, the following characteristics of operation were observed.

1. Under the microscope the particles emitted light intermittently, giving a scintillating appearance.
2. In some tubes, the light output was greater with the aluminum at a negative potential, but in other cases it was greater with the aluminum positive. Similarly, electrode polarity affected the number of particles emitting light and the rate of scintillation of individual particles.
3. Practically all the common phosphors luminesced to a greater or less extent.
4. Similar results could be obtained with the same aluminized phosphors when the cathode-ray tube vacuum was destroyed and pressure raised to atmospheric.

A sample operating at atmospheric pressure was made as follows. A willemite phosphor screen was set on a thin 0.007-inch piece of glass having a transparent conductive coating on the opposite side. The phosphor was then aluminized by conventional methods and a dc voltage applied between the aluminum coating and the transparent coating. When heated with a hot air blast, application of 2,000 volts dc caused a current of 700 ma to flow through an area of 2 cm,[2] giving a luminance of 1.5-foot lamberts.

Very briefly the dc electroluminescence action would seem to be one in which high fields are produced across the individual particles sufficient to cause luminescence,[1-3] but by means of the resistive layer adjacent to the particles, each particle is prevented from reaching destructive breakdown by the current limiting effect of the series resistance. This protective action is somewhat analogous to the behavior of the plastic binder in conventional ac electroluminescence where each individual particle is protected by the high impedance of the surrounding dielectric material.

F. H. NICOLL and B. KAZAN
RCA Labs., Radio Corporation of America
Princeton, N. J.

* Received by the IRE, April 6, 1955.

[1] K. W. Boer and U. Kummel, "Luminesence of single crystals of CdS in strong dc fields," *Z. Physik. Chem.*, vol. 200, pp. 193–198; September, 1952.

[2] R. W. Smith, "Radiation from CdS crystals generated by dc electric fields," *Phys. Rev.*, vol. 93, p. 347; January, 1954.

[3] P. Zalm, G. Diemer and H. A. Klasens, "Electroluminescent ZnS phosphors," *Philips Res. Rep.*, vol. 9, pp. 81–108; April, 1954.

"Further Analysis of Transmission-Line Directional Couplers"*

I feel that this work[1] represents a very useful extension of the conditions for obtaining infinite directivity for mismatched transmission lines; the extension being for the heavy coupling case.

However, in order to fully appreciate how this additional work fits into the overall pattern of my work[2] and what its ramifications might be, I would like to make the following comments.

First, it is an easy matter to justify Mr. Knechtli's derivations on a physical basis. This is so because it is clear that transmission lines in close proximity (i.e. heavy coupling) will affect the impedance of both of the transmission lines because of the added mutual loading effects. Hence, for the heavy coupling case it would be expected that additional corrective terms involving the coefficient of coupling between the lines should appear. Concerning this point, I would like to point out that if one only knew that for the light coupling case the normalized impedance product was equal to unity, he would well be able to achieve infinite directivity in the laboratory even for heavy coupling. This is possible because if one realizes that to get infinite directivity with mismatched transmission lines, it is an easy matter to "tune" the load of the secondary line to compensate for any mismatch even though the mismatch might come from the proximity of the primary line. If the lines are heavily coupled, one would then find that for infinite directivity the normalized impedance product would deviate somewhat from unity. I do not wish to undervalue Mr. Knechtli's contribution, but merely to point out that once one appreciates mismatched lines can be made to achieve infinite directivity, the additional mismatch due to the proximity effects would normally be expected to be tuned out.

Next, I would like to point out that the scattering matrix which I have derived[3] and listed below, is in no way changed by the generalization of the mismatch conditions.

$$s = \left[\begin{array}{cc:cc} \bar{\gamma} & j\beta_3 & 0 & j\beta_2 \\ j\beta_3 & \bar{\gamma}^* & j\beta_2 & 0 \\ \hdashline 0 & j\beta_2 & \bar{\gamma} & -j\beta_3 \\ j\beta_2 & 0 & -j\beta_3 & \bar{\gamma}^* \end{array}\right].$$

The derivation of this matrix would be identical even if one assumed the heavy coupling conditions. All that is necessary is that conditions B and C of (35) of my paper merely are replaced by Mr. Knechtli's more general equations given by his (8a) and (8b). This substitution should thus extend the general scattering matrix which I derived, to the heavy loaded case.

A third point worth mentioning in order to avoid any possible confusion, is that the analysis for the lumped circuit coupler which I have made is general and includes the heavy coupling case. This is because for the lumped circuit coupler, network theory was used and any degree of mutual coupling is handled thereby, although admittedly the basic concepts in the lumped coupler were conceived from the transmission line analysis. I might point out along this line that in the laboratory couplings as high as −1 db were achieved while maintaining good agreement with the theoretical calculations.[4]

Lastly, I would like to mention an interesting application, particularly for the light coupling case, is that of measuring the impedances of transmission lines. For example, if one either knows the characteristic impedance of the primary transmission line or determines it by proper matching, then by coupling a secondary line to this network it is possible to measure the impedance of the secondary line. For the light coupling case, all that is required is to tune the termination of line 1 (Z_{L2}) and the termination at terminal 3 (Z_{L3}), such that infinite directivity occurs, by measuring. Since $Z_{L2}Z_{L3}$ is equal to the product of the characteristic impedances of the two lines, it is possible to solve for the unknown characteristic impedance. This relation is another way of expressing:

$$Z_{22}Z_{33} = 1$$

namely:

$$Z_{L2}Z_{L3} = Z_{01}Z_{03}.$$

While the same method is applicable for heavily-coupled transmission lines, (8a) and (8b) of Mr. Knechtli's paper would be required for the exact solution and, for this case, since the coupling coefficient is not negligible, more information is obviously needed to accurately determine the impedance of the secondary line.

W. L. FIRESTONE
Motorola, Inc.
Chicago, Ill.

* Received by the IRE, May 16, 1955.

[1] R. C. Knechtli, PROC. IRE, vol. 43, pp. 867–869; July, 1955.

[2] W. L. Firestone, "Analysis of transmission-line directional couplers," vol. 42, pp. 1529–1538; October, 1955.

[3] *Ibid.*, eq. (44).

Rebuttal[5]

I completely agree with you about the physical significance of infinite directivity with strong coupling, about the general scattering matrix which you discussed, and about the validity of your analysis of lumped circuit couplers in the case of strong coupling. I should be very glad if you publish these comments, as they certainly clarify both our papers.

R. G. KNECHTLI
RCA Laboratories
Princeton, N. J.

[5] Received by the IRE, May 16, 1955.

Frequency Stable *LC* Oscillators*

In a recent paper by Clapp,[1] an argument leading to equation (40) suggests that the frequency change due to harmonic intermodulation is reduced if the L/C ratio of the resonator is increased. Substantially the same argument and conclusion appear in an earlier paper by Gouriet,[2] and since both authors appear to have misinterpreted Llewellyn,[3] comment seems justified.

The change of phase of the effective generator is the thing that matters, not the change of phase of the generator in series with the reactances used as mutuals to grid and anode circuits.

Assume that harmonic intermodulation produces a fundamental quadrature component i_2 so that the phase of the anode current is

$$\phi = \tan^{-1} i_2/i_1.$$

* Received by the IRE, February 28, 1955.

[1] J. K. Clapp, "Frequency stable *LC* oscillators," PROC. IRE, vol. 42, p. 1295; August, 1954.

[2] G. G. Gouriet, "High stability oscillator," *Wireless Eng.*, vol. XXVII, p. 105; April, 1950.

[3] F. W. Llewellyn, "Constant frequency oscilla-

Then, assuming that the Q of the tank circuit is reasonably high, and that equal capacitances C are used for grid and anode mutuals, the generated emf's will be

$$i_1/\omega C = IR \text{ in phase}$$

$$i_2/\omega C = I\Delta X \text{ in quadrature,}$$

where R is tank circuit resistance, I is tank current, and ΔX is a reactance "injected" into the tank circuit. Then

$$i_2/i_1 = \Delta X/R = \tan\phi$$

but

$$Q = \frac{\omega L}{R}$$

$$\therefore \quad \frac{\Delta X}{\omega L} = \tan\phi/Q$$

and

$$\frac{\Delta\omega}{\omega} = \tan\phi/2Q$$

that is to say, the fractional frequency change is independent of the L/C ratio.

NORMAN LEA
Res. Div., Marconi's Wireless Telegraph Company Ltd.,
Chelmsford, England.

Rebuttal[4]

J. K. Clapp, in his rebuttal, has conceded that the part of his paper with which I took issue is in error. We are, therefore, in agreement in principle and all that remains is to clear up some of the questions that Clapp has raised in his rebuttal.

First is the question of the circuit of Fig. 4. This is a very unsatisfactory equivalent circuit for the problem at hand. Since $Rg = -R_s$ there is no net resistance in the circuit. This results in an infinite Q and a discontinuous $df/d\phi$.

Clapp states that he is referring only to resonant operation. None the less he attempts to derive the quantity $df/d\phi$ for the circuit in Fig. 4. This quantity is the ratio of the displacement of the operating frequency from the resonant frequency to the amount of phase shift necessary to cause this displacement. Once the operating frequency is displaced from the resonant frequency, even by a differential amount, you no longer have resonant operation.

Clapp also states that he based his entire development on the circuit with the load connected. Eqs. (30) and (31) are based only on part of the circuit, Cg and Rg Eqs. (30) and (31) have no real meaning and since they were not derived from the entire circuit, (31) cannot be combined with (39), which was derived from the entire circuit.

It can be seen from the above that the basic error in the development from (30) to (40) was the mathematical combination of (31) which relates to only a portion of the circuit with (39) which was derived from the entire circuit. It was, of course, necessary to do this to derive $df/d\phi$ since as stated above $df/d\phi$ for the entire circuit of Fig. 4 is a discontinuous function.

It would have been much more satisfactory to have taken an equivalent circuit which separated the physical resistances and reactances of the circuit from the electronic resistances and reactances of the tube. Under these circumstances, which are representative of the actual operation of an oscillator, we may easily have the oscillator operating at a frequency other than that of the physical constants of the circuit.

I readily admit that the high-C Colpitts requires impractical circuit values for many cases. However, once we concede that even in the presence of distortion, stability at a given frequency does not depend upon the LC ratio, we see that we may avail ourselves of circuits such as those shown in Figs. 2 and 3. I do not consider these to be series-tuned circuits and according to statements previously attributed to Clapp,[5] he did not consider them to be series-tuned circuits. Lampkin[6] pointed out the advantages of tapping the tube across only a portion of the oscillator circuit many years ago and it is good engineering to do this when it is practicable but tapping the capacitive leg of the resonator circuit does not automatically make the oscillator a series-tuned oscillator.

My experiments consisted of comparative tests between two oscillators, at 2 mc, one of which is similar to the one shown in Fig. 1 and the other similar to the one shown in Fig. 2. The series-tuned oscillator requires an inductor approximately 20 times greater in inductance than the inductor required for the higher-C oscillator. According to (40) the high-L oscillator should have been very much more stable than the low-L oscillator. No appreciable difference between the oscillators could be found in runs of frequency deviation *vs* Eb, frequency deviation *vs* Ef, and frequency deviation *vs* time with all other conditions fixed. The Q's and impedances of the oscillator circuits were measured with an instrument of my own devising.[7]

Reference 1 is not available to me but the improvement in stability of 10 to 100 times mentioned in reference 4 was based upon the theoretical development which Clapp has conceded was in error.

I hope that the above remarks have clarified the situation so that we may have complete agreement on the stability of oscillators.

W. B. BERNARD
Commander, USN
4420 Narragansett Ave.,
San Diego 7, Calif.

[4] Received by the IRE, March 17, 1955.

[5] *QST*, p. 45; October, 1948.

[6] G. F. Lampkin, "An improvement in constant-frequency oscillators," PROC. IRE, vol. 27, pp. 199–201; March, 1939.

[7] W. B. Bernard, "Admittance analyzer," *Electronics*, vol. 28, pp. 107–109; August, 1950.

Surrebuttal[8]

The author is greatly indebted to Lea for so clearly pointing out the error in the original analysis of oscillator stability, with respect to phase shift resulting from harmonic intermodulation, as well as giving the correct analysis. Although W. B. Bernard questioned the correctness of the author's analysis, it was not clear where the basic error occurred.

All parties to this discussion are now agreed that the oscillator stability depends only upon the Q of the circuit and the magnitude of the impedances presented to the tube, not only with respect to variations in tube parameters, but with respect to the effects of harmonic intermodulation as well.

Commander Bernard has disregarded the comments of the first paragraph of my reply.[9] If $-Rg$, of Fig. 4, is removed, and a voltage e is inserted between the terminals, it is obvious that the circuit resistance is R_s and not zero; that the current is finite and not infinite; that Q is finite and not infinite, and that $df/d\phi$ is continuous and not discontinuous. If e is expressed in terms of the current as $-IRg$, none of these considerations is altered. If $-Rg$ is equal in magnitude to R_s, it does not imply zero net resistance in the circuit; it indicates that the energy supplied is equal to the energy lost, or that the current I is stable in magnitude with time.

In 1948, when the author expressed a belief that oscillators, such as those of Figs. 2 and 3 of the paper, were not series-tuned oscillators, the general relationships among different types of circuits were not appreciated. Contrary to Bernard's statement, tapping of the capacitative branch of the resonant circuit does result in a series-tuned oscillator.

In Fig. 2, for example, the variable capacitance Cv, can be replaced by a three-section variable capacitance, of capacitances in the same ratio as Cx, C_1, C_2, and of total capacitance equal to Cv. The voltage division across the sections of this variable capacitance will be the same as that across Cx, C_1, C_2. The respective fixed and variable sections can therefore be paralleled, giving the final equivalent of three capacitors in series. Since one of these is in series with the inductor and is not included between tube terminals, the circuit is a series-tuned oscillator, comparable to Fig. 1. The difference in the circuits is in the way that the impedance transformation varies as the tuning is changed. Similar remarks apply to the oscillator of Fig. 3.

Historically, the term "high-C" oscillator was first applied to either Colpitts or Hartley oscillators, and it has been used throughout in this sense by the author. Bernard has, however, included oscillators such as that of Fig. 2 of the paper under this designation. A better designation for Fig. 2 would be a "low-impedance series-tuned oscillator." As a result, there has been considerable confusion, and much tilting at windmills, concerning the relative performance of "high-C" and "series-tuned" oscillators. With an understanding of terms, there should be agreement on the remarks previously made on this subject.

Bernard's tests of "high-C" and "series-tuned" oscillators actually consisted of a comparison of two "series-tuned" oscillators. These tests indicated that the conclusions of the paper in regard to nonlinear distortion were incorrect, which has been admitted previously. These tests, however, gave no information as to the relative performance of "high-C" and "series-tuned" oscillators.

Bernard is not justified in concluding that the improved stability of the "series-tuned" oscillator is based on an incorrect theoretical development. Only that portion of the development covering the effects of harmonic inter-modulation was in error.

J. K. CLAPP
General Radio Co.
Cambridge, Mass.

[8] Received by the IRE, March 11, 1955; revision received March 30, 1955.

[9] J. K. Clapp, "Frequency stable LC oscillators," PROC. IRE, vol. 43, p. 876; July, 1955.

Impedance of Open- and Closed-Ridge Waveguide*

Ridge waveguide has found many applications in the microwave field because of its unusual cutoff properties and because it concentrates the electric field into a region where transit time is small.[1,2] If the dimensions of the ridge are small compared to a wavelength, and if this section is sufficiently removed from other boundaries so that its local fields are not disturbed, it is possible to calculate the cutoff frequency and the impedance of the waveguide by considering the re-entrant section as a lumped capacity and the remaining part of the structure as a transmission line in the transverse direction.

The cutoff frequency of closed-ridge waveguide was calculated by Cohn[1] using the method outlined above. The impedance was then calculated assuming a unidirectional transverse field in the waveguide. It was pointed out later[2] that the power flow along the discontinuity capacity had been neglected by Cohn. When this power flow is taken into account, a lower impedance is calculated. Only a few isolated experimental measurements were available to test the accuracy of the new calculation. Some time ago measurements of the voltage-current impedance of closed-ridge waveguide were made at Stanford University by setting up an analog of the waveguide on a rectangular co-ordinate Kron network board.[3] The results obtained there are compared in Table I with the calculations of Cohn[1] and Mihran[2] for a series of typical closed-ridge waveguides.

TABLE I

VOLTAGE-CURRENT IMPEDANCE OF CLOSED-RIDGE WAVEGUIDE WITH $a_1/b_1=2$

	$b_2/b_1=0.2$			$b_2/b_1=0.4$		
a_2/a_1	Cohn	Adams	Mihran	Cohn	Adams	Mihran
0.1	200	120	110	—	—	—
0.2	135	90	86	215	144	148
0.3	104	75	73	182	128	131
0.4	83	65	61.5	157	117	118
0.5	70	57	54	138	105	107

This table shows ample experimental evidence that the accuracy of the impedance calculation is greatly improved by the inclusion of a term taking into account power flow along the discontinuity capacity.

When ridge waveguide is used as a structure to interact with an electron stream, it is sometimes necessary to remove the gridded ridge top in order to minimize current interception.[4] An attempt was made to measure the loss of capacity resulting from the removal of the top from the ridge; this quantity was plotted in Fig. 5 of reference 2. This curve has recently come under suspicion, and new experimental and theoretical work have verified its inaccuracy. The ΔC's plotted in this curve are too high by a factor of two. Recent experimental measurements indicate that this correction is necessary. The same conclusion has been reached by studying two structures theoretically: one with infinitely thin ridge sides, and one with infinitely thick ridge sides. These two cases bound the case of most practical interest, i.e., an open-ridge guide in which the ridge sides have finite thickness. The theoretical results will be described briefly and will then be compared with the old and new experimental data.

The structures studied theoretically are shown in Fig. 1. It is assumed that the ridge top region is sufficiently far removed from other discontinuities (such as the corner at the bottom of the ridge or the side walls of the guide) so that its local fields are not disturbed. This is true in most practical cases. This means the ridge top can be studied independently of the remaining parts of the structure. The problem is most amenable to calculation if the rest of the guide is assumed to be infinitely far away. Thus the broken planes in Fig. 1 are assumed to extend to infinity.

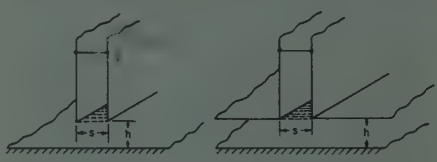

Fig. 1—(a) Rectangular ridge with infinitely thin side walls facing a plane. (b) Infinitely thick fins facing a plane.

These structures are admirably suited to study by the Schwarz-Christoffel transformation.[5] With the grid in place, the structure of Fig. 1(b) is simply a parallel plate capacitor. The capacity between the gridded region and the ground plane is $\epsilon_0 s/h$ mmfd per meter, where $\epsilon_0=8.85$ mmfd/meter. When the grid is removed, it can be shown[5] that the normalized capacity change is given by the following expression:

$$\frac{\Delta C}{\epsilon_0}=\frac{s}{h}-\frac{2}{\pi}\frac{s}{h}\tan^{-1}\frac{2h}{s}-\frac{2}{\pi}\ln\left[1+\left(\frac{s}{2h}\right)^2\right]. \qquad (1)$$

This normalized capacity change is plotted in Fig. 2 as a function of s/h, the ratio of the slot width to slot height above the ground plane, and is marked "infinitely thick fins."

An expression for the capacity of the structure of Fig. 1(a) without the grid can be obtained in terms of simple functions.[5] An exact expression for the capacitance of the structure with the grid in place has been obtained in terms of elliptic functions by Davy.[6] If $s/h>1$, the local fields at the edges of the ridge do not interact appreciably, and the capacity may be expressed in terms of simpler functions. If this restriction is observed, the normalized capacity change of the structure of Fig. 1(a) when the grid is removed is given by:

$$\frac{\Delta C}{\epsilon_0}=\frac{s}{h}+0.084-\frac{4}{\pi}\ln\left[\frac{h}{s}\frac{\pi}{\sinh^2\theta}\right] \qquad (s/h>1), \quad (2)$$

where

$$\frac{h}{s}=\frac{1}{2\pi}(2\theta+\sinh 2\theta).$$

Eq. (2) is plotted in Fig. 2 as a function of s/h, and is marked "infinitely thin fins."

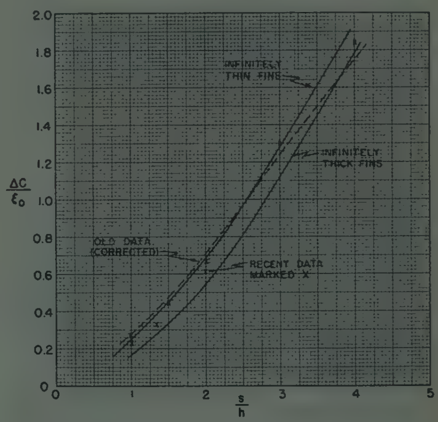

Fig. 2—Normalized capacity change as a function of the ratio of slot spacing to slot height above ground plane.

It is important to note that the curves plotted in Fig. 2 differ by a surprisingly small amount. This observation enables us to obtain the change in capacity involved when a bridging grid is removed from the ends of finite size conductors facing a ground plane, as in Fig. 3(a). The ΔC in this case must lie between the values obtained for the structures of Fig. 1(a) and Fig. 1(b). Since in practical cases, t/s would probably be small, practical ΔC values should be closer to the upper curve of Fig. 2 than the lower curve. It is interesting to note that the sharpened fin structure of Fig. 3(b) is also bounded by the cases shown in Fig. 1. This knowledge is not too useful, however, since the capacity of the gridded structure is not known.

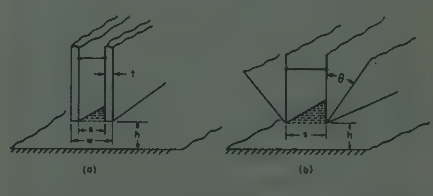

Fig. 3—(a) Fins of finite thickness facing a ground plane. (b) Sharpened fins facing a ground plane.

Recent experimental data are plotted in Fig. 2 as points marked by an "x." The ratios of fin thickness to fin spacing corresponding to these points range from 0.125 to 0.5. As predicted, the data tend to fall near the upper boundary curve. The dashed curve represents the data plotted in Fig. 5 of reference 2, reduced by a factor of two. This corrected curve is sufficiently close to the new data to indicate that an error of a

* Original manuscript received, April 11, 1955; revised manuscript received, June 1, 1955.

[1] S. B. Cohn, "Properties of ridge waveguide," PROC. IRE, vol. 35, pp. 783–788; August, 1947.

[2] T. G. Mihran, "Open- and closed-ridge waveguide," PROC. IRE, vol. 37, pp. 640–644; June, 1949.

[3] E. W. Adams, "Characteristics of Ridge Waveguide," Tech. Memo. No. 102, Elec. Res. Lab., Stanford Univ., Stanford, Calif.; May 31, 1951.

[4] T. G. Mihran, "The duplex traveling-wave klystron," PROC. IRE, vol. 40, pp. 308–315; March, 1952.

[5] T. G. Mihran, "Calculation of waveguide slot capacitance using the Schwarz-Christoffel transformation," Report No. RL-523, General Electric Research Laboratory; April, 1951.

[6] N. Davy, "On the field between equal semi-infinite rectangular electrodes or pole pieces," *Phil. Mag.*, vol. 35, pp. 819–840; December, 1944.

factor of two somehow entered into the original experimental work. Investigation has shown the source of the error was not in the reduction of the experimental data. The error apparently arose from incorrect calibration of the capacity measuring apparatus. In any case, the bounding curves of Fig. 2 now provide a simple and reasonably accurate way of determining the loading capacity of practical open-ridge waveguide.

T. G. MIHRAN
Electron Tube Section
General Elec. Co.
Schenectady, N. Y.

Measurement of Small Attenuations*

Small attenuations of the order of tenths of a db can be measured with a precision of about 10 per cent by a method which subtracts the outputs of two crystals and thus makes the measurement independent of small power fluctuations.

Square-wave modulated rf power from a well-buffed klystron is split in a magic T section (any suitable power divider could be used for this purpose). Proceeding outward from the T, each symmetrical arm (designated A and B) consists of a variable attenuator, a slotted section, and a tuned crystal mount. The outputs of the two crystals are combined and amplified as shown in Fig. 1 so as to produce a null when the outputs of the crystals are equal. The condensers are used to optimize the null by equalizing the capacitance across each half of the transformer input winding.

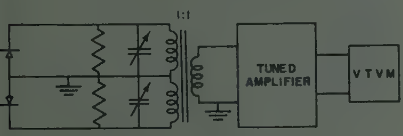

Fig. 1

The attenuator in arm A is adjusted to achieve a null and is then varied by an amount a_0 db which can be determined by observing the change in level of the output of the slotted section probe. The voltage v_0 caused by the a_0 db power change is read on the voltmeter. The attenuator is again adjusted for a null and the test section is inserted in arm A between the slotted section and the tuned crystal mount. If the voltage output caused by the attenuation of the test section is v_1 then this attenuation, a_1 db, is given as

$$a_1 = \frac{v_1 - v_n}{v_0 - v_n} a_0 \text{ db}, \tag{1}$$

where v_n is the null voltage.

Eq. (1) actually yields the insertion loss of the test section: however, if the generator and load are matched to the transmission line, then (1) yields the attenuation.

An attenuation measurement of a section of X-band guide was made at a frequency of 11 kmc. The vswr's of the tuned crystal mount, test section plus tuned mount, and when looking back toward the T were 1.02, 1.07, and 1.03 respectively. Six successive measurements yielded the following values. Each tabulated value of v_0 is actually the average of three consecutive readings.

v_n (volts)	0.2	0.2	0.2	0.2	0.2	0.3
a_0 (db)	0.2	0.2	0.2	0.2	0.2	0.2
v_0 (volts)	11.0	11.0	11.1	13.9	14.5	15.2
v_1 (volts)	4.7	4.1	5.0	5.4	5.8	5.8
a_1 (db)	0.083	0.072	0.088	0.076	0.078	0.074

The average value of a_1 is 0.079 db and the standard deviation is 0.006 db. Since the slight mismatches that were present can produce an uncertainty of about 0.01 db, one can conclude that the attenuation of the test section is 0.079 ± 0.016 db. This result compares, within the limits of error, to the value of 0.09 db, which was obtained at a frequency of 11 kmc by using a variable lossy short.[1]

One could use wollaston wire bolometers as the detectors at frequencies too high to permit the use of crystals. The circuitry to do this is shown in Fig. 2. The advantage gained by using wollaston wire elements as detectors is that they can be more readily broadbanded; consequently the measurement would not be overly sensitive to frequency variations of the rf source.

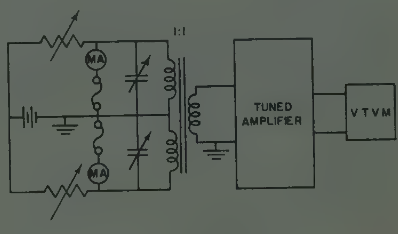

Fig. 2

This procedure can be readily extended to the measurement of attenuation by a substitution method, since changes in attenuation of 0.01 db can be detected as an observed change in the null. For example, if the variable attenuator in arm A were accurately calibrated, then the insertion loss of a test section is simply given as the change in the attenuation of this calibrated standard necessary to reproduce a null.

ACKNOWLEDGMENT

This work was supported by the Rome Air Development Center, Contract No. AF-30(602)-988. The author also wishes to acknowledge the aid of M. Sucher of the Microwave Research Institute.

L. O. SWEET
Microwave Res. Inst.
55 Johnson Street
Brooklyn, N. Y.

* Received by the IRE, May 23, 1955.

[1] H. M. Altschuler and A. A. Oliner, "Microwave Measurements with a Variable Short Circuit," Res. Rep. R-399-54, PIB-322; September, 1954.

Network Transformations Concerning Jaumann Networks*

It is well-known that the lattice network is equivalent to the network consisting of two arms associated with a three-winding ideal transformer, as shown in Fig. 1. This, often known as Jaumann network, has been used extensively to realize filters, especially piezoelectric filters, because of the simpler construction and less elements than that of the lattice network.

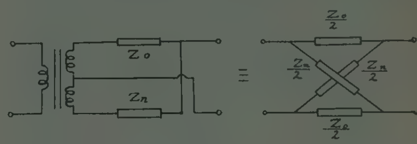

Fig. 1

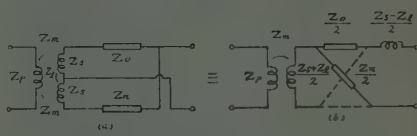

Fig. 2

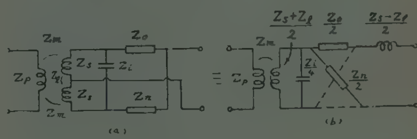

Fig. 3

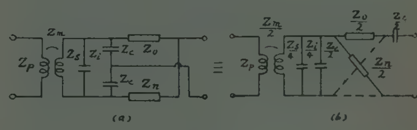

Fig. 4

In practice, however, no transformer is ideal. What effect will its imperfection have on the filter characteristics?

Another question concerning the Jaumann network is: What are the relationships between the modified connections shown in Figs. 3(a) and 4(a), which sometimes have been used in the high frequency range?

Probably the simplest and most satisfactory approach to these problems is to look for equivalent networks consisting of a lattice section, which is the essential part of the network, and some cascade sections due to both the imperfection of the transformer and the additional elements. Figs. 2–4 show the network transformations in this sense, among which the first one (Fig. 2) was already derived by Mason.[1]

MORIO ONOE
Inst. Ind. Sci., Univ. of Tokyo
Chiba-city, Japan

* Original manuscript received by the IRE, March 29, 1955; revised manuscript received, April 25, 1955.

[1] W. P. Mason, "Resistance compensated bandpass crystal filters for use in unbalanced circuits," *Bell Sys. Tech. Jour.*, vol. 16, pp. 423–436; October, 1937.

The Width of Coverage of a Radar Antenna*

During the development of a microwave vehicle speed indicator, consideration of the width of the coverage pattern of a radar antenna has indicated a property which at first sight may appear somewhat surprising, particularly if the expression "beamwidth" is loosely interpreted. Using a paraboloid antenna of about 18 inches diameter and a wavelength of 3 cm it has been found that satisfactory coverage of vehicles on both sides of a highway is obtained. To restrict the coverage to a single traffic lane (Fig. 1)

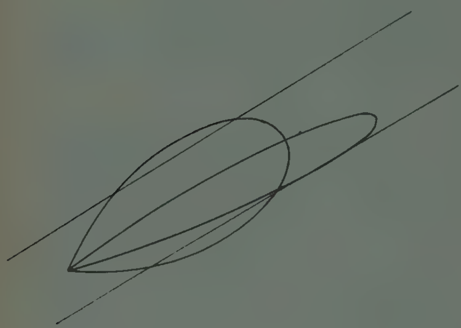

Fig. 1

it is necessary to reduce the width of the coverage diagram and the immediate suggestion may well be to increase the antenna size, reduce the beamwidth and hence the width of the coverage pattern. It can immediately be shown that variation of the antenna diameter has no effect on the maximum width of the coverage pattern. In fact, it appears that "the width of the coverage pattern produced by a radar antenna, of fixed shape and filling factor, at any fraction of the maximum range on a given target, is independent of the size of the antenna, provided it is large compared with the wavelength used."

This statement may readily be proved for patterns in the principal planes (Fig. 2).

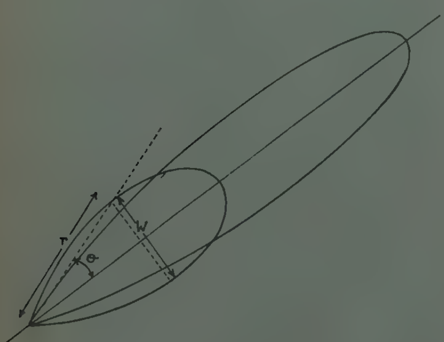

Fig. 2

The maximum range of a radar system is dependent on the antenna gain G

$$R_{\max} \propto \sqrt{G}$$

* Received by the IRE, March 14, 1955.

and

$$G = \frac{4\pi A f}{\lambda^2},$$

where

A is the area of the antenna aperture
λ is the wavelength
f is a factor depending on the energy distribution across the aperture.

So

$$R_{\max} \propto \sqrt{A}$$

If the antenna shape is fixed and "h" is the horizontal dimension

$$A \propto h^2,$$

and hence

$$R_{\max} \propto h.$$

Now the horizontal angular beamwidth is governed by the ratio of "h" and λ and it can be shown[1] that, if the same relative energy distribution is produced over apertures of different sizes, the same secondary field strength pattern is produced when it is regarded as a function of "u" where

$$\text{"}u\text{"} = \frac{\pi h}{\lambda} \sin\theta$$

and θ is an angle measured from the normal to the aperture.

It is also known that the field strength pattern produced by a radar antenna can be interpreted as a range diagram in which the maximum of the pattern corresponds to the maximum range as calculated or determined experimentally.

Let us refer to points on the radiated pattern such that the function of u has a value $(k)\times$(maximum value) i.e., u_0 determines $\pm\theta_0$, the angle at which the range is $(k)\times$(maximum range)

$$u_0 = \frac{\pi h}{\lambda} \sin\theta_0.$$

Now the width of the coverage pattern is

$$W = 2r \sin\theta$$

where r is the range considered and 2θ the full angular beamwidth at this range.

For a range which is a factor k of the maximum range,

$$W = 2k.\, R_{\max} \sin\theta_0$$
$$= k.\, h.\, \frac{\lambda u_0}{\pi h.}$$
$$\propto k\lambda u_0 \text{ which is a constant;}$$

in particular W is independent of the size of the antenna.

In practice the reduction in width of cover is readily obtained by reducing the receiver sensitivity to reduce the maximum range made available by an over-all increase in antenna size, or, more beneficially in the particular case referred to, by maintaining the initial vertical beamwidth and increasing only the horizontal aperture.

A. W. G. Court
Dominion Physical Lab.
Lower Hutt
New Zealand

[1] S. Silver, "Microwave Antenna Theory and Design," Radiation Lab. Ser. No. 12, McGraw-Hill Book Co., Inc., New York, N. Y.; 1949.

"Maximum Efficiency of Four-Terminal Networks"*

Mathis has described in the above paper[1] a direct geometric construction of finding the input impedance Z_A (or reflection coefficient Γ_A) of an arbitrary four-pole terminated in its conjugate-image impedance match. Employing reflection coefficient notation, this construction (which assumes that only the input reflection coefficient locus, (Γ'), corresponding to all possible reactive terminations of the four-pole has been drawn), is repeated in dashed lines in Fig. 1. In this connection further comments of interest can be made.

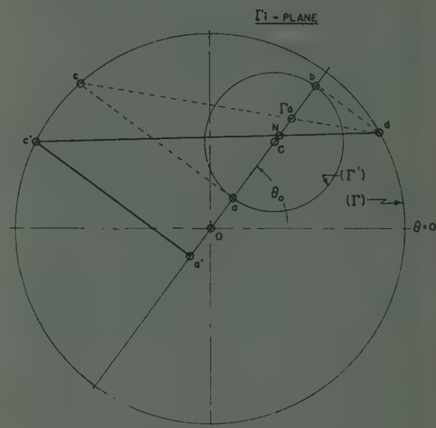

Fig. 1—Determination of maximum efficiency.

An additional, similar construction yields the maximum efficiency $\eta_{\max}$ directly: On the line OC (C is the center of the locus) determine a', the reflection of the point a in the origin 0 ($|a0| = |a'0|$). Erect $a'c'$ perpendicular to OC to intersect the unit circle, (Γ) at c'. The line $c'd$ intersects OC at N. The magnitude $|ON|$ (i.e., the magnitude of the reflection coefficient N) equals $\eta_{\max}$.

In a recent paper[2] the author has introduced the modified Wheeler network. Mathis' construction in conjunction with the one presented here yields three of the parameters of this representation (l_1, n_1 and $|\Gamma_\alpha|$) almost without computation:

$$l_1 = \theta_0/2\beta,$$
$$n_1^2 = \frac{1 + |\Gamma_A|}{1 - |\Gamma_A|}$$
$$|\Gamma_\alpha| = |ON|,$$

where θ_0 is the argument of, say, Γ_A and β is the propagation constant of the input transmission line of the four-pole in question.

It must be pointed out that both the constructions and the formulas discussed here apply equally well when the locus (Γ') encloses 0, the origin of the chart.

H. M. Altschuler
Microwave Research Inst.
Polytechnic Inst. of Bklyn.
Brooklyn, N. Y.

* Received by the IRE, March 4, 1955.

[1] H. F. Mathis, Proc. IRE, vol. 43, pp. 229–230; February, 1955.

[2] H. M. Altschuler, "A method of measuring dissipative four-poles based on a modified Wheeler network," *Trans. IRE.*, vol. MTT-3, pp. 30–36; January, 1955.

Measurement of Microwave Nonreciprocal Four-Poles*

Recent work on microwave ferrite and gas discharge devices has resulted in many new microwave four-terminal devices (four-poles) which are linear to a good approximation but which do not satisfy reciprocity. These devices may be termed microwave nonreciprocal four-poles (MNRFP). It is well known that the terminal behavior of such devices can be completely described by four complex parameters which are in general functions of frequency. It is the purpose of this note to describe a convenient method for measuring these parameters.

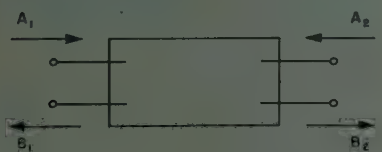

Fig. 1—Linear 4-pole.

Using the scattering matrix representation the linear equations which describe the MNRFP can be written (Fig. 1)

$$B_1 = S_{11}A_1 + S_{12}A_2 \tag{1}$$

$$B_2 = S_{21}A_1 + S_{22}A_2, \tag{2}$$

where the A's and B's are proportional to the complex amplitudes of the waves traveling into and out of the MNRFP and the S's are the elements of the scattering matrix which describe the terminal behavior of the MNRFP. The problem is to measure S_{11}, S_{12}, S_{21}, S_{22}. S_{11} is measured by placing a reflectionless load on terminals 2 and measuring the input reflection coefficient at terminals 1. S_{22} is measured similarly. If the device were reciprocal, S_{12} and S_{21} would be equal and could be measured by measuring the input reflection coefficient of the device with a known reflection coefficient connected to the output. It can be shown, however, that this method will not yield S_{21} and S_{12} separately when reciprocity is not satisfied. An obvious and straightforward way to measure S_{21} would be to excite the device at terminals 1 with a reflectionless load connected to terminals 2. Then $A_2=0$ and $S_{21}=B_2/A_1$. Since the waves associated with A_1 and B_2 are located in different waveguides and hence do not directly interfere with each other the measurement of their relative amplitudes and phases is rather difficult although it can be done using directional couplers to extract the waves from terminals 1 and 2 and then combining them and measuring their relative amplitude and phase.

The following method, which involves only the measurement of two-terminal reflection coefficients, is proposed for determining S_{12} and S_{21}. The microwave circuit of Fig. 2 provides excitation simultaneously at both terminal pairs with reflectionless (matched) equivalent generators. The purpose of the matched pads or matched Unilines (a commercial one-way pad) is to insure that both equivalent generators are reflectionless regardless of the signal source characteristics and to minimize signal source pulling. The two equivalent generators are coherent since they are derived from the same signal source. In the scattering matrix scheme a reflectionless generator is characterized completely by one complex number, B_g, which specifies the amplitude and phase, at a given reference plane of the wave issuing from the generator. Assume that the equivalent generators, at terminals 1 and 2, are characterized by B_{g1} and B_{g2} respectively.

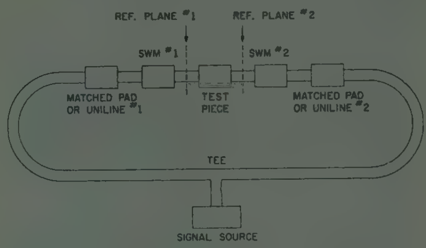

Fig. 2—Microwave circuit.

The joining condition will then be that $A_1=B_{g1}$ and that $A_2=B_{g2}$. Substituting in (1) and (2), we obtain

$$B_1/B_{g1} = S_{11} + (S_{12})B_{g2}/B_{g1}$$

and

$$B_2/B_{g2} = S_{22} + (S_{21})B_{g1}/B_{g2}.$$

Now B_1/B_{g1} and B_2/B_{g2} are just the quantities that are measured by the standing wave machines shown in Fig. 2. If the setup is physically symmetrical then $B_{g1}=B_{g2}$ and knowing S_{11} and S_{22}, S_{12} and S_{21} are obtained from the above.

In a practical setup it is rather difficult to produce the required symmetry and it is preferable to measure B_{g1}/B_{g2} as follows: The unknown 4 terminal device is replaced with a section of straight waveguide. The waves issuing from the two generators will interfere in the usual way and either standing wave machine (SWM) can then be employed to measure their relative phases and amplitudes at any convenient reference plane. The usual transformation to reference planes 1 and 2 then yields B_{g1}/B_{g2}.

The following procedure could be carried out to obtain fairly rapid measurements of all four parameters. (1) Measure B_{g1}/B_{g2} as outlined above, (2) insert the unknown MNRFP, replace SWM #2 with a matched load and measure S_{11} using SWM #1, (3) replace SWM #2 or put a straight section of waveguide in its place and measure B_1/B_{g1} with SWM #1. Calculate S_{12}, and (4) carry out steps 2 and 3 with the digits 1 and 2 interchanged. Note that two SWM's are not really needed.

A. C. MACPHERSON
Naval Res. Lab.
Washington 25, D. C.

* Original manuscript received by the IRE, April 18, 1955.

Magnetic Tuning of Klystron Cavities*

Reflex klystron oscillators are ordinarily modulated in frequency by applying a fluctuating voltage to the repeller. When the dc portion of the voltage is set at the center of the mode, the frequency modulation (FM) is approximately linear and the accompanying amplitude modulation (AM) depends upon the excursion of the modulating voltage. Amplitude modulation can be reduced to a minimum by limiting the modulating voltage to a small section of the mode. For many applications the AM characteristic of the klystron restricts the range of frequency deviation. This letter describes a method, suggested to us by C. W. Carnahan, Varian Associates, for very wideband frequency modulation with low amplitude modulation. In this method the resonant frequency of an X-band klystron with an external cavity is varied by applying a magnetic field to a ferrite in the cavity.

Fig. 1 shows the frequency deviation and power change as functions of the applied magnetic field when a piece of magnesium-manganese ferrite[1] is placed in the external cavity of a klystron similar to the VA-201.[2] A perturbation calculation gives results which roughly confirm the experimental measurements. As the field is increased, the mode of oscillation (ordinarily only 80 mc wide) shifts so that very wide deviations are possible.

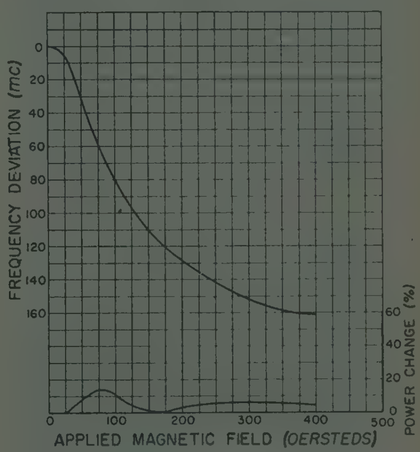

Fig. 1—Frequency deviation and power change as functions of the applied magnetic field for a ferrite in the external cavity of a klystron.

For less than 20 per cent power change, the maximum deviation is 160 mc compared to 15 mc using conventional reflector tuning. These properties make magnetic tuning of klystron cavities useful in wideband applications such as FM transmitters and radar systems.

These measurements were made using a magnetic field supplied by a magnet external to the cavity. Additional measurements have been made to show that this field can be supplied by a properly designed solenoid wound directly on the ferrite, with little interference with the resonant properties of the cavity.

The authors wish to thank C. A. Morrison for many helpful discussions.

J. C. CACHERIS and G. JONES
Diamond Ordnance Fuze Labs.
Washington 25, D. C.
L. DIEHL
ACF Electronics
Alexandria, Va.

* Received by the IRE, April 5, 1955.

[1] The magnesium-manganese ferrite is type R-1 manufactured by General Ceramics Corp., Keasby, N. J.

[2] Manufactured by Varian Associates, Palo Alto, Calif.

Reduction of Plasma Frequency in Electron Beams by Helices and Drift Tubes*

The behavior of klystrons, traveling-wave tubes and other long beam microwave devices at small signal levels can be conveniently described in terms of the coupling of circuit waves and space charge waves.[1] The propagation characteristics of the space-charge waves depend on the plasma frequency, which, in electron beams of uniform density and infinite extent, is a function of the electron density only. In beams of finite size in the vicinity of conductors or dielectric materials, the plasma frequency is reduced from the infinite beam value, ω_p, to the value ω_q. Graphs of the reduction factor ω_q/ω_p for round and flat beams have appeared in the literature,[2,3] and complete sets of curves for the general case of an annular beam in annular or cylindrical drift tubes, including solid and flat beams as limiting cases, are being published.[4]

The purpose of this communication is to point out the fact that the principal factor in the reduction of plasma frequencies in electron beams in either cylindrical drift tubes or in helices is due to the finite diameter of the beam. The presence of the drift tube or helix has relatively little effect in further reducing the plasma frequency for the usual cases of the beam diameter being about half the drift tube or helix diameter.

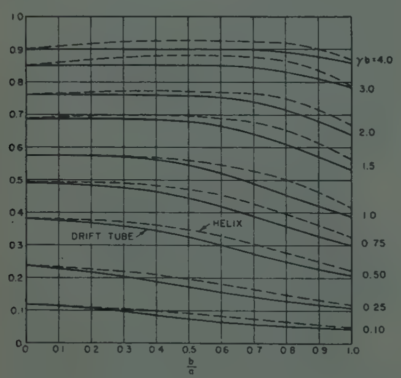

Fig. 1—The plasma frequency reduction factor, ω_q/ω_p, for solid electron beams as a function of the ratio of the beam radius b to a coaxial helix or drift tube of radius a for several values of γb.

In Fig. 1 the plasma frequency reduction factor ω_q/ω_p is plotted versus the ratio of the beam radius b to the helix or drift tube radius a with the argument $\gamma b = \omega b/u_0$ as a parameter, where ω is the signal angular frequency and u_0 is the electron velocity in the beam. The solid curves pertain to beams in conducting drift tubes and are reproduced.[5] Data for the dashed curves giving the helix reduction factors were calculated from the curves of the space charge parameter Q_s and the sheath helix impedance parameter K_s given by Pierce.[6] At small values of the product of the space charge parameter Q and the cube of the gain parameter C, the ratio of the plasma frequency to the signal frequency is given approximately by[7]

$$\omega_q/\omega = \sqrt{4QC^3},$$

which at a nonrelativistic electron velocity synchronous with the helix circuit wave can be rewritten in terms of the helix impedance and the beam perveance p as:

$$\omega_q/\omega = 22.48\sqrt{pQ'K'},$$

where Q' and K' are the quantities plotted along the ordinates.[8]

From the definition of the plasma frequency, it can readily be shown that the ratio of the unreduced plasma frequency to signal frequency is given in MKS units by

$$\omega_p/\omega = 174.1\sqrt{p}/\gamma b.$$

Thus from the ratio of the two last equations one finds, for solid beams in sheath helices,

$$\omega_q/\omega_p = 0.1291\gamma b\sqrt{Q'K'}.$$

From Fig. 1 it would appear that the helix reduces the plasma frequency by a smaller amount than does a drift tube of the same diameter. For traveling-wave tubes operating in the usual range of $\gamma b = 0.5$ to $\gamma b = 1.0$, there is less than 10 per cent difference between the plasma frequency for a beam in a helix of diameter about twice the beam diameter ($b/a \approx 0.5$) and that of the same beam in free space ($b/a = 0$).

G. M. Branch
Electron Tube Sec., General Electric Co.
Schenectady, N. Y.

* Received by the IRE, April 8, 1955.

[1] J. R. Pierce, "The wave picture of microwave tubes," *Bell Sys. Tech. Jour.*, vol. 33, pp. 1343–1372; November, 1954.

[2] D. A. Watkins, "Traveling-wave tube noise figure," Proc. IRE, vol. 40, pp. 65–70 (Fig. 6); January, 1952.

[3] J. W. Sullivan, "A wide-band tunable oscillator," Proc. IRE, vol. 42, 1658–1665; November, 1954.

[4] G. M. Branch and T. G. Mihran, "Plasma frequency reduction factors in electron beams," *Trans. IRE*, vol. ED-2 (In press).

[5] Branch and Mihran, *ibid.* (Fig. 2).

[6] J. R. Pierce, "Traveling-Wave Tubes," D. Van Nostrand Co., New York, N. Y., pp. 249–250; 1950.

[7] C. K. Birdsall and G. R. Brewer, "Traveling-wave tube characteristics for finite values of C," *Trans. IRE*, vol. ED-1, pp. 1–11 (eq. 9); August, 1954.

[8] Pierce, *op. cit.*, in Figs. A6.4 and A6.5.

Toward a Measure for Meaning*

The complete information measure set[1] which describes the intelligence communicated to the human operator should include a numeric measure for meaning of any given display and observer. The average meaning can be considered to be the amount of selective information which is stimulated in an average observer, and is dependent upon the real information stimulus as well as the retained information from past experience. In terms of aural display, meaning can be considered a measure of the difference between the articulation index of nonsense-syllables as opposed to monosyllable meaningful words measured under the same environmental noise conditions.[2] It appears that the repetition of nonsense-syllables to add repetitive redundancy does not account for the difference in articulation index and leaves a large measure of improvement yet to be accounted for. It, therefore, appears that the remainder is dependent upon the contextual redundancy of the memory.

Since it would seem "easier" to identify something which can be related directly to a "mental picture" as opposed to an abstract quantity, it seems probable that a primary component of meaning is pictorialism. A pictorial-symbolic continuum can be constructed wherein the pictorial end of the scale is a single point which represents the parameter as it is displayed in the real world, and the symbolic end of the scale is an infinite set of points which represent all various symbols which could be used to represent the same parameter. Only one dimension of this continuum is of immediate concern, that being, the line which terminates on the truly pictorial single point and connects all those increasingly symbolic displays which most directly relate to the mode of display as seen in the real world.

Each end of this single dimension symbolic-pictorial scale has advantages and disadvantages; for instance, a highly pictorial quality of altitude would lack the required sensitivity and accuracy for aircraft missions, such as in-air refueling; the highly symbolic end would require extensive training and increased latency time which might be intolerable in certain aircraft missions. Therefore, it seems reasonable to presume that there is some optimal point on this scale which should be chosen for the display of each parameter once the parameter, personnel available, etc. have been specified.

Any parameter in the real world is an ordered message set where a purely symbolic display would be unordered. The measure of this scale might then be considered to be the degree of order presented by the display as compared to that of the real world so as to allow percentage expression. This order is composed of two components which, in general, are independent. The first is repetitive redundancy, a measure of the pointer area in terms of elementary observable areas, etc., and the second is contextual redundancy in terms of alternative parameters which may be reinterpreted in terms of the parameter the observer is concerned with. This situation may be illustrated by the apparent altitude estimated from the size of a house based on the pilot's knowledge of the actual size of that house.

The degree of pictorialism may then be defined mathematically as the ratio of the weighted sum of repetitive and contextual redundancy to that contained in the real world display of this same parameter. (It is conceivable that a display may be more "pictorial" than the real world representation in that it may have a higher degree of order. It is judged that an observer would consider this to be a distorted picture and soon become unhappy with such a display.)

The work of Dr. K. V. Wilson, Control Systems Laboratory, University of Illinois, should be studied in an effort to relate his "similarity measure" to the "pictorialism measure" suggested above.

Much remains to be done in this field and it would be of distinct value if a proper pictorialism or meaning measure could be achieved so as to complete the defining sets of communication qualities[3] which can be used to analyze, evaluate, and guide the design of display configurations.

L. J. Fogel
Stavid Engineering, Inc.
Plainfield, N. J.

* Received by the IRE, April 11, 1955.

[1] Inclusive of the selective Shannon measure.

[2] I. J. Hirsh, E. G. Reynolds and N. Joseph, "Intelligibility of different speed materials," *Jour. Acoust. Soc. Amer.*, vol. 26, p. 530; July, 1954.

[3] L. J. Fogel, "A communication theory approach toward the design of aircraft instrument displays," 1955 IRE Convention Record, Part 5.

Contributors

S. V. Chandrashekhar Aiya (A'39–M'40–SM'43) was born in Saklaspur, India, on May 17, 1911. He received the B.Sc. degree in 1931 from Wilson College, Bombay and the B.A. in 1934 from Gonville and Caius College, Cambridge, Eng. with First Class Honours in Physics.

S. V. C. Aiya

He was professor of radio-physics at S.P. College, Poona from 1936 to 1942, and experimental physicist at the Cosmic Ray Research Unit of the Indian Institute of Science in Bangalore from 1942 to 1945. He is now professor of electrical communications at the College of Engineering, Poona. He has served on several government committees and been a member of authorities of the Universities of Bombay and Poona.

Mr. Aiya is a full member of the IEE.

❖

M. E. Amdursky was born in Rochester, N. Y., on October 7, 1922. He is a graduate of the Institute of Optics of the University of Rochester, having received a B.S. degree in 1944, and took graduate studies at New York University and City College of New York.

M. E. Amdursky

During World War II, he was active in the Manhattan District Project and in the Division of War Research.

In 1946, Mr. Amdursky joined the research staff of Philips Laboratories, Inc. at Irvington, N. Y., where he helped develop the Philips Protelgram television receiver. In 1949, he became a member of the research and development department of the Rauland Corp., where he is now project engineer in charge of color tube development.

Mr. Amdursky is a member of the Optical Society of America.

❖

G. Y. Chu (S'50–A'52) was born in Shanghai, China, in 1918. He received his B.S. in electrical engineering from Chiao Tung University.

G. Y. Chu

In 1946 he came to the United States to study at the Westinghouse Electric Corp. In 1947 he joined the Electrical Engineering Department of M.I.T. as a Research Assistant. He received the M.S. and Sc.D. degrees in electrical engineering in 1949 and 1953, respectively.

Mr. Chu joined Sylvania Electric Prod- ucts in 1953 and has worked on applications of semiconductor devices. He is now engineer in charge of the circuits and applications section of the semiconductor engineering department at Ipswich.

Mr. Chu is a member of Sigma Xi.

❖

W. A. Edson (M'41–SM'43) was born at Burchard, Neb., on October 30, 1912. He studied electrical engineering at the University of Kansas, receiving the B.S. and M.S. degrees in 1934 and 1935,.

W. A. Edson

The following two years Dr. Edson spent at Harvard University on a fellowship. Upon receiving his D.Sc. in communication engineering in 1937, he joined the systems development department of Bell Telephone Labs.

In 1941 Dr. Edson joined Illinois Institute of Technology as Assistant Professor of electrical engineering; then became Professor of physics at the Georgia Institute of Technology in 1945, and Professor of electrical engineering in 1946. From 1951 to 1952 he was Director of the School of Electrical Engineering. Since July, 1952, he has been Acting Professor of electrical engineering and Research Associate at the Applied Electronics Laboratory at Stanford University.

Dr. Edson is a member of the American Physical Society and the California Society of Professional Engineers.

❖

Walter G. Gibson (S'48–A'49) was born in San Mateo, California on July 18, 1924. Mr. Gibson received the Bachelor of Science degree in electrical engineering from the University of California in 1948.

W. G. Gibson

Since then Mr. Gibson has been a member of the technical staff of the RCA Laboratories Division, David Sarnoff Research Center, at Princeton, N.J.

Mr. Gibson is a member of Sigma Xi.

❖

H. A. Haus was born in Ljubljana, Yugoslavia, in 1925. He attended the Technische Hochschule in Graz, from 1946 to 1948 and studied one term at the Technische Hochschule in Vienna. He attended Union College, receiving his B.S. degree in 1949. He received his M.S. from the Rensselaer Polytechnic Institute in 1951 and his Sc.D. from the Massachusetts Institute of Technology in 1954.

H. A. Haus

He is now engaged in microwave tube research at M.I.T. and is also Assistant Professor of electrical engineering at M.I.T.

Dr. Haus is a member of Sigma Xi.

❖

R. C. Hergenrother (A'37–SM'52) was born on September 5, 1903, in Chemnitz, Germany. He received his A.B. from Cornell University in 1925. He went to Pennsylvania State College in 1927 as an instructor in physics, and there received the M.S. degree in 1928. He was awarded Ph.D. from the California Institute of Technology in 1931.

R.C. Hergenrother

Dr. Hergenrother held a Rockefeller Foundation Research Fellowship in physics at Washington University, St. Louis, Mo., from 1932 to 1934. From 1934 until 1945, he worked for the Hazeltine Corp. Since 1945 Dr. Hergenrother has been employed by the Raytheon Manufacturing Co., and is now head of klystron and storage-tube development in microwave and power tube operations.

He is a member of the American Physical Society, Sigma Xi, and Sigma Pi Sigma.

❖

C. T. Kohn was born in Ostrzeszów, Poland, in 1908. He received the Dipl.-Ing. degree in electrical engineering in 1932 from the Institute of Technology in Lwów.

C. T. Kohn

From 1934 to 1939 he was employed by the National Establishment for Tele- and Radiocommunications in Warsaw. After the war he was associated with the Signals Res. and Dev. Establishment in Christchurch, Eng.

In 1948 he joined the British Telecommunications Research Ltd., Taplow, Eng., where he has been working on transmitter design and precision electronic equipment.

❖

M. McWhorter (S'47–A'53) was born on January 8, 1926, in Norfolk, Va. He received his B.S. degree in 1949 from Oregon State College and his M.S. from Stanford University in 1950.

M. McWhorter

He then worked on wide-band amplifiers at Stanford and received his Ph.D. in 1953. From 1953 to 1954 he was a Research Associate at Stanford working in nuclear induction. Since that time he has been concerned with high-frequency, wide-band amplifiers at the Stanford Electronics Laboratory and an acting Assistant Professor since January,

C. W. Mueller (S'35–A'36–VA'39–SM '45) was born in New Athens, Ill., in 1912. He received the B.S. degree in electrical engineering from the University of Notre Dame in 1934, and the S.M. degree in electrical engineering from the Massachusetts Institute of Technology in 1936. From 1936 to 1938 Dr. Mueller was associated with the Raytheon Production Corporation. In 1938 he returned to M.I.T. where he received the degree of Sc.D. in physics in 1942. While at M.I.T., he worked on the development of gas-filled special-purpose tubes for counting operations. Since 1942 he has been a member of the RCA Research Laboratories, where he has been engaged in research on high-frequency receiving tubes and secondary electron emission phenomena.

C. W. Mueller

Dr. Mueller is a member of the American Physical Society and Sigma Xi.

❖

For a photograph and biography of J. M. Pettit, see page 1348 of the September, 1954 issue of the Proceedings of the IRE.

❖

R. G. Pohl was born in Chicago, Ill., on August 22, 1927. He obtained the A.B. degree in 1948 and the M.S. degree in 1950 from the University of Illinois.

R. G. Pohl

From 1948 to 1952 he was an Assistant in the Physics Department of the University of Illinois. From 1952 to the present he has been a research engineer in the research department of the Rauland Corp., conducting research and development work on semiconductor devices.

Mr. Pohl is a member of the American Physical Society, Alpha Kappa Psi and Pi Mu Epsilon.

❖

P. A. Redhead (A'47) was born in Brighton, Eng., on May 25, 1924. He graduated from Cambridge University in 1944 with the B.A. degree in physics. From 1944 to 1947 he was employed by the British Admiralty in work on proximity fuses and later on microwave tube development. In 1947 he joined the Radio and Electrical Engineering Division of the National Research Council of Canada, working in the field of physical electronics.

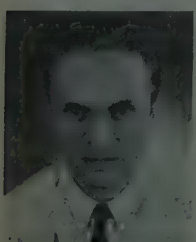

P. A. Redhead

Mr. Redhead is a member of the American Physical Society.

F. N. H. Robinson was born in 1925, at West Bromwich, Eng. and educated at Christ's College, Cambridge, England, where he received the B.A. degree in 1946. From 1945 to 1950, he was employed by the British Admiralty and where he was engaged in work on microwave tubes. Since 1950 he has been successively Nuffield Research Fellow and I.C.I. Research Fellow at the Clarendon Laboratory, Oxford, England.

F. N. H. Robinson

During the fall of 1954 and spring of 1955, he was on leave of absence from Oxford to work in the Electronics Research Department of Bell Telephone Laboratories.

❖

A. C. Schroeder (A'38–SM'46–F'54) was born at West New Brighton, Staten Island, N. Y., on February 28, 1915. He received the B.S. degree in electrical engineering from the Massachusetts Institute of Technology in 1937, and the M.S. degree from the same institution that year.

A. C. Schroeder

He joined the Radio Corporation of America in 1937, and is now engaged in television research at the RCA Laboratories in Princeton, N. J.

Mr. Schroeder is a member of the AAAS, and Sigma Xi.

❖

For a photograph and biography of R. P. Stone, see page 1572 of the October, 1954 issue of the Proceedings of the IRE.

❖

C. S. Szegho (A'41–SM'51–F'52) was born in Hungary, on March 15, 1905. He received his M.S. and Dr. of Engineering degrees in 1927 and 1931, respectively, from the Institute of Technology in Munich and Aachen.

C. S. Szegho

Shortly after arriving in the United States Dr. Szegho became, for seven years, head of the cathode-ray tube research department of Baird Television Co. In 1942 Dr. Szegho joined the Rauland Corp. in Chicago as director of research. His work covers cathode-ray tubes and other electronic and solid-state devices.

In addition to being a member of IRE Dr. Szegho is a member of the APS

F. J. Tischer was born in Plan, Austria, in 1913. He received his preparatory education at the Realgymnasium in Budweis and attended the University of Prague from 1932 to 1938. In 1937 he received the Master's degree in electronics and was awarded the Ph.D. degree in technical sciences from the University of Prague in 1938.

F. J. Tischer

He then joined the Telefunken Laboratories, Berlin, where he worked in the field of television and microwaves. In 1941, he founded the Tischer Physical Research Laboratory at Budweis and Aigen, Austria.

Dr. Tischer joined the staff of the Royal Institute of Technology in Stockholm, Sweden in 1947, where he directed the activities in microwave research. In 1954 he came to the United States and has since been conducting research in microwaves with the Research Division, Ordnance Missile Laboratories, Redstone Arsenal, Army Guided Missile Center.

❖

W. M. Webster (A'48–SM'54) was born in Warsaw, N. Y. in 1925. He studied physics at Rensselaer Polytechnic Institute, and at Union College. He received the B.S. degree in physics from Union College, and the Ph.D. degree from Princeton University.

W. M. Webster

He joined the RCA Laboratories Division at Princeton, N. J., in 1946. In November, 1954, Dr. Webster transferred to the RCA Tube Division at Harrison, N. J.

Dr. Webster is a member of Sigma Xi and received the Editor's Award in 1953.

❖

W. Welsh was born at Toronto, Can., in 1915. He graduated from the Ottawa Technical High School, after which he opened a radio sales and service business.

W. Welsh

During the war, while with the Royal Canadian Air Force, he was engaged in development work on remotely-controlled communications receivers and carrier-shift teletype.

At the end of the war he resumed his original sales and service business, and has made a specialty of custom television antenna installations.

He is a senior member and a past president of the Ottawa chapter of the Radio

IRE News and Radio Notes

Johnson Receives ESD Outstanding Young Engineer Award

E. Calvin Johnson, electronics research engineer for Bendix Aviation Research Laboratories, has been awarded The Engineering Society of Detroit's annual award to the outstanding young engineer for 1955. Dr. Johnson was presented the award at ESD's 19th annual meeting on June 8. The award is made each year to a young engineer who the Society feels is outstanding not only in his job but in his initiative, background, and "off the job" activities.

Dr. Johnson received the Bachelor's Degree from Georgia Institute of Technology and the Master's and Doctor's degree from M.I.T. His work has been directed toward the development of electronic computors and controls for industrial and military applications.

Joining the Research Laboratories Division, Bendix Aviation Corporation in 1951 as a Senior Engineer, he was later made Project Engineer, and at present supervises a group of engineers as well as being project manager on several other development projects.

Helping to organize the IRE Detroit Chapter, Dr. Johnson was its first chairman. He is also an associate member of the American Institute of Electrical Engineers.

Radio Fall Meeting Schedule

The Radio Fall Meeting schedule has been revised as follows: 1955: October 17–19, Hotel Syracuse, Syracuse, New York. 1956: October 15–17, Hotel Syracuse, Syracuse, New York (originally scheduled for Toronto). 1957: October 21–23, King Edward Hotel, Toronto, Canada. 1958: Exact dates not set, Sheraton Hotel, Rochester, New York.

International College of Surgeons Soon Honor Dr. Alfred N. Goldsmith

The Board of Trustees of the International College of Surgeons has unanimously accorded Alfred N. Goldsmith, Editor Emeritus of the Proceedings Of The IRE, an Honorary Fellowship for his achievements and contribution to science and the welfare of mankind.

The degree and insignia will be conferred on Dr. Goldsmith at the Twentieth Assembly of the United States and Canadian Sections on September 15 in Philadelphia, Pennsylvania.

November Eastern Joint Computer Conference to be Held in Boston, Massachusetts

Computers in business and industrial systems is the theme of the 1955 Eastern Joint Computer Conference and Exhibition to be sponsored by the IRE, American Institute of Electrical Engineers, and the Association for Computing Machinery at the Hotel Statler, Boston, November 7–9.

Technical papers are aimed toward businessmen interested in using electronic computers and clerical machines for payrolls, accounts receivable, inventory problems; to plant engineers interested in using electronic computers to control oil refineries, chemical plants, machine tools, materials-handling equipment; and to engineers and makers of computing and data processing systems and components.

Exhibits will include electronic data processing systems, process control systems, storage systems, input-output equipment, conversion devices, and sensing devices.

Discussing the Symposium on Normal Mode Theory, held July 5–7 at the San Diego Navy Electronics Labora-

Calendar of Coming Events

SRI and Nat. Ind. Conf. Board Symposium on Electronics in Automatic Production, Sheraton-Palace, San Francisco, Calif., Aug. 22–23.

URSI Symposium on Solar Eclipses and the Ionosphere, Royal Society, Burlington House, London, England, Aug. 22–24

IRE-West Coast Electronic Manufacturers' Association WESCON, Civic Auditorium, San Francisco, California, Aug. 24–26

Emporium Section Sixteenth Annual Summer Seminar, Emporium, Pa. August 26–28

Society for Industrial and Applied Mathematics Second General Meeting, U. of Mich. Ann Arbor, Mich., Aug. 30–Sept. 1

IRE-ISA Tenth Annual Instrument Conference, Shrine Auditorium, Los Angeles, Calif., Sept. 12–16

Association for Computing Machinery, Annual Meeting, Moore School of Electrical Engineering, U. of Pa., Sept. 14–16

IRE Professional Group on Nuclear Science—Second Annual Meeting, Oak Ridge National Labs., Oak Ridge, Tenn., Sept. 14–17.

IRE Cedar Rapids Section Symposium on Automation, Cedar Rapids, Ia., Sept. 17

RETMA Automation Symposium, U. of Pennsylvania, Philadelphia, Pa., Sept. 26–27

PG on Vehicular Communications Sixth Annual Meeting, Multnomah Hotel, Portland, Ore., Sept. 26–27

IMSA Annual Convention, Hotel Seneca, Rochester, N. Y., Sept. 26–29

IRE-AIEE Conference on Industrial Electronics, Rackham Memorial Building, Detroit, Michigan, Sept. 28–29

National Electronics Conference, Hotel Sherman, Chicago, Ill., October 3–5

Audio Engineering Society Convention, Hotel New Yorker, New York City, Oct. 12–15

IRE-RETMA Radio Fall Meeting, Hotel Syracuse, Syracuse, N. Y., Oct. 17–19

PG on Electron Devices Annual Technical Meeting, Shoreham Hotel, Washington, D. C., Oct. 24–25

GAMM and NTG-VDE International Conference on Electronic Digital Computers, and Data Processing, Darmstadt, Germany, Oct. 25–27

IRE East Coast Conference on Aeronautical and Navigational Electronics, Lord Baltimore Hotel, Baltimore, Md., Oct. 31–Nov. 1

IRE Kansas City Section Electronics Conference, Kansas City, Kansas, Nov. 3–4

IRE-AIEE-ACM Eastern Joint Computer Conference, Hotel Statler, Boston, Nov. 7–9

IRE-AIEE-ISA Electrical Techniques in Medicine and Biology, Shoreham Hotel, Washington, D. C., Nov. 14–16

IRE-PGCS Symposium on Aeronautical Communications—Civil and Military; Utica, New York, Nov. 21–22

PGI and Atlanta Section Data Processing Symposium, Hotel Biltmore, Atlanta, Ga., Nov. 28–30

SEVENTH REGION TECHNICAL CONFERENCE AND SHOW

Over 1,600 people attended the Annual Seventh Region Technical Conference and Trade Show last April in Phoenix, Arizona. The keynote address was delivered by J. W. McRae while Stephen C. Shadegg of S. K. Research Laboratories spoke at the conference luncheon. Social activities included a ladies' luncheon and fashion show, sight seeing trips, a Wild West Banquet, and Western Party.

Thirty-five technical papers were presented in the following categories: *Engineering Management*, Myrl Stearns, Session Chairman; *Semiconductors*, V. E. Bottom, Session Chairman; *Specialized Components and Measurement Techniques*, T. L. Martin, Session Chairman; *Electron Tubes*, W. C. Carnahan, Session Chairman; *Missile Electronics I*, J. A. Chambers, Session Chairman; *Missile Electronics II*, G. C. Rich, Session Chairman.

In the student paper competition first prize of $75.00 was won by Merlin H. MacKenzie for his paper, "A Portable Instrument for the Study of the Sodium Flash Phenomena." Second prize of $25.00 was won by R. D. Egan for "A Method for Studying the Distribution of Sporadic E Over Short Distances."

This year's conference chairman is Allen M. Creighton while Joseph M. Pettit is Director of the Seventh Region. Committee Chairmen include: Paul W. Sokoloff, *Section Chairman;* William R. Saxon, *Vice-Chairman;* Wallace R. Hitt, *Arrangements Committee;* C. L. McClanathan, *Exhibits Committee;* Norman Fenton, *Facilities Committee;* H. J. Werst, *Publications Committee;* Greg Berens and John Hammond, *Publicity Committee;* C. A. Debel, *Registration Committee;* Virgil A. Cuckler, *Special Events Committee;* V. E. Bottom, *Student Sessions Committee;* R. W. Elsner, *Technical Program Committee;* and Mrs. Fred Dreste, *Women's Activities Committee.*

Stephen Shadegg, of S. K. Research Laboratories, speaker at the Conference luncheon.

C. F. Meyer (*left*), was the Arrangements Chairman and A. M. Creighton acted as the Conference Chairman.

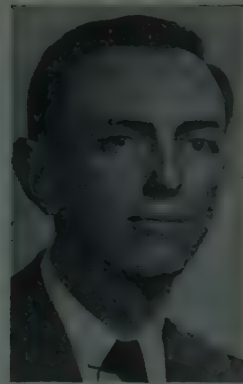

Joseph M. Pettit, Director of the Seventh Region for this year.

Left to right, Virgil E. Bottom, Chairman of the Student Sessions Committee, presents Raymond D. Egan, Stanford U. with the Second Prize Award in the student paper competition. Behind him is Merlin H. MacKenzie of Oregon State College who won first prize. Six papers were presented at the Student Sessions, and Harry E. Stewart, who is Professor of Electrical Engineering at the University of Arizona, presided.

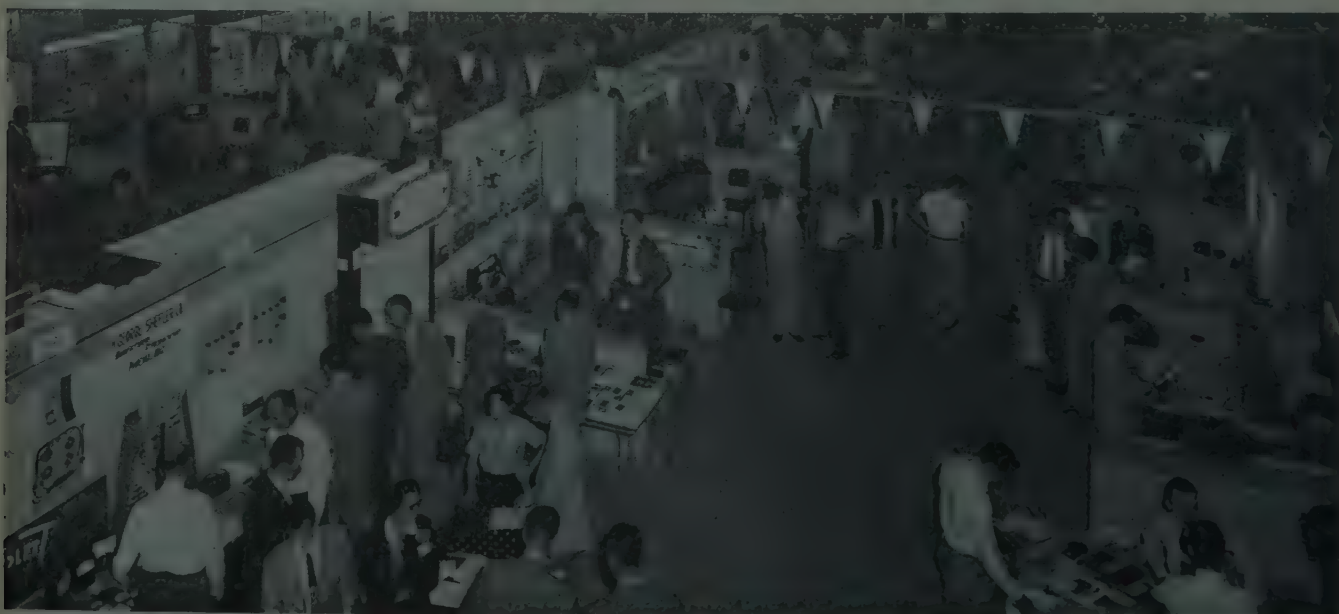

The Seventh Region Trade Show, held in conjunction with the Technical conference, was popular with conference members and visitors. Eighty-three booths were occupied by exhibitors who displayed equipment indicating advances in the electronics industry. Chairman of the Exhibits Committee was George L. McClanathan.

Nuclear Engineering and Science Congress Will Meet This Coming December

U. S. and foreign engineers, representatives from business and technical societies, universities, government bureaus, AEC contractors, and industrial corporations will present nearly 300 papers in 50 sessions covering practically every phase of peacetime uses for atomic energy at the Nuclear Engineering and Science Congress in Cleveland, December 12–16.

Coordinating the arrangements for the Congress is the Engineers Joint Council under the leadership of Thorndike Saville, Dean of the College of Engineering, New York University and President of EJC. Technical sessions will be held at the Cleveland Public Auditorium, while the International Atomic Exposition will be presented in the building's five exhibit halls.

Preliminary plans for the program include speakers and topics covering Canadian, English, Austrialian and South African nuclear developments. England's Harwell project and Atomic Energy of Canada, Ltd., are both represented in the line-up of technical papers. Dr. Katz and E. Paul Lange, EJC Secretary, said the Program Committee had grouped the 292 papers to be presented into 50 general topic headings. Prominent among these session topics are the "where and how" of atomic power plants with emphasis on safety and selection of site; radiation hazards and their controls; pros and cons of the varied proposed power plant types; atomic reactors for research purposes and radiation laboratories; radioisotopes and tracer techniques for industry; medicine and agriculture; disposal of radioactive wastes; what to do about radioactive fall-outs; uranium geology—where uranium is and how to discover it.

Reactor models of the latest design will be shown in the Exposition. Several of these are still undergoing last minute design changes and will be completed only a short time before the Atomic Show opens on December 10. The Atomic Exposition is sponsored by the American Institute of Chemical Engineers and headed by B. F. Dodge of Yale University.

Guests at Frequency Control Symposium Banquet

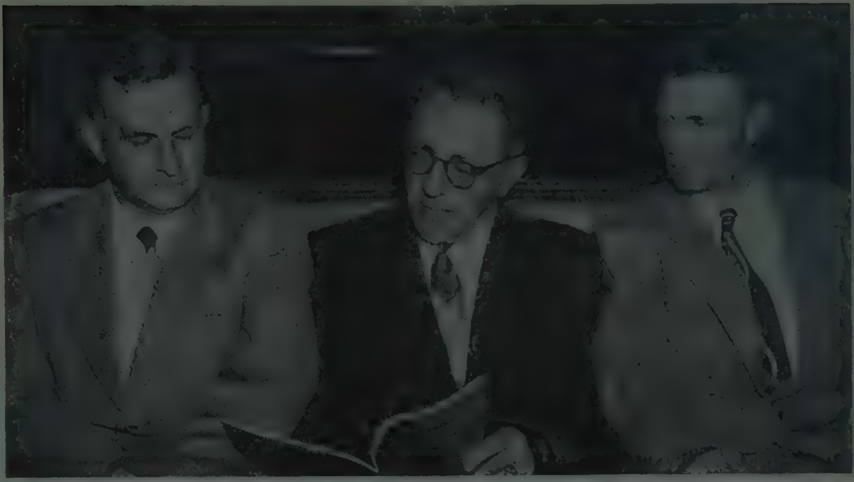

The Frequency Control Symposium, sponsored by Signal Corps Engineering Laboratories of Fort Monmouth, was held recently at Asbury Park, N. J. Shown together at the banquet are (*left to right*): E. A. Gerber, Chief of the Frequency Control Branch; Willy Ley, guest speaker; and Clarence Searls, Director of the Symposium.

Symposium on Reliability and Quality Control in Electronics Will Meet this Winter in Washington

The Second National Symposium on Reliability and Quality Control in Electronics will be held in Washington, D. C., January 9–10, 1956. The symposium will be sponsored by the PG on Reliability and Quality Control, American Society for Quality Control, and Radio Electronic Television Manufacturer's Association.

"A Progress Report on Reliability" is the theme of the symposium which will include four formal sessions, two panels, and two luncheons.

J. W. Greer, Bureau of Ships in Washington D. C., is General Chairman of the symposium while F. W. Weiland, Inspector of Naval Material in Baltimore, is Co-Chairman. Other chairmen include: D. A. Hill, Program Chairman; J. Dorfman, Chairman of Moderators; F. R. Stansel, Finances Chairman; A. Warsher, Speakers' Hospitality Chairman; V. Wouk, General Publicity and Advance Registration; A. F. Cone, West Coast Publicity; and P. K. McElroy, Transactions Chairman.

D. A. Hill to be Program Chairman

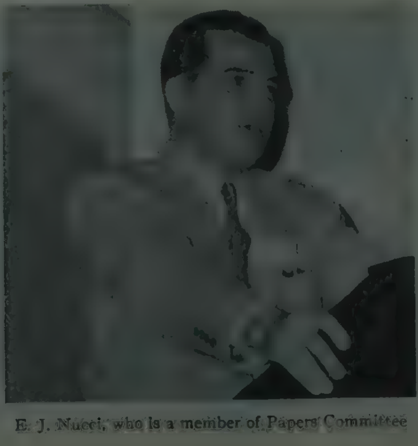

E. J. Nucci, who is a member of Papers Committee

Conference on Electrical Insulation to Meet in October at Pocono Manor, Pennsylvania

The annual meeting of the Conference on Electrical Insulation will be held at Pocono Manor Inn, Pocono Manor, Pa., October 17–19. For those planning to attend the conference reservations may be made directly with the inn.

The Chairman of the Program Committee for this year's meeting is Harry A. Sharbaugh, General Electric Company, P. O. Box 1088, Schenectady, New York. Those interested in presenting papers at the meeting may submit titles and abstracts to Dr. Sharbaugh not later than August 15. The committee urges that papers be submitted well in advance of the deadline. In addition to the brief abstract, a summary of the paper should be prepared for inclusion in the Annual Report. This summary, two to four double spaced typewritten pages long, plus a few figures if needed, should be in the hands of the Program Chairman not later than the meeting date which is October 17.

Round table discussions are being planned on subjects chosen to give a well rounded program for the meeting as a whole. Suggestions for topics may be sent to Dr. Sharbaugh. A new feature at this year's meeting will be the presentation of of the first J. B. Whitehead Memorial Lecture. This lecture will be a part of the technical program and the lecturer, to be chosen by the Executive Committee, will be announced later.

Members of the conference will receive the *Annual Report and Digest of Literature on Dielectrics* and will pay a $5.00 fee either at the meeting or by mail to the National Research Council. Non-members attending the meeting will pay a $3.00 registration fee but will not receive the publications. It has been announced that no registration fee will be required of students attending the meeting but not wishing the publications.

IRE and WCEMA to Sponsor WESCON this August

Noel Porter

Albert Morris

Donald Harris

Shouldering the burden of organizing this year's WESCON is a board of directors working under the chairmanship of Noel E. Porter of the Hewlett-Packard Company of Palo Alto. Other members of the board are Donald B. Harris, Stanford University, *Convention Vice-Chairman;* Norman H. Moore, Litton Industries, *Show Vice-Chairman;* Walter E. Noller, Lynch Carrier Systems, Inc., *Secretary-Treasurer;* W. D. Hershberger, College of Engineering, University of California at Los Angeles; C. Frederick Wolcott, Gilfillan Brothers, Inc; Thomas P. Walker, Triad Transformer Corporation; and Leon B. Ungar, Ungar Electric Tools, Inc. Business Manager is Mal Mobley, Jr., and the Chairman of the San Francisco Section is Albert Morris.

General MacArthur Will Open WESCON from N. Y. This Month

General Douglas MacArthur, Chairman of the board of directors of Remington-Rand, will officially open WESCON, in San Francisco, on August 24. Speaking from his headquarters in New York before television and news reel cameras, the General will discuss the role of electronics in the nation's economy, stressing in particular WESCON's contributions to the industry and the historical background of electronics in the San Francisco Bay Area.

Following the General's nation-wide remarks, and after he has signaled, by remote control, the opening of the Show and Convention, Elmer E. Robinson, Mayor of San Francisco, speaking over TV-telephone, will thank the General for his participation. This will be the first public demonstration of the TV-telephone communication system. It will be in operation between the city's Civic auditorium, Show headquarters and the Fairmont Hotel, where convention activities will be centered. Radio, television, industry, and newspaper representatives, who will be invited to participate, will not only see the image of the person to whom they are talking on the screen, but also one of themselves.

E. W. Engstrom, Executive Vice-President of research and engineering for RCA and IRE Fellow, will deliver the major address at WESCON's All-Industry Luncheon, on Friday, August 26. Other features of the luncheon will be the appearance of Bernard M. Oliver of the Hewlett-Packard Company as toastmaster, the introduction of leaders of the IRE and WCEMA, the presentation of the Annual Achievement Award of the Seventh Region and the announcement of WCEMA scholarship winners. The Show and Convention, which is expected to attract some 20,000 people, will be held August 24–26. Convention activities will feature a technical program consisting of 160 papers and 32 technical sessions, field trips, All-Industry Cocktail Party and Women's Activities. The Show itself will consist of more than 580 exhibits, representing the products of more than 650 manufacturers, and will be the largest in the history of WESCON,

A complete schedule of field trips has been announced by Noel E. Porter, WESCON Chairman. The program was arranged by W. M. Silhavy and Jack Ingersoll, co-chairmen of the WESCON field trips committee. During the afternoon of the opening day, August 24, there will be a tour of the Scientific Division of Beckman Instruments, Inc. In the evening, visitors will see the University of California Radiation Laboratory in Berkeley. On Thursday, WESCON visitors will be welcomed to Eitel-McCullough during the morning. In the afternoon, they will visit the Ampex Corporation. The Stanford Research Institute in Palo Alto will be opened on Friday morning. A tour of the Hewlett-Packard plant will be made Friday afternoon.

Time and Motion Study and Management Clinic to Meet

The Nineteenth Annual Time and Motion Study and Management Clinic, sponsored by the Industrial Management Society, will be held November 9–11 at the Sherman Hotel, Chicago. More than 2,000 are expected to attend.

Inquiries may be addressed to the Industrial Management Society, 35 East Wacker Drive, Chicago 1, Illinois.

Chicago Host to International Automation Exposition

The potentialities of automation will be studied at close range at the Second International Automation Exposition, in the Chicago Navy Pier, November 14–17. Since automatic production has developed far beyond application to single pieces of equipment, the equipment on display indicates the possibilities of applying automatic production to plant and lab operations.

The Second International Automation Exposition also will provide an opportunity for manufacturers of instruments and devices for measurement, analysis, inspection, testing, computing, and automatic control to display latest advances.

Copies of the floor plan may be obtained from the Exhibit Director of the Second International Automation Exposition, 845 Ridge Avenue, Pittsburgh 12, Pa.

Eight Members of Buffalo Section Visit Air Development Center at Griffiss AFB

The Buffalo Section recently toured the Rome Air Development Center. Shown here are (*left to right*): C. J. Borkowski, Morris Handelsman, Chief of the Rome Radar Lab., G. F. Buranich, Walter Tanner, W. L. Kinsell, E. L. Price, E. F. Clune, N. A. Champness, H. W. Kasper, and Ernest Storrs, Chief of the Navigation Lab.

Banquet Marks Section Status of Northwest Florida

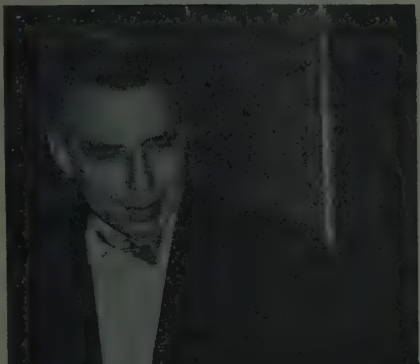

The Northwest Florida Subsection, which recently achieved Section status, celebrated the occasion with a charter meeting and banquet. Harry W. Wells, Director of the Southeastern Region, greeted the new Section at the dinner meeting which was held at the Shoreline Hotel in Silver Beach, Florida. He remarked on the extent and intensity of the technical effort going on in the area between Tallahassee and the Alabama line and congratulated the Armament Center on the progress being made in development testing of all Air Force armament.

Brigadier General Edward P. Mechling, Commander of the Air Force Armament Center at Eglin Air Force Base, also spoke to the 82 Section members and their guests. Active in support of the IRE in the Northwest Florida area, General Mechling spoke to the diners on the importance of professional activity to major engineering efforts.

Prior to the banquet General Mechling invited Mr. Wells to tour the technical facilities of the Armament Center. Attractions of the tour were the new million dollar, high-speed, electronic computer installation and its central time signal system. The visitors also saw several armament test range installations and were briefed on the instrumentation development program.

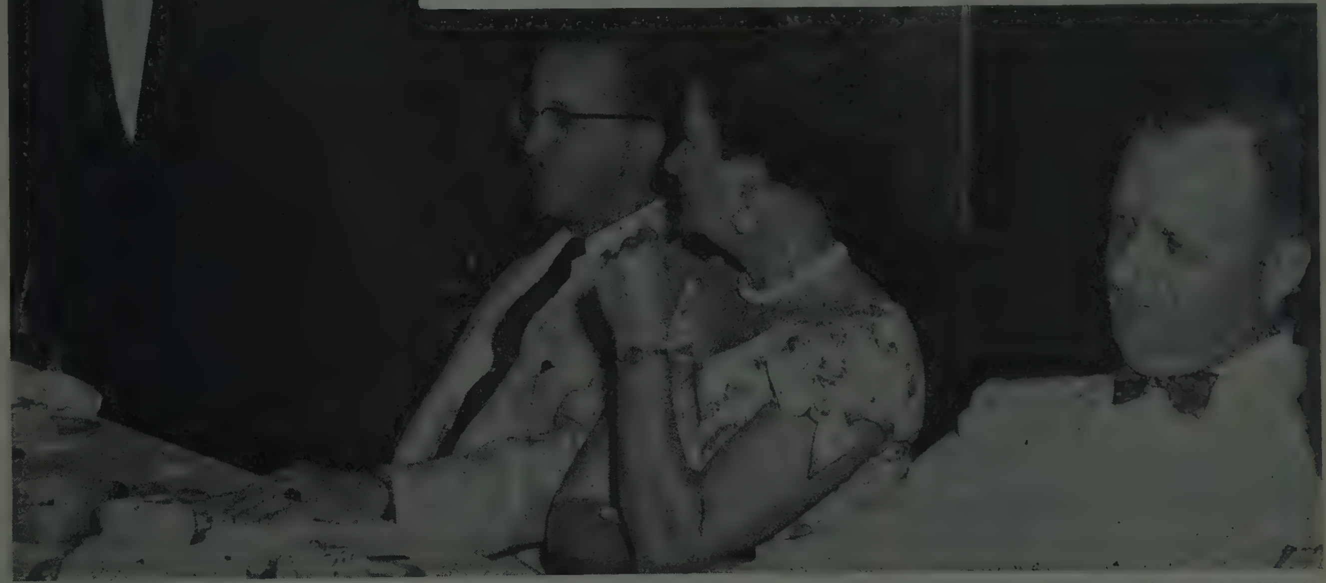

Harry W. Wells, *far left*, Director of the Southeastern Region, welcomes the new Northwest Florida Section at the Charter Banquet. On his left are Kenneth Huntley, Chairman of the Section and a senior engineer of the Air Force Armament Center, and Mrs. Huntley. Next is Brigadier General P. Mechling, Commander of the Air Force Armament Center. The Charter Meeting was held as a dinner with the Armed Forces Communication and Electronics Association, Eglin Chapter.

November 4 Deadline for 1956 IRE Convention Papers

Prospective authors should submit the following: a 100 word abstract, in triplicate, including title of paper, name, and address; a 500 word summary in triplicate, including title of paper, name, and address. Please indicate the field in which the paper falls: Aeronautical and Navigational Electronics, Antennas and Propagation, Audio, Automatic Control, Broadcast and Television Receivers, Broadcast Transmission Systems, Circuit Theory, Communications Systems, Component Parts, Electron Devices, Electronic Computers, Engineering Management, Industrial Electronics, Information Theory, Instrumentation, Medical Electronics, Microwave Theory and Techniques, Nuclear Science, Production Techniques, Reliability and Quality Control, Telemetry and Remote Control, Ultrasonics Engineering, Vehicular Communications.

Send material to Russel R. Law, 1956 Technical Program Committee, IRE, 1 East 79 St., N. Y. 21, N. Y.

Broadcast Symposium to be Held this September in Washington

The Fifth Annual Broadcast Symposium of the PG on Broadcast Transmission Systems will be held in Washington, D. C. on September 23 and 24. The technical program will be built around new techniques in the field of broadcasting. In standard broadcasting attention will be directed toward remote control of directional antenna systems and automatic programming practices. In FM broadcasting, new trends in multiplexing will be examined with the accent on operational experience. In television the latest features in color programming, lighting, and higher power transmitting equipment will be the subject of papers and discussion.

A banquet will be held on Friday evening, September 23 and speakers discussing, "Whither UHF and the VHF-UHF TV Allocation Structure," will be guests of the evening.

Sessions will be held in the Hamilton Hotel, 14th and K Streets, N.W. Washington, D. C. and registration will be $2.00. Advance reservations for the banquet will be requested by September 15th.

Deadline for submission of papers is August 15. Chairman of the Steering Committee is Oscar Reed, Jr., new Chairman of the Administrative Committee of the PGBTS. Ralph N. Harmon is Chairman of the Technical Program Committee, and Lewis Winner is Chairman of the Papers Review Committee.

Detroit Site for Conference on Industrial Electronics

A Conference on Industrial Electronics will be held in Detroit, Michigan, September 28–29. It will be sponsored by the American Institute of Electrical Engineers and the IRE Professional Group on Industrial Electronics. Some 300 engineers will gather in Detroit during the two-day session to discuss automation, industrial measurement problems, and new control system applications. A total of sixteen papers have been tentatively scheduled for the four technical sessions to be held in the Engineering Society of Detroit Auditorium.

Co-chairmen of the conference are S. Sterling of S. Sterling Company and H. S. Mika of Ford Motor Company. Official convention headquarters will be

Continued on page 1026

the Park Sheraton Hotel and G. N. Gerrara, 8106 West Nine Mile Road, Oak Park 37, Michigan, is Chairman of the Hotel and Registration Committee. The registration fee will be $3.00 and all registrants will receive copies of the *PGIE Transactions*.

OBITUARY

Francis J. Brott, Director of Engineering for KOMO Radio and KOMO-TV, died recently. Mr. Brott was Chief Engineer for KOMO, Fisher's Blend Station, Inc., the Seattle NBC Affiliate Station, since it was organized in 1926; he became Director of Engineering for both KOMO Radio and KOMO-TV in November, 1952.

Becoming interested in radio during a visit to the 1915 World's Fair, he obtained his first amateur license in 1916. Starting with amateur call 7ED, he has operated on 7AD, licensed in 1919, 7XS in 1922–23, and W7NK, his present call. Five of the original broadcast station transmitters in the Pacific Northwest were built by him, as well as two early broadcast stations, KFIY and KGCL, which were built, owned and operated by him in Seattle.

In 1920 over amateur station 7AD using an Edison cylinder phonograph and telephone microphone, he was the first to broadcast music. In 1921 Mr. Brott became Seattle's first radio announcer on 7AD.

On June 3, 1929 he broadcast the first television pictures ever seen in Seattle.

As Chief Engineer for KOMO, he installed the original 1000 watt transmitter at Fisher Flouring Mills in the fall of 1926, and has designed and built many of KOMO's technical facilities during the past 28 years. A new 5000 watt transmitter installation was supervised by Mr. Brott in 1936. Four complete studio installations have been made during his tenure at KOMO, including a $1,000,000 six-studio plant, the present 50 kw transmitter and directional antenna system installed on Vashon Island, and the new KOMO-TV studios and transmitter.

TECHNICAL COMMITTEE NOTES

The **Antennas and Waveguides** Committee met at IRE Headquarters on May 11 with H. Jasik presiding. A motion expressing the appreciation of the committee for the efforts and leadership of the outgoing chairman, Phillip H. Smith, was unanimously passed. There was a brief review of the subcommittee structure. Subcommittee 2.4 on Waveguide and Waveguide Component Measurements presented drafts of material for *Methods of Measurements*, comprising discussions on Measurement of Delay Time, Measurement of Power Handling Capacity, and Measurement of Q.

D. E. Maxwell presided at the **Audio Techniques** Committee meeting at IRE Headquarters on May 24. The Proposed *Standard on Audio Systems and Components Methods of Measurement of Gain, Loss Amplification, Attenuation and Frequency Response* was approved by the committee.

The **Facsimile** Committee met at the Times Building on May 20 with Chairman K. R. McConnell presiding. The major portion of the meeting time was spent rechecking the *Proposed Standards on Facsimile: Definitions of Terms*.

J. E. Ward presided at a meeting of the **Feedback Control Systems** Committee at the MIT Faculty Club on May 10. The committee discussed the establishment of Subcommittee 26.2 on Methods of Measurement for Feedback Control Systems. The major part of the meeting was occupied by a discussion of the work to be done by the new subcommittee; the scope and suggested initial procedure of the sub were established.

The **Radio Frequency Interference** Committee met at IRE Headquarters on May 19 with R. M. Showers, the Chairman, presiding. The committee discussed at length the work that had been done on interference in Europe and in other organizations, after which there was a detailed report of the work being done by the subcommittees under the Radio Frequency Interference Committee.

Books

Circuits and Networks by Glenn Koehler

Published (1955) by the Macmillan Co., 60 Fifth Ave., N. Y., N. Y. 336 pages+5 page index+x pages. Illus. $9\frac{1}{4} \times 6\frac{1}{4}$. $6.50.

This text, which is intended for a one-semester course for students who are already familiar with ac circuit theory, discusses many of the important topics in network analysis and also certain selected topics in network synthesis. The scope of the book is evident from the chapter titles, which follow: "Methods for Analyzing and Solving Circuits and Networks," "Network Theorems," "Properties of Simple Frequency-Selective Circuits," "Coupled Circuits," "Four-Terminal Network Analyses and Impedance Matching," "Filters, Attenuators and Equalizers," "Transmission-Line Parameters," "Transmission Line Analysis," "High Frequency Transmission Lines," "Transformers and Reactors." Evidently none of the topics can be accorded a comprehensive treatment, and have the book stay within the time objectives of the author. One has the feeling throughout that the treatments are just barely adequate.

There are many places where this reviewer takes issue with the author, sometimes on philosophical grounds, often on technical grounds. Some examples follow. In Chapter One where Phasor Algebra is introduced, sinusoids are discussed as conjugate rotating phasors, and it is these time dependent functions which are called phasors, and are later written as complex numbers which are not functions of time. Likewise phasor impedance, a quantity that is independent of the time, is also written as a complex number. The significance of the complex number in network analysis is never adequately discussed.

The discussion of the node analysis in circuit theory is quite inadequate. Moreover, the entire concept of duality, which follows naturally from a critical examination of the mesh and the node analyses, is not mentioned. The relation between dual and inverse networks is similarly missing. Moreover, the discussion in Chapter Six on filters proceeds without any indication of the importance of inverse networks in filter theory. An introduction to inverse networks does appear in Chapter Seven.

The discussion of magnetic coupling in Chapter Four, and the subsequent considerations in Chapter Eleven, leaves much to be desired. The analysis of the transformer in terms of self- and mutual-inductance is included, but even when the commercial power transformer is discussed in Section 11-8, no mention is made of the "machinery" analysis of transformers, nor of the relation between the "networks" and the "machinery" analyses of such a device.

The author, in his discussion of transmission lines in Chapter Nine and Ten, overlooks a number of important features of transmission lines. He fails to point out the relation of the phasor diagrams which show the composition of the potential or current at any point on the line in terms of the logarithmic spirals representing the incident and reflected components, and the standing wave distribution on the line. The standing wave ratio of potential or current of the lossless line and the location of the maxima and minima are obtained directly from an inspection of the phasor diagrams, which become ellipses in this case. It is felt, in fact, that too little emphasis has been given to the traveling waves on the line, and their relation to the resulting standing waves that exist.

Despite the detailed criticisms that can be made of the text, the topical coverage is generally satisfactory. Further, in view of the one-semester course objective of the text, the author has achieved a considerable measure of success in meeting this objective.

SAMUEL SEELY
Syracuse University
Syracuse, New York

Handbook of Piezoelectric Crystals for Radio Equipment Designers by John P. Buchanan

Published (1954) by Office of Technical Services, U.S. Dept. of Commerce, Washington, D. C. 524 pages+8 page index+iv pages. Illus. $8\frac{1}{2} \times 10\frac{1}{2}$. PB-No. 111586.

This handbook combines under one cover an unusually complete treatise on the origin, development, and application of piezoelectric elements for stabilized frequency control. It should be of equal value both for military and commercial applica-

tions, to the crystal engineer and to the crystal manufacturer. The specifications of many standardized and popular types of crystal units, both with and without temperature control, are described in detail, together with typical using circuits. As stated in the introduction, "The purpose of this manual is to provide the design and development engineer of military electronic equipment with a reference handbook containing background material, circuit theory, and components data related to the application of piezoelectric crystals for the control of radio frequencies."

The volume includes a factual account of the early discoveries of piezoelectric properties, with the subsequent developments which led to achieving the present degree of stabilized frequency control. This historical account is presented in a most entertaining manner with illustrations and diagrams which add to one's interest and comprehension of the text.

Although this book does treat thoroughly the mathematical analysis of piezoelectric elements and their associated circuits, it is not overburdened with highly technical data, thus enhancing its value to all classes of personnel associated with the crystal industry.

In our opinion, those who have so successfully contributed to the contents and authenticity of this handbook are to be congratulated on a very valuable and complete publication, one which fully satisfies an urgent need existing for many years. The painstaking care and thought which have gone into its preparation are illustrated by the very complete alphabetical index covering 8½ pages, the 883 bibliographical references and 5 full pages of manufacturer's crystal unit designations and related frequency control items. We strongly recommend this handbook to every student both as a text book of piezoelectricity and a reference manual for standardized types of crystal units with recommended using circuits, to every student of crystallography.

E. M. Washburn
RCA Victor
Camden, N. J

Abstracts of Transactions of the I.R.E.

The following issues of "Transactions" have recently been published, and are now available from the Institute of Radio Engineers, Inc., 1 East 79th Street, New York 21, N.Y. at the following prices. The contents of each issue and, where available, abstracts of technical papers are given below.

Sponsoring Group	Publication	Group Members	IRE Members	Non-Members*
Vehicular Communications	PGVC-5	$1.50	$2.25	$4.50

*** Public libraries and colleges may purchase copies at IRE Member rates.**

Vehicular Communications
PGVC-5, June, 1955

Management of Communications in Industry—J. G. McKinley

The Communications Engineer's Role in American Railroading—J. N. Albertson

A Multichannel Crystal Oscillator—Alwin Hahnel

City of Houston Vehicular Communications System—R. D. Thornton

This paper is a general description of the radio communications system being used by the City of Houston, Texas. As early as 1926, the first experiments in the use of radio for police work in Houston made use of a commercial broadcast station, which interrupted regular programs when necessary. Today, communications and electronic work for most city departments is done by this agency, although the division is a section of the Police Department. The operation of three FM transmitters and receivers into a single antenna, and the problems encountered with intermodulation are outlined.

A Communications Consulting Engineer's Notebook—V. J. Nexon

The Operational Fixed Microwave Council—C. D. Campbell and J. E. Keller

Mobile Radio Changes the Pace of the Nation—Merle E. Floegel

The purpose of this paper is to direct attention to the many uses of radio communication systems, some of them unusual and seldom heard of, and to show how organizations, through the use of radio, are better able to coordinate their activities and thus provide a quicker more efficient service to the public.

Radio Equipment Which Meets the Challenge of 6 and 12 Volt Vehicles—K. E. H. Backman

Design, Installation and Maintenance of 1,000 Unit Base-Mobile System—J. S. Stover

License or License—Edwin L. White

A Three Channel Common Carrier Radio Mobile System to Serve Industry—D. R. Gehrig

To show the Communication Engineer's role in American Industry, an example is made of the engineering, installation and maintenance of a three-frequency mobile system covering the oil basin of Indiana, Illinois and Kentucky. In this instance, the so-called "Tri-State" Mobile Telephone System, it was first necessary to determine the Industry's communication needs; analyze these data, manufacture specific equipment, establish transmitter sites and control points and set up traffic handling procedures.

The need for the system was two-fold. An area adjacent to an existing general highway mobile cell needed to be covered and the existing cell was overloaded. Another cell on the same frequency would only aggravate conditions in the overloaded portion. The new "Tri-State" system was devised so that each of nine base stations operated on one of three frequencies. Since, at the time the system was being engineered, there were no three-frequency mobile units available, a special set had to be designed and manufactured to meet the requirements of the system. Co-channel overlap was alleviated in this system by making no adjacent cells operate on the same frequency. The customer was required to select the right channel as he moved across the area.

Studies made of actual results indicate that more traffic is being handled per station in this system than in the usual area coverage (highway) system. Only through cooperation of user, manufacturer and supplier together with their engineers could an adequate system have been provided.

Effect of Front End Receiver Design on Over-All Performance—A. G. Manke

Front end receiver selectivity is defined as the selectivity preceding the second converter in communications receivers. The effects of high IF and RF selectivity are analyzed separately to show how receiver performance suffers or is improved as each of these selectivities are varied for a given set of conditions in the low IF amplifier. The minimum selectivity each of these amplifiers must have, in order to obtain a specific spurious response ratio in the first and second converter, is explained. Also discussed are the effects of gain vs. selectivity in the front end for adjacent and off-channel performance on desensitization, and the limits of improvement on desensitization of receivers with respect to transmitter noise. Intermodulation and gain in the RF amplifier is considered for threshold intermodulation, and also for high level intermodulation. The use of cavities and other methods for the elimination of intermodulation is considered, and the effects of these measures on system performance are compared.

A Squelch System Controlled by Signal-to-Noise Ratio—W. G. Klehfoth

Since the quality of communications is a function of signal-to-noise ratio, it follows that a squelch system will perform its intended function more proficiently if it operates directly as a function of this ratio. The threshold of operation of the commonly used carrier-operated system varies widely with changes in ambient noise conditions and receiver gain. This squelch system overcomes these objections to the carrier-operated squelch and may also prove useful for suppressed carrier systems. Formulas applicable to circuit operation and practical circuitry which will provide consistent operation for signal plus noise to noise ratios as low as 2 db are given. Results of field tests are also included.

Vehicular Radio Station Inspections—S. W. Norman

Of Communications Engineers, Mobile Radio, Management and Sealing Wax—Jeremiah Cortney

Abstracts and References

Compiled by the Radio Research Organization of the Department of Scientific and Industrial Research, London, England, and Published by Arrangement with that Department and the *Wireless Engineer*, London, England

NOTE: The Institute of Radio Engineers does not have available copies of the publications mentioned in these pages, nor does it have reprints of the articles abstracted. Correspondence regarding these articles and requests for their procurement should be addressed to the individual publications, not to the IRE.

The number in heavy type at the upper left of each Abstract is its Universal Decimal Classification number and is not to be confused with the Decimal Classification used by the United States National Bureau of Standards. The number in heavy type at the top right is the serial number of the Abstract. DC numbers marked with a dagger (†) must be regarded as provisional.

The Index to the Abstracts and References published in the PROC. I.R.E. from February, 1954 through January, 1955 is published by the PROC. IRE, April, 1955, Part II. It is also published by *Wireless Engineer* and included in the March, 1955 issue of that journal. Included with the Index is a selected list of journals scanned for abstracting with publishers' addresses.

ACOUSTICS AND AUDIO FREQUENCIES

534.2:551.510.52 1846
Sound Propagation into the Shadow Zone in a Temperature-Stratified Atmosphere above a Plane Boundary—D. C. Pridmore-Brown and U. Ingard. (*Jour. Acous. Soc. Amer.*, vol. 27, pp. 36–42; January, 1955.) "The sound field in the 'shadow zone' (diffraction region) formed over a plane boundary in an atmosphere with a constant vertical temperature gradient is analyzed both theoretically and experimentally."

534.232:546.431.824–31 1847
On the Contribution of a Contained Viscous Liquid to the Acoustic Impedance of a Radially Vibrating Tube—D. H. Robey. (*Jour. Acous. Soc. Amer.*, Vol. 27, pp. 22–25; January, 1955.) Theoretical investigation of cylindrical $BaTiO_3$ transducers for use in fluids. Equations are derived expressing the impedance presented to the cylinder by the contained liquid and the resonance frequencies for longitudinal and coupled radial vibrations for a nonviscous liquid.

534.26+538.566:535.42 1848
Green's Functions for the Cylinder and the Sphere—Franz. (*See* 1955.)

534.322.1 1849
Audibility Limits for Nonlinear Distortion in the Transmission of Instrumental Music—G. Gässler. (*Frequenz*, vol. 9, pp. 15–25; January, 1955.) Theoretical and experimental investigations are reported, consideration being confined to instruments producing sounds with harmonically related components. The levels at which nonlinear distortion becomes audible are shown in loudness contour diagrams for various combinations of tones.

534.614–8:621.372.552 1850
Novel Uses of the Ultrasonic Light Cell—N. B. Terry, H. Mumford and D. G. Halloway. (*A.T.E. Jour.*, vol. 11, pp. 2–16; January, 1955.) Experiments are described which demonstrate the use of an ultrasonic light cell as filter and as a waveform corrector of the type described by Linke (1178 of 1953). A method of measuring the wave velocity of a modulated ultrasonic wave in liquids is discussed.

534.75 1851
Perstimulatory Auditory Fatigue for Continuous and Interrupted Noise—E. C. Carterette. (*Jour. Acous. Soc. Amer.*, vol. 27, pp. 103–111; January, 1955.)

534.75 1852
Perstimulatory Fatigue as Measured by Heterophonic Loudness Balances—J. P. Egan. (*Jour. Acous. Soc. Amer.*, vol. 27, pp. 111–120; January, 1955.)

534.75 1853
Influence of Stimulus Duration on the Pure-Tone Threshold during Recovery from Auditory Fatigue—J. F. Jerger. (*Jour. Acous. Soc. Amer.*, vol. 27, pp. 121–124; January, 1955.)

534.75 1845
Channels of Reception in Pitch Discrimination—A. G. Pikler and J. D. Harris. (*Jour. Acous. Soc. Amer.*, vol. 27, pp. 124–131; January, 1955.) Experiments are reported indicating that, for subjects with normal hearing, the degree of pitch discrimination is the same for both ears, for binaural hearing, and for bone conduction.

534.75 1855
Pitch Perception for Certain Periodic Auditory Stimuli—W. R. Thurlow and A. M. Small, Jr. (*Jour. Acous. Soc. Amer.*, vol. 27, pp. 132–137; January, 1955.) Report of experiments on the perception of pitch with pulsed tones.

534.78 1856
Transmission of the Vocal Cavities—J. van den Berg. (*Jour. Acous. Soc. Amer.*, vol. 27, pp. 161–168; January, 1955.) "The transmission of the vocal cavities has been determined for eleven cardinal vowels of the I.P.A., using a hemilaryngectomized subject. A special throat loudspeaker with pick-up was constructed and was fitted in the throat of the subject, leaving a gap beneath it for normal breathing."

534.78 1857
Imitation of Dutch Vowels and Words by a Hemilaryngectomized Subject using a Throat Loudspeaker as a Pseudolarynx—J. van den Berg. (*Jour. Acous. Soc. Amer.*, vol. 27, pp. 169–172; January, 1955.)

534.78 1858
As Instantaneous Pitch-Period Indicator—L. O. Dolanský. (*Jour. Acous. Soc. Amer.*, vol. 27, pp. 67–72; January, 1955.) Circuit arrangements for analyzing speech sounds are discussed. Marker pulses derived from the speech waveform are used to indicate the beginnings of the individual pitch periods.

534.845 1859
A Tentative Method for the Measurement of Sound Transmission Losses in Unfinished Buildings—A. C. Raes. (*Jour. Acous. Soc. Amer.*, vol. 27, pp. 98–102; January, 1955.) An arrangement for testing the transmission properties of a wall under construction comprises a loudspeaker distant at least 6 feet from the wall and a microphone close to each side of the wall. Pure tones with exponentially increasing or decreasing amplitude are used. Results of measurements are reported for several types of construction.

621.395.623.64 1860
Factors determining the Sound Attenuation produced by Earphone Sockets—J. Zwislocki. (*Jour. Acous. Soc. Amer.*, vol. 27, pp. 146–154; January, 1955.) Discussion of the design of earphone sockets to attenuate extraneous noise as far as possible without unduly reducing the transmission of sound from the earphone to the ear. Experiments indicate that for frequencies below 700 cps the mass of the system and the impedance of the flesh under the earphone cushion are the limiting factors; for frequencies above 700 cps bone conduction is the determining factor.

621.395.623.64 1861
Development of a Semiplastic Earphone Socket—J. Zwislocki. (*Jour. Acous. Soc. Amer.*, vol. 27, pp. 155–161; January, 1955.) A headphone design combining comfort with high attenuation of extraneous noise is described.

621.395.623.7 1862
Theater Loudspeaker System incorporating an Acoustic-Lens Radiator—J. G. Frayne and B. N. Locanthi. (*Jour. Soc. Mot. Pic. Telev. Eng.*, vol. 63, pp. 82–85; September, 1954. Discussion, p. 85.) Description of a loudspeaker with uniform distribution up to high frequencies over a wide horizontal angle, as required for the presentation of stereophonic sound. The radiator comprises arrays of elements similar to those used in microwave lenses, as discussed by Kock and Harvey (5 of 1950).

621.395.625.3 1863
'Wow' in Sound Reproduction Systems—C. B. Sacerdote, M. Caciotti and G. Sacerdote. (*Onde Élect.*, vol. 35, pp. 62–70; January, 1955.) Magnetic systems are considered. Wow and flutter are defined and methods of measurement described. Mechanical properties of

tapes are discussed. Subjective tests of the threshold of perception for wow are mentioned. The effects of re-recording are examined.

621.395.625.3(083.74) 1864
Absolute Measurement of Signal Strength on Magnetic Recordings—R. Schwartz, S. I. Wilpon and F. A. Comerci. (*Jour. Soc. Mot. Pic. Telev. Engr.*, vol. 64, pp. 1–5; January, 1955, Discussion, p. 5.) The method under development involves the use of a nonmagnetic loop to determine the absolute surface induction at 400 cps. This single absolute measurement is then related to the corresponding relative surface-induction measurement, which is one of a series made over a range of frequencies up to about 6 kc.

ANTENNAS AND TRANSMISSION LINES

621.315.212:621.397.7 1865
Color-Television Coaxial Cable Termination and Equalization—W. B. Whalley. (*Jour. Soc. Mot. Pic. Telev. Eng.*, vol. 64, pp. 8–12; January, 1955.) "This paper describes (a) the development of multi-element terminations to match the variation of cable impedance with frequency, (b) the design of networks to compensate for amplifier input capacitance, and (c) the provision of precise amplitude equalizers to compensate for cable attenuation."

621.315.212:621.397.7:621.317.3 1866
Evaluation of Pulse-Reflection Curves for determining the Length and True Magnitude of Inhomogeneities in Wide-Band Cables—Krügel. (*See* 2052.)

621.372:621.315.6 1867
Investigations on Dielectric Waveguides in Rod or Tube Form—P. Mallach. (*Fernmeldetech. Z.*, vol. 8, pp. 8–13; January, 1955.) Waveguides excited in an HE_{11} mode are investigated. The phase constant, attenuation, and spread of the external field are calculated for dielectrics with permittivity about 1.3, and the maximum concentration of field obtainable is estimated. Results obtained by direct measurement of the field are presented graphically, and suggestions are made for the design of low-loss supports for tubular waveguides.

621.372.8 1868
Propagation of Microwave through an Imperfectly Conducting Cylindrical Guide filled with an Imperfect Dielectric—S. K. Chatterjee. (*Jour. Indian Inst. Sci.*, Section B, vol. 37, pp. 1–9; January, 1955.) General expressions are derived for the attenuation and phase constants for the hybrid wave EH_{11}.

621.372.8 1869
Transformation of a Frequency Equation in Corrugated-Wave guide Theory—C. C. Grosjean. (*Nuovo Cim.*, vol. 1, pp. 174–192; January 1955. In English.) A procedure is described for simplifying the equation given by Walkinshaw (177 of 1949).

621.372.8 1870
Experimental Verification of a Frequency Equation for Corrugated Waveguides—C. C. Grosjean and V. J. Vanhuyse. (*Nuovo Cim.*, vol. 1, pp. 193–200; January 1, 1955. In English.) To verify the accuracy of the theory given by Grosjean (1869 above), measurements were made of the resonance frequency of a terminated iris-loaded guide, for various values of guide diameter and iris diameter. Explanations are advanced for discrepancies noted.

621.372.8:537.226 1871
Problems of Propagation in Cylindrical Systems—M. Jouguet. (*Câbles B Trans.*, vol. 9, pp. 3–39; January, 1955.) General formulas are derived and are applied to the particular cases of (a) imperfectly conducting circular waveguide, (b) infinite wire conductor supporting surface waves, and (c) hollow dielectric cylinders; analysis indicates that in case (c) no wave can propagate. (EH) modes in two-dielectric lines are investigated; the $(EH)_{1,0}$ mode may have any frequency. See also 964 of 1954.

621.396.67 1872
The Skeleton Slot Aerial System, Designs for H.F. and V.H.F. Applications—B. Sykes. (*Short Wave Mag.*, vol. 12, pp. 594–598; January, 1955.) For hf, with purely resistive 500-Ω feed, design specifications given are: length /width ratio 3:1; ratio of width to conductor diameter 32:1; length of sides 0.56 λ. An antenna for 18.5 mc covers the 14–22-mc band when tuned feeders are used; minimum conductor diameter is 1 inch. Dimensions for bands between 7 and 44 mc and between 115 and 530 mc are listed. λ/4-stub matching is necessary in vhf designs; optimum performance for stacked arrays is achieved with wavelength spacing. See also 2858 of 1954 (Dent).

621. 396.67:517.512.2 1873
Further Investigations into Iterated Sine and Cosine Integrals and their Amplitude Functions with Reference to Antenna Theory—E. Hallén. [*Kungl. tek. Högsk. Handl.* (*Stockholm*), no. 89, 44 pp; 1955. In English.] Includes tables of functions discussed.

621.396.67.029.5 1874
Dual-Frequency Operation of a Loaded Vertical Medium-Frequency Radiator—A. J. McKenzie, W. H. Hatfield and V. F. Kenna. [*Proc. IRE*, (*Australia*), vol. 16, pp. 4–11; January, 1955.] " A method is described for loading a vertical broadcasting aerial for optimum operation at two different frequencies. The design construction and adjustment of a radiator of this type for the Australian National System is discussed in detail."

621.396.673 1875
Input Resistance of L.F. Unipole Aerials with Radial Wire Earth Systems—J. R. Wait and W. A. Pope. (*Wireless Eng.*, vol. 32, pp. 131–138; May, 1955.) The method described previously (334 of March) is extended to deal with antennas of length <λ/4 with top loading.

621.396.677.73 1876
The Propagation of Electromagnetic Waves in a Pyramidal Horn—G. Piefke. (*Z. angew. Phys.*, vol. 6, pp. 499–507; November, 1954.) Analysis for a pyramidal horn of square cross section is simplified by considering a nearly equivalent spherical pyramid. With an aperture semi-angle of 26.57 degrees the field components for an H_{10} wave are evaluated exactly. Representing the curve at the aperture by a sine function gives a maximum error of 1 per cent. In the distant field the wavelength is equal to the free-space wavelength and the field-strength amplitude decreases as $1/r$ for transverse components and as $1/r^2$ for longitudinal components, where r is measured from the apex. The longitudinal component increases with decreasing aperture angle or increasing order of wave mode. In the near field the wavelength rapidly approaches infinity in the direction of the apex; the smaller the aperture angle or the higher the wave mode the larger is the near-field amplitude and consequently the greater the attenuation through losses at the walls.

621.396.677.833.2 1877
Quasi-Fraunhofer Gain of Parabolic Antennas—R. F. H. Yang. (Proc. IRE, vol. 43, p. 486; April, 1955.) A note showing how the measured gain varies with distance from the antenna for several assumed tapered aperture illuminations.

AUTOMATIC COMPUTERS

681.142+621-52 1878
I.V.A. [Royal Swedish Academy of Engineering Sciences] Director's Annual Report on Progress in Research and Technology: Part 4—Computers and Automation—E. Velander. [*IVA* (*Stockholm*), vol. 26, pp. 36–45; 1955.] Includes a description of the BESK digital computer and notes on the industrial uses of computers and automation.

681.142 1879
Analogue Computation in the Service of Industry—J. Hoffmann. [*Rev. HF* (*Brussels*), vol. 2, pp. 321–340; 1954.]

681.142 1880
Coefficient Errors in Analogue Computers—H. Fuchs. (*Wireless Eng.*, vol. 32, p. 142; May, 1955.) Brief analysis is presented facilitating assessment of the accuracy of individual computers.

681.142 1881
The Use of a Reflected Code in Digital Control Systems—F. A. Foss. (*Trans. IRE*, vol. EC-3, pp. 1–6; December, 1954.)

681.142 1882
A Permanent High-Speed Store for Use with Digital Computers—R. D. Ryan. (*Trans. IRE*, vol. EC-3, pp. 2–5; September, 1954.) Information is stored in the form of spots arranged in a coordinate grid on a slide, and is picked up by a flying-spot system. Reliable operation should be possible with a digit spacing of 1 μs if phosphors with low decay time are used. Advantages of the system are high storage density and commercial availability of the components.

681.142 1883
System Design of the SEAC and DYSEAC—A. L. Leiner, W. A. Notz, J. L. Smith and A. Weinberger. (*Trans. IRE*, vol. EC-3, pp. 8–23; June, 1954.) Standard design procedures developed during the work on the SEAC and DYSEAC digital computers cover (a) system specifications, (b) functional plans, and (c) wiring plans. Similarity between these design procedures and data-processing procedures carried out by such computers indicates that existing computers could be used to produce the wiring plans for new models.

681.142 1884
The Universal Relay-Computer (URR1) of the Institute for Low-Frequency Engineering at the Vienna Technische Hochschule—H. Zemanek. (*Elektrotech. u. Maschinenb.*, vol. 72, pp. 6–12; January 1, 1955.) The simple binary-scale digital computer described was primarily designed to demonstrate principles for the basic arithmetical operations and the extraction of roots. The input is via perforated tape, and electromechanical relays are used both in the store and the computer parts. The times required are 150 ms for addition and 4 seconds for multiplication.

681.142 1885
Checking Codes for Digital Computers—J. M. Diamond. (Proc. IRE, vol. 43, pp. 487–488; April, 1955.)

681.142:538.221 1886
A Radio-Frequency Nondestructive Readout for Magnetic-Core Memories—B. Widrow. (*Trans. IRE*, vol. EC-3, pp. 12–15; December, 1954.)

681.142:621.318.134 1887
New Ferrite-Core Memory uses Pulse Transformers—W. N. Papian. (*Electronics*, vol. 28, pp. 194–197; March, 1955.)

681.142:621.372 1888
Asymmetrical Finite Difference Network for Tensor Conductivities—L. Tasny-

Tschiassny. (*Quart. Appl. Math.*, vol. 12, pp. 417–420; January, 1955.) An extension of the technique described by Macneal (1331 of 1954).

CIRCUITS AND CIRCUIT ELEMENTS

621.314.7:[621.318.57+621.373.52 1889
Junction-Transistor Trigger Circuits—J. E. Flood. (*Wireless Eng.*, vol. 32, pp. 122–130; May, 1955.) The junction transistor with earthed emitter is sufficiently similar to the thermionic tube with earthed cathode to enable it to be used in conventional trigger circuits. Details are given of bistable, monostable and emitter-coupled trigger circuits, multivibrators, a scale-of-two circuit and a blocking oscillator. Pulses of duration down to about 10 μs can be produced. Power consumption is of the order of 1 mw per stage.

621.316.722.4 1890
Rotary and Slider Potentiometers with Variable Characteristic—J. A. Reppich. (*Elektrotech Z., Edn B*, vol. 7, pp. 8–9; January 21, 1955.) Any resistance/slider-position characteristic can be approximated by connecting suitable resistors in parallel with short sections of the potentiometer.

621.316.8:621.396.822 1891
Investigations of Current Noise in Resistors—H. Bittel and L. Storm. (*Z. angew. Phys.*, vol. 7, pp. 27–32; January, 1955.) Report of noise-voltage measurements over the frequency range 30 cps–300 kc. With film resistors the mean square noise voltage usually varies approximately inversely as frequency; for resistors exhibiting such a frequency variation the noise is proportional to the direct voltage applied. Deviations from this frequency dependence are accompanied by deviations from this voltage dependence, as reported by Macfarlane (4087 of 1947). The behavior of wire resistors is similar. The statistical distribution of amplitude of the current noise agrees with the distribution function for thermal noise, indicating that its nature is Gaussian.

621.318.43 1892
Linear Reactor Chart—R. Lee. (*Electronics*, vol. 28, pp. 208, 210; March, 1955.) Design data are presented for iron-core reactors with inductance unaffected by variations of dc through the winding or alternating voltage across it.

621.318.57:621.327.42:535.215 1893
Light-Sensitive Neon-Tube Circuits—J. Braunbeck. (*Radio-Electronics*, vol. 26, pp. 136, 138; January 1955.) The decrease in the striking voltage and the slight increase in the dark current produced by external illumination in low-voltage (<100 v) neon lamps is made use of in switching, lf-relaxation-oscillator, and other circuits. High-power illumination glow lamps may also be suitable.

621.372 1894
A Mathematical Technique for the Analysis of Linear Systems—R. Boxer. (PROC. IRE, vol. 43, p. 489; April, 1955.) Comment on 363 of March (Ragazzini and Bergen).

621.372.412:621.314.7 1895
Calculation of the Oscillation Frequency of a Quartz Crystal maintained by a Transistor—G. Briffod. [*Compt. Rend. Acad. Sci. (Paris)*, vol. 240, pp. 841–842; February 21, 1955.] Calculations are made for high-Q and for low-Q crystals. Values of the frequency variation are tabulated for a range of values of detuning of the oscillator circuit connected to the transistor collector.

621.372.414.029.63 1896
An R.F. Resonant Circuit for Use at 300–1000 Mc/s.—F. C. Isely. (*Tele-Tech and Electronic Ind.*, vol. 14, section 1, pp. 60–62, 136; January, 1955.) Circuits of inductive-line type with a tuning range >2:1 have been designed without metallic sliding or rotating contacts. The construction may be of low-loss plastic, with plated or printed conductors. Eccentric "coaxial" or two-wire arrangements are used.

621.372.5 1897
Understanding the Gyrator—L. M. Vallese. (PROC. IRE, vol. 43, p. 483; April, 1955.) An equivalent Π-network is used to show that gyrators can be simply realized by means of current or voltage generators.

621.372.5 1898
RLC Lattice Transfer Functions—A. D. Fialkow and I. Gerst. (PROC. IRE, vol. 43, pp. 462–469; April, 1955.)

621.372.5 1899
A General Theory of Wideband Matching with Dissipative 4-Poles—R. LaRosa and H. J. Carlin. (*Jour. Math. Phys.*, vol. 33, pp. 331–345; January, 1955.)

621.372.5 1900
Effect of a Radio Pulse Signal on Resonant Circuits—J. Marique. (*Onde élect.*, vol. 35, pp. 55–61; January, 1955.) Calculations are made of the time required to establish the signal in a circuit of given bandwidth and time constant. It is not possible to establish any simple relation between these parameters except in the case when the signal frequency is the same as the resonance frequency. The influence of signal duration is studied. The results are of importance in connection with radiotelegraphy, and explain the occurrence of maxima at the beginning and end of each signal.

621.372.5 1901
Transformation for Constant-Impedance Networks—H. J. Orchard. (*Wireless Eng.*, vol. 32, pp. 139–141; May, 1955.) "Certain constant-impedance networks having a restricted range of variation of loss often contain components which are difficult to manufacture. The transformation which is described overcomes this difficulty at the expense of two extra resistors in the network and a small amount of frequency-independent loss added to the characteristics. Another application is the absorption of inductor dissipation in special cases."

621.372.54.012 1902
A Chart for Analyzing Transmission-Line Filters from Input Impedance Characteristics—H. N. Dawirs. (PROC. IRE, vol. 43, pp. 436–443; April, 1955.) Use of Smith-chart techniques is demonstrated.

621.372.542 1903
Compilation of a Filter Catalogue—E. Glowatzki. (*Frequenz*, vol. 8, pp. 296–299; October, 1954.) A discussion of the desirable features of a catalog in which all numerical data required in designing reactance quadripoles by the insertion-loss method are assembled. An appendix gives formulas linking the reflection factor and four insertion-loss parameters. Values of the insertion-loss parameters are tabulated for values of reflection coefficient ranging from 0 per cent to 100 per cent in unit steps.

621.372.552:534.614–8 1904
Novel Uses of the Ultrasonic Light Cell—Terry, Mumford and Holloway. (*See* 1850.)

621.373 1905
The Generation of Undamped Electrical Oscillations in Series and Parallel Oscillatory Circuits—H. Pfeifer. (*Z. angew. Phys.*, vol. 6, pp. 508–510; November, 1954.) A formal analytical treatment showing the types of negative-resistance characteristic necessary for generating sinusoidal oscillations in the two types of circuit. See also 2602 of 1953 (Steimel).

621.373 1906
On the Extension of the Principle of Imaginary Power Balance of Harmonics to Circuits with Continuous Spectra—J. Groszkowski. (*Bull. Acad. Polon. Sci.*, classe 4, vol. 2, no. 3, pp. 131–135; 1954. In English.) Extension of the principles given in a previous paper on the interdependence of frequency variations and harmonic content in oscillators (PROC. IRE, vol. 21, pp. 958–981; July, 1933).

621.373.4 1907
The Nonlinear-Theory Approach to Resistance-Capacitance Oscillators—J. Groszkowski. (*Bull. Acad. Polon. Sci.*, classe 4, vol. 2, no. 4, pp. 185–188; 1954. In English.) Exact calculations can be made using nonlinear theory based on the balance of the reactive power of the harmonics involved. The analysis indicates that the frequency stability when operating near the limit conditions is generally better with RC than with CR networks.

621.373.4 1908
The Influence of Grid Current upon Valve Oscillator Frequency—L. Lukaszewicz. (*Bull. Acad. Polon. Sci.*, classe 4, vol. 2, pp. 177–180; 1954. In English.) Analysis indicates that when the intensity of harmonics in the oscillator anode and grid circuits is low, the fundamental component of grid current is the main factor influencing oscillation frequency. Grid-current harmonics have a greater influence than anode-current harmonics.

621.373.4:621.316.726 1909
Frequency Stabilization of Valve Oscillators in Respect of Grid Current, Amplification Factor and Load—L. Lukaszewicz. (*Bull. Acad. Polon. Sci.*, classe 4, vol. 2, pp. 181–184; 1954. In English.) Formulas are derived for determining the values of stabilizing reactances for series connection in the grid, anode and load circuits.

621.373.4:621.365.55 1910
The Operation and Loading Characteristics of Valve Oscillators for Dielectric Heating—V. L. Atkins. (*Electronic Eng.*, vol. 27, pp. 106–111 and 164–169; March and April, 1955.)

621.373.4.029.63:621.385.3' 1911
Designing Stable Triode Microwave Oscillators—J. G. Stephenson. (*Electronics*, vol. 28, pp. 184–187; March, 1955.) Two circuit-constructional arrangements are described using a planar triode Type-2C40 and suitable respectively for operation at frequencies of 1–1.5 kmc and 3 kmc.

621.373.421 1912
Perturbations in Nonlinear Filtered Systems. Applications to the Theory of Oscillators—V. Belevitch. [*Rev. HF*, (*Brussels*), vol. 2, pp. 341–348; 1954.] Conventional methods of studying feedback-amplifier stability can be applied to "separable" filtered systems comprising a nonlinear frequency-independent unit followed or preceded by a linear selective circuit [2044 of 1954 (Cahen) and back references]. The theory of free and synchronized modes is extended to the case of frequency division. Stability is investigated by introducing two different coefficients for the in-phase and quadrature components of the perturbation voltage, so that the system can be treated as an amplifier with two feedback loops. The method is applied to determine the effect on the output of a tube oscillator due to lf modulation at the grid.

621.373.43:621.385.15 1913
Pulse Generator using Secondary-Electron-Emission Valves—E. Baldinger and N. Nicolet. (*Z. angew. Math. Phys.*, vol. 5, pp. 508–511; November 15, 1954.) The generator described produces positive and negative voltage pulses with duration adjustable between

10^{-7} and 10^{-5} second and a rise time of about 1.3×10^{-8} second, as well as cro beam-brightening and sweep voltages.

621.373.44 1914
A Versatile Pulse Shaper—K. E. Wood. (*Electronic Eng.*, vol. 27, p. 188; April, 1955.) Comment on 1294 of June (Kaufer).

621.373.52 1915
Transistor Waveform Generators—F. Butler. (*Electronic Eng.*, vol. 27, pp. 170–173; April, 1955.) Design of circuits using point-contact and junction transistors is considered on the basis of analogies with thermionic-tube circuits. Experimental af tuned-circuit, crystal-controlled and blocking oscillators are described.

621.374.43 1916
Fractional Frequency Generation by Regenerative Modulation—D. Makow. (*Canad. Jour. Technol.*, vol. 33, pp. 41–55; January, 1955.) The circuit theory is similar to that presented previously for frequency multiplication (1295 of June). An arrangement is described producing six frequencies lower than input as well as others higher than input.

621.375.2:621.318.57 1917
A High-Speed Waveform-Sampling Circuit—G. D. Bergman and D. M. MacKay. (*Electronic Eng.*, vol. 27, pp. 160–163; April, 1955.) Pulsed sampling circuits are discussed for obtaining a quantized output corresponding to a continuously varying input voltage. A cathode follower with negative feedback is used to provide an arrangement giving satisfactory operation with sampling pulses of short duration and small amplitude. A diode-switch circuit leads from the cathode follower to the input of a sign-reversing amplifier between whose input and output terminals the storage capacitor is connected.

621.375.2.029.3 1918
Design for a 20-Watt High-Quality Amplifier—W. A. Ferguson. (*Wireless World*, vol. 61, pp. 223–227; May, 1955.) Discussion with emphasis on the output stage and with special reference to the application of Type-EL84 output pentodes.

621.375.2.029.3 1919
Amplifiers and Preamplifiers—C. G. McProud. (*Audio*, vol. 39, pp. 23–60; January, 1955.) "A practical discussion covering the operation, design, construction, and testing of all types of amplifiers used in home music systems, and a presentation of the interesting features of commercially available products."

621.375.221 1920
Selectivity and Delay Distortion in High-Frequency Amplifiers—W. Nonnenmacher. (*Frequenz*, vol. 8, pp. 313–318; October, 1954.) In designing wide-band amplifiers or filters, a compromise must be reached between the conflicting requirements of linearity of phase characteristic, maximum amplification, and selectivity. Normalized curves for the attenuation, phase and transient-response characteristics of four different amplifiers with four tuned coupling circuits are presented and discussed from the point of view of design to meet specific requirements. The four types of amplifier considered are (a) those with single-tuned circuits, (b) those with flat phase characteristic, (c) power-law, and (d) Tchebycheff.

621.375.222 1921
Parallel-Series Amplifier—R. Peretz. [*Rev. HF* (*Brussels*), vol. 2, pp. 349–358; 1954.] High amplification, stability and low output impedance are achieved in a direct-coupled circuit containing only two resistances, one in the common cathode lead of a parallel-connected double triode, the other, R_P, as the anode load of the first triode, whose anode is also connected directly to the grid of a third triode in series with the second. The output voltage is that between the anode of the second triode and the reference voltage input. Under appropriate conditions, amplification $A = -g_mR_P/2$, where g_m refers to the slope of the double triode. The operation of the circuit is analyzed and its application as an amplifier for an analog computer, a voltage stabilizer or a dc amplifier is described.

621.375.232:[621.397.7:535.623 1922
Studio Amplifier Design for Color Television—J. O. Schroeder. (*Electronics*, vol. 28, pp. 154–158; March, 1955.) Distribution amplifiers with highly linear phase characteristics over a wide frequency range are obtained by using multistage feedback amplifiers with *RC* couplings having different time constants.

621.375.3 1923
High-Speed Magnetic Amplifiers—R. E. Wright. (*Electronic Eng.*, vol. 27, p. 188; April, 1955.) Comment on 670 of April. An alternative arrangement using a junction transistor for coupling is described.

621.375.3 1924
A Survey of Magnetic Amplifiers—C. W. Lufcy. (PROC. IRE, vol. 43, pp. 404–413; April, 1955.) Principles of operation and basic circuits are described, and applications are indicated.

621.375.4:621.314.63 1925
Diode Amplifier—A. W. Holt. (*Radio-Electronic Engng.*, vol. 24, pp. 18–19, 33; January, 1955.) See 987 of May.

621.376.332:621.372.2 1926
Delay Line Subcarrier Discriminator—K. A. Morgan and R. F. Blake. (*Electronics*, vol. 28, pp. 203–205; March, 1955.) The frequency discriminator described uses a multivibrator triggered by the direct input signal and stopped by the delayed signal, producing pulses whose spacing is a function of signal phase. Designed primarily for telemetering, it is useful also for automatic correction of wow and flutter in tape recorders.

GENERAL PHYSICS

537.2 1927
An Electrostatic Problem involving a Nonlinear Fluid Dielectric—R. Cade. (*Proc. Phys. Soc.*, vol. 68, pp. 1–9; January 1, 1955.) "An approximate calculation is made of the electrostatic couple on an anisotropic dielectric sphere influenced by a uniform field and immersed in a slightly nonlinear fluid dielectric."

537.212 1928
Slit-Middle-Plate Capacitors: a Contribution to the Technique of Calculation of Potential Fields—E. Kreyszig. (*Z. angew. Phys.*, vol. 7, pp. 13–17; January, 1955.) A numerical calculation is made for a system comprising two parallel plates distant respectively 8 cm and 4 cm on opposite sides of a third parallel plate with a slit 5 cm wide. The results are compared with electrolyte-trough measurements.

537.228.1 1929
Theory of the Diffusion of Light by Strongly Piezoelectric Crystals—J. Chapelle and L. Taurel. [*Compt. Rend. Acad. Sci.* (*Paris*), vol. 240, pp. 743–745; February 14, 1955.] Expressions are derived for the variations of electric susceptibility produced in the crystal by passage of a wave of thermal agitation.

537.311.31 1930
Kinetic Temperature of Electrons in Metals and Anomalous Electron Emission—V. L. Ginzburg and V. P. Shabanski. [*Compt. Rend. Acad. Sci.* (*URSS*), vol. 100, pp. 445–448; January 21, 1955. In Russian.] The effect of strong electric fields on metals is to raise the temperature θ of the electrons above that of the lattice. The symmetrical part of the electron energy distribution is a Fermi distribution function; the asymmetric part is negligible in the cases considered. Quantitative estimates of the effect of the electron-temperature rise on conduction and emission are briefly discussed. See also 675 and 676 of April (Shabanski).

537.311.31:537.315.8 1931
Effect of Strong Electrostatic Fields on the Resistance of Tungsten Wires in High Vacua—W. J. Deshotels and A. H. Weber. (*Phys. Rev.*, vol. 97, pp. 66–73; January 1, 1955.) Wires of diameter 0.004 and 0.00045 inch were subjected to negative and positive radial fields of strength up to 9×10^6 and 1.4×10^6 v/cm respectively. The resistance decreased abruptly on applying the field and increased abruptly on removing it, regardless of its sign; the change of resistance was proportional to the square of the field strength. No explanation of the effect has been found. Slight increases of resistance during steady application of the field are associated with temperature increases attributed to effects of ion-, photo- and field-emission currents.

537.311.33:537.312.8 1932
The Theory of the Magnetoresistance Effects in Polar Semiconductors—B. F. Lewis and E. H. Sondheimer. (*Proc. Roy. Soc. A*, vol. 227, pp. 241–251; January 7, 1955.) Theory developed previously for conduction in polar semiconductors [381 of 1954 (Howarth and Sondheimer)] is extended to deal with effects occurring in the presence of a magnetic field. Hall coefficient and magnetoresistance effect are shown graphically as functions of the magnetic field strength and of the temperature and degree of degeneracy of the electron gas. At low temperatures the magnetoresistance effect may become very large, contrary to the prediction of the free-path theory.

537.311.62 1933
Theory of Skin Effect in Constant Magnetic Field—M. Ya Azbel'. [*Compt. Rend. Acad. Sci.* (*URSS*), vol. 100, pp. 437–440; January 21, 1955. In Russian.] The surface impedance is calculated for the case of a metal surface parallel to the magnetic field. An analogous treatment for a normal field was given earlier by Azbel' and Kaganov (2624 of 1954).

537.311.62 1934
Current Distribution in Cylindrical Conductors of Circular Cross-Section—G. Freud. (*Acta. Tech. Acad. Sci. Hungaricae*, vol. 10, nos. 3/4, pp. 397–406; 1955. In German.) A calculation is made of the current distribution and Joule heating for the conductor in a uniform alternating magnetic field.

537.52 1935
The Electron Avalanche and its Development in the Self-Maintained Discharge—H. Raether. (*Z. angew. Phys.*, vol. 7, pp. 50–56; January, 1955.) A survey of the primary and secondary processes leading to breakdown in a parallel-plate system in a gas.

537.52 1936
Departure from Paschen's Law of Breakdown in Gases—W. S. Boyle and P. Kisliuk. (*Phys. Rev.*, vol. 97, pp. 255–259; January 15, 1955.)

537.52 1937
Breakdown Processes in Nitrogen, Oxygen, and Mixtures—E. L. Huber. (*Phys. Rev.*, vol. 97, pp. 267–274; January 15, 1955.)

537.523 1938
Influence of Insulating Films on the Corona Current and Breakdown Voltage of Spark Gaps—C. H. Hertz. (*Ark. Fys.*, vol. 9, part 1, pp. 1–28; January 20, 1955. In German.) Experiments are reported in which a

point-to-plate discharge path was used, the plate being coated with lacquer or other insulator; observed breakdown voltages are in some cases lower than with an uncoated plate. An explanation of the results is presented.

537.523 1939

The Effect of Lacquer Films on the A.C. Corona on Points and Wires—C. H. Hertz. (*Ark. Fys.*, vol. 9, part 1, pp. 29–37; January 20, 1955. In German.)

537.523 1940

Two Different Breakdowns between a Positive Electrode with Small Curvature and a Plane—R. Siksna. (*Ark. Fys.*, vol. 9, part 1, pp. 77–82; January 20, 1955.) Experiments made using loops of different radii in combination with a plane are described.

537.523 1941

Some Peculiarities of the Current-Potential Characteristics of Positive Corona Discharge—R. Siksna. (*Ark. Fys.*, vol. 9, part 1, pp. 83–91; January 20, 1955.)

537.523.3 1942

Indication of the Development Stages of Positive Corona Discharge in the Atmospheric Air—H. Norinder and R. Siksna. [*IVA* (*Stockholm*), vol. 26, pp. 46–57; 1955. In English.] Experimental technique is described for investigating the development of the discharge by means of the various optical, acoustic and electrical effects involved; the correlation between these effects is demonstrated.

537.523.5:538.561 1943

Radiation of Plasma Noise from Arc Discharge—T. Takakura, K. Baba, K. Nunogaki and H. Mitani. (*Jour. Appl. Phys.*, vol. 26, pp. 185–189; February, 1955.) Radiation from cold-cathode dc arc discharges in air has been observed at frequencies of 3.3 kmc, 190 mc, 15 mc and 1.5 mc. The oscillation is thought to be generated by periodic electron emission from the cathode caused by a small perturbation of the potential gradient due to variation of the ion sheath potential.

537.525 1944

Electron Resonance in Gas Discharges—D. J. E. Ingram and J. G. Tapley. (*Phys. Rev.*, vol. 97, pp. 238–239; January 1, 1955.) Brief description of experiments in which absorption lines were observed by paramagnetic-resonance technique, using a cavity resonator constructed so that the gas discharge occupied the region of maximum microwave magnetic-field strength. The results indicate that this may constitute a sensitive method for studying the variation of concentration of free ions.

537.525 1945

Space-Charge Effects in a High-Frequency Discharge: Part 1—M. Chenot. (*Jour. Phys. Radium*, vol. 16, pp. 54–61; January, 1955.) Details of experimental work on the effect reported in 2189 of 1952. The current flowing in a circuit connecting the external electrodes and including a high resistance R is measured, and its relation to the applied voltage and to the p.d. between the internal electrodes examined. When R is very high, discontinuities in the characteristic and hysteresis effects are observed with change in applied voltage. The latter are studied in further detailed oscillograms. A theoretical explanation of the results is discussed.

537.525:621.396.822 1946

Noise of Gas Discharge Plasma—S. Kojima, K. Takayama and A. Shimauchi. (*Jour. Phys. Soc. Japan*, vol. 9, pp. 802–804; September/October, 1954.) Measurements were made in the frequency range 1–10 mc on a 60-ma discharge in a 45-cm tube containing argon and Hg vapor at a pressure of about 2mm Hg; probe currents of 83 and 220 μa were used. Current noise was approximately proportional to $1/f$, as with semiconductors. See also 1133 of 1951 (Kojima and Takayama).

537.525.083 1947

An Evaluation of Plasma-Ion Temperature—O. Shimada. (*Jour. Phys. Soc. Japan*, vol. 9, pp. 874–876; September/October, 1954.) Measurements made by the double-probe and other methods are reported.

537.533.8 1948

Energy Distributions of Field-Dependent Secondary Electrons—F. A. Brand and H. Jacobs. (*Phys. Rev.*, vol. 97, pp. 81–84; January 1, 1955.) Report of an experimental investigation of the emission from thin films of MgO; a retarding-field technique was used. The energy distribution was found to be Maxwellian, with values ranging from zero to 90 ev and average values of 10 to 20 ev, depending on the applied field. The method is useful for determining the surface potential of the emitter.

537.56:538.566 1949

Experiments on the Behavior of an Ionized Gas in a Magnetic Field—W. H. Bostick and M. A. Levine. (*Phys. Rev.*, vol. 97, pp. 13–21; January 1, 1955.) Probe measurements in a plasma comprising electrons and helium ions in a toroidal tube with a toroidal magnetic field reveal an oscillatory current which is interpreted as indicating fluctuations of ion concentration consistent with magnetohydrodynamic waves of the type described by Alfvén (2777 of 1950). Microwave measurements on a toroidal cavity resonator indicate that the degree of diffusion control in helium at low pressure is very much less than expected from the classical theory of ambipolar diffusion of ions and electrons in a magnetic field. The diffusion-coefficient/magnetic-field curve passes through a minimum at about 600 G. Tentative explanations of the experimental results are advanced.

538.222:621.372.413 1950

Various Ways of using Cavity Resonators in Paramagnetic Resonance—J. Uebersfeld. (*Jour. Phys. Radium*, vol. 16, pp. 78–79; January, 1955.) Note on operating conditions for greatest sensitivity in signal detection, the cavity resonator not being matched to the guide. Cases considered are (a) oscillator tuned to cavity resonance frequency: ratio of reflected to incident power 1:3; and (b) oscillator frequency varying around resonance frequency.

538.3 1951

Field Equations for a Fluid/Electromagnetic-Field System—Pham Mau Quân. [*Compt. Rend. Acad. Sci.*, (*Pairs*), vol. 240, pp. 598–600; February 7, 1955.] A relativistic generalization is presented of the macroscopic equations of electromagnetism.

538.3 1952

Cauchy's Problem in Relation to a Fluid /Electromagnetic-Field System—Pham Mau Quân. [*Compt. Rend. Acad. Sci.* (*Paris*), vol. 240, pp. 733–735; February 14, 1955.] Equations derived previously (1951 above) are studied by an analysis of Cauchy's problem.

538.566 1953

Reflection of a Transient Electromagnetic Wave at a Conducting Surface—J. R. Wait and C. Froese. (*Jour. Geophys. Res.*, vol. 60, pp. 97–103; March, 1955.) A treatment of oblique-incidence reflection from the plane interface of a dissipative medium. The inversion of the Laplace transforms can only be carried out in closed form in special cases. Series solutions are developed for the general case and numerical results are presented graphically. A possible application of the results to the case of a lightning-discharge waveform and reflection from a sharply bounded inosphere is noted.

538.566:517 1954

An Integral Equation governing Electromagnetic Waves—P. R. Garabedian. (*Quart. Appl. Math.*, vol. 12, pp. 428–433; January, 1955.) The problem discussed is that of determining the solution of the Helmholtz equation $\Delta u+k^2u=0$ for the region outside a simple closed-curve boundary at which values of u or its normal derivatives are prescribed. By introducing a suitable parameter, constructed by conformal mapping, the problem is reduced to a new Fredholm integral equation whose solution is independent of conditions inside the boundary. Scattering cross section is discussed.

538.566:535.42]+534.26 1955

Green's Functions for the Cylinder and the Sphere—W. Franz. (*Z. Naturf.*, vol. 9a, pp. 705–716; September, 1954.) The investigation of diffraction [1665 of 1953 (Franz and Deppermann)] is continued. The exact expression for the Green's function is split into two parts corresponding respectively to the geometrical-optics wave and the surface wave. A semi-asymptotic solution is thus obtained which is valid for quite small obstacles. The surface waves are shown to be identical with the residual waves discussed by Watson and by van der Pol and Bremmer in connection with wireless telegraphy.

538.566:535.42/.43 1956

Backscattering from Wide-Angle and Narrow-Angle Cones—L. B. Felsen. (*Jour. Appl. Phys.*, vol. 26, pp. 138–151; February, 1955.) "Solutions are obtained for the diffraction of the waves radiated by scalar and vector point sources on the axis of a semi-infinite cone. The scalar problems are solved by the method of characteristic Green's functions to yield directly various alternative representations whose different convergence properties are discussed; the vector problem is solved by an application of spherical transmission line theory. To evaluate the plane wave scattering observed far from the cone tip, a highly convergent contour integral representation is selected and evaluated approximately for the special case of backscattering from cones having large and small apex angles. The results for the large-angle cone exhibit the transition from a backscattered spherical wave to a plane wave as the cone degenerates into an infinite plane."

538.566:535.42 1957

Measurement of Microwave Diffraction from a Long Slit in a Thin Conducting Plane—J. L. Hirshfield and C. M. Zieman. (*Jour. Appl. Phys.*, vol. 26, pp. 135–137; February, 1955.) An outline is given of technique used to produce a uniform incident plane wave. Results of measurements of the intensity of the diffraction field are shown graphically for longitudinal and transverse polarization of the incident wave.

538.566:535.42 1958

Diffraction by Apertures—C. Huang, R. D. Kodis and H. Levine. (*Jour. Appl. Phys.*, vol. 26, pp. 151–165; February, 1955.) Theoretical and experimental investigations are reported of the diffraction of plane em waves by circular and elliptical apertures in plane screens. Integral equations are derived for the distribution over the apertures and the aperture transmission coefficient is determined by a variational method. The closeness of the agreement between experimental and theoretical results shows that the method is capable of providing good approximations to the actual field values. The measurements were made in the 24-kmc band, using an image-plane technique.

538.566:535.42 1959

The Edge Conditions and Field Representation Theorems in the Theory of Electromagnetic Diffraction—A. E. Heins and S. Silver. (*Proc. Camb. Phil. Soc.*, vol. 51, part 1, pp. 149–161; January, 1955.) Discussion is

presented relevant to the case of a perfectly conducting screen of infinite extent with an aperture of finite area. Order conditions are developed which must be satisfied by the field components in the neighborhood of the edge as a consequence of the requirement that the total energy in a finite volume must be finite. The boundary-value problem is formulated as a pair of simultaneous integral equations. From the solution for the edge region, the functional form of the local fields can be determined without assuming a particular type of expansion. An indeterminacy present in the system of local integral equations can be removed when the local behavior of certain field components is known in detail.

538.566:537.311.31:539.23 1960

Simultaneous Partial Absorption, Reflection and Transmission of a Uniform Plane Wave by a Thin Metal Layer—M. Gourceaux. [*Compt. Rend. Acad. Sci.* (*Paris*), vol. 240, pp. 952–953; February 28, 1955.] Simple analysis is used to derive expressions for the energy reflected, transmitted and absorbed, for a normally incident wave. For given conductivity, the absorbed energy has a maximum value of half the incident energy at a particular value of thickness, the reflected and transmitted energies being then equal.

538.6:536.7 1961

Thermodynamical Theory of Galvanomagnetic and Thermomagnetic Phenomena—R. Fieschi. (*Nuovo Cim.*, vol. 1, *Supplement*, no. 1, pp. 1–47; 1955. In English.)

539.152.2:538.569.4 1962

Spin-Echo Memory Device—S. Fernbach and W. G. Proctor. (*Jour. Appl. Phys.*, vol. 26, pp. 170–181; February, 1955.) "A proton-rich sample placed in a strong inhomogeneous magnetic field of mean strength H_o was subjected to a pattern of relatively weak radio-frequency pulses at the Larmor frequency of the protons in the field H_o. The pattern was then recalled by applying a strong r.f. pulse at a later time as in the spin-echo technique. It is shown both mathematically and experimentally that such a series of pulses, varying in amplitude can be 'memorized' by the spin system of protons for times as long as one second and then repeated, preserving both shape and relative amplitude." Spin echoes are discussed by Hahn in *Phys. Rev.*, vol. 80, pp. 580–594; November 15, 1950.

621.3.032.44 1963

The Distribution of Temperature along a Thin Rod Electrically Heated in Vacuo: Part 5—Time Lag—S. C. Jain and K. S. Krishnan. (*Proc. Roy. Soc. A*, vol. 227, pp. 141–154; January 7, 1955.) Expressions obtained previously (417 of March) for the steady-state temperature distribution are used to study the increase of temperature accompanying a small increase in heating current. Over a considerable region near the center of the rod the temperature variation can be completely represented by a simple exponential law involving a single relaxation time, whose magnitude can be readily calculated. This method is compared with that based on the Fourier expansion; the latter can be adapted for general use by introducing an effective length to replace the actual length of the rod. For a given temperature at the center the relaxation time varies inversely as the ratio of surface to volume, and is thus smaller for a ribbon filament than for one of circular cross section, as observed by Prescott and Morrison (*Rev. Sci. Instr.*, vol. 10, p. 36; 1939).

GEOPHYSICAL AND EXTRATERRESTRIAL PHENOMENA

523.16 1964

Radio Astronomy in Hawaii—G. Reber. [*Nature* (*London*), vol. 175, pp. 78–79; January 8, 1955.] Observations are being made of cosmic noise at frequencies near 20, 30, 50 and 100 mc, using a Lloyd's-mirror technique. The interference patterns observed are discussed in relation to the nature of the sources and to ionospheric and solar variations.

523.16:523.72 1965

Interferometer Observations of Solar Radiation at 9350 Mc/s—I. Alon, J. Arsac and J. L. Steinberg. [*Compt. Rend. Acad. Sci.* (*Paris*), vol. 240, pp. 595–598; February 7, 1955.] The distribution of brightness over the solar disk has been studied by observations at Marcoussis subsequent to those reported previously (3272 of 1953). The sensitivity of the system was sufficient for reliable measurements of interference of magnitude down to 2.5 per cent. The results confirm that (a) at this frequency the sun's apparent diameter is slightly greater than for the visible disk, and (b) limb brightening is present.

523.16:523.72:621.396.677.3 1966

New Array for Radio-Astronomical Observations of the Sun's Brightness at 9350 Mc/s—J. Arsac. [*Compt. Rend. Acad. Sci.* (*Paris*), vol. 240, pp. 942–945; February 28, 1955.] Equipment installed at Marcoussis comprises four identical parabolic mirrors of diameter 1.1 m located respectively at 0, a, $4a$ and $6a$ along an E-W line, where $a=58\lambda$; the four antennas are connected to a single receiver by lines of equal length. The over-all length of this array is 11.2 m, as compared with 15 m for a continuous mirror to give the same half-power lobe width. The arrangement enables the first six Fourier harmonics of the brightness distribution over the sun to be observed at true amplitude.

550.372 1967

The Apparent Specific Resistance of an Inclined Plane Stratum—A. Huber. (*Arch. Met. A, Wien*, vol. 8, pp. 95–112; January 7, 1955.)

550.38(47) 1968

Fundamental Types of Geomagnetic Activity—V. M. Mishin. [*Compt. Rend. Acad. Sci.* (*URSS*), vol. 100, pp. 53–56; January 1, 1955. In Russian.] K indices obtained from observations at Irkutsk (geomagnetic latitude $\phi=41$ degrees), Watheroo ($\phi=-$M.41 degrees), Slutsk ($\phi=56$ degrees) and Tashkent ($\phi=32$ degrees) are compared and discussed. The average K indices and St-variations for Irkutsk are presented graphically.

550.384 1969

Establishment of a New Process of Terrestrial Demagnetization—Period of the Latest Demagnetization-Remagnetization Cycles recorded for our Planet—C. Gaibar-Puertes. (*Geofis. pura appl.*, vol. 29, pp. 22–56; September/December, 1954. In Spanish.) Analysis of figures from observatories covering the whole world indicates oscillations in the intensity of the terrestrial magnetic field since 1885; an average period of 50 years is inferred for the remagnetization-demagnetization cycles.

550.385 1970

Solar Corpuscles responsible for Geomagnetic Disturbances—J. C. Pecker and W. O. Roberts. (*Jour. Geophys. Res.*, vol. 60, pp. 33–44; March, 1955.) A qualitative hypothesis is presented.

550.385 1971

Annual Variation of the Magnetic Elements—R. P. W. Lewis, D. H. McIntosh and R. A. Watson. (*Jour. Geophys. Res.*, vol. 60, pp. 71–74; March, 1955.)

550.385 1972

Note on the Occurrence of World-Wide S.S.C.'s during the Onset of Negative Bays at College, Alaska—J. P. Heppner. (*Jour. Geophys. Res.*, vol. 60, pp. 29–32; March, 1955.) S. s.c.'s (sudden commencements followed by a period of storminess) may have an atmospheric source which is related to sudden changes in auroral activity.

550.385:523.746 1973

Geomagnetic Activity and Sunspots—P. Simon. [*Compt. Rend. Acad. Sci.* (*Paris*), vol. 240, pp. 940–942; February 28, 1955.] Analysis of observations by the method of superposed epochs shows that geomagnetic activity following the central meridional passage of certain sunspots is related more closely to their rf radiation than to their eruptive intensity.

550.385:523.755 1974

Correlation between the Solar Corona and the Geomagnetism for the Remarkable M-Regions in 1950–1953—T. Shimazaki. [*Jour. Radio Res. Labs* (*Japan*), vol. 1, pp. 51–61; June, 1954.]

551.510.52:621.396.11.029.62 1975

On the Distribution of Refractive Index in the Lower Atmosphere in Japan—K. Tao and Y. Baba. [*Jour. Radio Res. Labs* (*Japan*), vol. 1, pp. 17–28; June, 1954.] Radiosonde data for heights up to 3 km are analyzed. Contour maps show the derived distribution of k (effective earth radius factor) for day and night in each month of the year; the k distribution is closely related to the movement of the air mass. Predicted values of field-strength for 150 mc over a 125-km path are generally greater for summer than for winter, in agreement with observed values.

551.510.53 1976

Tidal Oscillations of the Lower Stratosphere—D. H. Johnson. (*Quart. Jour. R. Met. Soc.*, vol. 81, pp. 1–8; January, 1955.) Diurnal and semidiurnal variations of wind occurring in the lower stratosphere appear to be associated with solar tides. The semidiurnal variation in the stratosphere is in phase with and of comparable magnitude to the semidiurnal variation at the earth's surface. The diurnal variation in the stratosphere is of similar magnitude to the semidiurnal variation.

551.510.535 1977

Viscosity in the High Atmosphere—D. G. Yerg. (*Jour. Geophys. Res.*, vol. 60, pp. 87–94; March, 1955.)

551.510.535 1978

Widespread Diurnal Variations of Effective Slope of the Ionosphere—H. A. Whale. [*Nature* (*London*), vol. 175, pp. 77–78; January 8, 1955.] Measurements have been made at Seagrove Radio Research Station, N.Z., of the bearing and elevation angles of signals received on 9.315 mc from ZQD, Nandi, Fiji, distant 2,000 km almost magnetically north, and on 9.660 mc from VLQ9, Brisbane, Queensland, distant 2,250 km almost magnetically west. From these measurements the effective slopes of the ionosphere are found to be related at places about 1,500 km apart and the average diurnal variation of these slopes is determined.

551.510.535 1979

Storms in the Ionosphere—E. V. Appleton. (*Endeavour*, vol. 14, pp. 24–28; January, 1955.) A general survey of existing knowledge and theories of the world-wide disturbances in the upper structure of the ionosphere observed at times of magnetic storms. The effects on long-distance short-wave communication are briefly indicated.

551.510.535 1980

Behaviour of the Ionosphere at Rome during the Period 1948–1953—P. Dominici. (*Ann. Geofis.*, vol. 7, pp. 503–520; October, 1954.) Ionosphere records obtained at Rome are analyzed; the normal variations are established. Predicted values of f_2F_0 are shown graphically.

551.510.535 1981

Movement of the F-Region—K. Toman.

(*Jour. Geophys. Res.*, vol. 60, pp. 57–70; March, 1955.) Using three spaced receivers, continuous recordings were made in Massachusetts, during the period August, 1952–December, 1953 of a vertical-incidence and two oblique-incidence 3.5 mc pulse transmissions, the base lines for the latter being 62 km and 109 km in directions roughly W-E and NW-SE. Horizontal speed and direction of winds in the F region were determined from the time displacement of echoes. At an average virtual height of 215 km average speed was 362 km/h and mean direction nearly parallel to the earth's magnetic field. Monthly averages of mean direction showed a semiannual period with maximum deviation E of N around the equinoxes. Monthly averages of speed, varying between 250 and 600 km/h, showed an annual period with higher values in winter than in summer. Speed increased with height.

551.510.535 1982

Intermediate Layers of Ionization between the E and F_1 Layers of the Ionosphere over Ahmedabad (23 degrees N, 72.6 degrees E)—R. G. Rastogi. (*Proc. Indian Acad. Sci.*, Section A, vol. 40, pp. 158–166; October, 1954.) Observations are reported indicating the regular occurrence of two intermediate layers with virtual heights of 125 km and 140 km respectively. Both layers exhibit magneto-ionic splitting. The variation of the critical frequencies with the sun's zenithal angle obeys a $\cos^n$ law, the value of n being about 0.38. True heights and thicknesses of the layers are determined for some cases; the values of true heights are in good agreement with rocket observations.

551.510.535 1983

Geomagnetic Control of the F_1 Region of the Ionosphere—M. Ghosh. (*Jour. Geophys. Res.*, vol. 60, pp. 115–116; March, 1955.) Noon values of f_0F_1 and f_0F_2 for March, June and December of 1947 and 1951 plotted against geomagnetic latitude show the same type of geomagnetic control. The equatorial dip in the f_0F_1 curves is more pronounced in the year of higher sunspot activity. See also 2938 of 1954.

551.510.535:523.3 1984

A Measurement at Ottawa of the Change in Height with Lunar Time of the E Region of the Ionosphere—C. A. Littlewood and J. H. Chapman. (*Canad. Jour. Phys.*, vol. 33, pp. 11–16; January, 1955.) "The method used by Appleton and Weekes to detect the lunar variation of height of the E region of the ionosphere has been used to determine the amplitude and phase of the lunar height variation at Ottawa. Observations were made from October to December, 1952. A sinusoidal variation of height of 1.5 km amplitude and 12 h period was observed. The maximum height occurred about six hours after lunar transit. This result differs in phase by six hours from that observed in Cambridge in 1938."

550.510.535:523.5:621.396.11 1985

Continuous Radar Echoes from Meteor Ionization Trails—V. R. Eshleman, P. B. Gallagher and A. M. Peterson. (Proc. IRE, vol. 43, p. 489; April, 1955.) Preliminary results are presented of experiments giving support to the view that meteoric ionization is the most important factor in extended-range vhf propagation.

551.594.5.:621.396.11.029.53/.62 1986

Interpretations of Radio Reflections from the Aurora—H. G. Booker, C. W. Gartlein and B. Nichols. (*Jour. Geophys. Res.*, vol. 60, pp. 1–22; March, 1955.) Report and discussion of measurements made at Ithaca, N.Y. Pulse radar experiments at 104 mc show that (a) reflections occur only during auroras having ray structure; (b) the transmitted beam must be directed roughly normal to the rays; (c) echoes are complex. Cw signals at various frequencies between 2.4 and 144 mc showed a rate of fading roughly proportional to frequency, i.e. much higher than the fading rate for normal ionospheric conditions. Observations are interpreted as indicating that echoes are due to scattering from numerous auroral columns of ionization; fading is due to wind-like motion of these columns. Other interpretations are critically discussed. Reasons are given for the possible occurrence of auroral reflection at F-region as well as E-region levels.

551.594.5:621.396.11.029.62 1987

More about V.H.F. Auroral Propagation—R. Dyce. (*QST*, vol. 39, pp. 11–15, 118; January, 1955.) Radio amateur reports of auroral propagation at 144 mc since 1951 indicate an extended communication range along E-W direction rather than N-S. Automatic recordings at 50 mc show a predominance of auroral reflection around 6 PM and 2 AM EST, an unexplained dip in the diurnal curve at midnight, a marked seasonal trend, and a decrease in occurrences from 1952 to 1954. In cw and radar experiments at College, Alaska, in 1953, echoes came from far north of the auroral zone, with ranges above 400 km, and never from the south; reflections probably occurred at heights of 100 km; angles of elevation were low no matter where visible auroras occurred.

550.38 1988

Variations of the Terrestrial Magnetic Field in Hungary. [Book Review]—G. Barta. Publishers: Akadémiai Kiadó, Budapest, 1954, 146 pp., Ft. 60. (*Acta Tech. Acad. Sci. Hungaricae*, vol. 10, nos. 3/4, pp. 508–512; 1955. In Russian, English, French and German.) The text of this survey is given in Hungarian, Russian and German.

LOCATION AND AIDS TO NAVIGATION

621.396.969.3 1989

Radar in Inland Traffic—A. Esau and K. Brocks. (*Fernmeldetech. Z.*, vol. 8, pp. 1–7; January, 1955.) Report on a commercial British-made marine-radar equipment which was tested on inland waterways, roads and railways. The PPI display proved to be useful in river navigation and in the control of a railway marshalling yard. While the horizontal beam-width (1.7 degrees to half-power), wavelength (3.2 cm) and pulse repetition rate (1,000 per second) were satisfactory, modifications are required to reduce the pulse duration ($\sim 10^{-7}$ seconds at present), vertical beam-width (23 degrees) and the radiated pulse power (7 kw); the scanning rate requires to be increased.

MATERIALS AND SUBSIDIARY TECHNIQUES

535.5 1990

Theory of Vapour-Jet Vacuum Pump—V. I. Skobelkin and N. I. Yushchenkova. (*Zh. Tekh. Fiz.*, vol. 24, pp. 1879–1891; October, 1954. Correction, *ibid.*, vol. 25, p. 366; February, 1955.) The action of a supersonic-jet pump is considered in two stages: (a) determination of the structure of the vapor jet, and (b) investigation of the diffusion of gas in such a jet. Pumping speeds calculated from the formulas derived are in good agreement with experimental results.

535.37 1991

Motion of Conduction Electrons in Luminescent Crystals—D. Curie. (*Jour. Phys. Radium*, vol. 16, pp. 77–78; January, 1955.) Note discussing phosphorescence mechanisms and their terminology and the proportion of ejected electrons with free path $>10^{-6}$ cm.

535.37 1992

The Effect of Superposing a Small Alternating Excitation on the Steady Excitation of a Luminescent Material—K. F. Stripp and R. H. Bube. (*Jour. Appl. Phys.*, vol. 26, pp. 251–252; February, 1955.)

535.37 1993

Optical Properties of Calcium Metaantimoniate—J. Janin and R. Bernard. [*Compt. Rend. Acad. Sci.* (*Paris*), vol. 240, pp. 614–615; February 7, 1955.] Properties of this phosphor activated with Pb or Mn are discussed; an inaccuracy in a previous paper (158 of 1954) is noted.

535.37+535.215]:534–8 1994

Effect of Ultrasonic Radiation on the Conductivity and Fluorescence of ZnS and CdS Crystals—L. Herforth and J. Krumbiegel. (*Naturwiss.*, vol. 42, p. 39; January, 1955.) Experiments indicate that exposure of the crystals to ultrasonic radiation produces a rapid reversible reduction of photoconductivity but has no effect on the luminescence intensity.

535.37:546.482.21 1995

Infrared Emission Band and Kinetics of Semiconductor Processes in CdS in the Region of Temperature Quenching of Luminescence—V. A. Arkhangel'skaya. [*Compt. Rend. Acad. Sci.* (*URSS*), vol. 100, pp. 233–235; January 11, 1955.] Oscillograms are presented of the rise and decay of luminescence and conductivity at temperatures between about 20 degrees and 200 degrees C. The rise and decay times are of the order of a few milliseconds. Relaxation in the infrared (about 950 mμ) band is slower than that for the red luminescence.

535.37:621.317.373 1996

Measurements of Luminescence Decay Time on Excitation by Electrons—W. Hanle and H. G. Jansen. (*Z. Naturf.*, vol. 9a, pp. 791–797; September, 1954.) Modifications are described for converting the method of Rohde (1504 of 1954) into an absolute method. Further measurements on organic phosphors indicate that decay time depends on grain size, degree of purity, and type of excitation.

537.224 1997

Naphthalene Electrets and the Origin of their Homocharge—W. Baldus. (*Z. angew. Phys.*, vol. 6, pp. 481–489; November, 1954.) Experiments are reported on naphthalene, a nonpolar substance which exhibits the characteristic charge reversal and permanent electrification of electrets. This homocharge is conditioned by the electrode material and is suppressed if the sample is insulated by glass plates in the polarizing field. The internal field immediately after establishment of the homocharge is determined quantitatively, the change of sign being explained by the disappearance of a field component initially due to ordered and oriented dipoles. Space charge distribution within the electret is evaluated.

537.226:546.212 1998

Dielectric Properties of Water Adsorbed by Silica Gel at Cm λ—J. Le Bot and S. Le Montagner. (*Jour. Phys. Radium*, vol. 16, pp. 79–80; January, 1955.) Results of experiments at 10.37 cm λ using the method previously developed (2067 of 1953) show that the formula relating the frequency of maximum Debye absorption to absolute temperature is also valid at cm λ. The mean activation energy of the adsorbed water is 12.5 kcal/mol.

537.227 1999

Aging of the Properties of Barium Titanate and Related Ferroelectric Ceramics—W. P. Mason. (*Jour. Acous. Soc. Amer.*, vol. 27, pp. 73–85; January, 1955.) Variations with time of the dielectric constant and other electrical and elastic properties of various titanates have been observed. At room temperature such variations may continue for over a year, but stabilization can be hastened by heating the material. The aging is due to a reduction in the effective polarization caused by a slow temperature-induced motion of the domain walls; this is borne out by calculations.

537.227 2000
Effect of Mechanical Pressure on Dielectric Properties of a Ferroelectric Ceramic—E. V Sinyakov and I. A. Izhak. [*Compt. Rend. Acad. Sci.* (*URSS*), vol. 100, pp. 243–246; January 11, 1955. In Russian.] Experimental results show that pressure increase (up to 600 kg/cm²) the spontaneous polarization decreases and induced polarization remains constant; the fractional variation of permittivity with pressure is -1.7×10^{-4} cm² kg^{-1} at room temperature and -5.4×10^{-4} cm² kg^{-1} at the Curie point, determined at 1 mc in a weak field, and -3.10×10^{-4} and 5.8×10^{-4} cm² kg^{-1}, respectively, at 50 cps in a field of 700 v/cm. The Curie point rises 2.8×10^{-8} degrees C. per kg/cm² increase of pressure. Results are presented graphically.

537.227:546.431.824–31:535.343.2 2001
Optical Behaviours of Multi-domain Single Crystal of $BaTiO_3$ in Dependence on Temperature—T. Horie, K. Kawabe and S. Sawada. (*Jour. Phys. Soc. Japan*, vol. 9, pp. 823–825; September/October, 1954.) Report of measurements of the transmission and absorption characteristics of samples about 20 μ thick in the temperature range from -120 degrees C. to $+150$ degrees C.

537.311.33+621.315.6 2002
Recombination Processes in Insulators and Semiconductors—A. Rose. (*Phys. Rev.*, vol. 97, pp. 322–333; January 15, 1955.) The terminology used to describe recombination processes is studied, and variations are noted as between the terms used in connection with luminescence, photoconductivity and semiconductors. Most of the recombination occurs at discrete states in the forbidden energy zone, which may be ground states or shallow trapping states; the latter cause the observed decay time of free carrier concentrations to exceed the lifetime of a free carrier. To account for certain anomalous phenomena such as infrared quenching, the "superlinear" photocurrent/illumination characteristic, and the enhancement of photoconductivity on addition of recombination centers, it may be necessary to assume the existence of more than one class of ground states. Energy-level models for various possible cases are examined.

537.311.33 2003
Amsterdam Conference on Semiconductors—(*Physica*, vol. 20, pp. 801–1140; November, 1954.) The text of 65 papers is given and brief reports presented at the conference. These include reviews of the experimental evidence of band structure in Ge and Si, the surface properties of semiconductors (mainly Ge), the chemical and electronic aspects of impurity centers in Ge and Si, the electrical and optical properties of the PbS group, ZnS, and a large number of intermetallic compounds. Results of new determinations of various constants, including resistivity, Hall constant and thermoelectric power, are also reported. Abstracts of some of the papers are given below.

537.311.33 2004
The Electronic and Optical Properties of the Lead Sulphide Group of Semiconductors—R. A. Smith. (*Physica*, vol. 20, pp. 910–929; November, 1954.) Experimental results are reviewed and an attempt is made to clarify their interpretation.

537.311.33 2005
Fluctuations in the Number of Charge Carriers in a Semiconductor—R. E. Burgess. (*Physica*, vol. 20, pp. 1007–1010; November, 1954.) The brief treatment presented takes into account only the influence of recombination via the donors or acceptors responsible for determining n and p, the number of electrons in the conduction band or holes in the valence band respectively. Thermodynamic and statistical approaches show that when n and p are large numbers their fluctuations have Gaussian-type distribution.

537.311.33 2006
Complex Index of Refraction of Semiconducting Surfaces—P. H. Miller, Jr., and J. R. Johnson. (*Physica*, vol. 20, pp. 1026–1028; November, 1954.) Simple formulas are given for (a) the reflectivity near the Brewster minimum in terms of the complex refractive index $n(1+i\alpha)$, when $\alpha\ll1$, (b) the reflectivity at the minimum and (c) the angle between the incident ray and the incident ray at the minimum. The effect of a thin surface layer is also considered. The experimental setup consists of a modified spectrometer with fixed light source and detector, constant deviation being obtained by use of an aluminized mirror fixed at an angle to the semiconductor surface investigated. See also 1304 of 1953 (Pikus).

537.311.33:[546.28+546.289 2007
Modulation of the Surface Conductance of Germanium and Silicon by External Electric Fields—G. G. E. Low. (*Proc. Phys. Soc.*, vol. 68, pp. 10–16; January 1, 1955.) Experiments similar to those reported by Shockley and Pearson for thin semiconductor films (*Phys. Rev.*, vol. 74, pp. 232–233; July 15, 1948.) have been made on single-crystal specimens of n- and p-type Ge and on p-type Si. Voltage pulses applied capacitively to the specimen produce rapid variations of its conductance, with corresponding variations of the emf across it in the presence of a sweeping current; these variations are recorded oscillographically. The observed conductance changes and their time dependence provide information concerning the surface barrier and the relaxation phenomena associated with departures from electronic and ionic equilibrium.

537.311.33:[546.28+546.289 2008
Measurement of Carrier Lifetimes in Germanium and Silicon—D. T. Stevenson and R. J. Keyes. (*Jour. Appl. Phys.*, vol. 26, pp. 190–195; February, 1955.) A method is used in which the bar-shaped sample is illuminated by a pulse of light and the current decay curve is displayed on an oscilloscope. Analysis of the solution of the diffusion equation yields methods of measuring the bulk lifetime, the surface recombination velocity and the diffusion constant.

537.311.33:[546.28+546.289 2009
Ground State of Impurity Atoms in Semiconductors having Anisotropic Energy Surfaces—M. A. Lampert. (*Phys. Rev.*, vol. 97, pp. 352–353; January 15, 1955.) An approximate calculation is made of the binding energy of the impurity ground state using experimentally determined values of effective electron mass; the energy contours are assumed to be symmetrically located ellipsoids. Theoretical and experimental results are compared with conduction-band electrons and donor impurities in Ge and Si.

537.311.33:[546.28+546.289 2010
Plastic Deformation of Germanium and Silicon by Torsion—E. S. Greiner. [*Jour. Metals* (*New York*), vol. 7, section 2, pp. 203–205; January, 1955.]

537.311.33:546.28 2011
Ionization and solubility in Semiconductors—H. Reiss and C. S. Fuller. (*Phys. Rev.*, vol. 97, pp. 559–560; January 15, 1955.) Based on the theory of Reiss (*Jour. Chem. Phys.*, vol. 21, p. 1209; 1953.) concerning the effects of hole-electron equilibrium on solubility, a formula is derived relating the concentration of donors in a semiconductor to the concentration of acceptors. Calculated and observed values are compared for B-doped Si saturated with Li.

537.311.33:546.28 2012
Effect of Crystal Distortion upon Change of Resistivity of Silicon by Heat Treatment—W. C. Dash. (*Phys. Rev.*, vol. 97, p. 354; January 15, 1955.) Results of experiments suggest that structural imperfections of the crystal retard the appearance of n-type carriers in crystals heated at 450 degrees C.

537.311.33:546.28 2013
Trapping of Minority Carriers in Silicon: Part 1—P-Type Silicon—J. A. Hornbeck and J. R. Haynes. (*Phys. Rev.*, vol. 97, pp. 311–321; January 15, 1955.) Photoconductivity decay curves obtained after cutting off illumination demonstrate the existence of two sets of electron traps of different depths in p-type Si at room temperature. The traps are distributed within the body of the specimen rather than at the surface. An energy-level model is developed to fit the results. In low-resistivity specimens recombination of electrons from the deeper traps is proportional to the square of hole concentration. The deep trap concentration is roughly proportional to conductivity.

537.311.33:[546.289+546.3–1–28–681 2014
Melting Point of Germanium and the Constitution of Some Ge-Ga Alloys—E. S. Greiner and P. Breidt, Jr. [*Jour. Metals* (*New York*), vol. 7, section 2, pp. 187–188; January, 1955.]

537.311.33:546.289 2015
Measurements of Injection Ratio of Point Contacts on Germanium—P. C. Banbury and J. Houghton. (*Proc. Phys. Soc.*, vol. 68, pp. 17–21; January 1, 1955.) Measurements were made on n-type specimens, using the method described by Shockley et al. (380 of 1950). Injection ratio γ was found to be insensitive to the nature of the contact material, to the contact thrust, and to the carrier concentration of the Ge over the limited range investigated. In all cases measured, γ decreased with increasing emitter current over the range 0.5 to 30 ma. A slight decrease of γ with increasing humidity of the ambient air was also observed.

537.311.33:546.289 2016
The Effective Surface Recombination of a Germanium Surface with a Floating Barrier—A. R. Moore and W. M. Webster. (Proc. IRE, vol. 43, pp. 427–435; April, 1955.) One-dimensional analysis is used to examine the possibility of reducing surface recombination velocity s by special surface treatments; three types considered are (a) electroplated metal layer, (b) Ge layer of opposite conductivity, and (c) Ge layer of higher conductivity of same type. Calculations indicate that s should be of the order of 1 cm for cases (b) and (c) and $>1{,}000$ cm for case (a). Measurements of s on alloyed junction surfaces indicate that their apparent recombination velocity is nearly the same as that of the adjacent untreated surfaces, e.g. 300–500 cm. The discrepancy is attributed to lateral current flow due to gradients parallel to the interface, which are neglected in the one-dimensional theory. This effect is discussed in relation to erroneous values of carrier lifetime which have been obtained from diffusion measurements.

537.311.33:546.289 2017
Carrier Extraction in Germanium—J. B. Arthur, W. Bardsley, M.A.C.S. Brown and A. F. Gibson. (*Proc. Phys. Soc.*, vol. 68, pp. 43–50; January 1, 1955.) Extraction may be expected to occur in an n-type crystal when the sweeping voltage applied is of a magnitude such that the transit time of holes is very much shorter than the hole lifetime. A distinction is drawn between this effect and the depletion of minority carriers at a reverse-biased rectifying contact. Techniques are described in which large changes of carrier concentration are produced in near-intrinsic Ge by extraction; use of direct and of pulsed fields is considered. The effect may have important implications for the design of new semiconductor devices.

537.311.33:546.289 2018
The Electrical Properties of Germanium Semiconductors at Low Temperatures—H. Fritzsche and K. Lark-Horovitz. (*Physica*, vol.

20, pp. 834–844; November, 1954.) Low-temperature effects including an anamalous maximum in the Hall effect and a change in the slope of the log-resistivity/inverse-temperature curve were reinvestigated using single crystals of *n*- and *p*-type Ge with various carrier concentrations. The experimental setup is described and results are presented graphically. The observations are consistent with a model which assumes conduction in two energy bands, one of which is the usual conduction or valence band, the other a band with a very small mobility. The sharp decrease of this mobility with decreasing impurity content suggests that the observed characteristics may be due to conduction in an impurity band.

537.311.33:546.289 **2019**

Recombination and Trapping of Carriers in Germanium—H. Y. Fan, D. Navon and H. Gebbie. (*Physica*, vol. 20, pp. 855–872; November, 1954.) Report of experiments at temperatures between liquid-nitrogen and room temperature. Consideration is mainly confined to *n*-type and *p*-type single crystals with no intentionally introduced lattice imperfections or impurities other than the commonly used impurities of the 3rd and 5th groups of elements. The results indicate that carrier lifetime decreases with reduction of temperature, but much faster in *n*-type than in *p*-type material. These results are discussed in terms of recombination through trapping states.

537.311.33:546.289 **2020**

Diffusion Constant of Carriers in Germanium—A. Many. (*Physica*, vol. 20, pp. 985–989; November, 1954.) Results are presented of determinations of the diffusion constant by measurement of injected-carrier lifetime in rectangular filaments with rough surfaces. The method used differs from that of Shockley and Haynes, as modified by Prince (1462 of 1954), in that the diffusion perpendicular to rather than along the direction of the drift is determined. Surface effects are thus completely eliminated. The hole mobility and the temperature dependence of the diffusion constant of holes are in agreement with those found by Prince; for electrons the values obtained are appreciably different.

537.311.33:546.289 **2021**

Galvano-magnetic Effects in Germanium at High Frequencies—B. Donovan and G. Reichenbaum. (*Physica*, vol. 20, pp. 993–995; November, 1954.) A brief report is presented on experimental determinations of the relative change of resistivity in a magnetic field and the Hall coefficient for a selection of Ge samples. Frequencies up to 3 mc were used; in all cases the results were found to be independent of frequency.

537.311.33:546.289:538.214 **2022**

Magnetic Susceptibility Measurements on Germanium between Room Temperature and Liquid Hydrogen Temperatures—A. van Itterbeek, L. de Greve and W. Duchateau. (*Appl. Sci. Res.*, vol. B4, no. 4, pp. 300–308; 1955.) Results obtained are compared with those of Stevens and Crawford (1467 of 1954); a large measure of agreement is found. At liquid hydrogen temperatures there is a marked variation of the susceptibility associated with the paramagnetic term for the ionized impurity [1476 of 1954 (Bush and Mooser)].

537.311.33:546.289:621.314.632 **2023**

Properties of Metal to Germanium Contacts—C. V. Bocciarelli. (*Physica*, vol. 20, pp. 1020–1025; November, 1954.) A discussion is presented of the electrical properties of plates and evaporated contacts; repeatable characteristics are obtainable.

537.311.33:546.431 31 **2024**

Structure in Optical Absorption of Barium Oxide Films—R. J. Zollweg. (*Phys. Rev.*, vol. 97, pp. 288–290; January 15, 1955.) "Measurements of the optical absorption of BaO films at temperatures between 15 degrees K and 370 degrees C are reported. Four absorption peaks between 3.8 eV and 4.5 eV are found for measurements at liquid nitrogen temperature or below."

537.311.33:546.482.21 **2025**

Controlled Preparation and X-Ray Investigation of Cadmium Sulfide—F. Schossberger. (*Jour. Electrochem. Soc.*, vol. 102, pp. 22–26; January, 1955.)

537.311.33:546.482.21:535.215 **2026**

Photoelectric Properties of Evaporated Cds Films W. Veith. (*Z. angew. Phys.*, vol. 7, pp. 1–7; January, 1955.) Films with high photoconductivity can be obtained by evaporation; Cu and Ag are used as sensitizers. Experiments are described which enable the structure of the film and the photoconduction mechanism to be understood.

537.311.33:[546.817.221+546.817.231 +546.817.241 **2027**

The Hall Coefficient, Electrical Conductivity and Magneto-Resistance Effect of Lead Sulphide, Selenide and Telluride—E. H. Putley. (*Proc. Phys. Soc.*, vol. 68, pp. 22–34; January 1, 1955.) Procedure and results are described for measurements of Hall coefficient and conductivity of single crystals and natural specimens of PbS, PbSe and PbTe over the temperature range 77 degrees–1,000 degrees K; some measurements at 20 degrees K are also described. The magnetoresistance effect was measured on some specimens at temperatures between 20 degrees and 300 degrees K. The results are consistent with accepted semiconductor theory. *See* also 2028 below.

537.311.33:[546.817.231+546.817.241 **2028**

Thermoelectric and Galvanomagnetic Effects in Lead Selenide and Telluride—E. H. Putley. (*Proc. Phys. Soc.*, vol. 68, pp. 35–42; January 1, 1955.) Measurements of the thermoelectric power and of the Peltier, Nernst, Ettinhausen and Righi-Leduc effects are reported. The results are in accordance with accepted semiconductor theory. Values of the coefficients calculated from the Hall coefficient and conductivity of the specimen are in good agreement with the measured coefficients. The effective mass of carriers in PbSe is estimated. *See* also 2027 above.

537.311.33:546.817.231 **2029**

Hall Effect and Electrical Conductivity of Lead Selenide—E. Hirahara and M. Murakami. (*Jour. Phys. Soc. Japan*, vol. 9, pp. 671–681; September/October, 1954.) Measurements in the temperature range from 500 degrees C. to −180 degrees C. are reported. Results for *p*-type specimens are analyzed taking account of scattering from both lattice and impurity centers and of the temperature dependence of Fermi energy. Errors of approximation in calculating Fermi energies of impurity semiconductors with both *p*- and *n*- type conduction are discussed.

537.311.33:548.0:535.34 **2030**

Infrared Lattice Absorption in Ionic and Homopolar Crystals—M. Lax and E. Burstein. (*Phys. Rev.*, vol. 97, pp. 39–52; January 1, 1955.) Evidence is discussed relevant to the possibility that appreciable deformation of the charge distribution about the atoms results from lattice vibration. This deformation introduces a second-order electric moment, whose effect on the infrared absorption is analyzed. In the case of diamond, Si and Ge, part of the absorption is due to this effect, the remainder being due to impurity-induced first-order electric moments. The second-order effect also affords an explanation of the side bands in the absorption and reflection spectra of the alkali halides, but not of the observed broadening of the main absorption line.

538.221 **2031**

Neutron Diffraction Studies of the Magnetic Structure of Alloys of Transition Elements—C. G. Shull and M. K. Wilkinson. (*Phys. Rev.*, vol. 97, pp. 304–310; January 15, 1955.) Data on scattering and magnetic moments are presented for members of the alloy series Fe-Cr, Ni-Fe, Co-Cr and Ni-Mn.

538.221 **2032**

Theory of the Faraday and Kerr Effects in Ferromagnetics—P. N. Argyres. (*Phys. Rev.*, vol. 97, pp. 334–345; January 15, 1955.) A treatment based on the energy-band theory of metals is presented.

538.221 **2033**

Relation between the Temperature of a Ferromagnetic Body and the Heat dissipated in its Interior by an Alternating Field—G. Ribaud and D. Bordier. [*Compt. Rend. Acad. Sci.* (*Paris*), vol. 240, pp. 703–707; February 14, 1955.] From measurements on hollow Ni and Fe cylinders heated by an internal resistor and located inside a hf coil, curves are derived showing the power dissipated as a function of temperature. The curve rises from room temperature to Curie temperature, when it drops sharply to a low value corresponding to a nonmagnetic metal. The effect is attributed to an increase of initial permeability with temperature.

538.221 **2034**

Magnetic Hysteresis in Annealed Nickel-Cobalt Alloys—M. Yamamoto, S. Taniguchi and K. Hoshi. (*Sci. Rep. Res. Inst. Tohoku Univ., Ser. A*, vol. 6, pp. 539–550; December, 1954.) Hysteresis curves determined ballistically are shown for Ni-Co alloy specimens containing between 0.6 per cent and 99.86 per cent Co. γ-phase alloys containing >25 per cent Co show hysteresis loops of the constricted form similar to those of annealed perminvars and permalloys. The characteristic may be explained by the stabilization of domain walls due to the appearance of an ,additional uniaxial anisotropy along the directions of magnetization vectors during annealing. Results are presented graphically and references to earlier work on other physical properties of Ni-Co alloys are given.

538.221:621.317.411.029.64 **2035**

Measurement of the Complex Permeability of Carbonyl Iron Powders at 4000 Mc/s—A. Nishioka and H. Okamoto. (*Jour. Phys. Soc. Japan*, vol. 10, p. 79; January, 1955.) Measurements are reported on four samples with different particle sizes, the powders being dispersed in polystyrol. The variation with particle size is discussed briefly in relation to skin effect.

538.221:621.318.134 **2036**

Magnetic Rotation Phenomena in a Polycrystalline Ferrite—D. Park. (*Phys. Rev.*, vol. 97, pp. 60–66; January 1, 1955.) The hf properties of polycrystalline ferrites are analyzed taking account of the interaction between neighboring crystallites. Expressions derived for the susceptibility lead to values in satisfactory agreement with those obtained experimentally by Brown and Gravel (2037 below).

538.221:621.318.134 **2037**

Domain Rotation in Nickel Ferrite—F. Brown and C. L. Gravel. (*Phys. Rev.*, vol. 97, pp. 55–59; January 1, 1955.) Permeability measurements were made on specimens prepared by sintering, at various temperatures, ferrite particles of dimensions between 0.5 and 1 μ. The results indicate that for such specimens the initial permeability and the rf dispersion

are due principally to rotation of the crystallite magnetic moments in an equivalent anisotropy field.

538.221:621.318.134 2038

The g-Factor of Ferromagnetic Spinels—Y. Kojima. (*Sci. Rep. Res. Inst. Tohoku Univ., Ser. A*, vol. 6, pp. 614–622; December, 1954.) An experimental investigation is reported of ferromagnetic resonance in Ni-Zn and Mn-Zn binary ferrites and Ni ferrite aluminates of various compositions, at frequencies of about 9.4, 19.2 and 28.9 kmc. The observed variation of the g-factor with composition is in good agreement with theoretical results, except in $NiFe_{2-x}Al_xO_4$ at $x>0.72$. The frequency dependence of the g-factor is mainly determined by the porosity of the specimen. Results are presented graphically.

538.221:621.318.134 2039

Ferromagnetic Resonance in Nickel Ferrite between One and Two Kilomegacycles [per second]—H. Suhl. (*Phys. Rev.*, vol. 97, pp. 555–557; January 15, 1955.) Resonance in the band considered is obtained by a special experimental arrangement producing a particularly low effective field. Some results are presented.

538.652:538.221 2040

The Magnetostriction Constants of Silicon Steel: Part 2—H. Takaki and Y. Nakamura. (*Jour. Phys. Soc. Japan*, vol. 9, pp. 748–752; September/October, 1954.) Part 1: 785 of March. Further measurements show that the magnetostriction constant λ 100, after decreasing nonlinearly as the Si content is increased up to 2 per cent, rises sharply at Si values between 2 per cent and 3 per cent, and then shows little change up to 4 per cent Si.

621.315.616 2041

Dielectric Constants and Mechanical Losses of High Polymers—H. Thurn. (*Z. angew. Phys.*, vol. 7, pp. 44–47; January, 1955.) Small discontinuities are observed in the dielectric-constant/temperature characteristic for strongly and for weakly polar high polymers; the temperature points at which the discontinuities occur depend on frequency. For a given frequency, the ultrasonic-absorption /temperature characteristic exhibits a maximum and the ultrasonic-velocity/temperature characteristic slopes steeply at the same points. The cause of the discontinuities is thought to be variation of the freedom of motion of weakly polar partial groups.

621.318.122 2042

The Magnetic Properties and their Temperature Dependence of Ferromagnetic Alloys with an Order-Disorder Transformation—T. Taoka and T. Ohtsuka. (*Jour. Phys. Soc. Japan*, vol. 9, pp. 712–729; September/October, 1954.) Measurements made on samples at different fixed degrees of order, and particularly in the transformation temperature range, are reported and discussed. In Ni_3Fe the Curie point, saturation magnetization and magnetostriction all increase with the formation of the superlattice. In Ni_3Mn the Curie point increases from below room temperature in the disordered state to over 490 degrees C. in the ordered state; saturation magnetostriction is very small; large long-period magnetic aftereffects occur at intermediate states of order.

621.318.2.042.15 2043

Influence of Additives in the Production of High Coercivity Ultra-Fine Iron Powder—E. W. Stewart, G. P. Conard II and J. F. Libsch. (*Jour. Metals (New York)*, vol. 7, section 2, pp. 152–157; January, 1955.) Magnesium formate, cadmium formate, cadmium oxide, stannous oxide or tin formate, when added in the correct proportion to ferrous formate prior to its reduction, inhibit sintering and markedly improve the magnetic properties of the compacts produced from the resulting powders.

669.871.4 2044

Purification of Gallium by Zone-Refining—D. P. Detwiler and W. M. Fox. [*Jour. Metals (New York)*, vol. 7, section 2, p. 205; January, 1955.] The method involves cleaning the surface by acid leaching, followed by zone refining to remove metallic impurities.

53 2045

Dielectrics and Waves. [Book Review]—A. R. von Hippel. Publishers: Chapman and Hall, London, Eng. 284 pp., 128s. (*Wireless Eng.*, vol. 32, p. 143; May, 1955.) A treatment in which the physics and electrical engineering aspects are combined.

537.311.33+621.314.7 2046

Halbleiter-Probleme Vol. I. [Book Review]—W. Schottky (Ed.). Publishers: F. Vieweg and Sohn, Brunswick, W. Germany, 1954, 387 pp., DM 28.80. (*Fernmeldetech. Z.*, vol. 8, p. 62; January, 1955.) A collection of papers presented at the semiconductor conference of the German Physical Societies at Innsbruck in Autumn, 1953.

MATHEMATICS

517.948 2047

The Solution by Iteration of Nonlinear Integral Equations—M. Lotkin. (*Jour. Math. Phys.*, vol. 33, pp. 346–355; January, 1955.)

519.2:530.16 2048

Distribution of the Extreme Values of the Sum of n Sine Waves phased at Random—S. O. Rice. (*Quart. Appl. Math.* vol. 12, pp. 375–381; January, 1955.)

519.24 2049

Practical Analysis of Sequences of Observations or Empirical Functions—O. M. J. Mittmann. (*Arch. Met. A, Wien*, vol. 8, pp. 113–120; January 7, 1955.) A method is described for finding the variance of the average of any empirical sequence of numbers, based on the assumption that as the sequence tends to infinity the standard deviation tends to zero.

MEASUREMENTS AND TEST GEAR

621.314.7.001.4 2050

A Point-Contact Transistor Test Set—R. S. Hill. [*Elec. Eng., (New York)*, vol. 74, section 1, pp. 59–62; January 1955.] Detailed operating instructions are presented relative to the tests described by Wooley (1092 of May).

621.317 2051

Precision Electrical Measurements—L. Hartshorn. [*Nature (London)*, vol. 175, pp. 57–58; January 8, 1955.] Report of symposium held at the National Physical Laboratory in November, 1954.

621.317.3:621.315.212:621.397.5 2052

Evaluation of Pulse-Reflection Curves for determining the Length and True Magnitude of Inhomogeneities in Wide-Band Cables—L. Krügel. (*Fernmeldetech. Z.*, vol. 8, pp. 14–18; January, 1955.) A "dc" and an "ac" pulse were used; the former approximated a one-quarter-cycle sinusoidal voltage of duration 4×10^{-8} second between zero and maximum, the latter a similar pulse but of duration 1.8×10^{-8} second. Examples of typical waveforms of pulses reflected at faults of various lengths at distances up to about 3 km from the instrument are discussed.

621.317.3+621.396.621:621.396.822 2053

On Power Spectra and the Minimum Detectable Signal in Measurement Systems—J. J. Freeman. (*Jour. Appl. Phys.*, vol. 26 pp. 236–240; February, 1955.) A least upper bound for the minimum detectable value of a signal received in noise is specified in terms of the first and second moments of the rectified output. The power spectrum of the rectified output and the impedance characteristic of the output meter together enable the first and second moments of the meter deflection to be determined in two specified modes of operation.

621.317.328(083.74) 2054

Study of the Very-High-Frequency Field-Intensity Standard—T. Yagara and G. Kondo. [*Jour. Radio Res. Labs (Japan)*, vol. 1, pp. 63–71; June, 1954.] The use of a crystal voltmeter in the standard-antenna method of field-strength measurement is discussed and experimental results obtained at different frequencies by this method and the standard-field method are compared. The former is preferred. Replacing the crystal voltmeter by a vacuum thermocouple gave similar results at 55 mc. See also 3090 of 1950 (Greene and Solow) and 154 of 1951 (King).

621.317.33.029.6 2055

Techniques for the Measurement of Impedances at Metre and Decimetre Wavelengths and their Use for studying the Dielectric Properties of Solids and Liquids—A. Lebrun. [*Ann. Phys. (Paris)*, vol. 10, pp. 16–70; January/February, 1955.] A comprehensive account is given of resonance methods involving variation of the length of a section of transmission line. Compared with cavity-resonator methods, these have the advantage of covering a wide frequency band with a single apparatus. Results obtained with some normal saturated alcohols are reported. 74 references.

621.317.335.029.62/.63 2056

Measurements of Materials at Ultrahigh Frequencies—H. Schwan and K. Li. [*Trans. AIEE*, Part I, *Communication and Electronics*, vol. 73, pp. 603–607; 1954. Digest, *Elec. Eng. (New York)*, vol. 74, section 1, p. 64; January, 1955.] Discussion of methods involving measurements of standing waves resulting from reflection of energy from a dielectric sample indicates that small sample thickness and open-circuit techniques are desirable for determining the dielectric properties of high-permittivity materials over the frequency range 100–1,000 mc.

621.317.335.3:621.372.8 2057

Methods of Measuring Dielectric Constants based upon a Microwave Network Viewpoint—A. A. Oliner and H. M. Altschuler. (*Jour. Appl. Phys.*, vol. 26, pp. 214–219; February, 1955.) Measurement procedures are discussed in which the dielectric sample is located within a waveguide; the admittance determinant of the quadripole system thus constituted is simply related to the required dielectric constant.

621.317.337:621.372.412 2058

Application of Frequency Modulation to the Determination of the Quality Factor Q of Piezoelectric Crytstals—H. Mayer. [*Compt. Rend. Acad. Sci. (Paris)*, vol. 240, pp. 612–614; February 7, 1955.] The signal from a frequency-shift oscillator is applied in push-pull across a potentiometer, while the voltage from the oscillating crystal is superposed at one terminal only of the potentiometer. A tapping on the potentiometer is adjusted so that the output comprises only the voltage due to the crystal; this is amplified, detected and applied to a cro. The crystal may be in the form of a few grains vacuum-sealed between the plates of a capacitor. A formula is presented by means of which the Q of the crystal can be calculated from the photographed oscillogram.

621.317.361:621.317.755 2059

A Method for Accurate Determination of Frequency—L. Horn. (*Frequenz*, vol. 8, pp. 304–306; October, 1954.) The cro timebase

frequency is derived from the mains, and the signal of unknown frequency, up to 2 mc, is passed through a pulse former and a counter circuit. When the unknown frequency is a multiple or certain fraction of the timebase frequency, a stationary stepped pattern is obtained. With a slight adjustment in experimental arrangement phase can also be measured.

621.317.361:621.396.822 2060
Short-Time Frequency Measurement of Narrow-Band Random Signals by Means of a Zero Counting Process—H. Steinberg, P. M. Schultheiss, C. A. Wogrin and F. Zweig. (*Jour. Appl. Phys.*, vol. 26, pp. 195–201; February, 1955.) Further consideration of the problem of determining the true frequency of a signal represented by a power spectrum, when measured over a finite time interval [206 of January (Schultheiss et al.)]. A third method now discussed consists of counting the zeros of the signal in the specified interval. For a Gaussian power spectrum the figure of merit of the arrangement used, defined by output-variance/sensitivity-squared [2168 of 1945 (Rice)], is comparable with those of the autocorrelator and frequency discriminator.

621.317.373:621.317.755 2061
A Direct Method of Phase Measurement on the Cathode-Ray Tube—D. Karo. (*Brit. Jour. Appl. Phys.*, vol. 6, pp. 10–12; January, 1955.)

621.317.42 2062
New Method for Measurement of Magnetic-Field Distribution—U. Dolega, H. Pfeifer and A. Lösche. (*Z. angew. Phys.*, vol. 7, pp. 12–13; January, 1955.) A nuclear-resonance method is described. A twin-coil system is used to ease the requirement for high time constancy of the field under examination.

621.317.42 2063
The Förster Probe for Measurement of Strong Magnetic Fields—F. Brandstaetter. (*Elektrotech. u. Maschinenb*, vol. 72, pp. 12–15; January 1, 1955.) A lf differential method suitable for measurements up to 4,000 oersted is described. The probe comprises two parallel carbonyl-iron cores each carrying a primary and a secondary; the primaries are wound to produce magnetization in the same sense, the secondaries are wound in opposition. In use, one of the cores is in the field, the other is outside it. Using the ancillary oscillator (~10 kc) and amplifier circuits described, direct indication of the field strength can be obtained.

621.317.7:621.383 2064
On the Theory of Photoelectric Compensators and their Accuracy—A. Kelen. (*Appl. Sci. Res.*, vol. B4, no. 4, pp. 278–284; 1955.)

621.317.7:621.383 2065
A Photoelectric Compensator with Good Zero Stability—A. Kelen. (*Appl. Sci. Res.*, vol. B4, no. 4, pp. 285–288; 1955.)

621.317.725 2066
An Inverted-Triode Voltmeter for the Measurement of Negative Voltages—R. Génin. (*Jour. Phys. Radium*, vol. 16, pp. 74–75; January, 1955.)

621.317.729 2067
The Rubber Membrane and the Solution of Laplace's Equation—W. Fulop. (*Brit. Jour. Appl. Phys.*, vol. 6, pp. 21–23; January, 1955.) Examination of the theory of the rubber membrane, as used e.g. for investigating es fields, indicates that Laplace's equation holds without restriction.

621.317.755 2068
Measurement of Time Constants with the Cathode-Ray Oscillograph—R. Gullien and H. Mayer. [*Compt. Rend. Acad. Sci.* (*Paris*), vol. 240, pp. 739–741; February 14, 1955.] A method described by Tolstoi and Feofilov is discussed. A voltage with a known adjustable time constant is applied to the cro X plates; the trace, which is in general a transcendental curve, becomes a straight line when the time constant of the unknown voltage applied to the Y plates becomes equal to that of the X-plate voltage. Circuit methods for improving the attainable accuracy are considered, and an outline is given of a suitable arrangement.

621.317.761 2069
High Precision Automatic Frequency Comparator and Recorder—J. M. Shaull. (*Tele-Tech. and Electronic Ind.*, vol. 14, section 1, pp. 58–59, 134; January, 1955.) Description of apparatus in use at the N.B.S. enabling frequency differences of the order of 1 part in 10^{11} to be detected and recorded. The improvement in sensitivity as compared with apparatus and methods described previously (1731 of 1953) is obtained by use of an auxiliary cavity-type type multiplier-converter unit, permitting comparison at about 1 kmc instead of 100 mc.

621.385.001.4 2070
Quality Screening for Audio-Frequency Impulse Noise and Microphonism—R. J. Wohl and S. Winkler. [*Elec. Eng.*, (*New York*), vol. 74, section 1, pp. 54–56; January, 1955.] Test gear described includes a pendulum tapper for exciting valves to produce af noise, and indicating circuits using biased thyratrons to operate neon lamps. Procedure adopted for trials on 100 unselected tubes is described. Unsatisfactory tubes are eliminated with greater facility than by use of procedures based on a statistical approach. See also *Proc. Nat. Elect. Conf.*, *Chicago*, vol. 9, pp. 119–129; 1953. (Wohl et al.)

OTHER APPLICATIONS OF RADIO AND ELECTRONICS

531.77:[621.387:621.318.57 2071
A High-Speed Revolution Counter—E. L. Harrington. (*Electronic Eng.*, vol. 27, pp. 142–146; April, 1955.) An instrument designed for measuring the rotational speed of gas turbines to within ±1 revolution per minute at 20,000 revolutions per minute operates by counting a frequency proportional to speed over a 1-second sampling period, at sampling intervals of 3 seconds. The counter uses dekatrons.

534.143:529.78:621.314.7 2072
Electronic Clock using Transistors—N. Boyer. [*Electronique* (*Paris*), no. 98, pp. 20–22; January, 1955.] A self-maintained-pendulum precision clock is described in which the electrical maintaining mechanism operates without contacts, using instead a transistor as a relay. The only power supply required is a 1.5-v cell. Other possible applications relating to the maintenance of mechanical oscillations are indicated briefly.

616.006.4:534.2–8 2073
Ultrasonic Ranging Speeds Cancer Diagnosis—J. J. Wild and J. M. Reid. (*Electronics*, vol. 28, pp. 174–180; March, 1955.)

651–52+681.142 2074
I.V.A. [Royal Swedish Academy of Engineering Sciences] Director's Annual Report on Progress in Research and Technology: Part 4—Computers and Automation—Velander. (See 1878.)

621.316.71 2075
The Automatic Factory—a Critical Examination—S. A. June J. D. Bardis, L. H. Lurio, L. S. Polander, O. Sagedahl, H. A. Sklenar, and B. K. Yenkin. (*Instruments and Automation*, vol. 27, part 1, pp. 1952–1997; December, 1954, vol. 28, pp. 110–114 and 277–279; January and February, 1955.) Automatic processes used in industry were analyzed. Apart from cost, the main obstacle to fully automatic operation is the difficulty in assembly of parts.

621.317.39.082:621.38 2076
Electronic Indicators of Mechanical Quantities—L. A. Goncharski. (*Uspekhi Fiz. Nauk*, vol. 55, pp. 81–100; January, 1955.) A review is presented of the author's work on measurement of small displacements (827 of April) and of work published in other countries on accelerometers, tensometers, manometers, etc. 17 references.

621.319.339 2077
The Calculation of Voltage Surges in a Van de Graaff Generator—B. Millar. (*Brit. Jour. Appl. Phys.*, vol. 6, pp. 13–15; January, 1955.)

621.365.54:621.385.002.2 2078
High-Frequency Induction Heating—[*Metal Ind.* (*London*), vol. 86, p. 52; January 21, 1955.] Application of the hf heating process to the brazing of thermionic-tube components is described briefly. The parts are placed in an atmosphere of forming gas during the process. A 25-kw generator operating at a frequency of 2 mc is used.

621.365.65 2079
A New Application of Dielectric Heating—A. Blake. (*Plastics*, vol. 20, pp. 31–32; January, 1955.) The use of dielectric heating in the manufacture of rollers for leather tanning, printing, etc. is discussed. The method of mold manufacture is described.

621.373.4:621.365.55 2080
The Operation and Loading Characteristics of Valve Oscillators for Dielectric Heating—V. L. Atkins. (*Electronic Eng.* vol. 27, pp. 106– and 164–169; March and April, 1955.)

621.384.611:621.372.413 2081
Microtron Resonators—H. F. Kaiser. (*Jour. Frank. Inst.*, vol. 259, pp. 25–46; January, 1955.) Q, shunt resistance and optimum size are discussed for various simple resonator shapes for use with the microtron (electron cyclotron). The design of confocal ellipsoidal-hyperboloidal resonators is considered, and an equation given relating resonator dimensions and operating frequency which has proved satisfactory for practical use.

621.384.612 2082
Synchrotron Oscillations induced by Radiation Fluctuations—M. Sands. (*Phys. Rev.*, vol. 97, pp. 470–473; January 15, 1955.)

621.385.83:537.533 2083
The Influence of the Space Charge in an Electron Beam accelerated in a Constant Electrostatic Field up to Energies of Several MeV—M. Sangster. (*Appl. Sci. Res.*, vol. B4, no. 4, pp. 261–270; 1955.) The development of an electron gun to give high-intensity current pulses is discussed. Calculation shows that, at an average field strength of 10^6 v/m in the acceleration tube, space charge begins to play a dominating part at a current density of 2 a/cm². Advantages are gained by making the first electrodes of larger diameter than the succeeding ones.

621.387.424 2084
Gas Discharge Mechanism of Halogen-Quenched Counters—D. van Zoonen. (*Appl. Sci. Res.*, vol. B4, pp. 237–248; 1955.)

621.387.424 2085
Corona Threshold and the Range of Velocities of Pulse Spread in Geiger Counters—L. B. Loeb. (*Phys. Rev.*, vol. 97, pp. 275–277; January 15, 1955.)

629.113.06:621.383.27 2086
Scanning Disk improves Auto Headlight Dimmer—J. Rabinow. (*Electronics*, vol. 28, pp. 170–173; March, 1955.) Description of an automatic arrangement capable of detecting headlights at 1,500 feet and tail lights at 300 feet; by interposing a motor-driven scanning disk in front of the multiplier photocell the dimming control action is made independent of the general illumination level.

681.81:621.37/.38 2087

Some Recent Developments in American Electronic Musical Instruments—A. Douglas. (*Electronic Eng.*, vol. 27, pp. 154–159; April, 1955.) An account of developments in the direction of improved tonal synthesis and increased flexibility of control.

PROPAGATION OF WAVES

621.396.11 2088

On the Radio Wave Propagation in a Stratified Atmosphere—R. Yamada. (*Jour. Phys. Soc. Japan*, vol. 10, pp. 71–77; January, 1955.) Analysis is presented for propagation in a single-surface duct, the refractive-index profile being given by the expression $a+bh+ch^2$.

621.396.11:550.510.535:523.5 2089

Continuous Radar Echoes from Meteor Ionization Trails—Eshleman, Gallagher and Peterson. (*See* 1985.)

621.396.11.029.55:523.5 2090

Observations of Distant Meteor-Trail Echoes followed by Ground Scatter—W. L. Hartsfield. (*Jour. Geophys. Res.*, vol. 60, pp. 53–56; March, 1955.) "Observations of backscatter on 13.7 Mc/s over a southeasterly path from Sterling, Virginia, revealed the existence of meteor-trail reflections just ahead of the main body of the backscatter, demonstrating that the latter was from the ground in these instances. The existence of apparent two-hop backscatter without the appearance of one-hop was noted in a number of cases. Possible reasons for this behavior are discussed."

621.396.11.029.55:621.396.824 2091

Some Considerations on the Measurement of Bearing of the Incoming Short Waves: Part 1.—I. Kasuya. [*Jour. Radio Res. Labs.* (*Japan*), vol. 1, pp. 29–40; June, 1954.] During undisturbed ionospheric conditions in early February, 1954 measurements were made with crdf equipment and U-Adcock antennas of the variations in the bearing of standard-frequency 4-mc AO signals at four stations distant between 340 and 920 km from the transmitter. Results are compared with muf data for E and F regions. Difficulties of df in the skip zone are noted. Twilight effect in lateral deviation δ was observed on a short-distance N-S path. A sudden 20-db increase in signal strength at Akita in the evening coincided with a sudden increase in δ at Sendai, distant about 170 km SSE.

621.396.11.029.62:551.594.5 2092

More about V.H.F. Auroral Propagation—Dyce. (*See* 1987.)

621.396.11.029.62:621.317.328 2093

Measurements of Field Intensity of V.H.F. Radio Waves behind Mt. Fuji—T. Kono, Y. Uesugi, M. Hriai, S. Niwa and H. Irie. [*Jour. Radio Res. Labs* (*Japan*), vol. 1, pp. 1–15; June, 1954.] The "diffraction gain of a mountain" (obstacle gain), defined as the ratio of the actual field-strength to that calculated for a smooth spherical earth, was investigated in May, 1954 using FM and frequency-shift transmissions at 159.49 mc with horizontal polarization. Receivers were located at distances up to 200 km behind Mt. Fuji, which is 3,780 miles high and effectively 80 km from the transmitter. At Ise Bay, 180 km from Mt. Fuji, the maximum gain was about 85 db. Fading was generally slight. Path profiles and field-strength records are shown.

621.396.81.029.6 2094

V.H.F. and U.H.F. Reception: Effects of Trees and Other Obstacles—J. A. Saxton and J. A. Lane. (*Wireless World*, vol. 61, pp. 229–232; May, 1955.) A summary is presented of published experimental results and of some previously unpublished work on propagation in the frequency range from about 100 mc to 3 kmc. The results are extended, by calculation, down to 30 mc. For a continuous wood the attenuation is of the order of 0.02 db/m at 30 mc rising to about 0.5 db/m at 3 kmc. Below 1 kmc the attenuation rate is slightly greater with vertical polarization than with horizontal polarization. For single obstacles, such as a tree or a building, diffraction effects result in considerable spatial variations of field-strength in the shadow region.

621.396.812.3:621.39.001.11 2095

Information Theory Aspects of Propagation through Time-Varying Media—Feinstein. (*See* 2103.)

RECEPTION

621.396.62.029.62:621.376.333 2096

Design for an F.M. Tuner—S. W. Amos and G. G. Johnstone. (*Wireless World*, vol. 61, pp. 159–163 and 216–222; April and May, 1955.) The tuner, designed for the BBC vhf service, to cover the 87.5–100-mc frequency range, uses a ratio-detector; reasons for preferring this to the Foster-Seeley discriminator are given. A complete circuit diagram, lists of components and layout photographs are presented, and the operation and constructional details are discussed in some detail.

621.396.621 2097

The Siemens S.S.B. Receiver KW2/6—E. Schulz, D. Leypold and H. Schreiber. (*Frequenz*, vol. 8, pp. 306–313; October, 1954.) Designed for long-distance reception of telephony in two independent channels on either side of a suppressed carrier or for ssb reception of dsb transmissions. Two models cover the ranges 2.5–20 mc and 4–28 mc respectively. Frequency constancy of $\Delta f/f \leqq 10^{-7}$ is achieved.

621.396.621+621.317.3:621.396.822 2098

On Power Spectra and the Minimum Detectable Signal in Measurement Systems—Freeman. (*See* 2053.)

621.396.621:621.396.822 2099

The Effect of a Random Noise Background upon the Detection of a Random Signal—H. S. Heaps. (*Canad. Jour. Phys.*, vol. 33, pp. 1–10; January, 1955.) " A Noise distributed in phase and power according to a Rayleigh law is studied in terms of its effects upon the detectability of a signal of similar phase and amplitude distributions. An expression is derived for the probability distribution of the ratio of the power of the signal plus noise to that of the noise in the absence of the signal. The corresponding result is given for the ratio of the averages over several observations. Also derived is the probability distribution of the fractional change in noise plus signal power due to a given fractional change in signal power."

621.396.621.54:621.314.7 2100

Design of Transistorized High-Gain Portable—W. E. Sheehan and J. H. Ivers. (*Electronics*, vol. 28, pp. 159–161; March, 1955.) An 8-transistor superheterodyne receiver is described, capable of delivering 100 mw undistorted output.

STATIONS AND COMMUNICATION SYSTEMS

621.376.55:621.396.41 2101

Modulator Equipment for a 24-Channel P.P.M.-System—K. Steinbuch, H. Endres and H. Reiner. (*Fernmeldetech. Z.*, vol. 8, pp. 38–43; January, 1955.)

621.39.001.11 2102

Effect of Heisenberg's Principle on Channel Capacity—R. J. Solomonoff. (PROC. IRE, vol. 43, p. 484; April, 1955.) Analysis shows that the value found for the energy necessary to transmit one bit of information is not appreciably increased by introducing quantum-mechanics considerations.

621.39.001.11:621.396.812.3 2103

Information Theory Aspects of Propagation through Time-Varying Media—J. Feinstein. (*Jour. Appl. Phys.*, vol. 26, pp. 219–229; February, 1955.) "The channel capacity of a communications system which utilizes wave propagation through a time-varying medium such as the ionosphere or troposphere is evaluated in terms of the statistical properties of the medium and of the noise. The signal fading in such a system reduces the capacity. Rayleigh fading is found to give rise to an equivalent signal to noise ratio of 1.72, while shallow fading of the Gaussian type augments the noise in the channel by a fraction of the signal power proportional to the fading depth. An optimum manner of band width subdivision is shown to exist when selective fading is present. Information theory concepts are broadened to include the possibility of multiple reception at spaced receiving sites, and the consequent increase in theoretical channel capacity is computed as a function of the number of such sites and the signal statistics. The method of maximum likelihood is utilized to obtain optimum combinatorial laws for the multiple signals. The commonly employed maximum signal selection diversity system is shown to perform as well as the optimum system in the presence of Rayleigh fading, for a small number of receiving sites."

621.395.66:621.385.4/.5 2104

Automatic Valve-Emission Monitor—J. Boura. (*A.T.E. Jour.*, vol. 11, pp. 49–51; January, 1955.) A monitoring system applicable to multichannel carrier systems is described. The rise in screen potential due to a decrease in cathode emission is used to operate an alarm. The basic circuit of the monitor and alarm is described; a miniature cold-cathode metering diode is used.

621.396.41 2105

Radio-Link Transmission with Reference to International Recommendations for Long-Distance [telephone] Communication—H. Werrmann. (*Elektrotech. Z., Edn. A*, vol. 76, pp. 64–72; January 1, 1955.)A discussion of multichannel radiotelephone systems, and the various modulation methods used, with particular reference to the limitations imposed by noise. A brief account is also given of CCIR and CCIF recommendations made at Geneva in 1954, on standardization of equipment. See also *Tech. Mitt. schweiz. Telegr.-TelephVerw*, vol. 33, pp. 35–38; January 1, 1955.

621.396.41.029.64:621.376.3 2106

Method for improving the Performance of Radiotelephone Links—C. Ducot. (*Onde élect.*, vol. 35, pp. 41–54; January, 1955.) CCIF recommendations on multiplex links are examined with particular reference to thermal and intermodulation noise. Experimental results are presented for a 48-channel link of length 12.5 km using a double FM system with a carrier frequency of 3.5 kmc and a final frequency deviation of ± 5 mc; high output power is obtained using the multireflection oscillator tube described by Coeterier (2628 of 1947). The performance of double and simple FM systems is compared.

621.396.44 2107

Short-Haul Carrier-Current Systems—J. Jacot. (*Tech. Mitt. schweiz. Telegr.-Teleph-Verw.*, vol. 33, pp. 8–17 and 70–83; January 1 and February 1, 1955. In French.) A review of systems in use or under development in Europe and the U.S.A. The manner in which various factors affect the choice of a particular system is indicated.

621.396.5:621.311.6 2108

Battery-Powered Subscribers' Radio Telephone—N. A. Lockley and R. A. Glover. (*A.T.E. Jour.*, vol. 11, pp. 62–74; January, 1955. Digest, *Elec. Jour.*, vol. 154, p. 203; January 21, 1955.) Lightweight FM radiotelephone equipment with normal dialing facilities is described, for operation at frequencies between 54 and 88 mc. A 12-v accumulator is used, 90

and 120 V hv being obtained by means of a vibrator unit. Cyclic switching reduces the stand-by consumption to 2.16 Ah per day. A rf output of 500 mw ensures reliable operation over a distance of 17–20 miles. In use the equipment and accumulator are mounted on the antenna pole and connected by a two-wire line to the subscriber's instrument. An AM system operating at 160 mc is also briefly described.

621.396.61/.62 2109
Two-Way U.H.F. Pack Set uses Helmet Antenna—D. C. Jensen and M. Schwartz. (*Electronics*, vol. 28, pp. 150–153; March, 1955.) A compact 23-tube transmitter/receiver Type-AN/PRC-14, for military use, is described. Operation is in the band 225–400 mc; about 1,750 channels are available, but only one of four pre-set crystal-controlled frequencies can be selected at a time. Ground-to-air communication over a distance of 110 miles has been achieved.

621.396.65.029.63 2110
P.P.M. Radio-Link Equipment—O. Laaff and O. Bettinger. (*Fernmeldetech. Z.*, vol. 8, pp. 43–48; January, 1955.) Equipment for the frequency range 2.1–2.3 kmc is briefly described with block diagrams.

621.396.712.2:534.86 2111
Broadcasting-Studio Engineering—today and tomorrow—E. Vogl. [*Radio Tech.* (*Vienna*), vol. 31, pp. 3–7; January, 1955.] Both centralized and decentralized studio control systems are briefly discussed; the latter system is the one preferred in Austria. The gain/frequency characteristic of the studio amplifiers should be adjustable, so that the apparent loudness /frequency characteristic of the original can be reproduced at a given intensity level.

621.396.931 2112
Single Sideband for Mobile Communication—A. Brown and R. H. Levine. [*Proc. IRE* (*Australia*), vol. 16, pp. 12–17; January, 1955. *Convention Record IRE*, Part 2, pp. 123–128; 1953.] The advantages of the ssb system are indicated and simple arrangements are described.

SUBSIDIARY APPARATUS

621–526 2113
Three Examples of Electrical-Servomechanism Engineering—E. Gerecke. (*Z. angew. Math. Phys.*, vol. 5, pp. 443–465; November 15, 1954.) Servomechanism system design problems treated by graphical methods, which are explained, include regulation of the output voltage of a constant-speed independently excited dc generator and two cases of motor speed control.

621.314.63 2114
Component Design Trends—Metallic Rectifiers approach Infinite Life—F. Rockett. (*Electronics*, vol. 28, pp. 162–166; March, 1955.) Developments in Cu_2O, Se, Si, Ge and TiO_2 rectifiers are surveyed; new designs give reduced size and longer life together with higher operating-temperature, output-current and reverse-voltage ratings.

621.316.722.078.3 2115
Highly Stable Medium-Voltage Direct and Alternating Sources for Test Purposes—H. Helke and R. Stenzel. (*Z. angew. Phys.*, vol. 6, pp. 521–528; November, 1954.) A review of methods of stabilizing supply voltages up to about 1 kv, and a note on methods of measuring small changes of alternating voltage. See also 2227 of 1954 (Helke).

621.316.722.1 2116
A Cascode Amplifier Degenerative Stabilizer—V. H. Attree. (*Electronic Eng.*, vol. 27, pp. 174–177; April, 1955.) Description of stabilizers with modified-cascode shunt amplifiers having gain $>1,000$.

621.319.3 2117
Generation of High Voltage by Charge Transport on Rotating Insulator Surfaces—W. Herchenbach. (*Z. angew. Phys.*, vol. 7, pp. 32–43; January, 1955.)

TELEVISION AND PHOTOTELEGRAPHY

621.397.2:621.376.53 2118
System for the Transmission of Two [television] Programmes Simultaneously or of a Colour Signal—G. A. Boutry, P. Billard and L. Le Blan. (*Onde élect.*, vol. 35, pp. 5–21; January, 1955.) Two-channel PAM is used in a dot-sequential system, the pulses in the combined signal being alternately positive and negative as described previously [1176 and 1561 of 1954 (Le Blan)] so as to double the over-all channel capacity. Diode separators are used at the receiver. Methods for reducing crosstalk are discussed.

621.397.61/.62 2119
Russian Colour Television—(*Wireless World*, vol. 61, pp. 127–128; March, 1955.) A digest is presented of recently published accounts of the Moscow experimental color-television transmitter and of the color-television receiver "Raduga." A 525-line frame-sequential system operating in the 76-88-mc band is used; the 150 single-color frames per second give 25 line-interlaced color pictures per second. The transmitter is described by N. Belyaev in *Radio, Moscow*, pp. 31–32; May, 1954; the receiver by V. Semenov and N. Baldin, *ibid.*, pp. 33–35; May, 1954, and pp. 32–36; November, 1954, (where a complete circuit diagram and constructional details are given), and No. 12, pp. 37–40; December, 1954. (alignment procedure). In an article by K. Sergeichuk entitled "Contemporary Radio Technique" (*Radio, Moscow*, pp. 5–7; April, 1955) it is indicated that a compatible color-television system using a three-color tube is under development.

621.397.62:621.314.7 2120
Transistorized Portable [television] Receiver—G. B. Herzog and R. D. Lohman. (*Radio-Electronics*, vol. 26, pp. 43–45; January, 1955.) This experimental receiver is designed for single-channel reception at 67.25 mc. It uses a superheterodyne circuit, with no rf stage. Transistors and crystal diodes replace thermionic tubes throughout. Circuit diagrams are shown and the operation is described. The power input requirement of 13 w includes 3.6 w for the Type-5FP4 cathode ray tube heater. The total weight is 27 pounds.

621.397.621:621.375.232 2121
Feedback I. F. Amplifiers—J. Rasmussen and P. V. Iversen. (*Wireless World*, vol. 61, p. 213; May, 1955.) Comment on 568 of March (Jewitt). In IF amplifiers for televisoin the tube and circuit losses are not negligible and design calculations should therefore be based on the formulas for the Π network. Experimentally determined selectivity curves for a feedback and a stagger-tuned amplifier using the calculated values of components are shown.

621.397.7:535.623 2122
Subject-Lighting Contrast for Color Photographic Films in Color Television—F. T. Percy and T. G. Veal. (*Jour. Soc. Mot. Pic. Telev. Eng.*, vol. 63, pp. 90–94; September, 1954.)

621.397.8 2123
Quality Characteristics of Television Pictures—E. Menzer and H. Voelkel. (*Elektrotech Z.*, *Edn.*, *B*, vol. 7, pp. 13–19; January 21, 1955.) Various picture faults are illustrated and their causes are briefly discussed.

TRANSMISSION

621.396.61 2124
Modern Fifty-Kilowatt Broadcast Transmitter—W. M. Witty. (*Electronics*, vol. 28, pp. 168–169; March, 1955.) Features of the transmitter are (a) use of a Doherty amplifier modified for grounded-grid operation, and (b) use of a 5-kw driver which is itself a complete transmitter, with switching arrangements for reduced-power operation.

621.396.61:621.396.932 2125
Circuit and Operation of Emergency Transmitters—H. Geschwinde and E. Huttmann. (*NachrTech.*, vol. 5, pp. 38–40; January, 1955.) An East German two-tube automatically-keyed 80-w marine emergency transmitter for the frequency band 410–550 kc is discussed. Use of a 220-v 500-cps supply for anode and screen, obtained from a 24-v battery via a converter and transformer, results in the production of sidebands at ± 500 cps of the carrier frequency. Carrier suppression is obtained by connecting the grids of the two pentodes in push-pull and the anodes in parallel.

TUBES AND THERMIONICS

621.314.63 2126
Anomalous Forward Switching Transient in *p-n* Junction Diodes—N. T. Jones, R. H. Kingston and S. F. Neustadter. (*Jour. Appl. Phys.*, vol. 26, pp. 210 213; February, 1955.) "A delay in the flow of forward current when a grown-crystal *p-n* junction diode is switched from reverse to forward bias is explained on the basis of an extra *p-n* barrier in the grown-crystal bar. This effect was observed in 10 out of 24 production units, while no such anomaly was found in fused-junction diodes. A mathematical theory of the effect gives good agreement with the experimental results."

621.314.63 2127
Measurement of Minority Carrier Lifetime and Surface Effects in Junction Devices—S. R. Lederhandler and L. J. Giacoletto. (*Proc. IRE*, vol. 43, pp. 477–483; April, 1955.) A current pulse in the forward direction is applied to a *p-n* junction, injecting minority carriers. At the end of the pulse the junction is open-circuited by means of a thermionic diode, and the voltage decay characteristic is observed. The method is useful for measurements on junction devices in course of manufacture, and permits estimation of absolute values of surface recombination velocity. See also 887 of 1954 (Gossick).

621.314.63:537.311.33 2128
Planar [-junction] Germanium Diodes—A. Puzhai. [*Radio* (*Moscow*), pp. 27–28; January, 1955.] Current/voltage characteristics for temperatures of 20 degrees, 50 degrees and 70 degrees C. are given of four Russian-made In/Ge junction diodes. A section drawing of their construction is also shown.

621.314.63:546.28 2129
Silicon Alloy Junction Diode as a Reference Standard—D. H. Smith. [*Trans. AIEE* Part I, *Communication and Electronics*, vol. 73, pp. 645–651; 1954, Digest, *Elec. Eng.* (*New York*), vol. 74, section 1, p. 43; January, 1955.] Results of measurements on a number of Si junction diodes indicate that they can serve as low-voltage reference sources when biased beyond saturation point in either the forward or the reverse direction. Specimens with reverse saturation voltages of 4–6 v are suitable, having low characteristic slope and low temperature coefficient of slope.

621.314.63:546.28 2130
High-Voltage Silicon Diodes—L. G. Rubin and W. D. Straub. (PROC. IRE, vol. 43, p. 490; April, 1955.) Characteristics of some experimental grown-junction diodes are presented. Performance comparable to that of tube rectifiers can be obtained using high-resistivity Si.

621.314.632+621.314.7 2131
Double Base expands Diode Applications—J. J. Suran. (*Electronics*, vol. 28, pp. 198–202; March, 1955.) See 2535 of 1954 (Aldrich and Lesk).

621.314.632:546.289 2132

Long-Period Effects in Germanium Crystal Rectifiers—M. Kikuchi. (*Jour. Phys. Soc. Japan*, vol. 9, pp. 665–670; September/October, 1954.) Measurements were made, using a pendulun switching technique, on some fifty Type-IN34 diodes illuminated by a tungsten lamp. 60–70 per cent exhibited all three of the following phenomena: (a) photo-after-effect [2794 of 1954 (Kikuchi and Onishi)]; (b) current creep; (c) photocurrent creep. The remainder showed none of these effects. Typical decay curves exhibit two distinct phases with characteristic time constants of 30–50 seconds and 200–300 seconds respectively. The effects are explained as due to traps, not necessarily at the surface of the crystal, and possibly produced by electrical forming.

621.314.7+621.314.63 2133

Intrinsic Barrier Transistor—W. C. Hittinger, J. W. Peterson and D. E. Thomas. (PROC. IRE, vol. 43, p. 487; April, 1955.) Brief note of the performance of experimental *p-n-i-p* transistors [2799 of 1954 (Early)]. A unit oscillating stably at 465 mc has been produced. Corresponding results were obtained with *p-i-n* diodes.

621.314.7.001.4 2134

A Point-Contact Transistor Test Set—R. S. Hill. [*Elec. Eng.* (*New York*), vol. 74, section 1, pp. 59–62; January, 1955.] Detailed operating instructions are presented relative to the tests described by Wooley (1092 of May).

621.314.7.012.6:621.317.755 2135

Displayed Transistor Characteristics—H. W. Loeb and N. W. Morgalla. (*A.T.E. Jour.*, vol. 11, pp. 38–48; January, 1955.) A 'cro characteristic-curve tracer is described and some of the design considerations are discussed.

621.383.2:546.36.86 2136

Relation of Antimony Transmission and the Photoelectric Yield of Cs-Sb—M. Rome. (*Jour. Appl. Phys.*, vol. 26, pp. 166–169; February, 1955.) The investigation reported is relevant to the control of the thickness of semitransparent Cs-Sb photocathodes in accordance with their optical transmission. Results of transmission measurements on Sb films of different thicknesses are shown graphically for blue, red and white illumination. Discontinuities in the curves appear at a phase change in the Sb, when the transmission is about 30 per cent. The Sb films were next activated with Cs, and measurements were made of the photoelectric yield. For reverse illumination the peak response occurs with films of thickness corresponding to 5.5–6 μg/cm².

621.383.42 2137

Photoelectric Effect in Selenium Photocells at Low Temperatures—G. Blet. [*Compt. Rend. Acad. Sci.* (*Paris*), vol. 240, pp. 962–963; February 28, 1955.] Measurements have been made over the range 88 degrees–295 degrees K. For a given excitation wavelength the sensitivity varies in the same sense as the temperature. For a given temperature, the sensitivity /wavelength characteristic passes through a maximum.

621.383.5 2138

InSb Photovoltaic Cell—G. R. Mitchell, A. E. Goldberg and S. W. Kurnick. (*Phys. Rev.*, vol. 97, pp. 239–240; January 1, 1955.) Measurements are reported on a *p-n*-junction cell produced by crystal-pulling technique. Noise spectra are shown for the cell at 77 degrees K, (a) exposed to room-temperature radiation, and (b) shielded.

621.383.5:546.23:538.639 2139

Photomagnetoelectric Effect in Selenium Barrier-Layer Photocells—G. Blet. [*Compt. Rend. Acad. Sci.* (*Paris*), vol. 240, p. 743; February 14, 1955.] When a magnetic field is applied parallel to the plane of the illuminated more marked as the excitation wavelength increases.

621.385.001.4 2140

Quality Screening for Audio-Frequency Impulse Noise and Microphonism—Wohl and Winkler. (*See* 2070.)

621.385.002.2:621.365.54 2141

High-Frequency Induction Heating—(*See* 2078.)

621.385.029.6 2142

Concerning the Noise Figure of a Backward-Wave Amplifier—T. E. Everhart. (PROC. IRE, vol. 43, pp. 444–449; April, 1955.) Calculations show that the minimum noise figure is about the same for the backward-wave amplifier as for the ordinary traveling-wave tube, i.e. about 6 db. Results of measurements of noise figure as a function of gain support the theory.

621.385.029.6 2143

The "M"-Type Carcinotron Tube—R. R. Warnecke, P. Guenard, O. Doehler and B. Epsztein. (PROC. IRE, vol. 43, pp. 413–424; April, 1955.) The magnetron-type carcinotron is investigated theoretically and experimentally. By taking account of space charge, the theory is brought into agreement with experimental results on starting current, variation of efficiency with coupling impedance, and parasitic oscillations. The "rising-sun" effect is observed as in ordinary magnetrons. Figures obtained for a tube with the line curved into a circle and with permanent-magnet focusing indicate that power output of several hundred watts is obtainable over a frequency band greater than half an octave in the 3-kmc region. See also 1828 of July (Epsztein).

621.385.029.6 2144

Method for Measurement of Ripple in Electron Beams—J. Berghammer. (*Frequenz*, vol. 9, pp. 25–28; January, 1955.) A sliding diaphragm with parallel-sided slit is used; this arrangement does not require highly accurate centering with respect to the electron beam. A brief description is given of the special tube used for the measurements, and some results are presented.

621.385.029.6 2145

Power Flow in Electron Beam Devices—W. H. Louisell and J. R. Pierce. (PROC. IRE, vol. 43, pp. 425–427; April, 1955.) A formula for the power flow at low signal levels is derived which includes the contribution corresponding to the Poynting vector and that corresponding to the kinetic energy of the electrons.

621.385.029.6 2146

On the Possibility of Amplification in Space-Charge-Potential-Depressed Electron Streams—W. R. Beam. (PROC. IRE, vol. 43, pp. 454–462; April, 1955.) A more rigorous analysis is presented for the single ribbon beam than that of Kent (1945 of 1954). The results confirm that no growing waves can be produced in single-beam vm tubes, even with the velocity distribution corresponding to the presence of space charge. This conclusion is also confirmed by measurements of the amplitude of space-charge waves at points along a drift tube. Where gain is observed, it is probably due to interaction of the beam with a second electron stream produced by reflection at a low-potential collector and again in the region of the gun.

621.385.029.6 2147

Modes and Operating Voltages of Interdigital Magnetrons—A. Singh. (PROC. IRE, vol. 43, pp. 470–476; April, 1955.) Methods are discussed for obtaining operation over a desired frequency spectrum, with particular attention to modes of nonzero order. The relation between the frequencies of various modes [illegible] experimentally. The consequences of phase reversal at certain locations in the anode are analyzed; use of phase-shifting fingers as described by Crawford and Hare (2987 of 1947) does not ensure operation at only one voltage for one mode. A more effective method is to use a large number of fingers without phase reversal.

621.385.029.6:538.691 2148

Relativistic Dynamics of a Charged Particle in Crossed Magnetic and Electric Fields with Application to the Planar Magnetron—L. Gold. (*Jour. Appl. Phys.*, vol. 26, pp. 253–254; February, 1955.) Correction to papers abstracted in 3203 and 3401 of 1954.

621.385.029.62/.63 2149

A Magnetless "Magnetron"—A. Versnel and J. L. H. Jonker. (*Philips Res. Rep.*, vol. 9, pp. 458–459; December, 1954.) The tube comprises two coaxial cylindrical electrodes, with the outer one at a lower potential and an electron gun between them. The inner electrode is divided into an even number of longitudinal strips, the ends of alternate strips being connected to two points on the cylinder axis, which are in turn connected to the ends of two short-circuited Lecher wires. This combination forms a resonant structure. With a suitably chosen electron velocity, the tube acts as an oscillator. Outputs of some tens of milliwatts were obtained in the range 72–130 cmλ.

621.385.029.63/.64 2150

The Mitron—an Interdigital Voltage-Tunable Magnetron—J. A. Boyd. (PROC. IRE, vol. 43, pp. 323–338; March, 1955.) The magnetron described is tunable in the range 1.5–3.5 kmc by varying the anode potential; it is associated with an external cavity and is adaptable to mounting in a waveguide structure. It has an output of about 200 mw and can be used for measurement purposes or as local oscillator for a microwave receiver. A pure tungsten cathode gives better operation than either an oxide-coated or a thoriated-tungsten cathode. The high power output depends on keeping the anode-to-anode capacitance low and the external circuit impedance high.

621.385.029.63/.64 2151

Application of Recurrent-Network Equivalent Circuit in determining the Attenuation of Helical Transmission Lines loaded by Resistive Coatings—M. Müller. (*Fernmeldetech. Z.*, vol. 8, pp. 29–34; January, 1955.) The line considered comprises a conducting helix of radius a, a coaxial resistive cylinder of radius b and a coaxial conducting cylinder of radius d, where $d>b>a$. Characteristics calculated using the formulae derived are in good agreement with experimental characteristics of traveling-wave tubes obtained by Webber (2378 of 1950). The analysis also shows that the resistance required for maximum attenuation is proportional to the delay of the line and that the specific attenuation depends strongly on the separation (b-a).

621.385.029.63/.64 2152

History, Classification and Physics of Very-High-Frequency Electron Valves—W. Kleen. (*Elektrotech. Z.*, *Edn A*, vol. 76, pp. 53–64; January 1, 1955.) Tubes for frequencies above 1 kmc are surveyed. 52 references.

621.385.032.2:537.533 2153

Pin-Hole Camera Investigation of Electron Beams—C. C. Cutler and J. A. Saloom. (PROC. IRE, vol. 43, pp. 299–306; March, 1955.) The technique described is useful in designing guns for high-density beams. Transverse distribution of density and velocity are investigated by passing the beam through a pinhole aperture followed by a current detector which may consist of a fluorescent screen or a further aperture associated with a collector. Results of observations on some Pierce-type guns are reported; various arrangements of beam-

forming auxiliary electrodes are illustrated. At high perveance values bombardment of the cathode by positive ions may be serious. Initial transverse velocity components are the fundamental cause of nonideal flow.

621.385.032.2:537.533 2154
Thermal Velocity Effects in Electron Guns—C. C. Cutler and M. E. Hines. (PROC. IRE, vol. 43, pp. 307–315; March, 1955.) The effects are studied theoretically in relation to the experimental work on Pierce-type guns described by Cutler and Saloom (2150 above). Expressions are derived for the beam spread resulting from the transverse velocities and for the magnification produced by the pinhole device.

621.385.032.213 2155
Patch Effect for the Thermionic Emission from Polycrystalline Tantalum—W. B. LaBerge, R. J. Munick, J. A. Dezoteux, J. F. Whalen and E. A. Coomes. (*Jour. Appl. Phys.*, vol. 26, pp. 241–243; February, 1955.) Schottky plots for dc-aged Ta filaments exhibit breaks at high as well as low field strength. Dc etch patterns on certain faces of the crystal grains appear at the higher break point. The results are discussed in the light of theory given by Herring and Nichols (3407 of 1949).

621.385.032.213 2156
Electron Velocities with the Hollow Cathode—W. Veith. (*Naturwiss.* vol. 42. pp. 40–41; January, 1955.) Experiments were made using a special tube with a cathode acting simultaneously as an emitter of usual type and as a hollow cathode. The results confirm that electron velocities much greater than ordinary emission velocities occur within the hollow cathode.

621.385.032.216 2157
International Congress to mark the Fiftieth Anniversary of the Oxide Cathode—(*Le Vide*, Jan. 1955, Vol. 10, No. 55, pp. 318–400.) The text is given of the following further papers:
"Long-Life Valves,"—W. Dahlke (pp. 318–335). German version included.
"Long-Life Oxide-Coated Cathodes,"—S. Takada and S. Fujino (pp. 336–339). English version included.
"The Oxide Cathode in Very-Long-Life Valves,"—G. Saintesprit and P. Meunier (pp. 340–346).
"Comparison of Thoria Cathodes and Alkaline-Earth Oxide Cathodes,"—G. Mesnard (pp. 347–351).
"Semiconductor Properties of the Thoria Cathode,"—S. Takahashi (pp. 352–354). English version included.
"Thoriated Tungsten Cermet Cathode for Pulse Magnetrons,"—L. J. Cronin. (pp. 355–359). English version included.
"Statistical Observation of the Performance of Oxide-Cathode Valves in the French Long-Distance Telephone System,"—J. Eldin (pp. 360–361).
"Poisoning of Oxide Cathodes,"—H. Pentotet (pp. 362–365).
"Failure of Emission from Oxide Cathodes,"—K. Amakasu, T. Imai and M. Asano (pp. 366–379). English version included.
"Influence and Measurement of the Degree of Vacuum in Oxide-Cathode Valves,"—J. Bailleuil-Langlais (pp. 380–383).
"Deterioration of the Oxide Cathode by Evolution of Gas from the Anode under Electron Bombardment,"—T. Imai (pp. 384–393). English version included.
"Determination of the Sulphur Content in Nickel,"—T. R. Andrew and C. H. R. Gentry (pp. 394–400). English version included.
For previous list see 1526 of June.

621.385.032.216 2158
Measurement and Theoretical Study of Electrical Conductivity and Hall Effect in Oxide Cathodes—R. Forman. (*Phys. Rev.*, vol. 96, pp. 1479–1486; December 15, 1954.) Results of measurements over the temperature range 500 degrees–1,000 degrees K indicate that the Hall coefficient is negative, with a maximum between 600 degrees and 800 degrees. Electron mobility is high at temperatures over 700 degrees and decreases rapidly with decreasing temperature. Magnetoresistive effects were observed, of intensity depending on temperature and on the porosity of the cathode. The results are consistent with the porous semiconductor model proposed by Loosjes and Vink (3208 of 1950).

621.385.032.216 2159
Evaporation of Barium and Strontium from Oxide-Coated Cathodes—L. A. Wooten, A. E. Ruehle and G. E. Moore. (*Jour. Appl. Phys.*, vol. 26, pp. 44–51; January, 1955.) Measurements are reported indicating that the rate of evaporation from filamentary cathodes is strongly affected by chemical reducing agents in the Ni support, as well as by the composition of the anode and grid, but is not affected by space current. No correlation is observed between the rate of evaporation and the thermionic activity of individual cathodes. The material evaporated from commercial cathodes is mainly Ba metal, and contains <5 per cent Sr, <2 per cent BaO, and <0.01 per cent SrO.

621.385.032.216 2160
Heat Transfer through Oxide-Cathode Materials—A. E. Pengelly. (*Brit. Jour. Appl. Phys.*, vol. 6, pp. 18–20; January, 1955.) Measurements indicate a value of about 0.4×10^{-3} W. cm.$^{-1}$ degree C.$^{-1}$ for the true thermal conductivity of typical oxide-cathode materials. The sum of the absorption and scattering coefficients estimated from the results is such that for a coating about 0.1 mm thick the fraction of the radiation leaving the base metal and passing straight through the coating is about 1/3 for BaO, about 1/9 for SrO, and considerably less for mixtures investigated.

621.385.1 2161
Valve Noise produced by Electrode Movement—J. J. Glauber: P. A. Handley and P. Welch. (PROC. IRE, vol. 43, p. 488; April, 1955.) Comment on 1970 of 1954 and authors' reply.

621.385.3/.5:621.396.822 2162
The Nature of the Uncorrelated Component of Induced Grid Noise—T. E. Talpey and A. B. Macnee. (PROC. IRE, vol. 43, pp. 449–454; April, 1955.) Theoretical and experimental investigations indicate that a major portion of the uncorrelated component of induced grid noise is caused by fluctuations in the number of electrons reflected by the anode with sufficient energy to enable them to return through the grid. The corresponding change in the tube input admittance is discussed. A table shows measured values of induced grid noise for 11 typical receiving tubes.

621.385.3.029.6 2163
Input Conductance of the Type-2C40 Disk-Seal Triode with Grounded at U.H.F.—C. Colani. (*Frequenz.* vol. 8, pp. 293–296; October, 1954.) Comparison of the input conductance deduced from measurements at 2 kmc with the computed conductance shows that the actual values of transit angle are only about half those computed. Assuming a constant grid-cathode transit angle of 150 degrees, measured and computed conductances are in good agreement. The usual transit-angle/mutual-conductance relation does not hold, probably because of island formation in front of the cathode.

621.385.832 2164
Infrared speeds Erasure of Dark-Trace Tubes—F. Holborn and G. Hodowanec. (*Electronics*, vol. 28, pp. 170–171; February, 1955.)

621.385.832 2165
Measurement of the Luminescent Screen Potential of Cathode-Ray Tubes—W. Berthold. (*Fernmeldetech. Z.*, vol. 8, pp. 19–21; January, 1955.) The potential measured by an external es attracted-filament voltmeter arrangement, in which the plate was constituted by the screen, was found to be in good agreement with results deduced from luminosity measurements.

621.385.832 2166
Beam-Hugging Plates for Unlimited Cathode Ray Deflection—H. E. Kallmann. (PROC. IRE, vol. 43, p. 485; April, 1955.) Cathode-ray tubes can be designed with long and closely spaced plates to have good deflection sensitivity without limiting the maximum deflection by using lateral pre-deflection and twisting the closely spaced plates.

621.385.832:537.533:535.37 2167
Secondary Emission from Luminescent Screens in Cathode-Ray Tubes—K. H. J. Rottgardt, W. Berthold and H. Dietrich. (*Z. angew. Phys.*, vol. 6, pp. 560–563; December, 1954.) Experimental results indicate that the decrease of the sticking potential of a (ZnCd)S screen on irradiation by the beam electrons is probably due to removal of the adsorbed-gas surface layer. The sticking potential may be restored to its original value by introducing hydrogen but not by oxygen.

MISCELLANEOUS

621.3:061.1 2168
The "Mark of Quality" for Electrical Engineering Materials and Equipment [in Italy]—P. Anfossi. (*Ricerca Sci.*, vol. 25, pp. 234–343; February, 1955.) Note on the inauguration of an institute having authority to issue "Mark-of-Quality" certificates to manufacturers of electrical equipment.

621.3:061.3 2169
1955 IRE National Convention Program—(PROC. IRE, vol. 43, pp. 347–377; March, 1955.) Includes abstracts of the papers presented.

621.39(44) 2170
Brief Account of the C.N.E.T. [Centre National d'Etudes des Télécommunications]—[(*Électronique* (*Paris*), no. 100, pp. 25–29; March, 1955.] The C.N.E.T. is an interdepartmental research organization administered by the French Post Office but including sections serving all the other government departments with an interest in telecommunications. The documentation service covers a wide field and is responsible for the publication of *Les Annales des Télécommunications* as well as an internal journal.

621.396:378.9 2171
Education and Training of Radio Engineers—E. Williams. [*Nature* (*London*) vol. 175, pp. 279–280; February 12, 1955.] Report of discussion at a meeting of the British Institution of Radio Engineers. See also *Jour Brit. IRE*, vol. 15, pp. 154–160; March, 1955.

413=00+621.3:083.73) 2172
International Electrotechnical Dictionary [Book Review]—Publishers: International Electrotechnical Commission, Geneva, Switzerland; 70 pp., S.Fr. 8. (*Fernmeldetech. Z.*, vol. 8, p. 62; January, 1955.) Part 1 comprises 70 pages of alphabetically arranged terms and definitions in French and English together with translations of the terms into German, Italian, Spanish, Polish and Swedish. Part 2 comprises indexes in the seven languages.

621.38 2173
Advances in Electronics, Vol. V [Book Review]—L. Marton (Ed.). Publishers: Academic Press, New York, N.Y. and Academic Books, London, Eng. 1953, 420 pp., $9.50 or 76s. (*Proc. Phys. Soc.*, vol. 68, pp. 59–60; January 1, 1955.) This volume contains eight review articles, including one on steady-state theory

Membership

(Continued from page 94A)

Jacobs, J. E., 6230 S. 116, Hales Corners, Wis.
Jahn, D. M., Sperry Gyroscope Co., Great Neck, L. I., N. Y.
Jakowatz, C. V., 10 Cornelius Ave., Schenectady 9, N. Y.
Janik, J. L., Box 92, Vivian, La.
Janiszewski, F. A., Bell Telephone Laboratories, 463 West St., New York, N. Y.
Jarvis, D. T., 3481 Gray Ave., Detroit 15, Mich.
Jasberg, J. H., Hansen Laboratories, Stanford University, Stanford, Calif.
Jennett, N. E., Jr., Box 506-R, R.F.D. 2, Camarillo, Calif.
Jensen, P. A., Jr., 904 N. Overlook Dr., Alexandria, Va.
Jensen, R. S., 306D Talbot Laboratory, University of Illinois, Urbana, Ill.
Joerger, J. C., 7509 S. Boer Ave., Whittier, Calif.
Johnson, F. H., 71 Washington Pl., Ridgewood, N. J.
Johnson, G. S., 3015 Santa Clara, S.E., Albuquerque, N. Mex.
Johnson, L., 2710 S. Anthony Blvd., Fort Wayne, Ind.
Johnson, S. O., General Electric Co., Bldg. 7, Syracuse 1, N. Y.
Johnson, V. N., 1652 S. Edgemoor, Wichita 17, Kans.
Johnston, G. D., 1535 Ruie Rd., N. Tonawanda, N. Y.
Jones, W. N., Whitehall Beach, R.F.D. 2, Annapolis, Md.
Jorgensen, S. W., 75 Pitt St., Boston, Mass.
Kafalas, C., 37 Edgewood Rd., Ardsley, N. Y.
Kalkman, E. C., 437 W. Longwood Dr., Haddonfield, N. J.
Kaluzna, I. J., 1422 W. Farwell, Chicago 26, Ill.
Kamm, E., 68-09 Booth St., Forest Hills 75, L. I., N. Y.
Kaplan, J., 720 Ave. U, Brooklyn 23, N. Y.
Kappauf, E. F., 1346 Decker St., Valley Stream, L. I., N. Y.
Kasai, G. S., 2682 S. Menlo Ave., Los Angeles 7, Calif.
Katchky, M., 9 Avion Ave., Toronto, Ont., Canada
Katz, E. S., 245 Woodlawn Ter., Collingswood, N. J.
Katz, L., 228 N. Regent St., Port Chester, N. Y.
Kauffman, C. W., 25 Park St., Montclair, N. J.,
Kaufman, H., Mathematics Department, Engineering Bldg., McGill University, Montreal 2, Que., Canada
Kavanaugh, J. C., Officers Mail Section, c/o Det 1. 11 CHS, APO 124, c/o Postmaster, New York, N. Y.
Kearney, L. E., 629 Parkside Ave., Elmhurst, Ill.
Kebby, M. H., 203 Wyndham Dr., Redwood City, Calif.
Keen, H. S., 697 Waypark Ave., E. Hempstead, L. I., N. Y.
Kelsay, W. D., 7211 Coronado Ave., Dallas 14, Tex.
Kentner, C. D., R.F.D. 1, Kresson Rd., Marlton, N. J.
Kerney, R. W., U.S. Naval Ordnance Plant, 21 & Arlington, Indianapolis 8, Ind.
Kershner, S. W., A. D. Ring & Co., 342 Munsey Bldg., Washington 4, D. C.
Kiefer, C. F., Jr., 285 McCinkey Dr., Kenmore 17, N. Y.
Kienker, J. E., 4252 Woodbine Ave., Dayton 10, Ohio
Kieselbach, R., R.F.D. 1, West Chester, Pa.
Kilby, J. S., 315 S. Dean Rd., Milwaukee 11, Wis.
Kilgore, W., 1206—21 Ave., Altoona, Pa.
Kilpatrick, L. L., 12864 Morning Ave., Downey, Calif.
Kimball, L. L., 419 Kensington Rd., Baltimore 29, Md.

(Continued on page 102A)

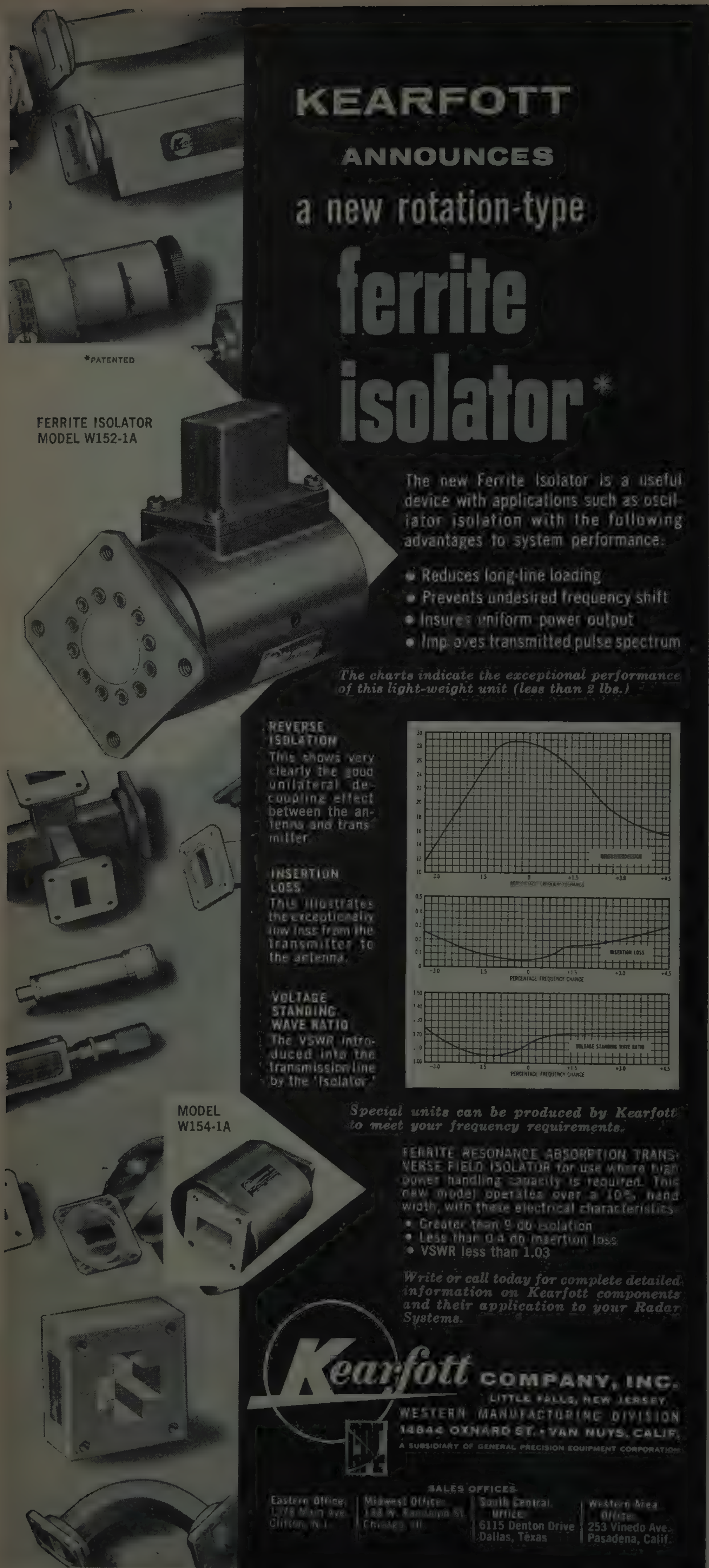

Membership

(Continued from page 100A)

Kimel, H., 8274 Williiams Ave., Philadelphia 19, Pa.
Kinder, H. R., 619 Yale Ave., Baltimore 29, Md.
King, F. H., 38 Pleasant St., Holyoke, Mass.
King, F. H., Bell Telephone Laboratories, Murray Hill, N. J.
King, H. E., Court F-31-C2 Stadium Ter., Champaign, Ill.
King, W. P., 11012 Cone La., Silver Spring, Md.
Kirchmayer, L. K., General Electric Co., Analytical Division, Syracuse, N. Y.
Kirksey, T. W., 2216 Ansborough Ave., Waterloo, Iowa
Kirkwood, R. L., 249 Lowell Ave., Palo Alto, Calif.
Klane, C. H., 5 Hampton Rd., Melrose 76, Mass.
Klein, H., 69-11A—188 St., Apt. 2B, Flushing, L. I., N. Y.
Klingaman, G. W., Lynnport, Pa.
Klotzbaugh, G. A., 600 Churchill Ave., Pittsburgh 35, Pa.
Knapp, R. L., Ridge Rd., R.F.D. 9, York, Pa.
Knights, C. F., 6 Slocum Ave., Port Washington, L. I., N. Y.
Knopoff, L., Institute of Geophysics, University of California, Los Angeles 24, Calif.
Knox, R. M., 99 Hermosa Ave., Hermosa Beach, Calif.
Koch, R. C., 3724 N. Oxford St., Indianapolis 18, Ind.
Koeblitz, W. E., 1462 Maple Rd., Cleveland Heights 21, Ohio
Koether, G. H., Jr., 108 Third Ave., S.E., Glen Burnie, Md.
Koffman, H. J., 75-31—198 St., Flushing, L. I., N. Y.
Kolding, A. R., Bell Telephone Laboratories, Rm. 2B-410, Murray Hill, N. J.
Kolodner, M., 4825 Gransback St., Philadelphia 20, Pa.
Koontz, C. E., 316 W. Olney Rd., Norfolk 7, Va.
Korn, S. J., 1597 Jesup Ave., New York 52, N. Y.
Kovacs, F. M., 66 Cambridge Rd., Whitesboro, N. Y.
Krauss, S. L., 141 Homan Ave., Elkhart, Ind.
Kravetz, A. J., University of Toronto 5, Ont., Canada
Krcek, J. A., 3509 N. Quebec St., Arlington, Va.
Kres, A. J., 16911 Valleyview Ave., Cleveland 11, Ohio
Kreuder, N. L., 9764 Cabanas Ave., Tujunga, Calif.
Krimsky, W. J., 4232 Avenue "M", Brooklyn 34, N. Y.
Kroencke, E. A., Jr., 8200 Riggs St., Overland Park, Kans.
Kroger, M. G., 428 S. Grove Ave., Oak Park, Ill.
Krulikoski, S. J., Jr., Bendix Aviation Corp., Research Laboratories, 4855 Fourth Ave., Detroit 1, Mich.
Ksiazek, F. T., 1768—41 St., Pennsauken, N. J.
Kudo, F. M., 8012 Dalesford Rd., Towson 4, Md.
Kulesha, K. J., 927 Commonwealth Dr., Teaneck, N. J.
Kunnes, H., 30 Arcadia, Rd., Apt. 27-J, Hackensack, N. J.
Kurss, H., 2044 Pacific St., Brooklyn 33, N. Y.
Kurtz, L. A., 7123 W. 94 St., Los Angeles 45, Calif.
Labagh, E. L., 455 Dorchester Rd., Ridgewood, N. J.
Laikevich, A., 311 Hickory St., Kearny, N. J.
Laitinen, L. K., 1520 N. Indiana, Kokomo, Ind.
Laitinen, W. R., 17 Russell Ave., S., Minneapolis 5, Minn.
Lamy, R. H., 110 Woodward Ave., Kenmore, N. Y.
Land, D. W., 724 Gates St., W. Chicago, Ill.
Landauer, W. E., 812 Middle Neck Rd., Great Neck, L. I., N. Y.

(Continued on page 104A)

Membership

(Continued from page 102A)

Landers, T. P., 5 Porter Rd., E. Longmeadow, Mass.
Lane, C. A., 5345 Coolidge Ave., Culver City, Calif.
Lane, J. F., Jr., 110 Adams St., Lexington 73, Mass.
Lane, J. H., Grubb Rd., R.D. 2, Malvern, Pa.
Langdon, J. G., 521 E. 126 St., Hawthorne, Calif.
Langford, J. W., Jr., Dept. of Elect. Eng., Univ. of Mass., Amherst, Mass.
Langston, G. A., 3512 Wayne Ave., Dayton 10, Ohio
Langston, J. F., 7444 Fay Ave., La Jolla, Calif.
Larisch, R. W., 35 Continental Ave., Morristown, N. J.
Larson, H. T., 8820 Bellanca Ave., L. A. 45, Calif.
Latson, F. W., c/o The Vitro Corp. of Amer. 962 Wayne Ave., Silver Spring, Md.
Lattin, W. J., 1209 W. 15th St., Owensboro, Ky.
Laurent, J. A., Jr., G.E. Co. Bldg. ML, 40 Federal St., Wesy Lynn, Mass.
Laurien, I. M., 210 Victoria Blvd., Kenmore 17, N. Y.
Lavier, E. C., 3301 W. Coquelin Terr., Chevy Chase, Md.
Lawn, F., E. Freehold Rd., R. R. 2, Freehold, N. J.
Lawson, E. J., 2519 Wilkins Ave., Balto, 3, Md.
Lebell, D., 3186 Barrington Ave., L. A. 66, Calif.
Lederer, P. S., 11408 Sherrie Lane, Silver Spring, Md.
Lee, Chi-Yuan, Bell Tel. Labs., 463 West St., N. Y., N. Y.
Lee, J. L., Union Depot Bldg. P.O. Box 629, Galveston, Tex.
Lee W. S., Kirk Rd., Bucks Co., Ivyland, Pa.
Lehnert, W. E., 5209 Minnehaha Blvd., Minn. 10, Minn.
Leibowitz, S., 362, W. Bowery, Akron, Ohio
Lemnios, W. Z., 11 Summer St., Newburyport, Mass.
Leo, R. E., 3361 Waverly St., Palo Alto, Calif.
Lester, V. R., 956 Dewey Circle, Biloxi, Miss.
Levine, A. M., 10 Terr. Circle, Gr. Neck, L. I., N. Y.
Levine, S., 98 Beechwood Ave., W. Long Branch, N. J.
Levinson, E., 213-02—73 Ave., Bayside 64, L. I., N. Y.
Lewi, J. B., 12733 Appleton Way, L. A., Calif.
Lewis, A. M., 1433 Hartford Ave., Akron 20, Ohio
Ley, B. J., 3225—163 St., Flushing, L. I., N. Y.
Lichty, J. R., 212 N. Cignes St., Los Angeles 54, Calif.
Liddiard, G. E., 820 Chalcedony St., San Diego 9, Calif.
Lietzan, A. A., 6815 Eighth Ave., L. A., 43, Calif.
Lindsay, J. T., 230 So. Ave., Van Wert, Ohio
Lockhart, H. H., 18 Robinhood Rd., Natick, Mass.
Lockwood, Lawrence W., Apt. 5, 16 E. 58 St., N. Y. C.
Logan, R. W., c/o Dorne & Margolin, Inc., 30 Sylvester St., Westbury, L. I., N. Y.
Loiterman, L., 270 Harrison Ave., Jersey City 4, N. J.
Lome, J. B., 441 E. 26th St., Paterson 4, N. J.
Long, L. A., 1247 S.E. Powell Blvd., Portland 2, Ore.
Long, R. G., 3 Paul St., Natick, Mass.
Lopuch, A. J., 617 Fifth Ave., N. Great Falls, Mont.
Lorentz, E. F., Comm. Radio Equip. Co., 1319 F St., N.W., Rm. 810, Wash. 4, D. C.
Lorenz, R. J., 924 Sweetbriar Dr., Bucknell Manor, Alexandria, Va.
Lothes, R. N., Elec. Eng. Research, D-3 Comstock Lane, Syracuse Univ., Syracuse 10, N. Y.

(Continued on page 106A)

THEY'RE HERE!

FERRAMIC® "Q"

THREADED PERM-TUNING CORES

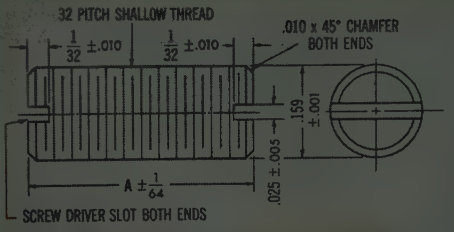

PART. NO.	DIMENSION A
F606-1	.250
EE-F606-2	.375

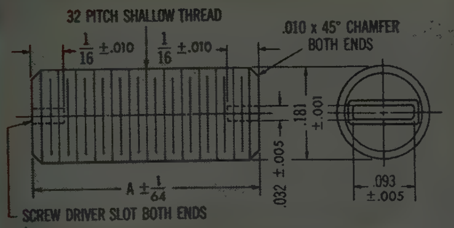

PART. NO.	DIMENSION A
EE-F607-1	.312
F607-2	.375

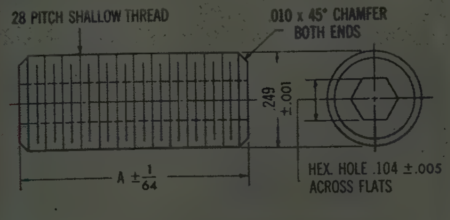

PART. NO.	DIMENSION A
EE-F608-1	.375

...Economy—engineered by GENERAL CERAMICS to M. P. A. Standard 11-53T

Following two years of intensive research and development by General Ceramics specialists, three standard threaded perm-tuning cores are now available from stock. These standard cores are offered in several lengths to meet industry's diversified requirements. Call, wire or write for quotations, today!

MAGNETIC PROPERTIES

PROPERTIES	UNIT	"Q"
Initial Perm. at 1 mc/sec.	—	125
*Max. Perm.	—	400
*Sat. Flux Density	Gauss	3300
*Residual Mag.	Gauss	1800
*Coercive Force	Oersted	2.1
Temp. Coef. of Initial Perm.	%/°C	.10 max.
Curie Point	+°C	350
Vol. Resistivity	ohm-cm.	High
Loss Factor:	$\frac{1}{u_0 Q}$	
At 1 mcs/sec.	—	.000020
At 5 mcs/sec.	—	.000050

*Measurements made on D.C. Ballistic Galvanometer with Hmax = 25 oersteds. Above data is based on nominal values.

GENERAL CERAMICS CORPORATION STEATITE INSULATORS

General CERAMICS CORPORATION
TELEPHONE: VALLEY 6-5100
GENERAL OFFICES and PLANT: KEASBEY, NEW JERSEY

MAKERS OF STEATITE, ALUMINA, ZIRCON, PORCELAIN, SOLDERSEAL TERMINALS, "ADVAC" HIGH TEMPERATURE SEALS, CHEMICAL STONEWARE, IMPERVIOUS GRAPHITE, FERRAMIC MAGNETIC CORES

Membership

(Continued from page 104A)

Louden, W. C., 1363 Grantleigh Rd., So. Euclid 21, Ohio
Louer, P. E., 847—13 St., Newport, News, Va.
Lounsberry, E. P., 1967 Maplewood Ave., Overlook Hills, Willow Grove, Pa.
Lucas, D. T., Raytheon Manufacturing Co., 4935 Fullerton Ave., Chicago 39, Ill.
Luke, L. M., 16 Woodridge Ct., 599, No. Park, Ont. Canada
Lund, N., Bell Tel. Labs., Mountain Ave., Murray Hill, N. J.
Lundquist, F. E., 2928½ Upper Highwood Dr., Billings, Mont.
Lynch, F. R., 5704 Greer Ave., St. Louis 20, Mo.
MacDonald, W. L., 65 Glen Ellen, Ventura, Calif.
MacGregor, R. R., Tower Dr., Darien, Conn.
MacKimmie, G. B., 5171 Westmore St., Montreal, Que. Canada
MacLean, W., 254 Henry St., Brooklyn 2, N. Y.
MacLean, T. W., 1428 S. Cedar St., Spokane, Wash.
Macklin, T. G., 23390 Ostronic Dr., Woodland Hills, Calif.
Madeley, P. E., 5449 Hidalgo St., Houston, Tex.
Maeshner, E., 6545 Alat Vista Dr., El Cerrito 9, Calif.
Magid, M., 2001 S. Garth Ave., L. A. 34, Calif.
Magnuson, R. W., Librascope, Inc., 1607 Flower St., Glendale, Calif.
Mallett, J. D., 522, Almar Ave., Pacific Palisades, Calif.
Mallin, J. A., 217 Hillside Terr., Great Kills 8, Staten Is., N. Y.
Malmberg, P., Nucleonics Div. Code 7240, Naval Research Lab., Wash. 25, D. C.
Marburger, W. G., 2308 Oakland Dr., Kalamazoo, Mich.
Marchetta, P., 8109—20 Ave., Adelphi Knolls, W. Hyattsville, Md.
Maron, I., 107 C Walworth Pk., Apts., Haddonfield, N. J.
Marosz, M. J., 10207 S. Hopeland Ave., Downey, Calif.
Marriner, A. W., 734 Hillsdale Ave., Hillsdale, N. J.
Marsh, W., 1264 Harbert, Memphis 4, Tenn.
Marshall, B. O., Jr., Mellon Inst., 4400 Fifth Ave., Pitts. 32, Pa.
Marshall, J. R., 2 Meadow Rd., Raymond, Me.
Martin, P. J., 2301 Cathedral Ave., N.W., Apt. 304, Wash. 8, D. C.
Martin, F. C., Jr., 1227 Chalcedony St., San Diego 9, Calif.
Martin, R. R., No. Ave., Pleasant Valley, N. Y.
Martin, W. L., 5230 Norwich Ave., Van Nuys, Calif.
Mason, D. R., 20 Condit Pl., Morristown, N. J.
Massy, F. M., 131 E. 238 St., New York 70, N. Y.
Master, W. R., Vickers, Inc., 1400 Oakman Blvd., Detroit 32, Mich.
Matarese, J., 4144 Paulding Ave., New York 66, N. Y.
Match, M. J., 16 Parkwold Dr., W., Valley Stream, L. I., N.Y.
Mathers, G. C., 23161 Payne Ct., Mountain View, Calif.
Mathews, E., 110-19—196 St., St. Albans 12, L. I., N. Y.
Mathwich, H. R., 257-C Haddon Hills Apts., Haddonfield, N. J.
Mattern, J., 837 Stamford Rd., Baltimore, Md.
Matthews, J. G., Bell Telephone Laboratories, Whippany, N. J.
Maurer, J. W., Box 288, Consaul Rd., R.F.D. 1, West Albany, N. Y.
Maximoff, B. S., 1512 N. Wells St., Chicago 10, Ill.
McCann, F. A., 635 N. Grevillea Ave., Hawthorne, Calif.

(Continued on page 108A)

Every part that AUTOMATIC *uses . . .* AUTOMATIC *makes!*

That's why the K-TRAN gives you the highest performance possible at the lowest price

IF you are designing AM, FM and TV receivers, you'll find 3 big advantages resulting from our policy of making every part of our K-Tran* and J-Tran* I.F. Transformer under our own roof:

1. It assures you of the lowest cost possible for an I.F. Transformer of highest electrical performance.

2. It assures you of highest quality construction throughout.

3. It assures you of speedy deliveries because we have no production "bottlenecks" and we maintain an ample inventory of broadly interchangeable standard catalog K-Trans.

That's why we make them this way. It's good business for you . . . good business for us, and enables us to completely control the quality of the product.

Automatic makes the shields, the iron and ferrite cores, the coil forms, the silvered mica capacitors, the high temperature plastic supports, the terminals, with the same skilled workmanship that created K-Tran, the original ¾″ I.F. Transformer in 1945, and has kept it the standard of the industry ever since.

The many types of the K-Tran are all assembled from the same components, hence are immediately available for orders of any size. These types meet every requirement of tube complement and circuit variations in Radio and TV receivers (particularly 262 KC, 455 KC, 10.7 MC, 21 MC and 44 MC).

Be sure you have the 56-page Manual, "K-Tran* and J-Tran*", which gives full engineering information, and explains the 8 distinct advantages of the K-Tran. You'll design better AM, FM, and TV receivers if you do. Write for it today.

*T.M. Reg. U.S. Pat. Off.

AUTOMATIC MANUFACTURING CORPORATION

65 GOUVERNEUR ST., NEWARK 4, N.J.

MASS PRODUCERS OF ELECTRONIC COMPONENTS

5249 WEST DIVERSEY AVE., CHICAGO 39, ILL.

Every Part Automatic uses . . . Automatic Makes.

IRE Membership

(Continued from page 106A)

McCarthy, C. J., Hq. Air Research & Development Command, Baltimore, Md.
McCloud, W. W., 17054 Bollinger Dr., Pacific Palisades, Calif.
McConaughy, R. L., 27 Pettit Ave., Merrick, L. I., N. Y.
McCown, W. E., Libby Owens, Ford Glass Co., Technical Bldg., 1701 E. Broadway, Toledo, Ohio
McDermid, W. L., IBM Corp., Box 554, Vestal, N. Y.
McDonough, S. L., 12 Lorfield Dr., Snyder 21, N. Y.
McFall, C. H., Jr., 41 Newport Ave., Warwick, Va.
McFee, R., Craftsman Farms, Morris Plains, N. J.
McGee, C. G., 35 Hewitt St., Willimantic, Conn.
McGuigan, J. H., Bell Telephone Laboratories, Murray Hill, N. J.
McIlvaine, D. K., 554 Arlington Ave., Des Plaines, Ill.
McKelvie, J. L., PSC Applied Research, Ltd., 1500 O'Connor Dr., Toronto 16, Ont., Canada
McLeod, W. W., Jr., 14 Dexter Rd., Lexington 73, Mass.
McMorrow, C. F., 1317 Maple Ave., Haddon Heights, N. J.
McNamara, T. J., 6 Corwin St., Dorchester, Mass.
Meaney, M. H., Jr., National Broadcasting Co., Rm. 503, 30 Rockefeller Pl., New York 20, N. Y.
Medwin, A. H., 641 Parson St., Easton, Pa.
Meehan, J. D., 539 W. Fulton St., Long Beach, L. I., N. Y.
Meiners, W. H., Box 270, R.F.D. 1, Pharr, Tex.
Melius, F. G., 1385 Portland Ave., St. Paul 3, Minn.
Mendoza, D. C., 155 S. E. Maple St., Beaverton, Ore.
Menes, M., Westinghouse Research Laboratories, Ardmore Blvd., E. Pittsburgh, Pa.
Menger, W. M., 5962 Willow Glen, Houston 21, Tex.
Merenda, C. T., 8508—17 Ave., Brooklyn 14, N. Y.
Merrill, G. E., 903 Spring St., Santa Rosa, Calif.
Merrill, R. B., 425 Chestnut St., Moorestown, N. J.
Merritt, N. A., 899 Montauk Ave., New London, Conn.
Mesak, C., 720 Lomita St., El Segundo, Calif.
Messner, G. P., 1641 Menlo Ave., Los Angeles 6, Calif.
Mettler, R. F., 3701 Connecticut Ave., N.W., Apt. 906, Washington 8, D.C.
Meyerhoff, A. A., 138 Seafield Rd., Southbourne, Bournemouth, Hants., England
Meyers, K. D., 108 W. Pomfret St., Carlisle, Pa.
Meyerson, M., 75 Morris Ave., Manasquan, N. J.
Miccioli, A. R., 62 Third Ave., New London, Conn.
Michalenko, A., University of Saskatchewan, Saskatoon, Sask., Canada
Middleton, M., Jr., 3336 Bookman Ave., Pittsburgh 27, Pa.
Miedke, R. C., 3140 Carroll Dr., S.E., Cedar Rapids, Iowa
Miller, C. N., 3029 Nichols, San Diego 6, Calif.
Miller, C. J., Box 274, R.F.D. 6, Rock Hill Beach, Pasadena, Md.
Miller, E. F., 8033 Harbury, Long Beach 8, Calif.
Miller, H. A., 17 Arlington Rd., Natick, Mass.
Miller, J. B., 2016 Franklin Ave., Middleton, Wis.
Miller, J. W., Braddock Acres, R.F.D. 3, Box 523-J, Alexandria, Va.

(Continued on page 110A)

Membership

(Continued from page 108A)

Miller, M., 924 Grassmere Ave., Wanamassa, N. J.
Miller, P. G., 7506 Exter Rd., Bethesda 14, Md.
Miller, R. E., 818 Hemphill St., Ypsilanti, Mich.
Miller, R. F., 2458—18 St., Cuyahoga Falls, Ohio
Millstone, S. D., 1522 N. Van Ness Ave., Los Angeles 28, Calif.
Milton, O., 9024 Los Arboles Ave., N.E., Albuquerque, N. Mex.
Mitchell, L. W., Suite 2828, 1 N. La Salle St., Chicago 2, Ill.
Moffitt, G. R., Jr., 43 Glenwood Ave., Hartford 12, Conn.
Monfon, L., Yuan Guan Electric Co., Bank of China Bldg., Rm. 303, 4 Queen's Rd., Central, Hong Kong
Monroe, J. C., 15206 Dickens St., Sherman Oaks, Calif.
Montalvo, E., 1019 Opal St., San Diego 9, Calif.
Montgomery, J. N., III, 4943 N. 33 Rd., Arlington 7, Va.
Montgomery, R. A., 1830-100, N.E., Bellevue, Wash.
Moore, F. B., 300 College Hill Apts., Huntsville, Ala.
Moore, G. F. D., 961 Mitchell Ave., Elmhurst, Ill.
Moore, W. C., 201 Pennsylvania Ave., Winston-Salem, N. C.
Morgan, E. D., 2124—31 Pl., S.E., Washington 20, D. C.
Morgan, R. E., 2410 Broadway, Schenectady 6, N. Y.
Morgan, W. A., Box 642, Union, N. Y.
Morken, D. A., 218 Newton Rd., Rochester 13, N. Y.
Morris, J. C., 1654 State St., New Orleans 18, La.
Morrison, A. I., 710-N Maple Ave., Burbank, Calif.
Moses, K., 160 Terrace Ave., Hasbrouck Heights, N. J.
Mountain, J. E., 9 Coolidge Ave., White Plains, N. Y.
Mueller, A. J., 16 Granville Ave., Park Ridge, Ill.
Mueller, H. W., 2354 N. 71 St., Milwaukee 10, Wis.
Mumford, E. R., Box 108, R.F.D. 1, Annapolis, Md.
Munn, E. H., Jr., Box 5A, R.F.D. 4, Coldwater, Mich.
Murphy, G. G., 153 Rockhill Rd., Clifton, N. J.
Murphy, R. P., 14 Waldron Ave., Nyack, N. Y.
Mutch, J. J., 2500 E. Strathmore Ave., Baltimore 14, Md.
Myers, W. A., 720 Corlett Ave., Compton 3, Calif.
Nachfolger, N., 4359 Esplanade Ave., Montreal, Que., Canada
Nash, C. C., Jr., Maple Dr., Fayetteville, N. Y.
Nash, R. W., 12 Alice St., M.R. 97, Binghamton, N. Y.
Nauss, B. M., 19501 Arminta St., Reseda, Calif.
Nawalinski, T. E., 1552 Knoxville Ave., San Diego, Calif.
Needle, J. S., 1230 White St., Ann Arbor, Mich.
Neilsen, I. R., Pacific Union College, Department of Physics, Box 32, Angwin, Calif.
Neikin, A., 4383 Coleridge St., Pittsburgh 1, Pa.
Nelson, E. A., 2104 Jefferson Ave., St. Paul 5, Minn.
Nelson, F. H., 406 Crest Rd., Oreland, Pa.
Nelson, H. C., Polytechnic Research & Development Co., 202 Tillary St., Brooklyn, N. Y.
Nelson, J. L., 115 E. 21 St., Brooklyn, N. Y.

(Continued on page 113A)

IRE Membership

(Continued from page 110A)

Nelson, M. D., 6 RCA Ind. Ser. Labs., 711 Fifth Ave., New York 22, N. Y.
Neubert, H. A., Jr., 119 N. Childs St., Woodbury, N. J.
Neudorfer, W. L., RCA Field Engineer, Box 441, Hamilton Field, Calif.
Newborg, D. S., RCA Victor Division, 718 Keith Bldg., Cleveland 15, Ohio
Newton, S. H., 208 Avenue C, Redondo Beach, Calif.
Nichols, R. F., Box 123, Excelsior, Minn.
Nickles, R. W., Radio Station KFAL, Fulton, Mo.
Nielsen, G. A., 1942 Patricia Dr., Concord, Calif.
Nigg, D. J., 4923 W. 78 Pl., Prairie Village 15, Kans.
Noland, A. R., c/o Gilfillan Bros., Inc., 1815 Venice Blvd., Los Angeles 6, Calif.
Norsell, H. C., 6671 Vista Del Mar, Playa Del Rey, Calif.
Norton, M. H., 10 Addison Rd., Fairfax, Va.
Nowogrodski, M., 895 West End Ave., Apt. 9C, New York 25, N. Y.
Nozick, S., 268 S. Second St., Brooklyn 11, N. Y.
Nunn, E. C., 2706 Aldrich Ave., N., Minneapolis 11, Minn.
Nurre, H. H., Jr., 7466 Brightwood Dr., Affton 23, Mo.
Nutter, M. J., 14072 Riverview, Detroit 23, Mich.
Oakes, W. S., Rt. 1, Pattersonville, N. Y.
Obenland, D. K., R.F.D. 1, Eightyfour, Pa.
Oberrender, G. F., Jr., 710 Williamson Bldg., Cleveland 14, Ohio
O'Bryan, R. L., 757 Devonshire Dr., Oxnard, Calif.
Ocheret, R., 247-46—76 Ave., Bellerose, L. I., N. Y.
Odekirk, M. D., 555 Geneva Ave., Claremont, Calif.
Odessey, P. H., Polarad Electronics Corp., 100 Metropolitan Ave., Brooklyn 11, N. Y.
Oesterle, A. G., Jr., 96 Sheldon St., Wyckoff, N. J.
Ogletree, W. A., Street Rd., Southampton, Pa.
O'Hea, J. T., 31-A Buckner, Ft. Leavenworth, Kan.
Olin, I. D., 1233 Valley Ave., S.E., Washington 20, D.C.
Olson, D. R., 3310 Dogwood Ct., Birmingham, Mich.
Olson, W. J., 3019 Walnut St., Huntington Park, Calif.
Opperman, R. H., 540 Muscatel N. E., Albuquerque, N. Mex.
Orazio, A. F., 287 North St., Herricks, New Hyde Park, L. I., N. Y.
Oster, R. E., 3012 Shadow Wood Dr., Dallas 8, Tex.
Ottinger, G. L., 630 Sansome St., San Francisco 26, Calif.
Owen, W. E., Engineering School, Louisiana Polytechnic Institute, Ruston, La.
Owens, A. T., 228 Pine Spring Rd., Falls Church, Va.
Owings, J. L., 1163 Maplecrest Circle, Gladwyne, Pa.
Pacent, H. C., 59 Orchard Farm Rd., Port Washington, L. I., N. Y.
Paddison, L. J., 911 Parkland Circle, Albuquerque, N. Mex.
Paisley, S. R., 15 Grandview Ave., Toronto, Ont., Canada
Paley, W. D., 73-55 260 St., Glen Oaks, L. I., N. Y.
Paller, J. L., 14031 Weddington St., Van Nuys, Calif.
Palmer, L. N., Box 298, Griffiss AFB, Rome, N. Y.

(Continued on page 114A)

Membership

(Continued from page 113A)

Palmer, P. J., 47 Cedrus Ave., Roslindale 31, Mass.
Palmer, R. T., 88 Broad St., Boston 10, Mass.
Palmquist, M. L., Jr., 8026 N. Sepulveda, Van Nuys, Calif.
Panetta, A. R., 139 Willow St., West Acton, Mass.
Papas, C. H., 4616 Angeles Vista Blvd., Los Angeles 43, Calif.
Parkinson, J. A., Rm. 457, 80 E. Jackson, Chicago 4, Ill.
Parks, J. V., 1815 E. 74 Terrace, Kansas City 30, Mo.
Parks, R. J., 4334 Bel Air Dr., La Canada, Calif.
Parr, A. F. W., 63 Bedford Rd., Pleasantville, N. Y.
Paschetto, D. D., 18 Myrtle Ave., Ramsey, N. J.
Passera, A. L., 200 Lexington St., Hampton, Va.
Pastell, D. L., 303 Cleveland Ave., McDaniel Crest, Wilmington, Del.
Paul, D. R., 675 Sara Dr., Washington, Pa.
Pearlman, L., 933 New York Ave., Brooklyn 3, N. Y.
Peckhart, M. A., 619 Austin Ave., Downers Grove, Ill.
Peghiny, J. W., 966-B Suburban Pkwy., Portsmouth, Va.
Pelavin, M. H., 65-39—108 St., Apt. D-2, Forest Hills 75, L. I., N. Y.
Pelitsch, E. J., 63-12 Forest Ave., Ridgewood, Brooklyn 27, N. Y.
Penrose, R. M., 378 Dewry Ave., Willowdale, Ont., Canada
Penton, R. E., 2090 Claremont Avenue, Apt. 39, NDG, Montreal, Que., Canada
Perecinic, W. S., 2014 Drexel St., Apt. 203, Hyattsville, Md.
Perkins, D. W., 210 Newfield Rd., Dewitt, N. Y.
Perkins, G. O., 314 W. Zeralda St., Philadelphia 44, Pa.
Perlsweig, A. M., 95 W. Broadway, Salem, N. J.
Perry, M. A., 8 Godwin Ave., Fairlawn, N. J.
Peterson, N. J., 212 N. Vignes St., Los Angeles, Calif.
Peterson, R. M., 509 S. W. Oak St., Portland 4, Ore.
Peterson, R. E., 809 Conklin Rd., Binghamton, N. Y.
Petkof, B., 2147 'O' St., N.W., Washington, D. C.
Petrich, L. G., Bell Telephone Labs., Whippany, N. J.
Pfeffer, I., 1009 N. Sweetzer Ave., Los Angeles 46, Calif.
Pfund, C. E., 5218 Danbury Rd., Bethesda 14, Md.
Phillips, E. V., 170 S. Michillinda, Sierra Madre, Calif.
Phillips, G. D., 533 Empire Ave., Benton Harbor, Mich.
Pierce, E. W., 1261 Corbin Rd., Toledo 12, Ohio
Pierce, R. L., Route 1, Box 256, McFarland, Wis.
Pierson, A. L., III, 5304 Chenevert St., Apt. 4, Houston 4, Tex.
Pinnow, R. L., 2244 N. 67 St., Wauwatosa 13, Wis.
Pitzer, R. L., 20 Grandview Ave., Arcadia, Calif.
Platt, S., 309 Ave. C, Apt. 4D, New York 9, N. Y.
Pochmerski, D., Star Route, Colts Neck Rd., Freehold, N. J.
Polcyn, S. J., Jr., 97-22—63 Dr., Rego Park, L. I., N. Y.
Pollack, H. W., 16 Helen Ave., Plainview, L. I., N. Y.

(Continued on page 117A)

Membership

(Continued from page 114A)

Pomon, J. D., 531 S. Lewis Ave., Lombard, Ill.
Porter, G. R., 645 Summit St., Winston-Salem, N. C.
Porter, W. R., 412 S. Parton, Santa Ana, Calif.
Porterfield, E. A., R.F.D. 1, N. Greenwich Rd., Armonk, N. Y.
Portz, H. G., 2014 E. Genesee St., Syracuse, N. Y.
Powell, M., Jr., Rd. 2, Vestal, N. Y.
Prasil, A., 245 Oaklawn Dr., Rochester 17, N. Y.
Pravda, M. F., 1856 State St., Schenectady, N. Y.
Preti, L. L., 1755 Meadow Lane, East Meadow, L. I., N. Y.
Price, R. C., 918 Stratford Court, Westbury, L. I., N. Y.
Primich, R. I., Radio Physics Lab., Defence Research Board, Ottawa, Ont., Canada
Prince, M. J., Upper Air Research Lab., Univ. of Rhode Island, Kingston, R. I.
Prothers, L. T., 8722 Reading Ave., Los Angeles 45, Calif.
Pruett, J. W., 11621 Highland View Ct., Mountain View, Calif.
Purcell, C. J., 1464 Schletti St., St. Paul 3, Minn.
Putz, J. L., Electronics Research Lab., Stanford Univ., Stanford, Calif.
Quance, F. R., 313 Herrick Ave., Teaneck, N. J.
Quigley, A. J., 1019 N. Frances St., South Bend 17, Ind.
Ragni, V. F., 14 Miller Rd., Farmingdale, L. I., N. Y.
Rainville, L. E., Rm. 318, Bldg. 15, Div. 8, Hughes Aircraft Co., Culver City, Calif.
Ralls, J. W., Lippincott and Smith, 24 California St., San Francisco 11, Calif.
Ramler, W. J., 163 Chandler Ave., Elmhurst, Ill.
Ramsey, R. C., RR-2, Box 355, Buchanan, Mich.
Randall, J. E., Dept. of Physiology, Ohio State University, Columbus 10, Ohio
Rankowitz, S., 51 Bell Ave., Brookhaven Nat'l. Lab., Upton, L. I., N. Y.
Ransom, R. A., 1025 Connecticut Ave., Washington 6, D. C.
Raymond, J. L., Box 2095, Inglewood, Calif.
Raynes, H. D., 4400 Kenwood Ave., Baltimore 6, Md.
Read, R. A., Jr., 211 S. Waiola Ave., La Grange, Ill.
Reade, R. B., RCA Victor Division, Bldg. 15-4, Camden 2, N. J.
Reale, E. P., 49 Corby, Toronto, Ont., Canada
Record, F. A., 92 Forest St., Danvers, Mass.
Rector, C. V., 112 W. Jefferson St., Tipton, Ind.
Reed, B. S., 6722 Santa Anita, Dallas, Tex.
Reed, R. H., 5812 Compass Drive, Los Angeles 45, Calif.
Reese, J. R., 1723 Old Welsh Rd., Meadowbrook, Pa.
Reichenthal, A., Exeter Hotel, Seattle 1, Wash.
Reinsmith, G. M., 131 W. Pleasant Ave., Syracuse 5, N. Y.
Relf, K. E., 3347 Jameson Dr., Pittsburgh 27, Pa.
Reque, S. G., 1250 Garner Ave., Schenectady 9, N. Y.
Rescoe, J. M., 14 Halsey Way, Natick, Mass.
Rethoret, R. H., 1390 Ouimet St., Apt. 3, Norgate, Ville St. Laurent, P.Q., Canada
Reukauf, D. C., Box 113, Riverdale, Md.
Rhea, H. E., 39 War Admiral Lane, Media, Pa.
Rhodes, H. A., 5 Aldon Terrace, Bloomfield, N. J.
Ricardi, L. J., 1 Lodge Rd., Natick, Mass.
Rich, E. A., 49 Homestead Ave., West Springfield, Mass.

(Continued on page 118A)

Membership

(Continued from page 117A)

Richard, V. W., Box 77-A, R. D. 1, Sherwood Lane, Havre De Grace, Md.
Richards, C. A., 802 Drexel Ave., Ft. Wayne 5, Ind.
Richardson, C. M., Apt. 10 B, Winoka Village, Huntington Station, L. I., N. Y.
Richman, P. L., 65 Central Park West, New York, N. Y.
Richter, F., 268 So. Felton St., Philadelphia 39, Pa.
Ridgely, N. R., Jr., 5811 Namakagan Rd., Washington 16, D. C.
Rigby, S., 721 Rugby Rd., Brooklyn 30, N. Y.
Riley, J. C., 2039 S. E. Yamhill St., Portland 15, Ore.
Riley, R. N., 120 Oakdale Ave., Baltimore 28, Md.
Ringlee, R. J., 39 Highlawn Dr., Pittsfield, Mass.
Ritzow, N. R., Route 5, Box 351, Waukesha, Wis.
Rizzo, J. E., 8-24 Chester St., Fairlawn, N. J.
Roach, C. L., 486 Sanford Ave., St. Lambert, Montreal 23, Que., Canada
Roberts, R. E., 10721 La Rosa, Temple City, Calif.
Robertson, A. J. L., Concordia College, Physics Department, Moorhead, Minn.
Robertson, D. J., 166 Arundel Rd., Paramus, N. J.
Robidoux, F. T., 4630 Park Dr., Houston 3, Tex.
Robinson, K. W., Palmer Physical Lab., Princeton, N. J.
Robinson, W. A., 102 Tyndall Ave., Apt. 14, Toronto, Ont., Canada
Rodewald, M. V., 2565 N. Second St., Milwaukee 12, Wis.
Roeger, R. E., 1300 Elmwood Rd., Mayfield Heights, Cleveland 24, Ohio
Roessing, E. F., 211 W. Washington St., Napoleon, Ohio
Rogers, D. C., Star Route, Box 3453, Spenard, Alaska
Rogers, P. H., 1714 Chandler Dr., Ann Arbor, Mich.
Rohr, J. G., 254 West 64th Ave., Philadelphia 26, Pa.
Rohrer, C., Jr., 429 W. Lakewood, Peoria, Ill.
Rolnik, J. A., 78 Second Pl., Brooklyn 31, N. Y.
Romero, R. F., 533 Taylors Lane, Mamaroneck, N. Y.
Rorden, R. J., 11846 Mississippi Ave., Los Angeles 25, Calif.
Rosar, M. T., 33 Merry Lane, Westbury, L. I., N. Y.
Rosett, E., Apt. K-15, 14-20 Chandler Dr., Fairlawn, N. J.
Ross, D. K., 7912 Bonhomme, St. Louis 5, Mo.
Ross, H. M., 2420—19 St., Broadview, Ill.
Roth, H. H., 15 Edwards St., Roslyn Heights, L. I., N. Y.
Roth, J. E., Jr., 604 W. 178 St., New York 33, N. Y.
Rothe, F. S., 1175 Oxford Pl., Schenectady 8, N. Y.
Rottner, A. W., 111 Edwards Rd., Box 46, Breton Woods, N. J.
Rowland, C. A., Jr., 765 N. Wheeler St., St. Paul 4, Minn.
Royce, H. W., 706 Fairway Dr., Baltimore 4, Md.
Rubinoff, M., Moore School of Electrical Engineering, Univ. of Pennsylvania, Philadelphia 4, Pa.
Ruddock, K. A., Box 51, Jerome, Ariz.
Ruedisueli, R. W., 2 Decker Rd., Ossining, N. Y.
Ruina, J., Control Systems Lab., University of Illinois, Urbana, Ill.

(Continued on page 132A)

Communications

Opportunities exist at Ramo-Wooldridge for professional communications personnel in the following categories:

At Ramo-Wooldridge New Techniques in Communications Are Being Developed

In this age of fast moving transportation and shrinking distances, communication of ideas, plans, and actions becomes steadily more critical. New techniques are urgently needed to provide better means for transmitting information from point to point. Engineers and Physicists of the Communications Division of The Ramo-Wooldridge Corporation are applying advanced methods of system analysis to complex military communication problems. Basically new techniques are being developed to provide better answers to long standing needs for greater transmission capacity, better presentation of information, and higher system reliability in communication systems.

The military challenge of today sets the pace for the industrial development of tomorrow. New techniques in picture transmission, facsimile, information coding, and bandwidth compression are revealing new horizons in the world of communications.

ELECTRICAL ENGINEERS AND PHYSICISTS *qualified to conduct advanced analysis and development work in one or more of these fields: Video or radio frequency amplifiers, networks, pulse forming and shaping circuits, magnetic recording and reproduction, low and medium power transmitters, application of information theory, receiver design, communication and navigation systems engineering.*

MECHANICAL ENGINEERS *having from eight to fifteen years experience in the design and development of precision mechanical assemblies and electro-mechanical mechanisms. Experience in the design for production of miniaturized airborne communication equipment especially desirable. The minimum educational requirement is a B.S. degree in mechanical engineering.*

Consideration must be given to whether relocation of applicant will disrupt other important military work.

COMMUNICATIONS DIVISION

The Ramo-Wooldridge Corporation

8820 BELLANCA AVENUE • LOS ANGELES 45, CALIFORNIA

Membership

(Continued from page 118A)

Rupp, E. W., Jr., 412 Hook Place, Ithaca, N. Y.
Ruppel, A. E., 118 Wilson St., Lynbrook, L. I., N. Y.
Russell, W. D., 3005 Barclay Ave., Apt. 2, Montreal, Que., Canada
Ruvin, A. E., 211 Wyngate Dr., Massapequa, L. I., N. Y.
Ryerson, J. L., 3 Park Ave., Holland Patent, N. Y.
Sabin, W. D., 501 N. Allen St., Mesa, Ariz.
Sadowsky, S. S., Bldg. 6, Electronics Park, Syracuse, N. Y.
Saffitz, I. M., 680 Hawthorne St., West Hempstead, L. I., N. Y.
St. Jean, L. E., 66 Fisher Rd., Arlington 74, Mass.
Salzman, C. F., Jr., 28 Knollwood Ave., Stamford, Conn.
Sample, G. A., 211 Fair St., Ithaca, N. Y.
Samson, C. A., 4334 E. 55 St., Seattle 5, Wash.
Samuels, J. C., Bldg. 22, Apt. 3, Ross Ade, W. Lafayette, Ind.
Sanborne, J. M., 1875 Langham Rd., Columbus 12, Ohio
Sander, M. H., 1446 Thomas Barbour Dr., Eau Gallie, Fla.
Sanderson, R. F., 2421, Chinook Rd., Waukegan, Ill.
Sard, E. W., 74-27—220 St., Flushing 64, L. I., N. Y.
Sartor, J. O., Jr., 4512 McKinney Ave., P.O. Box 8081, Dallas 5, Tex.
Saur, Richard D., 5 Dorset Lane, South Farmingdale, L. I., N. Y.
Sayer, T. C., 1620 Roumfort Rd., Philadelphia 19, Pa.
Schafer, H. G., 8535 Chestnut Oak Rd., Baltimore 4, Md.
Schager, R. J., 5650 N. Delaware St., Indianapolis 20, Ind.
Scharfman, H., 43 Neillian Way, Bedford, Mass.
Schede, R. W., 86 Outer Dr., Oak Ridge, Tenn.
Scherer, B. L., 10 Revere Dr., Stamford, Conn.
Schmertz, R. C., Jr., 1740 Broadway, New York, N. Y.
Schmidt, B. F., 8306 Georgetown Ave., Los Angeles 45, Calif.
Schmidt, J. N., 9253 S. True Ave., Rivera, Calif.
Schneider, R. M., 221 Linden Blvd., Brooklyn 26, N. Y.
Schoenberg, J. P., 138 Tennis Ave., Ambler, Pa.
Scholfield, W. D., Canadian General Electric Co., 830 Lansdowne Ave., Toronto, Ont., Canada
Schorr, M. G., 5 West Slope Lane, Hamden, Conn.
Schreiber, O. W., U. S. Navy Electronics Lab., San Diego 52, Calif.
Schreiber, W. F., Technicolor Motion Picture Cor., 6311 Romaine St., Hollywood, Calif.
Schrettenmueller, R. F., 2 Primrose Dr., New Hyde Park, L. I., N. Y.
Schulman. J. R., 10704 Lockridge Dr., Silver Spring, Md.
Schulz, R. F., 315 N. Lincoln, Hinsdale, Ill.
Schwab, P. E., 1701 Widener Pl., Philadelphia 41, Pa.
Schwalbe, J. H., 866 Chestnut St., Franklin Square, L. I., N. Y.
Schwantes, R. C., 581 Eleventh Ave., N.W., New Brighton, Minn.
Schwartz, E. D., 3787 Mohawk, Pasadena 10, Calif.
Sciorra, A. F., 95 Homestead Rd., Tenafly, N. J.

(Continued on page 136A)

ith your future in mind

Check the chart below for positions which interest you most...

FIELDS OF ENGINEERING ACTIVITY	TYPE OF DEGREE AND YEARS OF EXPERIENCE PREFERRED											
	Electrical Engineers			Mechanical Engineers			Physical Science			Chemistry Ceramics Glass Technology Metallurgy		
	1-2	2-3	4+	1-2	2-3	4+	1-2	2-3	4+	1-2	2-3	4+
SYSTEMS (*Integration of theory, equipments, and environment to create and optimize major electronic concepts.*)												
AIRBORNE FIRE CONTROL			W						W			
DIGITAL DATA HANDLING DEVICES			C			C			C			
MISSILE AND RADAR			M			M			M			
INERTIAL NAVIGATION			M			M			M			
COMMUNICATIONS			C I						C I			
DESIGN • DEVELOPMENT												
COLOR TV TUBES—Electron Optics—Instrumental Analysis—Solid States (Phosphors, High Temperature Phenomena, Photo Sensitive Materials and Glass to Metal Sealing)	L	L	L	L	L	L	L	L	L	L	L	L
RECEIVING TUBES—Circuitry—Life Test and Rating—Tube Testing—Thermionic Emission	H	H	H		H	H		H	H		H	H
SEMI-CONDUCTORS—Transistors—Semi-Conductor Devices	H	H	H				H	H	H			
MICROWAVE TUBES—Tube Development and Manufacture (Traveling Wave—Backward Wave)		H	H		H	H		H	H		H	H
GAS, POWER AND PHOTO TUBES—Photo Sensitive Devices—Glass to Metal Sealing	L	L	L	L	L	L	L	L	L	L	L	L
AVIATION ELECTRONICS—Radar—Computers—Servo Mechanisms—Shock and Vibration—Circuitry—Remote Control—Heat Transfer—Sub-Miniaturization—Automatic Flight—Design for Automation—Transistorization	C X	C F X	M C F X	C X	C F X	M C F X	C X	C F X	M C F X			
RADAR—Circuitry—Antenna Design—Servo Systems—Gear Trains—Intricate Mechanisms—Fire Control	C X	M C F X	M C F X	C X	M C F X	M C F X	C X	M C F X	M C F X			
COMPUTERS—Systems—Advanced Development—Circuitry—Assembly Design—Mechanisms—Programming	C	C F X	M C F X	C	C F	M C F X	C	C F	M C F			
COMMUNICATIONS—Microwave—Aviation—Specialized Military Systems	C	C F	M C F		C F	M C F		C F	M C F			
RADIO SYSTEMS—HF-VHF—Microwave—Propagation Analysis—Telephone, Telegraph Terminal Equipment		I	I F		I	I F		I	I F			
MISSILE GUIDANCE—Systems Planning and Design—Radar—Fire Control—Shock Problems—Servo Mechanisms		M F	M F		M F	M F		M F	M F			
COMPONENTS—Transformers—Coils—TV Deflection Yokes (Color or Monochrome)—Resistors	C	Z C X	Z C X	C	Z C	Z C	C	C	C		Z	Z
MACHINE DESIGN Mech. and Elec.—Automatic or Semi-Automatic Machines		L	L		L	L		L	L			

Location Code

C—Camden, N. J.—in Greater Philadelphia near many suburban communities.
F—Florida—on east central coast.
H—Harrison, N. J.—just 18 minutes from downtown New York.
I—International Div.—New York City and Overseas.
L—Lancaster, Pa.—about an hour's drive west of Philadelphia.
M—Moorestown, N. J.—quiet, attractive community close to Phila.
W—Waltham, Mass.—near the cultural center of Boston.
X—Los Angeles, Calif.—west coast electronics center.
Z—Findlay, Ohio—pleasant, small midwestern town.

Please send resume of education and experience, with location preferred, to:

Mr. John R. Weld, Employment Manager
Dept. A-13H, Radio Corporation of America
30 Rockefeller Plaza
New York 20, N.Y.

RCA®

RADIO CORPORATION of AMERICA

Membership

(Continued from page 132A)

Scott, R. E., 13 Heath's Bridge Rd., Concord, Mass.
Scrafford, R. L., 523 N. Alameda, Las Cruces, N. Mex.
Seay, P. A., c/o Reeves Instrument Corp., 215 E. 91 St., New York 28, N. Y.
Seckler, H. N., Bell Telephone Labs., Whippany, N. J.
Secord, A. H., 9 Cotswold Crescent, Willowdale, Ont., Canada
Sees, J. H., Route 7, Burlington, N. C.
Seideman, I. M., 4524 E. 25 St., Tulsa, Okla.
Seidler, R. L., Jeffrie Trail, Whippany, N. J.
Seidler, S. W., 134 Haven Ave., New York 32, N. Y.
Sellars, R. F., U. S. Naval Ordnance Test Station, China Lake, Calif.
Sencenbaugh, D. W., 22 Chestnut Hill Rd., Groton, Conn.
Sensenig, W. A., 124 Anderson Pkwy., Cedar Grove, N. J.
Setzer, L. E., 5865 Kings Rd., Los Angeles 56, Calif.
Sevian, E. A., Dynamic Anal. & Con. Lab., Massachusetts Institute of Technology, Cambridge 39, Mass.
Shallon, [illegible] C., 13060 Morningside Way, Los Angeles 66, Calif.
Shank, R. R., Dunham Lab. of Electrical Engineering, Yale University, New Haven, Conn.
Shapiro, H., 1201 E. California St., Pasadena 4, Calif.
Shapiro, M. D., 3872 Maple Ave., Northbrook, Ill.
Shearer, R. W., Box 2830, Term. Annex, Los Angeles 54, Calif.
Shectman, N., 714 Graisbury Ave., Haddonfield, N. J.
Sheets, M. J., 1017 S. Frederick St., Apt. 1423, Arlington 4, Va.
Shekel, J., 330 Westgate West, Cambridge 39, Mass.
Shelton, E. J., Jr., 57 Donna Rd., Needham 92, Mass.
Shelton, J. T., 1207 Foyer Ave., Cheyenne, Wyo.
Shepherd, J. F., 101 Channing Ave., Cradock, Va.
Sheppard, J. J., Jr., 2677 Belvidere Ave., Seattle 6, Wash.
Shields, R. A., Jr., 210 Farrand Ave., Highland Park 3, Mich.
Shipek, R. H., 513 E. 125 St., Seattle 55, Wash.
Shively, H. G., 1223 Berwin St., Akron 10, Ohio
Shub, Lionel, 41 Park Dr., Boston 15, Mass.
Shuey, C. W., 2627 McNally St., Altadena, Calif.
Sibley, H. C., Jr., 4288 Canal Rd., Spencerport, N. Y.
Sidnam, R. D., 330 East Dr., Oak Ridge, Tenn.
Siegmund, E. L., 14 Wellington Rd., Greenvale, L. I., N. Y.
Siemen, H. A., 8540 Bustleton Ave., Philadelphia 24, Pa.
Sievers, E. S., 1662 Hillhurst Ave., Los Angeles 27, Calif.
Silbert, W. C., 22631 Sunnyside, St. Clair Shores, Mich.
Silva, A. D., Jr., Columbus Process Co., Inc.
Silverman, B. P., c/o Friden Calculating Machines, San Leandro, Calif.
Silverman, E., 321 Forest Ave., Willow Grove 8, Pa.
Silverman, H. M., 3515 Greenly St., Silver Spring, Md.
Simone, C. F., 114 Franklin St., Apt. 2-C2, Morristown, N. J.
Simonton, L. J., 1879 Newton St., N.W., Washington 10, D. C.

(Continued on page 137A)

Membership

(Continued from page 136A)

Simpson, F. W., 342 McKay St., Apt. 4, Ottawa, Ont., Canada
Singer, E., Newfield Ave., Stamford, Conn.
Sloan, G. H., Treble Cove Rd., North Billerica, Mass.
Small, B., 50-15—175 Pl., Flushing, L. I., N. Y.
Smith, A. W., 2535 W. Fifth St., Los Angeles 57, Calif.
Smith, B. D., Jr., 452 Swann Ave., Alexandria, Va.
Smith, B. H., 184 Concord Ave., Belmont, Mass.
Smith, C. H., Jr., Electronic and Nuclear Physics Dept., Westinghouse Research Laboratories, East Pittsburgh, Pa.
Smith, D. I., 196 San Felipe St., Pomona, Calif.
Smith, H. H., 33-22 209 St., Bayside, L. I., N. Y.
Smith, H. H., 175 Manor Dr., Mill Valley, Calif.
Smith, O. H., 5456 N. Hopkins St., Apt. 1, Milwaukee 16, Wis.
Smith, R. S., 704½ South Cottage Grove, Urbana, Ill.
Smith, R. J., Jr., 506 W. Hildebrand Ave., San Antonio 12, Tex.
Smith, Z. R., 109 Sunset Ave., La Grange, Ill.
Smithline, H., 658 Thoreau Ter., Union, N. J.
Smith-Vaniz, W. R., Jr., Prince's Pine Rd., Norwalk, Conn.
Smyth, F. J., Airborne Instruments Lab., 160 Old Country Rd., Mineola, L. I., N. Y.
Snow, C. A., Jr., Middle St., Middletown, Conn.
Snyder, H. H., 129 Union St., Montclair, N. J.
Snyder, W. G., Weaverville, Calif.
Snyder, W., Box 1238, Palo Alto, Calif.
Soltes, A. S., 33 Hagar Lane, Waltham 54, Mass.
Sorensen, W. N., 10110 Tappan Dr., St. Louis 15, Mo.
Spencer, D. L., 1959 Rosemary Hills Dr., Apt. 1, Silver Spring, Md.
Spencer, R. H., Massachusetts Institute of Technology, Bldg. 32, Cambridge 39, Mass.
Spenser, C. W., 611 Northampton Dr., Silver Spring, Md.
Spergel, P., 171 Colonial Ave., Williston Park, L. I., N. Y.
Spiegel, R. E., 175 E. 151 St., New York 51, N. Y.
Spittal, W. R., 185 Bellmore St., Floral Park, L. I., N. Y.
Sprecher, N. D., 7639 Xerxes Ave. S., Minneapolis 23, Minn.
Spriggs, J. O., 9903 Thornwood Rd., Kensington, Md.
Stancliff, V. A., 145 Dessa Dr., Hamden 17, Conn.
Staniforth, A., Box 227, R.R. 1, Ottawa, Ont., Canada
Stannard, G. E., 3 Whitney Dr., Paxton, Mass.
Stansfield, F. H., 3061 Edwin Ave., Apt. 4E, Fort Lee, N. J.
Starkey, M. J., 1200—17 St., Manhattan Beach, Calif.
Staub, D. W., 5707 Second St., S.E., Washington 21, D. C.
Stauder, L. F., Box 1413, University of Notre Dame, Notre Dame, Ind.
Steele, C. W., 959 Waverly, Palo Alto, Calif.
Steele, R. B., 20 Pine Way, New Providence, N. J.
Steen, D. R., 34-57 Silverton Ave., Wantagh, L. I., N. Y.
Steiger, B. F., 24 Webster Ave., Summit, N. J.
Stern, E., 2314 Holland Ave., Bronx 67, N. Y.
Stevens, R. R., Michigan Bell Telephone Co., Rm. 313, 118 Clifford, Detroit 26, Mich.

(Continued on page 139A)

(Continued from page 137A)

Stimson, J. D., 2777 Fleur Dr., San Marino, Calif.
Stone, N. T., 4412—16 Ave., S., Minneapolis 7, Minn.
Strom, L. D., 3720 Dunhaven Rd., Dallas 20, Texas
Stumpf, R. J., 6176 Cleon Ave., North Hollywood, Calif.
Sturrock, J. K., Box 237, R.C.A.F., Stat. Rockcliffe, Rockcliffe, Ont., Canada
Sublette, I. H., 132 Wayne Ave., Haddonfield, N. J.
Sulkowski, E. L., Grandview Dr., R. D. 2, Canonsburg, Pa.
Sullivan, R. P., 1541 Hollywood, Grosse Pointe Woods 36, Mich.
Sulzer, P. G., 10605 St. Paul St., Kensington, Md.
Sund, H. E., Jr., Box 421, Los Gatos, Calif.
Suter, S. G., 5625 Rural St., Pittsburgh 6, Pa.
Svendsen, E. C., USN, San Francisco Naval Shipyard, Code 125, San Francisco, Calif.
Swift, I. H., 602 B, Essex Circle, China Lake, Calif.
Sylvester, G. E., 20060 Lime Crest Dr., Covina, Calif.
Szabo, W., Reeves Soundcraft Corp., Disc. Div., 204 Walnut St., Allentown, Pa.
Szegda, A., 561 E. Cass St., Joliet, Ill.
Taglauer, E. R., 3048 Lyndale Ct., Edgewood, Covington, Ky.
Talcott, M. S., 1115 34 Ave., Seattle 22, Wash.
Talkin, A. I., Diamond Ord. Fuze Labs., Washington 25, D. C.
Tanana, E. J., 4845 W. 24 Pl., Cicero, Ill.
Tanenbaum, M. S., 518 Hawthorne St., Massapequa, L. I., N. Y.
Tanigawa, N. F., 45-235 Haunani Pl., Kaneohe, Oahu, Hawaii
Taskett, D. A., 1164 Laurel St., Berkeley 8, Calif.
Teal, E. E., 4002 Drummond, Houston 25, Tex.
Tedder, P. M., Rt. 3, Box 58, Gainesville, Fla.
Teetzel, F. M., R.R. 1, Oxford, Ohio
Teich, P. J., 201 S. Midler Ave., Syracuse 6, N. Y.
Terrell, J. M., Jr., 5003 Newport Dr., Chattanooga 11, Tenn.
Tesno, R. R., 142 Gubernat Dr., S. Plainfield, N. J.
Thatcher, T. W., Jr., Bell Telephone Labs., 463 West St., N. Y. 14, N. Y.
Theodore, C., 1019 Gettysburg, Fresno, Calif.
Thomas, M. W., 1400 N.E. 45 St., Oklahoma City, Okla.
Thomas, W. P., Jr., 228 Woodbine Ave., Syracuse, N. Y.
Thompson, A. G., Rt. 2, Norwood, Vill., Bellevue, Wash.
Thompson, E. M., 2521 Central Ave., Alameda, Calif.
Thompson, Everett E, 6 E. Richard Dr., Pine Bluff, Ark.
Thompson, J. H., 307 Rose Ave., Pittsburgh 35, Pa.
Thompson, L. G., 2735 Hillview Rd., Broomall, Pa.
Thompson, P., 325 22 St., N.E., Cedar Rapids, Iowa
Thompson, A., 1642 S.W. Westwood Dr., Portland 1, Ore.
Tice, T. E., 2214 Jervis Rd., Columbus 21, Ohio
Tickell, E. B., 923 N. La Brea Ave., Los Angeles 38, Calif.
Tisdale, G. E., Box 328, New Canaan, Conn.
Todes, R. S., 3822 S. Cross Dr., Baltimore 7, Md.
Tom, H., Box 3532 MCLI, USAF INST. OF TECH., Wright-Patterson AFB, Ohio

(Continued on page 140A)

IRE Membership

(Continued from page 139A)

Tomcik, D. J., R.R. 2, Buchanan, Mich.
Toms, E. C., Graybar Elec. Co., Inc., Sixth & Cary Sts., Richmond 19, Va.
Toukdarian, R. Z., 1487 W. Harding Ave., Pasadena 7, Calif.
Tracy, T. J. R., 3645 Gaspar Dr., Dallas, Texas
Trelewicz, E. R., 7931 71 Ave., Glendale 27, L. I., N. Y.
Troell, R. E., 115 N. Pleasant Ave., Ridgewood, N. J.
Tucker, J. W., 603 N. View Ter., Alexandria, Va.
Turnbull, H. A., Fed. Comm. Com., Washington 25, D. C.
Turner, K. A., 14 Ralston Ave., Toronto 6, Ont., Canada
Underberger, G. M., 6213 Alonzo Ave., Reseda, Calif.
Updike, O. L., Jr., 1329 W. Birch St., Oxnard, Calif.
Urbank, J. G., 108 Rockville Centre Pky., Oceanside, L. I., N. Y.
Vaccaro, F. E., 112 N. Munn Ave., E. Orange, N. J.
Van Cott, J. M., 705 Sylvan Rd., Winston-Salem, N. Car.
Vanderburgh, A., Jr., 52 Massachusetts Ave., Cambridge 39, Mass.
Van Dusen, H. J., 256 Pilgrim, Highland Park 3, Mich.
Van Nice, R. I., 1021 N. Lang Ave., Pittsburgh 8, Pa.
Van Tilbury, J. D., 1930 Seventh Ave., Marion, Iowa
Vavra, P. H., 18 Trincard Rd., Hampton, Va.
Veburg, J. C., Friendsville Stage, Binghamton, N. Y.
Veit, F., 78-08 75 St., Glendale, L. I., N. Y.
Vene, J. M., 220 E. Jefferson, Fort Wayne, Ind.
Versoy, I. R., Jr., Niantic River Rd., Waterford, Conn.
Verven, S. J., 4 Case Ct., Poughkeepsie, N. Y.
Vignos, J. P., 908 Colonial Blvd. N.E., Canton 4, Ohio
Vlcek, D. H., Ades Project Office, 220 Church St., New York 13, N. Y.
Vosteen, R. E., 473 Backus Rd., Webster, N. Y.
Wadlin, M. L., R.C.A. Labs. Div., Princeton, N. J.
Wagner, R. L., 105 Lane Ave., Caldwell, N. J.
Wagner, T. C. G., 5123 Newport Ave., Washington 16, D. C.
Wahl, A., 1228 Lansdowne Ter., Plainfield, N. J.
Walder, B., Lake Allandale, Peekskill, N. Y.
Walker, A. C., Control Elect. Co., Inc., 1925 New York Ave., Huntington Station, L. I., N. Y.
Waller, E. E., 2321 Oak St., Northbrook, Ill.
Wallmark, M., Dept. of Electronics, Royal Inst. of Tech., Stockholm 70, Sweden
Wambsganss, B., Box 1635, Stanford, Calif.
Ward, W. P., 1881 Cornelia St., Ridgewood, Brooklyn 27, N. Y.
Warner, H., 2316 Armstrong Ave., Holmes, Pa.
Warren, Chas. W., 37 Mali Dr., N. Plainfield, N. J.
Warshaw, C. H., 7643-A Washington Lane, Elkins Park, Pa.
Washburn, B. W., 403 Truman, N. E., Albuquerque, N. Mex.
Wassilik, E. J., 100 Clearview Dr., N. Syracuse, N. Y.
Watts, C. B., Jr., 90 Church St., Winchester, Mass.
Wearden, P. L., 235 Canterbury Dr., Beaumont, Texas
Weaver, J. L., 1433 Glen Moore Circle, Lancaster, Pa.
Webb, J. C., Box 368, Newburgh, N. Y.

(Continued on page 142A)

What Opportunities in Electronics are on the Horizon at GENERAL ELECTRIC?

Huge antenna used with new radar height-finder needs a room all its own above the control center in the radome building erected in Arctic climates. Air pressure supports the rubberized glass fabric radome "balloon." Entrance to the radome is through an air lock chamber.

Advances in electronics are so rapid at General Electric that today's predictions appear tomorrow as equipment bearing the GE symbol.

The opportunities created by the scope and pace of the field are increased at General Electric by the facilities and range of professional advantages which GE engineers enjoy.

This means that GE electronics engineers have incentives, satisfactions and rewards that lead to accelerated personal development and advancement in the company.

ENGINEERS · PHYSICISTS

Positions available in the following fields:

Advanced Development, Design, Field Service and Technical Writing in connection with:

MILITARY RADIO & RADAR • MULTIPLEX MICROWAVE MOBILE COMMUNICATION • SEMI CONDUCTORS • ELECTRONIC COMPONENTS • TELEVISION, TUBES & ANTENNAS

Bachelor's or advanced degree in Electrical or Mechanical Engineering, physics, and experience in electronics industry necessary.

Please send resume to:
Dept. 8-5-P — Technical Personnel

GENERAL ELECTRIC

ELECTRONICS PARK, SYRACUSE, N. Y.

SUPERVISOR

for

APPLICATION ENGINEERING

for major manufacturer of
Electronic Tubes
Location: Eastern Seaboard

SHOULD HAVE ABOUT 10 YEARS EXP IN THESE FIELDS. SALARY OPEN.

- Wonderful plant location
- Unusual company benefits
- Outstanding opportunities for professional progress

Traveling and moving expenses paid. All replies confidential. Send resume, Box I.R.E. 1034, 221 W. 41st St., New York, N.Y.

ELECTRONIC DEVELOPMENT ENGINEERS

CHALLENGING DESIGN & DEVELOPMENT POSITIONS FOR CREATIVE ENGINEERS

These positions are tailor-made for highly imaginative engineers who enjoy problems of more than ordinary difficulty—problems that require a maximum of individual electronic creativity. Men selected will be entrusted with the complete electronic or electromechanical design and development tasks (initial circuits, systems, components, or product design) entailed in carrying a prototype project from original conception to its completion.

REQUIREMENTS: Senior and Intermediate engineers with degrees and 4 to 8 years' experience; Junior engineers with degrees and 1 to 3 years' experience, capable of growing with our long-range, electronic design and development program in the following fields:

(1) ANALOG COMPUTER
(2) RADAR BEACONS
(3) MAGNETIC AMPLIFIERS
(4) ELECTRO-OPTICS
(5) MISSILE SYSTEMS
(6) SERVOS
(7) FIRE CONTROL SYSTEMS

Interviews will be arranged at convenient locations.

Send resume to:

AVION DIVISION
OF ACF INDUSTRIES INCORPORATED

Route 17, Paramus, N.J. COlfax 1-4100

Membership

(Continued from page 140A)

Weckwerth, H. A., 39 Gressing Ct., Cedar Grove, N. J.
Wehner, J. H., Allen B. DuMont Labs., Inc., 2 Main Ave., Pássaic, N. J.
Weil, K., 32-10 93 St., Jackson Heights, L. I., N. Y.
Weil, T. A., 14 Linden Gardens, Wellesley 81, Mass.
Weiner, S. L., Archer Ave., Stamofrd, Conn.
Weisbrod, S., 4326 Hill St., San Diego 7, Calif.
Weise, D. S., 705 Lees Lane, Collingswood, N. J.
Weissman, E., 730 W. 183rd St., New York 33, N. Y.
Welber, I., 30 Edward Ct., New Providence, N. J.
Weller, B. L., R.D. 2, Stepney, Conn.
Wells, M., Box 6087, Cleveland 1, Ohio
Wentworth, J. W., 383 Tavistock Blvd., Haddonfield, N. J.
Werts, L. C., Loyola University of Los Angeles, 7101 W. 80 St., Los Angeles 45, Calif.
Wesley, C. A. E. Ridge, Ridgefield, Conn.
Westbrook, E. P., 36 Linden Pl., Nutley, N. J.
Westbrook, R. D., 3456 E. Scarborough, Cleveland Heights 18, Ohio
Westcott, V. C., R.F.D. 1, Concord, Mass.
Westlake, P. R., 230 E. California St., Pasadena 5, Calif.
Westphal, W. B., M.I.T. Rm. 4-244, Cambridge 39, Mass.
Westrate, M. C., Commonwealth Assoc., 252 W. Cortland, Jackson, Mich.
Wexler, C. H., 10 Hopson St., Utica, N. Y.
Wexler, M. P., 4762 Belwood GN, Baltimore 27, Md.
Wheatland, D. P., Six Dininity Ave., Cambridge 38, Mass.
Wheatley, W. A., 237 Edison Ave., Ypsilanti, Mich.
Wheeler, F. K. B., CINCPACFLT, Code 54, Navy 128, F.P.O. San Francisco, Calif.
Wheeler, M. S., 1506 Midvale Ave., Baltimore 28, Md.
Whitaker, J. L., 8460 Abilene Terr., La Mesa, Calif.
White, E. A., Rd. 1, Forest Greens, Aberdeen, Md.
White, R. F., 4831 Highland Ave., Downers Grove, Ill.
Wade, Orison, 4858 Atlanta Dr., San Diego 15, Calif.
Wick, R. S., 213 Clover Ridge Dr., Syracuse 6, N. Y.
Wickliffe, P. R., Jr., Bell Telephone Labs., Murray Hill, N. J.
Wieder, H. H., U.S. Naval Ord. Lab., Corona, Calif.
Wieland, C. W., 541 S. El Molino Ave., Pasadena 5, Calif.
Wiener, W. A., 8 Bayview Ave., Islip, L. I., N. Y.
Wildermuth, J. L., 4010 Tennyson Rd., University Park, Hyattsville, Md.
Wilkinson, J. D., 2406 Ross Ave., Dallas 1, Texas
Williams, A. M., 2006 Milam St., Amarillo, Texas
Williams, C., 4028 Via Largavista, Palos Verdes Estates, Calif.
Williams, D. G., Boxboro Depot Rd., Littleton, Mass.
Williams, J. R. L., Apartado 700, Madrid, Spain
Williams, L. L., III, 105 E. Lenox St., Chevy Chase 15, Md.
Williams, R. B., Jr., 3348 Van Fleet Pkwy., Toledo 6, Ohio
Williams, W. S., 1630 Glen Keith Blvd., Baltimore 4, Md.
Williiamson, R. G., 22 Melrose Ave., E. Norwalk, Conn.

(Continued on page 143A)

(Continued from page 142A)

Williston, S. S., 43 South St., Williamsburg, Mass.
Wilshinsky, I., 113 Ravine Dr., Matawan, N.J.
Wilson, L. F., 15 Sunnie Terr., W. Caldwell, N. J.
Wilson, M. S., Willarch Rd., S. Lincoln, Mass.
Wilson, R. F., Gen. Elec. X-Ray Dept., 4855 Elect. Ave., Milwaukee 14, Wis.
Wilson, W. D., 6245 Adobe Dr., San Diego 15, Calif.
Wimmer, A. A., 1059 Maple Lane, Herricks, New Hyde Park, L. I., N. Y.
Wimmer, P. L., 539 Melody Lane, R.R. 5, Vienna, Va.
Winans, R. C., Bell Tel. Labs., Inc., Whippany, N. J.
Winchell, R. W., 902 Whittier Dr., Beverly Hills, Calif.
Windus, W. A., 2921 Soutter Ave., S.E., Cedar Rapids, Iowa
Winklestein, R. A., 159 Frederick St., Lake Allandale, Peekskill, N. Y.
Wise, D. O., Jr., Box 455, Univ. Br., Coral Gables, Fla.
Woestman, J. W., 331 Leconey Ave., Palmyra, N. J.
Wolf, S. B., 21200 Kipling Ave., Oak Park 37, Mich.
Wolfe, H. T., 5706 Ross St., Oakland 18, Calif.
Wolfe, J. A., 21 Coulton Park, Needham, Mass.
Wolff, J. R., 7541 S. Essex Ave., Chicago 49, Ill.
Wolfthal, D. A., 270 Ft. Washington Ave., New York 32, N. Y.
Wolman, L. L., 7917 Ranchito St., Van Nuys, Calif.
Wolotkin, A., 299 E. Mt. Eden Ave., New York 57, N. Y.
Wolter, Herbert R., 225 72 St., N. Bergen, N. J.
Wood, A. G., 288 Bear Ridge Rd., Pleasantville, N. Y.
Wood, Barton C.. Natl. Bur. of Standards, Div. 74,03, Corona, Calif.
Wood, I. E., Bell Tel. Labs., Murray Hill, N. J.
Woodbridge, D. E., R.D. 2, Carter Rd., Princeton, N. J.
Woodcock, C. A. ,8476 Pine Rd., Rossmoyne, Ohio
Woodruff, T. E., Hughes Aircraft, Florence-At-Teal, Culver City, Calif.
Woodson, W. L., 19044 Schoolcraft, Reseda, Calif.
Woodward, R. H., 46 Prospect St., Belmont 78, Mass.
Worster, J. R., Butler Town Rd., Oakdale, Conn.
Worthington, D. T., 318 Hamilton Ave., Rome, N. Y.
Wright, W. W., 429 Montgomery Ferry Dr., N.E., Atlanta, Ga.
Wulfsberg, K. N., 58 Concord Rd., Bedford, Mass.
Yale, W. H., 3 N. Clover Dr., Great Neck, N. Y.
Yeager, J. R., 909 Helmsdale Rd., Cleveland 12, Ohio
Yeutter, C. S., 731 Park Ave., Oradell, N. J.
Yewdall, G. E., 610 Chestnut St., Palmyra, N. J.
Yingst, T. E., 321 E. Roseville Rd., Lancaster, Pa.
Yoder, D. R., Raytheon Mfg. Co., 622 S. La Brea Ave., Los Angeles 36, Calif.
Yost, K. E., Dayton, Ind.
Yostpille, J. J., c/o Bell Tel. Labs., 473 West St., New York 14, N. Y.
Young, C. H., St. Mary's Co., Hollywood, Md.
Zebrowitz, S., 4417 Spruce St., Philadelphia 4, Pa.
Zecher, R. O., 213 Oakley Dr., Syracuse 5, N. Y.
Zeller, H. R., 2905 N. Ridgeway Ave., Chicago 18, Ill.

(Continued on page 145A)

ELECTRONICS ENGINEERS

Emerson

OFFERS

"A CAREER with a PRESENT as well as a FUTURE!"

in the fields of

- Radar
- Antennas
- Fire Control
- Network Theory
- Servo-Amplifiers
- Pulse Techniques
- Analog Computers
- Magnetic Amplifiers
- Microwave Techniques
- Electronic Countermeasures

Emerson's new air-conditioned Main Office and Engineering Laboratories, Jersey City, New Jersey.

Emerson's new air-conditioned Research Laboratories Washington, D.C.

SUBMIT RESUME (According to Location Preferred) TO:

Mr. R. I. Hoffman, Engineering Personnel Manager

EMERSON RADIO & PHONOGRAPH CORP.

14th and Coles Streets, Jersey City 2, N.J.

OR

Dr. R. E. Wilson

EMERSON RESEARCH LABORATORIES

701 Lamont Street, N.W. Washington 10, D.C.

ENGINEERS

ELECTRONIC

Experience in research & development of pulse circuitry, computing components and servo systems.

SYSTEMS (E. E.)

For work in the development of airborne navigational equipment.

MECHANICAL

2-3 years' experience in the design of precision instruments.

DESIGNERS

ELECTRONIC
ELECTRO-MECHANICAL
MECHANICAL

1. Electronic or electrical packaging. Knowledge of sub-miniaturized techniques. Work is associated with servos, amplifiers and computers.
2. Mechanical or electro-mechanical packaging of precision flight instruments.

The modern facilities and congenial atmosphere at Kollsman, designers of America's finest aircraft instruments, provide an environment conducive to truly creative work.

Please submit complete resumes to Employment Manager.

kollsman INSTRUMENT CORPORATION

80-08 45th AVENUE, ELMHURST, NEW YORK • SUBSIDIARY OF *Standard* COIL PRODUCTS CO. INC.

CAREER OPENINGS AT NORTH AMERICAN AVIATION, INC.

Instrumentation

Engineers apply. Analytic and experimental techniques for the selection and application of instruments for the static and dynamic measurement of displacement, force, pressure, etc.

Knowledge of transducers, amplifiers and recording equipment is essential.

E.E. or PHYSICS degree and 3 to 5 years experience preferred.

Maximum personal benefits include paid vacations and sick leave.

For more information contact Mr. Nance, Engineer Personnel Office.

NORTH AMERICAN AVIATION, INC.

S.E. Cor., International Airport, L.A. 45, Calif.

NORTH AMERICAN AVIATION HAS BUILT MORE AIRPLANES THAN ANY OTHER COMPANY IN THE WORLD.

Membership

(Continued from page 143A)

Zellmer, N. A., 268 Elm, Apt. 3, San Carlos, Calif.
Zemanek, J., Jr., 2106 Melbourne, Dallas 24, Texas
Zetrouer, W. F., II, Rt. 2, Gainesville, Fla.
Zimbel, N. S., 77 Montvale Rd., Newton Center, Mass.
Zobel, E. R., 1304 Mohawk, Bismark, N. Dak.
Zohn, R. L., 512 Gilpin Rd., Willow Grove, Pa.
Zukin, A. S., 2700 Butler Ave., Los Angeles 64, Calif.
Zurbriggen, J. H., 1454 High School Dr., St. Louis 17, Mo.
Zweifler, I., 812 Jefferson St., Woodmere, L. I., N. Y.
Zweizig, J. R., 4216 York Blvd., Los Angeles 65, Calif.

The following elections to the Associate grade were approved to be effective as of July 1, 1955:

Bader, J. M., 135 Division Ave., Levittown, L. I., N. Y.
Badger, A. H., 2341 N. Main, Royal Oak, Mich.
Baird, D. R., 416 Rainbow Dr., Kokomo, Ind.
Bartlett, W. F., Officers' Mess, Royal Air Force, Linton-on-Ouse, York, England
Bisko, T., 51 Avenue "B," Battle Creek, Mich.
Breland, M. H., 8107 Kenwood Dr., Norfolk 5, Va.
Briel, L. A., 18700 Saticoy St., Reseda, Calif.
Bruder, R. M., 523 Rockledge Rd., Ottawa, Ont., Canada
Brugman, W. E., 7501 El Manor Ave., Los Angeles 45, Calif.
Brunsting, A. W., 8316 S. Throop St., Chicago 20, Ill.
Bumpass, R. C., 1318 Vine Ave., Martinez, Calif.
Burton, R. E., Apt. 1508, 1300 Oakland Rd., Cedar Rapids, Iowa
Byle, B. J., State Highway 23, Mountain View, N. J.
Campbell, G. S., 3806 St. Elmo Ave., Chattanooga 9, Tenn.
Cashman, D. J., 535 May St., Waukegan, Ill.
Caulkins, D. C., 2527 Eaton Rd., Cleveland Heights 18, Ohio
Chapman, S. J., Sun Life of Canada, Box 6075, Montreal, Que., Canada
Chen, D-B., RCA, Bldg. 10-3, Camden 2, N. J.
Christiansen, E. M., 9 Sognegards alle, Hvidovre, Valby, Denmark
Cole, E. M., Sr., 1206 W. 52 St., Los Angeles 37, Calif.
Cooney, J. A., 53 Timber La., Levittown, L. I., N. Y.
Despathy, R. G., 320 Belmont St., Wollaston, Mass.
Dewig, E. L., U.C.L.A., School of Medicine, Biophysics, Los Angeles 24, Calif.
Deyerle, C. D., 4549 Lesher Dr., Dayton, Ohio
Dodgson, W. W., Jr., Radiation, Inc., Box Q, Melbourne, Fla.
Dombro, L., 2256 Walton Ave., New York 53, N. Y.
Duffy, J. M., 126 Brookline St., Lynn, Mass.
Edam, D. M., Box 97, Star Route, Destin, Fla.
Feinland, S., 436 Logan St., Brooklyn 8, N. Y.
Fields, I. L., 4049 Eastway Rd., South Euclid 21, Ohio
France, R. W., 9147 Hastings Ave., Los Angeles 45, Calif.
Francisco, G. E., Jr., 284 N. Gould Rd., Apt. 1-C, Columbus 9, Ohio
Fredericks, C. F., Rothenburg Rd., Meadow Park, Poughkeepsie, N. Y.
Friedman, S. N., 26 Post St., Yonkers 5, N. Y.
George, E. W., 30214 Westlawn Dr., Bay Village, Ohio
Ghiron, H., 1200 Fifth Ave., New York, N. Y.

(Continued on page 146A)

Membership

(Continued from page 145A)

Gilbertson, O. E., Box 41, O'Fallon, Ill.
Golding, J., 52 Elm St., Newark 5, N. J.
Goldman, E. M., 201-6504 Wilson Blvd., Falls Church, Va.
Hall, F. E., 3205 Northway Dr., Baltimore 14, Md.
Hamilton, J. M., Jr., 1620 Tropic St., Titusville, Fla.
Harrap, V., 25 Gleneverest Rd., Apt. 6, Toronto, Ont., Canada
Harrison, W. F., Jr., 1327 Dartmouth Dr., N.E., Albuquerque, N. Mex.
Hobstetter, J. P., 11 W. Monument, Dayton 2, Ohio
Hooker, R. H., Receipt Control Sec., Supply Div., Naval Research Laboratory, Washington 25, D. C.
Johnson, H. B., 4516 W. 17 St., Los Angeles 19, Calif.
Johnson, J. H., 46 Walnut Ave., Rockville Centre, L. I., N. Y.
Kasvand, T., 75½ Bay St., S., Hamilton, Ont., Canada
Kay, W. L., E. I. duPont, Pigments Dept., Newport, Del.
Kladke, W. F., Jr., 32 Wrexham Ct., S., Tonawanda, N. Y.
Kobold, J. W., c/o WCIA-TV, Champaign, Ill.
Krantz, K. B., 1653 Eighth St., N.W., Cedar Rapids, Iowa
Krug, R. E., 814 W. Wisconsin Ave., Milwaukee 3, Wis.
Lees, K. C., 19 Beloeil Ave., Outremont, Que., Canada
Leidy, H. W., 123 Vesper Ave., Westmont 7, N. J.
Levandosky, J. R., USS Carter Hall, LSD 3, c/o FPO, San Francisco, Calif.
Levin, M. H., 19 Brookledge St., Roxbury 21, Mass.
Louderback, H. W., Jr., RCA Repr., Com. Serv. Lant., Box 9, Bldg. 142, Norfolk 11, Va.
McCreanor, R. A., J. & L. Research Laboratory, 900 Agnew Rd., Pittsburgh 27, Pa.
McGrail, J. G., 4924 W. Adams St., Chicago 44, Ill.
McNeil, J. F., 296 Wisconsin Ave., E. Dubuque, Ill.
Maresca, T. J., 613 S. Meadow St., Ithaca, N. Y.
Masters, W. C., R.F.D. 2, Walhalla, S. C.
Matlack, R C., Bell Tel. Labs., 463 West St., New York 14, N. Y.
Maung, U. A., 17 Link Rd., Churchill P.O., Rangoon, Union of Burma
Michaelson, A. C., 9571 W. Pico Blvd., Los Angeles 35, Calif.
Mitchell, G. W., 3620—44 Ave., S.W., Seattle 16, Wash.
Moss, J. F., Jr., 1017 N. Marengo Ave., Pasadena 3, Calif.
Murr, W. C., 658—22 St., Richmond 9, Calif.
Nations, H. T. R.F.D. 3, Candler, N. C.
Neiland, A. C., 111-47—116 St., S. Czone Park 20, L. I., N. Y.
Newhouse, G. H., 7218 W. 91 St., Los Angeles 45, Calif.
Obenchain, T. I., 1901 N. 17 St., Boise, Idaho
Oertli, E. H., 36 Kreuzstrasse, Zurich 8, Switzerland
Okonski, E. S., Cornell Aeronautical Laboratory, 4455 Genesee St., Buffalo 21, N. Y.
Oliphant, A. J., 39 St. Baldreds Rd., N. Berwick, E. Lothian, Scotland
Ozarka, R. J., 223 Judson Ave., Besenville, Ill.
Parent, G. J. C., 4625 Wellington, Verdun, Que., Canada
Paterson, R. C., Box 573, Alexandria, Va.
Pease, L. A., 1430 Alametos, San Antonio 1, Texas
Peden, J. E., Sandborn, Ind.

(Continued on page 149A)

Membership

(Continued from page 146A)

Pehrson, C. R., 101 Clark Ct., Del Paso Heights, Calif.
Peterson, D. L., 812 Daniels St., N.E., Cedar Rapids, Iowa
Peterson, H. C., 6303 Sligo Pkwy., Hyattsville, Md.
Petrik, J., D.O.T. Aeradio Station, Eldorado, Sask., Canada
Phillips, R. M., 227 Ridge Ave., Liverpool, N. Y.
Pollack, P., 1225 Avenue R, Brooklyn 29, N. Y.
Quinn, D. L., 37 Laird Dr., Trenton, Ont., Canada
Ramage, W. W., 132 Arch St., Verona, Pa.
Ramsey, R. G., 3337 Training Sq., Box 270, Scott AFB, Ill.
Rasmussen, T. J., 30 Beatevej, Copenhagen, Valby, Denmark
Raymond, S. O., c/o Raymond Engineering Lab., Inc., Smith St., Middletown, Conn.
Rial, M. E., 12127 Selfridge Rd., Silver Spring, Md.
Rickey, F. B., Box 244, Gilbert, Ariz.
Robbins, C. M., Box 321, Colorado Springs, Colo.
Rock, P., Box 62, R.F.D. 6, Alexandria, Va.
Rywak, J., Northern Electric Co., Ltd., Belleville, Ont., Canada
Sacerdoti, G., 12 Via Porpora, Rome, Italy
Sanders, J. W., 724 Theresa Dr., Fort Worth, Texas
Sauvie, W. J. J., Box 9049, TAS, Fort Bliss, Texas
Schick, F. T., 47 Ossining Rd., Pleasantville, N. Y.
Scholer, R. M., 1109 Almeria, Coral Gables, Fla.
Schumacher, M. W., Denver, Iowa
Schwartz, E. R., 261-08 Langston Ave., Glen Oaks, L. I., N. Y.
Scott, V. P., Jr., 4821 Butler St., Pittsburgh 1, Pa.
Scratchley, W. P., Jr., 19 Williams Dr., W. Paterson, N. J.
Segelstrom, C. V., 4 MacArthur Blvd., Danvers, Mass.
Sentner, P. J., Box 336, Emporium, Pa.
Sharpe, B. R., 1233 W. Peachtree, Cocoa, Fla.
Shaw, L. R., Box 107, Rockledge, Fla.
Sherwin, L. W., 5807 Willowton Ave., Baltimore 14, Md.
Smith, C. E., 11748 Kiowa Ave., Los Angeles 49, Calif.
Smith, G. F., 2896 W. 41 Ave., Vancouver 13, B.C., Canada
Snell, B. N., Jr., 20 Clinton Pl., Utica, N. Y.
Somes, G. W., 1247 Savoy St., San Diego 7, Calif.
Soohoo, E. L., 385 River St., Waltham, Mass.
Sparkman, L. E., PCT, 1883-D AACS I&M Sqdn., APO 862, c/o Postmaster, New York, N. Y.
Stearns, W. P., 8120 Hannett, N.E., Albuquerque, N. Mex.
Steenhausen, D. R., 4826 Washington Blvd., Chicago 44, Ill.
Thompson, V. L., Box 440, R.F.D. 1, Ketchamtown Rd., Wappingers Falls, N. Y.
Turney, G. M., R.F.D. 4, Trenton, Ont., Canada
Valentine, E., 1900 S. Peninsula Dr., Daytona Beach, Fla.
Vertar, J. A., 20 Pike Rd., Bentleyville, Pa.
Viterisi, D. P., 1546 Fourth Ave., S. E., Cedar Rapids, Iowa
Wagner, R. J., 7711 Kelly St., Pittsburgh 21, Pa.
Walters, G. E., Stavid Engineering Co., Watchung, N. J.
Ward, A. L., III, 1803 W. Monticito Way, San Diego 3, Calif.
Welch, J. D., 2131 First Ave., W., Cedar Rapids, Iowa
Welker, C. M., 705 Backus, Jackson, Mich.

(Continued on page 152A)

News-New Products

These manufacturers have invited PROCEEDINGS readers to write for literature and further technical information. Please mention your I.R.E. affiliation.

(Continued from page 152A)

include an Automatic Transistor Noise Figure Meter, which measures noise figure of all types of transistors and transistor amplifiers on a direct reading basis, a Transistor Alpha Tester, which gives a direct reading of the dynamic value of alpha, and tests for alpha cut-off, and a Transistor Comparison Tester, which performs comparison tests on transistors and diodes. Also described is a Noise Figure Calibrator, which supplies noise figure values for calibration and reference.

Transistor-Transformer

Redesign of a miniature interstage transistor transformer has produced a new model $\frac{1}{3}$ smaller than the recent prototype, according to **Telex, Inc., E-A Division,** Telex Park, St. Paul 1, Minn.

Now measuring only $\frac{3}{8} \times \frac{3}{8} \times \frac{3}{8}$ inch, the transformer has numerous industrial uses in audio amplifiers, hearing aids, control circuits and other transistorized circuitry.

Only the #8901 transistor interstage model is available at the present time, but output and input models are available by special request. All three types are readily available in a fractionally larger size.

Impedance of the interstage primary is 20,000 ohms, and the secondary is 1,000 ohms. Frequency response is ±3 db from 150 to 15,000 cps with 0.25 milliamperes (dc) in the primary. This transformer will handle up to 0.5 milliwatts.

For additional information and prices write Dept. KP, Telex, Inc.